frontiers | Research Topics

Insights in cardiac rhythmology 2022

Edited by
Matteo Anselmino and Hung-Fat Tse

Published in
Frontiers in Cardiovascular Medicine

ISSN 1664-8714
ISBN 978-2-8325-3876-0
DOI 10.3389/978-2-8325-3876-0

About Frontiers

Frontiers is more than just an open access publisher of scholarly articles: it is a pioneering approach to the world of academia, radically improving the way scholarly research is managed. The grand vision of Frontiers is a world where all people have an equal opportunity to seek, share and generate knowledge. Frontiers provides immediate and permanent online open access to all its publications, but this alone is not enough to realize our grand goals.

Frontiers journal series

The Frontiers journal series is a multi-tier and interdisciplinary set of open-access, online journals, promising a paradigm shift from the current review, selection and dissemination processes in academic publishing. All Frontiers journals are driven by researchers for researchers; therefore, they constitute a service to the scholarly community. At the same time, the *Frontiers journal series* operates on a revolutionary invention, the tiered publishing system, initially addressing specific communities of scholars, and gradually climbing up to broader public understanding, thus serving the interests of the lay society, too.

Dedication to quality

Each Frontiers article is a landmark of the highest quality, thanks to genuinely collaborative interactions between authors and review editors, who include some of the world's best academicians. Research must be certified by peers before entering a stream of knowledge that may eventually reach the public - and shape society; therefore, Frontiers only applies the most rigorous and unbiased reviews. Frontiers revolutionizes research publishing by freely delivering the most outstanding research, evaluated with no bias from both the academic and social point of view. By applying the most advanced information technologies, Frontiers is catapulting scholarly publishing into a new generation.

What are Frontiers Research Topics?

Frontiers Research Topics are very popular trademarks of the *Frontiers journals series*: they are collections of at least ten articles, all centered on a particular subject. With their unique mix of varied contributions from Original Research to Review Articles, Frontiers Research Topics unify the most influential researchers, the latest key findings and historical advances in a hot research area.

Find out more on how to host your own Frontiers Research Topic or contribute to one as an author by contacting the Frontiers editorial office: frontiersin.org/about/contact

Insights in cardiac rhythmology: 2022

Topic editors

Matteo Anselmino — University of Turin, Italy

Hung-Fat Tse — The University of Hong Kong, Hong Kong, SAR China

Citation

Anselmino, M., Tse, H.-F., eds. (2023). *Insights in cardiac rhythmology: 2022*. Lausanne: Frontiers Media SA. doi: 10.3389/978-2-8325-3876-0

Table of contents

frontiers in Cardiovascular Medicine

BRIEF RESEARCH REPORT
published: 24 March 2022
doi: 10.3389/fcvm.2022.836288

Impact of the COVID-19 Pandemic and Public Restrictions on Outcomes After Catheter Ablation of Atrial Fibrillation

*Daehoon Kim, Hee Tae Yu, Tae-Hoon Kim, Jae-Sun Uhm, Boyoung Joung, Moon-Hyoung Lee and Hui-Nam Pak**

Yonsei University College of Medicine, Yonsei University Health System, Seoul, South Korea

Background: Here we aimed to analyze changes in the outcomes of atrial fibrillation (AF) catheter ablation (AFCA) during the coronavirus disease 2019 (COVID-19) pandemic and examine the relationship between rhythm outcomes and the stringency of government social distancing measures.

Methods: We included 453 patients who underwent *de novo* AFCA between May 2018 and October 2019 (pre-COVID-19 era) and 601 between November 2019 and April 2021 (COVID-19 era). The primary outcome was late recurrence, defined as any episode of AF or atrial tachycardia documented after a 3-month blanking period. A multivariable Cox regression analysis was performed to estimate the relative hazards of AF recurrence in the two eras.

Results: In the study population (24.3% women; median age, 60 years), 660 (62.6%) patients had paroxysmal AF. Among those with paroxysmal AF, the late recurrence rate was significantly lower in the COVID-19 era than in the pre-COVID-19 era [9.4% vs. 17.0%, respectively, log-rank P = 0.004; adjusted hazard ratio (HR) 0.56, 95% confidence interval (CI) 0.35–0.90] during a median follow-up of 11 months. In patients with persistent AF, the late recurrence rate did not significantly differ between the pre-COVID-19 and COVID-19 era groups (18.9% vs. 21.5%, respectively; log-rank P = 0.523; adjusted HR 0.84, 95% CI 0.47–1.53) during the median follow-up of 11 months.

Conclusion: A decrease in AF recurrence after catheter ablation was observed in patients with paroxysmal AF during the COVID-19 outbreak, whereas no change was observed in those with persistent AF.

Keywords: atrial fibrillation, COVID-19, pandemic, catheter ablation, rhythm outcome

OPEN ACCESS

Edited by:
Junbeom Park,
Ewha Womans Medical Center,
South Korea

Reviewed by:
François Regoli,
University of Zurich, Switzerland
Alexis Hermida,
University Hospital Center (CHU)
of Amiens, France

****Correspondence:***
Hui-Nam Pak
hnpak@yuhs.ac

Specialty section:
This article was submitted to Cardiac Rhythmology, a section of the journal Frontiers in Cardiovascular Medicine

Received: *15 December 2021*
Accepted: *02 March 2022*
Published: *24 March 2022*

Citation:
Kim D, Yu HT, Kim T-H, Uhm J-S, Joung B, Lee M-H and Pak H-N (2022) Impact of the COVID-19 Pandemic and Public Restrictions on Outcomes After Catheter Ablation of Atrial Fibrillation. Front. Cardiovasc. Med. 9:836288. doi: 10.3389/fcvm.2022.836288

INTRODUCTION

Severe acute respiratory syndrome coronavirus-2, which causes coronavirus disease 2019 (COVID-19), has affected over 2 million people worldwide (1). As a result, many countries have implemented public health restrictions to mitigate its spread. In Korea, non-pharmaceutical interventions (NPIs), including compulsory mask-wearing, social distancing, and enhanced screening and testing, were implemented in February 2020, the early phase of the outbreak (**Supplementary Figure 1A**) (2).

Electrophysiologic issues, including arrhythmias or device-related issues, have been increasingly recognized as a manifestation of COVID-19. While the need for services from electrophysiology laboratories continues to increase, a recent consensus paper recommended canceling or postponing elective cases during the pandemic (3). However, little is known about the impact of the COVID-19 pandemic and associated public health restrictions on clinical outcomes of catheter ablation for atrial fibrillation (AF).

METHODS

Study Population

This single-center retrospective observational study aimed to analyze changes in the outcomes of AF catheter ablation (AFCA) during the COVID-19 pandemic and examine the relationship between rhythm outcomes and the stringency of government social distancing measures. We included 453 consecutive patients who underwent *de novo* AFCA between May 2018 and October 2019 (18 months of the pre-COVID-19 era) and 601 between November 2019 and April 2021 (18 months of the COVID-19 era) at Severance Cardiovascular Hospital, a tertiary referral center in the Republic of Korea (**Supplementary Figures 1B,C**). The study protocol adhered to the Declaration of Helsinki and was approved by our institutional review board. Written informed consent was obtained from all patients (ClinicalTrials.gov: NCT02138695). The exclusion criteria were: (1) permanent AF refractory to electrical cardioversion; (2) AF with valvular disease $\geq$ grade 2; (3) a previous cardiac surgery with concomitant AF surgery or AFCA; and (4) empirical extra-pulmonary vein (PV) ablations other than the typical circumferential PV isolation. All antiarrhythmic drugs (AADs) were discontinued for at least five half-lives, and amiodarone was stopped at least 4 weeks before the procedure.

Echocardiographic Evaluation

All patients underwent transthoracic echocardiography (Sonos 5500, Philips Medical System, Andover, MA or Vivid 7, GE Vingmed Ultrasound, Horten, Norway) prior to their ablation. Chamber size, left ventricular ejection fraction, transmitral Doppler flow velocity, and the ratio of early diastolic peak mitral inflow velocity to early diastolic mitral annular velocity (E/Em) were acquired according to the American Society of Echocardiography guidelines (4).

Electrophysiological Mapping and Radiofrequency Catheter Ablation

Intracardiac electrograms were recorded using a Prucka CardioLab Electrophysiology system (General Electric Medical Systems, Inc., Milwaukee, WI, United States). Three-dimensional electroanatomic mapping (NavX, St. Jude Medical, Inc., Minnetonka, MN, United States; CARTO, Biosense-Webster, Inc., Diamond Bar, CA, United States) was performed using a circumferential PV mapping catheter (Lasso, Biosense-Webster Inc.) through a long sheath (Schwartz left 1, St. Jude Medical, Inc.). Transseptal punctures were performed, and multiview pulmonary venograms were obtained. The details of the AFCA technique were described previously (5, 6). All patients underwent circumferential PV isolation (CPVI) during the *de novo* procedure. Two-thirds of the patients (62.1%) underwent the creation of a cavotricuspid isthmus block during the *de novo* procedure. Systemic anticoagulation was achieved with intravenous heparin to maintain an activated clotting time of 350–400 s during the procedure. After completion of the protocol-based ablation, the procedure was completed when no recurrence of AF was observed within 10 min after cardioversion with isoproterenol infusion (5–10 μg/min depending on β-blocker use, target sinus heart rate, 120 bpm) (6). Complications were defined according to the 2017 HRS (Heart Rhythm Society)/EHRA (European Heart Rhythm Association)/APHRS (Asia Pacific Heart Rhythm Society)/SOLAECE (Latin American Society of Cardiac Stimulation and Electrophysiology) expert consensus (7). Detailed definitions of the complications have been described previously (8).

Follow-Up and Atrial Fibrillation Recurrence

We discharged patients not taking AADs except for those who had recurrent extra-PV triggers after the AFCA procedure, symptomatic frequent atrial premature beats, non-sustained atrial tachycardia, or an early recurrence of AF on telemetry during the admission period. Electrocardiography was performed for all patients visiting the outpatient clinic 1, 3, 6, and 12 months after AFCA and every 6 months thereafter or whenever symptoms developed. Twenty-four-hour Holter recordings were performed at 3, 6, and 12 months and every 6 months thereafter. Patients who reported episodes of palpitations suggestive of arrhythmia recurrence underwent Holter monitoring or event monitoring recordings.

The primary outcome was late recurrence defined as any episode of AF or atrial tachycardia (AT) lasting at least 30 s after a 3-month blanking period. Early recurrence was defined as any documentation of AF or AT recurrence on ECG within the 3-month blanking period. Follow-up lasted up to January 31, 2020 for the pre-COVID-19 era group and July 31, 2021, for the COVID-19 era group with equal follow-up durations for the groups with a minimum follow-up of 3 months (**Supplementary Figure 1B**).

Statistical Analysis

Continuous variables are summarized as median (interquartile range), while categorical variables are summarized as frequencies (percentages). A Kaplan–Meier analysis with the log-rank test was used to calculate AF recurrence-free survival over time across groups. Multivariable Cox regression analysis was performed to estimate the relative hazards of AF recurrence. The following variables were adjusted: age, sex, duration of AF, body mass index, CHA_2DS_2-VASc, medical history, antiarrhythmic drug use, alcohol use, echocardiographic parameters, an inflammatory marker, ablation lesion set, and follow-up duration (variables in **Table 1**). The proportional hazards assumption was tested based on Schoenfeld residuals (9).

TABLE 1 | Baseline characteristics of patients with paroxysmal and persistent atrial fibrillation undergoing catheter ablation.

Variables	Paroxysmal AF (*n* = 660)				Persistent AF (*n* = 394)			
	Overall (*n* = 660)	Pre COVID-19 era (*n* = 318)	COVID-19 era (*n* = 342)	*P*-value	Overall (*n* = 394)	Pre COVID-19 era (*n* = 135)	COVID-19 era (*n* = 259)	*P*-value
Age, years	60 (52–67)	59 (51–66)	61 (54–68)	0.018	61 (53–67)	58 (50–65)	61 (55–68)	0.001
Female, *n* (%)	179 (27.1)	84 (26.4)	95 (27.8)	0.760	77 (19.5)	27 (20.0)	50 (19.3)	0.975
AF duration, months	15 (7–36)	14 (7–36)	15 (7–36)	0.628	20 (9–48)	19 (9–47)	20 (9–48)	0.746
BMI, kg/m^2	24.6 (22.9–26.7)	24.5 (22.8–26.6)	24.7 (23.1–26.7)	0.562	25.3 (23.3–27.4)	25.7 (23.7–27.5)	25.2 (23.0–27.2)	0.092
CHA_2DS_2-VASc score	1 (0–2)	1 (0–2)	1 (0–2)	0.140	2 (1–2.75)	2 (1–2)	2 (1–3)	0.019
Comorbidities, *n* (%)								
Heart failure	54 (8.2)	22 (6.9)	32 (9.4)	0.317	102 (25.9)	32 (23.7)	70 (27.0)	0.553
Hypertension	298 (45.2)	150 (47.2)	148 (43.3)	0.354	208 (52.8)	65 (48.1)	143 (55.2)	0.220
Diabetes mellitus	92 (13.9)	47 (14.8)	45 (13.2)	0.625	75 (19.0)	27 (20.0)	48 (18.5)	0.828
Stroke	53 (8.0)	19 (6.0)	34 (9.9)	0.084	37 (9.4)	10 (7.4)	27 (10.4)	0.428
TIA	6 (0.9)	4 (1.3)	2 (0.6)	0.617	1 (0.3)	0 (0.0)	1 (0.4)	1.000
Vascular disease	20 (3.0)	10 (3.1)	10 (2.9)	1.000	24 (6.1)	3 (2.2)	21 (8.1)	0.036
Current drinking, *n* (%)	158 (23.9)	93 (29.2)	65 (19.0)	0.003	121 (30.7)	46 (34.1)	75 (29.0)	0.352
Total alcohol intake per week in current drinkers, g	51.8 (17.7–148.9)	64.8 (19.4–155.4)	51.8 (15.5–103.6)	0.155	77.7 (17.7–207.2)	90.7 (24.2–207.2)	77.7 (17.8–155.4)	0.544
Drinking frequency per week	1.5 (0.9–2.5)	1.5 (1.0–3.0)	1.0 (0.8–2.0)	0.190	2.0 (1.0–3.0)	2.0 (1.0–3.5)	1.5 (1.0–3.0)	0.375
AAD use prior to the ablation, *n* (%)								
Class Ic	378 (57.3)	189 (59.4)	189 (55.3)	0.316	158 (40.1)	51 (37.8)	107 (41.3)	0.568
Class III	306 (46.4)	142 (44.7)	164 (48.0)	0.441	264 (67.0)	98 (72.6)	166 (64.1)	0.112
Echocardiographic parameters								
LA dimension, mm	39 (35–43)	38 (35–43)	39 (36–43)	0.331	43 (39–46)	44 (40–48)	43 (39–45)	0.011
LV ejection fraction,%	65 (61–69)	65 (61–69)	65 (62–69)	0.448	62 (57–66)	61 (56–65)	62 (58–67)	0.030
E/Em	9.1 (7.4–11.8)	9.0 (7.2–11.1)	9.3 (7.6–12.3)	0.133	9.0 (7.3–11.5)	8.4 (7.4–10.6)	9.4 (7.4–12.0)	0.009
hsCRP, mg/dL	0.60 (0.30–1.10)	0.70 (0.40–1.37)	0.50 (0.20–1.00)	< 0.001	0.70 (0.40–1.35)	0.80 (0.60–1.72)	0.60 (0.20–1.20)	< 0.001
CPVI, *n* (%)	660 (100.0)	318 (100.0)	342 (100.0)	1.000	394 (100.0)	135 (100.0)	259 (100.0)	1.000
CTI, *n* (%)	399 (60.5)	206 (64.8)	193 (56.4)	0.035	256 (65.0)	111 (82.2)	145 (56.0)	< 0.001
Follow-up duration, months	11 (6–15)	11 (7–15)	12 (6–15)	0.898	11 (6–15)	11 (7–15)	11 (6–14)	0.609

Values are presented as median (interquartile range) or n (%).
AAD, antiarrhythmic drug; AF, atrial fibrillation; BMI, body mass index; CPVI, circumferential pulmonary vein isolation; CTI, cavotricuspid isthmus; E/Em, ratio of the peak mitral flow velocity of the early rapid filling to the early diastolic velocity of the mitral annulus; hsCRP, high sensitive C-reactive protein; LA, left atrium; LV, left ventricle; TIA, transient ischemic attack.

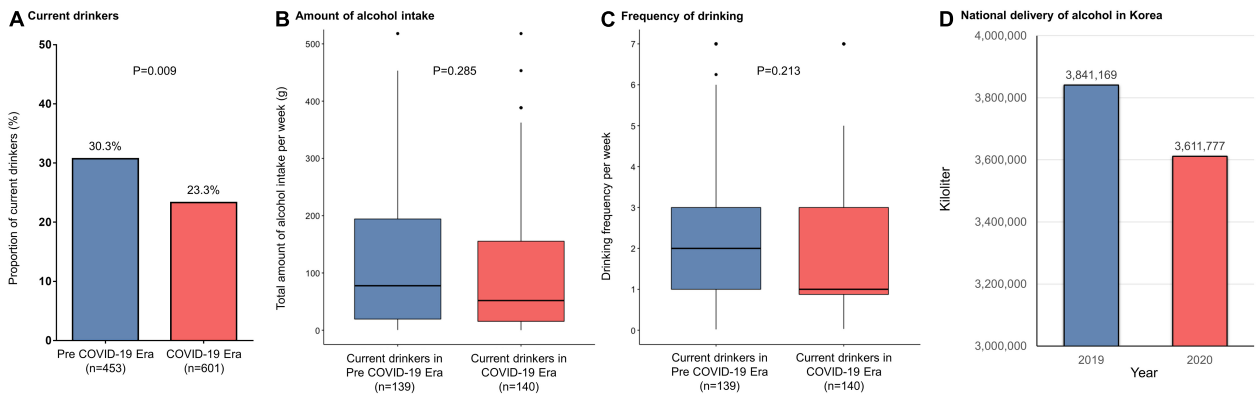

FIGURE 1 | (A) Proportion of current drinkers, **(B)** total alcohol intake per week, **(C)** frequency of drinking per week in atrial fibrillation patients undergoing catheter ablation, and **(D)** amounts of national alcohol deliveries in Korea. COVID-19, coronavirus disease 2019.

TABLE 2 | Clinical rhythm outcomes.

	Paroxysmal AF (*n* = 660)			Persistent AF (*n* = 394)		
	Pre COVID-19 era (*n* = 318)	COVID-19 era (*n* = 342)	*P*-value	Pre COVID-19 era (*n* = 135)	COVID-19 era (*n* = 259)	*P*-value
Follow-up months	11 (7–15)	12 (6–15)	0.898	11 (7–15)	11 (6–14)	0.609
Compliant to Holter monitoring	235 (73.9)	235 (68.7)	0.166	90 (66.7)	145 (56.0)	0.052
Post-ablation medication						
ACEi, or ARB, *n* (%)	105 (33.0)	100 (29.2)	0.335	43 (31.9)	110 (42.5)	0.052
Beta blocker, *n* (%)	134 (42.1)	146 (42.7)	0.949	79 (58.5)	154 (59.5)	0.942
Statin, *n* (%)	115 (36.2)	144 (42.1)	0.138	53 (39.3)	123 (47.5)	0.146
AAD use						
AADs at discharge, *n* (%)	93 (29.2)	76 (22.2)	0.048	70 (51.9)	95 (36.7)	0.005
AADs after 3 months, *n* (%)	116 (36.5)	87 (27.0)	0.013	84 (62.2)	106 (45.1)	0.002
AADs at final follow-up, *n* (%)	92 (28.9)	80 (25.2)	0.326	65 (48.1)	109 (47.4)	0.975
Early recurrence, *n* (%)	80 (25.2)	58 (17.0)	0.013	73 (54.1)	129 (49.8)	0.485
Recurrence type AF, *n* (% in early recur)	72 (90.0)	54 (93.1)	0.739	68 (93.2)	123 (95.3)	0.735
Recurrence type AT, *n* (% in early recur)	8 (10.0)	4 (6.9)		5 (6.8)	6 (4.7)	
Late recurrence, *n* (%)	54 (17.0)	32 (9.4)	0.005	29 (21.5)	49 (18.9)	0.636
Recurrence type AF, *n* (% in recur)	48 (88.9)	29 (90.6)	1.000	28 (96.6)	48 (98.0)	1.000
Recurrence type AT, *n* (% in recur)	6 (11.1)	3 (9.4)		1 (3.4)	1 (2.0)	
Cardioversion, *n* (% in recur)	10 (18.5)	1 (3.1)	0.083	12 (41.4)	12 (25.0)	0.211

AAD, antiarrhythmic drug; ACEi, angiotensin-converting enzyme inhibitor; AF, atrial fibrillation; ARB, angiotensin receptor blocker; AT, atrial tachycardia; COVID-19, coronavirus disease 2019.

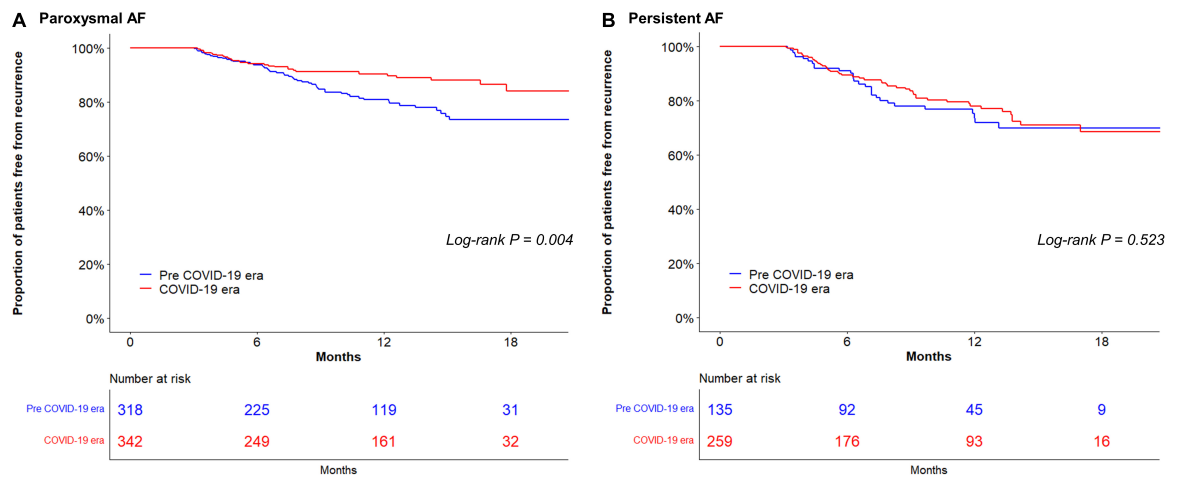

FIGURE 2 | Kaplan–Meier analysis of atrial fibrillation: (AF) recurrence-free survival in paroxysmal AF **(A)**; and in persistent AF **(B)**. AF, atrial fibrillation; COVID-19, coronavirus disease 2019.

A two-sided *P*-value of less than 0.05 was considered statistically significant. Statistical analyses were performed using R version 4.0.2 software (The R Foundation).[1]

RESULTS

In the study population (24.3% women; median age, 60 years), 660 (62.6%) had paroxysmal AF. Patients ablated in the COVID-19 era tended to be older and more frequently had a history of stroke than those in the pre-COVID-19 era group (**Table 1**). The proportion of current drinkers was lower in the COVID-19 era than in the pre COVID-19 era (23.3% vs. 30.3%, respectively; $P = 0.009$) (**Figure 1A**) whereas there were no differences in the amount of weekly alcohol intake (**Figure 1B**) and the frequency of drinking (**Figure 1C**) between the groups. Procedural complication rates did not differ between the pre-COVID-19 era (2.4%) and COVID-19 era (3.2%) groups ($P = 0.606$). There were no differences in the compliances to Holter monitoring between the pre-COVID-19 era and COVID-19 era groups (**Table 2**). Among those with paroxysmal AF, the

[1]www.R-project.org

rate of late recurrence was significantly lower in those ablated in the COVID-19 era than in those ablated in the pre-COVID-19 era (9.4% vs. 17.0%, respectively; $P = 0.005$) during a median follow-up of 11 months (**Table 2**). The cumulative incidence of late recurrence at 1 year of follow-up was significantly lower in the COVID-19 era group (9.8%) than in the pre-COVID-19 era group (19.2%; log-rank $P = 0.004$) (**Figure 2A**). In multivariable Cox regression, the patients ablated in the COVID-19 era were at a lower risk of recurrence than those ablated in the pre-COVID-19 era [adjusted hazard ratio (HR) 0.56; 95% confidence interval (CI), 0.35–0.90]. In patients with persistent AF, the recurrence rate did not significantly differ between the pre-COVID-19 and COVID-19 eras (18.9% vs. 21.5%, respectively; $P = 0.636$) during the median follow-up of 11 months (**Table 2**). There was no difference in the cumulative incidence of recurrence at 1 year of follow-up between the two eras (26.4% in the pre-COVID-19 era vs. 22.1% in the COVID-19 era; log-rank $P = 0.523$) (**Figure 2B**). Risk of late recurrence did not differ between the two eras in multivariable Cox regression (adjusted HR 0.84; 95% CI, 0.47–1.53).

DISCUSSION

The reasons for the association of the pandemic situation and public restrictions with a lower recurrence rate after AFCA in paroxysmal AF patients are unclear. After the implementation of NPIs in Korea, the monthly drinking rate, indicating the proportion of citizens who drink at least once a month for the past year, decreased from 59.9% in 2019 to 54.7% in 2020, the lowest value in the last 15 years (10). The Korean nationwide liquor delivery decreased from 3,841,169 kl in 2019 to 3,611,777 kl in 2020 (**Figure 1D**) (11). Takahashi et al. reported that alcohol reduction was associated with a 37% lower risk of recurrence after AFCA (12). In particular, the risk almost halved in those with paroxysmal AF (12). The proportion of current drinkers among patients with paroxysmal AF in this study was significantly higher in the pre-COVID-19 era (29.2%) than in the COVID-19 era (19.0%; $P = 0.003$), whereas there was no significant difference between 34.1% in the pre-COVID-19 era and 29.0% in the COVID-19 era among patients with persistent AF ($P = 0.352$). High-sensitivity C-reactive protein levels were also lower among patients undergoing AFCA in the COVID-19 era than those in the pre-COVID-19 era. Importantly, up-regulation of inflammatory biomarkers has been shown to be a valid predictor for AF recurrence (13, 14), and inflammation is known to alter atrial electrophysiology and structure to increase vulnerability to AF (15). Thus, changes in alcohol habits and systemic inflammation during the period of COVID-19 pandemic and associated social distancing might partly explain the results of this study.

This retrospective observational cohort study was performed at a single center and included patients using strict selection criteria for AF ablation; hence, our findings cannot be used to establish causal relationships. Although the follow-up period of this study was designed to enable a 3-month blanking period in all patients and to equalize follow-up durations between groups, there might be a discrepancy depending on the timing at which procedures were performed during the inclusion period. However, there were no differences in the follow-up durations between patients in the pre-COVID-19 and COVID-19 groups. In the pandemic period, the Korean medical system was under normal operation, and all elective AFCA procedures proceeded in the same manner as that before the pandemic without significant delay. Among the patients included this study, there were no differences in the compliances to Holter monitoring between the pre-COVID-19 era and COVID-19 era groups. In both paroxysmal AF and persistent AF patients, the uses of AADs at discharge and at 3 months of follow-up were more frequently observed in the pre-COVID-19 era than in the COVID-19 era, whereas there were no differences at the time of final follow-up. This difference might impact the outcomes.

CONCLUSION

This study reveals comparable outcomes of AFCA performed during the COVID-19 pandemic vs. the pre-pandemic period. Rather, a striking decrease in AF recurrence after catheter ablation was observed in patients with paroxysmal AF during the COVID-19 outbreak, whereas no change was observed in those with persistent AF.

DATA AVAILABILITY STATEMENT

The raw data supporting the conclusions of this article will be made available by the authors, without undue reservation.

ETHICS STATEMENT

The studies involving human participants were reviewed and approved by the study protocol adhered to the principles of the Declaration of Helsinki and was approved by the Institutional Review Board at Yonsei University Health System. The patients/participants provided their written informed consent to participate in this study.

AUTHOR CONTRIBUTIONS

H-NP contributed to the conception and design of the work, acquisition of data, and critical revision of the manuscript. DK contributed to the conception and design of the work, interpretation of data, and drafting of the manuscript. HTY, T-HK, J-SU, BJ, and M-HL contributed to the conception and design of the work and acquisition data. H-NP attested that all listed authors meet authorship criteria and that no others meeting the criteria have been omitted. All authors approved the final version to be published and agreed to be accountable for all aspects of

the work in ensuring that questions related to the accuracy or integrity of any part of the work are appropriately investigated and resolved.

FUNDING

This work was supported by a grant (HI21C0011) from the Ministry of Health and Welfare and a grant (NRF-2020R1A2B5B01001695) from the Basic Science Research Program run by the National Research Foundation of Korea (NRF) which was funded by the Ministry of Science, ICT and Future Planning (MSIP).

SUPPLEMENTARY MATERIAL

The Supplementary Material for this article can be found online at: https://www.frontiersin.org/articles/10.3389/fcvm.2022.836288/full#supplementary-material

REFERENCES

1. World Health Organization [WHO]. *Coronavirus Disease (COVID-19) Situation Reports*. (2021). Available online at: https://covid19.who.int/WHO-COVID-19-global-data.csv (accessed October 23, 2021).
2. Huh K, Jung J, Hong J, Kim M, Ahn JG, Kim JH, et al. Impact of nonpharmaceutical interventions on the incidence of respiratory infections during the coronavirus disease 2019 (COVID-19) outbreak in Korea: a nationwide surveillance study. *Clin Infect Dis*. (2021) 72:e184–91. doi: 10.1093/cid/ciaa1682
3. Lakkireddy DR, Chung MK, Gopinathannair R, Patton KK, Gluckman TJ, Turagam M, et al. Guidance for cardiac electrophysiology during the COVID-19 pandemic from the Heart Rhythm Society COVID-19 Task Force; Electrophysiology Section of the American College of Cardiology; and the Electrocardiography and Arrhythmias Committee of the Council on Clinical Cardiology, American Heart Association. *Circulation*. (2020) 141:e823–31. doi: 10.1161/CIRCULATIONAHA.120.047063
4. Nagueh SF, Smiseth OA, Appleton CP, Byrd BF III, Dokainish H, Edvardsen T, et al. Recommendations for the evaluation of left ventricular diastolic function by echocardiography: an update from the American Society of Echocardiography and the European Association of Cardiovascular Imaging. *J Am Soc Echocardiogr*. (2016) 29:277–314. doi: 10.1016/j.echo.2016.01.011
5. Kim D, Shim J, Kim YG, Yu HT, Kim TH, Uhm JS, et al. Malnutrition and risk of procedural complications in patients with atrial fibrillation undergoing catheter ablation. *Front Cardiovasc Med*. (2021) 8:736042.
6. Kim D, Hwang T, Kim M, Yu HT, Kim TH, Uhm JS, et al. Extra-pulmonary vein triggers at de novo and the repeat atrial fibrillation catheter ablation. *Front Cardiovasc Med*. (2021) 8:759967. doi: 10.3389/fcvm.2021.759967
7. Calkins H, Hindricks G, Cappato R, Kim YH, Saad EB, Aguinaga L, et al. 2017 HRS/EHRA/ECAS/APHRS/SOLAECE expert consensus statement on catheter and surgical ablation of atrial fibrillation. *Europace*. (2018) 20:e1–160. doi: 10.1093/europace/eux274
8. Lee JH, Yu HT, Kwon OS, Han HJ, Kim TH, Uhm JS, et al. Atrial wall thickness and risk of hemopericardium in elderly women after catheter ablation for atrial fibrillation. *Circ Arrhythm Electrophysiol*. (2021) 14:e009368. doi: 10.1161/CIRCEP.120.009368
9. Grambsch PM, Therneau TM. Proportional hazards tests and diagnostics based on weighted residuals. *Biometrika*. (1994) 81:515–26. doi: 10.1093/biomet/81.3.515
10. Korea Disease Control and Prevention Agency. *Community Health Survey Reports 2020*. (2021). Available online at: https://chs.kdca.go.kr/chs/stats/statsMain.do (accessed December 10, 2021).
11. Statistics Korea. *E-National Index*. (2021). Available online at: https://www.index.go.kr/potal/main/EachDtlPageDetail.do?idx_cd=2824 (accessed December 10, 2021).
12. Takahashi Y, Nitta J, Kobori A, Sakamoto Y, Nagata Y, Tanimoto K, et al. Alcohol consumption reduction and clinical outcomes of catheter ablation for atrial fibrillation. *Circ Arrhythm Electrophysiol*. (2021) 14:e009770. doi: 10.1161/CIRCEP.121.009770
13. Korodi S, Toganel R, Benedek T, Hodas R, Chitu M, Ratiu M, et al. Impact of inflammation-mediated myocardial fibrosis on the risk of recurrence after successful ablation of atrial fibrillation - the FIBRO-RISK study: protocol for a non-randomized clinical trial. *Medicine*. (2019) 98:e14504. doi: 10.1097/MD.0000000000014504
14. Richter B, Gwechenberger M, Socas A, Zorn G, Albinni S, Marx M, et al. Markers of oxidative stress after ablation of atrial fibrillation are associated with inflammation, delivered radiofrequency energy and early recurrence of atrial fibrillation. *Clin Res Cardiol*. (2012) 101:217–25. doi: 10.1007/s00392-011-0383-3
15. Zhou X, Dudley SC Jr. Evidence for inflammation as a driver of atrial fibrillation. *Front Cardiovasc Med*. (2020) 7:62. doi: 10.3389/fcvm.2020.00062

Conflict of Interest: The authors declare that the research was conducted in the absence of any commercial or financial relationships that could be construed as a potential conflict of interest.

Publisher's Note: All claims expressed in this article are solely those of the authors and do not necessarily represent those of their affiliated organizations, or those of the publisher, the editors and the reviewers. Any product that may be evaluated in this article, or claim that may be made by its manufacturer, is not guaranteed or endorsed by the publisher.

frontiers | Frontiers in Cardiovascular Medicine

ORIGINAL RESEARCH
published: 03 June 2022
doi: 10.3389/fcvm.2022.881446

QTc Dynamics Following Cardioversion for Persistent Atrial Fibrillation

Arwa Younis[1], Nofrat Nehoray[2], Michael Glikson[3], Christopher Bodurian[4], Eyal Nof[2], Nicola Luigi Bragazzi[5], Michael Berger[2], Wojciech Zareba[4], Ilan Goldenberg[4] and Roy Beinart[2]*

[1] Cardiac Electrophysiology and Pacing Section, Department of Cardiovascular Medicine, Cleveland Clinic, Cleveland, OH, United States, [2] Chaim Sheba Medical Center Affiliated to Sackler Medical School, Tel Aviv University, Ramat Gan, Israel, [3] Heart Center, Shaare Zedek Medical Center, Jerusalem, Israel, [4] Clinical Cardiovascular Research Center, University of Rochester, Rochester, NY, United States, [5] Laboratory for Industrial and Applied Mathematics, Center for Disease Modeling, York University, Toronto, ON, Canada

Background: Cardioversion (CV) for atrial fibrillation (AF) is common. We aimed to assess changes in QTc over time following electrical CV (ECV) for persistent AF, and to compare the benefit of using continuous Holter monitoring vs. conventional follow-up by ECG.

Methods: Prospective observational cohort study. We comprised 90 patients admitted to our center for elective ECV due to persistent AF who were prospectively enrolled from July 2017 to August 2018. All patients underwent 7-days Holter started prior to ECV. Baseline QTc was defined as median QTc during 1 h post ECV. The primary endpoint was QTc prolongation defined as QTc ≥500 ms, or ≥10% increase (if baseline QTc was >480 ms). Conventional monitoring was defined as 2-h ECG post ECV.

Results: Mean age was 67 ± 11 years and 61% were male. Median baseline QTc was 452 ms (IQ range: 431–479 ms) as compared with a maximal median QTc of 474 ms (IQ range: 433–527 ms; p <0.001 for the change in QTc from baseline). Peak median QTc occurred 44 h post ECV. The primary endpoint was met in 3 patients (3%) using conventional monitoring, compared with 39 new patients (43%) using Holter (p <0.001 for comparison). The Holter monitoring was superior to conventional monitoring in detecting clinically significant QTc prolongation (OR = 13; p <0.001).

Conclusions: ECV of patients with persistent AF was associated with increased transient risk of QTc prolongation in nearly half of the patients. Peak median QTc occurs during end of second day following ECV and prolonged ECG monitoring provides superior detection of significant QTc prolongation compared with conventional monitoring.

Keywords: persistent atrial fibrillation, cardioversion, safety, QT interval, QTc prolongation

OPEN ACCESS

Edited by:
Shimon Rosenheck, Hebrew University of Jerusalem, Israel

Reviewed by:
Stefan Michael Sattler, University of Copenhagen, Denmark
Lukas J. Motloch, Paracelsus Medical University, Austria

****Correspondence:***
Arwa Younis
or.younis@gmail.com
orcid.org/0000-0002-2485-5025

Specialty section:
This article was submitted to Cardiac Rhythmology, a section of the journal Frontiers in Cardiovascular Medicine

Received: *22 February 2022*
Accepted: *11 May 2022*
Published: *03 June 2022*

Citation:
Younis A, Nehoray N, Glikson M, Bodurian C, Nof E, Bragazzi NL, Berger M, Zareba W, Goldenberg I and Beinart R (2022) QTc Dynamics Following Cardioversion for Persistent Atrial Fibrillation. Front. Cardiovasc. Med. 9:881446. doi: 10.3389/fcvm.2022.881446

INTRODUCTION

Atrial fibrillation (AF) is the most common sustained arrhythmia worldwide and represents a major challenge in patients' management (1).

Rhythm control is the preferred strategy in patients with symptomatic AF. Electrical cardioversion (ECV) and pharmacological cardio-version (PCV) are widely used in order to restore sinus

rhythm (SR). ECV is more effective than PCV, particularly in persistent AF (2), and while proven to be a safe, in some cases it could lead to serious adverse events, including QT prolongation and Torsade de pointes (3, 4).

It has been suggested that persistent AF induces ventricular repolarization remodeling leading to transient QT prolongation following ECV (5). This might increase the risk for Torsade de pointes, especially when other QT prolonging conditions exists (4). Furthermore, the European Heart Society and the American Heart Association guidelines recommend the initiation of antiarrhythmic drug therapy 1–3 days before ECV to promote sustainable cardioversion (6, 7). In fact, many of these drugs have a potential of further QTc prolongation, increasing the risk even more (8). Currently, there are no guidelines specifying the time needed to monitor patients following ECV. The common practice is to watch the patients for 1–2 h following ECV, and thereafter to discharge them.

We hypothesized that patients with persistent AF on antiarrhythmic treatment might develop significant QTc prolongation following ECV during long-term monitoring. Therefore, in this prospective clinical study we aimed to (1) assess changes in QTc following ECV and to identify the time to maximal QTc prolongation, (2) to compare the current standard of care to 7-days Holter monitoring, and (3) to identify clinical predictors for clinically significant QTc prolongation.

METHODS

Study Patients

From 09/07/2017 to 27/08/2018, we prospectively enrolled consecutive patients with persistent AF who were admitted to the cardiology ward at the Chaim Sheba Medical Center (Tel Hashomer, Israel) for electiveECV. Our study inclusion criteria were: (1) age $\geq$18 years old, (2) symptomatic persistent AF/AFL (atrial fibrillation or atrial flutter), (3) baseline QTc $>$300 ms, (4) no contraindication for ECV, and (5) no contraindication for anticoagulation. Study exclusion criteria included: (1) recent initiation of medication that is well-known to prolong QTc, (2) recent increase in dose of potentially prolonging medication (other than the medication desired for the ECV), (3) pregnancy, (4) patients with congenital long QT syndrome, (5) baseline QTc $>$500 ms, and (6) history of Torsade de Points. Out of the 136 consecutive patients admitted to the award who met the inclusion criteria, 100 patients agreed to participate in the study. All enrolled patients were connected to a 7-day 3-lead Holter prior to ECV (in order to monitor QTc during AF) (**Figure 1A**).

All patients underwent transesophageal echocardiography (TEE) if effective anticoagulation status was not confirmed or upon physician discretion. In addition, all underwent transthoracic echocardiography (TTE) within 3 months prior to the study enrollment, or on the day of ECV. Of note, after connecting patients to Holter, ten patients (10%) were withdrawn from the study due to left atrial appendage thrombus or severe swirling in TEE (4 patients), Holter malfunction (3), failure to cardiovert to sinus rhythm (2) and a patient who spontaneously converted to sinus rhythm following TEE. All remaining 90 patients were successfully electrically cardioverter to sinus rhythm and were monitored according to the study protocol using the Holter for 7 days.

The protocol was approved by the institutional review board of the Chaim Sheba medical center (2711-15-SMC) affiliated to the University of Tel Aviv. All patients provided written informed consent. The primary hypothesis was that signifcant QTc prolongation can occur following ECV during 7 days of prolonged ECG monitoring, and that the use of Holter would be superior to the conventional protocol in detecting potentially clinically significant QTc prolongation.

Cardioversion

All patients were on antiarrhythmic drugs at baseline (Amiodarone 200 mg once daily, Sotalol 80–120 mg twice daily, Flecainide 100 mg twice daily, or Propafenone 150–225 mg three times daily). After light sedation with Midazolam (up to a maximum of 5 mg, based on the patient weight), all patients underwent ECV with 200 Joules using a biphasic defibrillator patches. If sinus rhythm was not achieved and upon discretion of the treating physician, antiarrhythmic drugs were given for 4–12 h (Amiodarone 900–1,200 mg, Flecainide 400 mg, Propafenone 450 mg). After several hours (12 h for Amiodarone, 4 h for Flecainide and Propafenone) an ECG was performed. If the patient was still in AF, ECV shock was re-delivered using the same sedation and shock protocol as described above. After achieving SR, patients were monitored for 2 h (conventional monitoring) and thereafter discharged home with Holter monitoring (**Figure 1B**). Patients were seen in office for clinical follow-up at 1–3 months following ECV.

QTc Measurement

The methods of computerized QT analysis and their reproducibility have been described in detail previously (9, 10). For this study, a 3 lead Life card CF (OSI systems) Holter was used and data were analyzed using the Spacelab Pathfinder SL software with measurements in lead number II. The Bazett formula was used to obtain heart rate-corrected values of parameters of QTc interval. Median QTc was given hourly. All measurements were adjudicated by electrophysiology fellow (AY) and by internal Emergency Medicine resident (NN). If a change between two consecutive measurements, calculated as $\frac{QTc\ second - QTc\ first}{QTc\ first} \times 100$, was $>$10%, a manual validation/correction was performed. Furthermore, manual adjustment was made for patients with pacemaker during pacing periods. In order to minimize the errors that may occur during short tachy-arrhythmic events, or secondary to diurnal variability, the median of every 4 h values was used. Accordingly, each patient had 6 measurements per day. Examples are listed in the **Supplementary Figure A**. In order to validate the results further, 10 random Holter strips were printed and evaluated blindly by a senior electrophysiologist (RB), and a fellow (AY), and the results were compared with the computerized results. The matching rate was 99.7%. Examples are listed in the **Supplementary Figures B,C**.

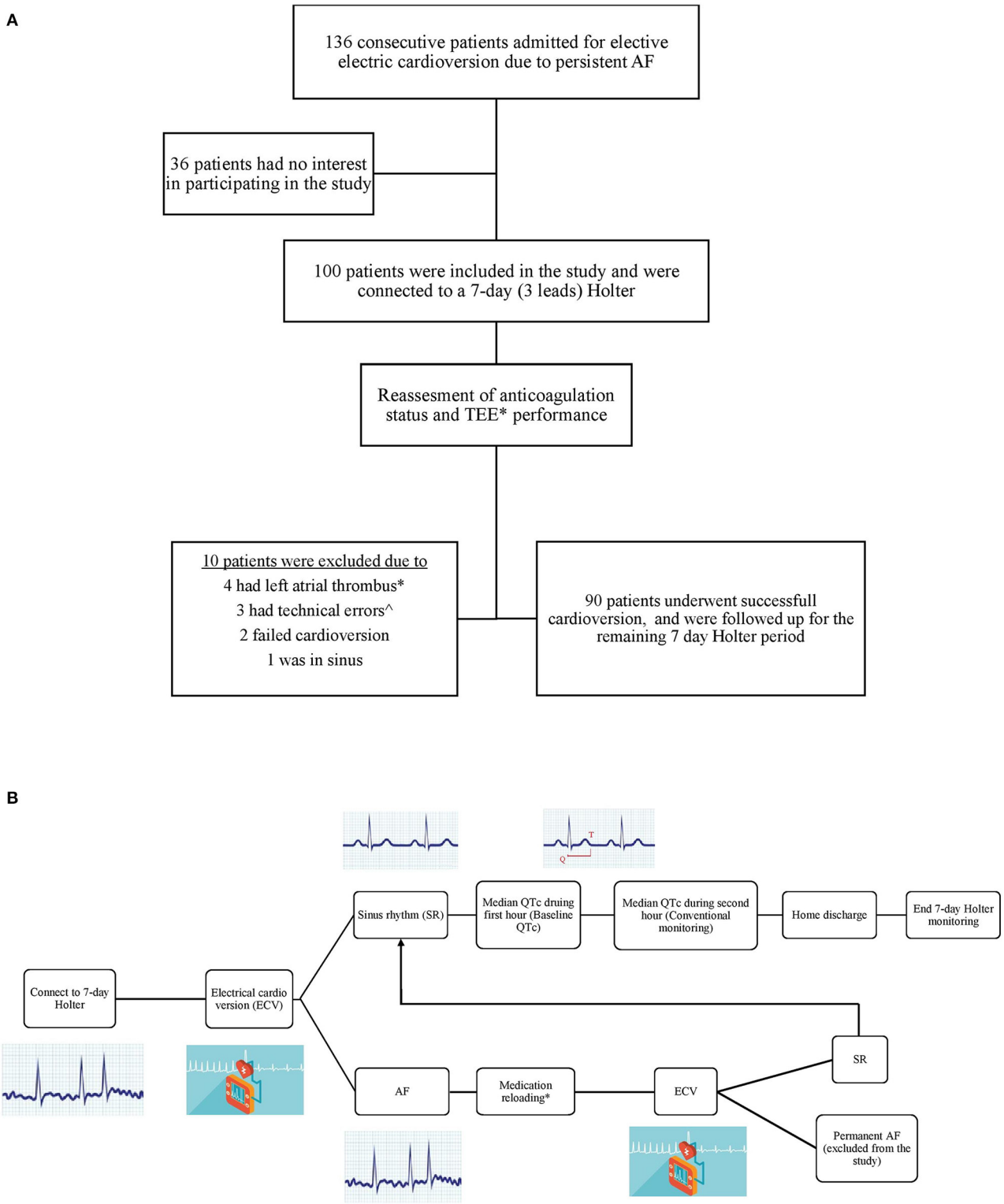

FIGURE 1 | (A) Study flow chart. **(B)** Patients management chart flow. *Trans esophageal echocardiography (TEE) was performed in two third of the patients due to their high risk profile. ^Two patients had very bad recordings quality, and in one patient lead three was disconnected prior to the CV and remained disconnected thereafter.

TABLE 1 | Baseline characteristics.

	Study cohort (No. = 90)	Study cohort		*P* value
		Significant QTc prolongation		
		No (No. = 48)	Yes (No.42)	
Male, %	55 (61)	26 (60)	27 (61)	0.83
Age, mean (SD)	67 ± 11	67 ± 12	67 ± 11	0.91
BMI, mean (SD), kg/m2	30 ± 5	29 ± 4	30 ± 5	0.44
Atrial flutter	7 (8)	5 (11)	2 (4)	0.25
Heart rate in AF, mean (SD), bpm	80 ± 20	78 ± 21	82 ± 20	0.56
Ischemic heart disease, %	19 (21)	8 (16)	12 (27)	0.30
CHF, %	30 (36)	12 (29)	18 (43)	0.25
TEE, %	63 (70)	31 (63)	32 (76)	0.67
EF, mean (SD), %	52 ± 12	54 ± 12	49 ± 14	0.11
LA size, mean (SD), cm	4.5 ± 0.4	4.5 ± 0.5	4.4 ± 1	0.64
Mitral regurgitation, %	56 (62)	23 (48)	33 (79)	0.049
Mitral stenosis, %	14 (15)	7 (15)	7 (17)	0.86
Aortic stenosis, %	12 (13)	6 (14)	6 (15)	0.87
SPAP, mean (SD), mmHg	34 ± 8	34 ± 8	35 ± 7	0.75
Diabetes, %	25 (28)	9 (19)	16 (36)	0.093
Hypertension, %	60 (67)	29 (67)	30 (68)	0.83
Renal disease, %	21 (23)	10 (24)	11 (25)	0.85
CHA_2DS_2VASc, mean (SD)	3.5 ± 1.5	3.3 ± 1.6	3.7 ± 1.7	0.32
ICD/CRTD, %	2 (2)	None	2 (4)	0.49
Pacemaker	11 (12)	5 (11)	6 (15)	0.74
ACE Inhibitor or ARB, %	47 (52)	22 (46)	25 (60)	0.64
Aldosterone, %	10 (11)	4 (9)	6 (15)	0.74
Beta-blocker, %	67 (74)	30 (63)	37 (88)	0.04
Calcium channel blocker, %	25 (28)	12 (26)	13 (29)	0.81
Digitalis, %	6 (7)	2 (4)	4 (9)	0.67
Amiodarone, %	60 (67)	30 (63)	30 (69)	0.83
Flecainide, %	20 (22)	10 (21)	10 (23)	0.79
Propafenone, %	5 (6)	4 (9)	1 (2)	0.36
Statins, %	39 (43)	21 (46)	18 (42)	0.56
NOAC, %	66 (73)	33 (69)	33 (76)	0.47
Warfarin, %	24 (27)	14 (30)	10 (23)	0.41
Creatinine, mean (SD), mg/dl	1 ± 0.3	1 ±0.3	0.9 ± 0.3	0.32
K, mean (SD), mg/dl	4.3 ± 0.4	4.3 ± 0.4	4.3 ± 0.4	0.73
Na, mean (SD), mg/dl	140 ± 4	140 ± 3	140 ± 2	0.49
Mg, mean (SD), mg/dl	2 ± 0.4	2± 0.2	2 ± 0.4	0.94

AF, atrial fibrillation; ACE, angiotensin converting enzyme; ARB, angiotensin receptor blocker; BMI, body mass index; CHF, congestive heart failure; COPD, chronic obstructive pulmonary disease; CRTD, cardiac resynchronization therapy with a defibrillator; ICD, implantable cardioverter defibrillator; EF, ejection fraction; LA, left atrial dimension; NOAC, novel oral anti-coagulant; SPAP, systolic pulmonic arterial pressure; TEE, trans-esophageal echocardiography.

Definitions and Endpoints

Baseline QTc was defined as the median QTc during the first hour post ECV. Conventional monitoring was defined as the Holter tracing at the second hour following ECV. Holter monitoring was defined as tracings starting from the beginning of the third hour following ECV throughout the end of the monitoring period. The primary endpoint was clinically significant QTc prolongation defined as; (1) new prolongation of QTc ≥500 ms (if baseline QTc was <480 ms) or (2) prolongation of QTc ≥10% if baseline QTc was >480 ms (11).

Statistical Analysis

Continuous variables are expressed as mean ± SD. Categorical data are summarized as frequencies and percentages. All variables were tested for normality using four tests; the Shapiro-Wilk (Shapiro & Wilk, 1965), the Kolmogorov-Smirnov test, Cramer von Mises test, and the Anderson-Darling test. All QTc values (during AF, after 2 h, and max) were all non-normal distributed. Therefore, we report median QTc instead of mean QTc. The test that was used to compare the medians was Wilcoxon rank Sum test. Median QTc baseline (first hour post ECV), median QTc during the second hour (conventional monitoring), and the median QTc every 4 consecutive hours (Holter monitoring) were displayed in a graph with 25%−75% confidence interval, while the Y axis is the QTc, and X axis is time from ECV.

We included 18 potential clinical, electrocardiographic, echocardiographic and laboratory binary risk factors for QTc prolongation (**Supplementary Table A**). Numeric variables were made binary by the use of cut points with the goal of finding simple, easily implemented predictors to be derived from them. Thresholds for categorization of numeric variables were based on the mean value. Univariate relationships between candidate covariates and a further event were assessed by *t* tests (2 for binary responses). The covariates with values of $P < 0.10$ were further evaluated by carrying out a best-subset regression analysis, examining the models created from all possible combinations of predictor variables, and using a penalty of 3.84 on the likelihood ratio 2 value for any additional factor included (corresponds to a *P* of 5% for a 1-df 2 test).

Detection rates were calculated as a fraction of all patients who had received 7-days Holter monitoring. The cumulative probability of AF was displayed according to the Kaplan-Meier method. The differences between detection rates for different monitoring intervals within each patient were tested using McNemar's test as appropriate. All statistical tests were two-sided, a *p*-value of <0.05 was considered statistically significant. Analyses were carried out with SAS software (version 9.4, SAS institute, Cary, North Carolina).

RESULTS

The baseline clinical characteristics of study patients are shown in **Table 1**. The mean age of the study cohort was 67 ± 11 years, 55 patients (61%) were male. The mean CHA_2DS_2VASc was 3.5 ± 1.5. Baseline mean heart rate in AF was 80 ± 20 bpm and median was 76 (IQR 64–92). In 7 patients (8%), ECV was performed

TABLE 2 | QTc values and atrial fibrillation recurrence rates based on the loading and re-loading of antiarrhythmic drugs.

	All patients (*N* = 90)			All patients (*N* = 90)		
	Prior loading of AAD (*N* = 36)	**No loading of AAD (*N* = 54)**	***p*-value**	**Reloading (*N* = 11)**	**No reloading (*N* = 79)**	***p*-value**
Amiodarone	26 (72)	NA		7 (64)	NA	
Flecanide/propafenone	10 (28)	NA		4 (36)	NA	
Max QTc prior to ECV	465 (446–500)	466 (440–494)	0.36	454 (424–483)	466 (445–500)	0.49
2 h post ECV	451 (433–471)	465 (432–500)	0.76	463 (422–494)	458 (433–494)	0.38
Max QTc	537 (472–590)	522 (475–555)	0.32	489 (451–523)	537 (481–580)	0.056
Patients with prologed QTc	22 (61)	24 (44)	0.13	2 (18)	43 (54)	0.066
Patients with AF recurrence	8 (22)	12 (22)	0.97	7 (64)	12 (15)	<0.001

AAD, antiarrhythmic medications; ECV, electrical cardioversion; AF, atrial fibrillation/flutter.

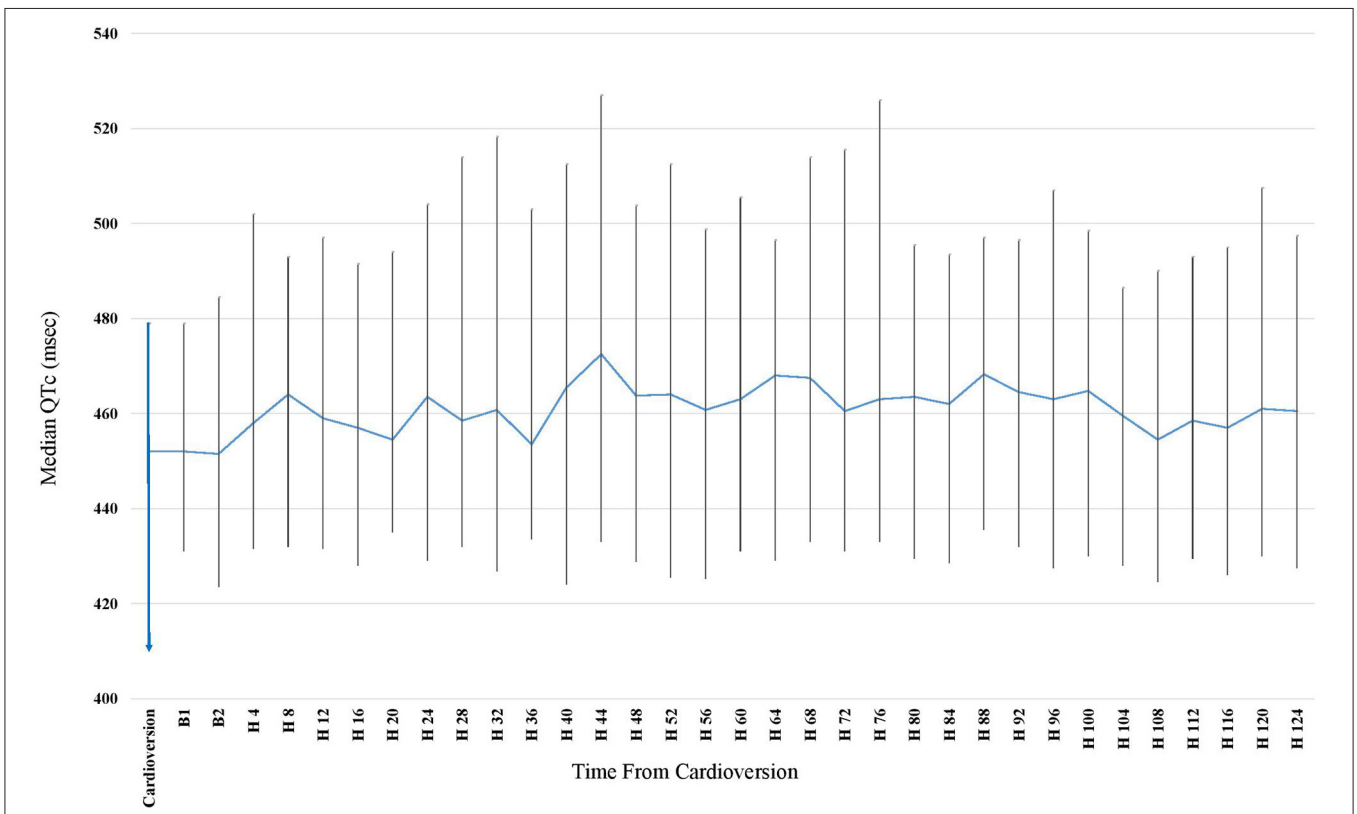

FIGURE 2 | Median QTc obtained by Continuous 7 days Holter following Elective Cardioversion (CV) for Persistent Atrial Fibrillation. Time Zero Represents the CV Time. At time 132 h post CV, 33 (37%) of the patients were no longer connected to the 7-days Holter (due to longer detection prior to CV). The rate of patients connected to the Holter became lower every further hour beyond the 132 h post CV, making it incorrect to calculate for means and draw conclusions from it. Therefore, the graph applies only until 128 h post CV.

due to persistent atrial flutter. Most patients had hypertension 60 (67%) and were likely to receive novel oral anti-coagulants 66 (73%). Amiodarone was the most common antiarrhythmic medication used prior to ECV (60 patients, 67%). Despite the fact that the vast majority of patients were on adequate anti-coagulation status, TEE was performed in 63 (70%) patients prior to CV, due to increased stroke risk in this population.

A total of 36 patients (40%) were treated with oral antiarrhythmic medication loading prior to the scheduled ECV (72% with amiodarone, and 28% with Class IC). Median max QTc was 537 (IQR 472–590) in the loading group and did not differ significantly from the no-loading group [522 (IQR 475–555); $p = 0.32$; **Table 2**].

TABLE 3 | Predictors for clinically significant QTc prolongation 7-day Holter vs. 2-h conventional monitoring.

End point	Hazard ratio	95% CI	*p*-value
Clinically significant QTc prolongation (39 events)			
Beta blocker	3.5	1.04-−12.3	0.042
Median QTc ≥ 450 during first hour post ECV	2.2	0.92-−5.2	0.093

TABLE 4 | Rates of clinically significant QTc during conventional monitoring and during 7-day Holter.

	New Clinically Significant QTc Prolongation	Percentage of new events	No. of remaining patients without QTc prolongation	McNemar's *p* for comparison with conventional monitoring
Conventional	3	3%	87	
First day	16	18%	71	0.0003
Second day	8	11%	63	0.025
Third day	7	11%	56	0.045
Fourth day	3	5%	53	NS
Fifth day	4	8%	49	NS
Sixth day	1	2%	48	NS
Seventh day	0	0%	48	NS
7 days Holter	39	43%	51	<0.001

Eleven patients did not convert to SR with the first electrical shock. Re-loading of the same anti-arrhythmic medication, as described in the methods section, was performed in them (8 patients with Amiodarone and 3 with Flecainide). Among them, 8 patients (5 Amiodarone, 3 Flecainide) converted to SR with the second ECV. The remaining 3 patients needed a third ECV with 360 Joules in order to convert to SR.

QTc Dynamics During Long-Term Holter Recording

Patients underwent long term Holter monitoring for an average of 6.2 ± 1.2 days. Median baseline QTc (defined as the median QTc during first hour after ECV) was 452 (IQR 413–477) ms and was significantly lower than the median QTc during the continuous Holter monitoring [467 (IQR 432–497) ms, $p = 0.01$ for comparison]. The maximal median QTc occurred 44 h post CV and was 474 (IQR 439–511) ms ($p < 0.001$ for comparison with baseline QTc). Following this peak, the QTc returned to the baseline QTc 132 h post ECV, with a median QTc of 458 (IQR 412–501) ms ($p = 0.58$ for comparison with baseline QTc) (**Figure 2**). The baseline clinical characteristics were similar between those who had significant prolongation within the 44 h post ECV and those who developed it after. A trend toward more Amiodarone use was seen in those who developed a later QTc prolongation (87% vs. 63%, $p = 0.07$). In 32 patients (35%), the median QTc reached new values ≥500 ms, and in 14 patients (16%) it even reached QTc ≥550 ms (baseline QTc was <480 ms).

Independent Predictors of QTc Prolongation

In best subset forward regression analysis only prior beta blocker usage (HR 3.5, 95% CI 1.04–12.3, $p = 0.042$) was found to be independent predictor for potentially clinically significant QTc prolongation. Baseline QTc ≥ 450 was significant enough to enter the final model ($p < 0.10$), however, in the final multiple regression model the *p*-value was not statistically significant (HR 2.2, 95% CI 0.89–5.2, $p = 0.09$) (**Table 3**).

During the 2 h following ECV (conventional monitoring), 3 (4%) patients met the primary endpoint. Among them, two patients had median QTc ≥ 500 ms (564 and 500 ms), and one had an increase of 11%. With the use of the 7-days Holter, significant QTc prolongation was detected in 39 patients (45%), significantly higher than the rate observed using the conventional monitoring period ($p < 0.001$). Notably, among the 87 patients without clinically significant QTc prolongation detected using conventional 2-h monitoring, sixteen patients (18%) developed new QTc prolongation during the first day, 8 patients (11%) during the second day, and the rest thereafter. Importantly, as shown in **Table 4**, more than half of the QTc prolongation were detected within the first 2 days. Notably, during the second day, 5 patients had QTc > 550 ms (baseline QTc was <480 ms in all of them).

Detection rates for every single day, and cumulative detection rates over the monitoring period are depicted in **Figure 3**. There was a strong recognizable pattern of detection rates favoring the first 48 h of the monitoring period.

Using McNemar test for comparison, the Holter monitoring was superior to conventional monitoring in detecting the PE with an OR of 13; 95% CI 5–65; $p < 0.001$.

Clinical Events and Death

During the study period, one patient died on the 5th day post ECV. The cause of the death was congestive heart failure exacerbation and pulmonary edema. This patient did not have clinically significant QTc prolongation. None of our patients had Torsade de points or sustained ventricular arrhythmia. No other significant clinical events were reported.

DISCUSSION

To the best of our knowledge this is the first observational prospective study that monitored closely the QTc interval following ECV in patients with persistent AF using 7-days Holter monitoring. The main finding of this study include (1) significant QTc prolongation that was detected in 47% of patients following ECV, (2) the maximal median QTc prolongation occurred during the second day (44 h following ECV), (3) there was a substantial increase in detection rates of clinically significant QTc prolongation using prolonged Holter monitoring compared with

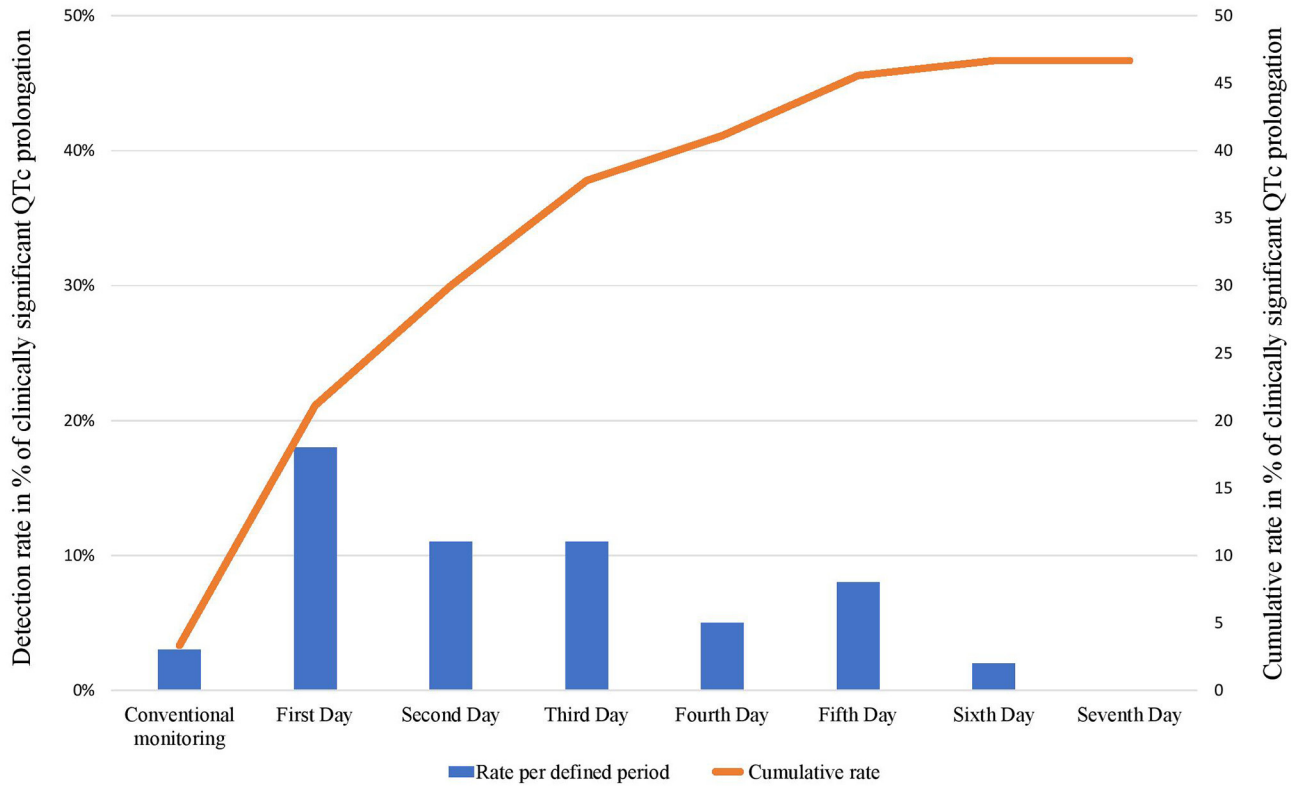

FIGURE 3 | Daily/conventional (columns) and cumulative (line) detection rates of clinically significant QTc prolongation following cardioversion during 7 days of Holter monitoring.

standard monitoring, and (4) chronic beta blockers and QTc $\geq$ 450 ms were the only predictors associated with significant QTc prolongation.

QTc Prolongation Following ECV

In our study, during prolonged monitoring using 7-days Holter, we were able to demonstrate a significant number of patients with new significant QTc prolongation following ECV. Our observations are in line with previous case series and small studies (12, 13). Houltz and colleagues had previously reported QTc prolongation up to a mean of 672 $\pm$ 26 ms in patients that, in fact, developed Torsade de pointes (14). In another study Choy and colleagues reported that QTc was prolonged from 405 $\pm$ 55 to 470 $\pm$ 67 ms following ECV (3). These reports, however, included a relatively small number of patients (<10 patients in average) or included patients who were treated with antiarrhythmic drugs, that are known to prolong the QTc significantly, such as Sotalol or Dofetilide. Notably, in our study, patients with these antiarrhythmic medications (Sotalol or Dofetilide) were excluded, and all patients with other antiarrhythmic medication were already on these drugs more than 1 week before enrollment in the study. The exact mechanisms of QTc prolongation following ECV remain unclear. Possible causes include: (1) bradycardia—several studies demonstrated that lower heart rates following ECV may prolong the QTc interval (11), however, in our study the median HR was similar between those with significant QTc prolongation when compared to those without (**Supplementary Table B**), however this might be influenced by the AF recurrence in some patients, (2) increased drug toxicity—changes in the neuro-hormonal status, such as change in sympathetic nervous activity and ANP were reported following ECV (15), and can potentially modulate the sensitivity to antiarrhythmic drugs (3), abrupt slowing of heart rates, following termination of fast ventricular rates, that may lead to QTc prolongation (16), (4) ventricular repolarization remodeling during AF—QTc during SR following ECV was reported to be significantly and transiently prolonged [although of limited in magnitude, the prolongation was substantial (approximately 15%) in some individuals (5)], and (5) ion channels modification—in several previous studies (17) an alterations in ion channels and several gene expressions in the atria and ventricle of patients with persistent AF were reported leading to change in QTc interval; In particular, the inward rectifier I(K1) channel, affecting the inward rectifier potassium current which regulates the terminal portion of phase 3 of the repolarization (18). Midazolam use and regardless the need to additional use/reloading of antiarrhythmic medication peri-cardioversion.

Holter Monitoring vs. Conventional Monitoring

Although the highest detection rate was observed during the first 24 h following ECV, a significant number of patients with QTc prolongation were detected thereafter. Furthermore, the maximum median QTc prolongation occurred during the second day (hour 44 post ECV), which attenuated thereafter, returning to baseline QTc. Similar findings were reported in a study that tested the QT/RR relationship following ablation of the atrioventricular junction in patients with AF. It demonstrated that the highest change in QTc was documented on the second day [(516 ± 51 ms on second day vs. 468 ± 26 ms baseline, $p = 0.02$) and (497 ± 37 ms on second day vs. 458 ± 25 ms baseline, $p = 0.02$)], afterwards the QTc normalizes with no statistical difference observed from days 3 to 7 at all heart rates (14). In light of our findings there might be a need for further monitoring beyond several hours post ECV in some individuals. In the past, and in accordance with this concept, the ACC/AHA/ESC 2006 Guidelines for the Management of Patients with AF recommended in hospital QT interval monitoring for 24–48 h following ECV in patients receiving drugs that prolong the QT interval. However, in the most recent AHA/ACC and ESC guidelines, the above-mentioned recommendations were omitted, and the monitoring time following ECV in patient on antiarrhythmic drugs became undefined. Hence, we believe that Holter monitoring or repeated ECGs are essential during the 48 h post ECV in some patients with persistent AF on antiarrhythmic drugs to identify patients with prolonged QTc.

Predictors Associated With Significant QTc Prolongation

We found that chronic Beta blocker usage was associated with clinically significant QTc prolongation. Surprisingly, no other independent clinical or demographic characteristic was found to be associated with QTc prolongation. Previous studies have demonstrated controversy regarding the effect of beta blocker on the QT interval. Studies in patients with long QT demonstrated that at faster heart rates, beta-blockers shortened the maximum QT interval and resulted in shorter QTc, whereas at slower heart rates beta-blockers lengthened the maximum QT interval and resulted in longer QTc (19). We believe that these results are consistent with our findings as the prolongations of the QT interval were most likely to occur during relative bradycardia post ECV. Furthermore, in patients with AF, Beta blocker medication may be a marker of a more resistant or more progressive AF disease with rapid ventricular response, resulting in the need for treatment with Beta blockers for rate management. In our study, we failed to show association between previously reported risk factors [female gender, age, potassium level, and magnesium level (20)] and the subsequent risk for QTc prolongation. We believe this is mainly due to the small number of our cohort.

Our study has several limitations. The major limitation is that the majority of the patients were already on antiarrhythmic medication which may affect the QTc duration. Yet these medications were baseline medication and were not initiated during the study. Another important limitation is the lack of control group which plays an important role in such a study. The detection of a higher percentage of patients with QTc prolongation over time might be caused by physiological QT variability, together with long observational period, yet we aimed to assess the benefit of further monitoring per patient, using the conventional monitoring period as our control measurement. Importantly, in our study, some patients had in addition to their AF an abnormal conduction system (bundle branch blocks or complete block and were therefore paced), which may have prolonged the QTc interval. Nevertheless, the use of individualized comparisons (patient level analysis—holter vs. baseline) allows to adjust for these cofounders, which are found also at baseline and not only during the holter recording. Some of the patients had AF recurrence (whether transient or persistent) which may affect the accuracy of the QTc calculation made by the software (using the Bazzet formula which may overestimate the QTc during tachycardia), however, we educated all the results with delta of more than 10%, and we used a 4 h median to correct for short episodes of tachyarrhythmia's or bradyarrhythmias. Data on EHRA score or AF duration was not captured, however all patients were symptomatic patients with persistent AF.

Unfortunately, the vast majority of our patients did not attend the 1–3 months office visit. Follow-up was performed remotely using the phone and addressed questions regarding clinical events (hospitalization, health care utilization for arrhythmia, and/or death). ECG was performed only in 13 patients. Information on QTc on the long term remained unknown. However none of our patient has reported on health care utilization for arrhythmia or other arrhythmia related hospitalizations.

CONCLUSION

ECV of patients with persistent AF was associated with increased transient risk of QTc prolongation in nearly half of the patients. Peak median QTc occurred during end of second day following ECV and prolonged ECG monitoring (by Holter or repeated ECGs) provided superior detection of significant QTc prolongation compared with conventional monitoring. In our study, this transient QTc prolongation did not result in clinical significant events.

DATA AVAILABILITY STATEMENT

The raw data supporting the conclusions of this article will be made available by the authors, without undue reservation.

ETHICS STATEMENT

The studies involving human participants were reviewed and approved by University of Tel Aviv. The patients/participants

provided their written informed consent to participate in this study.

AUTHOR CONTRIBUTIONS

AY, NN, MG, IG, and RB contributed to conception and design of the study, database, and drafting of the manuscript. CB, EN, NB, MB, and WZ contributed to the database, the enrollment, and the drafting of the manuscript. All authors contributed to the manuscript revision, read, and approved the submitted version.

FUNDING

This study was supported by a Research Grant from the Seymour Fefer Endowment.

SUPPLEMENTARY MATERIAL

The Supplementary Material for this article can be found online at: https://www.frontiersin.org/articles/10.3389/fcvm.2022.881446/full#supplementary-material

REFERENCES

1. Colilla S, Crow A, Petkun W, Singer DE, Simon T. Liu X. Estimates of current and future incidence and prevalence of atrial fibrillation in the US adult population. *Am J Cardiol.* (2013) 112:1142–7. doi: 10.1016/j.amjcard.2013.05.063
2. Van Gelder IC, Tuinenburg AE, Schoonderwoerd BS, Tieleman RG, Crijns HJ. Pharmacologic versus direct-current electrical cardioversion of atrial flutter and fibrillation. *Am J Cardiol.* (1999) 84:147R—51. doi: 10.1016/S0002-9149(99)00715-8
3. Choy AM, Darbar D. Dell'Orto S, Roden DM. Exaggerated QT prolongation after cardioversion of atrial fibrillation. *J Am Coll Cardiol.* (1999) 34:396–401. doi: 10.1016/S0735-1097(99)00226-0
4. Spearritt D. Torsades de pointes following cardioversion: case history and literature review. *Aust Crit Care.* (2003) 16:144–9. doi: 10.1016/S1036-7314(05)80037-2
5. Tan HL, Smits JP, Loef A, Tanck MW, Hardziyenka M, Campian ME. Electrocardiographic evidence of ventricular repolarization remodelling during atrial fibrillation. *Europace.* (2008) 10:99–104. doi: 10.1093/europace/eum270
6. January CT, Wann LS, Alpert JS, Calkins H, Cigarroa JE, Cleveland JC, Jr., et al. 2014 AHA/ACC/HRS guideline for the management of patients with atrial fibrillation: a report of the American College of Cardiology/American Heart Association Task Force on practice guidelines and the Heart Rhythm Society. *Circulation.* (2014) 130:e199–267. doi: 10.1161/CIR.0000000000000041
7. Kirchhof P, Benussi S, Kotecha D, Ahlsson A, Atar D, Casadei B, et al. 2016 ESC Guidelines for the management of atrial fibrillation developed in collaboration with EACTS. *Eur Heart J.* (2016) 37:2893–962. doi: 10.1093/eurheartj/ehw210
8. Roden DM. Drug-induced prolongation of the QT interval. *N Engl J Med.* (2004) 350:1013–22. doi: 10.1056/NEJMra032426
9. McLaughlin NB, Campbell RW, Murray A. Accuracy of four automatic QT measurement techniques in cardiac patients and healthy subjects. *Heart.* (1996) 76:422–6. doi: 10.1136/hrt.76.5.422
10. Savelieva I, Yi G, Guo X, Hnatkova K, Malik M. Agreement and reproducibility of automatic versus manual measurement of QT interval and QT dispersion. *Am J Cardiol.* (1998) 81:471–7. doi: 10.1016/S0002-9149(97)00927-2
11. Trinkley KE, Page RL. 2nd Lien H, Yamanouye K, Tisdale JE. QT interval prolongation and the risk of torsades de pointes: essentials for clinicians. *Curr Med Res Opin.* (2013) 29:1719–26. doi: 10.1185/03007995.2013.840568
12. Cellarier G, Deharo JC, Chalvidan T, Gouvernet J, Peyre JP, Savon N, et al. Prolonged QT interval and altered QT/RR relation early after radiofrequency ablation of the atrioventricular junction. *Am J Cardiol.* (1999) 83:1671–4, A7. doi: 10.1016/S0002-9149(99)00178-2
13. Faber TS, Zehender M, Van de Loo A, Hohnloser S, Just H. Torsade de pointes complicating drug treatment of low-malignant forms of arrhythmia: four cases reports. *Clin Cardiol.* (1994) 17:197–202. doi: 10.1002/clc.4960170410
14. Houltz B, Darpo B, Edvardsson N, Blomstrom P, Brachmann J, Crijns HJ, et al. Electrocardiographic and clinical predictors of torsades de pointes induced by almokalant infusion in patients with chronic atrial fibrillation or flutter: a prospective study. *Pacing Clin Electrophysiol.* (1998) 21:1044–57. doi: 10.1111/j.1540-8159.1998.tb00150.x
15. Salerno DM, Katz A, Dunbar DN, Fjeldos-Sperbeck K. Serum electrolytes and catecholamines after cardioversion from ventricular tachycardia and atrial fibrillation. *Pacing Clin Electrophysiol.* (1993) 16:1862–71. doi: 10.1111/j.1540-8159.1993.tb01821.x
16. Viskin S. Post-tachycardia QT prolongation: maladjustment of the QT interval to the normal heart rate. *Pacing Clin Electrophysiol.* (2003) 26:659–61. doi: 10.1046/j.1460-9592.2003.00114.x
17. Nattel S, Maguy A, Le Bouter S, Yeh YH. Arrhythmogenic ion-channel remodeling in the heart: heart failure, myocardial infarction, and atrial fibrillation. *Physiol Rev.* (2007) 87:425–56. doi: 10.1152/physrev.00014.2006
18. Anumonwo JM, Lopatin AN. Cardiac strong inward rectifier potassium channels. *J Mol Cell Cardiol.* (2010) 48:45–54. doi: 10.1016/j.yjmcc.2009.08.013
19. Bennett MT, Gula LJ, Klein GJ, Skanes AC, Yee R, Leong-Sit P, et al. Effect of beta-blockers on QT dynamics in the long QT syndrome: measuring the benefit. *Europace.* (2014) 16:1847–51. doi: 10.1093/europace/euu086
20. Tisdale JE, Jaynes HA, Kingery JR, Mourad NA, Trujillo TN, Overholser BR, et al. Development and validation of a risk score to predict QT interval prolongation in hospitalized patients. *Circ Cardiovasc Qual Outcomes.* (2013) 6:479–87. doi: 10.1161/CIRCOUTCOMES.113.000152

Conflict of Interest: The authors declare that the research was conducted in the absence of any commercial or financial relationships that could be construed as a potential conflict of interest.

frontiers | Frontiers in Cardiovascular Medicine

BRIEF RESEARCH REPORT
published: 23 June 2022
doi: 10.3389/fcvm.2022.906079

Clinical Validation of Automated Corrected QT-Interval Measurements From a Single Lead Electrocardiogram Using a Novel Smartwatch

*Diego Mannhart[1,2], Elisa Hennings[1,2], Mirko Lischer[1,2], Claudius Vernier[1,2], Jeanne Du Fay de Lavallaz[1,2], Sven Knecht[1,2], Beat Schaer[1,2], Stefan Osswald[1,2], Michael Kühne[1,2], Christian Sticherling[1,2] and Patrick Badertscher[1,2]**

[1] Department of Cardiology, University Hospital Basel, Basel, Switzerland, [2] Cardiovascular Research Institute Basel, University Hospital Basel, Basel, Switzerland

OPEN ACCESS

Edited by:
Alessandro Zorzi,
University Hospital of Padua, Italy

Reviewed by:
Giulia Brunetti,
University of Padua, Italy
Niccolo' Maurizi,
Careggi University Hospital, Italy

***Correspondence:**
Patrick Badertscher
patrick.badertscher@ubs.ch

Specialty section:
This article was submitted to Cardiac Rhythmology, a section of the journal Frontiers in Cardiovascular Medicine

Received: 28 March 2022
Accepted: 06 June 2022
Published: 23 June 2022

Citation:
Mannhart D, Hennings E, Lischer M, Vernier C, Du Fay de Lavallaz J, Knecht S, Schaer B, Osswald S, Kühne M, Sticherling C and Badertscher P (2022) Clinical Validation of Automated Corrected QT-Interval Measurements From a Single Lead Electrocardiogram Using a Novel Smartwatch. Front. Cardiovasc. Med. 9:906079. doi: 10.3389/fcvm.2022.906079

Introduction: The Withings Scanwatch (Withings SA, Issy les Moulineaux, France) offers automated analysis of the QTc. We aimed to compare automated QTc-measurements using a single lead ECG of a novel smartwatch (Withings Scanwatch, SW-ECG) with manual-measured QTc from a nearly simultaneously recorded 12-lead ECG.

Methods: We enrolled consecutive patients referred to a tertiary hospital for cardiac workup in a prospective, observational study. The QT-interval of the 12-lead ECG was manually interpreted by two blinded, independent cardiologists through the tangent-method. Bazett's formula was used to calculate QTc. Results were compared using the Bland-Altman method.

Results: A total of 317 patients (48% female, mean age 63 ± 17 years) were enrolled. HR-, QRS-, and QT-intervals were automatically calculated by the SW in 295 (93%), 249 (79%), and 177 patients (56%), respectively. Diagnostic accuracy of SW-ECG for detection of QTc-intervals ≥ 460 ms (women) and ≥ 440 ms (men) as quantified by the area under the curve was 0.91 and 0.89. The Bland-Altman analysis resulted in a bias of 6.6 ms [95% limit of agreement (LoA) –59 to 72 ms] comparing automated QTc-measurements (SW-ECG) with manual QTc-measurement (12-lead ECG). In 12 patients (6.9%) the difference between the two measurements was greater than the LoA.

Conclusion: In this clinical validation of a direct-to-consumer smartwatch we found fair to good agreement between automated-SW-ECG QTc-measurements and manual 12-lead-QTc measurements. The SW-ECG was able to automatically calculate QTc-intervals in one half of all assessed patients. Our work shows, that the automated algorithm of the SW-ECG needs improvement to be useful in a clinical setting.

Keywords: QTc, smartwatch, intelligent ECG, digital health, artificial intelligence, remote patient monitoring (RPM), single-lead ECG

INTRODUCTION

During the COVID-19 pandemic, the need for affordable and simple-to-use end-consumer solutions for health monitoring spiked (1). During the intake of certain medications, screening and monitoring for QT prolongation with frequent ECG checks is indicated and critical for patient safety. The Withings Scanwatch (SW, Withings Scanwatch, Withings SA, Issy les Moulineaux, France) offers automated analysis of the corrected QT-interval (QTc) remotely without the need for third-party software, manual measurement of SW-ECG or requiring different device positions during recording (2). Prior reports using other smart devices focused on the feasibility regarding manual measurements of the QT-interval *via* a single, six or more lead ECG (2–7). However, there is limited data available regarding the clinical validation of artificial intelligence (AI)-generated QT-measurements from commercially available smart devices (4, 5). We therefore sought to validate the use of automated SW-QTc-measurements in unselected patients referred to a cardiology service. The aim of this study was to compare automated QTc-measurements using a single lead ECG of a novel smart device compared to manual-measured QTc from a standard 12-lead ECG.

METHODS

We conducted a prospective, observational study enrolling consecutive adults (≥ 18 years) presenting to the University Hospital Basel from May 7 to June 18 2021 referred for obtaining a 12-lead ECG. The study was approved by the local ethics committee and complied with the Declaration of Helsinki. Written informed consent was provided by all participants. A trained nurse performed a 12-lead ECG immediately before or after instructing the patient in recording a single-lead ECG with the SW. These recordings were considered nearly simultaneously. To obtain a SW-ECG, patients were instructed to hold the stainless steel ring on the top case of the SW continuously for 30 s. Readings from the automated SW-algorithm (HR, PR-, and QT-interval plus QTc) were recorded and a PDF-file of the 30 s single-lead (lead I) SW-ECG was saved. QT-interval on the corresponding 12-lead ECG was manually interpreted by two blinded, independent cardiologists applying the tangent-method (8), using lead II or V5/V6 as suggested in previous work (6, 8, 9). Bazett's formula was used to calculate QTc (10). If the discrepancy between the two manual 12-lead ECG measurements was < 20 ms, the mean of the two was taken to compare against the AI-determined measurement. If there was a mismatch ≥ 20 ms between the two QT-measurements in the 12-lead ECG, a third cardiologist performed a re-measurement. In this case, the mean of the two measurements with the least difference of the three QT-measurements was used to compare against the AI-measurement.

Agreement between QTc-measurements (manual QTc on 12-lead ECG and AI-measured SW-ECG) were assessed applying the Bland-Altman method. Mean difference (bias) in the QTc-interval between the two methods was calculated, so was the lower and upper limits of agreement (LoA, defined as ± 1.96 standard deviations). The same method was applied to show discrepancy between the manual measurements of the 12-lead ECGs by the cardiologists. The percentage of AI-SW and manual measurements that differed < 15, > 20, and > 30 ms for QTc have also been calculated. Area under the receiver operator characteristic curve (AUC) was used to determine the efficacy of the algorithm to discriminate measurements ≥ 460 ms in women and ≥ 440 ms in men.

RESULTS

We enrolled 317 patients (48% female, mean age 63 ± 17 years, **Figure 1**). Clinical reasons for obtaining an ECG were routine check-up (n = 230; 73%), rhythm assessment (n = 24; 8%), QT-measurement (n = 16; 5%), ischemia (n = 4; 1%) and various

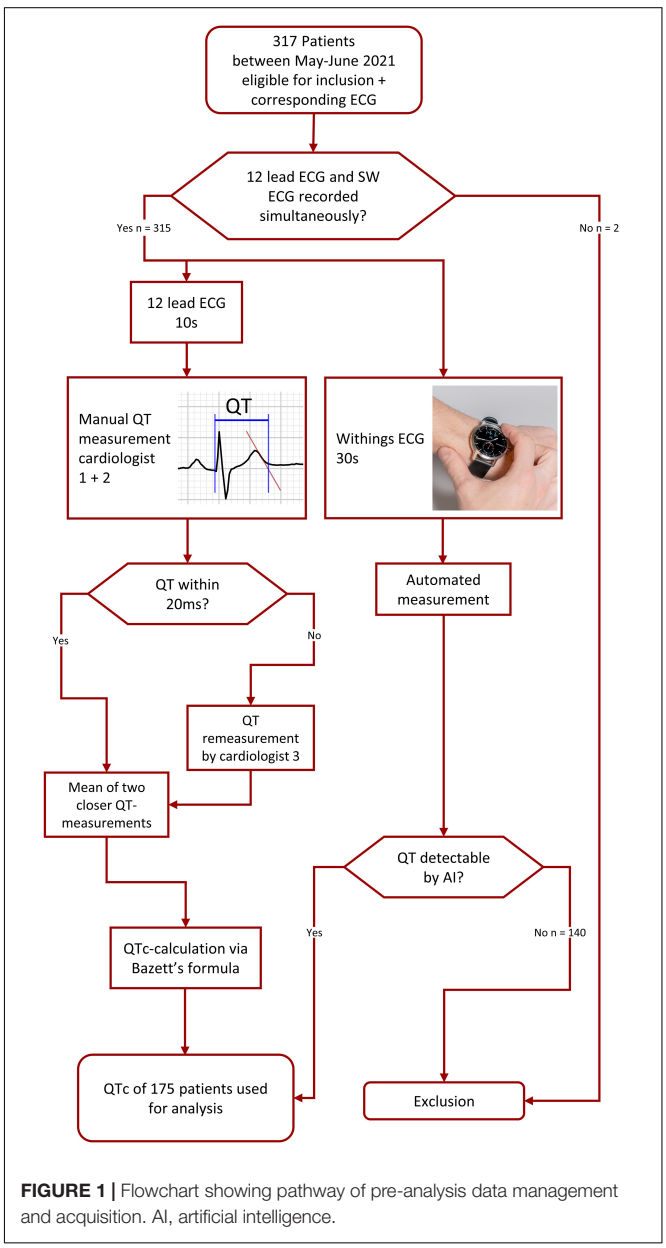

FIGURE 1 | Flowchart showing pathway of pre-analysis data management and acquisition. AI, artificial intelligence.

reasons (n = 43, 14%). The AI algorithm measured automatically the following intervals: HR, PR, QRS, and QTc. Among these 317 patients, HR, PR, QRS as well as QTc was automatically calculated by the SW in 295 (93%), 226 (71%), 249 (79%), and 177 patients (56%), respectively. Differences between patients with/without QTc measurements are highlighted in **Table 1**. Significantly more often the watch was able to detect and measure the QT-interval in younger women without a history of hypertension or heart failure. Reasons for missing automated QT measurement were technical artifacts (noise) such as fibrillation of the baseline or a moving/jumping baseline in 70 patients (50% of all missing), inconclusive recordings (27 cases, 19% of all missing), and tachy- or bradycardia (17 cases, 12% of all missing) amongst others. Manual measures of the QT-interval in the 12-lead ECG were possible in all patients. Two patients were excluded, since there was substantial time difference between ECG recordings. The 175 SW-ECG and 12-lead ECG were recorded within 63 s (95% CI 57–69 s) of each other. Median HR was 69 bpm (interquartile range 62–77). 21% of patients had a heart rate of $<$ 60 or $>$ 100 bpm. When comparing the HR calculated by the SW-AI with the HR manually measured by the cardiologists using the 12-lead ECG, we were able to report a bias of −0.14 bpm with 95% LoA of −8.95 and 7.86 bpm with 6 outliers using the Blant-Altman method. QT-prolonging drugs and/or beta-blocker were present in 70 of 175 patients (40.0%). QTc prolongation defined as $\geq$ 460 ms for women and $\geq$ 440 ms for men was noted in 7 (8%) of 91 women and in 10 (12%) of 84 men. AUC of correctly detecting measurements over 460 ms (women) by the SW was 0.91 (95% CI 85–97%) and for measurements over 440 ms (men) 0.89 (95% CI 83–96%). When comparing QTc measurements calculated by the SW-AI with the QTc measurements manually measured by the cardiologists using the 12-lead ECG, we were able to report a bias of 6.6 ms with 95% LoA of −59 and 72 ms using the Blant-Altman method (**Figure 2**). The disagreement for QTc measurements between the SW-AI and the manual measurements by the cardiologist using the 12-lead ECG was $<$ 15 ms in 38% cases, $>$ 20 ms in 54, and 29% of measurements had a disagreement $>$ 30 ms. In 12 patients (7%) the difference between the QTc-intervals was greater than the LoA. When only including patients with prolonged QTc interval defined as $\geq$ 460 ms for women and $\geq$ 440 ms for men, we were able to report a bias of 16 ms with 95% LoA of −78 and 111 ms using the Blant-Altman method. Among the 12 patients (7%) with a greater difference between the QTc-intervals than the LoA, 3 patients (2%) belonged to the subgroup of prolonged QT-intervals. Premature ventricular complexes and noise were observed in most of outliers. Examples are provided in circles in **Figure 2**. A total of 81 (46%) of patients presented with lower than 20 ms difference between the two QT-measurements in the 12-lead ECG, which is considered perfect (4). Differences between the manual QT-measurements of the cardiologists resulted in a bias of 0.13 ms (95% LoA −15 to 15 ms), measurements in 10 (6%) patients were outside the LoA. In 9 recordings, the remeasurement of a third cardiologist was necessary. A scatterplot showed a linear R2 of 0.94 between measurements of the cardiologists.

TABLE 1 | Baseline characteristics of patients available for analysis.

	Overall population (n = 317)	QT-interval detectable in SW-ECG (n = 177)	QT-interval not detectable in SW-ECG (n = 140)	
Female sex-no. (%)	151 (48)	93 (56)	58 (41)	$p < 0.05$
Mean age -yr	63.3 (± 17.2)	60.9 (± 18.5)	66.3 (± 14.9)	$p < 0.01$
≥65 yr-no. (%)	171 (54)	85 (48)	86 (61)	$p < 0.05$
BMI, kg/m^2	26.7 (± 5.2) n = 233	26.4 (± 5) n = 124	27.0 (± 5.5) n = 109	p = 0.44
Hypertension-no. (%)	159 (50)	77 (44)	82 (59)	$p < 0.01$
DM-no. (%)	71 (22)	38 (22)	33 (24)	p = 0.66
Stroke/TIA-no. (%)	16 (5)	10 (6)	6 (4)	p = 0.62
History HF-no. (%)	46 (15)	16 (9)	30 (21)	$p < 0.01$
CAD-no. (%)	87 (27)	42 (24)	45 (32)	p = 0.10
Sinus rhythm-no. (%)	242 (90)	165 (93)	119 (85)	$p < 0.05$
AF-no. (%)	33 (10)	12 (7)	21 (15)	$p < 0.05$
Indication for ECG				
Ischemia-no. (%)	4 (1)	1 (1)	3 (2)	
Rhythm-no. (%)	24 (8)	13 (7)	11 (8)	
QT-no. (%)	16 (5)	7 (4)	9 (6)	
Routine check-up-no. (%)	230 (73)	125 (71)	105 (75)	
Other -no. (%)	43 (14)	31 (18)	12 (9)	
Branch block				
Right BBB-no. (%)	20 (6)	10 (6)	10 (7)	p = 0.65
Left BBB-no. (%)	28 (9)	9 (5)	19 (14)	$p < 0.01$
Left AFB-no. (%)	9 (3)	7 (4)	2 (1)	p = 0.31

AF, atrial fibrillation; AFB, anterior fascicular block; BBB, bundle branch block; BMI, body mass index; CAD, coronary artery disease; DM, diabetes mellitus; ECG, electrocardiogram; HF, heart.

DISCUSSION

In this clinical validation of a direct-to-consumer smartwatch in a real world cohort of patients we report the following main findings: (1) The automated algorithm was able to measure QTc in 56% of cases. Main reasons for missing QTc measurements were technical artifacts. By manual review, QT-measurements were possible in additional 20% of SW-ECGs. Interestingly, more often the algorithm provided automated measurements in younger women without a history of hypertension or heart failure. It was more challenging for the algorithm to obtain interval measurements in abnormal ECGs, therefore impeding clinical application in patients at risk. In another study (6) using a multilead handheld device, it was shown, that QTc could be obtained by the device most frequent in lead II. Changing of the Scanwatch's position for recording might lead to more usable data. However, might also be difficult for patients to record. (2) We found fair to good agreement between automated-SW-ECG QTc-measurements and manual 12-lead-QTc measurements. This SW-AI algorithm tends to underestimate the QTc interval which has also been reported with another device (3). Consumers and healthcare providers need to be aware of this discrepancy when applying this

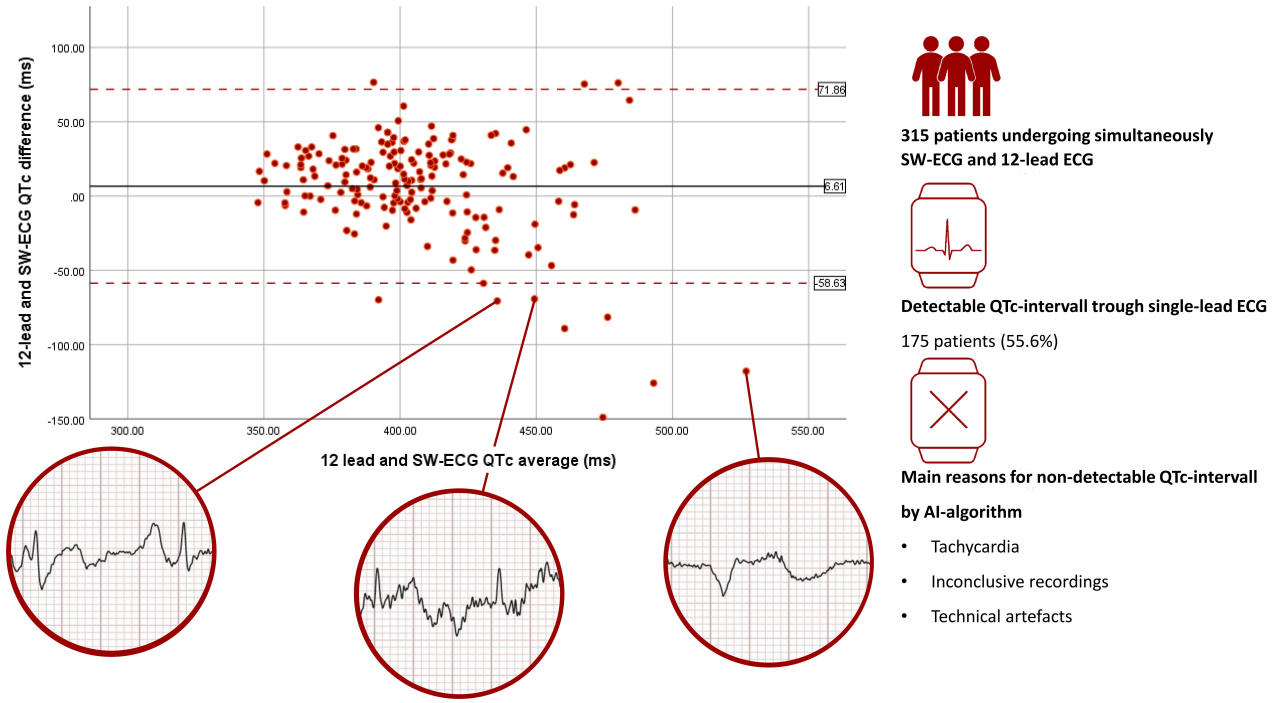

FIGURE 2 | Comparison of QT-interval measurements, manually measured QTc on a 12-lead ECG and automated SW-ECG. Measurement Agreement was analyzed using the Bland-Altmann Method. Bias is represented by the solid black line, limit of agreement is represented *via* d dashed red line. Sections of SW-ECG from outliners are shown in red circles. SW-ECG, Single-Lead Withings Electrocardiogram; QTc, corrected QT-interval; AI, Artificial Intelligence.

technology in real-world patients. (3) Adapting this smartwatch to a clinical setting such as the use of assisted measurement of QT-prolongation screening in pharmacies, we propose that until an improved algorithm is available, manual review is required in a high percentage of recordings to achieve conclusive findings and measurements. However, the SW-AI's abilities in measuring the heartrate indicate the possibilities of this technology.

Our findings corroborate and extend other studies investigating QTc-intervals through either device based single lead or device assisted multilead-ECG (2–5, 11, 12). This SW is currently the only single-lead open market device offering AI-based easy available QT-measurement. Contrary to the Kardia AliveCor 6L, a six-lead ECG, the Withings SW does not have an FDA-approval for QTc-measurements.

LIMITATIONS

Limitations of this study are as follows: First, although we were able to enroll 317 patients, this is a single center cohort study, we tested a single device on a single position and uniquely lead I was recorded. The comparison between the SW-ECGs lead I measurement and the 12-lead EKGs measurement of lead II could be responsible for the small bias, however, when comparing QTc-intervals measured in lead I from both SW- and 12-lead ECG, findings were confirmed with a bias of 0.7 ms with 95% LOA between −65 and 66 ms with 9 outliers reported. Second, while AI-determined QTc intervals from a single lead ECG can be accurate in monitoring changes in the QTc interval over time, it can never be as accurate for the measurement of the actual QTc when compared to a 12-lead ECG since factors like e.g., QT dispersion can never be accounted for. Third, the time-pressured recording could have contributed to an increased number of tracings of elevated noise possibly leading to a decrease of numbers of successful QT-measurements by the algorithm. No repeat measurements were taken, since they would have increased the time between recordings. This approach, however, allowed us to record the single lead ECG and 12-lead ECG within 63 s (95% CI 57–69 s) of each other. Fourth, despite being the most popular used method for measuring the QTc interval, the tangent method might underestimate the QTc interval as shown by Sharif et al. (13). However, this method was chosen since it allows the most reliable approach and reports a higher reproducibility. Fifth, despite being able to perform measurements within 63 s of each other, the gold standard would have been simultaneously recording SW-ECG and Holter-ECG allowing measurements of QT-intervals without any beat-by-beat variability (14).

CONCLUSION

In conclusion, utilization of single-lead SW-ECG for QTc monitoring could be practicable but still needs further validation, algorithm improvement and long-term research to be of possible use in a widespread clinical setting.

DATA AVAILABILITY STATEMENT

The raw data supporting the conclusions of this article will be made available by the authors, without undue reservation.

ETHICS STATEMENT

The studies involving human participants were reviewed and approved by the Ethikkommission Nordwest- und Zentralschweiz (EKNZ). The patients/participants provided their written informed consent to participate in this study.

AUTHOR CONTRIBUTIONS

CV, ML, DM, and EH were involved in data collection and analysis. DM and PB involved in the statistical analysis and wrote the initial manuscript. All authors read, reviewed, and edited the manuscript in the subsequent revision rounds.

ACKNOWLEDGMENTS

We thank all patients, nurses, and physicians involved in this study for their participation, support, and help.

REFERENCES

1. Giudicessi JR, Noseworthy PA, Friedman PA, Ackerman MJ. Urgent guidance for navigating and circumventing the QTc-prolonging and torsadogenic potential of possible pharmacotherapies for coronavirus disease 19 (COVID-19). *Mayo Clin Proc.* (2020) 95:1213–21. doi: 10.1016/j.mayocp.2020.03.024
2. Spaccarotella CAM, Migliarino S, Mongiardo A, Sabatino J, Santarpia G, de Rosa S, et al. Measurement of the QT interval using the apple watch. *Sci Rep.* (2021) 11:10817.
3. Cheung CC, Davies B, Gibbs K, Laksman ZW, Krahn AD. Multilead QT screening is necessary for QT measurement. *JACC Clin Electrophysiol.* (2020) 6:878–80. doi: 10.1016/j.jacep.2020.04.001
4. Garabelli P, Stavrakis S, Albert M, Koomson E, Parwani P, Chohan J, et al. Comparison of QT interval readings in normal sinus rhythm between a smartphone heart monitor and a 12-lead ECG for healthy volunteers and inpatients receiving sotalol or dofetilide. *J Cardiovasc Electrophysiol.* (2016) 27:827–32. doi: 10.1111/jce.12976
5. Strik M, Caillol T, Ramirez FD, Abu-Alrub S, Marchand H, Welte N, et al. Validating QT-interval measurement using the apple watch ECG to enable remote monitoring during the COVID-19 pandemic. *Circulation.* (2020) 142:416–8. doi: 10.1161/CIRCULATIONAHA.120.048253
6. Azram M, Ahmed N, Leese L, Brigham M, Bowes R, Wheatcroft SB, et al. Clinical validation and evaluation of a novel six-lead handheld electrocardiogram recorder compared to the 12-lead electrocardiogram in unselected cardiology patients (EVALECG Cardio). *Eur Heart J Digital Health.* (2021) 2:643–8.
7. Maurizi N, Fumagalli C, Cecchi F, Olivotto I. Use of smartphone-operated ECG for home ECG surveillance in COVID-19 patients. *Eur Heart J Digital Health.* (2021) 2:175–8.
8. Postema PG, de Jong JSSG, van der Bilt IAC, Wilde AAM. Accurate electrocardiographic assessment of the QT interval: teach the tangent. *Heart Rhythm.* (2008) 5:1015–8. doi: 10.1016/j.hrthm.2008.03.037
9. Salvi V, Karnad DR, Kerkar V, Panicker GK, Natekar M, Kothari S. Comparison of two methods of estimating reader variability in QT interval measurements in thorough QT/QTc studies. *Ann Noninvasive Electrocardiol.* (2014) 19:182–9. doi: 10.1111/anec.12136
10. Al-Khatib SM, LaPointe NMA, Kramer JM, Califf RM. What clinicians should know about the QT interval. *JAMA.* (2003) 289:2120–7. doi: 10.1001/jama.289.16.2120
11. Giudicessi JR, Schram M, Bos JM, Galloway CD, Shreibati JB, Johnson PW, et al. Artificial intelligence-enabled assessment of the heart rate corrected QT interval using a mobile electrocardiogram device. *Circulation.* (2021) 143:1274–86. doi: 10.1161/CIRCULATIONAHA.120.050231
12. Strik M, Ploux S, Ramirez FD, Abu-Alrub S, Jaïs P, Haïssaguerre M, et al. Smartwatch-based detection of cardiac arrhythmias: beyond the differentiation between sinus rhythm and atrial fibrillation. *Heart Rhythm.* (2021) 18:1524–32. doi: 10.1016/j.hrthm.2021.06.1176
13. Sharif H, O'Leary D, Ditor D. Comparison of QT-interval and variability index methodologies in individuals with spinal cord injury. *Spinal Cord.* (2017) 55:274–8. doi: 10.1038/sc.2016.118
14. Castelletti S, Dagradi F, Goulene K, Danza AI, Baldi E, Stramba-Badiale M, et al. A wearable remote monitoring system for the identification of subjects with a prolonged QT interval or at risk for drug-induced long QT syndrome. *Int J Cardiol.* (2018) 266:89–94. doi: 10.1016/j.ijcard.2018.03.097

Conflict of Interest: PB received research funding from the "University of Basel", the "Stiftung für Herzschrittmacher und Elektrophysiologie," the "Freiwillige Akademische Gesellschaft Basel", and Johnson & Johnson, all outside the submitted work and reports personal fees from Abbott. SK has received funding of the "Stiftung für Herzschrittmacher und Elektrophysiologie." CS Member of Medtronic Advisory Board Europe, and Boston Scientitic Advisory Board Europe, received educational grants from Biosense Webster and Biotronik, a research grant from the European Union's FP7 program and Biosense Webster, and lecture and consulting fees from Abbott, Medtronic, Biosense-Webster, Boston Scientific, Microport, and Biotronik all outside the submitted work. MK reports personal fees from Bayer, personal fees from Böhringer Ingelheim, personal fees from Pfizer BMS, personal fees from Daiichi Sankyo, personal fees from Medtronic, personal fees from Biotronik, personal fees from Boston Scientific, personal fees from Johnson & Johnson, personal fees from Roche, grants from Bayer, grants from Pfizer, grants from Boston Scientific, grants from BMS, grants from Biotronik, and grants from Daiichi Sankyo, all outside the submitted work. BS reports speaker's bureau for Medtronic.

The remaining authors declare that the research was conducted in the absence of any commercial or financial relationships that could be construed as a potential conflict of interest.

Publisher's Note: All claims expressed in this article are solely those of the authors and do not necessarily represent those of their affiliated organizations, or those of the publisher, the editors and the reviewers. Any product that may be evaluated in this article, or claim that may be made by its manufacturer, is not guaranteed or endorsed by the publisher.

frontiers | Frontiers in Cardiovascular Medicine

ORIGINAL RESEARCH
published: 28 June 2022
doi: 10.3389/fcvm.2022.917218

Universal Method of Compatibility Assessment for Novel Ablation Technologies With Different 3D Navigation Systems

Luigi Pannone[1†], Ivan Eltsov[1,2†], Robbert Ramak[1], David Cabrita[2], Marc Verherstraeten[3], Anaïs Gauthey[1], Antonio Sorgente[1], Cinzia Monaco[1], Ingrid Overeinder[1], Gezim Bala[1], Alexandre Almorad[1], Erwin Ströker[1], Juan Sieira[1], Pedro Brugada[1], Mark La Meir[4], Gian-Battista Chierchia[1‡] and Carlo de Asmundis[1‡]*

[1] Heart Rhythm Management Centre, Postgraduate Program in Cardiac Electrophysiology and Pacing, Universitair Ziekenhuis Brussel - Vrije Universiteit Brussel, European Reference Networks Guard-Heart, Brussels, Belgium, [2] Medtronic Inc, Minneapolis, MN, United States, [3] Boston Scientific, Marlborough, MA, United States, [4] Department of Cardiac Surgery, Universitair Ziekenhuis Brussel - Vrije Universiteit Brussel, Brussels, Belgium

Background: New technologies for ablation procedures are often produced by different companies with no cross-compatibility out of the box. This is not a negligible clinical problem since those separately developed devices are often used together. The aim of this study was to develop a bench-testing method to assess compatibility between the DiamondTemp ablation system (DTA) and the Rhythmia electroanatomic mapping system (EAM).

Methods: Different setups were tested. DTA was connected to the Rhythmia EAM using the following configurations: 3.1. An Ensite EPT GenConnect box (GCB) and Rhythmia Maestro GCB (Maestro GCB, native Rhythmia setup); 3.2. The Medtronic GCB-E and Maestro GCB; 3.3. The Medtronic GCB-E out via the Medtronic GCB-E directly to the Rhythmia at box 1 (pin A61 to A64).

Results: The DTA location was represented in real-time on the Rhythmia EAM. A proper tracking of the DTA was observed in all setups tested by visual comparison of physical catheter movements and its representation on EAM. In configuration 3.1, a significant shift was observed after the first radio frequency (RF) application; however, further applications caused no further shift. In setup 3.2, no significant shift was observed. The setup 3.3 showed a massive shift in the catheter position before ablation compared to baseline points acquired using the Orion catheter as a reference.

Conclusions: A universal and reproducible solution for compatibility testing between the various mapping systems and the ablation catheters has been described. DTA has been demonstrated as compatible with Rhythmia EAM with satisfactory results if a specific setup is used.

Keywords: catheter ablation, universal compatibility, DiamondTemp ablation system, Rhythmia electroanatomic mapping system, cardiac arrhythmias

OPEN ACCESS

Edited by:
Uğur Canpolat, Hacettepe University, Turkey

Reviewed by:
Ozcan Ozeke, Ankara City Hospital, Turkey
Hani Sabbour, Cleveland Clinic Abu Dhabi, United Arab Emirates

***Correspondence:**
Carlo de Asmundis
carlo.deasmundis@uzbrussel.be; carlodeasmundis@me.com

[†]These authors have contributed equally to this work and share first authorship
[‡]These authors have contributed equally to this work and share last authorship

Specialty section:
This article was submitted to Cardiac Rhythmology, a section of the journal Frontiers in Cardiovascular Medicine

Received: *10 April 2022*
Accepted: *23 May 2022*
Published: *28 June 2022*

Citation:
Pannone L, Eltsov I, Ramak R, Cabrita D, Verherstraeten M, Gauthey A, Sorgente A, Monaco C, Overeinder I, Bala G, Almorad A, Ströker E, Sieira J, Brugada P, La Meir M, Chierchia G-B and de Asmundis C (2022) Universal Method of Compatibility Assessment for Novel Ablation Technologies With Different 3D Navigation Systems. Front. Cardiovasc. Med. 9:917218. doi: 10.3389/fcvm.2022.917218

INTRODUCTION

The medical device industry is a fast-growing field and various companies are developing novel products to ensure precise and personalized treatment for cardiac arrhythmias.

New technologies are often produced by different companies with no cross-compatibility out of the box. This is not a negligible clinical problem since those separately developed devices are often used together. In the absence of a compatibility statement from the companies involved, their use may be considered "off label".

One of the most challenging clinical settings is the use of an ablation catheter with a 3D-electroanatomic mapping system (EAM), when both systems are produced by different, often competitive, manufacturers. These systems are intended to create 3D models of the dedicated heart chamber and to track the ablation catheters in the model with sufficient precision to deliver therapy.

All existing EAMs use 2 main catheter tracking technologies: magnetic field-based or impedance-based technology, either separately or in a hybrid mode (1).

The magnetic-based systems are using a magnetic field generator placed under the patient's table, which creates a magnetic field around the patient's heart. Catheters introduced into the patient have a magnetic sensor, constantly sending localization information based on the magnetic field measurements, which allows the system to track it and represent it in the 3D model. In this case, the catheter is developed by the manufacturer of the EAM, ensuring compatibility.

Impedance-based tracking allows visualizing and tracking virtually any catheter using the impedance measurement between the external patches and an electrode on the catheter. However, the precision of the tracking system may be influenced by external factors such as locator signal frequencies, system tracking algorithms, catheter electrode spacing, filter settings, cables, interface cables, and RF energy delivery. The hybrid tracking systems are using both the magnetic and impedance-based methods where magnetic tracking enhances localization accuracy and impedance measurement allows visualizing the third party catheters. The Rhythmia mapping system (Boston Scientific MA) is one of the most common EAMs, which uses a hybrid tracking algorithm.

The novel DiamondTemp^{TM} ablation system (DTA), (Medtronic Inc, Minneapolis, MN) and Rhythmia^{TM} EAM (Boston Scientific) are both CE-Marked and FDA-approved medical devices. The DTA has been validated by its manufacturer only in combination with Ensite Precision^{TM} System (Abbott, Inc., Chicago, Illinois) (2).

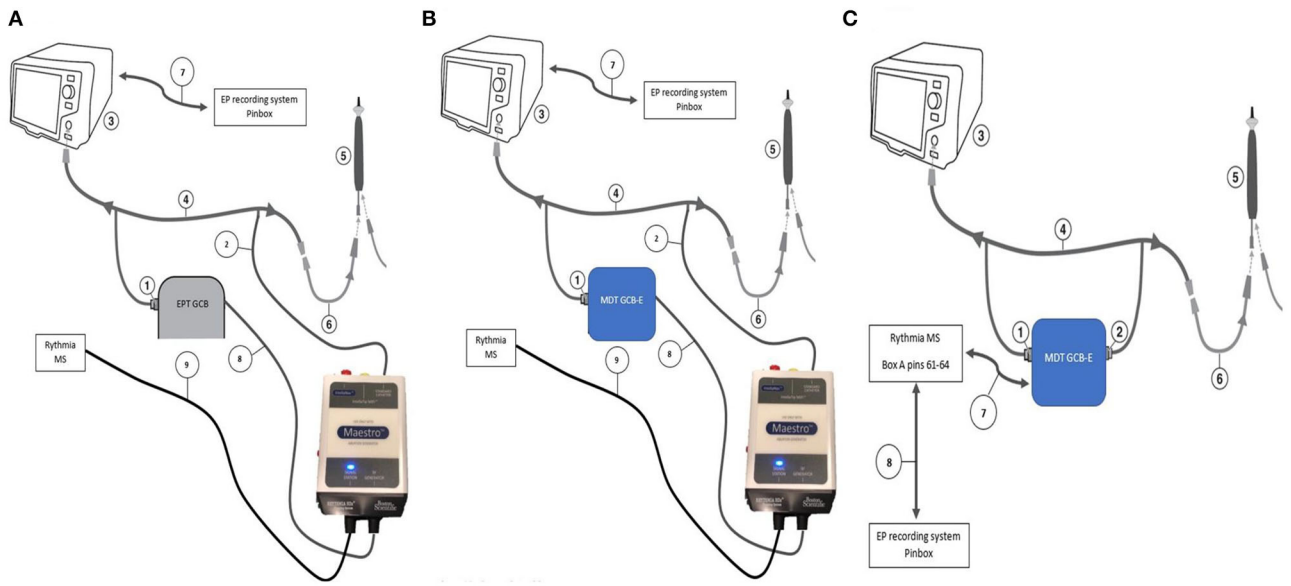

FIGURE 1 | DiamondTemp and Rhythmia connectivity configurations. **(A)** Setup 3.1. An EPT GCB and Rhythmia Maestro GCB (Maestro GCB, native Rhythmia setup). (1) 14-pin twist connector to RFG via the GCC; (2) 9-pin quick connector to DTC via the GCC to the DTC to RFG cable; (3) DTA RFG; (4) DTA GCC; (5) DTC; (6) DTC to RFG cable; (7) IC out cable; (8) 9-pin quick connector of the Maestro GCB; and (9) Connector from the Maestro GCB to the Rhythmia MS. **(B)** Setup 3.2. This configuration shows the best accuracy results—The catheter connection is connected to Rhythmia GCB using Genconnect cable and then to MDT GCB as shown in the picture. (1) 14-pin twist connector to RFG via the GCC; (2) 9-pin quick connector to DTC via the GCC to the DTC to RFG cable; (3) DTA RFG; (4) DTA GCC; (5) DTC; (6) DTC to RFG cable; (7) IC out cable; (8) 9-pin quick connector of the Maestro GCB; and (9) Connector from the Maestro GCB to the Rhythmia MS. **(C)** Setup 3.3. The MDT GCB-E and IC out via the MDT GCB-E directly to the Rhythmia IC in at box 1 (pin A61 to A64) (1) 14-pin twist connector to RFG via the GCC; (2) 9-pin quick connector to DTC via the GCC to the DTC to RFG cable; (3) DTA RFG; (4) DTA GCC; (5) DTC; (6) DTC to RFG cable; (7) IC out cable; and (8)Rhythmia IC out to the EP recording system.

The aim of this study was to develop a bench testing method to ensure the compatibility between the DTA and Rhythmia EAM.

METHODS

Ablation Catheter and Mapping System

The DTA ablation catheter is a 7.5-F irrigated radiofrequency (RF) catheter; the 4.1-mm composite tip electrode delivers RF. The ablation electrode tip is embedded with 2 interconnected diamonds which allow rapid RF delivery (due to isoelectric diamond properties) and shunting heath from externalized thermocouples. This allows accurate temperature measurement at the tip-tissue interface. The catheter operates in a temperature control mode and a dedicated RF generator (RFG) titrates rapidly the delivered power to the target temperature. The dual composite ablation tip behaves as a single electrode during ablation and the electrical insulation of the tip allows for high-resolution EGM sensing (3, 4).

Rhythmia™ is a high-density EAM that offers detailed insights into tissue electrical activity (5). Indeed, the reliability of electrogram annotation, the density of recorded electrograms, the low noise, and the enhanced characteristics of recording make Rhythmia™ a reliable tool in clinical practice (6).

Configurations for Compatibility Assessment

The following endpoints were evaluated for compatibility assessment: (1) there is no energy leak or a sudden shortcut within the proposed connectivity configuration, which ensures that the RF energy power and time shown on the device correspond to the delivered power and therapy duration, and (2) the DTA is correctly represented inside the 3D model, with a precise and reliable position not influenced by external factors, especially RF energy delivery. Four different configurations were tested.

The DTA can be connected to the navigation system either by using EGM out cables from the RF generator or by using special ablation connection boxes (provided by the mapping system manufacturer) to filter out RF energy so that it does not affect localization. DTA is using Maestro-type connectors and all the following experimental configurations are based on that.

Testing configurations:

1.0 DTA connected only to the DTA RFG - No GenConnect (GC) nor Genconnect Cable (GCC) connected to the DTA

1.1 An Ensite EPT GenConnect box (EPT GCB).

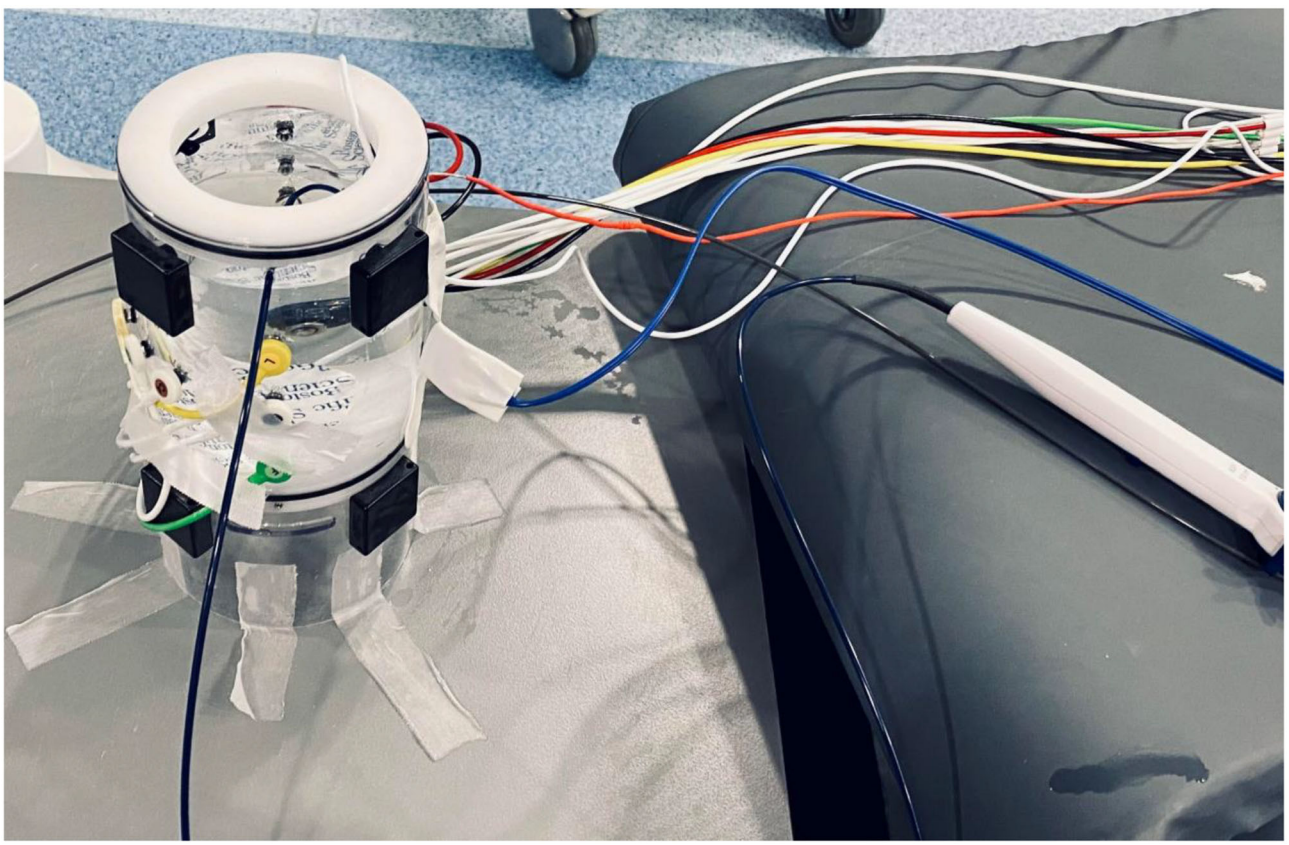

FIGURE 2 | Accuracy testing setup "*in vitro*". Dedicated testing phantom with all EAM cables connected, IntellaMap Orion catheter, and DiamondTemp ablation catheter submerged in the saline within the phantom.

1.2 The Medtronic (MDT) Generator Connection Box E (MDT GCB-E).
1.3 The MDT GCB-E and intracardiac (IC) signal out via the MDT GCB-E.

2.0 DTA not connected to a mapping system (MS) but connected to

2.1 An Ensite EPT GenConnect box (EPT GCB).
2.2 The Medtronic Generator Connection Box E (MDT GCB-E).
2.3 The MDT GCB-E and IC out via the MDT GCB-E.

3.0 DTA connected to the Rhythmia MS using (**Figure 1**)

3.1 An EPT GCB and Rhythmia Maestro GCB (Maestro GCB, native Rhythmia setup).
3.2 The MDT GCB-E and Maestro GCB.
3.3 The MDT GCB-E and IC out via the MDT GCB-E directly to the Rhythmia IC in at box 1 (pin A61 to A64).

Configurations 1.x and 2.x were used for functional and safety assessment only.

Functional and Safety Parameters Assessment

To assess the functional and safety parameters of the DTA with the different setups proposed, a calibrated electrosurgery analyzer "FLUKE Biomedical QA-ESII" was used. This device allows for the continuous measurement of power, current, peak-to-peak voltage (closed load only), and crest factor for each RF application. (7) The test and connectivity of the FLUKE Biomedical QA-ESII Electrosurgery Analyzer equipment to different components is performed in "continuous operation mode" with no footswitch. In this mode, the analyzer continues

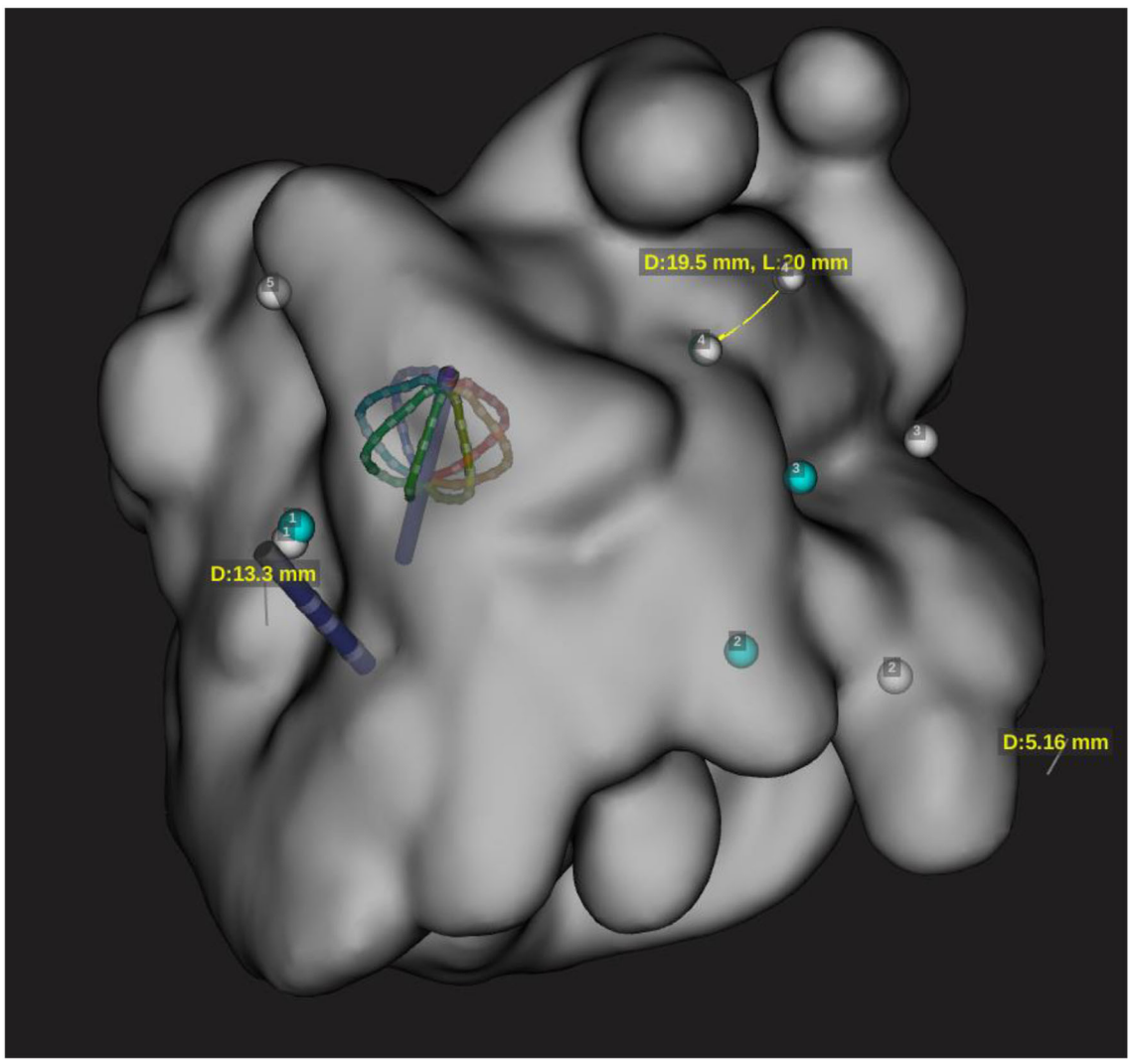

FIGURE 3 | Representation of both Orion and DT catheter in the 3D map on the EAM. This snapshot is showing catheter shift during RF application with configuration 3.1 and distance measurement of 19 mm for configuration 3.3.

TABLE 1 | Functional and safety parameters with different setups.

Functional and safety parameters observed with setup 0.0.					
Load (Ohm)		**50**		**150**	
Max power programed on RFG (W)	**50**	**30**	**15**	**50**	**30**
Difference between the power output indicated on RFG and the power measured at the tip of the DTC with the electrosurgery analyzer during ablation (W)	3	2	1	1	1
Functional and safety parameters observed with setup 1.1					
Load (Ohm)		**50**		**150**	
Max power programed on RFG (W)	**50**	**30**	**15**	**50**	**30**
Difference between the power output indicated on RFG and the power measured at the tip of the DTC with the electrosurgery analyzer during ablation (W)	3	3	1	1	1
Functional and safety parameters observed with setup 1.2					
Load (Ohm)		**50**		**150**	
Max power programed on RFG (W)	**50**	**30**	**15**	**50**	**30**
Difference between the power output indicated on RFG and the power measured at the tip of the DTC with the electrosurgery analyzer during ablation (W)	4	2	1	1	1
Maximum variation in current measured at the tip of the DTC using the electrosurgery analyzer between the 3 measurements performed (mA)	4	0	0	0	0
Functional and safety parameters observed with setup 3.1					
Load (Ohm)		**50**		**150**	
Max power programed on RFG (W)	**50**	**30**	**15**	**50**	**30**
Difference between the power output indicated on RFG and the power measured at the tip of the DTC with the electrosurgery analyzer during ablation (W)	4	3	1	1	1
Maximum variation in the current measured at the tip of the DTC using the electrosurgery analyzer between the 3 measurements performed (mA)	1	0	0	0	0
Functional and safety parameters observed with setup 3.2					
Load (Ohm)		**50**		**150**	
Max power programed on RFG (W)	**50**	**30**	**15**	**50**	**30**
Difference between the power output indicated on RFG and the power measured at the tip of the DTC with the electrosurgery analyzer during ablation (W)	4	3	1	1	1
Maximum variation in the current measured at the tip of the DTC using the electrosurgery analyzer between the 3 measurements performed (mA)	4	0	0	0	0
Load (Ohm)		**50**		**150**	
Functional and safety parameters observed with setup 3.3					
Load (Ohm)		**50**		**150**	
Max power programed on RFG (W)	**50**	**30**	**15**	**50**	**30**
Difference between the power output indicated on RFG and the power measured at the tip of the DTC with the electrosurgery analyzer during ablation (W)	4	3	1	1	1
Maximum variation in the current measured at the tip of the DTC using the electrosurgery analyzer between the 3 measurements performed (mA)	4	0	0	0	0
Load (Ohm)		**50**		**150**	

DTC, DiamondTemp catheter; RFG, radio frequency generator.

TABLE 2 | DiamondTemp catheter location after RF1, RF2 or RF3 for all setups tested.

CONTROL VALUES: baseline points	**Point 1**	**Point 2**	**Point 3**	**Point 4**	**Point 5**
Distance to baseline points before any other testing variables (mm)	NA	NA	NA	NA	NA
Distance to baseline points after reinsertion of the DTC in the phantom (mm)	NA	NA	NA	NA	NA
Distance to baseline points after reconnection of the DTC (mm)	0.0	0.0	0.0	0.0	0.0
Distance to baseline points after RF1 was performed (mm)	0.9	1.2	1.1	1.1	1.2
Distance to baseline points after reinserting the DTC following RF1 (mm)	0.4	0.6	1.0	1.4	1.2
Distance to baseline points after reconnecting the DTC following RF1 (mm)	0.4	0.6	1.0	1.4	1.2
Distance to baseline points after RF2 was performed (mm)	1.0	1.5	1.6	1.2	1.9
Distance to baseline points after reinserting the DTC following RF2 (mm)	0.5	0.4	1.2	1.6	1.0
Distance to baseline points after reconnecting the DTC following RF2 (mm)	0.5	0.4	1.2	1.6	1.0
Distance to baseline points after RF3 was performed (mm)	0.9	1.2	0.9	1.4	1.2
Distance to baseline points after reinserting the DTC following RF3 (mm)	0.5	0.8	1.0	1.8	1.6
Distance to baseline points after reconnecting the DTC following RF3 (mm)	0.5	0.8	1.0	1.8	1.6
Distance to baseline points after variables tested (mm)	NA	NA	NA	NA	NA
Quantitative data on Rhythmia MS reliability when connect to the DTA using setup 3.1					
Registered baseline points	**Point 1**	**Point 2**	**Point 3**	**Point 4**	**Point 5**
Distance to baseline points before any other testing variables (mm)	NA	NA	NA	NA	NA
Distance to baseline points after reinsertion of the DTC in the phantom (mm)	NA	NA	NA	NA	NA
Distance to baseline points after reconnection of the DTC (mm)	0.0	0.0	0.0	0.0	0.0
Distance to baseline points after RF1 was performed (mm)	0.5	0.5	1.2	2.5	12.4
Distance to baseline points after reinserting the DTC following RF1 (mm)	1.2	1.5	3.5	4.5	9.8
Distance to baseline points after reconnecting the DTC following RF1 (mm)	1.2	1.5	3.5	4.5	9.8
Distance to baseline points after RF2 was performed (mm)	1.5	1.0	4.0	9.6	10.5
Distance to baseline points after reinserting the DTC following RF2 (mm)	0.4	0.6	1.4	11.8	12.0
Distance to baseline points after reconnecting the DTC following RF2 (mm)	0.4	0.6	1.4	11.8	12.0
Distance to baseline points after RF3 was performed (mm)	2.9	2.8	4.9	10.0	10.2
Distance to baseline points after reinserting the DTC following RF3 (mm)	0.6	0.8	1.0	12.0	12.2
Distance to baseline points after reconnecting the DTC following RF3 (mm)	0.6	0.8	1.0	12.0	12.2
Distance to baseline points after variables tested (mm)	NA	NA	NA	NA	NA
Quantitative data on Rhythmia MS reliability when connect to the DTA using setup 3.2					
Registered baseline points	**Point 1**	**Point 2**	**Point 3**	**Point 4**	**Point 5**
Distance to baseline points before any other testing variables (mm)	NA	NA	NA	NA	NA
Distance to baseline points after reinsertion of the DTC in the phantom (mm)	NA	NA	NA	NA	NA

(Continued)

TABLE 2 | Continued

Quantitative data on Rhythmia MS reliability when connect to the DTA using setup 3.3					
Distance to baseline points after reconnection of the DTC (mm)	0.0	0.0	0.0	0.0	0.0
Distance to baseline points after RF1 was performed (mm)	0.9	1.2	1.1	3.1	3.2
Distance to baseline points after reinserting the DTC following RF1 (mm)	0.4	0.6	1.0	2.4	2.2
Distance to baseline points after reconnecting the DTC following RF1 (mm)	0.4	0.6	1.0	2.4	2.2
Distance to baseline points after RF2 was performed (mm)	1.0	1.5	1.6	3.2	3.9
Distance to baseline points after reinserting the DTC following RF2 (mm)	0.5	0.4	1.2	1.6	2.0
Distance to baseline points after reconnecting the DTC following RF2 (mm)	0.5	0.4	1.2	1.6	2.0
Distance to baseline points after RF3 was performed (mm)	0.9	1.2	0.9	3.4	4.2
Distance to baseline points after reinserting the DTC following RF3 (mm)	0.5	0.8	1.0	1.8	2.6
Distance to baseline points after reconnecting the DTC following RF3 (mm)	0.5	0.8	1.0	1.8	2.6
Distance to baseline points after variables tested (mm)	NA	NA	NA	NA	NA
Registered baseline points	**Point 1**	**Point 2**	**Point 3**	**Point 4**	**Point 5**
Distance to baseline points before any other testing variables (mm)	NA	NA	NA	NA	NA
Distance to baseline points after reinsertion of the DTC in the phantom (mm)	NA	NA	NA	NA	NA
Distance to baseline points after reconnection of the DTC (mm)	0.0	0.0	0.0	0.0	0.0
Distance to baseline points after RF1 was performed (mm)	17.2	15.5	21.5	24.5	25.5
Distance to baseline points after reinserting the DTC following RF1 (mm)	10.5	10.4	11.1	12.5	12.4
Distance to baseline points after reconnecting the DTC following RF1 (mm)	10.5	10.4	11.1	12.5	12.4
Distance to baseline points after RF2 was performed (mm)	18.5	21.0	22.0	24.7	32.5
Distance to baseline points after reinserting the DTC following RF2 (mm)	10.9	10.1	11.4	11.5	13.9
Distance to baseline points after reconnecting the DTC following RF2 (mm)	10.9	10.1	11.4	11.5	13.9
Distance to baseline points after RF3 was performed (mm)	20.2	20.7	21.2	25.0	30.0
Distance to baseline points after reinserting the DTC following RF3 (mm)	10.6	11.2	10.9	12.0	12.0
Distance to baseline points after reconnecting the DTC following RF3 (mm)	10.6	11.2	10.9	12.0	12.0
Distance to baseline points after variables tested (mm)	NA	NA	NA	NA	NA

DTC, DiamondTemp catheter; RF, radio frequency.

to perform measurements continuously. The test is interrupted by pressing the "stop" key. The analyzer acts like a meter during the test, showing increasing and decreasing values as received from the unit being tested, in this case, the DTA RFG. The DTA RFG is connected to the connection for the electrode outputs of internal variable resistance. An active connection (Red) is directly connected to the catheter tip alligator clip wired to the Red pin. The neutral connection is directly wired from the DTA neutral plate connection and the analyzer neutral pin (Black).

The functional and safety parameters of the DTA and its RFG were assessed at 3 different loads, namely 50 Ohms, 100 Ohms, and 150 Ohms, and 3 different maximum power outputs, namely 50 W, 30 W, and 15 Watts. For each load and maximum power output, 3 measurements were performed to assess the following parameters: (1) maximum power output indicated on the DTA RFG; (2) power output measured at the tip of the DiamondTemp catheter (DTC); (3) current measured at the tip of the DTC; (4) peak-to-peak voltage measured at the tip of the DTC; and (5) maximum current variation among the 3 measurements.

Assessing the DTA Reliability With EAM

The DTA reliability when using the Rhythmia^{TM} EAM was assessed as per the manufacturer's accuracy by testing work instruction using a dedicated EAM phantom. This ensured an

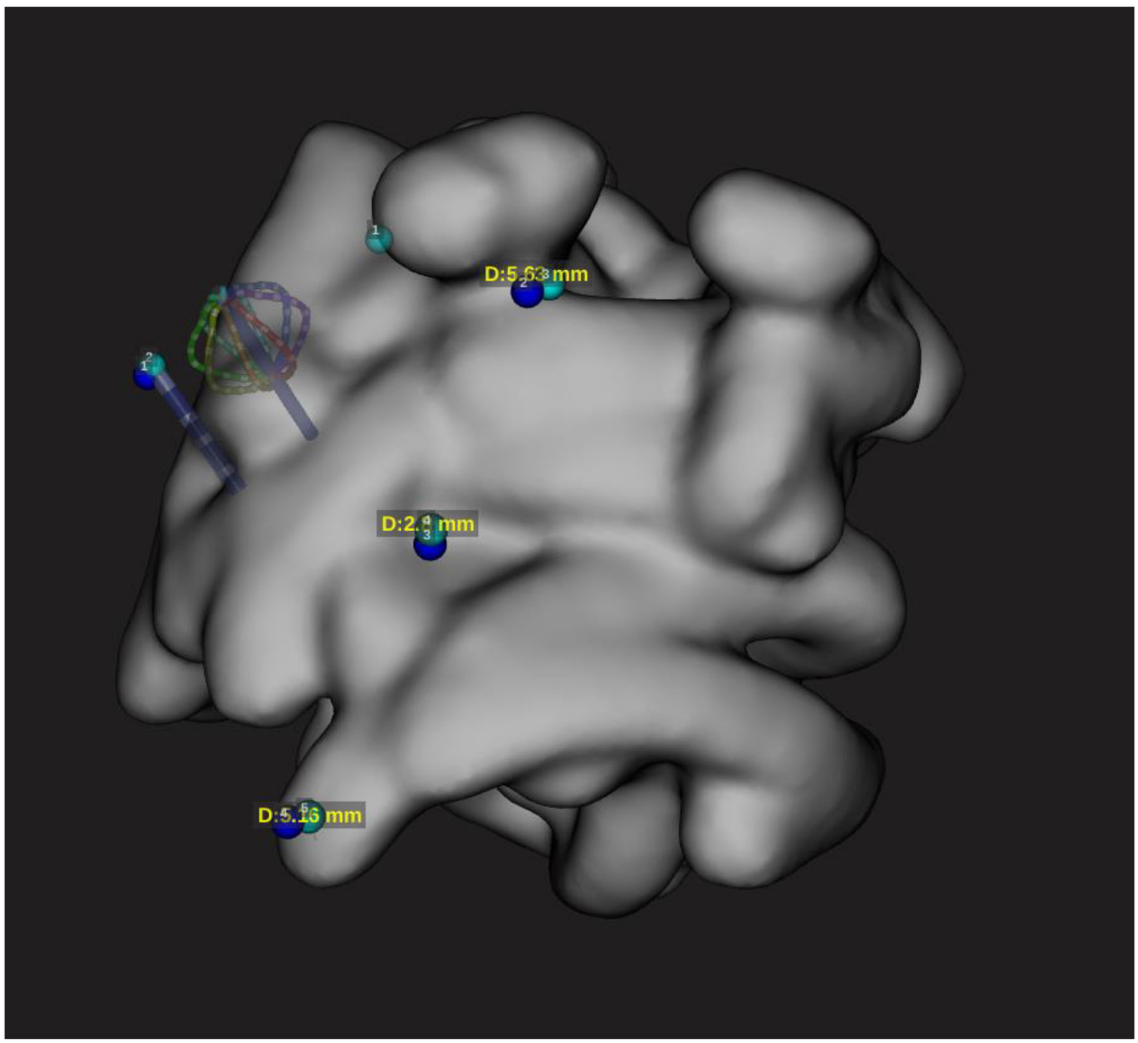

FIGURE 4 | Localization accuracy with minimal deviation according to configuration 3.2. The catheter positioned on the reference points is represented on the EAM with minimal difference to the reference sensor-enabled catheter.

accurate assessment of the EAM reliability using the DTA as this work instruction is normally used during the EAM installation prior to the certification for clinical use. Different components were connected to the DTA RFG and EAM according to the different setups to be tested (**Figure 2**).

The phantom anatomy was built using a dedicated high-resolution mapping catheter, Intellamap Orion (Boston Scientific). Reference locations from the phantom were reached with the tip of this catheter and the reference locations were added to the surface of the phantom as a baseline. Then the tracking of the DTA was verified by visual comparison of the physical catheter movements and its representation on the map (**Figures 3–5**).

Before testing any additional variables, points were collected on the EAM with the DTA manually positioned at the established reference locations. These were the baseline points for each setup that was tested.

To assess the reliability of the catheter location on the EAM, the DTA was placed back at each reference location and an additional point was collected. An assessment was made regarding the reproducibility of the baseline point locations by measuring the distance between tags (in mm) on the EAM.

For each setup, three different RF pulses were tested: (1) RF energy for 45 s with a target temperature of 60°C (longest application time and highest temperature allowed by the DTA in a clinical setting), with 0 s of power ramp delay, 1 s of pre-cooling, and 0 s of cooling post ablation (RF1); (2) RF energy for 10 s with a target temperature of 55°C (longest application time and highest temperature allowed by the DTA in a clinical setting) with 0 s of power ramp delay, 1 s of pre-cooling, and 0 s of cooling post ablation (RF2); or (3) RF energy for 5 s with a target temperature of 50°C (longest application time and highest temperature allowed by the DTA in a clinical setting) with 0 s of power

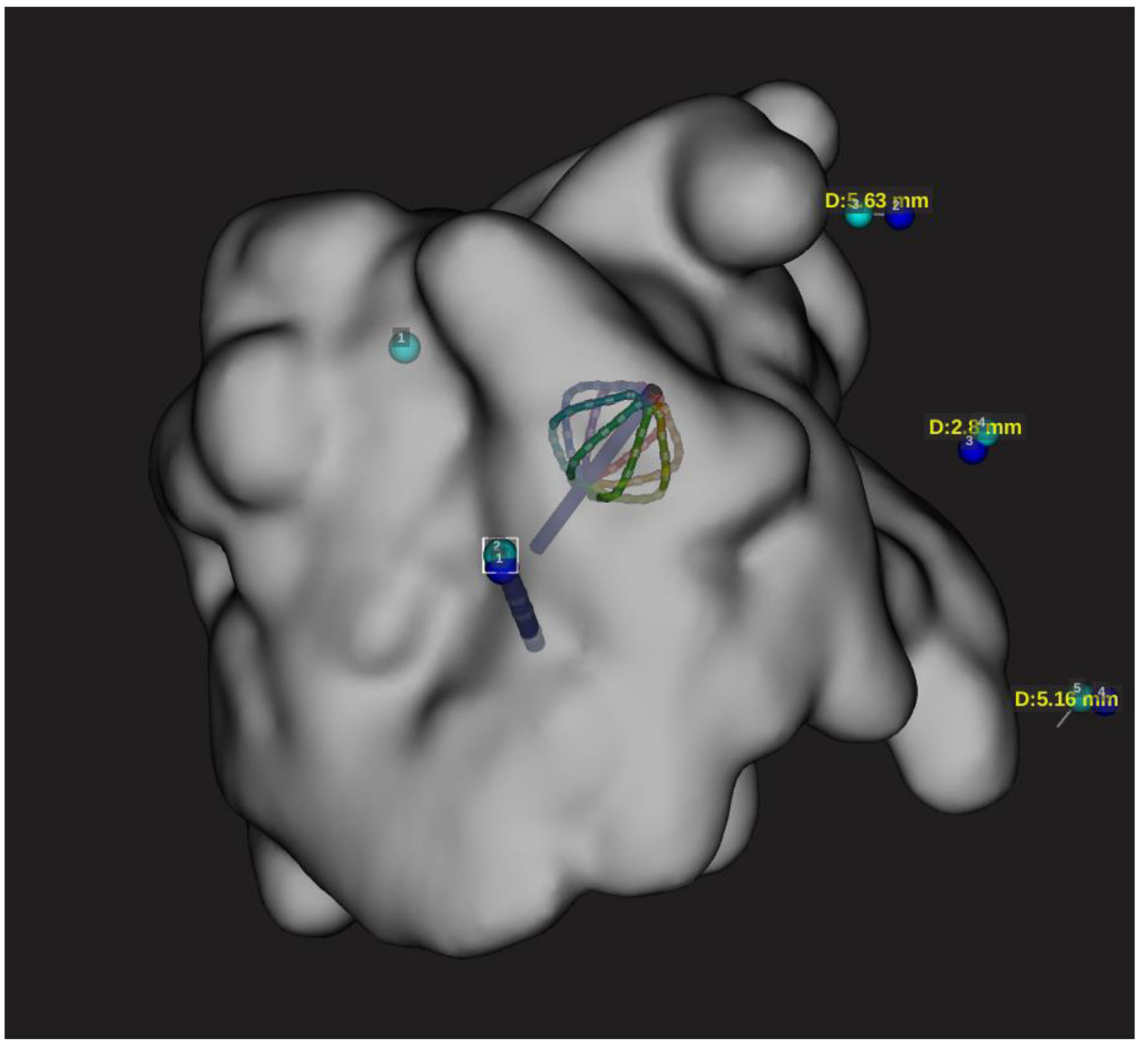

FIGURE 5 | Configuration 3.2 during RF delivery. Localization accuracy of DTA catheter on the EAM during RF application (50 w 30 s). This configuration has shown no catheter shift during RF application.

ramp delay, 1 s of pre-cooling, and 0 s of cooling post ablation (RF3).

Between each RF delivery, the DTA was removed and reinserted in the phantom and the DTA cable was disconnected and reconnected without moving the catheter.

After each RF application, the catheter was manually placed at each reference location by looking at the phantom directly. An additional point was collected at each reference location. Distance between every taken point and its corresponding baseline marker were measured using the EAM software.

Distance measurements (in mm) between baseline points and collected points were repeated for every reference location on the phantom model after each RF pulse. At the next step, the DTA was placed once again back at each reference location and an additional final point was collected.

Configurations and Connections of the DTA to the Rhythmia EAM

The original Rhythmia™ ablation setup has been modified to use DTA RFG by connecting DTA GCC and one of GCB to Maestro connections of the Maestro GCB. The reliability and accuracy of the DTA visualization on the Rhythmia™ EAM were based on the fact that the Rhythmia™ EAM has a hybrid-tracking mechanism. This hybrid mechanism uses an algorithm that calculates impedance values, from each electrode of nonmagnetic catheters, in the magnetic field map, created using the Orion catheter. This allows to accurately track nonmagnetic sensor-enabled catheters (6). The test was performed using the dedicated Boston Scientific Wet/Dry Tank corresponding to the Boston Scientific Work Instruction and accordingly to the EAM IFU (8).

A new ablation catheter has been configured in the EAM.

The anatomy shell and a Field Map were created using the Orion catheter as per IFU (1) to allow impedance tracking for 3rd party catheters. The DTA was connected to the Rhythmia™ EAM according to setup 3.1. Five fixed metallic points inside the wet tank were used as references, with points 3, 4, and 5 being the closest to the X-ray flat detector. To test the influence of magnetic distortion, the X-ray flat detector was kept in sufficient proximity to the phantom. Points 1 and 2 were not affected by the magnetic field distortion while points 3, 4, and 5 were, with 5 being the most affected location by magnetic distortion. All 5 points were found within the range of the Rhythmia™ EAM specifications. The Orion catheter was used to ensure the precision of all baseline points.

After preparation, the accuracy checks have been performed as described earlier.

Statistical Analysis

All variables were tested for normality with the Shapiro–Wilk test. Normally, the distributed variables were described as mean ± standard deviation and the groups were compared through ANOVA, paired *t*-test, or unpaired *t*-test as appropriate, while the non-normally distributed variables were described as median (Inter Quartile Range) and compared using the Kruskal–Wallis test, the Mann–Whitney test, or the Wilcoxon signed-rank test as appropriate. The categorical variables were described as frequencies (percentages) and compared by the Chi-squared test or Fisher's exact test as appropriate.

A p-value <0.05 was considered statistically significant.

The analysis was performed using R software version 3.6.2 (R Foundation for Statistical Computing, Vienna, Austria).

RESULTS

DTA Functional and Safety Parameters Assessment With Different Setups

The data collected on the functional and safety parameters of the DTA connected to the EPT GCB, different Medtronic R&D components, and the Rhythmia™ EAM are detailed in **Table 1**.

At the lowest load setting of 50 Ohm, a maximum discrepancy of 5W could be observed between the maximum power programmed to be delivered by the DTA RFG, the actual power output indicated on the DTA RFG, and the power output measured at the tip of the DTA.

Variations on the current output measured at the tip of the DTA by the RF analyzer could be observed between the three measurements performed with the same settings. All variations were within the limits specified by the manufacturer of the device (6). The results are summarized in **Table 1**.

DTA Location Accuracy With Rhythmia™ EAM

The DTA location was represented in real-time on the Rhythmia™ EAM while connected per IFU to the Maestro connection box. Proper tracking of the DTA was observed by visual comparison of the physical catheter movements and its representation on the EAM. This was consistent with all the setups tested.

TABLE 3 | Distances measured between the baseline points after each variable, for each setup tested.

Point 1 (*p*-value)	Baseline	Setup 3.1	Setup 3.2	Setup 3.3
Baseline	NA	0.99	1.00	<0.001
Setup 3.1	0.99	NA	0.99	<0.001
Setup 3.2	1.00	0.99	NA	<0.001
Setup 3.3	<0.001	<0.001	<0.001	NA
Point 2 (*p*-value)	**Baseline**	**Setup 3.1**	**Setup 3.2**	**Setup 3.3**
Baseline	NA	0.99	1.00	<0.001
Setup 3.1	0.99	NA	0.99	<0.001
Setup 3.2	1.00	0.99	NA	<0.001
Setup 3.3	<0.001	<0.001	<0.001	NA
Point 3 (*p*-value)	**Baseline**	**Setup 3.1**	**Setup 3.2**	**Setup 3.3**
Baseline	NA	0.93	1.00	<0.001
Setup 3.1	0.93	NA	0.93	<0.001
Setup 3.2	1.00	0.93	NA	<0.001
Setup 3.3	<0.001	<0.001	<0.001	NA
Point 4 (*p*-value)	**Baseline**	**Setup 3.1**	**Setup 3.2**	**Setup 3.3**
Baseline	NA	0.002	0.98	<0.001
Setup 3.1	0.002	NA	0.93	0.002
Setup 3.2	0.98	0.93	NA	<0.001
Setup 3.3	<0.001	0.002	<0.001	NA
Point 5 (*p*-value)	**Baseline**	**Setup 3.1**	**Setup 3.2**	**Setup 3.3**
Baseline	NA	<0.001	0.98	<0.001
Setup 3.1	<0.001	NA	0.003	0.025
Setup 3.2	0.98	0.003	NA	<0.001
Setup 3.3	<0.001	0.025	<0.001	NA

The accuracy of reference markers displayed on the Rhythmia™ EAM could not be assessed as the Rhythmia™ EAM does not have predefined information on their locations in the wet tank. The baseline points taken using the Intella Map Orion catheter's matrix were tracked using magnetic localization. The verification of the location of baseline points was established by taking points at the reference markers on the wet tank.

Although the catheter was reconnected after each RF energy delivery, no points were taken after the DTC reconnection because it was displayed in the same location it was found prior to its disconnection.

In setup 3.2, no major shifts were observed in the DTC location after RF1, RF2, or RF3 were performed with all setups tested (**Table 2**). The location of the DTC did not significantly shift in space when compared to baseline reference points. This was consistent after reinsertion and reconnection as well as following RF energy delivery. The distances measured between the baseline points after each variable, for each setup tested, are described in **Figures 4**, **5** and **Tables 2**, **3**.

Specific Observations Related to the Setup 3.1

In this configuration, a significant shift was observed after the first RF application (**Figure 3**); however, further applications caused not further shift. This may be linked to the fact that the EPT GCB used for testing was previously extensively used (**Tables 2**, **3**).

Observations Related to the Setup 3.2

In this configuration, no significant shift has been observed. All points were taken within the Rhythmia catheter location accuracy specifications (1) and were demonstrated to be accurate (**Figures 4**, **5**; **Tables 2**, **3**).

Specific Observations Related to the Setup 3.3

Setup 3.3 showed a massive shift in catheter position before ablation compared to baseline points acquired using the Orion catheter as a reference. The distance between the baseline points and the points taken after RF1 was over 10 mm. Further delivery of the RF energy caused more significant catheter shift (**Tables 2**, **3**).

DISCUSSION

The main results of the current study are as follows: (1) a universal method for compatibility assessment of the ablation catheters and navigation systems was described; (2) DTA is compatible with Rhythmia EAM with a safety and reliability profile within the specification; and (3) careful setup is mandatory to achieve good clinical outcomes as only setup 3.2 (**Figures 1**, **4**, **5**) demonstrated satisfactory results. Other tested configurations have shown significant accuracy mismatch with reference points taken using a sensor-enabled catheter. The shift was further increased during RF delivery.

The 3D mapping systems have become a standard tool for the diagnosis and treatment of various cardiac arrhythmias. They have multiple benefits like reducing radiation time and dose and improving the precision of ablation treatment (9). However, the use of third-party therapeutic catheters is limited as there is no compatibility out of the box. Extending the range of compatible ablation systems with various 3D mapping platforms allows innovative therapeutic modalities to be used without limitations, which may translate into a clinical benefit.

The *in vitro* compatibility assessment is a crucial step, which must be done prior to the clinical trial. The described method can be a universal solution for such compatibility testing since it is based on industry standards and manufacturer work instructions to evaluate all the parameters. Using only commercially available and CE-marked components during the evaluation makes further clinical use possible.

In the current study, compatibility testing for the DTA and the Rhythmia EAM was performed, assessing all the setups in terms of safety and functionality within specifications. However, in terms of location accuracy, only one setup has shown results within manufacturer specifications and the other 2 configurations were associated with a significant catheter representation shift. This is critical during ablation procedures, and setup 3.2 should be used for further clinical evaluation.

CONCLUSIONS

A universal and reproducible solution for compatibility testing between various mapping systems and ablation catheters has been described. DTA has been demonstrated to be compatible with Rhythmia EAM with satisfactory results if specific setup is used.

DATA AVAILABILITY STATEMENT

The original contributions presented in the study are included in the article/supplementary material, further inquiries can be directed to the corresponding author/s.

ETHICS STATEMENT

This study was reviewed and approved by Commissie Medische Ethiek, UZ Brussel.

AUTHOR CONTRIBUTIONS

Conception and design of the study: LP, IE, and CA. Substantial contributions to the acquisition of data for the study: RR, DC, MV, AG, AS, CM, IO, GB, AA, ES, JS, PB, ML, G-BC, and CA. Substantial contributions to the analysis of data for the study: LP, IE, and RR. Substantial contributions to the interpretation of data for the study and revising the draft of the work critically for important intellectual content: DC, MV, AG, AS, CM, IO, GB, AA, ES, JS, PB, ML, G-BC, and CA. Drafting the study: LP and IE. Final approval of the version to be published and agreement to be accountable for all aspects of the work in ensuring that questions related to the accuracy or integrity of any part of the study are appropriately investigated and resolved: LP, IE, RR, DC, MV, AG, AS, CM, IO, GB, AA, ES, JS, PB, ML, G-BC, and CA. All authors contributed to the article and approved the submitted version.

REFERENCES

1. Ellermann C, Frommeyer G, Eckardt L. Hochauflösendes 3-D-Mapping :Chancen und Limitationen des Rhythmia^{TM}-Systems [High-resolution 3D mapping : Opportunities and limitations of the Rhythmia^{TM} mapping system]. *HerzschrittmachertherElektrophysiol.* (2018) 29:284–92. doi: 10.1007/s00399-018-0580-0
2. *Medtronic: Instruction for Use—EPIX therapeutics—DiamondTemp Catheter.* (2021), Medtronic MN, USA. Available at: https://manuals.medtronic.com/content/dam/emanuals/crdm/M016135C001A_view.pdf
3. Iwasawa J, Koruth JS, Petru J, Dujka L, Kralovec S, Mzourkova K, et al. Temperature-controlled radiofrequency ablation for pulmonary vein isolation in patients with atrial fibrillation. *J Am Coll Cardiol.* (2017) 70:542–53. doi: 10.1016/j.jacc.2017.06.008

4. Ramak R, Lipartiti F, Mojica J, Monaco C, Bisignani A, Eltsov I, et al. Comparison between the novel diamond temp and the classical 8-mm tip ablation catheters in the setting of typical atrial flutter. *J Interv Card Electrophysiol.* (2022) 42:504–18 doi: 10.1007/s10840-022-01152-w
5. Nakagawa H, Ikeda A, Sharma T, Lazzara R, Jackman WM. Rapid high resolution electroanatomical mapping: evaluation of a new system in a canine atrial linear lesion model. *Circ ArrhythmElectrophysiol.* (2012) 5:417–24. doi: 10.1161/CIRCEP.111.968602
6. Anter E, McElderry TH, Contreras-Valdes FM Li J, Tung P, Leshem E, Haffajee CI, et al. Evaluation of a novel high-resolution mapping technology for ablation of recurrent scar-related atrial tachycardias. *Heart Rhythm.* (2016) 13:2048–55. doi: 10.1016/j.hrthm.2016.05.029
7. *Fluke Biomedical: QA-ES II Electrosurgical Analyzer—Users Manual.* (2006). United States: Fluke Corporation
8. *Boston Scientific: Rhythmia HDX Mapping System. Hardware Directions for Use.* (2016). MA, USA: Boston Scientific
9. Pani A, Giuseppina B, Bonanno C, et al. Predictors of Zero X-Ray Ablation for Supraventricular Tachycardias in a Nationwide Multicenter Experience. *Circ ArrhythmElectrophysiol.* (2018) 11:e005592. doi: 10.1161/CIRCEP.117.005592

Conflict of Interest: IE and DC are employees of Medtronic Inc. MV is employee of Boston Scientific. PB received compensation for teaching purposes from Biotronik. ML is consultant for Atricure. G-BC received compensation for teaching purposes and proctoring from Medtronic, Abbott, Biotronik, Boston Scientific, and Acutus Medical. CA receives research grants on behalf of the center from Biotronik, Medtronic, Abbott, LivaNova, Boston Scientific, AtriCure, Philips, and Acutus. CA received compensation for teaching purposes and proctoring from Medtronic, Abbott, Biotronik, Livanova, Boston Scientific, Atricure, and Acutus Medical Daiichi Sankyo.

The remaining authors declare that the research was conducted in the absence of any commercial or financial relationships that could be construed as a potential conflict of interest.

Publisher's Note: All claims expressed in this article are solely those of the authors and do not necessarily represent those of their affiliated organizations, or those of the publisher, the editors and the reviewers. Any product that may be evaluated in this article, or claim that may be made by its manufacturer, is not guaranteed or endorsed by the publisher.

frontiers | Frontiers in Cardiovascular Medicine

REVIEW
published: 30 June 2022
doi: 10.3389/fcvm.2022.942385

Left Atrial Cardiomyopathy – A Challenging Diagnosis

*Fabienne Kreimer and Michael Gotzmann**

University Hospital St. Josef-Hospital Bochum, Cardiology and Rhythmology, Ruhr University Bochum, Bochum, Germany

Left atrial cardiomyopathy (LACM) has been an ongoing focus of research for several years. There is evidence that LACM is responsible for atrial fibrillation and embolic strokes of undetermined sources. Therefore, the correct diagnosis of LACM is of clinical importance. Various techniques, including electrocardiography, echocardiography, cardiac magnetic resonance imaging, computed tomography, electroanatomic mapping, genetic testing, and biomarkers, can both identify and quantify structural, mechanical as well as electrical dysfunction in the atria. However, the question arises whether these techniques can reliably diagnose LACM. Because of its heterogeneity, clinical diagnosis is challenging. To date, there are no recommendations for standardized diagnosis of suspected LACM. However, standardization could help to classify LACM more precisely and derive therapeutic directions to improve individual patient management. In addition, uniform diagnostic criteria for LACM could be important for future studies. Combining several parameters and relating them seems beneficial to approach the diagnosis of LACM. This review provides an overview of the current evidence regarding the diagnosis of LACM, in which several potential parameters are discussed and, consequently, a proposal for a diagnostic algorithm is presented.

Keywords: atrial cardiomyopathy, diagnosis, atrial fibrillation, embolic stroke of undetermined source, diagnostic algorithm

OPEN ACCESS

Edited by:
Hung-Fat Tse,
The University of Hong Kong,
Hong Kong SAR, China

Reviewed by:
Roddy Hiram,
Université de Montréal, Canada
Robert Kiss,
McGill University, Canada

***Correspondence:**
Michael Gotzmann
michael.gotzmann@rub.de

Specialty section:
This article was submitted to Cardiac Rhythmology, a section of the journal Frontiers in Cardiovascular Medicine

Received: *12 May 2022*
Accepted: *14 June 2022*
Published: *30 June 2022*

Citation:
Kreimer F and Gotzmann M (2022) Left Atrial Cardiomyopathy – A Challenging Diagnosis. Front. Cardiovasc. Med. 9:942385. doi: 10.3389/fcvm.2022.942385

HIGHLIGHTS

- Left atrial cardiomyopathy (LACM) is a common disease associated with histopathological detectable structural and/or electrical changes in the myocardium of the left atrium.
- The clinical significance of LACM arises from its association with atrial fibrillation and embolic strokes of undetermined sources. Early detection of LACM may hence be important for the prevention of stroke.
- Various methods (including electrocardiography, echocardiography, cardiac magnetic resonance imaging, computed tomography, electroanatomic mapping, genetic testing, and biomarkers) have been investigated to establish the diagnosis of LACM. To date, however, there are no universally accepted recommendations.
- The present review presents the current evidence of the different methods and proposes an algorithm that could be used to diagnose LACM at present.
- The current work could help to make future research comparable and to unify diagnostic criteria of LACM.

Abbreviations: LACM, left atrial cardiomyopathy; AF, atrial fibrillation; APW, amplified P-wave; BMI, body mass index; CT, computed tomography; ECG, electrocardiography; f-wave, fibrillatory wave; HFpEF, heart failure with preserved ejection fraction; LA, left atrium/left atrial; MRI, magnetic resonance imaging; PA-TDI, duration total atrial conduction time assessed by tissue doppler imaging; PET-CT, positron emission tomography – computed tomography; PTFV1, P-wave terminal force in lead V1; PVI, pulmonary vein isolation.

INTRODUCTION

Cardiomyopathies can affect all parts of the heart to some extent, although there are types that predominantly involve one specific chamber (1). The idea of an left atrial cardiomyopathy (LACM) is not entirely new, but has recently become more significant and important (1, 2). Patients with lone atrial fibrillation (AF) and patients with embolic stroke of undetermined source (ESUS) are of particular interest because LACM is often suspected as an underlying disorder. Previous genetic studies identified genes that were associated with AF as well as electrical and structural left atrial (LA) remodeling, e.g., MYL4, Lamin-A, ETV1, Scn5a, Gja5, ErbB4, Tgfbr1/2, Igf1, TTN, numerous collagen genes (3–8). However, this probably only applies to a very small proportion of all patients with LACM. A detailed family history provides important and decisive clues in which patients genetic testing might be worthwhile.

Definition of Left Atrial Cardiomyopathy

In 2016, a position paper was published to define, characterize, and derive clinical implications of LACM (9). The expert group defined LACM as "any complex of structural, architectural, contractile or electrophysiological changes affecting the atria with the potential to produce clinically relevant manifestations" (9). The definition is broad and not disease-specific, as both risk factors and comorbidities may implicate and contribute to atrial changes (9). Therefore, a classification was introduced to classify LACM histopathological. Accordingly, LACM is divided into four categories: primarily cardiomyocyte-dependent (class I), primarily fibroblast-dependent (class II), mixed cardiomyocyte-fibroblast-dependent (class III) and primarily non-collagen deposits (class IV). Of course, mixed phenotypes are often present, and since this is a dynamic process, class variation over time is possible (9).

However, the heterogeneity of LACM causes difficulties not only in classification, but particularly in diagnosis. Several techniques have been described to diagnose LACM, e.g., electrocardiography (ECG), echocardiography, cardiac magnetic resonance imaging (MRI), computed tomography (CT), electroanatomic mapping, biomarkers, and genetic testing (9–12). Another complicating factor is that there are a variety of parameters that define LACM in different studies. To date, there is no randomized controlled trial that addresses LACM. Other studies that have attempted to identify parameters for the diagnosis of LACM so far are also extremely heterogeneous and thus difficult to compare. Most studies as well as the consensus paper focused on patients with AF or patients who have suffered stroke. The derived parameters should thus be considered cautiously, as a direct transferability to LACM may be questionable. However, combining the parameters and relating them might help to best approach the diagnosis of LACM.

The aim of this review is therefore to provide an overview of the current diagnostic options for an LACM, to highlight interrelationships of the different methodologies, and to discuss the clinical value.

CLINICAL IMPACT

Left Atrial Cardiomyopathy and Atrial Fibrillation

Left atrial cardiomyopathy and atrial fibrillation are closely related, but there is a controversy on whether AF is merely a marker of LACM. On the other hand, AF leads to AF and thus most likely promotes LACM, as AF *per se* can also cause atrial remodeling due to changes in ion channels and the development of atrial fibrosis (9). This mechanism conversely leads again to stabilization of AF and progression from lower to higher AF burden. Whereas very brief AF episodes do not alter the degree of fibrosis, longer lasting AF episodes may cause AF-induced LACM (9). Moreover, the presence of subclinical AF, particularly a higher burden, is significantly correlated with an increased thromboembolic risk (13). Therefore, the presumption exists that subclinical AF may be an early manifestation of LACM with increased risk of stroke and not the underlying cause of thromboembolic events (13).

"Lone" AF is also discussed as a possible marker of an existing LACM. "Lone" AF is diagnosed when there is no underlying explanation and other facilitating comorbidities (9). The risk of thromboembolism is lower, with a cumulative 15-year stroke risk of 1–2%, but it increases with the number of cardiovascular risk factors, e.g., age, male sex (9). In patients with "lone" AF, structural atrial remodeling, conduction disturbances, and morphological and inflammatory changes of atrial cardiomyocytes were described (9).

Left Atrial Cardiomyopathy and Embolic Stroke of Undetermined Source

Ischemic strokes are one of the most common causes of cardiovascular morbidity and mortality. A significant proportion of patients with ischemic stroke are suspected of embolic stroke without a specific embolic source being found (ESUS) (14). The clinical significance of ESUS results from the frequency of the disease and the fact that the recurrence risk for a new stroke is 4–5% per year despite antiplatelet agents (15).

A clinically significant therapeutic implication of this concept was that, because of the embolic genesis, oral anticoagulation rather than antiplatelet therapy might be beneficial for this group of patients.

By contrast, neither the NAVIGATE-ESUS trial comparing rivaroxaban with acetylsalicylic acid nor the RESPECT-ESUS trial with dabigatran demonstrated a statistically significant reduction in ischemic stroke or ischemic MRI lesions (16, 17). Similarly, the results of the ATTICUS trial, which were recently presented at the European Stroke Organisation Conference 2022 but not yet published, demonstrated that apixaban was not superior to acetylsalicylic acid in patients with ESUS and risk factors for cardiac thromboembolism (18).

However, a subgroup analysis of the NAVIGATE-ESUS trial demonstrated that patients with moderate and severe LA dilatation had a significant benefit from therapy with rivaroxaban (19). The results suggest that a proportion of patients with ESUS have LACM, which increases cardioembolic risk.

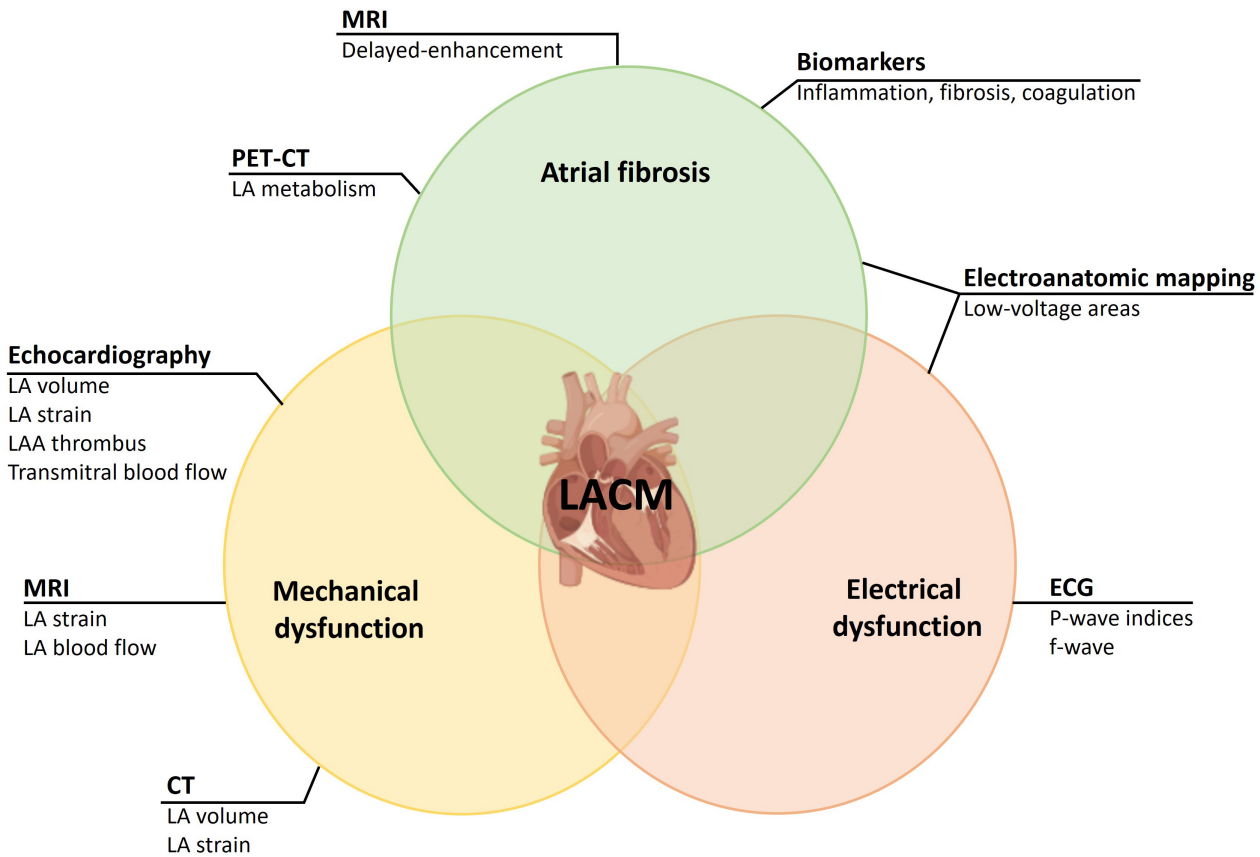

FIGURE 1 | Illustration of LACM as a composite entity of atrial fibrosis, mechanical dysfunction, and electrical dysfunction. Assessment of entities is achieved through different methods. CT, computed tomography; ECG, electrocardiology; f-wave, fibrillatory wave; LA, left atrial/let atrium; LAA, left atrial appendage; LACM, left atrial cardiomyopathy; MRI, magnetic resonance imaging; PET-CT, cardiac positron emission tomography – computed tomography.

The randomized-controlled ARCADIA trial will evaluate whether apixaban is superior to aspirin for prevention of recurrent stroke in patients with ESUS and LACM (20). According to the investigators, an LACM is defined by the presence of at least one of the following criteria: P-wave terminal force in lead V1 (PTFV1) > 5,000 μV*ms, Serum NT-proBNP > 250 pg/mL, LA diameter index ≥ 3 cm/m^2. Findings from the ARCADIA trial would have implications for secondary stroke prevention as well as primary prevention of LACM (20).

DEFINITION OF LEFT ATRIAL CARDIOMYOPATHY IN DIFFERENT STUDIES

Left atrial cardiomyopathy is both a clinical and histological diagnosis (9). The relationship between LACM and AF on the one hand and LACM and ESUS on the other suggests that correct diagnosis of LACM is of clinical benefit. As mentioned above, there is no uniform definition of LACM to date. Several studies have characterized the disease differently and used various methods:

For a correct diagnosis of LACM, histological examination of the atrial myocardium is required. Due to the invasive nature of a LA biopsy, this is an option in very few patients (for example, in mitral valve surgery). For an insight into the histology of the LA, we are thus dependent on methods that can detect fibrosis or scars. For this purpose, cardiac MRI, electroanatomic mapping in electrophysiologic studies, and PET-CT can be used. Further methods are dealing with the effects of an LACM on mechanical or electrical function. To detect mechanical dysfunction due to LACM, echocardiography may be considered in addition to CT and MRI. Furthermore, ECG parameters are suitable for the detection of electrical dysfunction, which in LACM may result from both functional and morphological changes in the LA (**Figure 1**). To what extent laboratory parameters are suitable to establish or enhance the likelihood of the diagnosis of LACM remains unclear. However, some laboratory parameters seem to be suitable to identify pathophysiological correlations (for example, LACM with immunological and inflammatory functions).

In conclusion, **Table 1** summarizes the different variables that have been used as markers of LACM in different studies.

TABLE 1 | Overview of different methods and variables for the assessment of LACM, and their associations to clinical outcomes and abnormal parameters.

Method	Parameter	Associations	References
Electrocardiography	f-wave	Abnormal echocardiographic parameters, SEC and thrombus in LA appendage, AF burden, age	(21–23)
	PTFV1	Ischemic stroke, AF, BMI, age, abnormal echocardiographic parameters	(24–37, 39)
	P-wave area	Ischemic stroke	(34)
	P-wave duration	Ischemic stroke, BMI, age, blood pressure	(34, 39)
	Advanced interatrial block	AF, Ischemic stroke	(25, 35, 38)
	Amplified P-wave duration	Abnormal echocardiographic parameters, LA appendage thrombus, major adverse cardiovascular events, AF, Recurrence of AF after ablation, low-voltage areas in electroanatomic mapping	(40–43)
	Artificial intelligence probability	Structural heart disease, abnormal echocardiographic parameters, AF, mortality	(45)
	Atrial premature complexes	Abnormal echocardiographic parameters	(46)
Transthoracic echocardiography	LA diameter	AF, ischemic stroke, major adverse cardiovascular events	(48–50)
	LA volume index	Major adverse cardiovascular events, AF, AF burden	(51–56)
	LA emptying fractions	AF, low-voltage areas in electroanatomic mapping, recurrence of AF after ablation	(43, 51, 57)
Doppler echocardiography	E-wave velocities	AF burden	(51, 52)
	A-wave velocities	AF	(51, 59)
	PA-TDI duration	AF, AF recurrence, thromboembolic events	(60)
3-D and 4-D echocardiography	LA volume index	Abnormal delayed-enhancement in MRI	(56)
	LA emptying fractions	Abnormal delayed-enhancement in MRI	(56)
	LA strain	Abnormal delayed-enhancement in MRI	(56)
Speckle-tracking echocardiography	LA strain	AF, AF burden, thromboembolic events, low-voltage areas in electroanatomic mapping, AF recurrence after ablation	(43, 57, 61–68)
	LA mechanical dispersion	AF, low-voltage areas in electroanatomic mapping	(64, 69)
Transesophageal echocardiography	LA appendage thrombus	Abnormal delayed-enhancement in MRI, LA appendage flow dynamics	(70, 71)
	SEC	Abnormal delayed-enhancement in MRI, LA appendage flow dynamics	(70, 71)
Cardiac MRI	LA strain	AF	(72–74)
Delayed- enhancement MRI	Delayed-enhancement in LA wall	AF, low-voltage areas in electroanatomic mapping, abnormal echocardiographic parameters, CHA2DS2-VASc score, ischemic stroke, major adverse cardiovascular events, AF recurrence after ablation	(75–86)
4-D flow MRI	LA blood flow velocities	AF burden, CHA2DS2-VASc score, age, abnormal echocardiographic parameters	(88–91)
CT	LA volume index	AF recurrence after ablation, reproducible in speckle-tracking echocardiography	(92, 93)
	LA strain	Reproducible in speckle-tracking echocardiography	(94–96)
	Image attenuation ratio	Low-voltage areas in electroanatomic mapping	(97)
PET-CT	18F-fluorodeoxyglucose activity	Ischemic stroke, AF, AF burden	(98, 99)
Electroanatomic mapping	Low-voltage areas	AF, CHA2DS2-VASc score, ischemic stroke, silent cerebral ischemia in MRI, AF recurrence after ablation, CRP, abnormal echocardiographic parameters	(100–110)
Biomarkers	Inflammation markers	AF, AF burden, AF recurrence after ablation, low-voltage areas in electroanatomic mapping, abnormal echocardiographic parameters	(112–121)
	Fibrosis markers	AF, AF recurrence after ablation, abnormal echocardiographic parameters, ischemic stroke	(105, 121–125)
	N-terminal pro-B-type natriuretic peptide	AF, abnormal echocardiographic parameters,	(114, 125–129)
	N-terminal pro-A-type natriuretic peptide	Low-voltage areas in electroanatomic mapping	(130)
	Aldosterone	AF	(131)
	Immunothrombosis markers	AF, major adverse cardiovascular events	(134–140)

AF, atrial fibrillation; BMI, body mass index; CRP, C-reactive protein; CT, computed tomography; f-wave, fibrillatory wave; LA, left atrial/left atrium; MRI, magnetic resonance imaging; PET-CT, cardiac positron emission tomography – computed tomography; PTFV1, P-wave terminal force in lead V1; SEC, spontaneous echo contrast.

ELECTROCARDIOGRAPHY

Introduction

An abnormal ECG may provide conduction disturbances and electrical remodeling. Studies analyzing ECG parameters defined LACM very heterogeneously. Associations with clinical outcomes (e.g., AF, ischemic stroke, major adverse cardiovascular events) and further imaging techniques evaluating LACM (e.g., abnormal echocardiographic parameters, low-voltage areas in electroanatomic mapping) were elaborated (**Table 1**).

Fibrillatory Waves (F-Waves)

The analysis of fibrillatory waves (f-waves) may be suitable for detecting both electrophysiological and structural changes in the atria. "Coarse" AF defined as amplitude of f-wave in lead V1 $\geq$ 1 mm is associated with decreased LA appendage ejection fraction and decreased maximal emptying velocity (21). In addition, higher incidences of spontaneous echo contrast and thrombus in the LA appendage were observed in the presence of "coarse" AF (22). Furthermore, patients with paroxysmal, persistent, and permanent AF had different f-wave frequencies of 5.7 ± 0.7, 6.1 ± 0.8, and 6.2 ± 0.6 Hz, respectively (23). Besides, the frequency was lower in older than in younger patients. Moreover, the amplitude of the f-wave correlates strongly with the LA volume measured by echocardiography (21) (**Figure 2C**).

P-Wave Indices

The P-wave represents the atrial depolarization of first the right atrium and then the LA, and is thus of particular interest with regard to atrial electrical remodeling (24). Interatrial excitation conduction disturbances via the Bachmann bundle can also be detected on the ECG. P-wave parameters comprise P-wave duration, P-wave dispersion, P-wave axis, P-wave voltage, P-wave area, interatrial block, and PTFV1 (24). First, several abnormal P-wave parameters are associated with the occurrence of AF. Second, they are predictive of ischemic stroke independent of AF, suggesting that they may reflect atrial remodeling irrespective of arrhythmogenesis (24). In addition, pathological P-wave parameters may be indicative of structural changes such as atrial enlargement (24).

P-Wave Terminal Force in Lead V1

An important electrocardiographic marker for atrial remodeling is the PTFV1. The P-wave in lead V1 is usually biphasic, whereby the second, negative term of the P-wave represents the excitation propagation in the LA. The PTFV1 is determined by multiplying the amplitude of the second term of the P-wave by the width of this term. A PTFV1 $\leq -4{,}000\ \mu V \times$ ms is considered pathological (24, 25). In the past, several studies demonstrated an association between an abnormal PTFV1 and the occurrence of later AF (25–28). Moreover, an abnormal PTFV1 has also been associated with cryptogenic or cardioembolic stroke independent of the presence of AF (29–32). Kamel et al. (33) revealed that an abnormal PTFV1 was more strongly associated with the occurrence of stroke than with the occurrence of AF. In contrast, P-wave area and duration were not associated with stroke occurrence (30, 33). However, a meta-analysis demonstrated an association between abnormal PTFV1, P-wave duration, maximum P-wave area, and the risk of ischemic stroke (34).

In contrast, Yamamoto et al. (35) were not able to prove a difference in prevalence of an abnormal PTFV1 among patients with cardioembolic stroke, lacunar stroke and control subjects.

Abnormal PTFV1 is also associated with functional remodeling. First, it is associated with low LA appendage ejection velocity in transesophageal echocardiography (36). Second, LA strain measured by speckle tracking echocardiography as a marker of functional atrial remodeling is significantly reduced in the presence of an abnormal PTFV1 (37). There is a negative correlation between the PTFV1 and the LA conduction strain. Surprisingly, atrial fibrosis quantified by using Masson's trichrome staining in atrial biopsies is significantly lower in patients with abnormal PTFV1. The results led to the suggestion that PTFV1 is possibly only a marker of electrical but not structural atrial remodeling (37) (**Figure 2A**).

P-Wave Duration and Advanced Interatrial Block

However, the maximal P-wave duration was significantly prolonged in patients with cardioembolic and lacunar strokes. A P-wave duration $\geq$ 120 ms and an advanced interatrial block, defined as P-wave duration $\geq$ 120 ms with simultaneous biphasic morphology in the inferior leads (35), were more frequent in the ischemic stroke groups than in the control group. At the same time, the presence of a P-wave duration $\geq$ 120 ms and an advanced interatrial block was associated with a higher likelihood for subsequent stroke, particularly of cardioembolic origin. The occurrence of an advanced interatrial block by itself is also associated with both the incidence of AF and the incidence of thromboembolic events (25, 38). Higher body mass index (BMI) and older age correlate with prolonged P-wave duration and abnormal PTFV1, whereas higher blood pressure correlate with prolonged P-wave duration and right P-wave axis deviation (39) (**Figures 2B,D**).

Novel Electrocardiography-Parameters

Recently, Müller-Edenborn et al. (40) conducted a study including patients with LA appendage thrombus to investigate an ECG-based diagnosis and staging of LACM using amplified P-wave (APW) analysis to stratify thromboembolic risk and cardiovascular outcome. Accordingly, LACM-stages were defined by APW duration, measured in digital ECG recordings from earliest beginning to latest activation in any of the 12 leads using standard amplification to 40–80 mm/mV and sweep speed of 100–200 mm/s, and P-wave morphology (40). No, moderate and extensive LACM were prevalent in 2.8, 21.1, and 76.1% of patients with LA appendage thrombi. The odds ratio for LA appendage thrombus was 24.6 ($p < 0.001$) per LACM-stage. Moreover, atrial contractile function, represented by LA appendage flow velocities, decreased with rising LACM-stages, while the occurrence of major adverse cardiovascular events increased (40). Abnormal APW duration is also associated with later onset of AF.

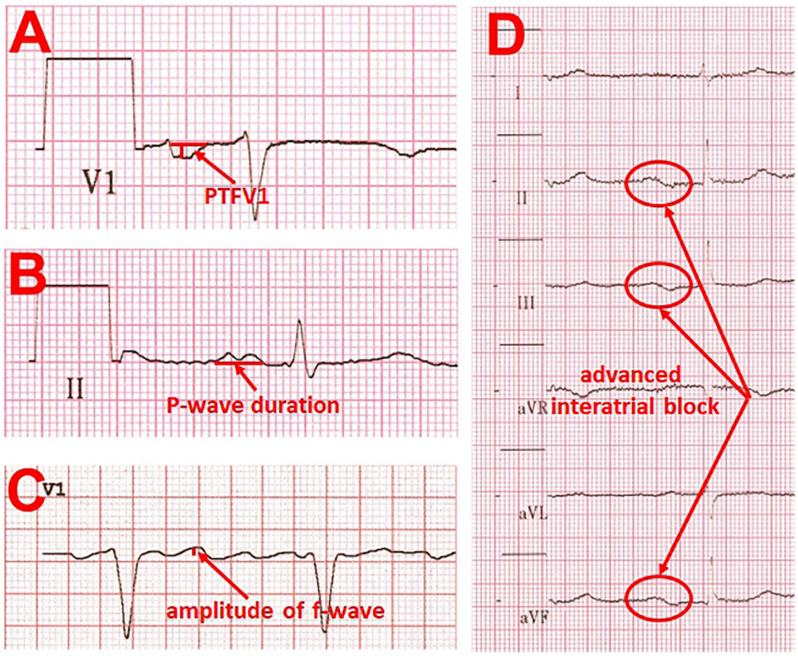

FIGURE 2 | Examples of ECG changes that are indicative of left atrial cardiomyopathy. **(A)** pronounced P-wave terminal force in lead V1 ≤ –4,000 μV × ms (multiplying the amplitude of the second term of the P-wave by the width of this term). **(B)** Prolonged P-wave duration (≥120 ms) and double peaked morphology. **(C)** "Coarse" atrial fibrillation with an amplitude of > 0.1 mV. **(D)** Example of an advanced interatrial block, defined as P-wave duration ≥ 120 ms with simultaneous biphasic morphology in the inferior leads.

An APW duration > 150 ms in patients with advanced heart failure with preserved ejection fraction (HFpEF) increased the risk for new-onset AF 10-fold (41). APW duration does not correlate with LA indexed volume but with recurrence-free survival after pulmonary vein isolation (PVI). Concordantly, an association has been demonstrated between electrophysiological evidence of LA low-voltage substrate and APW (41–43).

The duration of total atrial conduction time in non-invasive body surface electrocardiographic imaging correlated with the atrial activation time and extent of LA low-voltage substrate in endocardial contact mapping (44). Total atrial conduction time value of 148 ms identified an LACM with 91.3% sensitivity and 93.7% specificity, and the likelihood of arrhythmia recurrence after PVI was higher in patients with a total atrial conduction time > 148 ms (44).

Recently, a "novel artificial intelligence enabled ECG analysis" was performed to detect a possible LA myopathy in 613 patients with HFpEF (45). This method is based on a computer-assisted algorithm that analyzes data from raw 12-lead ECG signals and includes a statement about the probability of AF (45). Structural heart disease was more severe in patients with higher artificial intelligence probability of AF, with increased left ventricular hypertrophy, larger LA volumes, and decreased LA reservoir and booster strain in echocardiography. Each 10% increase in artificial intelligence probability resulted in a 31% higher risk of developing new-onset AF among patients with sinus rhythm and no prior AF. In the total population, each 10% increase in artificial intelligence probability led to a 12% higher risk of death (45).

Holter ECG may also provide evidence of LACM since excessive atrial premature complexes in patients with an ischemic stroke or a transient ischemic attack correlate with LA remodeling (46).

ECHOCARDIOGRAPHY

Transthoracic Echocardiography

Introduction

On the one hand, the positive correlation between LA enlargement and the occurrence of adverse cardiovascular outcomes is well known (9, 47). On the other hand, an enlarged LA is also associated with the incidence of AF (9). Echocardiography is the imaging technique of choice for the screening and follow-up of patients with abnormal LA morphology and function because of its widespread use, non-invasiveness and cost efficiency (9). Thus, echocardiography may be useful in detection of LACM. In studies investigating the utility of echocardiography, LACM was defined by demonstrating an association of abnormal LA size with mainly clinical outcomes such as AF, AF burden, recurrence of AF after ablation and ischemic stroke (**Table 1**).

Left Atrial Size

A widely used parameter for the estimation of LA size is the LA diameter (**Figure 3A**). In the AFFIRM study, an increasing

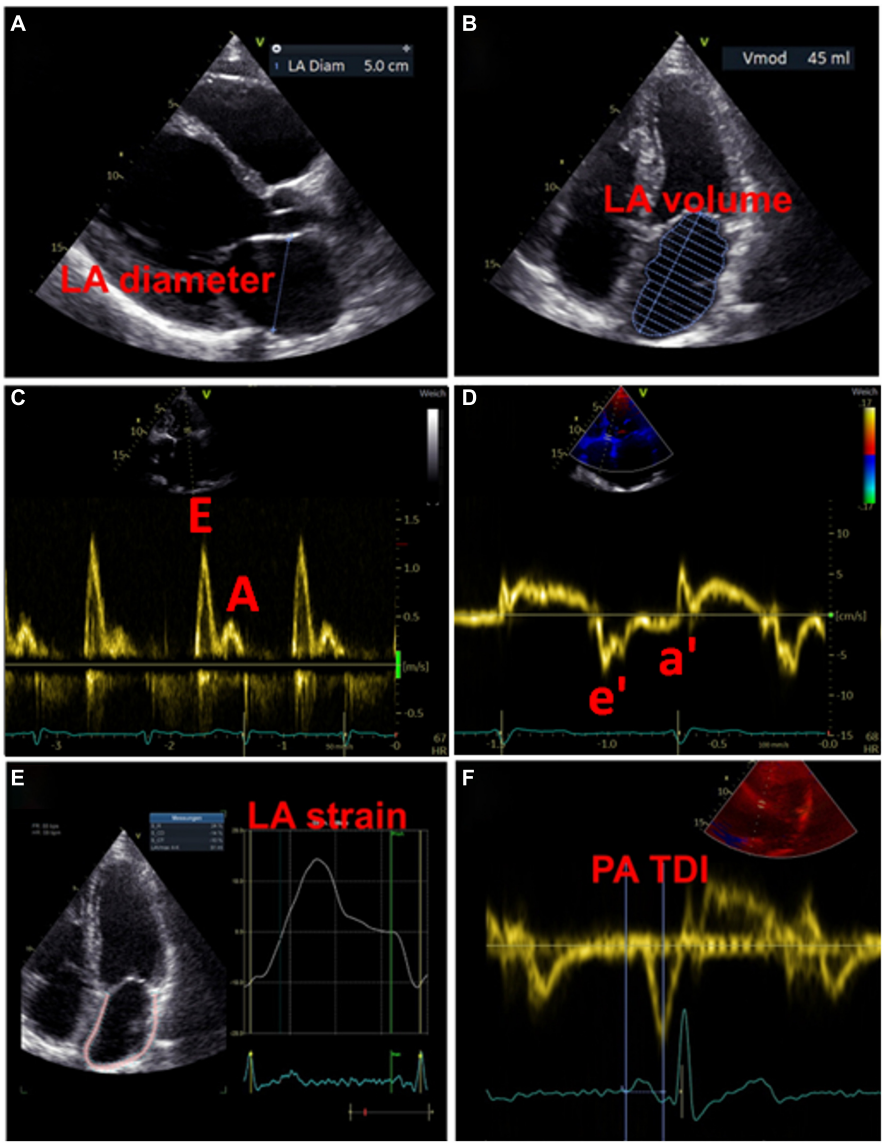

FIGURE 3 | Examples of echocardiographic measurements for the detection of left atrial cardiomyopathy. **(A)** Measurement of diameter in left atrial diastole. **(B)** Measurement of left atrial volume in left atrial diastole. **(C)** Transmitral inflow profile in left ventricular diastole: the first wave represents the E wave (passive inflow of blood into the left ventricle), the second wave represents the A wave (active contraction of the left atrium). **(D)** Tissue Doppler imaging of the movements of the left ventricular myocardium, in combination with the measurements from **(C)** the function of the atrium and the left ventricular end-diastolic pressure can be estimated. **(E)** Strain analysis of the left atrium. **(F)** Measurement of the PA-TDI interval from the beginning of the P-wave (as the onset of electrical activity of the atrium) to the peak of the a′-wave (mechanical response of atrial contraction).

LA diameter correlated with recurrent AF, but not with the risk of stroke (48). However, a meta-analysis revealed an association between a large LA diameter and the incidence of stroke and thromboembolic events (49). Moreover, large LA diameter and LA volume index were both demonstrated as predictive parameters for major adverse cardiovascular and thromboembolic events, particularly in young patients without AF (49, 50). The LA volume index is more precise and therefore more suitable for estimating atrial size (**Figure 3B**). Increased LA volume index has been described as a potential early marker of myocardial dysfunction and is often present in patients with AF, with increasing frequency in a higher AF burden (51, 52). Besides, the minimal LA volume strongly correlates with the incidence of new-onset AF and major adverse cardiovascular events compared to the maximal LA volume that seems to have no predictive effects (53–56).

In addition to abnormalities in LA size that represent structural remodeling, assessment of atrial function may provide further important indicators for the presence of LACM. Both enlarged LA and decreased LA emptying fractions are common phenomena in patients with AF, with a negative correlation between LA size and emptying fraction (51). Recently, Eichenlaub

et al. evaluated the LA emptying fraction in patients with AF for the diagnosis of LACM and prediction of arrhythmia recurrence after PVI (57). An LACM was defined as a LA low-voltage area $\geq$ 2 cm^2 at 0.5 mV threshold on endocardial contact mapping. Patients with LACM had lower LA emptying fractions than patients without LACM (27 vs. 41%, $p < 0.0001$) (43). Furthermore, LA emptying fraction < 34% was a significant predictor of both LACM, with an area under the curve of 0.846, and recurrence of arrhythmia after PVI (57).

Doppler Echocardiography

Additionally, the assessment of the LA function is possible by means of pulsed wave doppler measurements and tissue doppler imaging. Impaired LA function may be indicative of LACM, which was equated with clinical outcomes such as AF and AF burden in the studies that used doppler echocardiography (**Table 1**).

In the past, numerous echocardiographic parameters relating transmitral blood flow and diastolic myocardial motion have been investigated for association with LA function and clinical events (51, 52, 58, 59). However, no parameter and corresponding cut-off value have yet been identified as suitable for the diagnosis of LACM.

Whereas LA conduction function (represented by transmitral E-wave velocities) increases with higher AF burden, there is an opposite effect in LA contractile function (represented by transmitral A-wave velocities and mitral annular tissue Doppler a' velocities).

(51). There is an association between an increased ratio of the early [E] and late [A] diastolic filling waves and the risk of AF. Moreover, a U-shaped relationship between peak A-wave velocity and AF risk was described (59).

A reduced mitral annular "e"-wave velocity and an increased E/e ratio provide signs of impaired LV relaxation. There is evidence that the latter parameter is also suitable to assess LA function and pressure (52) (**Figures 3C,D**).

Total Atrial Conduction Time Assessed by Tissue Doppler Imaging Duration

Total atrial conduction time assessed by tissue doppler imaging duration, representing the echocardiographic derived total atrial conduction time, is an auspicious marker of both structural and electrical atrial remodeling, which is measured during sinus rhythm as the time interval between the onset of the P-wave in lead II on surface ECG and the peak of the A′ wave on tissue Doppler imaging (TDI) tracing of the lateral LA wall on echocardiography (60) (**Figure 3F**). Prolonged PA-TDI duration correlates with new-onset AF, post-operative AF and AF recurrence after rhythm control interventions (60). In patients with AF, assessment of thromboembolic risk has been improved by adding the PA-TDI duration value. To date, standard reference values for PA-TDI duration have not been established. Nevertheless, if each echocardiography laboratory determines its own normal values by routinely obtaining the PA-TDI value, risk assessment for AF-related outcomes may be improved (60).

3-Dimensional and 4-Dimensional Echocardiography

In the last few years, 3-dimensional and 4-dimensional echocardiography have improved the options of LA volume measurements. Studies using 3-dimensional and 4-dimensional echocardiography defined LACM by abnormal LA wall delayed-enhancement (**Table 1**). Recently, in a subanalysis of the LOOP trial investigating LA fibrosis by 4-dimensional echocardiography, an association of minimal LA volume, LA emptying fractions, and LA reservoir strain with LA late gadolinium enhancement measured by cardiac magnetic resonance imaging (MRI) was observed (56). LA emptying fractions had the strongest effect on predicting high LA late gadolinium enhancement and therefore LA fibrosis (56).

Speckle-Tracking Echocardiography

In recent years, speckle-tracking echocardiography has become a popular method for detecting early myocardial deformation by assessing the tissue movement (9). LA strain and strain rate imaging provide insights into functional remodeling of the atrium (**Figure 3E**). Studies evaluating the utility of speckle-tracking echocardiography defined LACM mainly by clinical definitions (e.g., AF, AF burden, AF recurrence, thromboembolic events) or by comparison with abnormal findings in electroanatomic mapping (**Table 1**).

In patients with severe mitral regurgitation, there was a strong correlation between the impairment of LA longitudinal deformation, as evaluated by the global peak atrial longitudinal strain, and the extent of LA fibrosis and remodeling (61). A reduced global longitudinal LA strain was described in patients with AF and presents a predictor for thromboembolism (62–64). There is evidence that a higher AF burden ($\geq$10%) is particularly associated with decrease in global longitudinal LA strain, which correlates with mean LA strain measured by mapping and may be improved after AF ablation (65). In the study of Eichenlaub et al. (57), a LA longitudinal strain rate < 23.5% predicted LACM, defined as LA low-voltage area $\geq$ 2 cm^2 at 0.5 mV threshold on endocardial mapping, with an area under the curve of 0.878, a sensitivity of 92.3% and specificity of 82.4%. In patients with LACM, LA strain rate during reservoir phase was significantly lower (15.2 vs. 29.4%, $p < 0.0001$) and showed a linear correlation with LACM amount (43).

Moreover, the addition of global longitudinal LA strain and LA volume index to the CHA2DS2-VASc score improves also the prediction of hospitalization and/or mortality (62).

Even in patients with sinus rhythm, restricted LA diastolic function, represented by the peak atrial longitudinal strain and the LA stiffness index, was strongly associated with low amplitude voltage areas measured by endocardial mapping (66).

By means of speckle-tracking echocardiography it is possible to specify the functional remodeling in different regions of the atrium. For example, a declined LA lateral wall longitudinal strain was found to be a predictor of arrhythmia recurrence after AF ablation (67). In patients with amyloidosis, the septal LA strain and strain rate were overall lower (68). Furthermore, lateral and septal LA strain rates were decreased in patients with heart failure compared to those without (68).

A higher LA mechanical dispersion, defined as the standard deviation (SD) of time to peak positive strain corrected by the R-R interval (SD-TPS, %), was described in patients with AF than in those without (64). Besides, SD-TPS was associated with the incidence of new-onset AF (64). The LA mechanical dispersion was also measured in patients with paroxysmal AF undergoing PVI. The SD-TPS was significantly higher in patients with low voltage areas, measured by mapping, and was simultaneously an independent predictor for low voltage areas (69).

Transesophageal Echocardiography

An important advantage of transesophageal echocardiography is the more precise assessment of the LA appendage. There is limited evidence on the correlation of transesophageal abnormalities and LACM which has been defined mainly by fibrosis determination using delayed-enhancement MRI. It was demonstrated that patients with LA appendage thrombus had a higher amount of LA fibrosis, diagnosed by late gadolinium enhancement MRI, in comparison to patients without thrombus (70). LA fibrosis was even higher in patients with spontaneous echo contrast than in those without. In addition, patients with high atrial fibrosis were more likely to have both thrombus and spontaneous echo contrast in the LA appendage (70). It is common knowledge that reduced LA/LA appendage flow dynamics and increased LA size are risk factors for the occurrence of thrombus and spontaneous echo contrast (71) (**Figure 4**).

CARDIAC MAGNETIC RESONANCE IMAGING

Introduction

Using MRI, LA volume and LA strain can be detected. Decreased LA strain measured by MRI is present in patients with AF (72). A modest correlation between speckle-tracking echocardiography and MRI obtained LA volume and LA strain has been observed (73, 74). There are systematic differences in measurements that should be taken into account as MRI measurements reveal higher values (73, 74).

Delayed-Enhancement Magnetic Resonance Imaging

Over recent years, delayed-enhancement MRI became the key method to detect atrial fibrosis. Studies aiming to define LACM by pathological delayed-enhancement MRI focused particularly on clinical definitions (e.g., AF, ischemic stroke, major adverse cardiovascular events) as well as on further imaging definitions (e.g., abnormal echocardiographic parameters, low-voltage areas in electroanatomic mapping) (**Table 1**).

In 2009, Oakes et al. established the Utah stage model to quantify LA fibrosis (75). Based on this model, four levels of severity are classified: Utah I, defined as $\leq$ 5% LA wall enhancement, Utah II, 5–20%, Utah III, 20–35%, and Utah IV, $>$35% (12) (**Figure 5**).

High correlations were discovered between delayed-enhancement MRI and histology from surgical biopsies for LA structural remodeling including interstitial and fatty fibrosis as well as total fibrosis and fat (76, 77). Native T1 corresponded with the extent of fibrosis from MRI and histology (76). Moreover, LA wall enhancement appeared to be greater in patients with AF than in patients without AF (77).

Regions of scar in the LA identified by delayed-enhancement MRI were noted to be associated with low-voltage areas in endocardial mapping (78).

A higher amount of LA late gadolinium enhancement is associated with decreased LA function as well as decreased LV diastolic function since significant correlations were described between LA late gadolinium enhancement and both LA ejection fraction and echocardiographic LV septal e′ and septal E/e′ (79). A correlation between delayed-enhancement and reduced LA function has also been demonstrated by speckle-tracking echocardiography. There was an inverse effect between the extent of LA wall fibrosis measured by delayed-enhancement MRI and LA strain and strain rate in speckle-tracking echocardiography, particularly LA midlateral strain and strain rate (80). Interestingly, patients with persistent AF presented with more fibrosis and less midseptal and midlateral strain compared to patients with paroxysmal AF (80). In general, the risk for new-onset atrial arrhythmias is higher by increasing amount of LA late gadolinium enhancement (79).

Patients with previous strokes and high-risk patients for stroke, reflected by a high CHA2DS2-VASc score, had a significantly higher proportion of LA fibrosis in delayed-enhancement MRI. LA fibrosis was an independent predictor of cerebrovascular events and significantly increased the predictive power of the CHA2DS2-VASc score (81). Rising Utah stage and more intense LA late gadolinium enhancement were associated with increased risk of major cardiovascular events, predominantly due to the increased risk of stroke or TIA (82). Interestingly, patients with ESUS present with similar amount of atrial fibrosis compared to patients with AF which supports the hypothesis that fibrosis is a major risk factor for ischemic stroke and LACM (83).

The extent of structural LA remodeling measured by delayed-enhancement MRI seems to be independent of the AF type (lone AF or non-lone AF) (84). The outcome after AF ablation was demonstrated to be significantly dependent on the degree of structural LA remodeling, with worse outcome at increasing Utah stage (84). With an increasing level of delayed-enhancement, AF recurrence after ablation occurred more frequently (75). Therefore, pre-ablation LA fibrosis assessment by delayed-enhancement MRI may predict the outcome (75). Another study examining the impact of LA fibrosis on the outcome after AF ablation demonstrated that the risk of recurrent arrhythmias appeared at higher LA fibrosis grades detected by delayed-enhancement MRI (77). The presence of higher LA fibrosis grades was also the best predictor for successful ablation, while increased LA volume and persistent AF had no predictive effect (77).

The DECAAF study evaluated the impact of LA fibrosis measured by delayed-enhancement MRI on the outcome after AF ablation (85). Among 329 patients undergoing AF ablation, the extent of LA fibrosis estimated by delayed-enhancement MRI

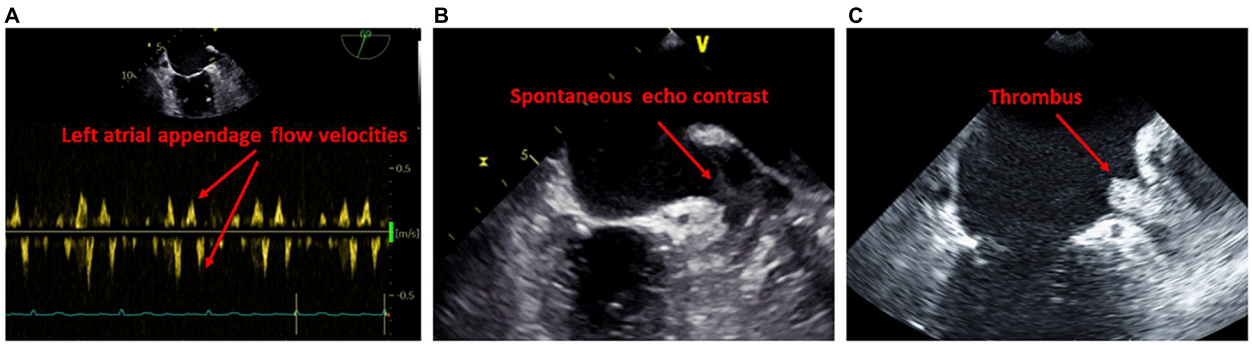

FIGURE 4 | Findings on transesophageal examination suggestive of left atrial cardiomyopathy. **(A)** Reduced blood flow in the ostium of the left atrial appendage. **(B)** Evidence of spontaneous echo contrast in the left atrial appendage. **(C)** Evidence of thrombus in the left atrial appendage.

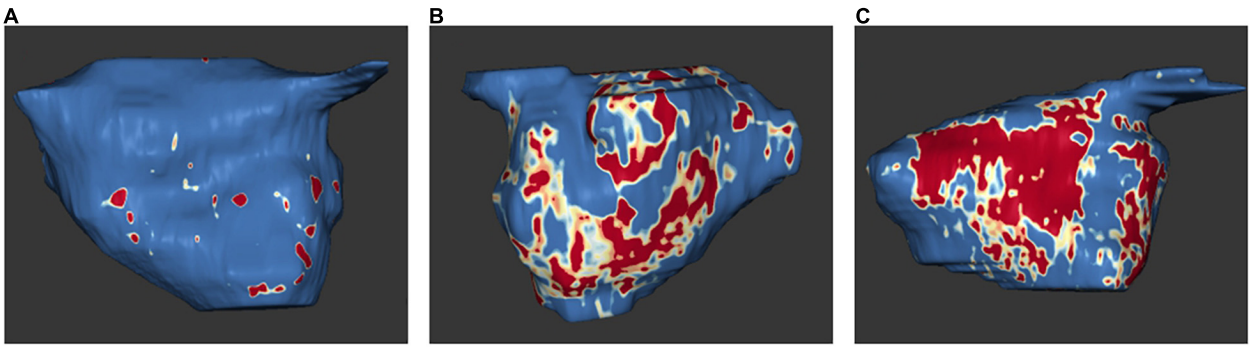

FIGURE 5 | Examples of MRI examinations of the left atrium: left atrial tissue fibrosis based on 3D delayed enhancement magnetic resonance imaging scans. Normal left atrial wall is displayed in blue, fibrotic changes are in red and white. Amounts of fibrosis as a percentage of the total left atrial wall volume. **(A)** Utah stage 1 (1%). **(B)** Utah stage 3 (27%). **(C)** Utah stage 4 (36%). *With the friendly support of Dr. Misagh Piran (Herz- und Diabeteszentrum Nordrhein-Westfalen, Ruhr-Universität Bochum).*

correlated significantly with the recurrence of arrhythmia (85). The prospective, randomized, multicenter DECAAF II study provides further insights into the value of preprocedural LA fibrosis estimation by delayed-enhancement MRI in patients with persistent AF experiencing AF ablation (86). The results, which were presented at the ESC Congress 2021 but not yet published, demonstrated that fibrosis-guided ablation was not superior to conventional PVI in reducing recurrence of AF (86).

4-Dimensional Flow Magnetic Resonance Imaging

4-dimensional flow MRI yields 3-dimensional volume sets over time (4-dimensional). This enables a precise quantitative evaluation of cardiovascular blood flows (87). In studies analyzing LA blood flow velocities, LACM has been equated with clinical definitions (e.g., AF burden), and further imaging definitions (e.g., abnormal echocardiographic parameters) (**Table 1**).

Contrasting data exist on blood flow velocities in patients with AF. On the one hand, there is evidence that patients with AF in history have a similar blood flow in the normal range at sinus rhythm compared to age-matched controls in measurements with 4-dimensional flow MRI (88, 89). On the other hand, there are findings that AF patients present with lower LA mean velocities and more often LA stasis compared to controls (90, 91).

Nevertheless, patients with persistent AF have a significant lower LA blood flow compared to AF patients at sinus rhythm (88). Moreover, a negative correlation was seen between increased CHA2DS2-VASc score and decreased mean LA velocity (89, 91). Interestingly, a correlation was described between LA blood flow indices, age and LA volume, but not with left ventricular ejection fraction (91).

CARDIAC COMPUTED TOMOGRAPHY

Cardiac Computed Tomography

It is well known that cardiac CT can be used for precise measurement of atrial volumes (9). A high correlation between LA volume index obtained by CT and speckle-tracking echocardiography has been observed (92). Moreover, LA volume index measured by CT is a predictor of AF recurrence after ablation (93).

Furthermore, it has recently been demonstrated that CT can also be applied for strain measurements. LA strain measured by

CT correlates strongly with strain measurements derived from speckle-tracking echocardiography (94–96).

In addition, structural changes of the atria can be detected by CT. Image attenuation ratio collected by CT predicts LA low-voltage areas in electroanatomic mapping which suggests that CT can help to assess fibrosis when contraindications for MRI exist (97).

Cardiac Positron Emission Tomography – Computed Tomography

In recent years, an association between atrial 18F-fluorodeoxyglucose activity in positron emission tomography – CT (PET-CT), previous ischemic stroke and LACM in non-AF individuals was demonstrated (98). LACM was defined either by increased atrial 18F-fluorodeoxyglucose uptake itself or by clinical outcomes, such as AF, AF burden, and stroke (**Table 1**).

Enhanced atrial activity was associated with ischemic stroke and LACM (98). In addition, higher atrial uptake of 18F-fluorodeoxyglucose was observed in patients with AF, whereas persistent AF showing higher atrial uptake than paroxysmal AF (99). Persistent AF is particularly associated with right atrial maximum standard uptake value and LA volume. Moreover, the right atrial target-to-background ratio of maximum standard uptake value to blood pool activity seems to be greater in patients with persistent AF than in those with paroxysmal AF (99). Data about the value of 18F-fluorodeoxyglucose PET-CT in patients with suspected LACM are very rare. 18F-fluorodeoxyglucose PET-CT could be useful to explore local atrial inflammation and to stratify the risk of subsequent stroke by monitoring disease activity in patients with AF. Nevertheless, a widespread use to detect LACM cannot be implemented. In oncologic patients undergoing PET-CT, this diagnostic tool can be used supplementally when additional LACM is suspected.

ELECTROANATOMIC MAPPING AND ABLATION

Introduction

Electroanatomic mapping is another valuable method providing additional insights into patients with presumed LACM. There a numerous studies aiming to define LACM by the presence of low-voltage areas and their association with clinical definitions (e.g., AF, AF recurrence, ischemic stroke) and with further imaging definitions (e.g., abnormal echocardiographic parameters) (**Table 1**).

Electrophysiological Findings in Left Atrial Cardiomyopathy

Patients with paroxysmal lone AF exhibit bi-atrial abnormalities including structural remodeling, conduction disorders, and sinus node dysfunction (100). Electrophysiological findings in these patients were enlarged atrial volumes, increased effective refractory period at multiple sites, increased conduction time along linear catheters, increased bi-atrial activation time, decreased conduction velocity, more frequent fractionated electrograms, increased corrected sinus node recovery time, and lower voltage (100).

Low-Voltage Areas

Patients with non-focal LA tachycardia presented with a high proportion of low-voltage areas in endocardial mapping, providing evidence for possible LACM (101) (**Figure 6**). An analysis of patients with fibrotic LACM revealed that severe fibrotic areas increased and maximum LA voltage decreased, with growing severity of fibrotic LACM (101).

An inverse relationship was found between lower mean LA voltage and higher CHA2DS2-VASc score (102). A significant association has been described between electroanatomic LA remodeling and the risk of stroke in patients with AF (102). In AF patients with previous stroke, low-voltages area as well as pre-existing silent cerebral ischemia were significantly larger detected by cerebral MRI after PVI, even after adjustment of CHA2DS2-VASc score (103). Whereas the mean LA volume/body surface area, particularly anterior LA, was greater, the LA endocardial voltage was lower in patients who suffered stroke (102).

Localization of the Low-Voltage Areas

Of particular interest is also the localization of the low-voltage areas. A relationship was described between anterior low-voltage areas and macro-re-entry mechanism by forming a conducting channel between the lower pole of the LA scar and the mitral valve annulus (101). Although the distribution of LA fibrosis is often variable, it is usually more pronounced anteriorly (104). Anterior severely fibrotic areas have been found to be more frequent and larger than posterior severely fibrotic areas (104). The knowledge that mainly the anterior LA is affected allows an individualized ablation approach that could complement the usual strategies (101).

Quantification of Low-Voltage Areas and Clinical Impact

A high percentage of low-voltage areas as well as fibrosis areas in the LA predicts recurrence of AF after catheter ablation (104–108). In patients with multiple ablations, AF recurrence rate was significantly higher in patients with low-voltage areas than without (36 vs. 6%, $p < 0.001$) (106). The size of fibrotic areas, fibrosis in the LA as well as in the right atrium, and decreased maximum voltage has negative impact on the ablation outcome (104). Furthermore, LA fibrosis areas correlated significantly with larger LA size, decreased ejection fraction, and higher C-reactive protein levels (107).

The modified APPLE score (one point for age $\geq$ 65 years, persistent AF, impaired estimated glomerular filtration rate $\leq$ 60 mL/min/1.73 m^2, LA volume $\geq$ 39 mL/m^2, and LA ejection fraction $<$ 31%) may be possible to estimate the success rate of catheter ablation (109).

Knowing that the degree of low-voltage areas is a key determinant of ablation success, individualized ablation approaches may be beneficial. Ablation of lesions with prominent activation features within/at the margins of low-voltage areas in addition to PVI might be more effective than the conventional strategy of PVI solely in patients with persistent AF (110). In

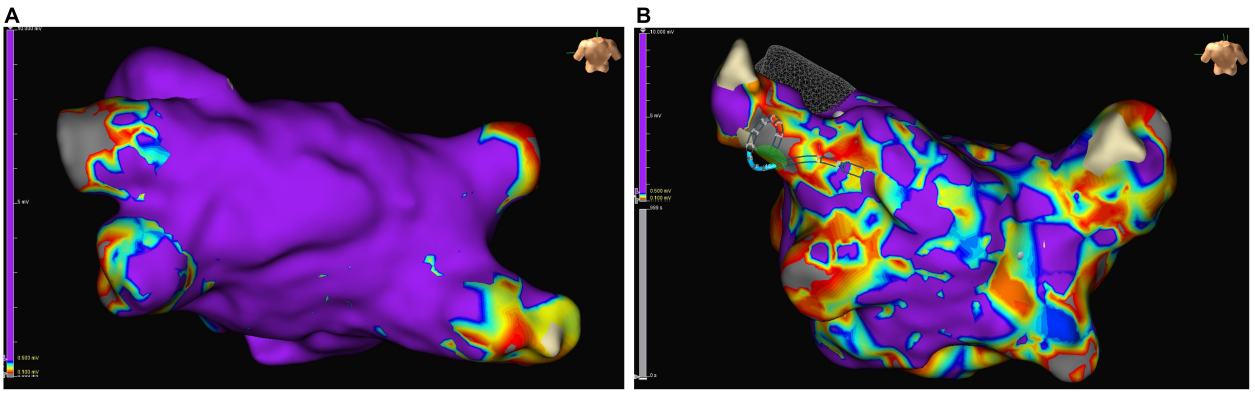

FIGURE 6 | Examples of low-voltage areas in endocardial mapping of left atrium in patients with sinus rhythm who underwent pulmonary vein isolation: normally conducting atrial myocardium is colored purple, low voltage areas (defined as zones with an amplitude of electrical perception of ≤ 0.5 mV) are colored differently. **(A)** Example of a left atrium almost without low voltage areas. **(B)** Example of a severely diseased left atrium with low voltage areas > 10%.

contrast, PVI alone appears to be sufficient for the treatment of patients with LA low-voltage < 10%, as no significant difference in success rate was demonstrated between patients with low-voltage who underwent PVI alone and patients who required PVI + selective low-voltage ablation (110).

Most studies evaluating the benefit of electroanatomic mapping for the assessment of LACM include patients with AF undergoing catheter ablation. There is strong evidence that patients with AF have both more low-voltage areas and severe fibrotic areas reflecting electrical and structural remodeling of the atrium (100–110) (**Figure 6**).

BIOMARKERS

Introduction

A number of circulating biomarkers have been proposed to estimate atrial remodeling and LACM (9, 111). Studies analyzing biomarkers defined LACM by clinical definitions (e.g., AF, AF burden, AF recurrence, stroke) as well as by further imaging definitions (e.g., low-voltage areas in electroanatomic mapping, abnormal echocardiographic parameters) (**Table 1**).

Marker of Inflammation

Atrial inflammation is discussed as a key factor for atrial fibrosis and the risk of AF (112). The metabolic syndrome is a well-known risk factor for inflammatory processes. Obesity, hypertension, and diabetes mellitus predispose to AF (9). Epicardial adipose tissue secretes proinflammatory and profibrotic cytokines as well as profibrotic microRNA which may promote the development of both AF and inflammation-induced LACM (112, 113). Proinflammatory IL-6 levels, MMP-9/TIMP-1 ratio as well as NF-AT3 and NF-AT4 mRNA and protein expression were significantly increased in patients with AF, particularly in persistent AF (114, 115). High sensitivity C-reactive protein was described as a predictor of arrhythmia recurrence after AF ablation (116).

Increased TGF-ß1 levels in monocytes were seen in patients who exhibited extensive low-voltage areas on endocardial mapping (117). Moreover, it has been demonstrated that higher serum TGF-ß1 levels correlated with the presence of AF and arrhythmia recurrence after AF ablation (118, 119). With increasing AF duration, serum TGF-ß1 levels declined (114). However, the predictive value of serum TGFß-1 level for the recurrence of arrhythmias seems to be only in patients with non-paroxysmal AF (120), and not all studies could demonstrate a risk for AF (121). The same applies to the concordance of serum TGF-ß1 levels and echocardiographic parameters. On the one hand, there is evidence about an inverse relationship between serum TGF-ß1 level and LA diameter (114), but on the other hand there are also findings that could not prove an association (119).

Marker of Fibrosis

Furthermore, it is suggested that specific fibrosis markers may be related to atrial remodeling. Surprisingly, Type III procollagen N terminal peptide, galectin-3, fibroblast growth factor 23, and type I collagen C terminal telopeptide were not predictors of arrhythmia recurrence after AF ablation (105). Type III procollagen N terminal peptide also revealed merely a slight positive trend with regard to AF risk (121). However, the combination of circulating biomarkers reflecting excessive myocardial collagen type-I cross-linking and deposition shows a predictive effect on higher AF prevalence, incidence, and recurrence after ablation (122). In addition, a negative correlation was described between galectin-3 and echocardiographic parameters assessing the LA, including LA volume and LA strain rate (123). ST-2 and apoptotic microparticles are also associated with increased LA volume index (124). Besides, galectin-3 and soluble ST-2 were significantly higher in patients with stroke and AF compared to patients with stroke without AF (125).

Atrial Peptides

N-terminal pro-B-type natriuretic peptide is a well-known indicator of congestive heart failure due to volume overload and

myocardial damage. N-terminal pro-B-type natriuretic peptide showed a strong correlation with echocardiographic parameters of LA remodeling and dysfunction, and was a significant but weak predictor of AF (125). Moreover, there is an association with AF burden (114). An inverse relationship was reported between higher levels of endothelin-1, N-terminal pro-B-type natriuretic peptide, troponin I and lower LA reservoir and contractile strain, suggesting that LA myopathy is associated with persistent congestion (126, 127). Oldgren et al. evaluated the ABC-stroke score, derived from the ARISTOTLE study, including age, biomarkers (N-terminal pro-B-type natriuretic peptide and high-sensitivity cardiac troponin), and clinical history (prior stroke) (128, 129). In anticoagulated patients with AF, the biomarker-based ABC stroke score was well applicable and generally more suitable than the CHA2DS2-VASc and ATRIA stroke scores (128).

N-terminal pro-A-type natriuretic peptide is a hormone released by the atria in response to increased atrial tension. Recently, Seewöster et al. introduced the novel biomarker-based ANP score (one point for age $\geq$ 65 years, N-terminal pro-A-type natriuretic peptide > 17 ng/mL, and persistent AF) which significantly predicted low-voltage areas in patients undergoing AF ablation (130).

Aldosterone and Renin

In patients with persistent AF, aldosterone levels and aldosterone/renin index decreased significantly after successful ablation of AF. It is worth noting that aldosterone and renin levels did not interact with duration of AF, LA diameter, mean heart rate, systolic blood pressure, age, New York Heart Association class, or left ventricular ejection fraction (131).

Marker of Immunothrombosis

The close interactions between the immune system and the coagulation cascade can be summarized under the term "immunothrombosis." On the one hand, the immune system initiates coagulation; on the other hand, local coagulation has pro-inflammatory and pro-fibrotic effects (132, 133). Thus, immunothrombosis might be an underlying mechanism of atrial remodeling and AF (134). In the last decades, several coagulation markers were described in patients with AF, with both impact on thromboembolism and bleeding risk. For example, abnormal levels of von Willebrand factor, D-dimer, growth differentiation factor 15, soluble p-selectin, coagulation factor Xa and endothelial nitric oxide synthase indicate endocardial remodeling (135–140). Nevertheless, a recent study was not able to demonstrate a correlation between immunothrombosis markers and incident AF after adjustment for cardiovascular risk factors (134). This may indicate that inflammation and immunothrombosis may be associated with AF by other cardiovascular risk factors, rather than AF *per se* (134).

Conclusion

Circulating biomarkers can provide evidence of inflammatory and fibrosis pathways in the atrium. However, there are sometimes conflicting results, and the inflammation- and fibrosis-related biomarkers are not specific. Therefore, the clinical value in the assessment of LACM is currently unclear, and routine screening seems questionable. However, future research investigating these pathways has potential, and treatment options

TABLE 2 | Overview of selected biomarkers with association to LACM, AF, and thromboembolic events.

Laboratory parameter	Up- or downregulation is associated with AF incidence	Associations	References
Aldosterone	↑	AF, AF recurrence after cardioversion	(131)
Aldosterone/renin	↑	AF, AF recurrence after cardioversion	(131)
Coagulation factor Xa	↑	AF, atrial remodeling	(139)
CRP	↑	AF recurrence after ablation	(116)
D-dimer	↑	Thromboembolic events in patients with AF	(140)
Endothelial nitric oxide synthase	↓	AF	(138)
Endothelin-1	↑	Abnormal echocardiographic parameters	(126, 127)
Galectin-3	↑	AF, stroke, abnormal echocardiographic parameters	(123, 125)
Growth differentiation factor 15	↑	AF	(137)
IL-6	↑	AF, AF burden	(114)
MMP-9	↑	AF, AF burden	(114)
MMP-9/TIMP-1	↑	AF, AF burden	(114)
NF-AT3	↑	AF, AF burden	(115)
NF-AT4	↑	AF, AF burden	(115)
N-terminal pro-A-type natriuretic peptide	↑	Low-voltage areas in electroanatomic mapping	(130)
N-terminal pro-B-type natriuretic peptide	↑	AF, AF burden, abnormal echocardiographic parameters	(114, 125–129)
Type III procollagen N terminal peptide	↑	AF	(121)
Soluble p-selectin	↑	AF	(135, 136)
Soluble ST-2	↑	AF, stroke, abnormal echocardiographic parameters	(124, 125)
TGF-ß1	↑	AF, AF burden, AF recurrence after ablation, low-voltage areas in electroanatomic mapping, abnormal echocardiographic parameters	(114, 117–121)
Troponin I	↑	Abnormal echocardiographic parameters	(126, 127)
Von Willebrand factor	↑	AF, stroke	(135, 136)

AF, atrial fibrillation; LACM, atrial cardiomyopathy; CRP, C-reactive protein; IL-6, interleukin 6; MMP-9, matrix metalloproteinase 9; NF-AT, nuclear factor of activated T cells; ST-2, suppression of tumorigenicity 2; TGF-ß1, transforming growth factor β 1; TIMP-1, tissue inhibitor of metalloproteinase 1.

could be identified that specifically intervene in the inflammatory and fibrosis regulatory circuits.

In conclusion, **Table 2** summarizes laboratory parameters that have been used as markers of LACM in different studies.

RISK FACTORS

Several risk factors for the development of AF as well as structural and electrical remodeling in terms of a possible LACM have been described. LACM may occur as a result of amyloidosis, hereditary muscular dystrophies, congestive heart failure, AF, obstructive sleep apnea, drugs, alcohol, myocarditis, genetic repolarization disturbances, aging, hypertension, obesity, diabetes mellitus, valvular heart disease (9, 127, 141–143) (**Figure 7**).

The newly developed AF-SCORE (+1 point for age $\geq$ 60 years and additional points for female sex [+1] and AF-persistency [+2]) enabled a good discrimination to identify fibrotic LACM and predicted arrhythmia-freedom after PVI (144). A low AF-SCORE $\leq$ 2 was more frequently observed in patients with paroxysmal AF of any age and in younger patients with persistent AF, irrespective of sex, and is associated with better PVI-only outcomes (144).

CRITICAL CONSIDERATIONS ON THE CONCEPT AND DIAGNOSIS OF LEFT ATRIAL CARDIOMYOPATHY

Diagnosis

The assessment of electrical, mechanical, and structural LA dysfunction seems feasible due to several diagnostic tools. However, single diagnostic procedures might not be sufficient for the diagnosis of LACM. In particular, because the diagnosis of LACM is challenging, a combination of parameters associated with LACM should be sought.

Clinical Endpoints

Most data were generated from studies that included patients with AF and/or with stroke. Because it is not yet completely understood how LACM can be diagnosed, there are very few studies that directly address LACM. Therefore, the parameters found to define LACM are vague and may not be specific. Focusing on patients with AF could be critical because it disregards subclinical LACM before the onset of AF.

Heterogeneity of Studies

It should also be considered that the comparability of the studies may not be given, because LACM and other parameters (e.g., low-voltage areas) were not defined standardized. Another critical consideration is that most studies equate LA myopathy with atrial cardiomyopathy in general. Perhaps, however, an atrial cardiomyopathy of the right atrium is different from an atrial cardiomyopathy of the LA. Unqualified transferability from the LA to the right atrium is not reasonable. Further investigation is required. Many studies concerning LACM analyzed only atrial fibrosis. However, fibrosis can also result from degenerative processes, increasing age, and other comorbidities. It is likely that LACM consists of a compound entity.

Therapeutic Consequences

Differentiation in terms of severity of LACM is important to identify high-risk patients. Possible differentiation could be achieved by the presence or absence of risk factors. It is uncontroversial that the presence of an LACM with concomitant multiple cardiovascular risk factors poses a high risk for major adverse cardiac events. However, it becomes more complicated in the absence of risk factors. This raises the question of whether a patient without risk factors but with evidence of LACM would benefit from therapy. Further outstanding issues address therapy and prevention strategies, which might include more aggressive rhythm control, close follow-up, or the prescription of oral anticoagulation. Conversely, a patient without risk factors also has a lower cardiovascular risk. Thus, it is interesting and indeed clinically very relevant to consider the impact of LACM by itself on stroke risk.

Left Atrial Cardiomyopathy and Atrial Fibrillation

The most extreme assumption would be that it is not AF itself that causes stroke but AF-associated LACM (1). Stroke prevention might become the key to therapeutic options. On the one hand, the identification of high-risk patients without previous AF is important, on the other hand, it could be evaluated whether patients with AF need oral anticoagulation at all. These considerations could also have implications for the use of oral anticoagulants after AF ablation. Conversely, there is also the possibility that patients with oral anticoagulants are not adequately managed (1).

Moreover, the presence of AF or the occurrence of thromboembolic events could already represent a later disease course of LACM. It is often assumed that LACM precedes the incidence of AF. Hence, diagnostic criteria of LACM are subsequently derived from predictors for the occurrence of AF. However, pre-existing AF may also trigger atrial remodeling. The landmark concept "AF begets AF" probably does not adequately address the diagnosis of LACM since there might be a bidirectional relationship between AF and atrial fibrosis (9). It is unknown why there are such large interindividual differences. Why does one patient persist in paroxysmal AF for several years while another progresses to persistent AF within a few weeks? Surprisingly, even patients with an extremely high amount of atrial fibrosis can present with paroxysmal instead of persistent AF (10). This "chicken and egg" situation, whether AF is a symptom of LACM or a trigger for LACM, cannot be conclusively resolved. However, it is important to be aware that one-sided considerations and assumptions can lead to a distortion of the complex clinical pattern of LACM.

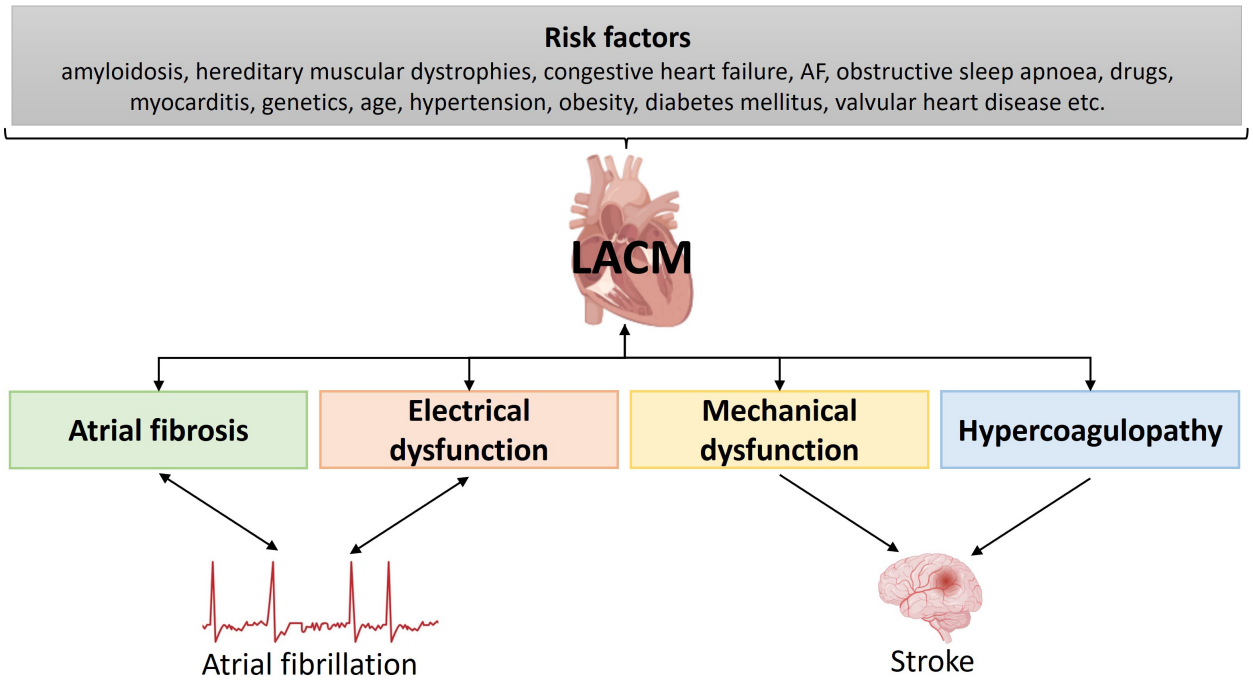

FIGURE 7 | Illustration of the underlying risk factors for left atrial cardiomyopathy. AF, atrial fibrillation; LACM, left atrial cardiomyopathy.

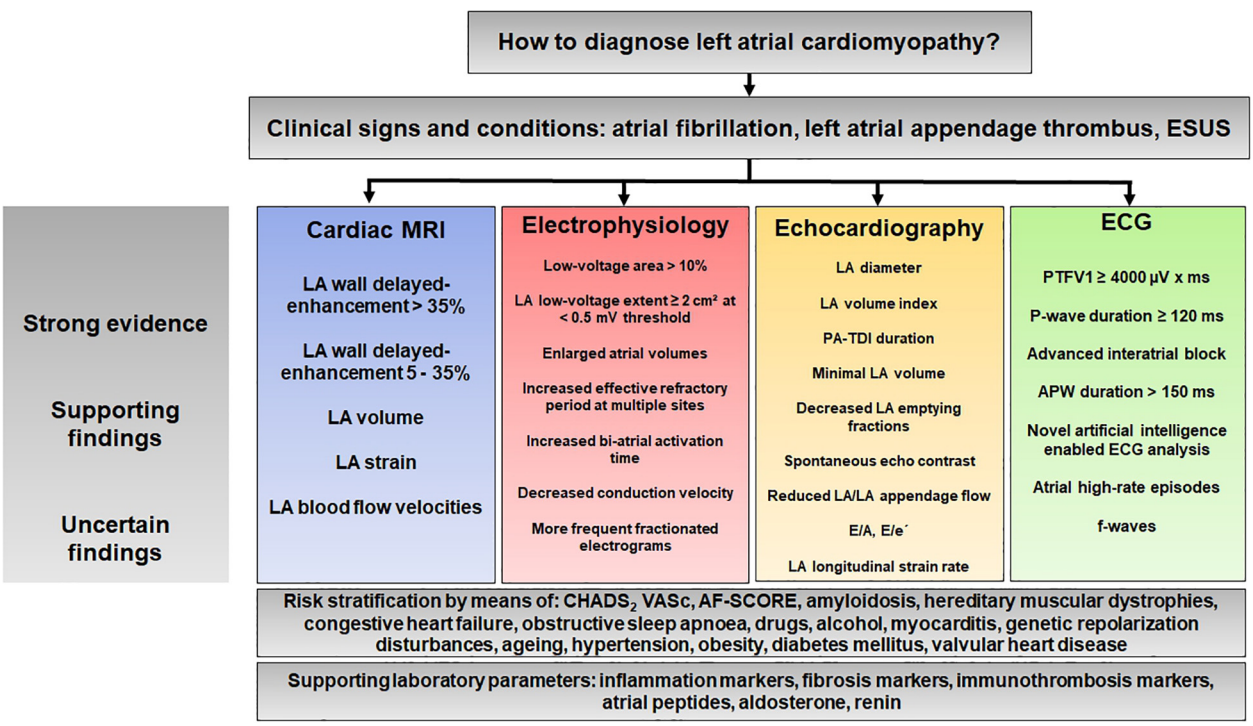

FIGURE 8 | Proposal for a diagnostic algorithm for atrial cardiomyopathy based on the results of previous studies. APW, amplified P-wave; ESUS, embolic stroke of undetermined source; LA, left atrium/left atrial; PA-TDI, total atrial conduction time assessed by tissue doppler imaging; PTFV1; P-wave terminal force in lead V1.

How to Diagnose Left Atrial Cardiomyopathy

Another reason for this elusive clinical pattern is the current classification of LACM, which is based on atrial histopathology (9). Although the classification has enormously helped to define LACM histopathological, it requires biopsies, which is difficult to implement and not reasonable in the clinical setting. There is hope that with improved clinical diagnostics, an improved classification might be possible (1). To date, there is no recommendation for the clinical diagnosis of LACM. In addition, the current classification does not yet provide any guidance for therapies and prevention strategies (9). Again, the question arises whether the management of patients can be improved by clinical diagnostics and clinical classification. This present review attempts to take a first step in this direction.

Randomized controlled trials could help to improve diagnostic and therapeutic options in the presence of LACM. This could also result in helpful advises for patient follow-up.

PROPOSAL FOR A DIAGNOSTIC ALGORITHM: HOW TO DIAGNOSE ATRIAL CARDIOMYOPATHY?

From the studies discussed in this review, a complex picture emerges of a disease that is difficult to diagnose. The main methods used to diagnose LACM are cardiac MRI, electrophysiological investigations, echocardiography, and ECG. In contrast, there are few studies with cardiac CT and PET-CT and many but inconsistent studies with biomarkers.

Although many questions remain, we would like to propose here a diagnostic algorithm that summarizes this review (**Figure 8**). This algorithm is intended to illustrate the complexity of the diagnostic process and may help to define uniform criteria for LACM in the future.

CONCLUSION

Studies specifically addressing LACM are extremely limited, and randomized controlled trials are lacking so far.

Our review represents an attempt to approach the diagnosis of LACM to define LACM more precisely by applying and combining several diagnostic criteria (**Table 1** and **Figure 8**). These criteria reflect the electrical, structural, and mechanical remodeling of the atria and can be obtained in clinical practice. The interrelationship of the diagnostic methods and the derived parameters is interesting and important regarding the diagnosis of LACM and provides the opportunity for improved assessment.

Further investigation is urgently needed to improve the diagnostic capabilities and management of patients with LACM.

AUTHOR CONTRIBUTIONS

FK and MG contributed to conception and design of the review. FK wrote the first draft of the manuscript. MG wrote sections of the manuscript. Both authors contributed to manuscript revision, read, and approved the submitted version.

ACKNOWLEDGMENTS

We acknowledge support by the Open Access Publication Funds of the Ruhr-Universität Bochum.

REFERENCES

1. Guichard J-B, Nattel S. Atrial cardiomyopathy: a useful notion in cardiac disease management or a passing fad? *J Am Coll Cardiol.* (2017) 70:756–65.
2. Bisbal F, Baranchuk A, Braunwald E, Bayés de Luna A, Bayés-Genís A. Atrial failure as a clinical entity: JACC review topic of the week. *J Am Coll Cardiol.* (2020) 75:222–32. doi: 10.1016/j.jacc.2019.11.013
3. Doñate Puertas R, Millat G, Ernens I, Gache V, Chauveau S, Morel E, et al. Atrial structural remodeling gene variants in patients with atrial fibrillation. *Biomed Res Int.* (2018) 2018:4862480.
4. Gudbjartsson DF, Holm H, Sulem P, Masson G, Oddsson A, Magnusson OT, et al. A frameshift deletion in the sarcomere gene MYL4 causes early-onset familial atrial fibrillation. *Eur Heart J.* (2017) 38:27–34. doi: 10.1093/eurheartj/ehw379
5. Peng W, Li M, Li H, Tang K, Zhuang J, Zhang J, et al. Dysfunction of myosin light-chain 4 (MYL4) leads to heritable atrial cardiomyopathy with electrical, contractile, and structural components: evidence from genetically-engineered rats. *J Am Heart Assoc.* (2017) 6:e007030. doi: 10.1161/JAHA.117.007030
6. Yamaguchi N, Xiao J, Narke D, Shaheen D, Lin X, Offerman E, et al. Cardiac pressure overload decreases ETV1 expression in the left atrium, contributing to atrial electrical and structural remodeling. *Circulation.* (2021) 143:805–20.
7. Zhang Y, Lin Y, Zhang Y, Wang Y, Li Z, Zhu Y, et al. Familial atrial myopathy in a large multigenerational heart-hand syndrome pedigree carrying an LMNA missense variant in rod 2B domain (p.R335W). *Heart Rhythm.* (2022) 19:466–75. doi: 10.1016/j.hrthm.2021.11.022
8. Zhu Y, Shi J, Zheng B, Liu H, Li C, Ju W, et al. Genetic findings in patients with primary fibrotic atrial cardiomyopathy. *Eur J Med Genet.* (2022) 65:104429. doi: 10.1016/j.ejmg.2022.104429
9. Goette A, Kalman JM, Aguinaga L, Akar J, Cabrera JA, Chen SA, et al. EHRA/HRS/APHRS/SOLAECE expert consensus on Atrial cardiomyopathies: definition, characterisation, and clinical implication. *J Arrhythm.* (2016) 32:247–78.
10. Kottkamp H. Human atrial fibrillation substrate: towards a specific fibrotic atrial cardiomyopathy. *Eur Heart J.* (2013) 34:2731–8. doi: 10.1093/eurheartj/eht194
11. Goldberger JJ, Arora R, Green D, Greenland P, Lee DC, Lloyd-Jones DM, et al. Evaluating the atrial myopathy underlying atrial fibrillation: identifying the arrhythmogenic and thrombogenic substrate. *Circulation.* (2015) 132:278–91.
12. Rivner H, Mitrani RD, Goldberger JJ. Atrial myopathy underlying atrial fibrillation. *Arrhythm Electrophysiol Rev.* (2020) 9:61–70.
13. Kreimer F, Mügge A, Gotzmann M. How should I treat patients with subclinical atrial fibrillation and atrial high-rate episodes? Current evidence and clinical importance. *Clin Res Cardiol.* (2022). doi: 10.1007/s00392-022-02000-7
14. Hart RG, Diener H-C, Coutts SB, Easton JD, Granger CB, O'Donnell MJ, et al. Embolic strokes of undetermined source: the case for a new clinical construct. *Lancet Neurol.* (2014) 13:429–38.
15. Ntaios G. Embolic stroke of undetermined source: JACC review topic of the week. *J Am Coll Cardiol.* (2020) 75:333–40. doi: 10.1016/j.jacc.2019.11.024

16. Hart RG, Sharma M, Mundl H, Kasner SE, Bangdiwala SI, Berkowitz SD, et al. Rivaroxaban for stroke prevention after embolic stroke of undetermined source. *N Engl J Med.* (2018) 378:2191–201.
17. Diener H-C, Sacco RL, Easton JD, Granger CB, Bernstein RA, Uchiyama S, et al. Dabigatran for prevention of stroke after embolic stroke of undetermined source. *N Engl J Med.* (2019) 380:1906–17.
18. Geisler T, Poli S, Meisner C, Schreieck J, Zuern CS, Nägele T, et al. Apixaban for treatment of embolic stroke of undetermined source (ATTICUS randomized trial): rationale and study design. *Int J Stroke.* (2017) 12:985–90. doi: 10.1177/1747493016681019
19. Healey JS, Gladstone DJ, Swaminathan B, Eckstein J, Mundl H, Epstein AE, et al. Recurrent stroke with rivaroxaban compared with aspirin according to predictors of atrial fibrillation: secondary Analysis of the NAVIGATE ESUS randomized clinical trial. *JAMA Neurol.* (2019) 76:764–73. doi: 10.1001/jamaneurol.2019.0617
20. Kamel H, Longstreth WT, Tirschwell DL, Kronmal RA, Broderick JP, Palesch YY, et al. The atrial cardiopathy and antithrombotic drugs in prevention after cryptogenic stroke randomized trial: rationale and methods. *Int J Stroke.* (2019) 14:207–14. doi: 10.1177/1747493018799981
21. Aysha MH, Hassan AS. Diagnostic importance of fibrillatory wave amplitude: a clue to echocardiographic left atrial size and etiology of atrial fibrillation. *J Electrocardiol.* (1988) 21:247–51. doi: 10.1016/0022-0736(88)90099-4
22. Li YH, Hwang JJ, Tseng YZ, Kuan P, Lien WP. Clinical significance of fibrillatory wave amplitude. A clue to left atrial appendage function in nonrheumatic atrial fibrillation. *Chest.* (1995) 108:359–63. doi: 10.1378/chest.108.2.359
23. Xi Q, Sahakian AV, Frohlich TG, Ng J, Swiryn S. Relationship between pattern of occurrence of atrial fibrillation and surface electrocardiographic fibrillatory wave characteristics. *Heart Rhythm.* (2004) 1:656–63. doi: 10.1016/j.hrthm.2004.09.010
24. Chen LY, Ribeiro ALP, Platonov PG, Cygankiewicz I, Soliman EZ, Gorenek B, et al. P-wave parameters and indices: a critical appraisal of clinical utility, challenges, and future research-a consensus document endorsed by the international society of electrocardiology and the international society for holter and noninvasive electrocardiology. *Circ Arrhythm Electrophysiol.* (2022) 15:e010435. doi: 10.1161/CIRCEP.121.010435
25. Kreimer F, Aweimer A, Pflaumbaum A, Mügge A, Gotzmann M. Impact of P-wave indices in prediction of atrial fibrillation-Insight from loop recorder analysis. *Ann Noninvasive Electrocardiol.* (2021) 26:e12854. doi: 10.1111/anec.12854
26. Huang Z, Zheng Z, Wu B, Tang L, Xie X, Dong R, et al. Predictive value of P wave terminal force in lead V1 for atrial fibrillation: a meta-analysis. *Ann Noninvasive Electrocardiol.* (2020) 25:e12739.
27. Li R, Yang X, Jia M, Wang D, Cui X, Bai L, et al. Effectiveness of P-wave ECG index and left atrial appendage volume in predicting atrial fibrillation recurrence after first radiofrequency catheter ablation. *BMC Cardiovasc Disord.* (2021) 21:164. doi: 10.1186/s12872-021-01930-w
28. Li TYW, Yeo LLL, Ho JSY, Leow AS, Chan MY, Dalakoti M, et al. Association of electrocardiographic P-wave markers and atrial fibrillation in embolic stroke of undetermined source. *Cerebrovasc Dis.* (2021) 50:46–53. doi: 10.1159/000512179
29. Kamel H, Hunter M, Moon YP, Yaghi S, Cheung K, Di Tullio MR, et al. Electrocardiographic left atrial abnormality and risk of stroke: northern manhattan study. *Stroke.* (2015) 46:3208–12.
30. Kamel H, Bartz TM, Longstreth WT, Okin PM, Thacker EL, Patton KK, et al. Association between left atrial abnormality on ECG and vascular brain injury on MRI in the cardiovascular health study. *Stroke.* (2015) 46:711–6.
31. Kamel H, O'Neal WT, Okin PM, Loehr LR, Alonso A, Soliman EZ. Electrocardiographic left atrial abnormality and stroke subtype in the atherosclerosis risk in communities study. *Ann Neurol.* (2015) 78:670–8. doi: 10.1002/ana.24482
32. Kohsaka S, Sciacca RR, Sugioka K, Sacco RL, Homma S, Di Tullio MR. Electrocardiographic left atrial abnormalities and risk of ischemic stroke. *Stroke.* (2005) 36:2481–3.
33. Kamel H, Soliman EZ, Heckbert SR, Kronmal RA, Longstreth WT, Nazarian S, et al. P-wave morphology and the risk of incident ischemic stroke in the multi-ethnic study of atherosclerosis. *Stroke.* (2014) 45:2786–8. doi: 10.1161/STROKEAHA.114.006364
34. He J, Tse G, Korantzopoulos P, Letsas KP, Ali-Hasan-Al-Saegh S, Kamel H, et al. P-wave indices and risk of ischemic stroke: a systematic review and meta-analysis. *Stroke.* (2017) 48:2066–72. doi: 10.1161/STROKEAHA.117.017293
35. Yamamoto S, Ono H, Motoyama H, Tachikawa H, Tagawa M, Akazawa K, et al. P-wave indices in Japanese patients with ischemic stroke: implication of atrial myopathy in subtype of ischemic stroke. *J Electrocardiol.* (2021) 66:18–22. doi: 10.1016/j.jelectrocard.2021.02.010
36. McConkey N, Malamas P, Norby FL, Plamenac J, Park R, Weigel F, et al. Abnormal P-wave terminal force in lead V1 is associated with low left atrial appendage ejection velocity. *J Electrocardiol.* (2021) 67:142–7. doi: 10.1016/j.jelectrocard.2021.06.011
37. Lebek S, Wester M, Pec J, Poschenrieder F, Tafelmeier M, Fisser C, et al. Abnormal P-wave terminal force in lead V1 is a marker for atrial electrical dysfunction but not structural remodelling. *ESC Heart Fail.* (2021) 8:4055–66. doi: 10.1002/ehf2.13488
38. Power DA, Lampert J, Camaj A, Bienstock SW, Kocovic N, Bayes-Genis A, et al. Cardiovascular Complications of Interatrial Conduction Block: JACC State-of-the-Art Review. *J Am Coll Cardiol.* (2022) 79:1199–211. doi: 10.1016/j.jacc.2022.01.030
39. Lehtonen AO, Langén VL, Puukka PJ, Kähönen M, Nieminen MS, Jula AM, et al. Incidence rates, correlates, and prognosis of electrocardiographic P-wave abnormalities - a nationwide population-based study. *J Electrocardiol.* (2017) 50:925–32. doi: 10.1016/j.jelectrocard.2017.07.004
40. Müller-Edenborn B, Minners J, Keyl C, Eichenlaub M, Jander N, Abdelrazek S, et al. Electrocardiographic diagnosis of atrial cardiomyopathy to predict atrial contractile dysfunction, thrombogenesis and adverse cardiovascular outcomes. *Sci Rep.* (2022) 12:576. doi: 10.1038/s41598-021-04535-7
41. Müller-Edenborn B, Minners J, Kocher S, Chen J, Zeh W, Lehrmann H, et al. Amplified P-wave duration predicts new-onset atrial fibrillation in patients with heart failure with preserved ejection fraction. *Clin Res Cardiol.* (2020) 109:978–87. doi: 10.1007/s00392-019-01590-z
42. Jadidi A, Müller-Edenborn B, Chen J, Keyl C, Weber R, Allgeier J, et al. The duration of the amplified sinus-P-wave identifies presence of left atrial low voltage substrate and predicts outcome after pulmonary vein isolation in patients with persistent atrial fibrillation. *JACC Clin Electrophysiol.* (2018) 4:531–43. doi: 10.1016/j.jacep.2017.12.001
43. Eichenlaub M, Mueller-Edenborn B, Minners J, Jander N, Allgeier M, Lehrmann H, et al. Left atrial hypertension, electrical conduction slowing, and mechanical dysfunction – the pathophysiological triad in atrial fibrillation-associated atrial cardiomyopathy. *Front Physiol.* (2021) 12:670527. doi: 10.3389/fphys.2021.670527
44. Eichenlaub M, Mueller-Edenborn B, Lehrmann H, Minners J, Nairn D, Loewe A, et al. Non-invasive body surface electrocardiographic imaging for diagnosis of atrial cardiomyopathy. *Europace.* (2021) 23:2010–9.
45. Verbrugge FH, Reddy YNV, Attia ZI, Friedman PA, Noseworthy PA, Lopez-Jimenez F, et al. Detection of left atrial myopathy using artificial intelligence-enabled electrocardiography. *Circ Heart Fail.* (2022) 15:e008176. doi: 10.1161/CIRCHEARTFAILURE.120.008176
46. Py A, Schaaf M, Duhamel S, Si-Mohamed S, Daher J, Altman M, et al. Atrial premature activity detected after an ischaemic stroke unveils atrial myopathy. *Arch Cardiovasc Dis.* (2020) 113:227–36. doi: 10.1016/j.acvd.2019.12.002
47. Hoit BD. Left atrial size and function: role in prognosis. *J Am Coll Cardiol.* (2014) 63:493–505.
48. Olshansky B, Heller EN, Mitchell LB, Chandler M, Slater W, Green M, et al. Are transthoracic echocardiographic parameters associated with atrial fibrillation recurrence or stroke? Results from the atrial fibrillation follow-up investigation of rhythm management (AFFIRM) study. *J Am Coll Cardiol.* (2005) 45:2026–33.
49. Froehlich L, Meyre P, Aeschbacher S, Blum S, Djokic D, Kuehne M, et al. Left atrial dimension and cardiovascular outcomes in patients with and without atrial fibrillation: a systematic review and meta-analysis. *Heart.* (2019) 105:1884–91.
50. Hirota N, Suzuki S, Arita T, Yagi N, Otsuka T, Kishi M, et al. Left atrial dimension and ischemic stroke in patients with and without atrial fibrillation. *Heart Vessels.* (2021) 36:1861–9.
51. Gupta DK, Shah AM, Giugliano RP, Ruff CT, Antman EM, Grip LT, et al. Left atrial structure and function in atrial fibrillation: ENGAGE AF-TIMI 48. *Eur Heart J.* (2014) 35:1457–65.

52. Yaramada P, Pai RG. Markers of atrial myopathy: widening the echocardiographic window for early detection of myocardial disease. *Echocardiography.* (2016) 33:177–8. doi: 10.1111/echo.13136
53. Schaaf M, Andre P, Altman M, Maucort-Boulch D, Placide J, Chevalier P, et al. Left atrial remodelling assessed by 2D and 3D echocardiography identifies paroxysmal atrial fibrillation. *Eur Heart J Cardiovasc Imaging.* (2017) 18:46–53.
54. Caselli S, Canali E, Foschi ML, Santini D, Di Angelantonio E, Pandian NG, et al. Long-term prognostic significance of three-dimensional echocardiographic parameters of the left ventricle and left atrium. *Eur J Echocardiogr.* (2010) 11:250–6. doi: 10.1093/ejechocard/jep198
55. Fatema K, Barnes ME, Bailey KR, Abhayaratna WP, Cha S, Seward JB, et al. Minimum vs. maximum left atrial volume for prediction of first atrial fibrillation or flutter in an elderly cohort: a prospective study. *Eur J Echocardiogr.* (2009) 10:282–6.
56. Olsen FJ, Bertelsen L, Vejlstrup N, Diederichsen SZ, Bjerregaard CL, Graff C, et al. Association between four-dimensional echocardiographic left atrial measures and left atrial fibrosis assessed by left atrial late gadolinium enhancement. *Eur Heart J Cardiovasc Imaging.* (2021) jeab275. doi: 10.1093/ehjci/jeab275 [Epub ahead of print].
57. Eichenlaub M, Mueller-Edenborn B, Minners J, Allgeier M, Lehrmann H, Allgeier J, et al. Echocardiographic diagnosis of atrial cardiomyopathy allows outcome prediction following pulmonary vein isolation. *Clin Res Cardiol.* (2021) 110:1770–80. doi: 10.1007/s00392-021-01850-x
58. Thomas L, Hoy M, Byth K, Schiller NB. The left atrial function index: a rhythm independent marker of atrial function. *Eur J Echocardiogr.* (2008) 9:356–62.
59. Vasan RS, Larson MG, Levy D, Galderisi M, Wolf PA, Benjamin EJ. Doppler transmitral flow indexes and risk of atrial fibrillation (the Framingham heart study). *Am J Cardiol.* (2003) 91:1079–83. doi: 10.1016/s0002-9149(03)00152-8
60. Müller P, Weijs B, Bemelmans NMAA, Mügge A, Eckardt L, Crijns HJGM, et al. Echocardiography-derived total atrial conduction time (PA-TDI duration): risk stratification and guidance in atrial fibrillation management. *Clin Res Cardiol.* (2021) 110:1734–42. doi: 10.1007/s00392-021-01917-9
61. Cameli M, Lisi M, Righini FM, Massoni A, Natali BM, Focardi M, et al. Usefulness of atrial deformation analysis to predict left atrial fibrosis and endocardial thickness in patients undergoing mitral valve operations for severe mitral regurgitation secondary to mitral valve prolapse. *Am J Cardiol.* (2013) 111:595–601. doi: 10.1016/j.amjcard.2012.10.049
62. Saha SK, Anderson PL, Caracciolo G, Kiotsekoglou A, Wilansky S, Govind S, et al. Global left atrial strain correlates with CHADS2 risk score in patients with atrial fibrillation. *J Am Soc Echocardiogr.* (2011) 24:506–12. doi: 10.1016/j.echo.2011.02.012
63. Tsai W-C, Lee C-H, Lin C-C, Liu Y-W, Huang Y-Y, Li W-T, et al. Association of left atrial strain and strain rate assessed by speckle tracking echocardiography with paroxysmal atrial fibrillation. *Echocardiography.* (2009) 26:1188–94.
64. Kawakami H, Ramkumar S, Nolan M, Wright L, Yang H, Negishi K, et al. Left atrial mechanical dispersion assessed by strain echocardiography as an independent predictor of new-onset atrial fibrillation: a case-control study. *J Am Soc Echocardiogr.* (2019) 32:1268–76.e3. doi: 10.1016/j.echo.2019.06.002
65. Walters TE, Nisbet A, Morris GM, Tan G, Mearns M, Teo E, et al. Progression of atrial remodeling in patients with high-burden atrial fibrillation: implications for early ablative intervention. *Heart Rhythm.* (2016) 13:331–9. doi: 10.1016/j.hrthm.2015.10.028
66. Pilichowska-Paszkiet E, Baran J, Sygitowicz G, Sikorska A, Stec S, Kułakowski P, et al. Noninvasive assessment of left atrial fibrosis. Correlation between echocardiography, biomarkers, and electroanatomical mapping. *Echocardiography.* (2018) 35:1326–34. doi: 10.1111/echo.14043
67. Mirza M, Caracciolo G, Khan U, Mori N, Saha SK, Srivathsan K, et al. Left atrial reservoir function predicts atrial fibrillation recurrence after catheter ablation: a two-dimensional speckle strain study. *J Interv Card Electrophysiol.* (2011) 31:197–206. doi: 10.1007/s10840-011-9560-6
68. Modesto KM, Dispenzieri A, Cauduro SA, Lacy M, Khandheria BK, Pellikka PA, et al. Left atrial myopathy in cardiac amyloidosis: implications of novel echocardiographic techniques. *Eur Heart J.* (2005) 26:173–9. doi: 10.1093/eurheartj/ehi040
69. Watanabe Y, Nakano Y, Hidaka T, Oda N, Kajihara K, Tokuyama T, et al. Mechanical and substrate abnormalities of the left atrium assessed by 3-dimensional speckle-tracking echocardiography and electroanatomic mapping system in patients with paroxysmal atrial fibrillation. *Heart Rhythm.* (2015) 12:490–7. doi: 10.1016/j.hrthm.2014.12.007
70. Akoum N, Fernandez G, Wilson B, McGann C, Kholmovski E, Marrouche N. Association of atrial fibrosis quantified using LGE-MRI with atrial appendage thrombus and spontaneous contrast on transesophageal echocardiography in patients with atrial fibrillation. *J Cardiovasc Electrophysiol.* (2013) 24:1104–9. doi: 10.1111/jce.12199
71. Asinger RW, Koehler J, Pearce LA, Zabalgoitia M, Blackshear JL, Fenster PE, et al. Pathophysiologic correlates of thromboembolism in nonvalvular atrial fibrillation: II. Dense spontaneous echocardiographic contrast (the stroke prevention in atrial fibrillation [SPAF-III] study). *J Am Soc Echocardiogr.* (1999) 12:1088–96. doi: 10.1016/s0894-7317(99)70106-9
72. Hopman LHGA, Mulder MJ, van der Laan AM, Demirkiran A, Bhagirath P, van Rossum AC, et al. Impaired left atrial reservoir and conduit strain in patients with atrial fibrillation and extensive left atrial fibrosis. *J Cardiovasc Magn Reson.* (2021) 23:131.
73. Benjamin MM, Munir MS, Shah P, Kinno M, Rabbat M, Sanagala T, et al. Comparison of left atrial strain by feature-tracking cardiac magnetic resonance with speckle-tracking transthoracic echocardiography. *Int J Cardiovasc Imaging.* (2021). doi: 10.1007/s10554-021-02499-3 [Epub ahead of print].
74. Pathan F, Zainal Abidin HA, Vo QH, Zhou H, D'Angelo T, Elen E, et al. Left atrial strain: a multi-modality, multi-vendor comparison study. *Eur Heart J Cardiovasc Imaging.* (2021) 22:102–10. doi: 10.1093/ehjci/jez303
75. Oakes RS, Badger TJ, Kholmovski EG, Akoum N, Burgon NS, Fish EN, et al. Detection and quantification of left atrial structural remodeling with delayed-enhancement magnetic resonance imaging in patients with atrial fibrillation. *Circulation.* (2009) 119:1758–67.
76. Bouazizi K, Rahhal A, Kusmia S, Evin M, Defrance C, Cluzel P, et al. Differentiation and quantification of fibrosis, fat and fatty fibrosis in human left atrial myocardium using ex vivo MRI. *PLoS One.* (2018) 13:e0205104. doi: 10.1371/journal.pone.0205104
77. McGann C, Akoum N, Patel A, Kholmovski E, Revelo P, Damal K, et al. Atrial fibrillation ablation outcome is predicted by left atrial remodeling on MRI. *Circ Arrhythm Electrophysiol.* (2014) 7:23–30.
78. Spragg DD, Khurram I, Zimmerman SL, Yarmohammadi H, Barcelon B, Needleman M, et al. Initial experience with magnetic resonance imaging of atrial scar and co-registration with electroanatomic voltage mapping during atrial fibrillation: success and limitations. *Heart Rhythm.* (2012) 9:2003–9. doi: 10.1016/j.hrthm.2012.08.039
79. Quail M, Grunseich K, Baldassarre LA, Mojibian H, Marieb MA, Cornfeld D, et al. Prognostic and functional implications of left atrial late gadolinium enhancement cardiovascular magnetic resonance. *J Cardiovasc Magn Reson.* (2019) 21:2.
80. Kuppahally SS, Akoum N, Burgon NS, Badger TJ, Kholmovski EG, Vijayakumar S, et al. Left atrial strain and strain rate in patients with paroxysmal and persistent atrial fibrillation: relationship to left atrial structural remodeling detected by delayed-enhancement MRI. *Circ Cardiovasc Imaging.* (2010) 3:231–9. doi: 10.1161/CIRCIMAGING.109.865683
81. Daccarett M, Badger TJ, Akoum N, Burgon NS, Mahnkopf C, Vergara G, et al. Association of left atrial fibrosis detected by delayed-enhancement magnetic resonance imaging and the risk of stroke in patients with atrial fibrillation. *J Am Coll Cardiol.* (2011) 57:831–8.
82. King JB, Azadani PN, Suksaranjit P, Bress AP, Witt DM, Han FT, et al. Left atrial fibrosis and risk of cerebrovascular and cardiovascular events in patients with atrial fibrillation. *J Am Coll Cardiol.* (2017) 70:1311–21.
83. Tandon K, Tirschwell D, Longstreth WT, Smith B, Akoum N. Embolic stroke of undetermined source correlates to atrial fibrosis without atrial fibrillation. *Neurology.* (2019) 93:e381–7.
84. Mahnkopf C, Badger TJ, Burgon NS, Daccarett M, Haslam TS, Badger CT, et al. Evaluation of the left atrial substrate in patients with lone atrial fibrillation using delayed-enhanced MRI: implications for disease progression and response to catheter ablation. *Heart Rhythm.* (2010) 7:1475–81. doi: 10.1016/j.hrthm.2010.06.030

85. Marrouche NF, Wilber D, Hindricks G, Jais P, Akoum N, Marchlinski F, et al. Association of atrial tissue fibrosis identified by delayed enhancement MRI and atrial fibrillation catheter ablation: the DECAAF study. *JAMA*. (2014) 311:498–506.
86. Marrouche NF, Greene T, Dean JM, Kholmovski EG, Boer LM, Mansour M, et al. Efficacy of LGE-MRI-guided fibrosis ablation versus conventional catheter ablation of atrial fibrillation: the DECAAF II trial: study design. *J Cardiovasc Electrophysiol.* (2021) 32:916–24. doi: 10.1111/jce.14957
87. Azarine A, Garçon P, Stansal A, Canepa N, Angelopoulos G, Silvera S, et al. Four-dimensional flow MRI: principles and cardiovascular applications. *Radiographics.* (2019) 39:632–48.
88. Fluckiger JU, Goldberger JJ, Lee DC, Ng J, Lee R, Goyal A, et al. Left atrial flow velocity distribution and flow coherence using four-dimensional FLOW MRI: a pilot study investigating the impact of age and pre- and postintervention atrial fibrillation on atrial hemodynamics. *J Magn Reson Imaging.* (2013) 38:580–7. doi: 10.1002/jmri.23994
89. Markl M, Lee DC, Furiasse N, Carr M, Foucar C, Ng J, et al. Left atrial and left atrial appendage 4D blood flow dynamics in atrial fibrillation. *Circ Cardiovasc Imaging.* (2016) 9:e004984.
90. Markl M, Carr M, Ng J, Lee DC, Jarvis K, Carr J, et al. Assessment of left and right atrial 3D hemodynamics in patients with atrial fibrillation: a 4D flow MRI study. *Int J Cardiovasc Imaging.* (2016) 32:807–15. doi: 10.1007/s10554-015-0830-8
91. Lee DC, Markl M, Ng J, Carr M, Benefield B, Carr JC, et al. Three-dimensional left atrial blood flow characteristics in patients with atrial fibrillation assessed by 4D flow CMR. *Eur Heart J Cardiovasc Imaging.* (2016) 17:1259–68. doi: 10.1093/ehjci/jev304
92. Kuraoka A, Ishizu T, Sato M, Igarashi M, Sato K, Yamamoto M, et al. Left atrial regional strain assessed by novel dedicated three-dimensional speckle tracking echocardiography. *J Cardiol.* (2021) 78:517–23. doi: 10.1016/j.jjcc.2021.07.002
93. Maier J, Blessberger H, Nahler A, Hrncic D, Fellner A, Reiter C, et al. Cardiac computed tomography-derived left atrial volume index as a predictor of long-term success of cryo-ablation in patients with atrial fibrillation. *Am J Cardiol.* (2021) 140:69–77. doi: 10.1016/j.amjcard.2020.10.061
94. Bernhard B, Grogg H, Zurkirchen J, Demirel C, Hagemeyer D, Okuno T, et al. Reproducibility of 4D cardiac computed tomography feature tracking myocardial strain and comparison against speckle-tracking echocardiography in patients with severe aortic stenosis. *J Cardiovasc Comput Tomogr.* (2022):S1934–5925. doi: 10.1016/j.jcct.2022.01.003 [Epub ahead of print].
95. Hirasawa K, Kuneman JH, Singh GK, Gegenava T, Hautemann D, Reiber JHC, et al. Comparison of left atrial strain measured by feature tracking computed tomography and speckle tracking echocardiography in patients with aortic stenosis. *Eur Heart J Cardiovasc Imaging.* (2021) 23:95–101.
96. Szilveszter B, Nagy AI, Vattay B, Apor A, Kolossváry M, Bartykowszki A, et al. Left ventricular and atrial strain imaging with cardiac computed tomography: validation against echocardiography. *J Cardiovasc Comput Tomogr.* (2020) 14:363–9.
97. Ling Z, McManigle J, Zipunnikov V, Pashakhanloo F, Khurram IM, Zimmerman SL, et al. The association of left atrial low-voltage regions on electroanatomic mapping with low attenuation regions on cardiac computed tomography perfusion imaging in patients with atrial fibrillation. *Heart Rhythm.* (2015) 12:857–64. doi: 10.1016/j.hrthm.2015.01.015
98. Su Y, Chen B-X, Wang Y, Li S, Xie B, Yang M-F. Association of atrial 18F-fluorodeoxyglucose uptake and prior ischemic stroke in non-atrial fibrillation patients. *J Nucl Cardiol.* (2022). doi: 10.1007/s12350-022-02903-y
99. Watanabe E, Miyagawa M, Uetani T, Kinoshita M, Kitazawa R, Kurata M, et al. Positron emission tomography/computed tomography detection of increased 18F-fluorodeoxyglucose uptake in the cardiac atria of patients with atrial fibrillation. *Int J Cardiol.* (2019) 283:171–7.
100. Stiles MK, John B, Wong CX, Kuklik P, Brooks AG, Lau DH, et al. Paroxysmal lone atrial fibrillation is associated with an abnormal atrial substrate: characterizing the "second factor". *J Am Coll Cardiol.* (2009) 53:1182–91.
101. Schaeffer B, Akbulak RÖ, Jularic M, Moser J, Eickholt C, Schwarzl JM, et al. High-density mapping and ablation of primary nonfocal left atrial tachycardia: characterizing a distinct arrhythmogenic substrate. *JACC Clin Electrophysiol.* (2019) 5:417–26. doi: 10.1016/j.jacep.2019.02.002
102. Park JH, Joung B, Son N-H, Shim JM, Lee MH, Hwang C, et al. The electroanatomical remodelling of the left atrium is related to CHADS2/CHA2DS2VASc score and events of stroke in patients with atrial fibrillation. *Europace.* (2011) 13:1541–9. doi: 10.1093/europace/eur135
103. Müller P, Makimoto H, Dietrich JW, Fochler F, Nentwich K, Krug J, et al. Association of left atrial low-voltage area and thromboembolic risk in patients with atrial fibrillation. *Europace.* (2018) 20:f359–65.
104. Schreiber D, Rieger A, Moser F, Kottkamp H. Catheter ablation of atrial fibrillation with box isolation of fibrotic areas: lessons on fibrosis distribution and extent, clinical characteristics, and their impact on long-term outcome. *J Cardiovasc Electrophysiol.* (2017) 28:971–83. doi: 10.1111/jce.13278
105. Begg GA, Karim R, Oesterlein T, Graham LN, Hogarth AJ, Page SP, et al. Left atrial voltage, circulating biomarkers of fibrosis, and atrial fibrillation ablation. A prospective cohort study. *PLoS One.* (2018) 13:e0189936. doi: 10.1371/journal.pone.0189936
106. Masuda M, Fujita M, Iida O, Okamoto S, Ishihara T, Nanto K, et al. Left atrial low-voltage areas predict atrial fibrillation recurrence after catheter ablation in patients with paroxysmal atrial fibrillation. *Int J Cardiol.* (2018) 257:97–101.
107. Verma A, Wazni OM, Marrouche NF, Martin DO, Kilicaslan F, Minor S, et al. Pre-existent left atrial scarring in patients undergoing pulmonary vein antrum isolation: an independent predictor of procedural failure. *J Am Coll Cardiol.* (2005) 45:285–92. doi: 10.1016/j.jacc.2004.10.035
108. Vlachos K, Efremidis M, Letsas KP, Bazoukis G, Martin R, Kalafateli M, et al. Low-voltage areas detected by high-density electroanatomical mapping predict recurrence after ablation for paroxysmal atrial fibrillation. *J Cardiovasc Electrophysiol.* (2017) 28:1393–402. doi: 10.1111/jce.13321
109. Seewöster T, Kosich F, Sommer P, Bertagnolli L, Hindricks G, Kornej J. Prediction of low-voltage areas using modified APPLE score. *Europace.* (2021) 23:575–80. doi: 10.1093/europace/euaa311
110. Jadidi AS, Lehrmann H, Keyl C, Sorrel J, Markstein V, Minners J, et al. Ablation of persistent atrial fibrillation targeting low-voltage areas with selective activation characteristics. *Circ Arrhythm Electrophysiol.* (2016) 9:e002962.
111. Linz D, Elliott AD, Marwick TH, Sanders P. Biomarkers and new-onset atrial fibrillation to assess atrial cardiomyopathy. *Int J Cardiol.* (2017) 248:208–10.
112. Packer M. Characterization, pathogenesis, and clinical implications of inflammation-related atrial myopathy as an important cause of atrial fibrillation. *J Am Heart Assoc.* (2020) 9:e015343. doi: 10.1161/JAHA.119.015343
113. Shaihov-Teper O, Ram E, Ballan N, Brzezinski RY, Naftali-Shani N, Masoud R, et al. Extracellular vesicles from epicardial fat facilitate atrial fibrillation. *Circulation.* (2021) 143:2475–93.
114. Stanciu AE, Vatasescu RG, Stanciu MM, Serdarevic N, Dorobantu M. The role of pro-fibrotic biomarkers in paroxysmal and persistent atrial fibrillation. *Cytokine.* (2018) 103:63–8. doi: 10.1016/j.cyto.2017.12.026
115. Zhao F, Zhang S, Chen Y, Gu W, Ni B, Shao Y, et al. Increased expression of NF-AT3 and NF-AT4 in the atria correlates with procollagen I carboxyl terminal peptide and TGF-β1 levels in serum of patients with atrial fibrillation. *BMC Cardiovasc Disord.* (2014) 14:167. doi: 10.1186/1471-2261-14-167
116. Malouf JF, Kanagala R, Al Atawi FO, Rosales AG, Davison DE, Murali NS, et al. High sensitivity C-reactive protein: a novel predictor for recurrence of atrial fibrillation after successful cardioversion. *J Am Coll Cardiol.* (2005) 46:1284–7.
117. Heinzmann D, Fuß S, Ungern-Sternberg SV, Schreieck J, Gawaz M, Gramlich M, et al. TGFβ is specifically upregulated on circulating CD14++ CD16+ and CD14+ CD16++ monocytes in patients with atrial fibrillation and severe atrial fibrosis. *Cell Physiol Biochem.* (2018) 49:226–34. doi: 10.1159/000492873
118. Kishima H, Mine T, Takahashi S, Ashida K, Ishihara M, Masuyama T. The impact of transforming growth factor-β1 level on outcome after catheter ablation in patients with atrial fibrillation. *J Cardiovasc Electrophysiol.* (2017) 28:402–9. doi: 10.1111/jce.13169

119. Tian Y, Wang Y, Chen W, Yin Y, Qin M. Role of serum TGF-β1 level in atrial fibrosis and outcome after catheter ablation for paroxysmal atrial fibrillation. *Medicine (Baltimore).* (2017) 96:e9210. doi: 10.1097/MD.0000000000009210
120. Wu C-H, Hu Y-F, Chou C-Y, Lin Y-J, Chang S-L, Lo L-W, et al. Transforming growth factor-β1 level and outcome after catheter ablation for nonparoxysmal atrial fibrillation. *Heart Rhythm.* (2013) 10:10–5.
121. Rosenberg MA, Maziarz M, Tan AY, Glazer NL, Zieman SJ, Kizer JR, et al. Circulating fibrosis biomarkers and risk of atrial fibrillation: the cardiovascular health study (CHS). *Am Heart J.* (2014) 167:723–8.e2. doi: 10.1016/j.ahj.2014.01.010
122. Ravassa S, Ballesteros G, López B, Ramos P, Bragard J, González A, et al. Combination of circulating type I collagen-related biomarkers is associated with atrial fibrillation. *J Am Coll Cardiol.* (2019) 73:1398–410. doi: 10.1016/j.jacc.2018.12.074
123. Wałek P, Grabowska U, Cieśla E, Sielski J, Roskal-Wałek J, Woñakowska-Kapłon B. Analysis of the correlation of galectin-3 concentration with the measurements of echocardiographic parameters assessing left atrial remodeling and function in patients with persistent atrial fibrillation. *Biomolecules.* (2021) 11:1108. doi: 10.3390/biom11081108
124. Dzeshka MS, Shantsila E, Snezhitskiy VA, Lip GYH. 3057Relation of atrial remodeling to circulating biomarkers of myocardial fibrosis and apoptotic microparticles in patients with atrial fibrillation and heart failure with preserved ejection fraction. *Eur Heart J.* (2019) 40:ehz745.0024.
125. Sieweke J-T, Pfeffer TJ, Biber S, Chatterjee S, Weissenborn K, Grosse GM, et al. miR-21 and NT-proBNP correlate with echocardiographic parameters of atrial dysfunction and predict atrial fibrillation. *J Clin Med.* (2020) 9:1118. doi: 10.3390/jcm9041118
126. Patel RB, Alenezi F, Sun J-L, Alhanti B, Vaduganathan M, Oh JK, et al. Biomarker profile of left atrial myopathy in heart failure with preserved ejection fraction: insights from the relax trial. *J Card Fail.* (2020) 26:270–5. doi: 10.1016/j.cardfail.2019.12.001
127. Patel RB, Lam CSP, Svedlund S, Saraste A, Hage C, Tan R-S, et al. Disproportionate left atrial myopathy in heart failure with preserved ejection fraction among participants of the PROMIS-HFpEF study. *Sci Rep.* (2021) 11:4885. doi: 10.1038/s41598-021-84133-9
128. Oldgren J, Hijazi Z, Lindbäck J, Alexander JH, Connolly SJ, Eikelboom JW, et al. Performance and validation of a novel biomarker-based stroke risk score for atrial fibrillation. *Circulation.* (2016) 134:1697–707.
129. Granger CB, Alexander JH, McMurray JJV, Lopes RD, Hylek EM, Hanna M, et al. Apixaban versus warfarin in patients with atrial fibrillation. *N Engl J Med.* (2011) 365:981–92.
130. Seewöster T, Büttner P, Zeynalova S, Hindricks G, Kornej J. Are the atrial natriuretic peptides a missing link predicting low-voltage areas in atrial fibrillation? Introducing the novel biomarker-based atrial fibrillation substrate prediction (ANP) score. *Clin Cardiol.* (2020) 43:762–8. doi: 10.1002/clc.23378
131. Goette A, Hoffmanns P, Enayati W, Meltendorf U, Geller J, Klein HU. Effect of successful electrical cardioversion on serum aldosterone in patients with persistent atrial fibrillation. *Am J Cardiol.* (2001) 88:906–9. doi: 10.1016/s0002-9149(01)01905-1
132. Engelmann B, Massberg S. Thrombosis as an intravascular effector of innate immunity. *Nat Rev Immunol.* (2013) 13:34–45.
133. Lazzerini PE, Capecchi PL, Laghi-Pasini F. Systemic inflammation and arrhythmic risk: lessons from rheumatoid arthritis. *Eur Heart J.* (2017) 38:1717–27. doi: 10.1093/eurheartj/ehw208
134. Tilly MJ, Geurts S, Donkel SJ, Ikram MA, de Groot NMS, de Maat MPM, et al. Immunothrombosis and new-onset atrial fibrillation in the general population: the Rotterdam study. *Clin Res Cardiol.* (2022) 111:96–104. doi: 10.1007/s00392-021-01938-4
135. Conway DSG, Pearce LA, Chin BSP, Hart RG, Lip GYH. Plasma von Willebrand factor and soluble p-selectin as indices of endothelial damage and platelet activation in 1321 patients with nonvalvular atrial fibrillation: relationship to stroke risk factors. *Circulation.* (2002) 106:1962–7. doi: 10.1161/01.cir.0000033220.97592.9a
136. Conway DSG, Pearce LA, Chin BSP, Hart RG, Lip GYH. Prognostic value of plasma von Willebrand factor and soluble P-selectin as indices of endothelial damage and platelet activation in 994 patients with nonvalvular atrial fibrillation. *Circulation.* (2003) 107:3141–5. doi: 10.1161/01.CIR.0000077912.12202.FC
137. Wallentin L, Hijazi Z, Andersson U, Alexander JH, de Caterina R, Hanna M, et al. Growth differentiation factor 15, a marker of oxidative stress and inflammation, for risk assessment in patients with atrial fibrillation: insights from the apixaban for reduction in stroke and other thromboembolic events in atrial fibrillation (ARISTOTLE) trial. *Circulation.* (2014) 130:1847–58. doi: 10.1161/CIRCULATIONAHA.114.011204
138. Bukowska A, Röcken C, Erxleben M, Röhl F-W, Hammwöhner M, Huth C, et al. Atrial expression of endothelial nitric oxide synthase in patients with and without atrial fibrillation. *Cardiovasc Pathol.* (2010) 19:e51–60.
139. Bukowska A, Zacharias I, Weinert S, Skopp K, Hartmann C, Huth C, et al. Coagulation factor Xa induces an inflammatory signalling by activation of protease-activated receptors in human atrial tissue. *Eur J Pharmacol.* (2013) 718:114–23. doi: 10.1016/j.ejphar.2013.09.006
140. Nozawa T, Inoue H, Hirai T, Iwasa A, Okumura K, Lee J-D, et al. D-dimer level influences thromboembolic events in patients with atrial fibrillation. *Int J Cardiol.* (2006) 109:59–65.
141. Lee H-C, Shin S-J, Huang J-K, Lin M-Y, Lin Y-H, Ke L-Y, et al. The role of postprandial very-low-density lipoprotein in the development of atrial remodeling in metabolic syndrome. *Lipids Health Dis.* (2020) 19:210.
142. McManus DD, Yin X, Gladstone R, Vittinghoff E, Vasan RS, Larson MG, et al. Alcohol consumption, left atrial diameter, and atrial fibrillation. *J Am Heart Assoc.* (2016) 5:e004060.
143. Voskoboinik A, Costello BT, Kalman E, Prabhu S, Sugumar H, Wong G, et al. Regular alcohol consumption is associated with impaired atrial mechanical function in the atrial fibrillation population: a cross-sectional MRI-based study. *JACC Clin Electrophysiol.* (2018) 4:1451–9. doi: 10.1016/j.jacep.2018.07.010
144. Müller-Edenborn B, Moreno-Weidmann Z, Venier S, Defaye P, Park C-I, Guerra J, et al. Determinants of fibrotic atrial cardiomyopathy in atrial fibrillation. A multicenter observational study of the RETAC (reseau Européen de traîtement d'arrhythmies cardiaques)-group. *Clin Res Cardiol.* (2021). doi: 10.1007/s00392-021-01973-1

Conflict of Interest: The authors declare that the research was conducted in the absence of any commercial or financial relationships that could be construed as a potential conflict of interest.

Publisher's Note: All claims expressed in this article are solely those of the authors and do not necessarily represent those of their affiliated organizations, or those of the publisher, the editors and the reviewers. Any product that may be evaluated in this article, or claim that may be made by its manufacturer, is not guaranteed or endorsed by the publisher.

frontiers | Frontiers in Cardiovascular Medicine

ORIGINAL RESEARCH
published: 13 July 2022
doi: 10.3389/fcvm.2022.949213

Multimodal Approach for the Prediction of Atrial Fibrillation Detected After Stroke: SAFAS Study

*Lucie Garnier[1,2], Gauthier Duloquin[1,2], Alexandre Meloux[2], Karim Benali[3], Audrey Sagnard[3], Mathilde Graber[1,2], Geoffrey Dogon[2], Romain Didier[2,3], Thibaut Pommier[2,3], Catherine Vergely[2], Yannick Béjot[1,2] and Charles Guenancia[2,3]**

[1] Department of Neurology, University Hospital, Dijon, France, [2] Pathophysiology and Epidemiology of Cerebro-Cardiovascular Diseases (EA 7460), Faculty of Health Sciences, Université de Bourgogne, Université de Bourgogne Franche-Comté, Dijon, France, [3] Department of Cardiology, University Hospital, Dijon, France

OPEN ACCESS

Edited by:
Hung-Fat Tse,
The University of Hong Kong,
Hong Kong SAR, China

Reviewed by:
Alexander Carpenter,
University of Bristol, United Kingdom
Mei Qiu,
Shenzhen Longhua District Central Hospital, China

***Correspondence:**
Charles Guenancia
charles.guenancia@gmail.com

Specialty section:
This article was submitted to Cardiac Rhythmology, a section of the journal Frontiers in Cardiovascular Medicine

Received: 20 May 2022
Accepted: 20 June 2022
Published: 13 July 2022

Citation:
Garnier L, Duloquin G, Meloux A, Benali K, Sagnard A, Graber M, Dogon G, Didier R, Pommier T, Vergely C, Béjot Y and Guenancia C (2022) Multimodal Approach for the Prediction of Atrial Fibrillation Detected After Stroke: SAFAS Study. Front. Cardiovasc. Med. 9:949213. doi: 10.3389/fcvm.2022.949213

Background: Intensive screening for atrial fibrillation (AF) has led to a better recognition of this cause in stroke patients. However, it is currently debated whether AF Detected After Stroke (AFDAS) has the same pathophysiology and embolic risk as prior-to-stroke AF. We thus aimed to systematically approach AFDAS using a multimodal approach combining clinical, imaging, biological and electrocardiographic markers.

Methods: Patients without previously known AF admitted to the Dijon University Hospital (France) stroke unit for acute ischemic stroke were prospectively enrolled. The primary endpoint was the presence of AFDAS at 6 months, diagnosed through admission ECG, continuous electrocardiographic monitoring, long-term external Holter during the hospital stay, or implantable cardiac monitor if clinically indicated after discharge.

Results: Of the 240 included patients, 77 (32%) developed AFDAS. Compared with sinus rhythm patients, those developing AFDAS were older, more often women and less often active smokers. AFDAS patients had higher blood levels of NT-proBNP, osteoprotegerin, galectin-3, GDF-15 and ST2, as well as increased left atrial indexed volume and lower left ventricular ejection fraction. After multivariable analysis, galectin-3 $\geqq$ 9 ng/ml [OR 3.10; 95% CI (1.03–9.254), p = 0.042], NT-proBNP $\geqq$ 290 pg/ml [OR 3.950; 95% CI (1.754–8.892, p = 0.001], OPG $\geq$ 887 pg/ml [OR 2.338; 95% CI (1.015–5.620), p = 0.046) and LAVI $\geq$ 33.5 ml/m^2 [OR 2.982; 95% CI (1.342–6.625), p = 0.007] were independently associated with AFDAS.

Conclusion: A multimodal approach combining imaging, electrocardiography and original biological markers resulted in good predictive models for AFDAS. These results also suggest that AFDAS is probably related to an underlying atrial cardiopathy.

Clinical Trial Registration: [www.ClinicalTrials.gov], identifier [NCT03570060].

Keywords: atrial fibrillation, stroke, atrial cardiopathy, biomarkers, Holter, echocardiography

INTRODUCTION

Atrial fibrillation (AF) is one of the most common causes of ischemic stroke. It is associated with a fivefold increased risk of stroke and accounts for more than one in five strokes (1, 2). However, many studies showed that even with continuous electrocardiographic monitoring (CEM), many AF episodes are not clinically diagnosed (3). It has been estimated that one third of patients with cryptogenic stroke may in fact have undetected asymptomatic AF (1, 4). In this setting, implantable cardiac monitors (ICM) are now commonly implanted in patients with cryptogenic stroke, in accordance with CRYSTAL-AF trial results (1). However, only one third of patients with ICM will eventually develop new-onset AF (5). Systematic anticoagulation in cryptogenic stroke patients failed to demonstrate a clinical benefit as compared to aspirin in the NAVIGATE-ESUS or RESPECT-ESUS trials (6, 7), supporting the emergence of a new concept known as AFDAS (Atrial Fibrillation Detected After Stroke and Transient Ischemic Attack). Although some studies tend to show that AFDAS has a different pathophysiology and embolic risk than AF, little is known about the underlying mechanisms of this condition (8).

Three components are involved in the development of all types of arrhythmia (9): the substrate, the modulator [the autonomic nervous system (ANS)] and the triggering factor(s). We thus aimed to approach systematically AFDAS pathophysiology in stroke patients using a multimodal approach combining clinical, imaging, biological and electrocardiographic markers:

- the atrial substrate (i.e. atrial cardiopathy), as assessed by left atrial dimensions, and by blood biomarkers of fibrosis (galectin-3, osteoprotegerin) and of cardiac remodeling (NT-pro-BNP),
- the modulator: ANS, assessed by heart rate variability,
- the triggers, as assessed by inflammatory mediators (CRP, ST2, GDF-15), the burden of premature atrial contractions and the presence of left ventricular dysfunction or acute myocardial injury.

Study Design and Population

We conducted a prospective study (SAFAS: Stepwise screening for silent Atrial Fibrillation After Stroke) in adult patients hospitalized between March 31, 2018, and January 18, 2020, in the stroke unit of the Dijon Bourgogne University Hospital. We included patients with ischemic stroke according to the World Health Organization criteria: a clinical syndrome characterized by a focal loss of cerebral or ocular function, of sudden onset, without obvious etiology at initial management and confirmed by imaging.

Patients with a history of AF or atrial flutter, as well as those with a pacemaker or an implantable cardioverter defibrillator with an atrial lead (not eligible for the stepwise screening strategy), adults under guardianship, pregnant or breastfeeding women, and those who refused to participate in the study were excluded. Patients who were not under the primary care area of the Dijon University Hospital (transfer to a department outside the University Hospital after acute management of stroke) were excluded because long-term external Holter screening could not be done.

Oral consent was obtained from all patients or their representative. This study was validated by a national ethics committee and conducted in accordance with the ethical principles of the Declaration of Helsinki and the recommendations of Good Clinical Practice (CPP Sud Méditerranée I n°2018-A00345-50, clinical trials NCT03570060).

Clinical, Biological and Imaging Data During Hospital Stay

Within 48 h of admission, we collected patients' demographic and clinical data. Upon admission to the stroke unit, patients underwent additional examinations, including brain and intra/extra-cranial vessel imaging, electrocardiogram (ECG), echocardiography [transthoracic with bubble test for patent foramen ovale (PFO) ± transesophageal] and a standard biological workup supplemented by sampling for biomarkers.

Biomarker Assay

Biological samples were stored in the stroke unit refrigerator at 3°C for a maximum of 24 h. Tubes were centrifuged at 3,500 rpm for 5 min at 4°C to recover the serum, and then aliquoted. The aliquots were then immediately transferred to the freezer (−80°C) until use. The assay was performed on thawed serum. The Enzyme-Linked Immuno-Sorbent Assay technique was used for galectin-3 (DGAL30, R&D systems, Minneapolis, United States) and the multiplex technique for osteoprotegerin (OPG), ST2, and GDF15 (R&D systems, Minneapolis, United States) following the manufacturer's recommendations.

Heart Rate Monitoring

Patients received continuous and sequential cardiac monitoring which included ECG at admission, CEM in the stroke unit, and long-term Holter ECG (SpiderFlash, Microport, France) during the entire stay in the neurology department. The SpiderFlash Holter allows the recording of arrhythmic episodes regardless of their duration, capturing the events and documenting them by means of ECG samples. The device was programmed to record every rhythmic event for 7 days, regardless of the duration of the supraventricular arrhythmia. An experienced cardiologist (CG) who was blinded to the patient's clinical data performed the Holter ECG analysis. If the diagnosis was uncertain, a second cardiologist, blinded to the first results, also analyzed the records. There was no discordance between the two analyses.

If no arrhythmia was detected and no etiology found for the ischemic stroke after the diagnostic workup, an ICM (REVEAL XT or Linq, Medtronic, United States) was indicated, as recommended by international guidelines in case of cryptogenic stroke (10). ICM detects AF by analyzing the irregularity and inconsistency of successive R-R intervals within a minimum time frame (5). Atrial fibrillation was defined according to European guidelines (11). Atrial flutter patients were included in the AF group.

Electrocardiographic Data

ECG: P-wave duration (ms) and *p*-wave terminal force (PTF) [amplitude of the terminal negative portion of the P-wave in V1 x the duration of the terminal negative portion of the *P*-wave in V1)].

Heart rate variability (HRV) on CEM tracings were measured as previously described (12): average pNN50 (marker of parasympathetic nervous system activation) corresponding to the proportion derived by dividing NN50 [the number of interval differences of successive sinus node depolarization (NN) intervals greater than 50 ms] by the total number of NN intervals, and SDNN [the standard deviation of all intervals between adjacent QRS complexes resulting from sinus node depolarization (NN)], on the first day of recording of the stroke unit CEM. Only sequences with normal QRS characteristics during 24 h (sinus rhythm) were analyzed for HRV study. If AF was diagnosed on the ECG at entry or on the first day of monitoring, ANS parameters were not analyzed.

Follow-Up

We collected the length of stay in each unit, where the patient was discharged to after hospitalization, any intercurrent hospital events, etiological diagnosis according to the TOAST classification (13) as well as the NIHSS score, modified Rankin score and discharge treatments.

Patients were contacted by phone at 3 months and seen for an outpatient visit at 6 months. Data was collected regarding vital status, current treatments, cardiovascular events (ischemic stroke, myocardial infarction, heart failure hospitalization, atrial fibrillation or atrial flutter), vascular or hemorrhagic recurrence, and any hemorrhagic event.

Patients implanted with an ICM had a follow-up cardiology consultation at 6 weeks and then every 3 months. If the patient was equipped with a remote monitoring system, the ICM data were analyzed every week and the patient was contacted if a rhythm disorder was detected. Decisions regarding the treatment of AF episodes were made by the attending physician.

Statistical Analysis

Continuous data were expressed as medians (25th–75th percentile) and dichotomous data as numbers (percentages). A Mann-Whitney test or Student's *t*-test was used to compare continuous data, and the Chi-square test or Fisher's test was used for dichotomous data. The optimal threshold to discriminate AF from the continuous data of interest was obtained with the receiver-operating characteristic (ROC) curve with the best sensitivity and specificity according to the Youden index. Variables entered into the multivariate model were chosen according to their univariate relationship with an inclusion and exclusion cut-off at 5%. Two multivariate backward stepwise logistic regression models were used, one to predict all recorded AFDAS from admission to 6-month follow-up (model 1) and the second one focusing on AFDAS diagnosed after the stay in the stroke unit, including HRV variables (model 2). A p-value < 0.05 was considered statistically significant. Analyses were performed using SPSS software (26.0, IBM Inc., United States).

RESULTS

Atrial Fibrillation Detected After Stroke Associated Factors

Among the 1,796 patients admitted to the stroke unit between March 2018 and January 2020, 265 were eligible for inclusion, and 240 were finally analyzed (**Figure 1**). During the 6 months of follow-up, 77 patients (32%) developed AFDAS and 163 patients (64%) maintained sinus rhythm. Clinical characteristics and complementary exam results are presented in **Tables 1**–**4**.

Compared with sinus rhythm patients, the patients who developed AFDAS were older ($p < 0.001$), were more often women, were less often active smokers ($p = 0.001$), had a higher NIHSS score on admission ($p = 0.001$), and were likely to have a premorbid mRS ≥ 2 ($p < 0.001$). The CHA_2DS_2VASc score at admission (calculated without including the current episode of stroke) was also higher in the AFDAS group ($p < 0.001$), and AFDAS patients were more likely to have undergone acute revascularization therapy by thrombolysis and/or mechanical thrombectomy ($p = 0.002$) (**Table 1**). On brain CT-scan imaging, the stroke location of patients with AFDAS more frequently involved the superficial middle cerebral artery territory ($p < 0.001$), especially when the insula was involved ($p = 0.003$).

AFDAS patients also had higher blood levels of NT-pro-BNP ($p < 0.001$) (**Table 2**). Plasma levels of OPG ($p < 0.001$), galectin-3 ($p = 0.026$), GDF 15 ($p = 0.001$) and ST2 ($p = 0.027$) were higher in AFDAS patients. Patients with AFDAS more frequently had LA dilatation as assessed by increased left atrial indexed volume (LAVI) ($p < 0.001$), and had lower LVEF ($p = 0.030$) (**Table 3**).

In patients without evidence of AF at admission or during CEM in the stroke unit, ($N = 158$), pNN50 ($p < 0.001$) and SDNN ($p = 0.007$), both calculated on the first day of the CEM, were higher in patients who subsequently developed AFDAS. AFDAS was also associated with higher burden of premature atrial contractions (PAC), ($p < 0.001$), non-sustained supraventricular tachycardias ($p < 0.001$) and premature ventricular contractions (PVC) ($p < 0.001$) on CEM.

We performed ROC curves analyses to assess the relationship and the best cut-off values between AF and the biological, imaging and electrocardiographic markers of atrial cardiopathy. After ROC curve, the best predictive value for AF was 887 pg/ml for OPG, 18,350 pg/ml for ST2, 1,320 pg/ml for GDF-15, 11 ng/ml for galectin-3, 290 pg/ml for NT-pro-BNP, 33.5 ml/m^2 for LAVI, 38 for SDNN and 11 for pNN50.

During the 6 months of follow-up, there were significantly more deaths in the AFDAS group than in the sinus rhythm group [10 (13%) vs. 3 (2%), $p = 0.001$]. There was also a trend toward more frequent bleeding in AF patients at 6 months. There was no difference in the recurrence rate of stroke or TIA.

Predictive Models for Atrial Fibrillation Detected After Stroke

Two multivariate models were performed, one to predict all recorded AFDAS (model 1) and another model (model

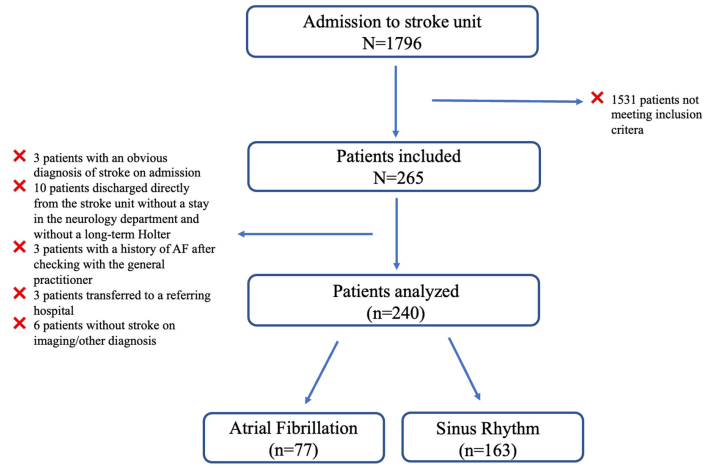

FIGURE 1 | Flow chart of the SAFAS study.

TABLE 1 | Clinical characteristics of patients [*n* (%) or median (IQR)].

	SR [*n* = 163 (68%)]	AFDAS [*n* = 77 (32%)]	*p*
Risk factors			
Age, years	65.79 (54.90–74.96)	81.27 (71.68–85.85)	<0.001
Age ≥ 77 years	31.00 (19.00)	49.00 (63.30)	<0.001
Female sex	68.00 (41.70)	45.00 (58.40)	0.015
BMI, kg/m^2	26.26 (23.75–29.19)	26.44 (23.10–29.79)	0.778
Obesity (BMI > 30 kg/m^2)	35.00 (21.90)	16.00 (22.9)	0.869
High blood pressure	86.00 (52.80)	50.00 (64.90)	0.076
Hypercholesterolemia	49.00 (30.10)	21.00 (27.30)	0.657
Diabetes	30.00 (18.40)	16.00 (20.80)	0.663
Active smoking	41.00 (25.20)	6.00 (7.90)	0.001
Active or withdrawn alcohol consumption	13.00 (8.00)	5.00 (6.70)	0.799
Obstructive sleep apnea	14.00 (8.60)	9.00 (11.80)	0.483
Previous kidney failure	2.00 (1.20)	3.00 (3.90)	0.331
Previous cancer	26.00 (16.00)	10.00 (13.00)	0.548
Recent infection (<1 month)	6.00 (3.70)	6.00 (7.90)	0.206
Cardiovascular history			
Stroke or TIA	25.00 (15.50)	13.00 (17.10)	0.757
Peripheral artery disease	2,00 (1.20)	1,00 (1.30)	1,000
Heart failure	5.00 (3.10)	5.00 (6.60)	0.296
Cardiac valve disease	7,00 (4.30)	6.00 (7.90)	0.357
Clinical data at admission			
Systolic pressure, mmHg	155.00 (138.25–175.00)	161.00 (139.50–178.50)	0.910
Diastolic pressure, mmHg	87.00 (75.25–95.00)	81.00 (70.00–92.50)	0.061
Blood glucose, g/l	1.17 (1.02–1.37)	1.11 (0.99–1.35)	0.288
NIHSS score	4.00 (1.00–7.00)	6.00 (3.00–12.75)	0.001
Premorbid mRS ≥ 2	20.00 (12.70)	28.00 (37.30)	<0.001
CHA_2DS_2VASc score	2.00 (1.00–4.00)	4.00 (2.00–4.00)	<0.001
Acute revascularization therapy	54.00 (33.10)	42.00 (54.50)	0.002

IQR, interquartile range; SR, sinus rhythm; BMI, Body mass index; TIA, transient ischemic attack; NIHSS, National Institute of Health Stroke Scale; mRS, modified Rankin scale.

2) focusing on AFDAS diagnosed after patients' stay in the stroke unit (> 48 h usually), including HRV variables (**Table 4**).

In model 1, among the variables significantly associated with AF in bivariate analysis, galectin-3 ≥ 9 ng/ml [OR 3.10; 95% CI (1.03–9.254), p = 0.042], NT-pro-BNP ≥ 290 pg/ml [OR

TABLE 2 | Biological, imaging and electrocardiographic characteristics of patients at admission [*n* (%) or median (IQR)].

	Sinus rhythm	AFDAS	*p*
Biological data			
CRP, mg/mL	2.90 (2.90–5.00)	2.95 (2.90–6.10)	0.269
Creatinine, μmol/l	72.00 (62.00–85.00)	74.00 (63.00–88.00)	0.476
Troponin, μg/l	0.02 (0.02–0.02)	0.02 (0.02–0.04)	0.417
NT-Pro-BNP, pg/ml	129.00 (60.00–331.00)	843.00 (303.25–2069.50)	<0.001
NT-pro-BNP ≥ 290 pg/ml	43.00 (28.70)	54.00 (77.10)	<0.001
TSH, μg/ml	1.32 (0.76–2.07)	1.16 (0.78–1.88)	0.772
Galectin 3, ng/ml	11.03 (8.24–14.33)	12.45 (10.03–16.29)	0.026
Galectin 3 ≥ 9 ng/ml	106.00 (68.40)	68.00 (88.30)	0.001
ST2, pg/ml	17147.90 (12932.97–26956.95)	21.202.68 (14708.56–31836.67)	0.027
ST2 ≥ 18,350 pg/ml	63.00 (39.90)	48.00 (63.20)	0.001
Osteoprotegerin, pg/ml	905.60 (757.07–1280.77)	1139.30 (912.92–1598.76)	<0.001
Osteoprotegerin ≥ 887 pg/ml	80.00 (50.60)	60.00 (77.90)	<0.001
GDF15, pg/ml	1573.64 (1003.80–2270.86)	2142.63 (1363.14-2931.12)	0.001
GDF15 ≥ 1,320 pg/ml	94.00 (59.90)	61.00 (79.20)	0.003
Imaging data			
Multi-territory stroke	19.00 (11.70)	6.00 (7.80)	0.360
Vertebro-basilar stroke	58.00 (35.60)	18.00 (23.40)	0.058
Bilateral stroke	15.00 (9.20)	6.00 (7.80)	0.718
Insular stroke	27.00 (16.60)	26.00 (33.80)	0.003
Cerebellar stroke	18.00 (11.00)	7.00 (9.10)	0.821
Thalamic stroke	9.00 (5.50)	5.00 (6.50)	0.773
Anterior choroidal stroke	10.00 (6.10)	0.00 (0.00)	0.033
CAA stroke	6.00 (3.70)	4.00 (5.20)	0.730
MCA superficial stroke	73.00 (44.80)	53.00 (68.80)	<0.001
MCA deep stroke	43.00 (26.40)	22.00 (28.60)	0.721
ECG data			
LBB (*n* = 180)	3.00 (2.40)	2.00 (3.50)	0.685
RBB (*n* = 180)	7.00 (5.70)	5.00 (8.80)	0.523
P-wave duration max, ms (*n* = 111)	100.00 (100.00–120.00)	120.00 (100.00–120.00)	0.570
PTF, mV.ms	4.00 (4.00–8.00)	6.00 (4.00–8.00)	0.407
PTF ≥ 4 mv.ms (*n* = 111)	41.00 (47.10)	17.00 (70.80)	0.063
PTF ≥ 5 mv.ms (*n* = 111)	38.00 (46.30)	20.00 (69.00)	0.051
PR duration, ms	168.00 (148.00–191.00)	172.00 (154.00–196.00)	0.214
QRS duration, ms	90,00 (82.50–98.00)	92.00 (82.00–108.00)	0.385
Corrected QTc duration, ms	423.00 (409.00–444.00)	435.00 (413.50–449.50)	0.189

IQR, interquartile range; SR, sinus rhythm; AF, Atrial fibrillation CRP, C-reactive protein; NT-pro-BNP, N-Terminal pro-brain natriuretic peptide; ST2, Suppression of Tumorigenicity 2; GDF15, growth differentiation factor 15; cerebral anterior artery; MCA, middle cerebral artery; ECG, electrocardiogram; LBB, left bundle branch block; RBB, right bundle branch block; PTF, p-wave terminal force.

3.950; 95% CI (1.754–8.892, $p = 0.001$], OPG ≥ 887 pg/ml [OR 2.338; 95% CI (1.015–5.620), $p = 0.046$] and LAVI ≥ 33.5 ml/m2 [OR 2.982; 95% CI (1.342–6.625), $p = 0.007$] were independently associated with AFDAS.

In model 2, including HRV variables, galectin-3 ≥ 9 ng/ml [OR 6.587; 95% CI (1.529–28.376) $p = 0.011$], NT-Pro-BNP ≥ 290 pg/ml [OR 4.676; 95% CI (1.655–13.210), $p = 0.004$], OPG ≥ 887 pg/ml [OR 3.350; 95% CI (1.060–10.590) $p = 0.040$] and pNN50 ≥ 11 [OR 8.260; 95% CI (2.795–24.406), $p < 0.001$] were independently associated with AFDAS after discharge from the stroke unit.

The ROC curves of these models illustrate their predictive performance for AFDAS in our cohort (**Figure 2**) [model 1: AUC 0.829, 95% CI (0.764–0.894); model 2: AUC 0.879, 95% CI (0.818–0.940)]. For model 1, the positive predictive value was 63% and the negative predictive value was 80%. For model 2, the positive predictive value was 71% and the negative predictive value was 83%.

DISCUSSION

The main results of this prospective study in ischemic stroke patients without previous AF or an obvious etiology at admission are as follows (**Figure 3**):

- Our sequential, continuous and early rhythm monitoring approach detected AFDAS in 32% of patients at 6 months of follow-up.

TABLE 3 | cardiac work-up [*n* (%) or median (IQR)].

	Sinus rhythm	AFDAS	*p*
CEM data (*n* = 224)	199.00 (88.84)	25.00 (11.16)	
PAC, day 1	1.00 (0.00–4.75)	9.00 (2.00–26.50)	<0.001
NSSVT, day 1	0.00 (0.00–1.00)	3.00 (1.00–9.00)	<0.001
NSVT, day 1	3.50 (1.00–7.00)	11.00 (2.50–23.00)	<0.001
pNN50 (*n* = 158)	2.00 (0.00–9.55)	14.11 (4.13–22.39)	<0.001
Sinus variability (SDNN) (*n* = 158)	29.08 (21.19–46.77)	41.67 (27.13–72.50)	0.002
pNN50 ≥ 11 (*n* = 158)	25.00 (21.40)	25.00 (61.00)	<0.001
SDNN ≥ 38 (*n* = 158)	36.00 (30.80)	27.00 (65.90)	<0.001
Echocardiographic data			
LA diameter, cm	3.60 (3.20–3.93)	4.10 (3.60–4.40)	<0.001
LA surface, cm^2	17.70 (15.05–22.20)	20.80 (17.03–25.87)	0.001
LA volume, mm^3	45,00 (35.30–61.25)	60.90 (42.00–81.60)	<0.001
LAVI, ml/m^2	25.84 (19.45–33.25)	35.80 (25.87–43.86)	<0.001
LAVI ≥ 33.5 ml/m^2 (*n* = 188)	32.00 (23.50)	32.00 (61.50)	<0.001
LVEF,%	60.00 (56.00–66.15)	59.90 (55.00–63.50)	0.030
PFO	26.00 (16.50)	2.00 (3.00)	0.004

SR, sinus rhythm; AF, atrial fibrillation; PAC, premature atrial contractions; NSSVT, non-sustained supra ventricular tachycardia; NSVT, non-sustained ventricular tachycardia; LAVI, left atrial indexed volume; LVEF, left ventricular ejection fraction; PFO, patent foramen ovale.

TABLE 4 | Univariate and multivariate analysis of AFDAS predictors.

	Univariate			Multivariate		
Variable	**OR**	**95% CI**	***p***	**OR**	**95% CI**	***P***
Model 1 (*n* = 240)						
Age ≥ 77 yo	7.45	4.06–13.67	<0.001			
Female sex	1.96	1.13–3.45	0.016			
Active smoking	0.26	0.10–0.63	0.003			
Insular stroke	2.57	1.37–4.81	0.003			
LAVI ≥ 33.5 ml/m^2	5.20	2.62–10.32	<0.001	2.982	1.34–6.63	0.007
PFO	0.16	0.04–0.68	0.013			
NT-pro-BNP ≥ 290 pg/ml	8.39	4.34–16.26	<0.001	3.950	1.75–8.89	0.001
Galectin-3 ≥ 9 ng/ml	3.49	1.61–7.57	0.002	3.101	1.04–9.25	0.042
ST2 ≥ 18,350 pg/ml	2.59	1.47–4.55	0.001			
OPG ≥ 887 pg/ml	3.44	1.85–6.41	<0.001	2.338	1.02–5.62	0.046
GDF15 ≥ 1,320 pg/ml	2.56	1.35–4.83	0.004			
Model 2 (*n* = 158)						
Age ≥ 77 yo	6.07	2.81–13.11	<0.001			
LAVI ≥ 33.5 ml/m^2	4.37	1.88–10.17	0.001			
NT-pro-BNP ≥ 290 pg/ml	6.83	3.05–15.32	<0.001	4.676	1.66–13.21	0.004
Galectin-3 ≥ 9 ng/ml	7.04	2.04–24.25	0.002	6.587	1.53–28.38	0.011
ST2 ≥ 18,350 pg/ml	2.56	1.23–5.36	0.012			
OPG ≥ 887 pg/ml	2.99	1.34–6.67	0.007	3.350	1.06–10.59	0.040
GDF15 ≥ 1,320 pg/ml	2.72	1.19–6.23	0.018			
PNN50 ≥ 11	5.75	2.67–12.39	<0.001	8.260	2.80–24.41	<0.001
SDNN ≥ 38*	4.34	2.04–9.33	<0.001			

*AF, atrial fibrillation; CI, confidence interval; HR, hazard ratio.*Not included in the multivariate analysis due to collinearity with PNN50 (R = -0.74).*

- Several clinical and imaging parameters, novel blood biomarkers (such as galectin-3 and osteoprotegerin), and electrocardiographic parameters such as PNN50 were associated with AFDAS. We can thus confirm the association between atrial cardiopathy markers and the new concept of AFDAS.
- The use of a multimodal approach based on the 3 key determinants of arrhythmia resulted in highly predictive

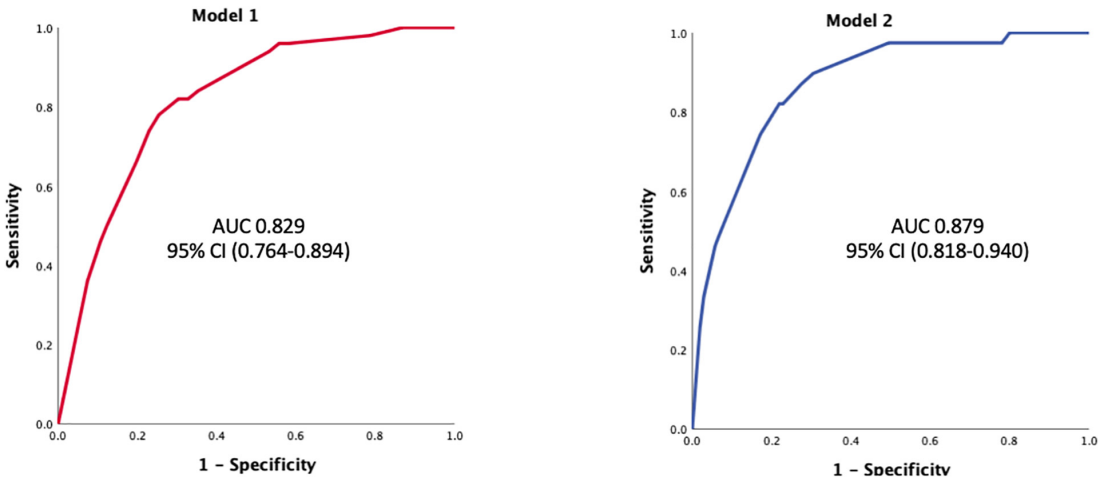

FIGURE 2 | ROC curve for models 1 and 2. Model 1 associates galectin-3 = 9 ng/ml; NT-pro-BNP ≥ 290 pg/ml; OPG ≥ 887 pg/ml and LAVI ≥ 33.5 ml/m^2 for all AFDAS prediction (*n* = 240). Model 2 associates galectin-3 ≥ 9 ng/ml; NT-Pro-BNP ≥ 290 pg/ml; OPG ≥ 887 pg/ml *and* pNN50 ≥ 11 for AFDAS occurring after a stay in the stroke unit: AUC, area under the curve. OPG, osteoprotegerin.

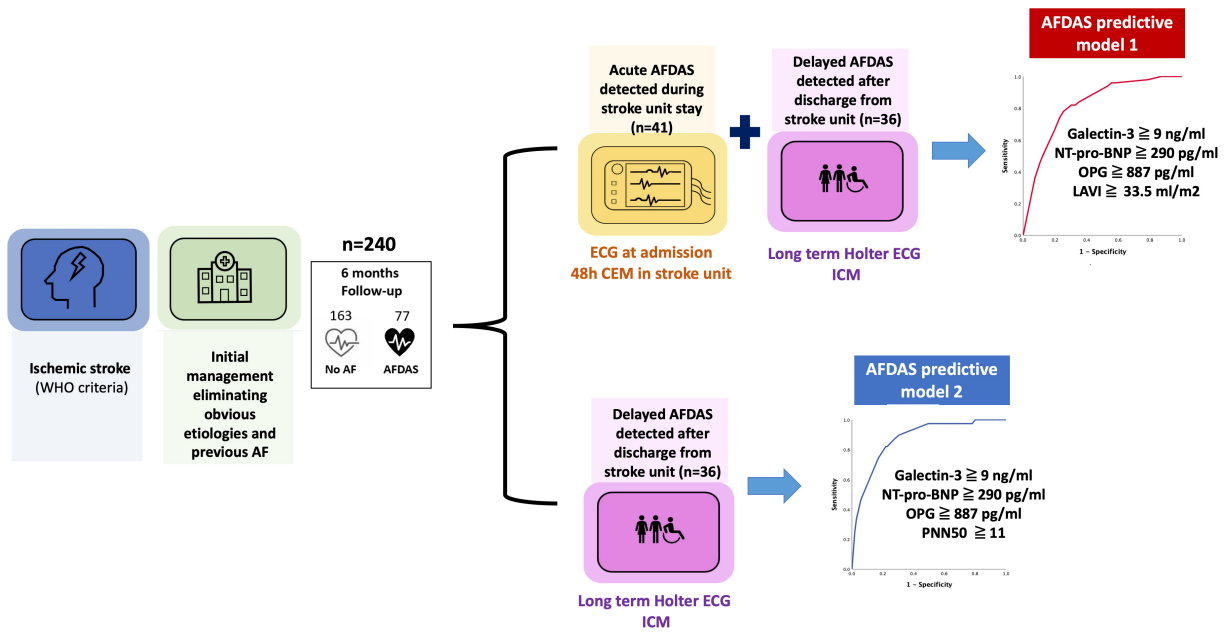

FIGURE 3 | SAFAS study main results.

models of AFDAS. These models could help to better stratify the screening strategy for AFDAS, especially for the use of ICM after hospitalization for stroke.

Left Atrial Substrate: Morphological, Biological and Electrical Assessment

Several studies have demonstrated the association between LA dilatation and AF. Some have even suggested that increased LAVI could be associated with stroke independently of AF onset (14). LA enlargement may promote blood stasis, endothelial damage and thrombus formation (15). This hypothesis is supported by recent data suggesting that atrial fibrosis increases thromboembolic risk regardless of atrial rhythm: this is the concept of atrial cardiopathy (16, 17). In our study, we found a strong association between LA remodeling and AFDAS, as assessed by LA dilatation (increased LA diameter, surface and LAVI). The optimal threshold of LAVI associated with the risk of AF occurrence was 33.5 ml/m^2. This threshold corresponds to the threshold of mild dilatation on echocardiography (18) and is close to the Carrazco study cut-off (30 ml/m^2) (19), but lower than

the threshold of 44–45 ml/m^2 found in some studies that have shown this association in the context of cryptogenic stroke (20).

In addition to LA dimensions, several research teams have suggested the use of electrocardiographic markers of atrial cardiopathy such as $PTFV_1$. This parameter has been associated with increased risk of AF after adjustment for other markers of atrial cardiopathy such as LA dimensions and NT-pro-BNP (21, 22). $PTFV_1$ may be a marker of atrial changes such as fibrosis and elevated filling pressure that are not fully revealed by echocardiographic or serum biomarker assessments. In our study, in a sample of patients (n = 111) in whom these measurements were feasible, we did not find a significant association between these ECG markers and AFDAS, contrary to LA dilatation or biomarkers of atrial substrate. This could be related to the population size or to the inclusion of more powerful markers of atrial cardiopathy in the prediction models.

Moreover, three biomarkers of atrial cardiopathy were associated with AFDAS in our study:

- In both predictive models, galectin-3, a biomarker of fibrosis (23), was independently associated with AFDAS. Galectin-3 blood levels are increased in AF patients, are independently correlated with LA volume (24) and predict AF onset and recurrence after AF ablation (25). Although the exact pathophysiological mechanisms by which galectin-3 promotes AF are still unclear, it appears to play an important role in fibrotic processes. It could therefore be a potential marker of interest for atrial cardiopathy.
- Osteoprotegerin is a protein is expressed in endothelial and smooth muscle cells and is involved in the regulation of the inflammatory response and remodeling of the extracellular matrix (26). Its association with AF was only recently suggested. Cao et al. showed that AF patients had higher atrial gene expression of the OPG/RANK/RANKL axis and a higher RANKL/OPG ratio, particularly in paroxysmal AF (27). This expression was also well correlated with markers of atrial remodeling including markers of apoptosis, pro-inflammatory factors, and the matrix metalloproteinase/tissue inhibitors of metalloproteinases system regulating extracellular matrix degradation (28). OPG could therefore be associated with AF through atrial remodeling processes, and could be suggested as a new marker of atrial cardiopathy.
- NT-proBNP levels are increased in stroke patients diagnosed with AF, and are reported to be higher in case of cardioembolic stroke (29, 30). In our study, NT-proBNP values over 290 pg/ml were significantly associated with the occurrence of AFDAS in both models, a threshold comparable to another study on cryptogenic stroke (30). Moreover, NT-proBNP levels > 250 pg/ml were used as a surrogate of atrial cardiopathy in the ARCADIA study (31). Finally, in the TARGET-AF study of stroke patients whose AF was detected by early and prolonged heart rate recordings, Suissa et al. suggested that low BNP levels could virtually exclude the risk of secondary AF (32). These findings suggest that this biomarker could be of great clinical value for targeted AF screening given its strong and independent predictive value of AFDAS in our study.

Taken together, these results suggest that these biomarkers could be of great clinical value for targeted AF screening and atrial cardiopathy diagnosis, given their strong and independent predictive value of AFDAS.

Modulator

The ANS acts as a modulator of AF onset through the modulation of atrial electro-physiological properties. Adami et al. demonstrated that patients with R-R interval variability after ischemic stroke had an increased risk of AF (33). In our second multivariate model, pNN50 $\geqq$ 11 was associated with an eightfold higher risk of AFDAS in patients without previous evidence of AF on ECG at admission or during CEM in the stroke unit. This analysis is particularly interesting because these data can be automatically extracted from CEM data in the stroke unit, making it feasible in routine clinical practice. We suggest that, if confirmed in further studies, temporal HRV measurements could be included in the cardiac work-up after stroke, similar to LAVI or NT-pro-BNP levels.

Atrial Fibrillation Triggers

Inflammation plays a role in the initiation, persistence and recurrence of AF. In our study, several inflammatory mediators know (ST2, GDF15, CRP) were associated with the occurrence of AF in bivariate analysis but did not remain significantly associated with AF in our predictive models. This suggests that the pathophysiology of AFDAS is more likely to involve chronic remodeling (atrial cardiopathy) rather that acute triggers such as inflammation or acute myocardial dysfunction.

Finally, the prognostic significance of AFDAS remains uncertain. Further studies are needed to assess the benefit of anticoagulants in AFDAS on the risk of stroke recurrence. In this regard, the ARCADIA trial, which aims to compare an anticoagulant strategy with apixaban vs. aspirin in patients with cerebral infarction of undetermined etiology with recognized markers of atrial cardiopathy (P-wave terminal force > 5,000 μV.ms in V1, serum NT-pro-BNP > 250 pg/mL, or left atrial diameter index ≥ 3 cm/m^2) (31) should add significant knowledge to this clinical issue.

Limitations

Our study has certain limitations. First, it was a monocentric study on a population based exclusively at the Dijon University Hospital, and we excluded patients referred by other hospitals, which limited the number of inclusions. In addition, some patients with ischemic stroke were not admitted to the stroke unit and therefore could not be included. The study follow-up was limited to 6 months in the study design, in contrast to some studies that completed up to 3 years of monitoring (1, 19). This could have led to an underestimation of AF incidence and to false negatives in the sinus rhythm group. However, in the study by Carrazco et al. 80% of AF cases were diagnosed within the first 6 months of screening (19).

CONCLUSION

In order to improve the cost-effectiveness of long-term external Holter recordings and ICM implantations, it is essential to target the patients most at risk of AFDAS, who should benefit from a prolonged rhythm screening strategy. Our multimodal approach combining imaging, electrocardiography and original biological markers of atrial cardiopathy resulted in good predictive models for AFDAS at 6-month follow-up. These results also suggest that AFDAS is probably not be an epiphenomenon related to the acute stroke but rather related to underlying atrial cardiopathy. Further studies are needed to evaluate the embolic risk and the indication for anticoagulation in these AFDAS patients.

DATA AVAILABILITY STATEMENT

The raw data supporting the conclusions of this article will be made available by the authors, without undue reservation.

ETHICS STATEMENT

The studies involving human participants were reviewed and approved by the CPP Sud Méditerranée I n°2018-A00345-50. Written informed consent for participation was not required for this study in accordance with the national legislation and the institutional requirements.

AUTHOR CONTRIBUTIONS

LG, GDu, AS, AM, GDo, RD, MG, YB, CV, and CG: substantial contributions to the conception, design of the work, the acquisition, analysis, and interpretation of data for the work. KB, TP, CV, YB, and CG: drafting the work and revising it critically for important intellectual content. All authors have substantially approved its submission to the journal and are prepared to take public responsibility for the work.

FUNDING

The SAFAS study was funded by an unrestricted grant from Microport CRM. The funder was not involved in the study design, collection, analysis, interpretation of data, the writing of this article or the decision to submit it for publication.

ACKNOWLEDGMENTS

We thank Suzanne Rankin for English revision of the manuscript.

REFERENCES

1. Sanna T, Diener HC, Passman RS, Di Lazzaro V, Bernstein RA, Morillo CA, et al. Cryptogenic stroke and underlying atrial fibrillation. *N Engl J Med.* (2014) 370:2478–86. doi: 10.1056/NEJMoa1313600
2. Sposato LA, Cipriano LE, Saposnik G, Vargas ER, Riccio PM, Hachinski V. Diagnosis of atrial fibrillation after stroke and transient ischaemic attack: a systematic review and meta-analysis. *Lancet Neurol.* (2015) 14:377–87. doi: 10.1016/S1474-4422(15)70027-X
3. Dilaveris PE, Kennedy HL. Silent atrial fibrillation: epidemiology, diagnosis, and clinical impact. *Clin Cardiol.* (2017) 40:413–8. doi: 10.1002/clc.22667
4. Hart RG, Diener HC, Coutts SB, Easton JD, Granger CB, O'Donnell MJ, et al. Embolic strokes of undetermined source: the case for a new clinical construct. *Lancet Neurol.* (2014) 13:429–38. doi: 10.1016/S1474-4422(13)70310-7
5. Brachmann J, Morillo CA, Sanna T, Di Lazzaro V, Diener HC, Bernstein RA, et al. Uncovering atrial fibrillation beyond short-term monitoring in cryptogenic stroke patients: three-year results from the cryptogenic stroke and underlying atrial fibrillation trial. *Circ Arrhythm Electrophysiol.* (2016) 9:e003333. doi: 10.1161/CIRCEP.115.003333
6. Diener HC, Sacco RL, Easton JD, Granger CB, Bernstein RA, Uchiyama S, et al. Dabigatran for prevention of stroke after embolic stroke of undetermined source. *N Engl J Med.* (2019) 380:1906–17. doi: 10.1056/NEJMoa1813959
7. Hart RG, Sharma M, Mundl H, Kasner SE, Bangdiwala SI, Berkowitz SD, et al. Rivaroxaban for stroke prevention after embolic stroke of undetermined source. *N Engl J Med.* (2018) 378:2191–201.
8. Sposato LA, Chaturvedi S, Hsieh CY, Morillo CA, Kamel H. Atrial fibrillation detected after stroke and transient ischemic attack: a novel clinical concept challenging current views. *Stroke.* (2022) 53:e94–103. doi: 10.1161/STROKEAHA.121.034777
9. Coumel P, Maison-Blanche P. Complex dynamics of cardiac arrhythmias. *Chaos Interdiscip J Nonlinear Sci.* (1991) 1:335–42. doi: 10.1063/1.165845
10. Kernan WN, Ovbiagele B, Black HR, Bravata DM, Chimowitz MI, Ezekowitz MD, et al. Guidelines for the prevention of stroke in patients with stroke and transient ischemic attack: a guideline for healthcare professionals from the American heart association/American stroke association. *Stroke.* (2014) 45:2160–236. doi: 10.1161/STR.0000000000000024
11. Kirchhof P, Benussi S, Kotecha D, Ahlsson A, Atar D, Casadei B, et al. 2016 ESC Guidelines for the management of atrial fibrillation developed in collaboration with EACTS. *Europace.* (2016) 18:1609–78. doi: 10.5603/KP.2016.0172
12. Sagnard A, Guenancia C, Mouhat B, Maza M, Fichot M, Moreau D, et al. Involvement of autonomic nervous system in new-onset atrial fibrillation during acute myocardial infarction. *J Clin Med.* (2020) 9:1481. doi: 10.3390/jcm9051481
13. Adams HP, Bendixen BH, Kappelle LJ, Biller J, Love BB, Gordon DL, et al. Classification of subtype of acute ischemic stroke. Definitions for use in a multicenter clinical trial. TOAST. Trial of Org 10172 in acute stroke treatment. *Stroke.* (1993) 24:35–41. doi: 10.1161/01.STR.24.1.35
14. Hamatani Y, Ogawa H, Takabayashi K, Yamashita Y, Takagi D, Esato M, et al. Left atrial enlargement is an independent predictor of stroke and systemic embolism in patients with non-valvular atrial fibrillation. *Sci Rep.* (2016) 6:31042. doi: 10.1038/srep31042
15. Anaissie J, Monlezun D, Seelochan A, Siegler JE, Chavez-Keatts M, Tiu J, et al. Left atrial enlargement on transthoracic echocardiography predicts left atrial thrombus on transesophageal echocardiography in ischemic stroke patients. *BioMed Res Int.* (2016) 2016:7194676. doi: 10.1155/2016/7194676
16. Calenda BW, Fuster V, Halperin JL, Granger CB. Stroke risk assessment in atrial fibrillation: risk factors and markers of atrial myopathy. *Nat Rev Cardiol.* (2016) 13:549–59. doi: 10.1038/nrcardio.2016.106
17. Kamel H, Healey JS. Cardioembolic stroke. *Circ Res.* (2017) 120:514–26. doi: 10.1161/CIRCRESAHA.116.308407
18. Lang RM, Badano LP, Mor-Avi V, Afilalo J, Armstrong A, Ernande L, et al. Recommendations for cardiac chamber quantification by echocardiography in adults: an update from the American Society of Echocardiography and the European association of cardiovascular imaging. *Eur Heart J Cardiovasc Imaging.* (2015) 16:233–70. doi: 10.1093/ehjci/jev014

19. Carrazco C, Golyan D, Kahen M, Black K, Libman RB, Katz JM. Prevalence and risk factors for paroxysmal atrial fibrillation and flutter detection after cryptogenic ischemic stroke. *J Stroke Cerebrovasc Dis Off J Natl Stroke Assoc.* (2018) 27:203–9. doi: 10.1016/j.jstrokecerebrovasdis.2017.08.022
20. Tsang TS, Barnes ME, Bailey KR, Leibson CL, Montgomery SC, Takemoto Y, et al. Left atrial volume: important risk marker of incident atrial fibrillation in 1655 older men and women. *Mayo Clin Proc.* (2001) 76:467–75. doi: 10.4065/76.5.467
21. Kamel H, Bartz TM, Elkind MSV, Okin PM, Thacker EL, Patton KK, et al. Atrial cardiopathy and the risk of ischemic stroke in the CHS (Cardiovascular Health Study). *Stroke.* (2018) 49:980–6. doi: 10.1161/STROKEAHA.117.020059
22. Kamel H, Hunter M, Moon YP, Yaghi S, Cheung K, Di Tullio MR, et al. Electrocardiographic left atrial abnormality and risk of stroke: Northern Manhattan study. *Stroke.* (2015) 46:3208–12. doi: 10.1161/STROKEAHA.115.009989
23. Yu L, Ruifrok WPT, Meissner M, Bos EM, van Goor H, Sanjabi B, et al. Genetic and pharmacological inhibition of galectin-3 prevents cardiac remodeling by interfering with myocardial fibrogenesis. *Circ Heart Fail.* (2013) 6:107–17. doi: 10.1161/CIRCHEARTFAILURE.112.971168
24. Gurses KM, Yalcin MU, Kocyigit D, Canpinar H, Evranos B, Yorgun H, et al. Effects of Persistent atrial fibrillation on serum galectin-3 levels. *Am J Cardiol.* (2015) 115:647–51. doi: 10.1016/j.amjcard.2014.12.021
25. Gong M, Cheung A, Wang Q, Li G, Goudis CA, Bazoukis G, et al. Galectin-3 and risk of atrial fibrillation: a systematic review and meta-analysis. *J Clin Lab Anal.* (2020) 34:e23104. doi: 10.1002/jcla.23104
26. Rochette L, Meloux A, Rigal E, Zeller M, Cottin Y, Vergely C. The role of osteoprotegerin in the crosstalk between vessels and bone: its potential utility as a marker of cardiometabolic diseases. *Pharmacol Ther.* (2018) 182:115–32. doi: 10.1016/j.pharmthera.2017.08.015
27. Cao H, Li Q, Li M, Od R, Wu Z, Zhou Q, et al. Osteoprotegerin/RANK/RANKL axis and atrial remodeling in mitral valvular patients with atrial fibrillation. *Int J Cardiol.* (2013) 166:702–8. doi: 10.1016/j.ijcard.2011.11.099
28. Cao H, Wang J, Xi L, Røe OD, Chen Y, Wang D. Dysregulated atrial gene expression of osteoprotegerin/receptor activator of nuclear factor-κB (RANK)/RANK ligand axis in the development and progression of atrial fibrillation. *Circ J Off J Jpn Circ Soc.* (2011) 75:2781–8. doi: 10.1253/circj.CJ-11-0795
29. Rodriguez-Yanez M, Arias-Rivas S, Santamaria-Cadavid M, Sobrino T, Castillo J, Blanco M. High pro-BNP levels predict the occurrence of atrial fibrillation after cryptogenic stroke. *Neurology.* (2013) 81:444–7. doi: 10.1212/WNL.0b013e31829d8773
30. Fonseca AC, Matias JS, Pinho e Melo T, Falcão F, Canhão P, Ferro JM. N-Terminal probrain natriuretic peptide as a biomarker of cardioembolic stroke. *Int J Stroke.* (2011) 6:398–403. doi: 10.1111/j.1747-4949.2011.00606.x
31. Kamel H, Longstreth W, Tirschwell DL, Kronmal RA, Broderick JP, Palesch YY, et al. The atrial cardiopathy and antithrombotic drugs in prevention after cryptogenic stroke randomized trial: rationale and methods. *Int J Stroke.* (2019) 14:207–14. doi: 10.1177/1747493018799981
32. Suissa L, Bresch S, Lachaud S, Mahagne MH. Brain natriuretic peptide: a relevant marker to rule out delayed atrial fibrillation in stroke patient. *J Stroke Cerebrovasc Dis.* (2013) 22:e103–10. doi: 10.1016/j.jstrokecerebrovasdis.2012.08.010
33. Adami A, Gentile C, Hepp T, Molon G, Gigli GL, Valente M, et al. Electrocardiographic RR interval dynamic analysis to identify acute stroke patients at high risk for atrial fibrillation episodes during stroke unit admission. *Transl Stroke Res.* (2018) 10:273–8. doi: 10.1007/s12975-018-0645-8

Conflict of Interest: The authors declare that the research was conducted in the absence of any commercial or financial relationships that could be construed as a potential conflict of interest.

Publisher's Note: All claims expressed in this article are solely those of the authors and do not necessarily represent those of their affiliated organizations, or those of the publisher, the editors and the reviewers. Any product that may be evaluated in this article, or claim that may be made by its manufacturer, is not guaranteed or endorsed by the publisher.

frontiers | Frontiers in Cardiovascular Medicine

TYPE Original Research
PUBLISHED 22 July 2022
DOI 10.3389/fcvm.2022.964694

OPEN ACCESS

EDITED BY
Marina Cerrone,
New York University, United States

REVIEWED BY
Ibrahim El-Battrawy,
Ruhr University Bochum, Germany
Michael Cutler,
Intermountain Medical Center Heart Institute, United States
Giuseppe Ciconte,
IRCCS San Donato Polyclinic, Italy

*CORRESPONDENCE
Federico Migliore
federico.migliore@unipd.it

†These authors share senior authorship

SPECIALTY SECTION
This article was submitted to Cardiac Rhythmology, a section of the journal Frontiers in Cardiovascular Medicine

RECEIVED 08 June 2022
ACCEPTED 30 June 2022
PUBLISHED 22 July 2022

CITATION
Migliore F, Martini N, Calo' L, Martino A, Winnicki G, Vio R, Condello C, Rizzo A, Zorzi A, Pannone L, Miraglia V, Sieira J, Chierchia G-B, Curcio A, Allocca G, Mantovan R, Salghetti F, Curnis A, Bertaglia E, De Lazzari M, de Asmundis C and Corrado D (2022) Predictors of late arrhythmic events after generator replacement in Brugada syndrome treated with prophylactic ICD.
Front. Cardiovasc. Med. 9:964694.
doi: 10.3389/fcvm.2022.964694

Predictors of late arrhythmic events after generator replacement in Brugada syndrome treated with prophylactic ICD

Federico Migliore[1]*, Nicolò Martini[1], Leonardo Calo'[2], Annamaria Martino[2], Giulia Winnicki[1], Riccardo Vio[1], Chiara Condello[1], Alessandro Rizzo[1], Alessandro Zorzi[1], Luigi Pannone[3], Vincenzo Miraglia[3], Juan Sieira[3], Gian-Battista Chierchia[3], Antonio Curcio[4], Giuseppe Allocca[5], Roberto Mantovan[5], Francesca Salghetti[6], Antonio Curnis[6], Emanuele Bertaglia[1], Manuel De Lazzari[1], Carlo de Asmundis[3†] and Domenico Corrado[1†]

[1]Department of Cardiac, Thoracic, Vascular Sciences and Public Health, University of Padova, Padova, Italy, [2]Department of Cardiology, Policlinico Casilino, Rome, Italy, [3]Heart Rhythm Management Centre, Postgraduate Program in Cardiac Electrophysiology and Pacing, Universitair Ziekenhuis Brussel-Vrije Universiteit Brussel, European Reference Networks Guard-Heart, Brussels, Belgium, [4]Division of Cardiology, Department of Medical and Surgical Sciences, Magna Graecia University, Catanzaro, Italy, [5]Department of Cardiology, S.Maria dei Battuti Hospital, Conegliano, Italy, [6]Spedali Civili Hospital, University of Brescia, Brescia, Italy

Introduction: Predictors of late life-threatening arrhythmic events in Brugada syndrome (BrS) patients who received a prophylactic ICD implantation remain to be evaluated. The aim of the present long-term multicenter study was to assess the incidence and clinical-electrocardiographic predictors of late life-threatening arrhythmic events in BrS patients with a prophylactic implantable cardioverter defibrillator (ICD) and undergoing generator replacement (GR).

Methods: The study population included 105 patients (75% males; mean age 45 ± 14years) who received a prophylactic ICD and had no arrhythmic event up to first GR.

Results: The median period from first ICD implantation to last follow-up was 155 (128–181) months and from first ICD Implantation to the GR was 84 (61–102) months. During a median follow-up of 57 (38–102) months after GR, 10 patients (9%) received successful appropriate ICD intervention (1.6%/year). ICD interventions included shock on ventricular fibrillation ($n = 8$ patients), shock on ventricular tachycardia ($n = 1$ patient), and antitachycardia pacing on ventricular tachycardia ($n = 1$ patient). At survival analysis, history of atrial fibrillation (log-rank test; $P = 0.02$), conduction disturbances (log-rank test; $P < 0.01$), S wave in lead I (log-rank test; $P = 0.01$) and first-degree atrioventricular block (log-rank test; $P = 0.04$) were significantly associated with the occurrence of late appropriate ICD intervention. At Cox-regression

multivariate analysis, S-wave in lead I was the only independent predictor of late appropriate ICD intervention (HR: 9.17; 95%CI: 1.15–73.07; $P = 0.03$).

Conclusions: The present study indicates that BrS patient receiving a prophylactic ICD may experience late appropriate intervention after GR in a clinically relevant proportion of cases. S-wave in lead I at the time of first clinical evaluation was the only independent predictor of persistent risk of life-threatening arrhythmic events. These findings support the need for GR at the end of service regardless of previous appropriate intervention, mostly in BrS patients with conduction abnormalities.

KEYWORDS

Brugada syndrome, implantable cardioverter-defibrillator, risk stratification, sudden cardiac death, complications

Introduction

Risk stratification and management of patients with Brugada syndrome (BrS), principally asymptomatic, still remain challenging (1–6). Many prognostic markers have been proposed, such as male gender, spontaneous type 1 BrS ECG pattern, positive electrophysiological study (EPS), fever, and resting situation (7–13). The role of genetic on risk stratification has been questioned. However, specific genetic mutations may be predictive, such as the combination of a SCN5A mutation with malignant arrhythmic events, ECG conduction abnormalities and the extent of the electrophysiological abnormalities (14, 15). In addition, ECG and imaging markers (16) seem to be useful for risk stratification. The predictive value of these parameters is based on non-invasive assessment of depolarization and repolarization parameters (17), such as: prolongation of PR interval (18), increase of QRS duration (19), fragmented QRS (f-QRS) (20, 21), S-wave in lead I (22), prolongation of QT interval or early repolarization (ER) pattern (23, 24). Even today, the implantable cardioverter-defibrillator (ICD) is the mainstay of treatment of BrS patients, although it is associated with high complication rates, including inappropriate shocks (IS) and lead failure (1–3, 25–27). Thus, when considering ICD implantation in BrS patients the risk/benefit balance should be considered. The subset of BrS patients requiring generator replacement (GR) who received a prophylactic ICD and did not experience appropriate interventions during the life of the first implantation rises challenging problems of management. Data on the arrhythmic outcome and predictors of late life-threatening arrhythmic events in this unique group of BrS patients after GR are incompletely established. The aim of the present long-term multicenter study was to assess the incidence and clinical-electrocardiographic predictors of late life-threatening arrhythmias in BrS patients treated with prophylactic ICD and undergoing GR.

Methods

The study population included BrS patients, with spontaneous or drug induced Type 1 ECG pattern who received a prophylactic ICD either transvenous ICD (TV-ICD) or subcutaneous ICD (S-ICD) and had no arrhythmic event up to first GR. The patients were enrolled at six centers (Cardiology Department of the University of Padova, Hospital of Conegliano, the University of Brescia, the University Hospital of Catanzaro, the Casilino Hospital of Rome and the Universitair Ziekenhuis Brussel), between January 1996 and September 2020. Herein, an ICD was defined as "prophylactic" when it was implanted in patients without prior sustained ventricular tachycardia (VT) or ventricular fibrillation (VF) who were considered at high risk of sudden cardiac death (SCD) on the basis of current recognized risk factors (1–10). In the case of a transvenous defibrillator implant, the type of venous access (subclavian, axillary, or cephalic vein), the type of lead fixation (passive or active), and the type of device (single or dual chamber) were at the discretion of the physician. Furthermore, the choice of implanting an S-ICD rather than a TV-ICD was also at discretion of the physician, according to current guidelines (28). Brugada syndrome was diagnosed as previously reported (1, 2). Provocative drug test using ajmaline (1 mg/kg in 5–10 min) or flecainide (2 mg/kg in 5 min) was administered intravenously to unmask the diagnostic ECG pattern of BrS in case of a non-diagnostic baseline electrocardiogram (1, 2). Family history of BrS, or sudden cardiac death (first-degree family member died suddenly at age <45 years old in the absence of known heart disease), medical history, physical examination, baseline ECG, results of provocative drug test, EPS when performed and indications for ICD implantation were collected in all patients. Underlying structural cardiac abnormalities were excluded in each patient. Patients presenting with syncope were considered as symptomatic. Syncope was defined as a non-traumatic transient loss of consciousness and spontaneous complete

recovery (29). The study was conducted in compliance with the Declaration of Helsinki, approved by the local ethics committee (Comitato Etico per la Sperimentazione Clinica, Azienda Ospedaliera di Padova, Italy) and all patients signed informed consent.

Electrocardiogram

Baseline 12-lead ECG (speed of 25 mm/s, 1 mV/10 mm gain, and 0.05–150 Hz filter) was recorded in each patient at the first clinical evaluation. The following parameters were recorded in leads II and V6: the RR interval, PQ interval, QRS duration, JT interval, and corrected QT interval. The QTc interval was calculated with the Bazett's formula. In leads V1 to V3, the maximal ST-segment elevation was measured at the J-point (STJ). An electrocardiogram was considered diagnostic of BrS if a coved-type ST-segment elevation of $\geq$2 mm (Type 1) was documented in $\geq$1 lead from V1 to V3 positioned in the 2nd, 3rd, or 4th intercostal space, in the presence or absence of a sodium-channel blocker. Conduction disturbances were defined as the presence of at least one of the following conduction abnormalities on basal ECG: first-degree atrio-ventricular (AV) block, prolonged QRS duration, f-QRS, and S-wave in lead I. A QRS interval duration >120 ms was considered prolonged. First-degree AV block was considered in the presence of a PR interval >200 ms. Left bundle branch block, right bundle branch block, left anterior fascicular block, and left posterior fascicular block were defined in accordance with current guidelines (30). Abnormal fragmentation of the QRS complex was defined as the presence of multiple spikes within the QRS complex as described previously (20). The presence of an S-wave $\geq$ 0.1 mV and/or >40 ms in lead I was examined as described previously (22). Early repolarization pattern was defined as an elevation of the J-point of at least 1 mm above the baseline level, in at least two consecutive inferior (II, III, aVF) or lateral (I, aVL, and V4 to V6) leads either as QRS slurring or notching (2, 23, 24). Two independent experienced electrophysiologists analyzed all the electrocardiograms. In cases of disagreement, a third physician was consulted.

Electrophysiological study

The EPS included basal measurements of conduction intervals (baseline AH and HV intervals) and programmed ventricular stimulation. The protocol used was at discerption of the center. A maximum of 3 ventricular extrastimuli (with minimum coupling interval of 200 ms) were delivered. A patient was considered inducible if a sustained ventricular arrhythmia, such as VF, VT, or monomorphic VT lasting >30 s or requiring termination because of hemodynamic compromise was induced. Inducibility at EPS was deemed as an indication for ICD implantation (1, 2).

Follow-up

The primary endpoint of the study was to assess the late arrhythmic outcome defined as a combined endpoint including cardiac arrest/sudden cardiac death (SCD) and appropriate ICD therapy which occurred after GR. Appropriate ICD therapy was defined as an ICD shock delivered in response to VT or VF or anti-tachycardia pacing (ATP) in response to VT and documented by stored intracardiac ECG data during outpatient evaluation or at the remote monitoring. The secondary endpoint was to evaluate a combined endpoint of device-related complications requiring surgical revision and IS after GR. Inappropriate shocks were defined as those delivered in the absence of ventricular arrhythmia.

Statistical analysis

Categorical variables were described as frequencies (percentages) and differences between groups were evaluated by using the X^2-test or the Fisher exact test as appropriate. Normal distribution of continuous variables was assessed by using the Shapiro-Wilk test. Continuous variables were expressed as mean $\pm$ standard deviation (SD) or median (25th−75th percentiles) for normally distributed and skewed variables, respectively, and compared with the Student's *t*-test or the Mann–Whitney *U*-test, as appropriate. The mean event rate per year was evaluated by the number of events occurring during the follow-up divided by the number of patients multiplied by the average duration of follow-up. Survival analysis was performed visually through Kaplan–Meier survival curves, which were later compared using the log-rank test. Patients were censored at the time of the first event or at the time of the last follow-up. Univariate analysis was performed using the Cox proportional hazards model. Variables with a $P < 0.05$ at univariate analysis were entered into the multivariate model. A $p < 0.05$ was considered statistically significant. Statistical analyses were conducted using STATA version 14.1 (STATA Corporation, College Station, TX, USA).

Results

Baseline clinical characteristics at enrolment

The study population consisted of 105 patients (79 males; 75%) with a mean age at first ICD implantation of 45 $\pm$ 14 years who underwent GR. Ninety-five patients (90.5%) received a TV-ICD and 10 patients (9.5%) an S-ICD. Table 1 shows the

10.3389/fcvm.2022.964694

TABLE 1 Clinical and electrocardiographic characteristics of the study population.

Variables	(*N* = 105)
Age at first implantation (years)	45 ± 14
Age at GR (years)	52 ± 14
Male sex, *n* (%)	79 (75)
Family history of BrS, *n* (%)	34 (32)
Family history of SCD, *n* (%)	48 (46)
Syncope, *n* (%)	61 (58)
History of AF, *n* (%)	25 (24)
Positive EPS	52/90 (58)
Basal electrocardiogram	
Spontaneous Brugada type 1, *n* (%)	53 (50)
Early repolarization, *n* (%)	4 (4)
QTc prolongation, *n* (%)	4 (4)
Conduction disturbances, *n* (%)	55 (52)
First degree AV block, *n* (%)	18 (17)
QRS fragmented or prolonged, *n* (%)	13 (12)
S-wave in lead I, *n* (%)	46 (44)

AF, atrial fibrillation; AV, atrioventricular; BrS, Brugada syndrome; EPS, electrophysiological study; GR, generator replacement; SCD, sudden cardiac death.

clinical characteristics of the study population. At enrollment, no patient had a history of previous cardiac arrest; 61 patients (58%) were symptomatic for syncope, 25 (24%) reported a history of paroxysmal atrial fibrillation (AF) and 44 (42%) were asymptomatic. A spontaneous type 1 ECG was documented in 53 patients (50%). A family history of BrS or SCD was ascertained in 34 (32%) and 48 (46%) patients, respectively. Of 90 patients (86%) undergoing EPS, 52 (58%) were inducible. All patients received a prophylactic ICD because of syncope ($n = 61$), inducibility at EPS ($n = 52$) or both. After the first ICD implantation 30 patients (28.5%) experienced a total of 37 device-related complications including IS ($n = 6$), lead failure ($n = 9$), pocket hematoma ($n = 8$), pocket infection ($n = 6$), pneumothorax ($n = 3$), device dislocation ($n = 2$), systemic infection ($n = 1$), lead dislocation ($n = 1$), cardiac perforation ($n = 1$). The median period from first ICD implantation to last follow-up was 155 (128–181) months and from first ICD implantation to the GR was 84 (61–102) months.

Electrocardiographic findings at first clinical evaluation

Table 1 shows the electrocardiographic findings of the study population. Conduction disturbances were found in 55 patients (52%) A first-degree AV block was documented in 18 patients (17%, mean PR duration 221 ± 16 ms). Prolonged QRS duration was observed in 9 subject (8%); 4 (4%) showed a f-QRS in leads V1, V2, V3 while 4 patients (4%) a prolonged QTc interval. Left anterior fascicular block was present in 7 patients (6%). A prominent S-wave in lead I was documented in 46 patients (44%). Early repolarization pattern was present in 4 patients (4%). No patient had a BrS pattern in leads other than V1–V3.

Generator replacement

No patient experienced major arrhythmic events including appropriate ICD intervention before GR. Reasons for GR were: battery depletion ($n = 86$; 82%), transvenous lead failure ($n = 9$; 8.5%), pocket infection ($n = 6$; 6%), device dislocation/cardiac perforation ($n = 3$, 2.8%) and systemic infection ($n = 1$;1%). Lead failure and infection were indication for transvenous lead extraction. The replacing device was the same type of ICD (TV-ICD or S-ICD) implanted at first in all patients.

Follow-up after generator replacement

The median follow-up after GR was 57 [38–102] months. Ten patients (9%) received successful ≥1 appropriate ICD intervention after GR (1.6%/year). The first intervention included shock on VF ($n = 8$ patients), shock on VT ($n = 1$ patient) and ATP on VT ($n = 1$ patient). Appropriate shocks occurred in 6 of the asymptomatic patients (6/44;13.6%; Figure 1). The median time to first appropriate ICD therapy was 108 (101–137) months from the first ICD implantation and 41 [25–55] after GR. Patients who experienced an appropriate ICD intervention had significantly more often a history of paroxysmal AF ($P = 0.01$) compared with patients without appropriate ICD intervention (Table 2). No significant difference between patients who did and did not have arrhythmic events during follow-up with regard to age, gender, family history for BrS or SCD and EPS result was observed. Among the ECG parameters, the presence of conduction abnormalities ($P = 0.001$) and S-wave in lead I ($P = 0.005$) were significantly associated with arrhythmic events (Table 2). At survival analysis, history of AF (log-rank test; $P = 0.02$), conduction disturbances (log-rank test; $P < 0.01$), S wave in lead I (log-rank test; $P = 0.01$) and first-degree AV block (log-rank test; $P = 0.04$) were significantly associated with the occurrence of late appropriate ICD intervention (Figures 2A–D). All patients without conduction disturbances had an uneventful follow-up for appropriate ICD intervention (Figure 2B).

After GR replacement 7 patients (6.6%) experienced a total of 12 device-related complications (1.7%/year) including IS ($n = 3$), lead failure ($n = 4$), pocket hematoma ($n = 1$), pocket infection ($n = 1$), and device dislocation ($n = 3$). Among patients with an S-ICD, 2 (20%) experienced IS. Univariate predictors of late arrhythmic events included a history of AF (HR: 4.11; 95% CI: 1.15–14.78; $P = 0.03$) and S-wave in lead

10.3389/fcvm.2022.964694

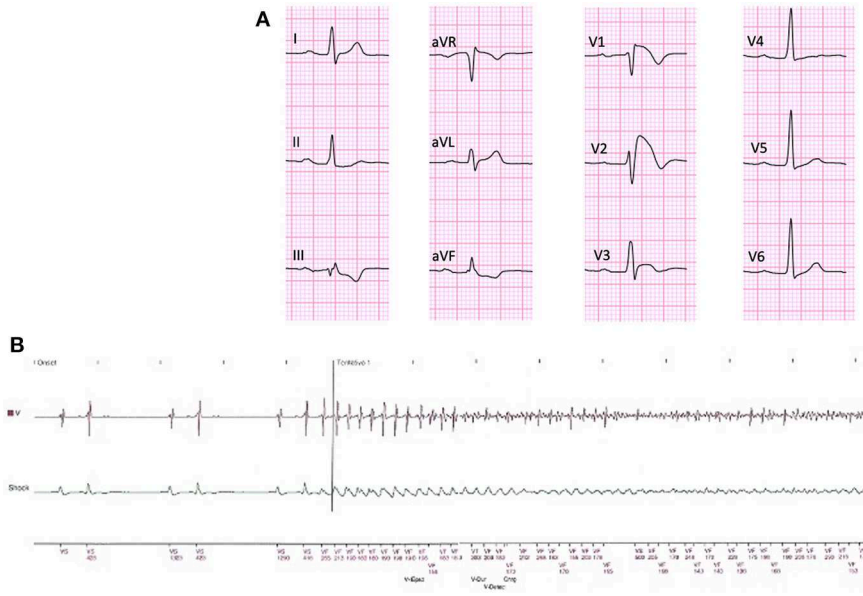

FIGURE 1
Baseline ECG of an asymptomatic BrS patient who experienced VF 4 years and 6 months after generator replacement. Note the presence of first-degree AV block and S-wave in lead I as well as spontaneous "coved type" ECG pattern in leads V1 and V2 **(A)**. Intracardiac electrocardiogram obtained from the transvenous ICD remote monitoring showing the onset of VF, triggered by a premature ventricular contraction and its offset by the ICD shock **(B)**.

TABLE 2 Baseline clinical and electrocardiographic findings according to late appropriate ICD intervention.

Variable	ICD therapy – ($N = 95$)	ICD therapy + ($N = 10$)	*P*-value
Age at GR (years)	45 ± 14	45 ± 15	0.79
Male sex, *n* (%)	71 (75)	8 (80)	1.00
Family history of BrS, *n* (%)	31 (33)	3 (30)	1.00
Family history of SCD, *n* (%)	43 (45)	5 (50)	1.00
Syncope, *n* (%)	57 (60)	4 (40)	0.31
History of AF, *n* (%)	19 (20)	6 (60)	0.01
Positive EPS	46 (55)	6 (86)	0.53
Basal electrocardiogram			
Spontaneous Brugada type 1, *n* (%)	48 (51)	5 (50)	1.00
Early repolarization, *n* (%)	3 (3)	1 (10)	0.33
QTc, *n* (%)	3 (3)	1 (10)	0.33
Conduction disturbances, *n* (%)	45 (47)	10 (100)	0.001
First degree AV block, *n* (%)	14 (15)	4 (40)	0.06
QRS fragmented or prolonged, *n* (%)	10 (10)	3 (30)	0.10
S-wave in lead I, *n* (%)	37 (39)	9 (90)	0.005

AF, atrial fibrillation; AV, atrioventricular; BrS, Brugada syndrome; EPS, electrophysiological study; GR, generator replacement; SCD, sudden cardiac death.

I (HR: 10.12; 95% CI: 1.28–79.97; $P = 0.02$) (Table 3). In the multivariate model, only S-wave in lead I remained a significant independent predictor of late arrhythmic outcome (HR: 9.17; 95% CI: 1.15–73.07; $P = 0.03$) (Table 3).

Discussion

The aim of the present long-term multicenter study was to assess the incidence and clinical-electrocardiographic predictors of late life-threatening arrhythmias in BrS patients treated with prophylactic ICD and undergoing GR. The main findings are the following: (1) over a long-term follow-up, the risk of late appropriate ICD therapy after GR remains clinically relevant in up to 9% of patients; (2) late arrhythmic events during follow-up were significantly associated with a history of AF and conduction abnormalities detected at baseline clinical evaluation (first-degree AV block and S-wave in lead I); (3) at multivariate analysis the presence of S-wave in lead I remained the only independent predictor of life-threatening arrhythmias. These findings support the need for GR at the end of service regardless of previous appropriate intervention, mostly in BrS patients with conduction abnormalities.

Risk stratification in BrS remains a clinical challenge. According to previous studies, history of cardiac arrest or syncope are the strongest predictors of SCD (4–10). The prognostic value of a history of familial SCD (1, 2), positive genetic testing for a SCN5A-gene mutation (1, 2) and history of AF (31) is less well-established. It is known that SCN5A-gene mutation is a major contributor of BrS.

TABLE 3 Univariate and multivariate cox regression analysis for predictors of late appropriate ICD intervention.

Variable	Univariate analysis		Multivariate analysis	
	HR (95% CI)	*P*-value	HR (95% CI)	*P*-value
Age <50 years-old at GR	1.21 (0.32–4.51)	0.78		
Male sex	1.38 (0.28–6.68)	0.69		
Family history of BrS	0.93 (0.23–3.75)	0.93		
Family history of SD	1.16 (0.34–4.02)	0.81		
Syncope	0.52 (0.15–1.86)	0.32		
History of AF	4.11 (1.15–14.78)	0.03	3.68 (0.98–13.63)	0.06
Positive EPS	1.12 (0.31–4.20)	0.86		
Spontaneous Brugada type 1	0.93 (0.27–3.24)	0.92		
QTc prolongation	1.15 (0.11–12.34)	0.91		
Early repolarization	3.54 (0.43–28.82)	0.24		
Conduction disturbances*	3.33 (0.89–12.45)	0.07		
First-degree AV block				
QRS fragmentated or prolonged	6.54 (0.79–53.93)	0.08		
S-wave in lead I	10.12 (1.28–79.97)	0.02	9.17 (1.15–73.07)	0.03

AF, atrial fibrillation; AV, atrioventricular; BrS, Brugada syndrome; EPS, electrophysiological study; GR, generator replacement; SCD, sudden cardiac death. *Cox regression could not be performed because no primary endpoint events occurred in patients without conduction disturbances.

However, only 20–30% of BrS patients carry mutations of SCN5A (1). Recently published data reported that other mutations, including SCN1B, SCN10A, and SNTB2 are also associated with BrS. Specific genetic mutations have been also related to specific genotype–phenotype association, including cardiac conduction dysfunction, AF, ventricular arrhythmias and susceptibility to sodium channel blockers (32–35). These findings may provide new opportunities to further elucidate the cellular disease mechanism of BrS, improve screening, and risk stratification.

ECG abnormalities both depolarization and repolarization, such as ER, increased QRS duration (19), f-QRS (20, 21), first degree AV block (18), and S-wave in lead I (22, 36) have been associated with a worse outcome. The role of EPS remains controversial (1, 2, 7–11). Our study reported that S-wave in lead I is an independent predictor of late arrhythmic events. Accordingly, the presence of this ECG abnormality should be added to the list of the ECG variables predicting a worse outcome in BrS who received a prophylactic ICD implantation.

ICD therapy in Brugada syndrome

To date, ICD remains the only therapy with proven efficacy in preventing SCD in BrS patients (1–3, 25–27). However, ICD implantation is not risk-free being associated with high rates of IS and device-related complications (25–27). Increase in diagnosis of patients with BrS has led to an increase of ICD implantations (1, 2). The decision to implant an ICD is not without risks given that up to 24% of BrS patients experience IS (25). Moreover, multiple GR procedures may be needed, with a potential increased rate of device-related complications, ranging from 15.9 to 36% (25–27). It is controversial whether device replacement is needed in patients who never experienced appropriate ICD therapy until the time of GR. Considering the ICD complications and cost, ICD replacement in patients without previous appropriate therapy should be evaluated carefully. Thus, the balance between the potential life-saving and the risk of complications after ICD replacement in asymptomatic BrS patients and without appropriate ICD intervention before GR remains to be established. Of note, in our study, appropriate shocks occurred in 13% of asymptomatic patients which is in line with previous long-term studies (25, 26). In our study, after ICD replacement ≥1 device-related complications requiring surgical revision occurred in 6.6% of patients.

A prior study by Kim et al. (37) reported the potential benefit of ICD therapy after GR in a small cohort of patients with BrS treated for either primary or secondary prevention. Our multicenter study confirmed and extended these previous observations by demonstrating in a large BrS population who received prophylactic ICD and did not experience appropriate ICD therapy, that the risk of late appropriate ICD therapy after GR remains significant in a clinically relevant proportion of cases, mostly in the presence of conduction abnormalities such as S-wave in lead I on basal ECG. According to the results of the present study, S-wave in lead I on basal ECG, may contribute to

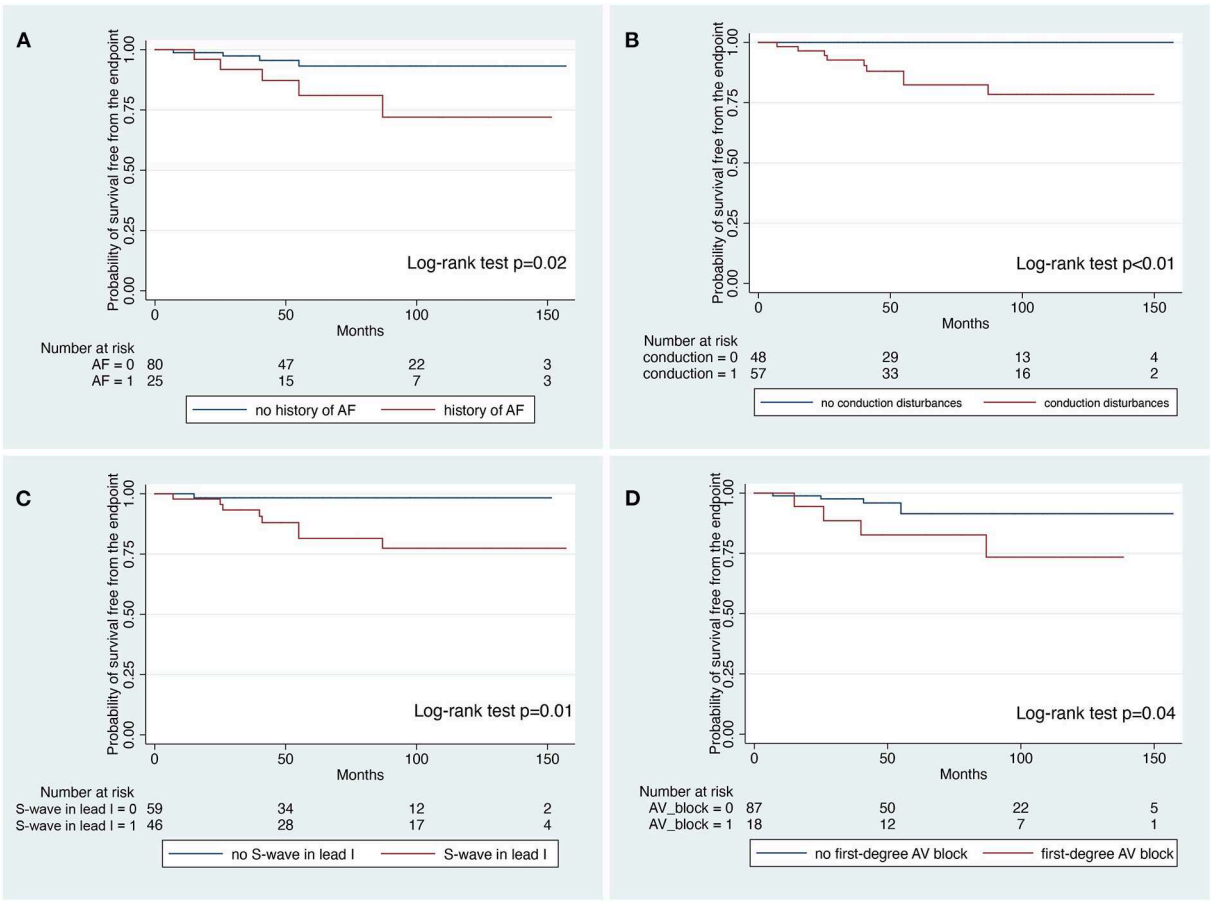

FIGURE 2
Kaplan–Meier analysis for survival free from the endpoint according to the presence of history of atrial fibrillation **(A)** conduction disturbances, **(B)** S-wave in lead I, **(C)** and first degree atrio-ventricular block **(D)**.

the accurate analysis of risk-benefit ratio when considering GR in BrS who received a prophylactic ICD implantation.

Subcutaneous implantable cardioverter-defibrillator is an alternative option to TV-ICD therapy to reduce lead-related complications (38). However, S-ICD in patients with BrS is associated with relatively high risk rate of IS (39), if one considers that in our study 2 patients of 10 patients (20%) with an S-ICD experienced IS due to signal oversensing. Most important, a sizeable proportion of patients with BrS are not eligible to S-ICD because they fail the pre-implantation screening (40).

Conduction abnormalities in Brugada syndrome

Although the potential prognostic role of the presence of different types of conduction abnormalities in BrS has been reported (18–22, 36), none of ECG conduction abnormalities are currently used for risk stratification. Recently, our study group, for the first time, demonstrated that first-AV block was an independent predictor of malignant arrhythmic events (18). A more recent meta-analysis by Pranata et al. confirms that first-degree AV block is associated with more frequent major arrhythmic events in BrS patients (41). In the present study, we found that among ECG abnormalities, patients who experienced malignant arrhythmic events after GR had more often conduction abnormalities including first-degree AV block at baseline ($P = 0.04$). At variance with our results, fQRS has been linked to poor prognosis in previous studies (16, 17). In a prospective study on 347 consecutive patients with BrS with spontaneous type 1 ECG pattern and no history of cardiac arrest, Calò et al. (22) found that the presence of an S-wave in lead I was a predictor of life-threatening ventricular arrhythmias. The potential prognostic value of this ECG conduction parameter was strengthened in a more recent study by Giustetto et al. (36) extending it to patients with drug-induced Type 1 ECG and

patients with previous cardiac arrest. According to our results the presence of S-wave in lead I on basal ECG is an independent predictor of ventricular arrhythmias. S-wave in lead I may be due to prolongation of the QRS complex, expression of a conduction delay localized in the right ventricular outflow tract (RVOT) (22). To this regard, several studies investigated the arrhythmogenic substrate in BrS patients and found that conduction abnormalities in the RVOT may represent a possible underlying arrhythmogenic substrate (17).

The results of the present and some previous studies confirmed that patients with BrS may exhibit variable degree of conduction abnormalities. Recently Migliore et al. found coexistence of Brugada repolarization abnormalities and conduction disturbances in a 35-year-old man who died suddenly. The histological examination demonstrated severe disruption by fibrous tissue of the proximal tract of both right and left bundle branches (18) suggesting the presence of underlying structural heart abnormalities in BrS. We can speculate, that the presence of underlying conduction disturbances associated with aging of the conduction system and drug interference on the conduction system itself could increase the arrhythmic risk in patients with BrS.

Study limitations

Limitations are present in our study. This is a retrospective multicenter study. Even with this very long follow-up there was a relatively small number of malignant arrhythmic events, and this might have affected the identification of unique predictors on multivariate analysis. Most of the ECG parameters analyzed in the study are dynamic, and the real prevalence of these parameters is difficult to evaluate. Moreover, EPS protocol and ICD implantation procedures were performed at discretion of the center protocol and physician. Finally, only few patients underwent genetic testing and no analysis combining genotype and arrhythmic risk was performed because, by study design, it was not a genotype–phenotype correlation study.

Conclusions

The present study indicates that BrS patients receiving a prophylactic ICD may experience late appropriate intervention after GR in a clinically relevant proportion of cases. S-wave in lead I on basal ECG at the time of first clinical evaluation was the only independent predictor of persistent risk of life-threatening arrhythmic events. These findings support the need for GR at the end of service regardless of previous appropriate intervention, mostly in BrS patients with conduction abnormalities.

Data availability statement

The raw data supporting the conclusions of this article will be made available by the authors, without undue reservation.

Ethics statement

The studies involving human participants were reviewed and approved by Local Ethics Committee: Comitato Etico per la Sperimentazione Clinica, Azienda Ospedaliera di Padova, Italy. The patients provided their written informed consent to participate in this study.

Author contributions

FM, NM, LC, and DC contributed to conception and design of the study. FM, NM, AM, GW, RV, CC, AR, LP, VM, JS, G-BC, ACurc, GA, RM, FS, ACurn, EB, and MD organized the database. RV and AZ performed the statistical analysis. FM, CA, LP, and DC wrote the first draft of the manuscript. FM, NM, LP, CA, and DC wrote the sections of the manuscript. All authors contributed to manuscript revision, read, and approved the submitted version.

Conflict of interest

VM received an educational grant from the Enrico and Enrica Sovena Fundation, Italy. G-BC received compensation for teaching purposes and proctoring from Medtronic, Abbott, Biotronik, Boston Scientific, Acutus Medical. CA receives research grants on behalf of the center from Biotronik, Medtronic, Abbott, LivaNova, Boston Scientific, AtriCure, Philips, Acutus, and received compensation for teaching purposes and proctoring from Medtronic, Abbott, Biotronik, Livanova, Boston Scientific, Atricure, Acutus Medical, and Daiichi Sankyo.

The remaining authors declare that the research was conducted in the absence of any commercial or financial relationships that could be construed as a potential conflict of interest.

Publisher's note

References

1. Priori SG, Wilde AA, Horie M, Cho Y, Behr ER, Berul C, et al. HRS/EHRA/APHRS expert consensus statement on the diagnosis and management of patients with inherited primary arrhythmia syndromes: document endorsed by HRS, EHRA, and APHRS in May 2013 and by ACCF. AHA, PACES, and AEPC in June 2013. *Heart Rhythm.* (2013) 10:1932–63. doi: 10.1016/j.hrthm.2013.05.014

2. Antzelevitch C, Yan GX, Ackerman MJ, Borggrefe M, Corrado D, Guo J, et al. J-Wave syndromes expert consensus conference report: Emerging concepts and gaps in knowledge. *J Arrhythm.* (2016) 32:315–39. doi: 10.1016/j.joa.2016.07.002

3. Brugada J, Campuzano O, Arbelo E, Sarquella-Brugada G, Brugada R. Present status of Brugada syndrome: JACC state-of-the-art review. *J Am Coll Cardiol.* (2018) 72:1046–59. doi: 10.1016/j.jacc.2018.06.037

4. Sieira J, Ciconte G, Conte G, Chierchia GB, de Asmundis C, Baltogiannis G, et al. Asymptomatic Brugada syndrome: clinical characterization and long-term prognosis. *Circ Arrhythm Electrophysiol.* (2015) 8:1144–50. doi: 10.1161/CIRCEP.114.003044

5. Probst V, Goronflot T, Anys S, Tixier R, Briand J, Berthome P, et al. Robustness and relevance of predictive score in sudden cardiac death for patients with Brugada syndrome. *Eur Heart J.* (2020) 42:1687–95. doi: 10.1093/eurheartj/ehaa763

6. Sieira J, Conte G, Ciconte G, Chierchia GB, Casado-Arroyo R, Baltogiannis G, et al. A score model to predict risk of events in patients with Brugada syndrome. *Eur Heart J.* (2017) 38:1756–63. doi: 10.1093/eurheartj/ehx119

7. Priori SG, Gasparini M, Napolitano C, Bella PD, Ottonelli AG, Sassone B, et al. Risk stratification in Brugada syndrome: results of the PRELUDE (PRogrammed ELectrical stimUlation preDictive valuE) registry. *J Am Coll Cardiol.* (2012) 59:37–45. doi: 10.1016/j.jacc.2011.08.064

8. Probst V, Veltmann C, Eckardt L, Meregalli PG, Gaita F, Tan HL, et al. Long-term prognosis of patients diagnosed with Brugada syndrome: results from the FINGER Brugada syndrome registry. *Circulation.* (2010) 121:635–43. doi: 10.1161/CIRCULATIONAHA.109.887026

9. Sieira J, Conte G, Ciconte G, de Asmundis C, Chierchia GB, Baltogiannis G, et al. Prognostic value of programmed electrical stimulation in Brugada syndrome: 20 years experience. *Circ Arrhythm Electrophysiol.* (2015) 8:777–84. doi: 10.1161/CIRCEP.114.002647

10. Delise P, Allocca G, Marras E, Giustetto C, Gaita F, Sciarra L, et al. Risk stratification in individuals with the Brugada type 1 ECG pattern without previous cardiac arrest: usefulness of a combined clinical and electrophysiologic approach. *Eur Heart J.* (2011) 32:169–76. doi: 10.1093/eurheartj/ehq381

11. Sroubek J, Probst V, Mazzanti A, Delise P, Hevia JC, Ohkubo K, et al. Programmed ventricular stimulation for risk stratification in the Brugada syndrome: a pooled analysis. *Circulation.* (2016) 133:622–30. doi: 10.1161/CIRCULATIONAHA.115.017885

12. Roterberg G, El-Battrawy I, Veith M, Liebe V, Ansari U, Lang S. Arrhythmic events in Brugada syndrome patients induced by fever. *Ann Noninvasive Electrocardiol.* (2020) 25:e12723. doi: 10.1111/anec.12723

13. El-Battrawy I, Lang S, Zhou X, Akin I. Different genotypes of Brugada syndrome may present different clinical phenotypes: electrophysiology from bench to bedside. *Eur Heart J.* (2021) 42:1270–2. doi: 10.1093/eurheartj/ehab070

14. Yamagata K, Horie M, Aiba T, Ogawa S, Aizawa Y, Ohe T, et al. Genotype-phenotype correlation of SCN5A mutation for the clinical and electrocardiographic characteristics of probands with Brugada syndrome: a Japanese Multicenter Registry. *Circulation.* (2017) 135:2255–70. doi: 10.1161/CIRCULATIONAHA.117.027983

15. Ciconte G, Monasky MM, Santinelli V, Micaglio E, Vicedomini G, Anastasia L, et al. Brugada syndrome genetics is associated with phenotype severity. *Eur Heart J.* (2021) 42:1082–90. doi: 10.1093/eurheartj/ehaa942

16. Pannone L, Monaco C, Sorgente A, Vergara P, Calburean PA, Gauthey A, et al. Ajmaline-induced abnormalities in Brugada syndrome: evaluation with ECG imaging. *J Am Heart Assoc.* (2022) 11:e024001. doi: 10.1161/JAHA.121.024001

17. Pannone L, Monaco C, Sorgente A, Vergara P, Calburean PA, Gauthey A, et al. High-density epicardial mapping in Brugada syndrome: depolarization and repolarization abnormalities. *Rhythm.* (2022) 19:397–404. doi: 10.1016/j.hrthm.2021.09.032

18. Migliore F, Testolina M, Zorzi A, Bertaglia E, Silvano M, Leoni L, et al. First-degree atrioventricular block on basal electrocardiogram predicts future arrhythmic events in patients with Brugada syndrome: a long-term follow-up study from the Veneto region of Northeastern Italy. *Europace.* (2019) 21:322–31. doi: 10.1093/europace/euy144

19. Ohkubo K, Watanabe I, Okumura Y, Ashino S, Kofune M, Nagashima K, et al. Prolonged QRS duration in lead V2 and risk of life-threatening ventricular arrhythmia in patients with Brugada syndrome. *Int Heart J.* (2011) 52:98. doi: 10.1536/ihj.52.98

20. Morita H, Kusano KF, Miura D, Nagase S, Nakamura K, Morita ST, et al. Fragmented QRS as a marker of conduction abnormality and a predictor of prognosis of Brugada syndrome. *Circulation.* (2008) 118:1697–704. doi: 10.1161/CIRCULATIONAHA.108.770917

21. De Asmundis C, Mugnai G, Chierchia GB, Sieira J, Conte G, Rodriguez-Manero M, et al. Long-term follow-up of probands with Brugada syndrome. *Am J Cardiol.* (2017) 119:1392–400. doi: 10.1016/j.amjcard.2017.01.039

22. Calo' L, Giustetto C, Martino A, Sciarra L, Cerrato N, Marziali M, et al. A new electrocardiographic marker of sudden death in Brugada syndrome: the S-wave in lead I. *J Am Coll Cardiol.* (2016) 67:1427–40. doi: 10.1016/j.jacc.2016.01.024

23. Takagi M, Yokoyama Y, Aonuma K, Aihara N, Hiraoka M. Clinical characteristics and risk stratification in symptomatic and asymptomatic patients with Brugada syndrome: multicenter study in Japan. *J Cardiovasc Electrophysiol.* (2007) 18:1244. doi: 10.1111/j.1540-8167.2007.00971.x

24. Takagi M, Aonuma K, Sekiguchi Y, Yokoyama Y, Aihara N, Hiraoka M. The prognostic value of early repolarization (J wave) and ST-segment morphology after J wave in Brugada syndrome: multicenter study in Japan. *Heart Rhythm.* (2013) 10:533–9. doi: 10.1016/j.hrthm.2012.12.023

25. Sacher F, Probst V, Maury P, Dabuty D, Mansourati J, Komatsu Y, et al. Outcome after implantation of a cardioverter-defibrillator in patients with Brugada syndrome: a multicenter study-part 2. *Circulation.* (2013) 128:1739–47. doi: 10.1161/CIRCULATIONAHA.113.001941

26. Conte G, Sieira J, Ciconte G, de Asmundis C, Chierchia GB, Baltogiannis G, et al. Implantable cardioverter-defibrillator therapy in Brugada syndrome: a 20-year single-center experience. *J Am Coll Cardiol.* (2015) 65:879–88. doi: 10.1016/j.jacc.2014.12.031

27. El-Battrawy I, Roterberg G, Liebe V, Ansari U, Lang S, Zhou X, et al. Implantable cardioverter-defibrillator in Brugada syndrome: Long-term follow-up. *Clin Cardiol.* (2019) 42:958–65. doi: 10.1002/clc.23247

28. Al-Khatib SM, Stevenson WG, Ackerman MJ, Bryant WJ, Callans DJ, Curtis AB, et al. AHA/ACC/HRS guideline for management of patients with ventricular arrhythmias and the prevention of sudden cardiac death: executive summary: a report of the American College of Cardiology/American Heart Association Task Force on Clinical Practice Guidelines and the heart rhythm society. *Heart Rhythm.* (2017) 2018:e190–252. doi: 10.1016/j.hrthm.2017.10.035

29. Brignole M, Moya A, de Lange FJ, Deharo JC, Elliot PM, Fanciulli A, et al. 2018 ESC Guidelines for the diagnosis and management of syncope. *Eur Heart J.* (2018). 39:1883–948. doi: 10.5603/KP.2018.0161

30. Surawicz B, Childers R, Deal BJ, Gettes LS, Bailey JJ, Gorgels A, et al. AHA/ACCF/HRS recommendations for the standardization and interpretation of the electrocardiogram: Part III: Intraventricular conduction disturbances: a scientific statement from the American Heart Association Electrocardiography and Arrhythmias Committee, Council on Clinical Cardiology; the American College of Cardiology Foundation; and the Heart Rhythm Society. Endorsed by the International Society for Computerized. *Electrocardiol J Am Coll Cardiol.* (2009) 53:976–81. doi: 10.1161/CIRCULATIONAHA.108.191095

31. Kewcharoen J, Rattanawong P, Kanitsoraphan C, Mekritthikrai R, Prasitlumkum N, Putthapiban P, et al. Atrial fibrillation and risk of major arrhythmic events in Brugada syndrome: a meta-analysis. *Ann Noninvasive Electrocardiol.* (2019) 24:e12676. doi: 10.1111/anec.12676

32. El-Battrawy I, Müller J, Zhao Z, Cyganek L, Zhong R, Zhang F, et al. Studying Brugada syndrome with an SCN1B variants in human-induced pluripotent stem cell-derived cardiomyocytes. *Front Cell Dev Biol.* (2019) 7:261. doi: 10.3389/fcell.2019.00261

33. El-Battrawy I, Albers S, Cyganek L, Zhao Z, Lan H, Li X, et al. A cellular model of Brugada syndrome with SCN10A variants using human-induced pluripotent stem cell-derived cardiomyocytes. *Europace.* (2019) 21:1410–21. doi: 10.1093/europace/euz122

34. Schmidt C, Wiedmann F, El-Battrawy I, Fritz M, Ratte A, Beller CJ, et al. Reduced Na+ current in native cardiomyocytes of a Brugada syndrome patient associated with β-2-syntrophin mutation. *Circ Genom Precis Med.* (2018) 11:e002263. doi: 10.1161/CIRCGEN.118.002263

35. El-Battrawy I, Lang S, Borggrefe M, Zhou XB, Akin I. Letter by El-Battrawy et al. Regarding Article, "The Brugada syndrome susceptibility gene HEY2 modulates cardiac transmural ion channel patterning and electrical heterogeneity". *Circ Res.* (2017) 121:e20. doi: 10.1161/CIRCRESAHA.117.311655

36. Giustetto C, Nangeroni G, Cerrato N, Rudic B, Tülümen E, Gribaudo E, et al. Ventricular conduction delay as marker of risk in Brugada Syndrome. Results from the analysis of clinical and electrocardiographic features of a large cohort of patients. *Int J Cardiol.* (2020) 302:171–7. doi: 10.1016/j.ijcard.2019.11.121

37. Kim JY, Kim SH, Kim SS, Lee KH, Park HW, Cho JG, et al. Benefit of implantable cardioverter-defibrillator therapy after generator replacement in patients with Brugada syndrome. *Int J Cardiol.* (2015) 187:340–4. doi: 10.1016/j.ijcard.2015.03.262

38. Knops RE, Olde Nordkamp LRA, Delnoy PHM, Boersma LVA, Kuschyk J, El-Chami MF, et al. Subcutaneous or transvenous defibrillator therapy. *N Engl J Med.* (2020) 383:526–36. doi: 10.1056/NEJMoa1915932

39. Casu G, Silva E, Bisbal F, Viola G, Merella P, Lorenzoni G, et al. Predictors of inappropriate shock in Brugada syndrome patients with a subcutaneous implantable cardiac defibrillator. *J Cardiovasc Electrophysiol.* (2021) 32:1704–11. doi: 10.1111/jce.15059

40. Conte G, Cattaneo F, de Asmundis C, Berne P, Vicentini A, Namdar M, et al. Impact of SMART pass filter in patients with ajmaline-induced Brugada syndrome and subcutaneous implantable cardioverter-defibrillator eligibility failure: results from a prospective multicentre study. *Europace.* (2021) 21:1410–21. doi: 10.1093/europace/euab230

41. Pranata R, Yonas E, Chintya V, Deka H, Raharjo SB. Association between PR Interval, First-degree atrioventricular block and major arrhythmic events in patients with Brugada syndrome - Systematic review and meta-analysis. *J Arrhythm.* (2019) 35:584–90. doi: 10.1002/joa3.12188

frontiers | Frontiers in Cardiovascular Medicine

TYPE Review
PUBLISHED 22 August 2022
DOI 10.3389/fcvm.2022.884767

OPEN ACCESS

EDITED BY
Shimon Rosenheck,
Hebrew University of Jerusalem, Israel

REVIEWED BY
Filippo Cademartiri,
Gabriele Monasterio Tuscany Foundation (CNR), Italy
Paolo Severino,
Sapienza University of Rome, Italy
Federico Migliore,
University of Padua, Italy

*CORRESPONDENCE
Jonathan Chrispin
chrispin@jhmi.edu

SPECIALTY SECTION
This article was submitted to Cardiac Rhythmology, a section of the journal Frontiers in Cardiovascular Medicine

RECEIVED 27 February 2022
ACCEPTED 02 August 2022
PUBLISHED 22 August 2022

CITATION
Xie E, Sung E, Saad E, Trayanova N, Wu KC and Chrispin J (2022) Advanced imaging for risk stratification for ventricular arrhythmias and sudden cardiac death.
Front. Cardiovasc. Med. 9:884767.
doi: 10.3389/fcvm.2022.884767

Advanced imaging for risk stratification for ventricular arrhythmias and sudden cardiac death

Eric Xie[1], Eric Sung[1,2], Elie Saad[1], Natalia Trayanova[1,2], Katherine C. Wu[1] and Jonathan Chrispin[1]*

[1]Division of Cardiology, Department of Medicine, Section of Cardiac Electrophysiology, Johns Hopkins University School of Medicine, Baltimore, MD, United States, [2]Department of Biomedical Engineering, Johns Hopkins University, Baltimore, MD, United States

Sudden cardiac death (SCD) is a leading cause of mortality, comprising approximately half of all deaths from cardiovascular disease. In the US, the majority of SCD (85%) occurs in patients with ischemic cardiomyopathy (ICM) and a subset in patients with non-ischemic cardiomyopathy (NICM), who tend to be younger and whose risk of mortality is less clearly delineated than in ischemic cardiomyopathies. The conventional means of SCD risk stratification has been the determination of the ejection fraction (EF), typically *via* echocardiography, which is currently a means of determining candidacy for primary prevention in the form of implantable cardiac defibrillators (ICDs). Advanced cardiac imaging methods such as cardiac magnetic resonance imaging (CMR), single-photon emission computerized tomography (SPECT) and positron emission tomography (PET), and computed tomography (CT) have emerged as promising and non-invasive means of risk stratification for sudden death through their characterization of the underlying myocardial substrate that predisposes to SCD. Late gadolinium enhancement (LGE) on CMR detects myocardial scar, which can inform ICD decision-making. Overall scar burden, region-specific scar burden, and scar heterogeneity have all been studied in risk stratification. PET and SPECT are nuclear methods that determine myocardial viability and innervation, as well as inflammation. CT can be used for assessment of myocardial fat and its association with reentrant circuits. Emerging methodologies include the development of "virtual hearts" using complex electrophysiologic modeling derived from CMR to attempt to predict arrhythmic susceptibility. Recent developments have paired novel machine learning (ML) algorithms with established imaging techniques to improve predictive performance. The use of advanced imaging to augment risk stratification for sudden death is increasingly well-established and may soon

have an expanded role in clinical decision-making. ML could help shift this paradigm further by advancing variable discovery and data analysis.

KEYWORDS

sudden cardiac death (SCD), ventricular arrhythmias, cardiovascular magnetic resonance (CMR), positron emission tomography (PET), single-photon emission computerized tomography (SPECT), computed tomography

Introduction

Sudden cardiac death is an unexpected death from a cardiac cause within a short period (typically an hour or less) from symptom onset or, if unwitnessed, within 24 h of last being seen alive (1, 2). While the incidence of SCD has gradually declined over the past decades, the annual incidence is ∼200,000–400,000 cases per year (the extensive range being attributable to the uncertainty of the cause of some deaths), amounting to around 15–20% of all deaths (3). Among patients with known cardiovascular disease (CVD), which represents about half of cases of SCD, ventricular arrhythmia (VA) is the leading mechanism of SCD in both ischemic cardiomyopathy (ICM) and non-ischemic cardiomyopathy (NICM). In ICM, obstructive coronary artery disease (CAD) leads to myocardial scarring, and regions of heterogeneous conduction serve as substrates for initiating ventricular tachycardia (VT). NICM encompasses diverse cardiac conditions that can result in scar formation or fibrosis, which along with electrophysiological remodeling, can result in VT or ventricular fibrillation (VF). The entity of ischemia but no CAD (INOCA) has also been described and remains an area of active investigation. Thus, far in clinical practice, primary prevention and risk reduction of SCD is accomplished with medical therapy and the implantable cardiac defibrillator (ICD), with slightly different approaches for patients with previously detected VA or resuscitated arrest. Guidelines for primary prevention ICD in both ICM and NICM are driven by clinical symptoms of heart failure and decreased ejection fraction (EF) <35% as derived by imaging (4). However, more useful prognostic data can be obtained from imaging than EF alone (5, 6).

Efforts to improve risk stratification for SCD, or even to reclassify risk assigned by EF, have been undertaken across all cardiac imaging modalities. Herein, we focus on the role of advanced imaging, namely cardiac magnetic resonance imaging (CMR), single-photon emission computer tomography (SPECT), and positron emission tomography (PET), and its application to risk stratification for SCD (Figure 1). We highlight unique techniques of each modality and their limitations, with particular attention to the patient subgroups that inform the utility and pathophysiology of each method (Table 1). For each study, we distinguish endpoints that are related though not interchangeable: while studies with SCD were emphasized in this review, we mention when cardiac death, all-cause mortality, or VA were the primary endpoint as they too are informative. We also describe current and future applications of machine learning (ML) in advanced imaging for SCD, from image acquisition to model construction.

Cardiac magnetic resonance imaging

Ventricular geometry and function

Chamber geometry has long been known to reflect the role of remodeling in CVD and, in turn, is associated with outcomes including VA (7, 8). Cardiac MRI has been described as the gold standard for structural and functional quantification of cardiac chambers (9, 10). Using CMR, geometry-based approaches to SCD risk stratification have emphasized these attributes, and measurements based on wall thickness have been found to distinguish patients with ICM who develop SCD (11). From a clinical standpoint, studies have suggested that at-risk patients may be inadvertently excluded from ICD as echocardiography overestimates EF when compared with CMR (12, 13). While every imaging modality is to some extent operator dependent, it is perhaps most prominently described in echocardiography as affecting interpretation (14). This highlights that LVEF thresholds may need to be individualized for different modalities, and CMR may be preferable to TTE for therapeutic decision-making in patients with intermediate-range LVEF (15). That said, EF < 35% as a selection criterion for primary prevention ICDs has routinely been critiqued for its low sensitivity and specificity in predicting VA and SCD. Furthermore, patients meeting these criteria encompass only 13% of all suffering SCD (16).

Role of LGE in ICM and CAD

CMR with LGE has developed as a means of characterizing myocardial tissue, and its value in prognosticating cardiovascular outcomes, including SCD, has been widely reviewed and increasingly well-established (17, 18). This has

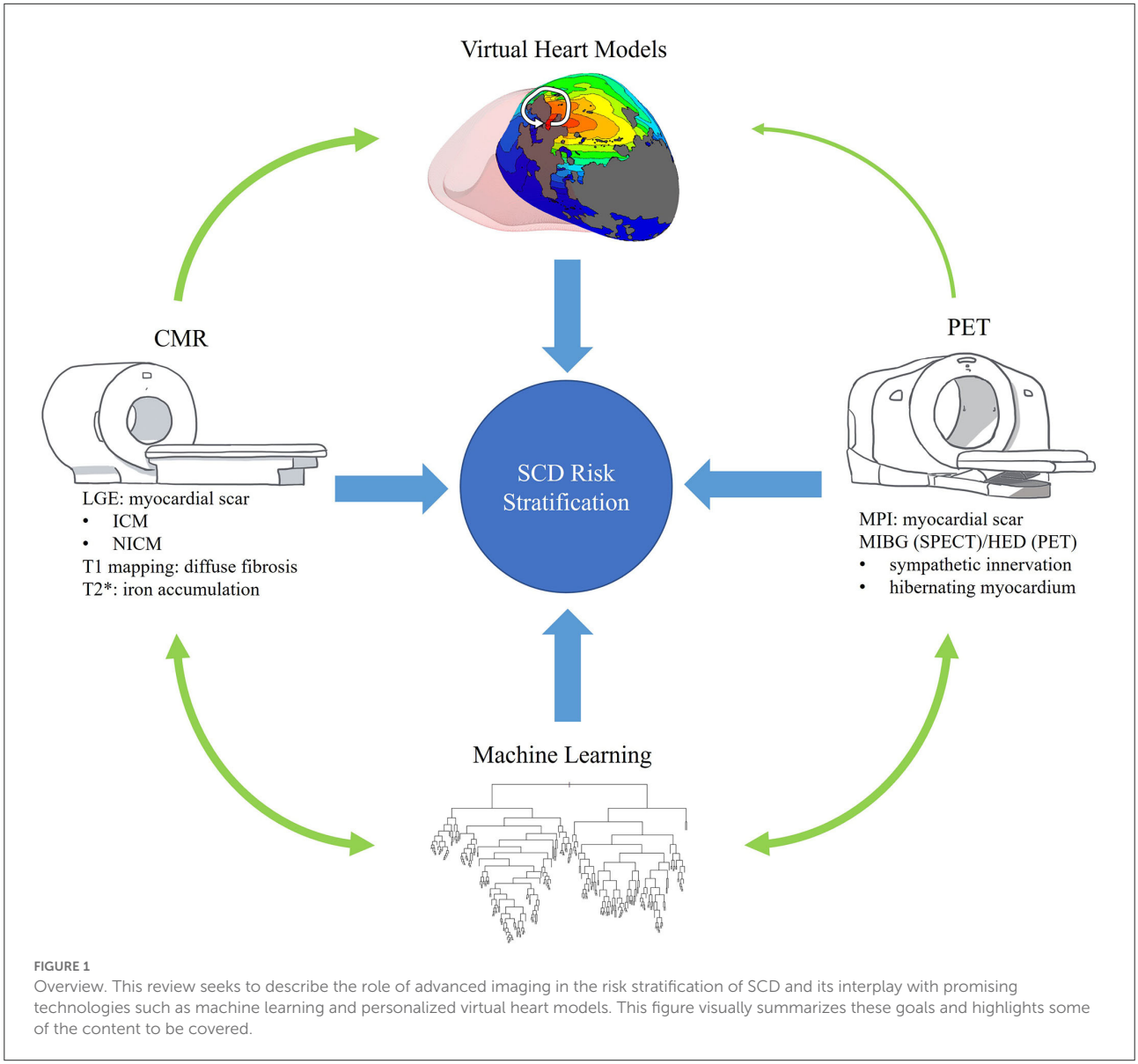

FIGURE 1
Overview. This review seeks to describe the role of advanced imaging in the risk stratification of SCD and its interplay with promising technologies such as machine learning and personalized virtual heart models. This figure visually summarizes these goals and highlights some of the content to be covered.

been demonstrated across a wide variety of phenotypes in both patients with ICM and NICM. In ICM, heterogeneous scar, also termed gray zone, is an independent predictor of VA and SCD in a number of studies of patients with ICD or undergoing ICD implantation (19–21). A recent retrospective study among 979 patients with CAD and majority EF with > 35% showed that gray zone mass was more strongly associated with SCD than LVEF (22). The same group showed that in a mixed ICM/NICM population with ICD and cardiac resynchronization therapy, the absence of myocardial fibrosis on visual assessment virtually excluded patients at risk of VA and SCD over 7 years follow-up and among those with scar, gray zone extent added predictive value and improved net reclassification (23). Likewise, a prospective study in a mixed population of ICM and NICM patients undergoing primary prevention ICD demonstrated that the combination of low gray zone mass and low high-sensitivity C-reactive protein identified a subgroup with very low risk for VA (24). In a similar population (mixed ICM/NICM with ICD), an analysis incorporating random survival forests for model construction showed LV scar mass as well as gray zone mass by LGE were top predictors for VA and SCD (25). The same study suggested a hierarchy of risk wherein no scar was less risky than scar, larger total/core scar had higher risk than smaller scar, and larger gray zone had higher risk than smaller gray zone for the same core scar size. Additional applications of LGE, beyond presence and extent, have also been developed, including LV entropy, a measure of the distribution of pixel intensity across the myocardium (26, 27). Amongst patients with CAD and

TABLE 1 Comparison of imaging modalities described in this review.

Modality	Sequences	Characteristics studied	Evaluation of structure	Evaluation of function	Tissue characterization	Cost
Echocardiography	2D	• LVEF • Strain	++	++	+	Low
CMR	LGE T1 T2*	• Strain • Scar • Diffuse fibrosis	+++	+++	+++	Moderate
SPECT	MIBG	• Scar • Viability • Innervation	+	+	++	High
PET	FDG HED	• Scar • Viability • Innervation	++	+	++	High

+ for fair, ++ for good, and +++ for excellent.

ICDs, entropy was a significant predictor for VA and SCD (27, 28). A mechanistically-minded approach in LGE has been identifying conducting channels, a nidus for VT as identified in CAD (29). A study in a mixed ICM/NICM population showed that the presence and mass of these channels were associated with the risk of VA and appropriate primary prevention ICD therapy (30).

Role of LGE in NICM

In NICM, the role of LGE for SCD risk stratification has been frequently studied in patients with dilated cardiomyopathy (DCM) and hypertrophic cardiomyopathy (HCM) (31–33).

LGE has been used to identify higher-risk patients who fall outside the EF criterion for primary prevention ICD (34). In a multivariate model for SCD in NICM, LGE had incremental prognostic value over clinical measures, whereas EF did not (35). Among HCM patients, LGE extent has been favorably compared with clinical risk models and, in some cases, exceeded the performance of these models (36–38). To define an LGE cut-off for risk stratification, various thresholds of LGE have been described. In HCM, LGE extent >10% identified patients with SCD rates up to an order of magnitude greater than predicted with clinical risk score (39). A further analysis using serial LGE imaging in DCM illustrated that amongst patients with fibrosis progression, the majority had minimal change in EF (<5%), ergo identifying a high-risk cohort for all-cause mortality not captured by LVEF alone (40). In a case series among athletes, LGE pattern, specifically involving the lateral LV wall, was also noted to correlate with increased risk of malignant arrhythmias (41). As in ICM, LV entropy in DCM patients with ICD significantly improved a clinical model for VA, although there was only one instance of SCD among these (26). Despite these advances and its prominence in the literature, LGE has yet to be included in clinical guidelines. A likely rationale for this is that there has yet to be a completed randomized control trial using LGE for risk stratification, though several are enrolling and underway (18, 31).

Proposed diagnostic guidelines for arrhythmogenic cardiomyopathies, which carry profound and inherent risk for VA and SCD, have included LGE patterns among other criteria (42). In arrhythmogenic right ventricular cardiomyopathy/dysplasia (ARVC/D) specifically, abnormal CMR findings including LGE were associated with increased VA (43). Advances in CMR may allow for improved RV assessment facilitating earlier disease detection and ergo risk stratification (44). Similarly in myocarditis, LGE presence and extent have been associated with increased risk of major adverse cardiac events, including VA and SCD (45, 46).

Shortcomings of LGE and alternative CMR sequences

While LGE is perhaps the most widely studied CMR method for SCD risk stratification, other CMR sequences have also been investigated, which may address certain shortcomings of LGE. An intrinsic limitation of gadolinium administration is toxicity, particularly among patients with renal insufficiency, though the degree of risk is controversial (47, 48). Fortunately, the most feared complication, nephrogenic systemic fibrosis, is exceedingly rare with modern gadolinium agents; a recent consensus statement from the American College of Radiology and the National Kidney Foundation leaves the decision for gadolinium administration in renal impairment to the clinician (49). LGE-CMR furthermore depends on several factors such as the timing of contrast injection and selection of scan parameters that can impact the interpretation of intensity values on imaging. Another limitation of LGE for risk stratification of SCD is

that a subset of patients with NICM who develop VF may not have LGE on CMR (50). Several alternative measures derived from CMR have been proposed that may address some of these limitations, including native T1 mapping and extracellular volume (ECV), which reflect diffuse fibrosis, a characteristic not captured by LGE (51, 52). In a prospective study of T1 mapping and LGE assessment in participants receiving ICDs, native T1 was independently associated with VA, although performed more poorly than LGE in reclassifying participants to a low-risk group (53). Among patients with DCM, native T1 was predictive of death independent of LGE, which was present only in 27% of the study population (54). Another study in HCM patients without LGE at CMR showed an association of native T1 with SCD, though it was limited by the small number of patients ($n = 5$) reaching this endpoint (55). Less well studied is T2* mapping, which combines spin-spin relaxation (T2) with magnetic field inhomogeneity to detect field distortions from the presence of materials such as iron (56). As such, it was traditionally applied to identify myocardial iron accumulation in iron storage diseases and considered arrhythmogenic in those populations (57). More recently, it has been suggested T2* may add to the assessment of fibrosis, although this has not yet been well-studied (58, 59). Thus, far, a small study of the association of T2* with VA in patients with HCM was negative (60). Yet another sequence, T2-weighted short-tau inversion recovery (T2w-STIR) has been used to assess myocardial edema in survivors of cardiac arrest. Presence of edema, hypothesized to represent a transient arrhythmogenic substrate, has been associated with fewer ICD shocks (61).

Innovative uses of CMR for personalized virtual heart models to predict VA and SCD risk

A more recent development in SCD risk stratification is the use of advanced imaging to build electrophysiologic virtual heart models, which can be used to simulate arrhythmias *in silico* (62). These 3D computational models entail a biophysical approach from the cell-scale to the organ-scale and are specific to each patient's disease and resultant remodeling. Perhaps uniquely among risk stratification methodologies, virtual hearts evaluate how triggers from different locations will interact with the substrate to initiate VA, potentially providing mechanistic insights into how and VAs can develop in the patient heart (63). This approach was initially demonstrated in patients with ICM and ICDs; wherein virtual hearts were superior to clinical risk factors in predicting VA (64). This work has also been extended in a small study of patients not meeting ICD implantation criteria, distinguishing patients with VT history from those without (65). These models make use of complex patterns of imaging data such as distribution and degree of fibrosis, as well as a fusion of different pulse sequences as was done with T1 mapping in HCM (66). It is worth noting these studies have all been retrospective thus far regarding event prediction. However, virtual heart technology has recently been used to prospectively identify VT ablation targets in a small cohort, extending the utility of CMR from predicting SCD risk to guiding therapy (67).

Nuclear imaging

Overview

Nuclear medicine presents another advanced imaging modality that has been applied for risk stratification of SCD (68). Single-photon emission computer tomography (SPECT) is commonly used in cardiology for myocardial perfusion imaging (MPI) to assess coronary patency (69). Among patients with CAD, composite scores of fixed and reversible perfusion defects determined *via* SPECT are independently associated with SCD, including patients with EF > 35% (70, 71). These results were also reproduced in patients without significant CAD (72). Positron emission tomography (PET) provides another method of MPI, with the degree of myocardial abnormalities, such as scar, ischemia, or hibernating myocardium, associated with cardiac death (although data on PET MPI and SCD specifically is sparse) (73, 74). Both PET and SPECT can be used to characterize myocardial scar, a similar substrate to what is assessed by LGE. In an unadjusted analysis, scar extent by SPECT was associated with SCD (75). A larger study using PET among patients with EF <35% showed that scar alone, and not reversible ischemia, was significantly associated with ICD firing and SCD (76). Interestingly in the study above, the scar alone was not a significant predictor for SCD after adjustment, although it is worth noting participants in this study had a considerably higher EF (70). Combining MPI with imaging of cardiac inflammation using (18) F-fluorodeoxyglucose (FDG) has identified higher risk NICM patients independent of LVEF and clinical markers (77). Other myocardial features associated with SCD that PET and SPECT can image include sympathetic innervation and hibernating myocardium (78–80).

Means of measuring sympathetic innervation and its significance

Assessment of innervation is conducted with radiolabeled catecholamines, most commonly iodine-123-labeled metaiodobenzylguanidine (MIBG) in SPECT though several tracers have also been studied for use with PET, most notably 11C-hydroxyephedrine (HED). Globally decreased uptake of

these tracers is thought to reflect the increased sympathetic tone, which can trigger malignant arrhythmias (81). However, regional reductions in uptake can be seen in sympathetic denervation caused by myocardial ischemia and are prevalent in CAD (82). Studies, primarily undertaken amongst patients with ICM, have demonstrated both global and regional approaches for risk stratification of SCD. A prospective study of patients with HFrEF showed that reduced global uptake of MIBG was significantly associated with potentially lethal arrhythmias and cardiac death (83). Using a different measure of reuptake, another group demonstrated that abnormal MIBG washout in HFrEF was associated with SCD specifically (though this group excluded the use of beta-blockers, perhaps limiting the generalizability of the study) (84). Using PET with HED, a study among ICM patients showed regionally reduced uptake; specifically, the volume of denervated tissue was associated with SCD (85). This was similarly demonstrated with regional MIBG washout being associated with SCD (86). The role of sympathetic denervation in HFpEF and NICM continues to be explored, and studies have shown decreased MIBG uptake is associated with increased mortality and readmission. However, the relationship with SCD is unclear (87–89).

Hibernating myocardium

Conceptually, hibernating myocardium describes regions of viable tissue with chronically reduced function and resting perfusion caused by chronic ischemia or recurrent (90). This is thought to be an arrhythmogenic substrate and has been associated with VA in porcine models (91, 92). In studies of patients with ischemic cardiomyopathy, the extent of hibernating myocardium has been associated with all-cause mortality and composite cardiac deaths (93, 94). However, in the aforementioned study of PET with HED in ICM, hibernating myocardium was not associated with SCD and was only rarely identified (85). It has been suggested that modern revascularization strategies and medical therapy may diminish the role of hibernating myocardium for risk stratification of SCD (95).

Future potential of hybrid imaging

It is worth briefly noting that hybrid PET/MRI scanners have become commercially available relatively recently (since 2010) and brought with them a unique set of technical challenges as well as clinical possibilities (96). Thus far, PET/MRI has been applied in similar roles as its constituent modalities—in perfusion and viability studies (97). An example comparing PET and CMR in the same patient, albeit not using a hybrid scanner, demonstrates the utility of each modality. PET/MRI has in particular been investigated for diagnosis of cardiac sarcoidosis and proof-of-concept demonstrated; it is speculated that the increased quality of data gathered with PET/MRI in sarcoid patients may 1 day be used for identification of those at greater risk for VA and death (98–101). However, the role of PET/MRI in risk stratification remains hypothetical, and no study has yet described the association of any PET/MRI measure with SCD (96).

Computed tomography

CT is presently a more accessible and generally lower cost modality than those previously mentioned. It provides higher spatial resolution and for certain purposes better temporal resolution as well. CT is perhaps most prominently used in cardiology for non-invasive assessment of the coronary arteries, the presence (or absence) of which is diagnostically significant and certainly a significant predictor of both VA and SCD (102). In terms of tissue characterization however, CT lags behind CMR, PET, and SPECT though developments are being made rapidly to improve this (103). It is also worth noting that there are patients in whom CMR may be contraindicated due to implants or foreign objects, or where ICD-related artifact is too limiting, in whom CT may provide a necessary alternative for risk stratification in the future.

CT has been used to detect fibrosis, such as by iodinated contrast enhancement (104). Scar qualification/quantification by CT has been favorably compared with LGE-CMR (105). A group recently used CT to map wall thinning to identify potential VT isthmuses in post-MI patients with a VT history, yielding 100% sensitivity when compared with gold-standard EP studies although with 50% positive predictive value (106). Similarly, regions of myocardial fat deposition as characterized by CT have been associated with VT circuit sites in patients with history of VA (107). CT has also been used to identify areas of lipomatous metaplasia after infarction which are associated with VA in experimental models (108). As with the previously mentioned modalities, CT has also been used for development of virtual heart models (109).

The emerging role of machine learning and artificial intelligence

Machine learning in image acquisition

In recent years, machine learning techniques have seen increasing integration within medicine, particularly as applied in imaging (110). This has specifically included applications across numerous modalities in cardiology, including CMR and nuclear imaging (111). The value of ML in the risk stratification of SCD can be appreciated at multiple stages of the imaging pipeline

(Table 2). ML has been used to enhance image processing on a granular level, such as by voxel denoising. In time-intensive modalities such as MRI, this has been shown to allow for a significant reduction of acquisition time while preserving quantitative metrics such as demonstrated in brain imaging of cerebral blood flow (112). On a more experimental level, ML has been applied in low-field MRI to address reconstruction using noisy data, which may increase CMR availability in less resource-rich environments (124, 125). Finally, as an analog in PET, the clinical utility of dynamic scans required for more rapid imaging and low count protocols minimizing radiation exposure in young patients is limited by poorer image quality (113). While hardware advances provide one means of addressing this challenge, a likely more cost-effective pathway is the utilization of ML to improve the quality of the reconstructed image (126). In parallel to improving image quality, ML has been used to lower the computational burden of contemporary post-processing techniques such as scatter correction in PET (114, 115). Another forward-looking application of ML is in attenuation and scatter correction for PET-only, SPECT-only, or hybrid PET/MRI imaging, as this is conventionally accomplished with simultaneous CT (116). This may increase the accessibility and capability of advanced imaging and allow for a broader range of patients to undergo risk stratification with these modalities.

TABLE 2 Incorporation of machine learning into advanced imaging.

Imaging steps	Role of ML	Examples of applications
Acquisition	• Increasing acquisition speed • Decreasing radiation exposure	• Voxel denoising in CMR (112) • Implementing low count (radiation) protocols for PET (113)
Processing	• Reducing computation burden • Automating labor-intensive analysis • Standardization	• Scatter correction (114, 115) • Synthetic CT (applied to PET, SPECT, and PET/MRI) (116) • Automated scar quantification (117) • Common algorithm for segmentation across multiple centers (118)
Feature extraction	• Generating novel features, texture analysis • Investigation of hypothetical markers	• ML-derived scar heterogeneity (119) • Generating hundreds of features from individual sequences (120)
Model construction	• Advanced analytics • Dimension reduction; identifying significant markers • Data synthesis	• Applying random survival forests (121) • Combining non-simultaneous PET, MRI modalities (122) • Unified analysis using EMR (123)

Machine learning in image processing

Perhaps more widely reported are clinician-facing advances in image analysis and interpretation using ML, described by the overarching term "computer vision" to include any automated interpretation of images (127). ML-based algorithms have been available in commercial software for segmentation for some time now. They are widely used for automated quantification of structure and function, for example, ventricular volumes and EF (128). Some of these data are, as previously mentioned, used in models for the prediction of SCD. However, automation has extended to tissue characterization as well. LGE segmentation, when performed manually, can be a labor-intensive process requiring significant training to mitigate subjectivity and inter-operator variability (129).

Nonetheless, manual segmentation has previously been considered the gold standard for accuracy, especially when compared with techniques based on older ML algorithms (130). More recent studies have demonstrated the feasibility of novel approaches, such as deep convolutional neural networks, for automated scar quantification approaching manual segmentation in subsets of patients such as those with ICM and HCM (117, 131). This has also shown promise in multicenter datasets, potentially addressing the challenge of practice standardization (118, 132).

Machine learning for feature extraction

Sequential to obtaining imaging measures is its interpretation and application to predicting cardiovascular endpoints. Techniques such as texture analysis may be applied to pre-existing LGE segmentation to obtain features beyond quantitative scar burden, such as measures of heterogeneity and shape, which have been proven valuable in conventional workflows (119, 133). Numerous extracted features and varying ML models have been evaluated for this role; in other words, ML can be used to identify novel predictors and implement novel prediction methods (134, 135). However, these extracted features are typically unrecognizable to the human eye, especially when obtained from composite, multistep analyses necessitating further selection to identify covariates with the strongest predictive value (119, 136). For example, in a cohort of patients with DCM, principal component analysis was applied across ventricular geometric models to derive shape-based features, which were integrated into a score that was shown to be independently associated with composite VA and SCD (137). Another study generated 608 features from LGE and T2 sequences in Takotsubo patients to predict outcomes, including MI and death (120). ML was also used for dimensionality

reduction in this study, which interestingly resulted in all LGE-derived features being discarded. Along these lines, a recent study used an unsupervised, deep learning approach on cine CMR among ICM patients to derive cardiac features that were then used as inputs in a separate deep neural network that successfully predicted VA risk (138). The inverse approach, using ML to generate pre-defined features, is also appreciable in recent literature. For example, ML-derived measures based on LGE, such as scar complexity, were associated with VA in a cohort where entropy was not a significant predictor (139).

Innovating the role of advanced imaging with machine learning

In the future, machine learning may be integrated into the risk stratification workflow from the point of image acquisition to patient-facing risk prediction models, and there are studies demonstrating this in principle. One example is incorporating manual measurements and segmentation with using ML for feature extraction and statistical model-building (134). Sophisticated virtual heart simulations incorporating both MRI and PET data, then using ML to synthesize imaging and clinical data for SCD prediction, have been shown to outperform existing risk models (122). This approach is not specific to VA or SCD outcomes, and it has also been used to predict improvement in EF after cardiac resynchronization therapy (140). Because of the sheer volume of data available to the clinician from the electronic medical record and conglomerate imaging, it seems increasingly likely that ML will play a central role in the fusion of data of different sources and risk modeling (123, 141–143).

Conclusion

As described in this review, there are numerous promising applications of advanced imaging to identify patients at risk of SCD. Some of the above techniques and sequences may likely be incorporated into clinical guidelines and ultimately into regular practice in the coming years. Machine learning may enable advances democratizing advanced imaging for at-risk patients, as has been achieved with CT screening in smoking. Physicians and cardiologists of the future will likely have a wide variety of complementary imaging modalities and analytic tools to identify SCD risk amongst different patient populations optimally.

Author contributions

EX and JC contributed to the conception, tables, and design of the manuscript. EX, ESu, ESa, and JC contributed to creation and editing of figures. All authors agree to be accountable for the content of the work. All authors contributed to the drafting, editing, and review of the manuscript. All authors contributed to the article and approved the submitted version.

Funding

The authors acknowledge funding from NIH (NIH/NHLBI R01HL103812 and R01HL132181 to KW and R01HL142496 and R01HL124893 to NT), Leducq Foundation (NT), and AHA (Predoctoral Fellowship to Esu).

Acknowledgments

The authors would like to thank Steven Xie for providing illustrations of the scanners in Figure 1.

Conflict of interest

The authors declare that the research was conducted in the absence of any commercial or financial relationships that could be construed as a potential conflict of interest.

Publisher's note

References

1. Zipes D, Wellens HJ. *Sudden Cardiac Death*. Berlin: Springer (2000). p. 621-45.

2. Adabag AS, Luepker RV, Roger VL, Gersh BJ. Sudden cardiac death: epidemiology and risk factors. *Nat Rev Cardiol.* (2010) 7:216–25. doi: 10.1038/nrcardio.2010.3

3. Kuriachan VP, Sumner GL, Mitchell LB. Sudden cardiac death. *Curr Probl Cardiol.* (2015) 40:133–200. doi: 10.1016/j.cpcardiol.2015.01.002

4. Al-Khatib SM, Stevenson WG, Ackerman MJ, Bryant WJ, Callans DJ, Curtis AB, et al. 2017 AHA/ACC/HRS guideline for management of patients with ventricular arrhythmias and the prevention of sudden cardiac death: a report of

the American College of Cardiology/American Heart Association Task Force on Clinical Practice Guidelines and the Heart Rhythm Society. *J Am Coll Cardiol.* (2018) 72:e91–e220.

5. Bertini M, Schalij MJ, Bax JJ, Delgado V. Emerging role of multimodality imaging to evaluate patients at risk for sudden cardiac death. *Circ Cardiovasc Imaging.* (2012) 5:525–35. doi: 10.1161/CIRCIMAGING.110.961532

6. Deyell MW, Krahn AD, Goldberger JJ. Sudden cardiac death risk stratification. *Circ Res.* (2015) 116:1907–18. doi: 10.1161/CIRCRESAHA.116.304493

7. Mann DL, Bristow MR. Mechanisms and models in heart failure: the biomechanical model and beyond. *Circulation.* (2005) 111:2837–49. doi: 10.1161/CIRCULATIONAHA.104.500546

8. Konstam MA, Kramer DG, Patel AR, Maron MS, Udelson JE. Left Ventricular remodeling in heart failure: current concepts in clinical significance and assessment. *JACC Cardiovasc Imaging.* (2011) 4:98–108. doi: 10.1016/j.jcmg.2010.10.008

9. Seraphim A, Knott KD, Augusto J, Bhuva AN, Manisty C, Moon JC. Quantitative cardiac MRI. *J Magn Reson Imaging.* (2020) 51:693–711. doi: 10.1002/jmri.26789

10. Lorenz CH, Walker ES, Morgan VL, Klein SS, Graham TP. Normal human right and left ventricular mass, systolic function, and gender differences by cine magnetic resonance imaging. *J Cardiovasc Magn Reson.* (1999) 1:7–21. doi: 10.3109/10976649909080829

11. Vadakkumpadan F, Trayanova N, Wu KC. Image-based left ventricular shape analysis for sudden cardiac death risk stratification. *Heart Rhythm.* (2014) 11:1693–700. doi: 10.1016/j.hrthm.2014.05.018

12. De Haan S, De Boer K, Commandeur J, Beek A, van Rossum A, Allaart C. Assessment of left ventricular ejection fraction in patients eligible for ICD therapy: discrepancy between cardiac magnetic resonance imaging and 2D echocardiography. *Neth Heart J.* (2014) 22:449–55. doi: 10.1007/s12471-014-0594-0

13. Pontone G, Guaricci AI, Andreini D, Solbiati A, Guglielmo M, Mushtaq S, et al. Prognostic benefit of cardiac magnetic resonance over transthoracic echocardiography for the assessment of ischemic and nonischemic dilated cardiomyopathy patients referred for the evaluation of primary prevention implantable cardioverter–defibrillator therapy. *Circ Cardiovasc Imaging.* (2016) 9:e004956. doi: 10.1161/CIRCIMAGING.115.004956

14. Alsharqi M, Woodward W, Mumith J, Markham D, Upton R, Leeson P. Artificial intelligence and echocardiography. *Echo Res Pract.* (2018) 5:R115–R25. doi: 10.1530/ERP-18-0056

15. Wu KC, Calkins H. Powerlessness of a number: why left ventricular ejection fraction matters less for sudden cardiac death risk assessment. *Circ Cardiovasc Imaging.* (2016) 9:e005519. doi: 10.1161/CIRCIMAGING.116.005519

16. Wellens HJ, Schwartz PJ, Lindemans FW, Buxton AE, Goldberger JJ, Hohnloser SH, et al. Risk stratification for sudden cardiac death: current status and challenges for the future. *Eur Heart J.* (2014) 35:1642–51. doi: 10.1093/eurheartj/ehu176

17. Wu KC, Weiss RG, Thiemann DR, Kitagawa K, Schmidt A, Dalal D, et al. Late gadolinium enhancement by cardiovascular magnetic resonance heralds an adverse prognosis in nonischemic cardiomyopathy. *J Am Coll Cardiol.* (2008) 51:2414–21. doi: 10.1016/j.jacc.2008.03.018

18. Wu KC. Sudden cardiac death substrate imaged by magnetic resonance imaging: from investigational tool to clinical applications. *Circ Cardiovasc Imaging.* (2017) 10:e005461. doi: 10.1161/CIRCIMAGING.116.005461

19. Schmidt A, Azevedo CF, Cheng A, Gupta SN, Bluemke DA, Foo TK, et al. Infarct tissue heterogeneity by magnetic resonance imaging identifies enhanced cardiac arrhythmia susceptibility in patients with left ventricular dysfunction. *Circulation.* (2007) 115:2006–14. doi: 10.1161/CIRCULATIONAHA.106.653568

20. Roes SD, Borleffs CJW, Geest RJvd, Westenberg JJM, Marsan NA, Kaandorp TAM, et al. Infarct tissue heterogeneity assessed with contrast-enhanced MRI predicts spontaneous ventricular arrhythmia in patients with ischemic cardiomyopathy and implantable cardioverter-defibrillator. *Circ Cardiovasc Imaging.* (2009) 2:183–90. doi: 10.1161/CIRCIMAGING.108.826529

21. Zeidan-Shwiri T, Yang Y, Lashevsky I, Kadmon E, Kagal D, Dick A, et al. Magnetic resonance estimates of the extent and heterogeneity of scar tissue in ICD patients with ischemic cardiomyopathy predict ventricular arrhythmia. *Heart Rhythm.* (2015) 12:802–8. doi: 10.1016/j.hrthm.2015.01.007

22. Zegard A, Okafor O, de Bono J, Kalla M, Lencioni M, Marshall H, et al. Myocardial fibrosis as a predictor of sudden death in patients with coronary artery disease. *J Am Coll Cardiol.* (2021) 77:29–41. doi: 10.1016/j.jacc.2020.10.046

23. Leyva F, Zegard A, Okafor O, Foley P, Umar F, Taylor RJ, et al. Myocardial fibrosis predicts ventricular arrhythmias and sudden death after cardiac electronic device implantation. *J Am Coll Cardiol.* (2022) 79:665–78. doi: 10.1016/j.jacc.2021.11.050

24. Wu KC, Gerstenblith G, Guallar E, Marine JE, Dalal D, Cheng A, et al. Combined cardiac magnetic resonance imaging and C-reactive protein levels identify a cohort at low risk for defibrillator firings and death. *Circ Cardiovasc imaging.* (2012) 5:178–86. doi: 10.1161/CIRCIMAGING.111.968024

25. Wu KC, Wongvibulsin S, Tao S, Ashikaga H, Stillabower M, Dickfeld TM, et al. Baseline and dynamic risk predictors of appropriate implantable cardioverter defibrillator therapy. *J Am Heart Assoc.* (2020) 9:e017002-e. doi: 10.1161/JAHA.120.017002

26. Muthalaly RG, Kwong RY, John RM, van der Geest RJ, Tao Q, Schaeffer B, et al. Left ventricular entropy is a novel predictor of arrhythmic events in patients with dilated cardiomyopathy receiving defibrillators for primary prevention. *JACC Cardiovasc Imaging.* (2019) 12:1177–84. doi: 10.1016/j.jcmg.2018.07.003

27. Androulakis AFA, Zeppenfeld K, Paiman EHM, Piers SRD, Wijnmaalen AP, Siebelink HJ, et al. Entropy as a novel measure of myocardial tissue heterogeneity for prediction of ventricular arrhythmias and mortality in post-infarct patients. *JACC Clin Electrophysiol.* (2019) 5:480–9. doi: 10.1016/j.jacep.2018.12.005

28. Gould J, Porter B, Claridge S, Chen Z, Sieniewicz BJ, Sidhu BS, et al. Mean entropy predicts implantable cardioverter-defibrillator therapy using cardiac magnetic resonance texture analysis of scar heterogeneity. *Heart Rhythm.* (2019) 16:1242–50. doi: 10.1016/j.hrthm.2019.03.001

29. Perez-David E, Arenal Á, Rubio-Guivernau JL. Castillo Rd, Atea L, Arbelo E, et al. Noninvasive identification of ventricular tachycardia-related conducting channels using contrast-enhanced magnetic resonance imaging in patients with chronic myocardial infarction. *J Am Coll Cardiol.* (2011) 57:184–94. doi: 10.1016/j.jacc.2010.07.043

30. Sánchez-Somonte P, Quinto L, Garre P, Zaraket F, Alarcón F, Borràs R, et al. Scar channels in cardiac magnetic resonance to predict appropriate therapies in primary prevention. *Heart Rhythm.* (2021) 18:1336–43. doi: 10.1016/j.hrthm.2021.04.017

31. Ganesan AN, Gunton J, Nucifora G, McGavigan AD, Selvanayagam JB. Impact of late gadolinium enhancement on mortality, sudden death and major adverse cardiovascular events in ischemic and nonischemic cardiomyopathy: a systematic review and meta-analysis. *Int J Cardiol.* (2018) 254:230–7. doi: 10.1016/j.ijcard.2017.10.094

32. Di Marco A, Anguera I, Schmitt M, Klem I, Neilan TG, White JA, et al. Late gadolinium enhancement and the risk for ventricular arrhythmias or sudden death in dilated cardiomyopathy: systematic review and meta-analysis. *JACC: Heart Failure.* (2017) 5:28–38. doi: 10.1016/j.jchf.2016.09.017

33. Kuruvilla S, Adenaw N, Katwal AB, Lipinski MJ, Kramer CM, Salerno M. Late gadolinium enhancement on cardiac magnetic resonance predicts adverse cardiovascular outcomes in nonischemic cardiomyopathy: a systematic review and meta-analysis. *Circ Cardiovasc Imaging.* (2014) 7:250–8. doi: 10.1161/CIRCIMAGING.113.001144

34. Halliday BP, Gulati A, Ali A, Guha K, Newsome S, Arzanauskaite M, et al. Association between midwall late gadolinium enhancement and sudden cardiac death in patients with dilated cardiomyopathy and mild and moderate left ventricular systolic dysfunction. *Circulation.* (2017) 135:2106–15. doi: 10.1161/CIRCULATIONAHA.116.026910

35. Klem I, Klein M, Khan M, Yang EY, Nabi F, Ivanov A, et al. Relationship of LVEF and myocardial scar to long-term mortality risk and mode of death in patients with nonischemic cardiomyopathy. *Circulation.* (2021) 143:1343–58. doi: 10.1161/CIRCULATIONAHA.120.048477

36. Greulich S, Seitz A, Herter D, Günther F, Probst S, Bekeredjian R, et al. Long-term risk of sudden cardiac death in hypertrophic cardiomyopathy: a cardiac magnetic resonance outcome study. *Eur Heart J Cardiovasc Imaging.* (2021) 22:732–41. doi: 10.1093/ehjci/jeaa423

37. Rowin EJ, Maron MS, Adler A, Albano AJ, Varnava AM, Spears D, et al. Importance of newer cardiac magnetic resonance-based risk markers for sudden death prevention in hypertrophic cardiomyopathy: An international multicenter study. *Heart rhythm.* (2021). doi: 10.1016/j.hrthm.2021.12.017

38. O'Mahony C, Jichi F, Pavlou M, Monserrat L, Anastasakis A, Rapezzi C, et al. A novel clinical risk prediction model for sudden cardiac death in hypertrophic cardiomyopathy (HCM risk-SCD). *Eur Heart J.* (2014) 35:2010–20. doi: 10.1093/eurheartj/eht439

39. Todiere G, Nugara C, Gentile G, Negri F, Bianco F, Falletta C, et al. Prognostic role of late gadolinium enhancement in patients with hypertrophic cardiomyopathy and low-to-intermediate sudden cardiac death risk score. *Am J Cardiol.* (2019) 124:1286–92. doi: 10.1016/j.amjcard.2019.07.023

40. Mandawat A, Chattranukulchai P, Mandawat A, Blood AJ, Ambati S, Hayes B, et al. Progression of myocardial fibrosis in nonischemic DCM and association

with mortality and heart failure outcomes. *JACC Cardiovasc Imaging.* (2021) 14:1338–50. doi: 10.1016/j.jcmg.2020.11.006

41. Zorzi A, Perazzolo Marra M, Rigato I, De Lazzari M, Susana A, Niero A, et al. Nonischemic left ventricular scar as a substrate of life-threatening ventricular arrhythmias and sudden cardiac death in competitive athletes. *Circ Arrhythm Electrophysiol.* (2016) 9:e004229. doi: 10.1161/CIRCEP.116.004229

42. Corrado D, Marra MP, Zorzi A, Beffagna G, Cipriani A, De Lazzari M, et al. Diagnosis of arrhythmogenic cardiomyopathy: the Padua criteria. *Int J Cardiol.* (2020) 319:106–14. doi: 10.1016/j.ijcard.2020.06.005

43. Deac M, Alpendurada F, Fanaie F, Vimal R, Carpenter J-P, Dawson A, et al. Prognostic value of cardiovascular magnetic resonance in patients with suspected arrhythmogenic right ventricular cardiomyopathy. *Int J Cardiol.* (2013) 168:3514–21. doi: 10.1016/j.ijcard.2013.04.208

44. Gandjbakhch E, Redheuil A, Pousset F, Charron P, Frank R. Clinical diagnosis, imaging, and genetics of arrhythmogenic right ventricular cardiomyopathy/dysplasia. *J Am Coll Cardiol.* (2018) 72:784–804. doi: 10.1016/j.jacc.2018.05.065

45. Gräni C, Eichhorn C, Bière L, Murthy VL, Agarwal V, Kaneko K, et al. Prognostic value of cardiac magnetic resonance tissue characterization in risk stratifying patients with suspected myocarditis. *J Am Coll Cardiol.* (2017) 70:1964–76. doi: 10.1016/j.jacc.2017.08.050

46. Georgiopoulos G, Figliozzi S, Sanguineti F, Aquaro GD, di Bella G, Stamatelopoulos K, et al. Prognostic impact of late gadolinium enhancement by cardiovascular magnetic resonance in myocarditis: a systematic review and meta-analysis. *Circ Cardiovasc Imaging.* (2021) 14:e011492. doi: 10.1161/CIRCIMAGING.120.011492

47. Pasquini L, Napolitano A, Visconti E, Longo D, Romano A, Tomà P, et al. Gadolinium-based contrast agent-related toxicities. *CNS Drugs.* (2018) 32:229–40. doi: 10.1007/s40263-018-0500-1

48. Schieda N, Blaichman JI, Costa AF, Glikstein R, Hurrell C, James M, et al. Gadolinium-based contrast agents in kidney disease: a comprehensive review and clinical practice guideline issued by the Canadian Association of Radiologists. *Can J Kidney Health Dis.* (2018) 5:2054358118778573. doi: 10.1177/2054358118778573

49. Weinreb JC, Rodby RA, Yee J, Wang CL, Fine D, McDonald RJ, et al. Use of intravenous gadolinium-based contrast media in patients with kidney disease: consensus statements from the American College of Radiology and the National Kidney Foundation. *Kidney Med.* (2021) 3:142–50. doi: 10.1016/j.xkme.2020.10.001

50. Voskoboinik A, Wong MCG, Elliott JK, Costello BT, Prabhu S, Mariani JA, et al. Absence of late gadolinium enhancement on cardiac magnetic resonance imaging in ventricular fibrillation and nonischemic cardiomyopathy. *Pacing Clin Electrophysiol.* (2018) 41:1109–15. doi: 10.1111/pace.13426

51. Kammerlander Andreas A, Marzluf Beatrice A, Zotter-Tufaro C, Aschauer S, Duca F, Bachmann A, et al. T1 Mapping by CMR imaging. *JACC Cardiovasc Imaging.* (2016) 9:14–23. doi: 10.1016/j.jcmg.2015.11.002

52. Messroghli DR, Moon JC, Ferreira VM, Grosse-Wortmann L, He T, Kellman P, et al. Clinical recommendations for cardiovascular magnetic resonance mapping of T1, T2, T2* and extracellular volume: a consensus statement by the Society for Cardiovascular Magnetic Resonance (SCMR) endorsed by the European Association for Cardiovascular Imaging (EACVI). *J Cardiovasc Magn Reson.* (2017) 19:1–24. doi: 10.1186/s12968-017-0389-8

53. Chen Z, Sohal M, Voigt T, Sammut E, Tobon-Gomez C, Child N, et al. Myocardial tissue characterization by cardiac magnetic resonance imaging using T1 mapping predicts ventricular arrhythmia in ischemic and non-ischemic cardiomyopathy patients with implantable cardioverter-defibrillators. *Heart Rhythm.* (2015) 12:792–801. doi: 10.1016/j.hrthm.2014.12.020

54. Puntmann VO, Carr-White G, Jabbour A, Yu C-Y, Gebker R, Kelle S, et al. T1-mapping and outcome in nonischemic cardiomyopathy. *JACC Cardiovasc Imaging.* (2016) 9:40–50. doi: 10.1016/j.jcmg.2015.12.001

55. Xu J, Zhuang B, Sirajuddin A, Li S, Huang J, Yin G, et al. MRI T1 mapping in hypertrophic cardiomyopathy: evaluation in patients without late gadolinium enhancement and hemodynamic obstruction. *Radiology.* (2020) 294:275–86. doi: 10.1148/radiol.2019190651

56. Lota AS, Gatehouse PD, Mohiaddin RH. T2 mapping and T2* imaging in heart failure. *Heart Fail Rev.* (2017) 22:431–40. doi: 10.1007/s10741-017-9616-5

57. van der Bijl P, Podlesnikar T, Bax JJ, Delgado V. Sudden Cardiac Death Risk Prediction: The role of cardiac magnetic resonance imaging. *Revista Española de Cardiología.* (2018) 71:961–70. doi: 10.1016/j.rec.2018.05.019

58. Triadyaksa P, Oudkerk M, Sijens PE. Cardiac T2* mapping: techniques and clinical applications. *J Magn Reson Imaging.* (2020) 52:1340–51. doi: 10.1002/jmri.27023

59. Gastl M, Gotschy A, von Spiczak J, Polacin M, Bönner F, Gruner C, et al. Cardiovascular magnetic resonance T2* mapping for structural alterations in hypertrophic cardiomyopathy. *Eur J Radiol Open.* (2019) 6:78–84. doi: 10.1016/j.ejro.2019.01.007

60. Gastl M, Gruner C, Labucay K, Gotschy A, Von Spiczak J, Polacin M, et al. Cardiovascular magnetic resonance T2* mapping for the assessment of cardiovascular events in hypertrophic cardiomyopathy. *Open heart.* (2020) 7:e001152. doi: 10.1136/openhrt-2019-001152

61. Zorzi A, Mattesi G, Baldi E, Toniolo M, Guerra F, Cauti FM, et al. Prognostic role of myocardial edema as evidenced by early cardiac magnetic resonance in survivors of out-of-hospital cardiac arrest: a multicenter study. *J Am Heart Assoc.* (2021) 10:e021861. doi: 10.1161/JAHA.121.021861

62. Trayanova NA, Pashakhanloo F, Wu KC, Halperin HR. Imaging-based simulations for predicting sudden death and guiding ventricular tachycardia ablation. *Circ Arrhythm Electrophysiol.* (2017) 10:e004743. doi: 10.1161/CIRCEP.117.004743

63. Sung E, Etoz S, Zhang Y, Trayanova NA. Whole-heart ventricular arrhythmia modeling moving forward: Mechanistic insights and translational applications. *Biophy Rev.* (2021) 2:031304. doi: 10.1063/5.0058050

64. Arevalo HJ, Vadakkumpadan F, Guallar E, Jebb A, Malamas P, Wu KC, et al. Arrhythmia risk stratification of patients after myocardial infarction using personalized heart models. *Nat Commun.* (2016) 7:1–8. doi: 10.1038/ncomms11437

65. Deng D, Arevalo HJ, Prakosa A, Callans DJ, Trayanova NA. A feasibility study of arrhythmia risk prediction in patients with myocardial infarction and preserved ejection fraction. *EP Europace.* (2016) 18(Suppl. 4):iv60–6. doi: 10.1093/europace/euw351

66. O'Hara RP, Binka E, Prakosa A, Zimmerman SL, Cartoski MJ, Abraham MR, et al. Personalized computational heart models with T1-mapped fibrotic remodeling predict sudden death risk in patients with hypertrophic cardiomyopathy. *Elife.* (2022) 11:e73325. doi: 10.7554/eLife.73325

67. Prakosa A, Arevalo HJ, Deng D, Boyle PM, Nikolov PP, Ashikaga H, et al. Personalized virtual-heart technology for guiding the ablation of infarct-related ventricular tachycardia. *Nat Biomed Eng.* (2018) 2:732–40. doi: 10.1038/s41551-018-0282-2

68. Juneau D, Erthal F, Chow BJW, Redpath C, Ruddy TD, Knuuti J, et al. The role of nuclear cardiac imaging in risk stratification of sudden cardiac death. *J Nucl Cardiol.* (2016) 23:1380–98. doi: 10.1007/s12350-016-0599-8

69. Mariani G, Bruselli L, Kuwert T, Kim EE, Flotats A, Israel O, et al. A review on the clinical uses of SPECT/CT. *Eur J Nucl Med Mol Imaging.* (2010) 37:1959–85. doi: 10.1007/s00259-010-1390-8

70. Piccini JP, Horton JR, Shaw LK, Al-Khatib SM, Lee KL, Iskandrian AE, et al. Single-photon emission computed tomography myocardial perfusion defects are associated with an increased risk of all-cause death, cardiovascular death, and sudden cardiac death. *Circ Cardiovasc Imaging.* (2008) 1:180–8. doi: 10.1161/CIRCIMAGING.108.776484

71. Piccini Jonathan P, Starr Aijing Z, Horton John R, Shaw Linda K, Lee Kerry L, Al-Khatib Sana M, et al. Single-photon emission computed tomography myocardial perfusion imaging and the risk of sudden cardiac death in patients with coronary disease and left ventricular ejection fraction >35%. *J Am Coll Cardiol.* (2010) 56:206–14. doi: 10.1016/j.jacc.2010.01.061

72. Adamu U, Knollmann D, Almutairi B, Alrawashdeh W, Deserno V, Vogt F, et al. Stress/rest myocardial perfusion scintigraphy in patients without significant coronary artery disease. *J Nucl Cardiol.* (2010) 17:38–44. doi: 10.1007/s12350-009-9133-6

73. Dorbala S, Di Carli Marcelo F, Beanlands Rob S, Merhige Michael E, Williams Brent A, Veledar E, et al. Prognostic value of stress myocardial perfusion positron emission tomography. *J Am Coll Cardiol.* (2013) 61:176–84. doi: 10.1016/j.jacc.2012.09.043

74. Dorbala S, Di Carli MF. Cardiac PET perfusion: prognosis, risk stratification, and clinical management. *Semin Nucl Med.* (2014) 44:344–57. doi: 10.1053/j.semnuclmed.2014.05.003

75. Morishima I, Sone T, Tsuboi H, Mukawa H, Uesugi M, Morikawa S, et al. Risk stratification of patients with prior myocardial infarction and advanced left ventricular dysfunction by gated myocardial perfusion SPECT imaging. *J Nucl Cardiol.* (2008) 15:631–7. doi: 10.1016/j.nuclcard.2008.03.009

76. Gupta A, Harrington M, Albert Christine M, Bajaj Navkaranbir S, Hainer J, Morgan V, et al. Myocardial scar but not ischemia is associated with defibrillator shocks and sudden cardiac death in stable patients with reduced left ventricular ejection fraction. *JACC Clin Electrophysiol.* (2018) 4:1200–10. doi: 10.1016/j.jacep.2018.06.002

77. Blankstein R, Osborne M, Naya M, Waller A, Kim CK, Murthy VL, et al. Cardiac positron emission tomography enhances prognostic assessments of patients with suspected cardiac sarcoidosis. *J Am Coll Cardiol.* (2014) 63:329–36. doi: 10.1016/j.jacc.2013.09.022

78. Zelt JG, deKemp RA, Rotstein BH, Nair GM, Narula J, Ahmadi A, et al. Nuclear imaging of the cardiac sympathetic nervous system: a disease-specific interpretation in heart failure. *JACC Cardiovas Imaging.* (2020) 13:1036–54. doi: 10.1016/j.jcmg.2019.01.042

79. Canty JM Jr, Suzuki G, Banas MD, Verheyen F, Borgers M, Fallavollita JA. Hibernating myocardium: chronically adapted to ischemia but vulnerable to sudden death. *Circ Res.* (2004) 94:1142–9. doi: 10.1161/01.RES.0000125628.57672.CF

80. Popescu CE, Cuzzocrea M, Monaco L, Caobelli F. Assessment of myocardial sympathetic innervation by PET in patients with heart failure: a review of the most recent advances and future perspectives. *Clin Transl Imaging.* (2018) 6:459–70. doi: 10.1007/s40336-018-0293-8

81. Fukuda K, Kanazawa H, Aizawa Y, Ardell JL, Shivkumar K. Cardiac innervation and sudden cardiac death. *Circ Res.* (2015) 116:2005–19. doi: 10.1161/CIRCRESAHA.116.304679

82. Malhotra S, Fernandez SF, Fallavollita JA, Canty JM. Prognostic significance of imaging myocardial sympathetic innervation. *Curr Cardiol Rep.* (2015) 17:62. doi: 10.1007/s11886-015-0613-9

83. Jacobson AF, Senior R, Cerqueira MD, Wong ND, Thomas GS, Lopez VA, et al. Myocardial iodine-123 meta-iodobenzylguanidine imaging and cardiac events in heart failure: results of the prospective ADMIRE-HF (AdreView Myocardial Imaging for Risk Evaluation in Heart Failure) study. *J Am Coll Cardiol.* (2010) 55:2212–21. doi: 10.1016/j.jacc.2010.01.014

84. Tamaki S, Yamada T, Okuyama Y, Morita T, Sanada S, Tsukamoto Y, et al. Cardiac Iodine-123 metaiodobenzylguanidine imaging predicts sudden cardiac death independently of left ventricular ejection fraction in patients with chronic heart failure and left ventricular systolic dysfunction. *J Am Coll Cardiol.* (2009) 53:426–35. doi: 10.1016/j.jacc.2008.10.025

85. Fallavollita James A, Heavey Brendan M, Luisi Andrew J, Michalek Suzanne M, Baldwa S, Mashtare Terry L, et al. Regional myocardial sympathetic denervation predicts the risk of sudden cardiac arrest in ischemic cardiomyopathy. *J Am Coll Cardiol.* (2014) 63:141–9. doi: 10.1016/j.jacc.2013.07.096

86. Yamamoto H, Yamada T, Tamaki S, Morita T, Furukawa Y, Iwasaki Y, et al. Prediction of sudden cardiac death in patients with chronic heart failure by regional washout rate in cardiac MIBG SPECT imaging. *J Nucl Cardiol.* (2019) 26:109–17. doi: 10.1007/s12350-017-0913-0

87. Aikawa T, Naya M, Obara M, Oyama-Manabe N, Manabe O, Magota K, et al. Regional interaction between myocardial sympathetic denervation, contractile dysfunction, and fibrosis in heart failure with preserved ejection fraction: 11C-hydroxyephedrine PET study. *Eur J Nucl Med Mol Imaging.* (2017) 44:1897–905. doi: 10.1007/s00259-017-3760-y

88. Katoh S, Shishido T, Kutsuzawa D, Arimoto T, Netsu S, Funayama A, et al. Iodine-123-metaiodobenzylguanidine imaging can predict future cardiac events in heart failure patients with preserved ejection fraction. *Ann Nucl Med.* (2010) 24:679–86. doi: 10.1007/s12149-010-0409-3

89. Seo M, Yamada T, Tamaki S, Watanabe T, Morita T, Furukawa Y, et al. Prognostic significance of cardiac 123I-MIBG SPECT imaging in heart failure patients with preserved ejection fraction. *JACC Cardiovasc Imaging.* (2021). doi: 10.1016/j.jcmg.2021.08.003

90. Kloner RA. Stunned and hibernating myocardium: where are we nearly 4 decades later? *J Am Heart Assoc.* (2020) 9:e015502. doi: 10.1161/JAHA.119.015502

91. Canty JM, Fallavollita JA. Hibernating myocardium. *J Nucl Cardiol.* (2005) 12:104–19. doi: 10.1016/j.nuclcard.2004.11.003

92. Fernandez SF, Ovchinnikov V, Canty JM Jr, Fallavollita JA. Hibernating myocardium results in partial sympathetic denervation and nerve sprouting. *Am J Physiol Heart Circ Physiol.* (2013) 304:H318–H27. doi: 10.1152/ajpheart.00810.2011

93. Uebleis C, Hellweger S, Laubender RP, Becker A, Sohn H-Y, Lehner S, et al. The amount of dysfunctional but viable myocardium predicts long-term survival in patients with ischemic cardiomyopathy and left ventricular dysfunction. *Int J Cardiovasc Imaging.* (2013) 29:1645–53. doi: 10.1007/s10554-013-0254-2

94. Desideri A, Cortigiani L, Christen Alejandra I, Coscarelli S, Gregori D, Zanco P, et al. The extent of perfusion–F18-fluorodeoxyglucose positron emission tomography mismatch determines mortality in medically treated patients with chronic ischemic left ventricular dysfunction. *J Am Coll Cardiol.* (2005) 46:1264–9. doi: 10.1016/j.jacc.2005.06.057

95. Malhotra S, Canty John M. Structural and physiological imaging to predict the risk of lethal ventricular arrhythmias and sudden death. *JACC Cardiovasc Imaging.* (2019) 12:2049–64. doi: 10.1016/j.jcmg.2019.05.034

96. Nensa F, Bamberg F, Rischpler C, Menezes L, Poeppel TD, la Fougère C, et al. Hybrid cardiac imaging using PET/MRI: a joint position statement by the European Society of Cardiovascular Radiology (ESCR) and the European Association of Nuclear Medicine (EANM). *Eur Radiol.* (2018) 28:4086–101. doi: 10.1007/s00330-017-5008-4

97. Rischpler C, Siebermair J, Kessler L, Quick HH, Umutlu L, Rassaf T, et al. editors. Cardiac PET/MRI: current clinical status and future perspectives. *Semin Nucl Med.* (2020) 50:260–9. doi: 10.1053/j.semnuclmed.2020.02.012

98. Hanneman K, Kadoch M, Guo HH, Jamali M, Quon A, Iagaru A, et al. Initial experience with simultaneous 18F-FDG PET/MRI in the evaluation of cardiac sarcoidosis and myocarditis. *Clin Nucl Med.* (2017) 42:e328–e34. doi: 10.1097/RLU.0000000000001669

99. Vita T, Okada DR, Veillet-Chowdhury M, Bravo PE, Mullins E, Hulten E, et al. Complementary value of cardiac magnetic resonance imaging and positron emission tomography/computed tomography in the assessment of cardiac sarcoidosis. *Circ Cardiovasc Imaging.* (2018) 11:e007030. doi: 10.1161/CIRCIMAGING.117.007030

100. Schneider S, Batrice A, Rischpler C, Eiber M, Ibrahim T, Nekolla SG. Utility of multimodal cardiac imaging with PET/MRI in cardiac sarcoidosis: implications for diagnosis, monitoring and treatment. *Eur Heart J.* (2014) 35:312. doi: 10.1093/eurheartj/eht335

101. Wisenberg G, Thiessen J, Pavlovsky W, Butler J, Wilk B, Prato F. Same day comparison of PET/CT and PET/MR in patients with cardiac sarcoidosis. *J Nucl Cardiol.* (2020) 27:2118–29. doi: 10.1007/s12350-018-01578-8

102. Sparrow P, Merchant N, Provost Y, Doyle D, Nguyen E, Paul N. Cardiac MRI and CT features of inheritable and congenital conditions associated with sudden cardiac death. *Eur Radiol.* (2009) 19:259–70. doi: 10.1007/s00330-008-1169-5

103. Mahida S, Sacher F, Dubois R, Sermesant M, Bogun F, Haïssaguerre M, et al. Cardiac imaging in patients with ventricular tachycardia. *Circulation.* (2017) 136:2491–507. doi: 10.1161/CIRCULATIONAHA.117.029349

104. Shiozaki AA, Senra T, Arteaga E, Martinelli Filho M, Pita CG, Ávila LFR, et al. Myocardial fibrosis detected by cardiac CT predicts ventricular fibrillation/ventricular tachycardia events in patients with hypertrophic cardiomyopathy. *J Cardiovasc Comput Tomogr.* (2013) 7:173–81. doi: 10.1016/j.jcct.2013.04.002

105. Langer C, Lutz M, Eden M, Lüdde M, Hohnhorst M, Gierloff C, et al. Hypertrophic cardiomyopathy in cardiac CT: a validation study on the detection of intramyocardial fibrosis in consecutive patients. *Int J Cardiovasc Imaging.* (2014) 30:659–67. doi: 10.1007/s10554-013-0358-8

106. Takigawa M, Duchateau J, Sacher F, Martin R, Vlachos K, Kitamura T, et al. Are wall thickness channels defined by computed tomography predictive of isthmuses of postinfarction ventricular tachycardia? *Heart Rhythm.* (2019) 16:1661–8. doi: 10.1016/j.hrthm.2019.06.012

107. Sasaki T, Calkins H, Miller CF, Zviman MM, Zipunnikov V, Arai T, et al. New insight into scar-related ventricular tachycardia circuits in ischemic cardiomyopathy: fat deposition after myocardial infarction on computed tomography–a pilot study. *Heart Rhythm.* (2015) 12:1508–18. doi: 10.1016/j.hrthm.2015.03.041

108. Mordi I, Radjenovic A, Stanton T, Gardner RS, McPhaden A, Carrick D, et al. Prevalence and prognostic significance of lipomatous metaplasia in patients with prior myocardial infarction. *JACC Cardiovasc Imaging.* (2015) 8:1111–2. doi: 10.1016/j.jcmg.2014.07.024

109. Sung E, Prakosa A, Aronis KN, Zhou S, Zimmerman SL, Tandri H, et al. Personalized digital-heart technology for ventricular tachycardia ablation targeting in hearts with infiltrating adiposity. *Circ Arrhythm Electrophysiol.* (2020) 13:e008912. doi: 10.1161/CIRCEP.120.008912

110. Giger ML. Machine learning in medical imaging. *J Am Coll Radiol.* (2018) 15:512–20. doi: 10.1016/j.jacr.2017.12.028

111. Quer G, Arnaout R, Henne M, Arnaout R. Machine learning and the future of cardiovascular care: JACC state-of-the-art review. *J Am Coll Cardiol.* (2021) 77:300–13. doi: 10.1016/j.jacc.2020.11.030

112. Xie D, Li Y, Yang H, Bai L, Wang T, Zhou F, et al. Denoising arterial spin labeling perfusion MRI with deep machine learning. *Magn Reson Imaging.* (2020) 68:95–105. doi: 10.1016/j.mri.2020.01.005

113. Wang T, Lei Y, Fu Y, Curran WJ, Liu T, Nye JA, et al. Machine learning in quantitative PET: A review of attenuation correction and low-count image reconstruction methods. *Physica Medica.* (2020) 76:294–306. doi: 10.1016/j.ejmp.2020.07.028

114. Gong K, Berg E, Cherry SR Qi J. Machine learning in PET: from photon detection to quantitative image reconstruction. *Proc IEEE.* (2019) 108:51–68. doi: 10.1109/JPROC.2019.2936809

115. Xiang H, Lim H, Fessler JA, Dewaraja YK, A. deep neural network for fast and accurate scatter estimation in quantitative SPECT/CT under challenging scatter conditions. *Eur J Nucl Med Mol Imaging.* (2020) 47:2956. doi: 10.1007/s00259-020-04840-9

116. Arabi H, AkhavanAllaf A, Sanaat A, Shiri I, Zaidi H. The promise of artificial intelligence and deep learning in PET and SPECT imaging. *Physica Medica.* (2021) 83:122–37. doi: 10.1016/j.ejmp.2021.03.008

117. Fahmy AS, Rausch J, Neisius U, Chan RH, Maron MS, Appelbaum E, et al. Automated cardiac MR scar quantification in hypertrophic cardiomyopathy using deep convolutional neural networks. *JACC Cardiovasc Imaging.* (2018) 11:1917–8. doi: 10.1016/j.jcmg.2018.04.030

118. Ghanbari F, Joyce T, Kozerke S, Guaricci A, Masci P, Pavon A, et al. Performance of a machine-learning algorithm for fully automatic LGE scar quantification in the large multi-national derivate registry. *Eur Heart J Cardiovasc Imaging.* (2021) 22 (Suppl. 2):jeab090. doi: 10.1093/ehjci/jeab090.023

119. Cheng S, Fang M, Cui C, Chen X, Yin G, Prasad SK, et al. LGE-CMR-derived texture features reflect poor prognosis in hypertrophic cardiomyopathy patients with systolic dysfunction: preliminary results. *Eur Radiol.* (2018) 28:4615–24. doi: 10.1007/s00330-018-5391-5

120. Mannil M, Kato K, Manka R, von Spiczak J, Peters B, Cammann VL, et al. Prognostic value of texture analysis from cardiac magnetic resonance imaging in patients with Takotsubo syndrome: a machine learning based proof-of-principle approach. *Sci Rep.* (2020) 10:20537. doi: 10.1038/s41598-020-76432-4

121. Wongvibulsin S, Wu KC, Zeger SL. Clinical risk prediction with random forests for survival, longitudinal, and multivariate (RF-SLAM) data analysis. *BMC Med Res Methodol.* (2020) 20:1–14. doi: 10.1186/s12874-019-0863-0

122. Shade JK, Prakosa A, Popescu DM, Yu R, Okada DR, Chrispin J, et al. Predicting risk of sudden cardiac death in patients with cardiac sarcoidosis using multimodality imaging and personalized heart modeling in a multivariable classifier. *Sci Adv.* (2021) 7:eabi8020. doi: 10.1126/sciadv.abi8020

123. Bhattacharya M, Lu D-Y, Kudchadkar SM, Greenland GV, Lingamaneni P, Corona-Villalobos CP, et al. Identifying ventricular arrhythmias and their predictors by applying machine learning methods to electronic health records in patients with hypertrophic cardiomyopathy (HCM-VAr-Risk Model). *Am J Cardiol.* (2019) 123:1681–9. doi: 10.1016/j.amjcard.2019.02.022

124. Koonjoo N, Zhu B, Bagnall GC, Bhutto D, Rosen M. Boosting the signal-to-noise of low-field MRI with deep learning image reconstruction. *Sci Rep.* (2021) 11:1–16. doi: 10.1038/s41598-021-87482-7

125. Campbell-Washburn AE, Ramasawmy R, Restivo MC, Bhattacharya I, Basar B, Herzka DA, et al. Opportunities in interventional and diagnostic imaging by using high-performance low-field-strength MRI. *Radiology.* (2019) 293:384–93. doi: 10.1148/radiol.2019190452

126. Ravishankar S, Ye JC, Fessler JA. Image reconstruction: from sparsity to data-adaptive methods and machine learning. *Proc IEEE.* (2019) 108:86–109. doi: 10.1109/JPROC.2019.2936204

127. Esteva A, Chou K, Yeung S, Naik N, Madani A, Mottaghi A, et al. Deep learning-enabled medical computer vision. *NPJ Digit Med.* (2021) 4:1–9. doi: 10.1038/s41746-020-00376-2

128. Leiner T, Rueckert D, Suinesiaputra A, Baeßler B, Nezafat R, Išgum I, et al. Machine learning in cardiovascular magnetic resonance: basic concepts and applications. *J Cardiovasc Magn Reson.* (2019) 21:1–14. doi: 10.1186/s12968-019-0575-y

129. McAlindon E, Pufulete M, Lawton C, Angelini GD, Bucciarelli-Ducci C. Quantification of infarct size and myocardium at risk: evaluation of different techniques and its implications. *Eur Heart J Cardiovasc Imaging.* (2015) 16:738–46. doi: 10.1093/ehjci/jev001

130. Engblom H, Tufvesson J, Jablonowski R, Carlsson M, Aletras AH, Hoffmann P, et al. A new automatic algorithm for quantification of myocardial infarction imaged by late gadolinium enhancement cardiovascular magnetic resonance: experimental validation and comparison to expert delineations in multi-center, multi-vendor patient data. *J Cardiovasc Magn Reson.* (2016) 18:1–13. doi: 10.1186/s12968-016-0242-5

131. Popescu DM, Abramson HG Yu R, Lai C, Shade JK, Wu KC, et al. Anatomically informed deep learning on contrast-enhanced cardiac magnetic resonance imaging for scar segmentation and clinical feature extraction. *Cardiovasc Digit Health J.* (2021). doi: 10.1016/j.cvdhj.2021.11.007

132. Fahmy AS, Neisius U, Chan RH, Rowin EJ, Manning WJ, Maron MS, et al. Three-dimensional deep convolutional neural networks for automated myocardial scar quantification in hypertrophic cardiomyopathy: a multicenter multivendor study. *Radiology.* (2020) 294:52–60. doi: 10.1148/radiol.2019190737

133. Aronis KN, Okada DR, Xie E, Daimee UA, Prakosa A, Gilotra NA, et al. Spatial dispersion analysis of LGE-CMR for prediction of ventricular arrhythmias in patients with cardiac sarcoidosis. *Pacing Clin Electrophysiol.* (2021) 44:2067–74. doi: 10.1111/pace.14406

134. Alis D, Guler A, Yergin M, Asmakutlu O. Assessment of ventricular tachyarrhythmia in patients with hypertrophic cardiomyopathy with machine learning-based texture analysis of late gadolinium enhancement cardiac MRI. *Diagn Interv Imaging.* (2020) 101:137–46. doi: 10.1016/j.diii.2019.10.005

135. Fei J-L, Pu C-L, Xu F-Y, Wu Y, Hu H-J. Progress in radiomics of common heart disease based on cardiac magnetic resonance imaging. *J Mol Clin Med.* (2021) 4:29–38. doi: 10.31083/j.jmcm.2021.01.801

136. Shu S, Wang C, Hong Z, Zhou X, Zhang T, Peng Q, et al. Prognostic value of late enhanced cardiac magnetic resonance imaging derived texture features in dilated cardiomyopathy patients with severely reduced ejection fractions. *Front Cardiovasc Med.* (2021) 8:766423. doi: 10.3389/fcvm.2021.766423

137. Balaban G, Halliday BP, Hammersley D, Rinaldi CA, Prasad SK, Bishop MJ, et al. Left ventricular shape predicts arrhythmic risk in fibrotic dilated cardiomyopathy. *Europace.* (2021). doi: 10.1093/europace/euab306

138. Krebs J, Mansi T, Delingette H, Lou B, Lima JAC, Tao S, et al. CinE caRdiac magneTic resonAnce to predIct veNTricular arrhYthmia (CERTAINTY). *Sci Rep.* (2021) 11:22683. doi: 10.1038/s41598-021-02111-7

139. Okada DR, Miller J, Chrispin J, Prakosa A, Trayanova N, Jones S, et al. Substrate spatial complexity analysis for the prediction of ventricular arrhythmias in patients with ischemic cardiomyopathy. *Circ Arrhythm Electrophysiol.* (2020) 13:e007975. doi: 10.1161/CIRCEP.119.007975

140. Khamzin S, Dokuchaev A, Bazhutina A, Chumarnaya T, Zubarev S, Lyubimtseva T, et al. Machine Learning prediction of cardiac resynchronisation therapy response from combination of clinical and model-driven data. *Front Physiol.* (2021) 2021:2283. doi: 10.1101/2021.09.03.458464

141. Cuocolo R, Perillo T, De Rosa E, Ugga L, Petretta M. Current applications of big data and machine learning in cardiology. *J Geriatr Cardiol.* (2019) 16:601. doi: 10.11909/j.issn.1671-5411.2019.08.002

142. Smole T, Žunkovič B, Pičulin M, Kokalj E, Robnik-Šikonja M, Kukar M, et al. A machine learning-based risk stratification model for ventricular tachycardia and heart failure in hypertrophic cardiomyopathy. *Comput Biol Med.* (2021) 135:104648. doi: 10.1016/j.compbiomed.2021.104648

143. Trayanova NA, Popescu DM, Shade JK. Machine learning in arrhythmia and electrophysiology. *Circ Res.* (2021) 128:544–66. doi: 10.1161/CIRCRESAHA.120.317872

frontiers | Frontiers in Cardiovascular Medicine

TYPE Review
PUBLISHED 14 September 2022
DOI 10.3389/fcvm.2022.844275

OPEN ACCESS

EDITED BY
Richard Hauer,
University Medical Center Utrecht, Netherlands

REVIEWED BY
Jordi Heijman,
Maastricht University, Netherlands
Viorel Mihalef,
Siemens Healthcare, United States
Yunlong Huo,
Shanghai Jiao Tong University, China

*CORRESPONDENCE
Matteo Anselmino
matteo.anselmino@unito.it

SPECIALTY SECTION
This article was submitted to Cardiac Rhythmology, a section of the journal Frontiers in Cardiovascular Medicine

RECEIVED 27 December 2021
ACCEPTED 22 August 2022
PUBLISHED 14 September 2022

CITATION
Anselmino M, Scarsoglio S, Ridolfi L, De Ferrari GM and Saglietto A (2022) Insights from computational modeling on the potential hemodynamic effects of sinus rhythm versus atrial fibrillation.
Front. Cardiovasc. Med. 9:844275.
doi: 10.3389/fcvm.2022.844275

Insights from computational modeling on the potential hemodynamic effects of sinus rhythm versus atrial fibrillation

Matteo Anselmino[1]*, Stefania Scarsoglio[2], Luca Ridolfi[3], Gaetano Maria De Ferrari[1] and Andrea Saglietto[1]

[1]Division of Cardiology, Department of Medical Sciences, "Città della Salute e della Scienza di Torino" Hospital, University of Turin, Turin, Italy, [2]Department of Mechanical and Aerospace Engineering, Politecnico di Torino, Turin, Italy, [3]Department of Environmental, Land, and Infrastructure Engineering, Politecnico di Torino, Turin, Italy

Atrial fibrillation (AF) is the most common clinical tachyarrhythmia, posing a significant burden to patients, physicians, and healthcare systems worldwide. With the advent of more effective rhythm control strategies, such as AF catheter ablation, an early rhythm control strategy is progressively demonstrating its superiority not only in symptoms control but also in prognostic terms, over a standard strategy (rate control, with rhythm control reserved only to patients with refractory symptoms). This review summarizes the different impacts exerted by AF on heart mechanics and systemic circulation, as well as on cerebral and coronary vascular beds, providing computational modeling-based hemodynamic insights in favor of pursuing sinus rhythm maintenance in AF patients.

KEYWORDS

atrial fibrillation, hemodynamics, beat-to-beat variability, systemic circulation, cerebral circulation, coronary circulation

Introduction

Atrial fibrillation (AF), the most common clinical tachyarrhythmia in adults, provokes a significant burden to patients, physicians, and healthcare systems worldwide. The Global Burden of Disease (GBD) Study estimates nearly 60 million prevalent AF cases in 2019 (nearly doubling the estimated prevalence in 1990) (1), with epidemiological projections foreseeing a further rise during the next decades (2). These alarming data urge the scientific community to attempt solving the clinical conundrum concerning the optimal management of this growing subset of patients.

The never-ending debate between those favoring sinus rhythm (SR) maintenance (*rhythm control*) over the simple treatment of symptoms related to high ventricular response AF (*rate control*) is yet not concluded. In the early 2000s, two randomized

clinical trials (AFFIRM and RACE) showed, with respect to hard cardiovascular endpoints, that rate control was non-inferior to rhythm control. Subsequent data pooled from a large population of patients (3) reported similar results, and the AF-CHF study (4) showed that, even in the presence of heart failure, rhythm control did not result superior to rate control. However, these trials were published before the widespread adoption of AF catheter ablation, and thus, the rhythm control option mostly included patients on anti-arrhythmic drugs (AADs). In the last decade, instead, AF catheter ablation has emerged as the most effective tool to maintain long-term SR, both as second-line therapy after failed AADs or as first-line approach (5, 6), potentially modifying the rhythm versus rate control benefits. In fact, a *post-hoc* analysis of the AFFIRM trial showed that SR rhythm maintenance was independently associated with improved survival, hinting that rhythm control might be prognostic, in case SR is maintained avoiding AADs side effects (7). In the past few years, albeit AF catheter ablation missed to statistically demonstrate its superiority on hard cardiovascular endpoints over AAD-based rhythm control strategy in the intention-to-treat analysis of a large clinical trial (CABANA) (8), the per-protocol analysis of the aforementioned study (characterized by high crossover rates between study arms), as well as several observational studies (9–11), showed that AF catheter ablation reduced all-cause mortality, stroke, and hospitalization. The EAST-AFNET 4 trial (12), published in 2020, eventually demonstrated that an early rhythm control approach, within the first 12 months since the first diagnosis, both by AADs and AF catheter ablation, was associated with improved survival compared to a standard approach (e.g., rate control, with rhythm control reserved to those patients still symptomatic despite rate control medications).

Clinical data focusing on the hemodynamic effects of AF are lacking and somewhat controversial, likely due to the challenge of obtaining precise measures in the specific districts (e.g., cerebral circulation) and of eliminating the numerous potential clinical confounders that limit the attempt of investigating arrhythmia-specific effects. The present review, sustained by the mounting data toward the prognostic benefit of SR maintenance, summarizes modeling-based evidence on the detrimental hemodynamic effects of AF on different circulatory districts to thoroughly argument why restoring SR in AF patients should be pursued. In particular, we focused on the three main aspects that have captured the most attention in the last decade, namely, heart mechanics and systemic circulation, cerebral hemodynamics, and coronary circle.

The efficiency of multiscale hemodynamic modeling for the description of the cardiovascular system has been widely recognized, and personalized computational hemodynamics is currently a reliable investigative tool in translational medicine (13–19). **Figure 1** shows a schematic representation of the main computational approaches, ranging from zero-dimensional (0D) to three-dimensional (3D), together with their mathematical features and hemodynamic outcomes. By simplifying the spatial description, in the 0D lumped-parameter model, each cardiovascular region is modeled through a combination of electrical counterparts: the viscous/dissipative effects are taken into account by the resistances (R), the distensibility/contractility effects are described by the compliances/elastances (C/E), and the inertial effects are considered by the inertances (L), leading to the most general 3-elements (or RLC circuit) Windkessel model. Through the electric analog, the only independent variable is time (t), and the 0D lumped-parameter model is suitable to investigate the temporal evolution of each cardiovascular compartment in terms of pressure (P), flow rate (Q), and blood volume (V). The one-dimensional (1D) distributed-parameter model identifies the vessel axis (x) as the preferential spatial direction and assumes the following hypotheses: the blood is Newtonian, incompressible, and characterized by constant density and kinematic viscosity; effects of suspended particles are neglected; vessels are asymmetrical, tapered, longitudinally tethered, with impermeable walls and only subject to small and radial deformations; flow is laminar; and pressure is uniform across the section. x and t (time) are the independent variables, while hemodynamics is described by the vessel area (A), pressure (P), and flow rate (Q). The 1D model, composed of the continuity, momentum, and constitutive equations, is able to capture a higher level of geometrical and viscoelastic details, as well as wave propagation in the arterial tree. Eventually, in the 3D model, the blood flow is governed by the three-dimensional continuity and momentum Navier-Stokes equations, which are discretized over the computational domain and usually solved by finite element/volume methods. In so doing, the temporal evolution of the 3D flow velocity and pressure fields over the whole spatial domain are obtained, making 3D modeling particularly promising to investigate the local hemodynamics of complex vascular morphologies in terms of flow velocity and wall shear stress-related parameters. Even though hemodynamic modeling cannot substitute or deny *in vivo* clinical findings, modeling-based data provide important insights for clinicians and lay the basis for future dedicated clinical studies (20–23).

Atrial fibrillation, heart mechanics, and systemic circulation

The AF induces several detrimental effects on systemic hemodynamics. The two main determinants of this noxious influence are (1) the fibrillatory atrial activation during AF that leads to ineffective atrial contraction and loss of atrial contribution to the ventricular filling ("atrial kick," normally contributing up to 20–30% of the volume) (24); and (2) the irregularity of the ventricular activation during AF (irregular RR intervals), as elegantly demonstrated in a seminal study by Clarke (25), published more than 20 years ago. In this study,

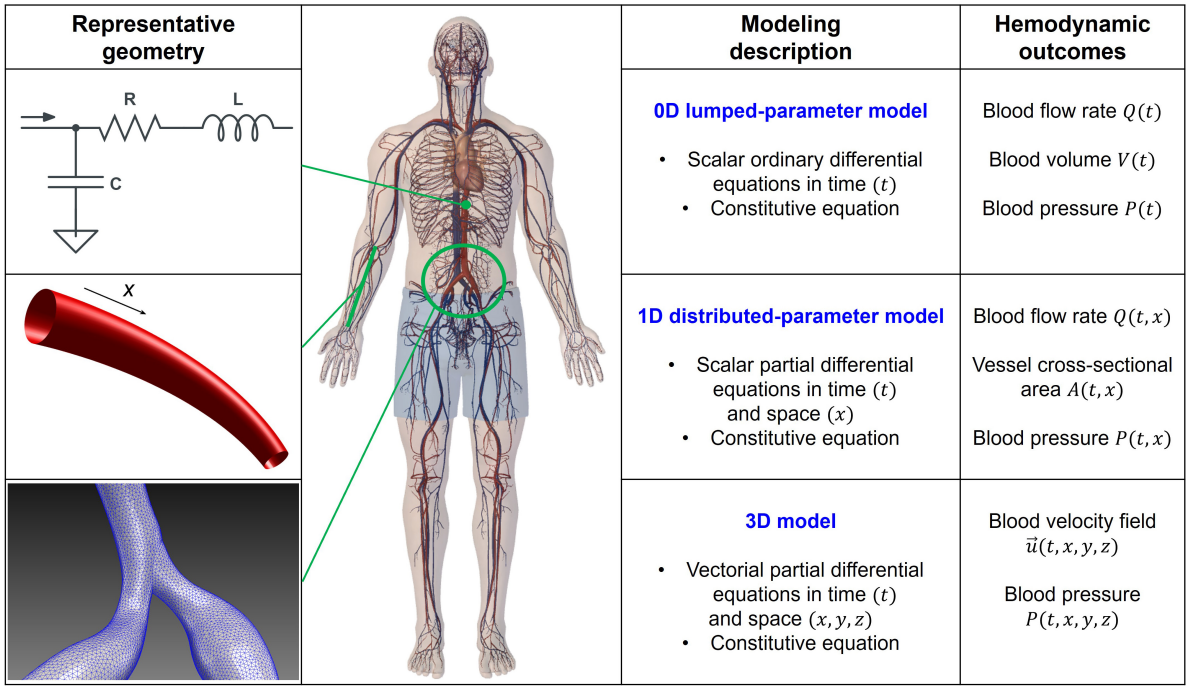

FIGURE 1
Scheme of the 0D, 1D, and 3D computational approaches: representative geometry, modeling description, and hemodynamic outcomes. RLC circuit accounts for dissipative (*R*, resistance), inertial (*L*, inertance), and elasticity (*C*, compliance) effects in the 0D model. Spatial coordinates (*x*, *y*, *z*) and time (*t*) are the independent variables, while volume (*V*), flow rate (*Q*), pressure (*P*), vessel cross-sectional area (*A*), and velocity field ($\vec{u}$=(*u*, *v*, *w*)) are the dependent variables and hemodynamic outcomes of the different models. Balance equations of mass and momentum are expressed in the differential form (0D: ordinary; 1D and 3D: partial), while constitutive equations rule the strain-stress relation between blood and wall vessel.

performed on 16 AF patients, compared to ventricular pacing at the same mean heart rate, during AF, the irregularity of RR intervals led to decreased cardiac output, increased pulmonary wedge pressure, and increased right atrial pressure.

However, despite these known effects, evidence on the global cardiovascular system response to AF remained scarce and controversial. Recently, a lumped-parameter AF modeling approach for the heart and systemic circulation was proposed (26), presenting the following potential advantages: first of all, AF's hemodynamic impact can be assessed in standardized conditions, without the potential confounding effect of other comorbidities; second, the most relevant cardiac variables, as well as hemodynamic parameters, can be monitored contemporaneously. The initial computational analysis investigated the hemodynamic response during AF at a given mean ventricular rate (75 bpm) in an ideal healthy male young adult, meaning that the model is not patient-specific, but model parameters are calibrated to reproduce the hemodynamic response of a generic healthy subject with common anthropometric and physical features (e.g., weight: 75 kg, height: 175 cm, age: 25 years old, sex: male). In this setup, AF induced a reduction in cardiac output, stroke volume, and ejection fraction, as well as an increase in left ventricular end-diastolic pressure and volume, left atrial pressures and volumes, and pulmonary vein pressure. Overall, while the right chambers appeared to be less affected by the arrhythmia, left ventricle pressure-volume loops clearly indicated reduced cardiac efficiency during AF compared to SR. A focus on the fluid dynamics of heart valves (27) showed that during AF, both atrioventricular valves do not seem to worsen their performance, while the arterial valves' efficiency is remarkably reduced.

A further step forward was to investigate the hemodynamic effects of different mean ventricular response rates. In fact, from a clinical standpoint, a clear heart rate target for AF patients, especially for those with the permanent form of arrhythmia, is lacking. A single randomized clinical trial, the Rate Control Efficacy in Permanent Atrial Fibrillation II (RACE II) (28), suggested that, in patients with permanent AF, lenient (targeting resting heart rate below 110 bpm) is not inferior to strict rate control (targeting resting heart rate below 80) both in terms of cardiovascular outcomes and quality of life. However, this clinical study presented several limitations, one out of all the modest difference in average heart rates achieved in the lenient and strict control groups (85 and 75 bpm, respectively) (29). Five different computational simulations, assuming resting conditions, with varying mean ventricular responses (50, 70,

90, 110, 130 bpm) were therefore performed (30). Interestingly, based on the lumped parameter model, slower ventricular responses during AF related to reduced left ventricular pressure increased stroke volume and ejection fraction, improved cardiac efficiency, and reduced oxygen consumption compared to higher ventricular rates. These results suggest that lowering ventricular rate during AF may partially blunt the detrimental hemodynamic impact exerted by the arrhythmia. Furthermore, an additional analysis was run to evaluate how the resting ventricular rate influenced the global cardiovascular systemic response to exercise with ongoing AF (31). Once again, the outcome of this exploration underlined that, in case of a slower basal ventricular response (70 bpm), compared to a higher one (100 bpm), the pulmonary venous pressure undergoes a dampened worsening (increase), and systemic blood pressure shows a more appropriate increase (as demanded by exertion).

The same computational framework was used to assess the hemodynamic impact of different left valvular heart diseases on systemic hemodynamics during AF (32). Several valvular pathologies (e.g., aortic stenosis, aortic regurgitation, mitral stenosis, and mitral regurgitation), with different grades of severity (i.e., mild, moderate, and severe), were simulated. Based on computational outcomes, regurgitant valvular diseases strongly affected AF hemodynamics (reduced cardiac output and systemic pressure, increased left ventricular volume, left atrial pressure, and pulmonary vein pressure), while aortic stenosis was the least impacting among the simulated valvular conditions. Given that AF is rarely an isolated pathology, in our opinion, these data provide a clear additional insight: if associated with comorbid conditions, such as valvular heart disease, AF may act as a further trigger toward hemodynamic decompensation.

More sophisticated multiscale approaches are able to grasp propagation and waveform alterations as well as regional variations of flow structure induced by AF. By comparing SR and AF at the same given mean ventricular rate (75 bpm), a multiscale 0D-1D modeling (33), which couples a 0D cardiac dynamics and a 1D description of the arterial tree, showed that the arterial system is not able to completely absorb the AF-induced variability. The sole heart rhythm variation promotes an alteration of the wave dynamics, which is amplified in the distal circulation, by modifying the interplay between forward and backward signals. The results suggest a possible vascular dysfunction due to prolonged exposure to irregular and extreme values. Recent 0D-3D multiscale studies (34), coupling 3D PC-MRI data for the aorta and a compact 0D model for the remaining circulation, showed that AF led to the modification of systemic blood perfusion and increase of the endothelial cell activation potential. Both these mechanisms can increase the risk of atherogenesis and thrombus formation in different regions from ascending to the thoracic aorta. Moreover, the concomitant presence of aortic aging further worsens flow circulation (35): in this case, AF exacerbates the vascular defects due to aging, which increases the possibility of cardiovascular diseases *per se*.

Notably, the aforementioned computational approaches focus on acute hemodynamic effects. Over longer time periods, the contractile impairment induced by fast and irregular ventricular rate (36) may induce arrhythmia-induced cardiomyopathy, and consequent detrimental systemic hemodynamic effects further magnify the hemodynamic alterations described. **Figure 2** graphically summarizes the main concepts of this section.

Atrial fibrillation and cerebral hemodynamics

Since at least three decades, it has been known that AF relates to a fivefold increased risk of stroke, compared to the general population (37). However, more recently, AF has shown to also relate to cognitive decline and dementia, independently from clinical cerebrovascular events (stroke or transient ischemic attack – TIA). A seminal work from Ott et al. (38), based on a cross-sectional analysis of a subgroup of patients in the Rotterdam Study, reported for the first time an independent association between AF and dementia. Thereafter, several prospective studies have been published, whose results have been recently integrated in a meta-analysis (39), demonstrating that AF is associated with a 28% increase in the risk of dementia compared to non-AF controls, net of the eventual intercurrent stroke/TIA during follow-up. However, the relative independent contribution of AF to dementia onset compared to other common dementia risk factors (e.g., age and hypertension) is to date not quantifiable. Another intriguing finding was that, when comparing the results to several previous analyses that assessed the risk of dementia without accounting for the possible occurrence of stroke/TIA during follow-up, the stroke-independent contribution to dementia seemed to be more prominent than the stroke-dependent one.

During the past years, several mechanisms have been proposed to explain the association between AF and cognitive decline (40). As reported by our group (41), AF patients present at cerebral magnetic resonance imaging (MRI) a significantly increased number of silent cerebral ischemia (SCIs) compared to a control group with a similar cardiovascular risk profile, and the burden of these lesions is proportional to the duration of the arrhythmia (paroxysmal to persistent). More recently, Conen (42) demonstrated that in 1,390 AF patients without previous cerebrovascular events, cerebral MRI showed the presence of different silent cerebral lesions in a significant number of patients, such as silent cerebral infarction in 30%, microbleeds in 22%, and white matter hyperintensities (WMHs) in 99% of the investigated population; the presence of these alterations, particularly silent infarctions and moderate-grade WMHs, was significantly associated with cognitive decline at multivariate

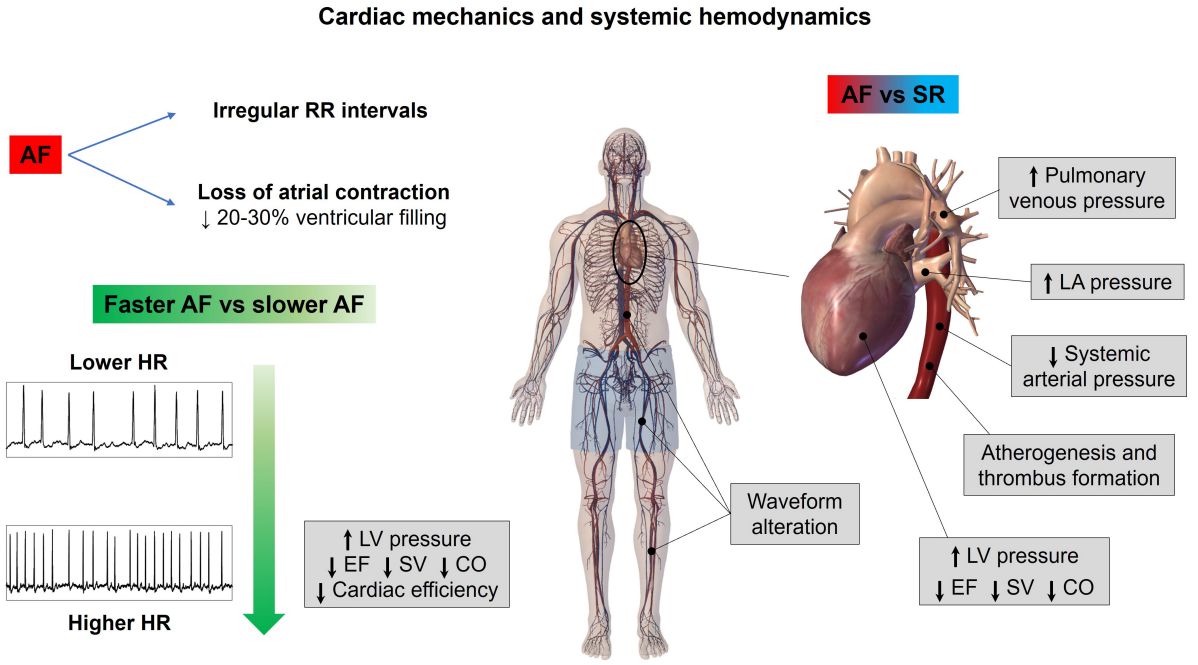

FIGURE 2
Atrial fibrillation effects on cardiac mechanics and systemic hemodynamics. AF, atrial fibrillation; CO, cardiac output; EF, ejection fraction; HR, heart rate; LA, left atrium; LV, left ventricle; SR, sinus rhythm; SV, stroke volume.

analysis. In addition, it was shown that AF is associated with smaller brain volumes as compared to non-AF patients, and this association was stronger in patients with persistent/permanent forms of AF and with increased time from the diagnosis of the disease (43).

This spectrum of AF-related cerebral phenotypic alterations can be broadly brought back to three possible phenomena: (1) subclinical micro-embolic events; the repetitive recurrence of these events, causing SCIs and WMHs, might contribute in reducing brain volume and affecting cognitive function; (2) oral anticoagulant therapy, particularly in case of warfarin therapy (44), may partly promote cerebral microbleeds; (3) the irregular rhythm may directly impact cerebral circulation, resulting in cerebral lesions (SCIs, microbleeds, WMHs) and atrophy.

Different from the first two mechanisms, the latter has seldom been investigated, most probably due to the evident technical difficulties in assessing the cerebral circle downstream of the Willis circle. Scant evidence from the end of the past century using transcranial Doppler (TCD) already suggested that AF might lower mean regional cerebral perfusion (45), but the scientific community had to wait until 2018 for the seminal work of Gardasdottir (46) for definitive proof. In this work, brain perfusion was estimated with phase contrast MRI in a large cohort of patients from the AGES-Reykjavik Study: individuals with persistent AF showed a reduced mean cerebral blood flow as compared to paroxysmal AF patients (in SR at the time of the MRI; −8%) and controls with no history of AF (−13%). In addition, in a subsequent experiment (47), the same group demonstrated that successful electrical cardioversion in persistent AF individuals was associated, after at least 10 weeks of SR maintenance, with an improvement of brain perfusion and cerebral blood flow measured by both arterial spin labeling (ASL) and phase contrast MRI, while no change in perfusion or blood flow was detected in those individuals where cardioversion was unsuccessful.

In addition to the reduction of the mean cerebral blood flow, AF with its irregular ventricular activation might also have a beat-to-beat impact on cerebrovascular circulation. This hypothesis has been demonstrated *in silico* (48). Based on a cerebral fluid-dynamics setup with two coupled lumped-parameter models (of the systemic and cerebral circulation, respectively), AF is related to transient and repetitive critical cerebral hemodynamic events in the distal cerebral circle, consisting of brief but incessant periods of deep cerebral hypoperfusions or hypertensive events. The repetitive occurrence of these critical events might at least partly explain the genesis of SCIs/WMHs (transient hypoperfusions) and cerebral microbleeds (transient hypertensive events), which could accumulate over time and determine the progressive cerebral damage linked to cognitive decline and dementia.

In vivo validation of these computational findings, given the limitations of the widely adopted noninvasive techniques assessing cerebral hemodynamics (TCD and cerebral ALS-MRI) (49, 50) not powered to assess beat-to-beat deep

microcirculatory dynamics, is challenging. Our group, for this aim, proposed spatially resolved near-infrared spectroscopy (SRS-NIRS) (51), a noninvasive technique mainly used to monitor cerebral tissue oxygenation in critical care, with the ability to provide a noninvasive assessment of the cerebral microcirculation with high temporal resolution, sensitive to beat-to-beat variations when used with a high sampling frequency (20 Hz). Cerebral SRS-NIRS and noninvasive systemic hemodynamic monitoring were recorded before and after elective electrical cardioversion in 53 AF/atrial flutter (AFL) patients (52), analyzing the total hemoglobin index (THI), a proxy of deep cerebral blood flow. In case of successful SR restoration, in front of a nonsignificant decrease in arterial blood, both hypoperfusive and hyperperfusive/hypertensive microcirculatory events were significantly reduced. These findings represent the first *in vivo* demonstration that SR restoration by ECV significantly improves cerebral microcirculation on a beat-to-beat level.

Additional intriguing insights on the association between AF and cognitive decline/dementia derive from an interesting 10-year follow-up study by Cacciatore (53). In this experience, AF patients presenting low (<50 bpm) compared to high (>90 bpm) median ventricular response were predictive of dementia onset. In fact, as suggested by computational data (54), higher ventricular rates relate to a progressive increase in critical cerebral hemodynamic events (hypoperfusions and hypertensive events) at the distal cerebral circle, while the excessively slow ventricular response is associated with systemic-proximal cerebral (up to the middle cerebral artery) hypoperfusions. Altogether, these findings, despite the results of the aforementioned RACE II trial, suggest that a rate control strategy aiming for a median ventricular response lower than 110 bpm appears more beneficial in terms of cerebral circulation. The main concepts of this section are illustrated in **Figure 3**.

Atrial fibrillation and coronary circulation

Patients with ongoing AF may present chest pain, ECG abnormalities, such as ST segment depression, and troponin release, even in the absence of classical obstructive epicardial coronary disease, particularly at high ventricular rates (55–57).

The coronary circulation presents some peculiar characteristics: the blood flow is mainly diastolic and a complex interaction occurs between the driving pressure (aortic pressure) and extravascular forces (intramural and endocavitary pressure) compressing the microvasculature of the different myocardial layers, in particular the subendocardium. In this setting, AF-related hemodynamics may determine blunted coronary flow reserve even in the presence of normal epicardial coronary arteries (55, 58).

The AF patients present downregulation of endothelial nitric oxide synthase (eNOS) (59), accounting for reduced nitric oxide-dependent vasodilation, as well as a potential influence on neurohumoral factors (60) [elevated levels of atrial natriuretic peptide (ANP) and brain natriuretic peptide (BNP), which mediate a shift of the vascular tone toward vasoconstriction], and increased sympathetic tone (61) (which increases coronary vascular resistance, reducing coronary flow reserve in response to increased myocardial energy demand). On top of these mechanisms, a direct detrimental hemodynamic effect may also relate to the irregular RR intervals, similar to the altered cerebral patterns of the microcirculatory perfusion, transient cerebral hypoperfusion, and hypertensive events, observed for the cerebral circulation during AF (48, 52, 54, 62). A computational multiscale (0D-1D) cardiovascular model including left heart mechanics and arterial tree fluid dynamics, together with a one-dimensional description of the epicardial coronary circulation, was designed (63). Based on this heart-arterial-coronary model, AF was simulated at different median ventricular responses (50, 70, 90, 110, 130 bpm), assessing the impact of the arrhythmia at different ventricular rates on the left anterior descending (LAD) flow waveform, as well as on coronary blood flow perfusion. The LAD flow waveform emerged as severely affected by AF, resulting, in particular, in a net decrease of coronary blood flow above 90–110 bpm. In addition, oxygen consumption monotonically increased with the ventricular rate (as estimated by rate pressure product), underlying how exceeding 90–110 bpm likely causes an imbalance in the oxygen supply-demand ratio.

To further study AF-related coronary microcirculation, a similar 1D-0D multiscale model of the entire human cardiovascular system enriched by detailed mathematical modeling not only of the epicardial coronary arteries but also of their downstream microcirculatory districts, subdivided into three layers (subepicardium, midwall, and subendocardium), has been designed (64). In this setting, AF and SR have been simulated at different ventricular rates (75, 100, 125 bpm), and the mean microcirculatory blood flow per beat across the different myocardial layers, in the districts downstream of the three coronary arteries [LAD; left circumflex artery, LCx; and right coronary artery, RCA], was compared. The major findings of this analysis were that the microcirculatory blood flow decreases across all myocardial layers, and at all ventricular rates, in AF compared to SR. In particular, the most affected were the subendocardial layers of the microcirculatory districts downstream of the left coronary arteries (LAD, LCx), where increased left endoventricular pressure during AF plays a role in increasing microvascular resistance of the subendocardial vessels. Of note, there was a more significant reduction of microvascular blood flow across all cardiac layers in AF simulations at the higher ventricular response (100, 125 bpm), as compared to the corresponding SR simulations, supporting

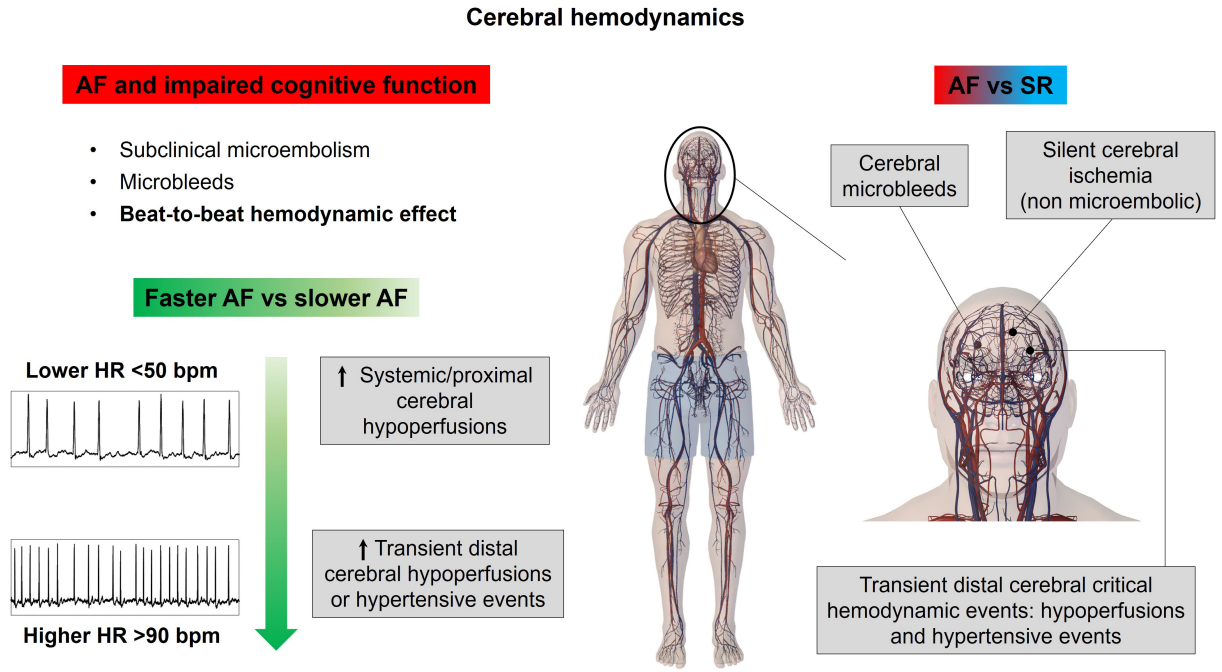

FIGURE 3
Atrial fibrillation effects on cerebral hemodynamics. AF, atrial fibrillation; HR, heart rate; SR, sinus rhythm.

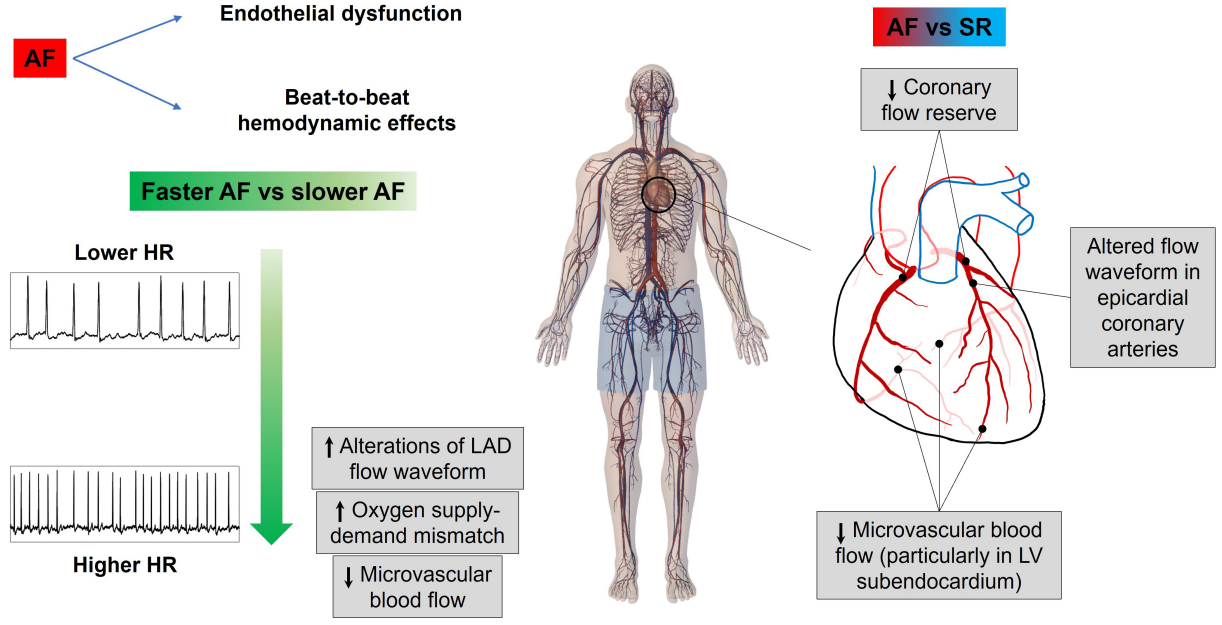

FIGURE 4
Atrial fibrillation effects on coronary hemodynamics. AF, atrial fibrillation; HR, heart rate; LAD, left anterior descending coronary artery; LV, left ventricle; SR, sinus rhythm.

the concept that fast ventricular rates during arrhythmia appear detrimental.

In the end, a 1D model of coronary circulation, with an assigned flow rate at the aorta root as an upstream boundary condition and constant pressure as a distal outflow boundary condition, was proposed to study the impact of different kinds of arrhythmias on coronary circulation (65). The authors found that coronary blood flow, defined as the net blood flow through left and right coronary arteries, was significantly affected by arrhythmias. In particular, during bigeminy, trigeminy, and quadrigeminy, coronary blood flow decreased by 28, 19, and 14% with respect to the baseline pacing at rest (60 bpm) and by 33, 22, and 17% with respect to pacing at 160 bpm, respectively.

Overall, these findings are concordant with the available evidence in the literature. Mechanically induced AF diminished coronary flow reserve particularly in the subendocardial layers of dog's hearts (subendocardial blood flow was reduced by 22%, while subepicardial blood flow was reduced by 9%) (66). Moreover, Kochiadakis elegantly demonstrated in humans (67), with the use of an intracoronary Doppler flow wire, reduced coronary flow reserve in experimentally induced AF compared to right atrial pacing at a similar heart rate, proving the critical role played by the irregular RR interval; interestingly, in the same study, it was also shown that, in case of AF with excessively short RR intervals, the ventricle may not generate enough pressure to open the aortic valve, corresponding to a markedly reduced coronary flow in that specific heartbeat. **Figure 4** resumes the main notions regarding how AF affects coronary circulation.

Limitations

Although computational modeling presents advantages in characterizing the hemodynamic impact exerted by AF, especially in those vascular regions—as the cerebral microcirculation—where the anatomical and structural complexity makes accurate clinical measures difficult to obtain, the following limitations need to be considered. First, the described hemodynamic modeling approaches predict acute hemodynamic effects, not taking into account possible chronic arrhythmia-induced hemodynamic compensatory mechanisms. Second, not all the cardiovascular models presented incorporate beat-to-beat autonomic response, and none of them considers the long-term effects of the autonomic nervous system. Third, the cardiovascular modeling approach is usually calibrated on a generic young healthy subject and validated against available AF hemodynamic literature data. While a number of mechanisms, such as posture and gravity effects, metabolic regulations, and cardiac electromechanics activity, would need to be included to account for different hemodynamic scenarios (from cardiac dysfunctions to astronautical applications), patient-specific cardiovascular modeling surely is emerging as a powerful tool to personalize and integrate cardiac care.

Conclusion

Growing scientific evidence, mainly based on cardiovascular modeling studies, points toward a relevant impact of AF on different aspects of physiological cardiovascular functioning, ranging from a broad impact on heart mechanics and systemic circulation to more specific influences on key vascular beds such as the cerebral and the coronary circles. Altogether, these data, if considered with the recent results of the EAST-AFNET 4 trial (12), highlight the critical role of sinus rhythm maintenance in improving not only patient's prognosis but also patient's hemodynamics, with likely benefit in cognitive function and ischemic symptoms. In addition, in case sinus rhythm could not be maintained over time, a strict rate control in permanent AF patients might be advisable to limit the hemodynamic impact of the arrhythmia.

Author contributions

MA and AS conceived the review. All authors wrote the article and approved the submitted version.

Acknowledgments

We thank "Compagnia di San Paolo" (https://www.compagniadisanpaolo.it) for the support granted to MA within the project "Progetti di Ricerca di Ateneo – 2016: Cerebral hemodynamics during atrial fibrillation (CSTO 60444)" and the grant "Ricerca locale anno 2019: Atrial fibrillation impact on coronary circulation" of the University of Turin, Italy.

Conflict of interest

The authors declare that the research was conducted in the absence of any commercial or financial relationships that could be construed as a potential conflict of interest.

Publisher's note

References

1. Roth GA, Mensah GA, Johnson CO, Addolorato G, Ammirati E, Baddour LM, et al. Global burden of cardiovascular diseases and risk factors, 1990-2019: Update from the GBD 2019 study. *J Am Coll Cardiol.* (2020) 76:2982–3021. doi: 10.1016/j.jacc.2020.11.010

2. Hindricks G, Potpara T, Dagres N, Arbelo E, Bax JJ, Blomström-Lundqvist C, et al. 2020 ESC Guidelines for the diagnosis and management of atrial fibrillation developed in collaboration with the European Association of Cardio-Thoracic Surgery (EACTS): The Task Force for the diagnosis and management of atrial fibrillation of the European. *Eur Heart J.* (2020) 42:373–498. doi: 10.1093/eurheartj/ehaa612

3. Caldeira D, David C, Sampaio C. Rate versus rhythm control in atrial fibrillation and clinical outcomes: Updated systematic review and meta-analysis of randomized controlled trials. *Arch Cardiovasc Dis.* (2012) 105:226–38. doi: 10.1016/J.ACVD.2011.11.005

4. Sterne JAC, Savoviæ J, Page MJ, Elbers RG, Blencowe NS, Boutron I, et al. RoB 2: A revised tool for assessing risk of bias in randomised trials. *BMJ.* (2019) 366:l4898. doi: 10.1136/bmj.l4898

5. Khan AR, Khan S, Sheikh MA, Khuder S, Grubb B, Moukarbel GV. Catheter ablation and antiarrhythmic drug therapy as first- or second-line therapy in the management of atrial fibrillation: Systematic review and meta-analysis. *Circ Arrhythmia Electrophysiol.* (2014) 7:853–60. doi: 10.1161/CIRCEP.114.001853

6. Saglietto A, Gaita F, De Ponti R, De Ferrari GM, Anselmino M. Catheter Ablation vs. Anti-arrhythmic drugs as first-line treatment in symptomatic paroxysmal atrial fibrillation: A systematic review and meta-analysis of randomized clinical trials. *Front Cardiovasc Med.* (2021) 8:664647. doi: 10.3389/fcvm.2021.664647

7. Epstein AE. Relationships between sinus rhythm, treatment, and survival in the atrial fibrillation follow-up investigation of rhythm management (AFFIRM) study. *Circulation.* (2004) 109:1509–13. doi: 10.1161/01.CIR.0000121736.16643.11

8. Packer DL, Mark DB, Robb RA, Monahan KH, Bahnson TD, Poole JE, et al. Effect of catheter ablation vs antiarrhythmic drug therapy on mortality, stroke, bleeding, and cardiac arrest among patients with atrial fibrillation: The CABANA randomized clinical trial. *JAMA J Am Med Assoc.* (2019) 321:1261–74. doi: 10.1001/jama.2019.0693

9. Friberg L, Tabrizi F, Englund A. Catheter ablation for atrial fibrillation is associated with lower incidence of stroke and death: Data from Swedish health registries. *Eur Heart J.* (2016) 37:2478–87. doi: 10.1093/EURHEARTJ/EHW087

10. Noseworthy PA, Gersh BJ, Kent DM, Piccini JP, Packer DL, Shah ND, et al. Atrial fibrillation ablation in practice: Assessing CABANA generalizability. *Eur Heart J.* (2019) 40:1257–64. doi: 10.1093/EURHEARTJ/EHZ085

11. Saglietto A, De Ponti R, Di Biase L, Matta M, Gaita F, Romero J, et al. Impact of atrial fibrillation catheter ablation on mortality, stroke, and heart failure hospitalizations: A meta-analysis. *J Cardiovasc Electrophysiol.* (2020) 5:1040–7. doi: 10.1111/jce.14429

12. Kirchhof P, Camm AJ, Goette A, Brandes A, Eckardt L, Elvan A, et al. Early rhythm-control therapy in patients with atrial fibrillation. *N Engl J Med.* (2020) 383:1305–16. doi: 10.1056/nejmoa2019422

13. Arts T, Delhaas T, Bovendeerd P, Verbeek X, Prinzen FW. Adaptation to mechanical load determines shape and properties of heart and circulation: The CircAdapt model. *Am J Physiol Heart Circ Physiol.* (2005) 288:H1943–54. doi: 10.1152/AJPHEART.00444.2004

14. Blanco PJ, Feijóo RA. A dimensionally-heterogeneous closed-loop model for the cardiovascular system and its applications. *Med Eng Phys.* (2013) 35:652–67. doi: 10.1016/J.MEDENGPHY.2012.07.011

15. Müller LO, Toro EF. A global multiscale mathematical model for the human circulation with emphasis on the venous system. *Int J Numer Method Biomed Eng.* (2014) 30:681–725. doi: 10.1002/CNM.2622

16. Mynard JP, Smolich JJ. One-dimensional haemodynamic modeling and wave dynamics in the entire adult circulation. *Ann Biomed Eng.* (2015) 43:1443–60. doi: 10.1007/s10439-015-1313-8

17. Heusinkveld MHG, Huberts W, Lumens J, Arts T, Delhaas T, Reesink KD. Large vessels as a tree of transmission lines incorporated in the CircAdapt whole-heart model: A computational tool to examine heart-vessel interaction. *PLoS Comput Biol.* (2019) 15:e1007173. doi: 10.1371/JOURNAL.PCBI.1007173

18. Mirramezani M, Shadden SCA. Distributed lumped parameter model of blood flow. *Ann Biomed Eng.* (2020) 48:2870–86. doi: 10.1007/S10439-020-02545-6

19. Caforio, F, Augustin CM, Alastruey J, Gsell MAF, Plank G. A coupling strategy for a first 3D-1D model of the cardiovascular system to study the effects of pulse wave propagation on cardiac function. *Comput Mech.* (2022):doi: 10.1007/S00466-022-02206-6 [Epub ahead of print].

20. Morris PD, Narracott A, Von Tengg-Kobligk H, Soto DAS, Hsiao S, Lungu A, et al. Computational fluid dynamics modelling in cardiovascular medicine. *Heart.* (2016) 102:18–28. doi: 10.1136/HEARTJNL-2015-308044/-/DC1

21. Kassab G, Guccione J. Editorial: Mathematical modeling of cardiovascular systems: From physiology to the clinic. *Front Physiol.* (2019) 10:1259. doi: 10.3389/FPHYS.2019.01259

22. Niederer SA, Lumens J, Trayanova NA. Computational models in cardiology. *Nat Rev Cardiol.* (2019) 16:100–11. doi: 10.1038/S41569-018-0104-Y

23. Scarsoglio S, Ridolfi L. A review of multiscale 0D-1D computational modeling of coronary circulation with applications to cardiac arrhythmias. *Rev Cardiovasc Med.* (2021) 22:1461–9. doi: 10.31083/J.RCM2204150

24. Alpert JS, Petersen P, Godtfredsen J. Atrial fibrillation: Natural history, complications, and management. *Annu Rev Med.* (1988) 39:41–52. doi: 10.1146/annurev.me.39.020188.000353

25. Clark DM, Plumb VJ, Epstein AE, Kay GN. Hemodynamic effects of an irregular sequence of ventricular cycle lengths during atrial fibrillation. *J Am Coll Cardiol.* (1997) 30:1039–45. doi: 10.1016/S0735-1097(97)00254-4

26. Scarsoglio S, Guala A, Camporeale C, Ridolfi L. Impact of atrial fibrillation on the cardiovascular system through a lumped-parameter approach. *Med Biol Eng Comput.* (2014) 52:905–20. doi: 10.1007/s11517-014-1192-4

27. Scarsoglio S, Camporeale C, Guala A, Ridolfi L. Fluid dynamics of heart valves during atrial fibrillation: A lumped parameter-based approach. *Comput Methods Biomech Biomed Engin.* (2016) 19:1060–8. doi: 10.1080/10255842.2015.1094800

28. Van Gelder IC, Groenveld HF, Crijns HJGM, Tuininga YS, Tijssen JGP, Alings AM, et al. Lenient versus strict rate control in patients with atrial fibrillation. *N Engl J Med.* (2010) 362:1363–73. doi: 10.1056/nejmoa1001337

29. Wyse DG. Lenient versus strict rate control in atrial fibrillation: Some devils in the details. *J Am Coll Cardiol.* (2011) 58:950–2. doi: 10.1016/j.jacc.2011.04.028

30. Anselmino M, Scarsoglio S, Camporeale C, Saglietto A, Gaita F, Ridolfi L. Rate control management of atrial fibrillation: May a mathematical model suggest an ideal heart rate? *PLoS One.* (2015) 10:e119868. doi: 10.1371/journal.pone.0119868

31. Anselmino M, Scarsoglio S, Saglietto A, Gaita F, Ridolfi L. A computational study on the relation between resting heart rate and atrial fibrillation hemodynamics under exercise. *PLoS One.* (2017) 12:e169967. doi: 10.1371/journal.pone.0169967

32. Scarsoglio S, Saglietto A, Gaita F, Ridolfi L, Anselmino M. Computational fluid dynamics modelling of left valvular heart diseases during atrial fibrillation. *PeerJ.* (2016) 4:e2240. doi: 10.7717/PEERJ.2240

33. Scarsoglio S, Gallo C, Ridolfi L. Effects of atrial fibrillation on the arterial fluid dynamics: A modelling perspective. *Meccanica.* (2018) 53:3251–67. doi: 10.1007/S11012-018-0867-6

34. Deyranlou A, Naish JH, Miller CA, Revell A, Keshmiri A. Numerical study of atrial fibrillation effects on flow distribution in aortic circulation. *Ann Biomed Eng.* (2020) 48:1291–308. doi: 10.1007/S10439-020-02448-6

35. Deyranlou A, Miller CA, Revell A, Keshmiri A. Effects of ageing on aortic circulation during atrial fibrillation; a numerical study on different aortic morphologies. *Ann Biomed Eng.* (2021) 49:2196–213. doi: 10.1007/S10439-021-02744-9

36. Raymond-Paquin A, Nattel S, Wakili R, Tadros R. Mechanisms and clinical significance of arrhythmia-induced cardiomyopathy. *Can J Cardiol.* (2018) 34:1449–60. doi: 10.1016/J.CJCA.2018.07.475

37. Wolf PA, Abbott RD, Kannel WB. Atrial fibrillation as an independent risk factor for stroke: The framingham study. *Stroke.* (1991) 22:983–8. doi: 10.1161/01.STR.22.8.983

38. Ott A, Breteler MMB, De Bruyne MC, Van Harskamp F, Grobbee DE, Hofman A. Atrial fibrillation and dementia in a population-based study: The Rotterdam study. *Stroke.* (1997) 28:316–21. doi: 10.1161/01.STR.28.2.316

39. Saglietto A, Matta M, Gaita F, Jacobs V, Bunch TJ, Anselmino M. Stroke-independent contribution of atrial fibrillation to dementia: A meta-analysis. *Open Hear.* (2019) 6:e000984. doi: 10.1136/openhrt-2018-000984

40. Madhavan M, Graff-Radford J, Piccini JP, Gersh BJ. Cognitive dysfunction in atrial fibrillation. *Nat Rev Cardiol.* (2018) 15:744–56. doi: 10.1038/s41569-018-0075-z

41. Gaita F, Corsinovi L, Anselmino M, Raimondo C, Pianelli M, Toso E, et al. Prevalence of silent cerebral ischemia in paroxysmal and persistent atrial fibrillation and correlation with cognitive function. *J Am Coll Cardiol.* (2013) 62:1990–7. doi: 10.1016/j.jacc.2013.05.074

42. Conen D, Rodondi N, Müller A, Beer JH, Ammann P, Moschovitis G, et al. Relationships of overt and silent brain lesions with cognitive function in patients with atrial fibrillation. *J Am Coll Cardiol.* (2019) 73:989–99. doi: 10.1016/j.jacc.2018.12.039

43. Stefansdottir H, Arnar DO, Aspelund T, Sigurdsson S, Jonsdottir MK, Hjaltason H, et al. Atrial fibrillation is associated with reduced brain volume and cognitive function independent of cerebral infarcts. *Stroke.* (2013) 44:1020–5. doi: 10.1161/STROKEAHA.12.679381

44. Umemura T, Mashita S, Kawamura T. Oral anticoagulant use and the development of new cerebral microbleeds in cardioembolic stroke patients with atrial fibrillation. *PLoS One.* (2020) 15:e0238456. doi: 10.1371/JOURNAL.PONE.0238456

45. Lavy S, Melamed E, Cooper G, Stern S, Keren A, Levy P. Effect of chronic atrial fibrillation on regional cerebral blood flow. *Stroke.* (1980) 11:35–8. doi: 10.1161/01.STR.11.1.35

46. Gardarsdottir M, Sigurdsson S, Aspelund T, Rokita H, Launer LJ, Gudnason V, et al. Atrial fibrillation is associated with decreased total cerebral blood flow and brain perfusion. *Europace.* (2018) 20:1252–8. doi: 10.1093/europace/eux220

47. Gardarsdottir M, Sigurdsson S, Aspelund T, Gardarsdottir VA, Forsberg L, Gudnason V, et al. Improved brain perfusion after electrical cardioversion of atrial fibrillation. *Europace.* (2020) 22:530–7. doi: 10.1093/europace/euz336

48. Anselmino M, Scarsoglio S, Saglietto A, Gaita F, Ridolfi L. Transient cerebral hypoperfusion and hypertensive events during atrial fibrillation: A plausible mechanism for cognitive impairment. *Sci Rep.* (2016) 6:28635. doi: 10.1038/srep28635

49. Naqvi J, Yap KH, Ahmad G, Ghosh J. Transcranial Doppler ultrasound: A review of the physical principles and major applications in critical care. *Int J Vasc Med.* (2013) 2013:629378. doi: 10.1155/2013/629378

50. Deibler AR, Pollock JM, Kraft RA, Tan H, Burdette JH, Maldjian JA. Arterial spin-labeling in routine clinical practice, part 1: Technique and artifacts. *Am J Neuroradiol.* (2008) 29:1228–34. doi: 10.3174/ajnr.A1030

51. Saglietto A, Scarsoglio S, Ridolfi L, Canova D, Anselmino M. Cerebral spatially resolved near-infrared spectroscopy (SRS-NIRS): Paving the way for non-invasive assessment of cerebral hemodynamics during atrial fibrillation. *Minerva Cardioangiol.* (2021) 69:124–6. doi: 10.23736/S0026-4725.20.05242-1

52. Saglietto A, Scarsoglio S, Canova D, Roatta S, Gianotto N, Piccotti A, et al. Increased beat-to-beat variability of cerebral microcirculatory perfusion during atrial fibrillation: A near-infrared spectroscopy study. *Europace.* (2021) 23:1219–26. doi: 10.1093/europace/euab070

53. Cacciatore F, Testa G, Langellotto A, Galizia G, Della-Morte D, Gargiulo G, et al. Role of ventricular rate response on dementia in cognitively impaired elderly subjects with atrial fibrillation: A 10-year study. *Dement Geriatr Cogn Disord.* (2012) 34:143–8. doi: 10.1159/000342195

54. Saglietto A, Scarsoglio S, Ridolfi L, Gaita F, Anselmino M. Higher ventricular rate during atrial fibrillation relates to increased cerebral hypoperfusions and hypertensive events. *Sci Rep.* (2019) 9:3779. doi: 10.1038/s41598-019-40445-5

55. Wijesurendra RS, Casadei B. Atrial fibrillation: Effects beyond the atrium? *Cardiovasc Res.* (2015) 105:238–47. doi: 10.1093/cvr/cvv001

56. Parwani AS, Boldt LH, Huemer M, Wutzler A, Blaschke D, Rolf S, et al. Atrial fibrillation-induced cardiac troponin I release. *Int J Cardiol.* (2013) 168:2734–7. doi: 10.1016/j.ijcard.2013.03.087

57. Van Den Bos EJ, Constantinescu AA, Van Domburg RT, Akin S, Jordaens LJ, Kofflard MJM. Minor elevations in troponin I are associated with mortality and adverse cardiac events in patients with atrial fibrillation. *Eur Heart J.* (2011) 32:611–7. doi: 10.1093/eurheartj/ehq491

58. Range FT, Schäfers M, Acil T, Schäfers KP, Kies P, Paul M, et al. Impaired myocardial perfusion and perfusion reserve associated with increased coronary resistance in persistent idiopathic atrial fibrillation. *Eur Heart J.* (2007) 28:2223–30. doi: 10.1093/eurheartj/ehm246

59. Cai H, Li Z, Goette A, Mera F, Honeycutt C, Feterik K, et al. Downregulation of endocardial nitric oxide synthase expression and nitric oxide production in atrial fibrillation: Potential mechanisms for atrial thrombosis and stroke. *Circulation.* (2002) 106:2854–8. doi: 10.1161/01.CIR.0000039327.11661.16

60. Tuinenburg AE, Van Veldhuisen DJ, Boomsma F, Van Den Berg MP, De Kam PJ, Crijns HJGM. Comparison of plasma neurohormones in congestive heart failure patients with atrial fibrillation versus patients with sinus rhythm. *Am J Cardiol.* (1998) 81:1207–10. doi: 10.1016/S0002-9149(98)00092-7

61. Wasmund SL, Li JM, Page RL, Joglar JA, Kowal RC, Smith ML, et al. Effect of atrial fibrillation and an irregular ventricular response on sympathetic nerve activity in human subjects. *Circulation.* (2003) 107:2011–5. doi: 10.1161/01.CIR.0000064900.76674.CC

62. Scarsoglio S, Saglietto A, Anselmino M, Gaita F, Ridolfi L. Alteration of cerebrovascular haemodynamic patterns due to atrial fibrillation: An in silico investigation. *J R Soc Interface.* (2017) 14:20170180. doi: 10.1098/rsif.2017.0180

63. Scarsoglio S, Gallo C, Saglietto A, Ridolfi L, Anselmino M. Impaired coronary blood flow at higher heart rates during atrial fibrillation: Investigation via multiscale modelling. *Comput Methods Programs Biomed.* (2019) 175:95–102. doi: 10.1016/j.cmpb.2019.04.009

64. Saglietto A, Fois M, Ridolfi L, De Ferrari GM, Anselmino M, Scarsoglio S. A computational analysis of atrial fibrillation effects on coronary perfusion across the different myocardial layers. *Sci Rep.* (2022) 12:841. doi: 10.1038/s41598-022-04897-6

65. Gamilov T, Kopylov P, Serova M, Syunyaev R, Pikunov A, Belova S, et al. Computational analysis of coronary blood flow: The role of asynchronous pacing and arrhythmias. *Mathematics.* (2020) 8:1205. doi: 10.3390/MATH8081205

66. Skalidis EI, Zacharis EA, Tsetis DK, Pagonidis K, Chlouverakis G, Yarmenitis S, et al. Endothelial cell function during atrial fibrillation and after restoration of sinus rhythm. *Am J Cardiol.* (2007) 99:1258–62. doi: 10.1016/j.amjcard.2006.12.044

67. Kochiadakis GE, Skalidis EI, Kalebubas MD, Igoumenidis NE, Chrysostomakis SI, Kanoupakis EM, et al. Effect of acute atrial fibrillation on phasic coronary blood flow pattern and flow reserve in humans. *Eur Heart J.* (2002) 23:734–41. doi: 10.1053/euhj.2001.2894

frontiers | Frontiers in Cardiovascular Medicine

TYPE Original Research
PUBLISHED 04 October 2022
DOI 10.3389/fcvm.2022.1016657

OPEN ACCESS

EDITED BY
Konstantinos Athanasios Gatzoulis,
National and Kapodistrian University of Athens, Greece

REVIEWED BY
Stefanos Archontakis,
Hippokration General Hospital, Greece
Emin Evren Özcan,
Dokuz Eylül University, Turkey

*CORRESPONDENCE
Anat Milman
anatmilman@gmail.com

†These authors have contributed equally to this work

SPECIALTY SECTION
This article was submitted to Cardiac Rhythmology, a section of the journal Frontiers in Cardiovascular Medicine

RECEIVED 11 August 2022
ACCEPTED 13 September 2022
PUBLISHED 04 October 2022

CITATION
Milman A, Leshem E, Massalha E, Jia K, Meitus A, Kariv S, Shafir Y, Glikson M, Luria D, Sabbag A, Beinart R and Nof E (2022) Occluded vein as a predictor for complications in non-infectious transvenous lead extraction. *Front. Cardiovasc. Med.* 9:1016657. doi: 10.3389/fcvm.2022.1016657

Occluded vein as a predictor for complications in non-infectious transvenous lead extraction

Anat Milman[1,2*†], Eran Leshem[1,2†], Eias Massalha[1,2], Karen Jia[2], Amit Meitus[2], Saar Kariv[2], Yuval Shafir[1,2], Michael Glikson[3,4], David Luria[4,5], Avi Sabbag[1,2], Roy Beinart[1,2] and Eyal Nof[1,2]

[1]Leviev Heart Institute, The Chaim Sheba Medical Center, Ramat Gan, Israel, [2]Sackler School of Medicine, Tel Aviv University, Tel Aviv, Israel, [3]The Jesselson Integrated Heart Center, Shaare Zedek Medical Center, Jerusalem, Israel, [4]Hebrew University in Jerusalem Medical School, Jerusalem, Israel, [5]Hadassah Medical Center, Heart Institute, Jerusalem, Israel

Background: The use of cardiovascular implantable electronic device (CIED) is steadily increasing, and complications include venous occlusion and fractured leads. Transvenous lead extraction (TLE) can facilitate the re-implantation of new leads.

Aims: This study aims to explore predictors and complications of non-infectious TLE.

Methods: This study involves a retrospective analysis and comparison of characteristics, complications, and outcomes of patients with and without occluded veins (OVs) undergoing TLE at our center.

Results: In total, eighty-eight patients underwent TLE for non-infectious reasons. Indications for TLE were lead malfunction (62; 70.5%) and need for CIED upgrade (22; 25%). Fourteen patients referred due to lead malfunction had an OV observed during venography. The OV group (36 patients) were significantly older (65.7 ± 14.1 vs. 53.8 ± 15.9, $p = 0.001$) and had more comorbidities. Ejection fraction (EF) was significantly lower for the OV group (27.5 vs. 57.5%, $p = 0.001$) and had a longer lead dwelling time (3,226 ± 2,324 vs. 2,191 ± 1,355 days, $p = 0.012$). Major complications were exclusive for the OV group (5.5% vs. none, $p = 0.17$), and most minor complications occurred in the OV group as well (33.3 vs. 4.1%, $p < 0.001$). Laser sheath and mechanical tools for TLE were frequently used for OV as compared to the non-occluded group (94.4 vs. 73.5%, respectively, $p = 0.012$). Procedure success was higher in the non-occluded group compared to the OV group (98 vs. 83.3%, respectively, $p = 0.047$). Despite these results, periprocedural mortality was similar between groups.

Conclusion: Among the TLE for non-infectious reasons, vein occlusion appears as a major predictor of complex TLE tool use, complications, and procedural success. Venography should be considered prior to non-infectious TLE to identify high-risk patients.

KEYWORDS

transvenous lead extraction, non-infectious, occluded vein, complications, venography

10.3389/fcvm.2022.1016657

What's new?

- Non-infectious causes are a prevalent indication for TLE in the current era. TLE is mainly performed due to lead malfunction and, to a lesser degree, due to the need for CIED upgrade.
- These subgroups of non-infectious TLE are inherently different, and the complication rate of TLE for CIED upgrade is considerably higher.
- The presence of an occluded vein is a major driving force for complex procedures, less procedural success, and abundant periprocedural complications.

Introduction

The use of cardiovascular implantable electronic device (CIED) has expanded over the 4 decades, with over a million new CIEDs being implanted worldwide annually (1, 2). Although these devices have revolutionized the management of patients with arrhythmias and conduction disorders, they are associated with various infectious and non-infectious complications, which may necessitate their removal (1, 3, 4). The leads of CIEDs are the weakest link of the device, with lead failure rates estimated to occur at a rate of 0.29–0.45% annually (2, 5). The most common causes of lead removal include infection, venous occlusion, and mechanical lead failure (1).

Transvenous lead extraction (TLE) is completed in a stepwise manner starting with manual traction of the leads (with or without locking stylets), mechanical tools, and progressing to powered tools such as laser sheaths (6, 7). Despite advances in lead removal, current estimates from large multi-center reports suggest that a clinical failure of lead extraction rates ranges from 2.3 to 3.3%, and major adverse events during lead extraction occur in up to 1.8% of patients (6, 7). Considering the significant risk of complications related to lead removal, the benefit of the patient must outweigh any surgical risks. Less contention exists regarding the necessity of removing infected leads; however, the risk-benefit ratio for non-infected lead removal indications has conflicting evidence (1). Many non-infectious indications for lead removal are currently categorized as class II indications (1), and decisions to progress to TLE remain challenging. These indications include lead failure, chronic pain, non-functional leads in young patients, symptomatic venous stenosis or occlusion, and device upgrades (1, 4). Using a large tertiary referral retrospective single-center cohort, we aimed to analyze the indications, predictors, and outcomes of non-infectious lead removal.

Materials and methods

Study population

This was a retrospective, single-center cohort study of patients who underwent lead extraction for non-infectious causes between 2011 and 2020 at Sheba Medical Center, Israel, a referral tertiary hospital. The clinical and procedural data were gathered prospectively from the procedural report and patients' records. This study included 88 consecutive patients who underwent non-infectious lead extraction (a total of 146 leads), between January 2011 and March 2020. Patients who presented with any signs of infection such as fever or positive bacterial culture were excluded from the analysis. The decision to perform TLE in these cases was left to the discretion of the treating team and was performed in cases where abandoning leads was not clinically justified. The study was approved by the Local Institutional Review Board.

TLE procedure

All TLE procedures were performed by qualified experienced operators with a cardiothoracic surgeon available on site. Procedures were performed under general anesthesia, with hemodynamic monitoring and transesophageal echocardiography (TEE). A large-bore femoral venous access was inserted in all patients in case femoral bailout was warranted and for the SVC bridging balloon wire after it became available. A stepwise approach was used in all patients as previously described by our group (8, 9). The TLE procedure was terminated after complete removal of the leads, when lead fragments could not be removed or in the event of a major complication.

Venography was routinely performed when a patient needed a CIED upgrade (22 patients) and in the rest by the discretion of the operator (26 patients). All patients without pre-procedural venography were retrospectively evaluated for vein occlusion by surveying the fluoroscopy data from the procedure. Some of the patients in the lead malfunction group had an occluded vein (OV) as observed by venography during the procedure ($n = 14$). We hypothesized that an OV is a significant contributor for the occurrence of complications during an extraction procedure, and thus, we regrouped all patients according to whether they were found to have an OV or not.

Definitions

Non-infectious causes for lead removal were categorized as having an indication for TLE because of a lead malfunction, occluded vein, or other cause. The primary analysis focused on

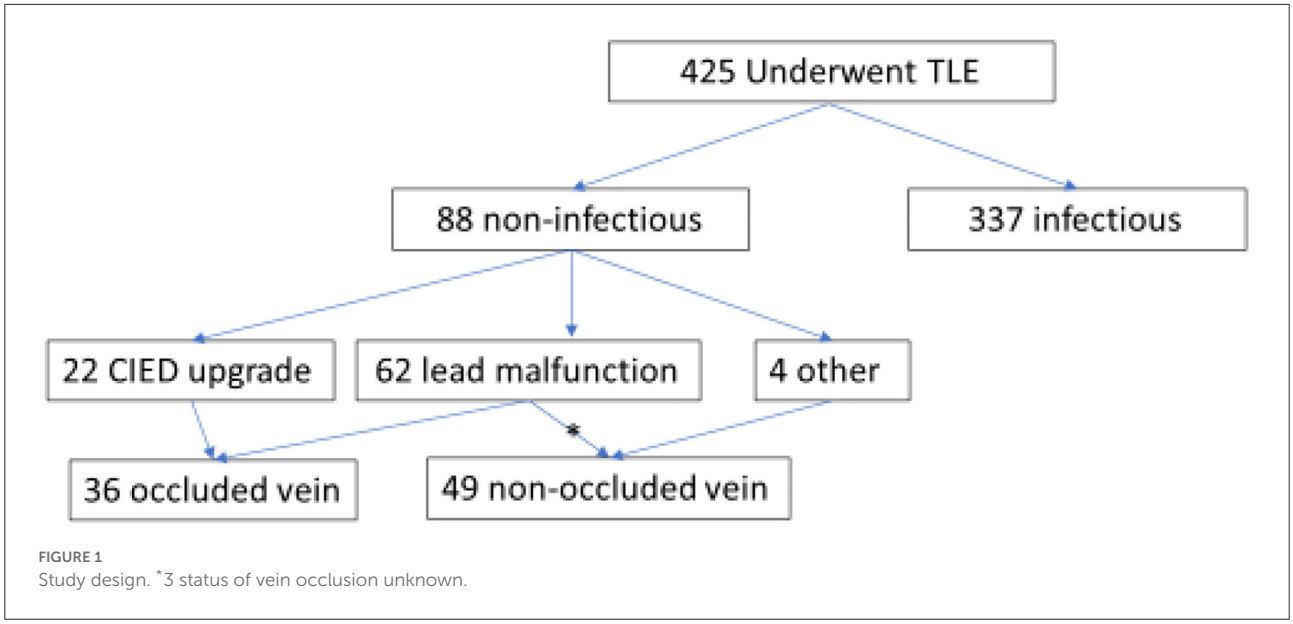

FIGURE 1
Study design. *3 status of vein occlusion unknown.

comparing the two major groups (lead malfunction and device upgrade in the setting of an OV).

TLE procedures were classified as *simple* (when complete removal of leads was achieved with simple traction including the need for locking stylet) or *complex* (when the former failed and the operator proceeded to the mechanical tool, powered sheaths, laser sheath, or femoral approach using a snare or ablation catheter). Different *time points* were ascribed for the periods from first *device implantation to extraction* (representing the oldest lead dwelling time) and *last intervention to extraction* (elapsed time from last pocket intervention to extraction).

Complications were divided into *major complications* (defined as life-threatening as tamponade, required surgical intervention, or result in death). Complications that did not meet the major complication criteria were classified as *minor complications*.

Success or failure was defined by radiological success results and not clinical success results (10). Patients were divided depending on the outcome of the extraction procedure. Success was defined only if the complete removal of all leads (including "lead tips") was achieved.

Patients were then regrouped according to the presence of an OV, regardless of whether the primary reason for non-infectious TLE was lead malfunction or device upgrade.

Follow-up

Patients were followed up until 1 May 2021. Mortality status was updated from Israel's population registry, a national registry updated regularly.

Statistical analysis

Categorical variables are reported in frequencies and percentages. All continuous variables were tested for normal distribution by the Kolmogorov-Smirnov test and by visualizing the Q–Q plot, plotting the distribution and variance of the residuals. Normally distributed continuous variables were reported as mean and standard deviation values, and differences between groups were assessed using the Student's *t*-test. Continuous variables not normally distributed were reported as median and interquartile range (IQR, 25th−75th percentiles) values, and significance was assessed using the Mann-Whitney U test or Kruskal Wallis test. All statistical tests were two-sided, and a $p < 0.05$ was considered significant.

A binomial multivariable logistic regression model analysis was employed to identify the predictors of the OV among TLE patients and the variables associated with periprocedural complication and mortality in patients undergoing TLE for non-infectious etiologies. The variables included in both models were prioritized based on statistical significance in the univariate analysis and those assumed to be clinically relevant based on previous publications and clinical plausibility.

Statistical analysis was performed using the SPSS software 27.0.0 (IBM, Armonk, NY, USA) and the R foundation statistical computing and graphics software (version 4.0.0).

Results

Study population

During the trial period, 88 patients underwent TLE procedures at the Sheba Medical Center for non-infectious

10.3389/fcvm.2022.1016657

TABLE 1 Patient characteristics of the entire cohort.

All patients	Overall	Non-infectious
Number of patients	425	88
Male sex	327 (76.9)	66 (75.0)
Age	65.5 ±15.7	58.4 ± 16.8
Smoking	140 (32.9)	16 (18.2)
Atrial fibrillation	149 (35.1)	32 (36.4)
Hypertension	223 (52.5)	40 (45.5)
Heart failure	191 (44.9)	34 (38.6)
Stroke	54 (12.7)	8 (9.1)
Vascular disease	238 (56.0)	43 (48.9)
Malignancy	28 (6.6)	3 (3.4)
Diabetes mellitus	178 (41.9)	24 (27.3)
EF (%) [median (IQR)]	38.0 [25.0, 60.0]	35.00 [25.0, 60.0]
Creatinine (mg/dl)	1.05 [0.84, 1.50]	0.95 [0.80, 1.19]
Hemoglobin (mg/dl)	11.54 (2.13)	13.05 (1.73)
C-Reactive protein (mg/dl)	24.70 [6.91, 74.97]	6.07 [1.88, 15.97]
Albumin (g/dl)	3.44 (0.80)	3.96 (0.52)
Device type		
CRT-D	108 (25.4)	19 (21.6)
CRT-P	11 (2.6)	3 (3.4)
ICD	139 (32.7)	40 (45.4)
PM	166 (39.1)	26 (29.5)
Number extracted leads		
1	105 (24.7)	46 (52.3)
2	186 (43.8)	29 (33.0)
3	101 (23.8)	13 (14.8)
Extraction success		
Full	390 (91.8%)	81 (92%)
Partial	21 (4.9%)	2 (2.3%)
Failure	14 (3.3%)	5 (5.7%)

indications (out of a total of 425 TLE procedures performed) and were included in this cohort (Figure 1). The mean age at extraction was 58.4 ± 16.9 years, and the majority (75%) were male patients with a median ejection fraction (EF) of 35% [25, 60%]. In the majority of the cohort, one lead was extracted (52.3%). The TLE was defined as fully successful in most procedures (92%). Patient baseline characteristics are presented in Table 1.

Extraction indication

The majority were extracted due to a non-functioning lead (70.5%). Further indications included device upgrade (25%) and four patients (4.5%) because of other causes (heart transplant, intractable pain, irradiation, and severe tricuspid regurgitation).

Lead malfunction compared to device upgrade

Table 2 provides the primary comparison of the two major groups of non-infectious indication for TLE for characteristics, complications, and extraction methods.

The TLE patients for device upgrade were significantly older than those with a lead malfunction (mean age 68.3 ± 12.6 vs. 55 ± 17.2, respectively, $p = 0.002$), had more vascular disease (68.2 vs. 43.5%, respectively, $p = 0.022$), had a higher creatinine level (1.25 ± 0.4 vs. 0.98 ± 0.4 mg/dl, respectively, $p = 0.005$), and had a lower EF (25 vs. 52.5%, respectively, $p < 0.001$). No difference was observed in the type of extracted device or number of leads, as well as lead dwelling time.

The extraction method used did not differ between these two groups, as well as the success rate of the procedure.

There were significantly more major and minor complications in the CIED upgrade group (minor 40.9 vs. 8.1%, respectively, $p < 0.001$ and major 9.1% vs. none, respectively, $p = 0.06$). One patient undergoing TLE for device upgrade perished during the procedure (due to SVC tear). Overall death during follow-up did not differ between the groups.

Occluded vein presence

We observed 14/62 patients (22.6%) from the lead malfunction group with an OV during the procedure. A new total of 36 patients in our cohort had an OV and were compared to 49 patients without OV. In 3/88 patients, data on OV could not be retrieved. These groups were compared accordingly as shown in Table 3.

Patients with an OV were significantly older (65.7 ± 14.1 vs. 53.8 ± 15.9, respectively, $p = 0.001$). Both groups had a majority of male patients undergoing TLE.

The OV group had a higher comorbidity prevalence such as atrial fibrillation (52.8% vs. 24.5% for the non-occluded group, $p = 0.018$), hypertension (66.7 vs. 30.6%, $p = 0.003$), and a trend toward more vascular disease (61.1 vs. 40.8%, $p = 0.07$). EF was significantly lower for the OV group (27.5 vs. 57.5% for the non-occluded group, $p = 0.001$).

The OV group had a lower hemoglobin (12.5 ± 1.5 vs. 13.6 ± 1.8 mg/dl, $p = 0.01$) and a lower albumin (3.8 ± 0.5 vs. 4.13 ± 0.5 g/dl, $p = 0.005$).

There was no difference in the type of CIED extracted or the number of leads. Lead dwell time in the OV group was longer compared to the non-occluded group (3,226 ± 2,324 vs. 2,191 ± 1,355 days, respectively, $p = 0.012$).

The methods used for TLE were significantly different between the groups with more complex methods used for OV as compared to the non-occluded group (94.4 vs. 73.5%,

10.3389/fcvm.2022.1016657

TABLE 2 Comparison of TLE due to lead malfunction or device upgrade in the setting of an occluded vein.

	Device upgrade	Lead malfunction	*P*-Value
Number of patients	22	62	
Male	16 (72.7)	48 (77.4)	0.879
Age	68.3 ± 12.6	55 ± 17.2	0.002
Smoking	3 (13.6)	13 (21.0)	0.4
Atrial fibrillation	10 (45.5)	22 (35.5)	0.533
Hypertension	14 (63.6)	25 (40.3)	0.13
Heart failure	8 (36.4)	25 (40.3)	0.509
Stroke	3 (13.6)	5 (8.1)	0.171
Vascular disease	15 (68.2)	27 (43.5)	0.022
Malignancy	1 (4.5)	1 (1.6)	0.174
Diabetes mellitus	8 (36.4)	15 (24.2)	0.476
EF (%) [median (IQR)]	25.00 [22.50, 30.00]	52.50 [35.00, 60.00]	<0.001
Creatinine (mg/dl)	1.25 ± 0.4	0.98 ± 0.4	0.005
Hemoglobin (mg/dl)	12.6 ± 1.6	13.2 ± 1.7	0.138
C-Reactive protein (mg/dl)	7.7 ± 10.5	17.2 ± 22.8	0.302
Albumin (g/dl)	3.8 ± 0.4	4 ± 0.5	0.086
Referral from other hospital	17 (77.3)	39 (62.9)	0.334
Device type			0.176
CRT-D	4 (18.2)	14 (22.6)	
CRT-P	2 (9)	1 (1.6)	
ICD	8 (36.4)	31 (50)	
PM	8 (36.4)	16 (25.8)	
Number extracted leads			0.314
1	9 (40.9)	37 (59.7)	
2	9 (40.9)	17 (27.4)	
3	4 (18.2)	8 (12.9)	
First device implant to extraction (days)	2,712.95 ± 1,803	2,545.6 ± 1,917.5	0.722
Last intervention to extraction (days)	1,454.2 ± 901.8	1,457.2 ± 970.6	0.99
Extraction type			0.21
Simple	2 (9.1)	14 (22.6)	
Complex	20 (90.9)	48 (77.4)	
Extraction success			0.54
Full	20 (90.9)	57 (91.9)	
Partial	0	2 (3.2)	
Failure	2 (9.1)	3 (4.8)	
Minor complication	9 (40.9)	5 (8.1)	<0.001
Major complication	2 (9.1)	0 (0.0)	0.06
Periprocedural death	2 (5.5)	1 (2)	0.38
Follow up time (days)	989 [353, 2,219]	1,365 [416, 2,259]	0.36
Death during follow up	5 (22.7)	7 (11.3)	0.363

respectively, $p = 0.012$). Radiological success was more common in the non-occluded group compared to the OV group (98 vs. 83.3%, respectively, $p = 0.047$; Figure 2).

Major complications were exclusively found in the OV group (two patients compared to none in the non-occluded vein, $p = 0.17$), and minor complications were more frequent in the OV group as well (33.3 vs. 4.1%, $p < 0.001$; Figure 3).

Periprocedural death during follow-up was similar (2% in the non-occluded vein group vs. 5.5% in the occluded group, $p = 0.38$; Figure 3).

10.3389/fcvm.2022.1016657

TABLE 3 Comparison according to occluded vein presence.

	No vein occlusion	Occluded vein	*P*-Value
Number of patients	49	36	
Male	37 (75.5)	27 (75.0)	1
Age	53.84 ± 15.91	65.69 ± 14.14	0.001
Smoking	9 (18.4)	7 (19.4)	0.471
Atrial fibrillation	12 (24.5)	19 (52.8)	0.018
Hypertension	15 (30.6)	24 (66.7)	0.003
Heart failure	17 (34.7)	17 (47.2)	0.205
Stroke	3 (6.1)	4 (11.1)	0.345
Vascular disease	20 (40.8)	22 (61.1)	0.07
Malignancy	2 (4.1)	1 (2.8)	0.481
Diabetes mellitus	11 (22.4)	13 (36.1)	0.286
EF (%) [median (IQR)]	57.5 [35, 60]	27.5 [25, 37.25]	0.001
Creatinine (mg/dl)	1.02 (0.39)	1.10 (0.36)	0.395
Hemoglobin (mg/dl)	13.56 (1.77)	12.54 (1.52)	0.01
C-Reactive protein (mg/dl)	16.39 (19.87)	12.61 (22.85)	0.627
Albumin (g/dl)	4.13 (0.52)	3.79 (0.48)	0.005
Referral from other hospital	28 (57.1)	28 (77.8)	0.08
Device type			0.187
CRT-D	11 (22.4)	8 (22.2)	
CRT-P	1 (2.1)	2 (5.6)	
ICD	26 (53.1)	12 (33.3)	
PM	11 (22.4)	14 (38.9)	
First device to extraction (days)	2,191 ± 1,355	3,226 ± 2,324	0.012
Last intervention to extraction (days)	1,438 ± 1,010	1,584 ± 981	0.528
Extraction type			0.012
Simple	13 (26.5)	2 (5.6)	
Complex	36 (73.5)	34 (94.4)	
Number of leads extracted			0.202
1	30 (61.2)	15 (41.7)	
2	13 (26.5)	14 (38.9)	
3	6 (12.2)	7 (19.4)	
Extraction success			0.047
Full	48 (98)	30 (83.3)	
Partial	0	2 (5.6)	
Failure	1 (2)	4 (11.1)	
Minor complication	2 (4.1)	12 (33.3)	<0.001
Major complication	0 (0.0)	2 (5.5)	0.17
Periprocedural death	1 (2)	2 (5.5)	0.38
Follow up time (days)	1,325 [432, 2,269]	1,218 [386, 2,053]	0.36
Death during follow up	6 (12.5)	7 (19.4)	0.38

A binomial multivariable logistic regression model was deployed to identify the clinical parameters associated with the presence of an OV. Older age [odds ratio (OR): 1.07 (95% CI: 1.01–1.13 per 1 year), $p = 0.01$] and hypertension [OR: 5.79 (95% CI: 1.68–20.08, $p < 0.01$)] were shown to be strongly correlated with vein occlusion. Lower left ventricular ejection fraction (LVEF) and the time elapsed from implantation to extraction were predictors for vein occlusion (Table 4).

A binomial multivariable backward regression model was performed to ascertain the predictors for periprocedural complications, including mortality. Patients with an OV had

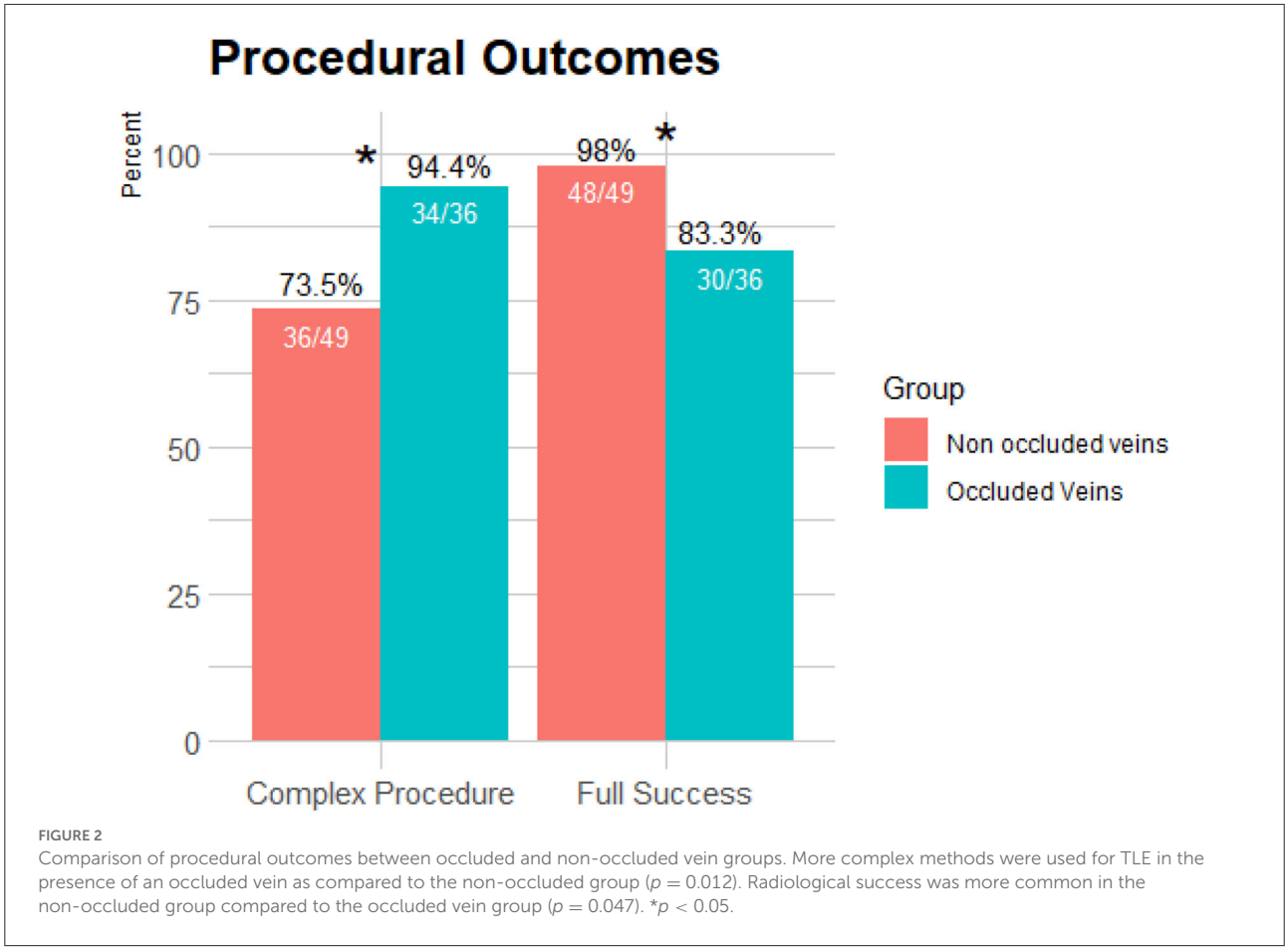

FIGURE 2
Comparison of procedural outcomes between occluded and non-occluded vein groups. More complex methods were used for TLE in the presence of an occluded vein as compared to the non-occluded group ($p = 0.012$). Radiological success was more common in the non-occluded group compared to the occluded vein group ($p = 0.047$). *$p < 0.05$.

significantly higher odds for periprocedural complications, including mortality [OR: 15.08 (95% CI: 2.76–82.2, $p < 0.01$) Table 5].

Discussion

Main findings of our study are as follows:

- TLE for non-infectious causes is a prevalent indication for TLE in the current era and is mainly performed due to lead malfunction and, to a lesser degree, due to the need for CIED upgrade.
- These subgroups of non-infectious TLE are inherently different, and the complication rate of TLE for CIED upgrade is considerably higher.
- Analysis according to the presence of an OV reveals that this factor is a major driving force for complex procedures, less procedural success, and abundant periprocedural complications.
- The present retrospective analysis of 88 consecutive patients undergoing TLE for non-infectious reasons emphasizes the importance of pre-procedural planning and venography to identify those with an OV, as these patients were found to have a worse outcome.

Non-infectious TLE

Patients referred for TLE for non-infectious reasons comprise a significant portion of those undergoing the procedure (6); however, they are underrepresented in the literature, and indications for appropriate extraction are all currently a class 2 indication (1).

In the ELECTRa European prospective cohort, the rate of TLE for a non-infectious etiology was found to be 47.3% of all TLE procedures (1,683/3,555) (6). The recently published CLEAR registry including eight Canadian centers showed that non-infectious reasons for TLE were the majority of cases, with only 48.6% of TLEs due to an infection (11). A recent study from the United Kingdom included a total of 1,151 patients, with 632 (54.9%) and 519 (45.1%) patients representing infective and non-infective indications, respectively (12).

Our cohort of 88 such patients represents a non-negligible fraction (21%), which is less than the aforementioned rates of

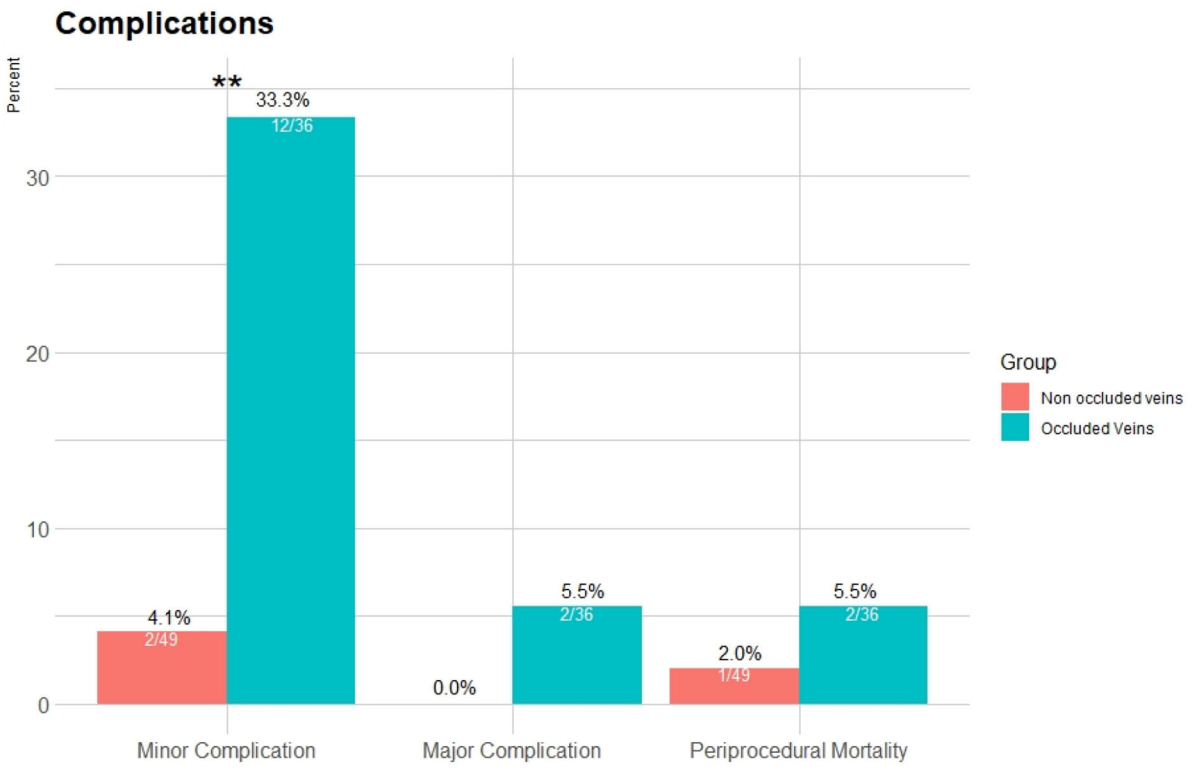

FIGURE 3
Complication rates for the occluded and non-occluded vein groups. Major complications were exclusive for the occluded vein group (2 patients), and minor complications were more frequent ($p < 0.001$). Periprocedural death during follow-up was similar ($p = 0.38$). **$p < 0.001$.

non-infectious TLE published. However, in Mayo Clinic, out of the 480 TLE performed between January 2001 and October 2012, 123 procedures (25.6%) were because of superfluous leads (13), and indications for extraction were malfunction in 41%, recall in 26%, and upgrade in 15% (13). Archontakis et al. (14) provided data from their high-volume reference center for CIED extractions in Athens, with a total of 242 consecutive patients undergoing TLE of which a minority was for non-infectious reasons (16.9%). This difference may be due to a strict adherence to current indications and a higher tendency to add leads in cases of lead malfunction of required upgrade.

Occluded veins

Patients with an OV were older and had more comorbidities such as atrial fibrillation, hypertension, and a borderline tendency for vascular disease. Not surprisingly, these patients also had a lower EF, as most of these patients were referred for a CIED upgrade. Our secondary analysis divided patients by results of venography, comparing the presence of OVs and the effect on the TLE procedure and outcome.

Predictors for occluded veins

Our findings reveal that advanced age, hypertension, decreased LVEF, and lead dwell time were significant predictors for an OV that will result in a more complex procedure with less favorable outcomes.

An important predictor for vein occlusion was lead dwell time, which was significantly longer in the OV group compared to those without an occlusion. This was also observed by Pieper et al. (15), when assessing venous obstruction in patients undergoing revision of CIED. The issue of the number of leads as a risk factor for an OV is debatable. The existence of multiple leads has previously been found to be a risk factor for developing venous thrombosis (16, 17), and thus, complete lead extraction is recommended whenever there are more than four leads on one side or five leads through the superior vena cava (SVC) (16). On the contrary, some studies failed to show a correlation between venous complications and lead burden (18, 19) in accordance with our findings. Moreover, Li et al. (19) found that infection (both systemic and local infection) and not the number of leads was associated with an increased risk of venous occlusion.

TABLE 4 Multivariate analysis of predictors for occluded veins.

Predictors	Univariate analysis			Multivariable analysis		
	Odds ratio	Confidence interval	*P*-Value	Odds ratio	Confidence interval	*P*-Value
Age	*1.05*	*1.02–1.09*	*0.002*	*1.07*	*1.01–1.13*	*0.018*
Atrial fibrillation	*3.2*	*1.29–1.83*	*0.01*	*1.49*	*0.43–5.07*	*0.52*
HTN	*4.12*	*1.65–10.29*	*0.002*	*5.79*	*1.67–20.08*	*0.006*
LVEF	*0.95*	*0.92–0.98*	*0.001*	*0.95*	*0.91–0.99*	*0.016*
Years (from first implantation to extraction)	*1.12*	*1.02–1.25*	*0.019*	*1.21*	*1.07–1.36*	*0.003*

HTN, hypertension; LVEF, left ventricular ejectin fraction.

TABLE 5 Multivariable regression (backward Wald) models of predictors for periprocedural complications and mortality.

Predictors	1st step model			Final step model		
	Odds ratio	Confidence interval	*P*-Value	Odds ratio	Confidence interval	*P*-Value
Age	*0.98*	*0.93–1.04*	*0.54*			
Male gender	*1.4*	*0.22–9.5*	*0.72*			
Atrial fibrillation	*0.13*	*0.02–0.81*	*0.29*	*2.4*	*0.06–1.01*	*0.052*
HTN	*4.8*	*0.98–23.8*	*0.052*	*3.60*	*0.84–15.4*	*0.084*
LVEF < 40%	*0.50*	*0.74–3.40*	*0.48*			
Years (from first implantation to extraction)	*1.09*	*0.95–1.26*	*0.21*			
Occluded vein	*15.03*	*1.86–121.8*	*0.11*	*15.08*	*2.76–82.2*	*0.002*

HTN, hypertension; LVEF, left ventricular ejectin fraction.

Results of OV procedures

The most clinically important findings of our analysis were the significantly more difficult procedures performed in the presence of OV, as reflected by the need to use more complex methods and the lower full success rate of the procedure. Complication rates were more frequent in the aforementioned group as well. Li et al. (19) demonstrated, although in a cohort of infected devices, that lead extraction was more challenging in patients with venous occlusion, requiring superior devices and longer time. Opposed to these findings, Boczar et al. (20) could not observe vein occlusion to influence the effectiveness, safety, and the use of additional devices during TLE procedures; however, their population was a mix of infected and non-infected devices, with a significantly higher rate of vein occlusion (36.1%).

Limitations

We acknowledge several limitations. This was a single-center retrospective cohort, and the results as such may not be generalized to other populations. Performing a TLE in these cases was left to the discretion of the treating physician team as was the decision to perform a pre-procedural venography. Of note, not all lead malfunction procedures had a venography prior to the procedure, mainly due to the fact that it was determined to proceed with TLE regardless of the venography results. No attempted venoplasty was performed in cases of venous occlusion, and these were referred for TLE.

Conclusion

The TLE for non-infectious reasons is common, and strict criteria and indications should be formalized. Vein occlusion appears as a major predictor for complex TLE tools use, complications, and procedural success. Venography should be considered prior to non-infectious TLE to identify venous occlusion and high-risk patients.

Data availability statement

The raw data supporting the conclusions of this article will be made available by the authors, without undue reservation.

Ethics statement

The studies involving human participants were reviewed and approved by The Chaim Sheba Medical Center, Tel Hashomer, Israel. The patients/participants provided their written informed consent to participate in this study.

Author contributions

AMi, EL, and EN contributed to conception and design of the study. AMi, KJ, SK, and YS organized the database. EM performed the statistical analysis. AMi and EL wrote the first draft of the manuscript. KJ wrote sections of the manuscript. All authors contributed to manuscript revision, read, and approved the submitted version.

Acknowledgments

The content of this manuscript has been presented as an e-poster at the European Heart Rhythm Association (EHRA) Congress 2022.

Conflict of interest

The authors declare that the research was conducted in the absence of any commercial or financial relationships that could be construed as a potential conflict of interest.

Publisher's note

References

1. Kusumoto FM, Schoenfeld MH, Wilkoff BL, Berul CI, Birgersdotter-Green UM, Carrillo R, et al. 2017 HRS expert consensus statement on cardiovascular implantable electronic device lead management and extraction. *Heart Rhythm.* (2017) 14:e503–51. doi: 10.1016/j.hrthm.2017.09.001

2. Providência R, Kramer DB, Pimenta D, Babu GG, Hatfield LA, Ioannou A, et al. Transvenous implantable cardioverter-defibrillator (ICD) lead performance: a meta-analysis of observational studies. *J Am Heart Assoc.* (2015) 4:e002418. doi: 10.1161/JAHA.115.002418

3. Khairy P, Landzberg MJ, Gatzoulis MA, Mercier LA, Fernandes SM, Côté JM, et al. Transvenous pacing leads and systemic thromboemboli in patients with intracardiac shunts: a multicenter study. *Circulation.* (2006) 113:2391–7. doi: 10.1161/CIRCULATIONAHA.106.622076

4. Gomes S, Cranney G, Bennett M, Li A, Giles R. Twenty-year experience of transvenous lead extraction at a single centre. *Europace.* (2014) 16:1350–5. doi: 10.1093/europace/eut424

5. Maisel WH. Transvenous implantable cardioverter-defibrillator leads: the weakest link. *Circulation.* (2007) 115:2461–3. doi: 10.1161/CIRCULATIONAHA.107.698597

6. Bongiorni MG, Kennergren C, Butter C, Deharo JC, Kutarski A, Rinaldi CA, et al. The European lead extraction ConTRolled (ELECTRa) study: a European heart rhythm association (EHRA) registry of transvenous lead extraction outcomes. *Eur Heart J.* (2017) 38:2995–3005. doi: 10.1093/eurheartj/ehx080

7. Wazni O, Epstein LM, Carrillo RG, Love C, Adler SW, Riggio DW, et al. Lead extraction in the contemporary setting: the LExICon study. An observational retrospective study of consecutive laser lead extractions. *J Am Coll Cardiol.* (2010) 55:579–86. doi: 10.1016/j.jacc.2009.08.070

8. Younis A, Glikson M, Meitus A, Arwas N, Natanzon SS, Lotan D, et al. Transvenous lead extraction with laser reduces need for femoral approach during the procedure. *PLoS ONE.* (2019) 14:e0215589. doi: 10.1371/journal.pone.0215589

9. Milman A, Zahavi G, Meitus A, Kariv S, Shafir Y, Glikson M, et al. Predictors of short-term mortality in patients undergoing a successful uncomplicated extraction procedure. *J Cardiovasc Electrophysiol.* (2020) 31:1155–62. doi: 10.1111/jce.14436

10. Bongiorni MG, Burri H, Deharo JC, Starck C, Kennergren C, Saghy L, et al. 2018 EHRA expert consensus statement on lead extraction: recommendations on definitions, endpoints, research trial design, data collection requirements for clinical scientific studies registries: endorsed by APHRS/HRS/LAHRS. *Europace.* (2018) 20:1217. doi: 10.1093/europace/euy050

11. Bashir J, Lee AJ, Philippon F, Mondesert B, Krahn AD, Sadek MM, et al. Predictors of perforation during lead extraction; results of the Canadian Lead ExtrAction risk (CLEAR) study. *Heart Rhythm.* (2021) 19:1097–103. doi: 10.1016/j.hrthm.2021.10.019

12. Mehta VS, Elliott MK, Sidhu BS, Gould J, Kemp T, Vergani V, et al. 2021. Long-term survival following transvenous lead extraction: importance of indication and comorbidities. *Heart Rhythm.* (2021) 18:1566–76. doi: 10.1016/j.hrthm.2021.05.007

13. Huang XM, Fu H, Osborn MJ, Asirvatham SJ, McLeod CJ, Glickson M, et al. Extraction of superfluous device leads: a comparison with removal of infected leads. *Heart Rhythm.* (2015) 12:1177–82.? doi: 10.1016/j.hrthm.2015.02.005

14. Archontakis S, Pirounaki M, Aznaouridis K, Karageorgopoulos D, Sideris K, Tolios P, et al. Transvenous extraction of permanent pacemaker and defibrillator leads: reduced procedural complexity and higher procedural success rates in patients with infective versus noninfective indications. *J Cardiovasc Electrophysiol.* (2021) 32:491–9.? doi: 10.1111/jce.14841

15. Pieper CC, Weis V, Fimmers R, Rajab I, Linhart M, Schild HH, et al. Obstruction in asymptomatic patients undergoing first implantation or revision of a cardiac pacemaker or implantable cardioverter-defibrillator: a retrospective single center analysis. *Rofo.* (2015) 187:1029–35. doi: 10.1055/s-0035-1553351

16. van Rooden CJ, Molhoek SG, Rosendaal FR, Schalij MJ, Meinders AE, Huisman MV. Incidence and risk factors of early venous thrombosis associated with permanent pacemaker leads. *J Cardiovasc Electrophysiol.* (2004) 15:1258–62. doi: 10.1046/j.1540-8167.2004.04081.x

17. Santini M, Di Fusco SA, Santini A, Magris B, Pignalberi C, Aquilani S, et al. Prevalence and predictor factors of severe venous obstruction after cardiovascular electronic device implantation. *Europace.* (2016) 18:1220–6. doi: 10.1093/europace/euv391

18. Bracke F, Meijer A, Van Gelder B. Venous occlusion of the access vein in patients referred for lead extraction: influence of patient and lead characteristics. *Pacing Clin Electrophysiol.* (2003) 26:1649–52. doi: 10.1046/j.1460-9592.2003.t01-1-00247.x

19. Li X, Ze F, Wang L, Li D, Duan J, Guo F, et al. Prevalence of venous occlusion in patients referred for lead extraction: implications for tool selection. *Europace.* (2014) 16:1795–9. doi: 10.1093/europace/euu124

20. Boczar K, Zabek A, Haberka K, Debski M, Rydlewska A, Musial R, et al. Venous stenosis and occlusion in the presence of endocardial leads in patients referred for transvenous lead extraction. *Acta Cardiol.* (2017) 72:61–7. doi: 10.1080/00015385.2017.1281545

frontiers | Frontiers in Cardiovascular Medicine

TYPE Original Research
PUBLISHED 07 November 2022
DOI 10.3389/fcvm.2022.1036574

OPEN ACCESS

EDITED BY
Roberto Rordorf,
San Matteo Hospital Foundation (IRCCS), Italy

REVIEWED BY
Ida Iafelice,
Istituto Clinico Città Studi (ICCS), Italy
Stefano Coli,
AOU Parma, Italy

*CORRESPONDENCE
Massimiliano Marini
massimiliano.marini@apss.tn.it

†These authors have contributed equally to this work and share first authorship

SPECIALTY SECTION
This article was submitted to Cardiac Rhythmology, a section of the journal Frontiers in Cardiovascular Medicine

RECEIVED 04 September 2022
ACCEPTED 19 October 2022
PUBLISHED 07 November 2022

CITATION
Marini M, Pannone L, Branzoli S, Tedoldi F, D'Onghia G, Fanti D, Sarao E, Guarracini F, Quintarelli S, Monaco C, Graffigna A, Bonmassari R, La Meir M, Chierchia GB and de Asmundis C (2022) Left atrial function after standalone totally thoracoscopic left atrial appendage exclusion in atrial fibrillation patients with absolute contraindication to oral anticoagulation therapy. *Front. Cardiovasc. Med.* 9:1036574. doi: 10.3389/fcvm.2022.1036574

Left atrial function after standalone totally thoracoscopic left atrial appendage exclusion in atrial fibrillation patients with absolute contraindication to oral anticoagulation therapy

Massimiliano Marini[1,2*†], Luigi Pannone[2†], Stefano Branzoli[3,4], Francesca Tedoldi[1], Giovanni D'Onghia[1], Diego Fanti[1], Emanuele Sarao[1], Fabrizio Guarracini[1], Silvia Quintarelli[1], Cinzia Monaco[2], Angelo Graffigna[3], Roberto Bonmassari[1], Mark La Meir[4], Gian Battista Chierchia[2] and Carlo de Asmundis[2]

[1]Department of Cardiology, S. Chiara Hospital, Trento, Italy, [2]Heart Rhythm Management Centre, Postgraduate Program in Cardiac Electrophysiology and Pacing, Vrije Universiteit Brussel, Universitair Ziekenhuis Brussel, Brussels, Belgium, [3]Department of Cardiac Surgery, S. Chiara Hospital, Trento, Italy, [4]Department of Cardiac Surgery, Vrije Universiteit Brussel, Universitair Ziekenhuis Brussel, Brussels, Belgium

Background: Left atrial appendage (LAA) is a common source of thrombi in patients with atrial fibrillation (AF). The effect on left atrial (LA) function of the Totally Thoracoscopic (TT)-LAA exclusion with epicardial clip is currently unknown. This study aims at evaluating the effect of TT-LAA exclusion on LA function.

Methods: Standalone TT-LAA exclusion with the clip device was performed in 26 patients with AF and contraindication to oral anticoagulation (OAC). A 3D CT scan, trans-esophageal echocardiography, spirometry and cerebrovascular doppler ultrasound were performed preoperatively. Clip positioning and LAA exclusion were guided and confirmed by intraoperative trans-esophageal echo. To evaluate LA function, standard transthoracic echocardiography and 2D strain of LA were performed before surgery, at discharge and at 3-month follow-up.

Results: The mean CHA_2DS_2-VASc and HASBLED scores were 4.6 and 2.4 respectively. There were no major complications during the procedure. At median follow-up of 10.3 months, 1 (3.8%) non-cardiovascular death, 1 (3.8%) stroke and 4 (15.4%) cardiovascular hospitalizations occurred. At 2D strain of LA, the reservoir function decreased significantly at discharge, compared to baseline and recovered at 3-months follow-up. Furthermore, NT-proBNP

increased significantly after the procedure with a return to baseline after 3 months. Changes in E/A were persistent at 3 months.

Conclusion: Our data in a small cohort suggest that TT-LAA exclusion with epicardial clip can be a safe procedure with regards to the atrial function. The LAA amputation impairs the reservoir LA function on the short term, that recovers over time.

KEYWORDS

left atrial appendage exclusion, oral anticoagulation therapy, totally thoracoscopic surgery, atrial fibrillation, left atrial appendage

Introduction

Atrial fibrillation (AF) is the most common sustained arrhythmia in humans and oral anticoagulation (OAC) to prevent ischemic stroke in AF patients with high CHA_2DS_2-VASc risk score is a guideline-recommended therapy (1, 2).

Despite the recent advances in pharmacological stroke prevention the perceived risk of OAC-associated bleeding may result in significant under prescription or under dosage of this therapy (3). The surgical exclusion of the left atrial appendage (LAA) is a therapeutic strategy for stroke prevention in AF patients with an absolute contraindication to OAC or a high risk of life-threatening bleeding on OAC or antiplatelet therapy (APT) (3) and unsuitable for percutaneous LAA occlusion. This intervention effect on left atrial (LA) function has not been studied. The LAA produces vasoactive neuroendocrine hormones activated by stretch-sensitive receptors (4) and this suggests a role in cardiovascular homeostasis as a "decompression chamber." LAA closure results in an increase LA size and mean pressure from animal models and human studies (5). Recent techniques have been introduced to assess the LA function such as two-dimensional speckle tracking echocardiography (2D STE), and specifically the strain and strain rate parameters. Through these parameters, the three LA function stages (reservoir, conduit and contractile) can be assessed.

This study aims at evaluating the effect of totally thoracoscopic (TT)-LAA exclusion on the LA function, evaluated with 2D STE.

Materials and methods

Patient population

This observational and retrospective study enrolled patients with AF at high risk for ischemic stroke and at high risk of life-threatening bleeding on OAC or APT or with a contraindication to long-term OAC. All patients underwent TT-LAA exclusion in the period between March 2020 and June 2021 at S. Chiara Hospital, Trento, Italy.

Inclusion criteria were: (1) AF defined following current guidelines (1); (2) Patients deemed at high risk for ischemic stroke, defined as CHADSVASC $>$ 1 or $\geq$ 2 if female sex; and (3) contraindication to long term OAC/APT, defined as at least one of the following: HASBLED $>$ 3, previous severe bleeding on OAC/APT or refractory anemia; or (4) refractory LAA thrombosis or recurrent stroke despite different OAC therapies (1). Previous severe bleeding was defined as at least one of the following:, diffuse gastrointestinal hemorrhage requiring transfusions or prior cerebral hemorrhage or other bleeding scenario with BARC $>$ 1 (6).

Final decision on inclusion in the study was taken by the "AF Heart Team," including a cardiac surgeon, a cardiologist, neurologist/neurosurgeon and referring physician following current guidelines on LAA exclusion (6).

All patients underwent preoperative computed tomography (CT) with 3-dimensional reconstruction, transthoracic and transesophageal echocardiography (TEE) to rule out thrombi in the LAA and to exclude other cardiac surgery indications for structural or functional heart diseases. Spirometry and bilateral carotid ultrasound doppler were also performed during the preoperative work out. Clinical history and laboratory data were collected and analyzed. Patient provided written informed consent to the procedure. The study complied with the Declaration of Helsinki as revised in 2013; the ethic committee approved the study.

Surgical procedure

All patients were treated using the video assisted thoracoscopic LAA exclusion approach with Atriclip PRO2 device (AtriCure Inc., Mason, OH). The procedure has been previously described in details (7). Briefly, patients were placed in a supine position, selective right lung ventilation was chosen with double lumen ventilation and intraoperative

TEE monitoring to evaluate and guide the correct device positioning. Three 12 Fr thoracoscopic access ports were used, including the following: (1) a camera port placed along the mid axillary line at mid sternal level and (2) working ports, placed along the anterior axillary line in the third intercostal space and in the intercostal space at the intersection between the line in the middle of anterior and midaxillary line and a sagittal line crossing the xiphoid process. After insufflation with CO_2, visualization of the intrathoracic anatomy, and freeing of adhesions, the opening of the pericardium was performed. The LAA was mobilized and the base measured with a dedicated sizer to select the device size. The AtriClip PRO2 (Atri-Cure Inc., West Chester, OH) device was positioned using the dedicated deployment device and deployed under TEE guidance and camera visualization.

Echocardiographic analysis

Echocardiographic analysis was performed in all patients by experienced cardiologists, a specific protocol was compiled, and the echocardiographic measurements were obtained following current guidelines (8). Standard 2D measurements were performed using GE Vivid E9 or GE Vivid E80, (GE-Healthcare, Chicago, Illinois) and LA deformation was evaluated with a 2D STE software. All images were acquired in a DICOM format and digitally stored for offline analysis. Two different experienced cardiologists performed offline analysis. Echocardiographic parameters analyzed included the following: LV end diastolic volume (EDV), left ventricular (LV) ejection fraction (LVEF), LA volume indexed to body surface area (BSA), mitral peak velocity in early diastole (E) and in late diastole (A), average (mean of septal and lateral) early diastolic mitral annulus velocity (e') estimated by tissue Doppler. Simpson's biplane method of discs was used to perform volumetric calculation of both LV and LA. All measurements were performed following ASE guidelines (9).

Two-dimensional speckle tracking echocardiography

Two-dimensional speckle tracking echocardiography was performed with a standard protocol following current guidelines (10). The apical four-chamber view was utilized for the strain measurements of LA and LV. Briefly, first the LA endocardium edge was traced manually and then the tracings based on the 2D STE were generated by the software, **Figure 1**. The mean deformation (strain) expressed in percentage was then calculated by the software. The reservoir function of the LA (LA reservoir strain) was calculated as the maximal wall deformation of LA during LV systole as compared to the end diastole, that was considered as preset reference point (11). 2D STE LA strain refers to reservoir strain if not otherwise specified. In patients with permanent AF, atrial strain was performed during ongoing AF. In patients with non-permanent AF, atrial strain was performed during sinus rhythm. Global longitudinal strain (GLS) of LV was measured as the longitudinal shortening of the myocardium (change in length compared to the baseline length).

Follow-up

Periprocedural adverse events were registered. Thoracoscopic access was evaluated after 10 days from the procedure. Clinical evaluations included laboratory work-out at pre-discharge and after 3 months and physical examination. A protocol echocardiogram was performed at baseline (pre-surgery), at pre-discharge (after surgery) and at 3 months. At 3 months follow-up, a cardiac synchronized CT scan or TEE were also performed to measure the size of the residual stump, if any and to assess the efficacy of LAA exclusion. A satisfactory outcome was considered as a residual stump < 1 cm (12). The primary endpoint was LA function, defined with 2D STE at pre-discharge and at 3 months. Secondary endpoints were the following: all-cause mortality, cardiovascular hospitalizations and stroke at long-term follow-up.

Statistical analysis

Descriptive statistics are reported as medians and interquartile range (IQR) for non-normally distributed continuous variables or mean $\pm$ standard deviation for normally distributed continuous variables. *T*-test was used to compare numerical normal variables, and Wilcoxon test for non-parametric variables. The categorical variables were compared by Chi-squared test or Fisher's exact test and described as frequencies and percentages. A p-value < 0.05 was considered significant for all tests. The analysis was performed using R software version 3.6.2 (R Foundation for Statistical Computing, Vienna, Austria).

Results

Patient population

The study enrolled 26 consecutive patients (77.3 $\pm$ 6 years, 76.9% males). The mean HAS-BLED and CHA_2DS_2-VASc scores were 2.4 $\pm$ 0.6 and 4.6 $\pm$ 1.1 respectively. Permanent AF was present in 8 patients (30.8%). The indication

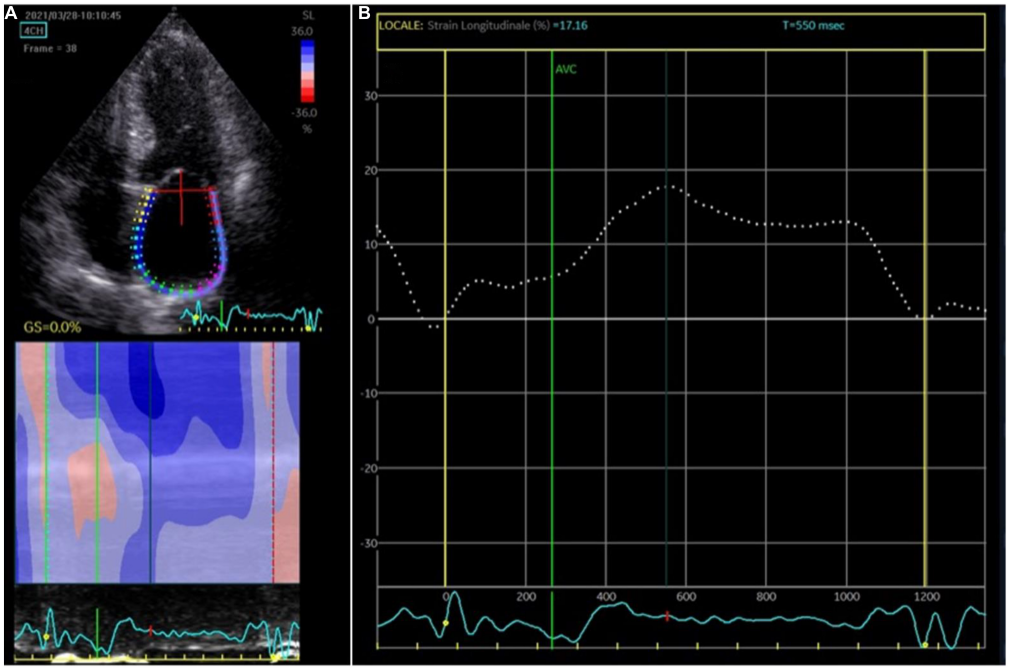

FIGURE 1
Atrial strain measurement. **(A)** The apical four-chamber view was utilized for the strain measurements of the left atrium (LA); the edge of the LA endocardium was manually traced. **(B)** The software generated tracings based on the 2D strain of LA. The mean deformation (strain) is expressed in percentage and calculated by the software.

TABLE 1 Baseline characteristics.

	Overall (N = 26)
Age (years)	77.3 (6.0)
Sex (M) (n, %)	20 (76.9%)
BMI	25.6 (4.7)
BSA	1.9 (0.2)
Permanent AF (n, %)	8 (30.8%)
CHA2DS2-VASc score	4.6 (1.1)
HASBLED score	2.4 (0.6)
Stroke/TIA history (n, %)	6 (23.1%)
Diabetes (n, %)	7 (26.9%)
Hypertension (n, %)	25 (96.2%)
Heart failure (n, %)	9 (34.6%)
CKD (HASBLED definition) (n, %)	3 (11.5%)
Peripheral vascular disease (n, %)	15 (57.7%)
COPD (n, %)	3 (11.5%)
NYHA II–III (n, %)	21 (80.8%)
Follow-up (months)	10.3 (4.7)

AF, atrial fibrillation; BMI, body mass index; BSA, body surface area; CKD, chronic kidney disease; COPD, chronic obstructive pulmonary disease; TIA, transient ischemic attack.

for LAA exclusion was the following: history of cerebral hemorrhage (n = 10), diffuse gastrointestinal hemorrhage requiring transfusions (n = 4), clinical scenario of high bleeding risk (n = 4), refractory anemia (n = 3), other bleeding scenarios (n = 2), refractory LAA thrombosis (n = 1) and recurrent stroke despite different OAC therapies (n = 2). Baseline characteristics are summarized in Table 1.

Surgical treatment

A total of 26 patients underwent thoracoscopic LAA exclusion. Mean operation time (skin-to-skin) was 69.2 ± 18.5 min. No deaths procedure-related or pulmonary morbidity were observed. No patient required conversion to mini thoracotomy. Intraoperative TEE showed complete LAA exclusion with minimal residual stump (<1 cm) in all cases. Following the procedure, no patients were prescribed OAC, APT or heparin. There were no major complications during and after the procedure.

Laboratory and echocardiographic changes

Compared with baseline, NT-proBNP was significantly higher at pre-discharge evaluation (1000.3 ± 950.1 pg/ml vs. 3170.2 ± 2011.6 pg/ml, p < 0.001); after 3 months there was no differences in NT-proBNP

TABLE 2 Laboratory and echocardiographic data during follow-up.

	Baseline (N = 26)	Pre-discharge (N = 26)	P-value (baseline vs. pre-discharge)	3 months follow-up (N = 26)	P-value (baseline vs. 3 months follow-up)	P-value (pre-discharge vs. 3 months follow-up)
NT-proBNP (pg/ml)	1000.3 (950.1)	3170.2 (2011.6)	<0.001	1509.5 (1444.3)	0.17	0.005
Creatinine (mg/dl)	1.4 (0.9)	1.5 (1.1)	0.86	1.7 (1.7)	0.46	0.56
Hb (g/dl)	12.3 (1.5)	12.0 (1.5)	0.37	12.5 (2.2)	0.75	0.34
LVEF (%)	58.9 (8.4)	58.1 (6.5)	0.72	56.3 (9.2)	0.32	0.46
GLS (%)	16.8 (4.5)	14.6 (4.2)	0.11	15.3 (4.2)	0.28	0.59
EDV (ml)	103.7 (27.7)	108.8 (33.2)	0.57	113.8 (27.9)	0.24	0.60
E wave (m/s)	0.8 (0.3)	0.9 (0.2)	0.48	0.8 (0.3)	0.99	0.47
A wave (m/s)	0.89 (0.2)	0.81 (0.3)	0.44	0.61 (0.3)	0.005	0.08
E/A	0.9 (0.3)	1.1 (0.3)	0.25	1.3 (0.4)	0.004	0.07
dT (ms)	165.0 (42.7)	168.0 (49.4)	0.83	183.2 (39.2)	0.16	0.28
E' (m/s)	0.1 (0.0)	0.1 (0.0)	0.31	0.1 (0.0)	0.17	0.74
E/e'	13.1 (6.8)	12.7 (6.8)	0.85	10.6 (3.0)	0.14	0.20
PAPs	33.7 (11.7)	33.4 (13.5)	0.96	30.6 (9.7)	0.47	0.55
LA volume index	59.3 (33.0)	56.6 (26.9)	0.76	59.2 (28.3)	0.99	0.76
LA reservoir strain	16.9 (7.7)	11.8 (8.0)	0.028	18.6 (10.5)	0.55	0.017

dT, deceleration time; EDV, end-diastolic volume; GLS, global longitudinal strain; Hb, hemoglobin; LA, left atrium; LVEF, left ventricular ejection fraction; PAPs, systolic pulmonary artery pressure.

TABLE 3 2D strain results for permanent vs. non-permanent atrial fibrillation patients.

	Non-permanent AF (N = 18)	Permanent AF (N = 8)	Overall (N = 26)	P-value
LA reservoir strain baseline	19.9 (7.0)	10.1 (4.2)	16.9 (7.7)	0.003
LA reservoir strain pre-discharge	14.2 (8.6)	6.6 (2.2)	11.8 (8.0)	0.023
LA reservoir strain 3 months follow-up	20.5 (9.9)	11.0 (10.7)	18.6 (10.5)	0.11

AF, atrial fibrillation; LA, left atrium.

value compared with baseline (p = 0.17) (Table 2). There were no significant differences in creatinine and hemoglobin at pre-discharge and at 3-months follow-up (Table 2).

The 2D STE of LA measured at pre-discharge decreased significantly compared with the baseline values (11.8 ± 8% vs. 16.9 ± 7.7%, p = 0.028) with a recovery at 3-months (18.6 ± 10.5% vs. 16.9 ± 7.7%, p = 0.55) (Table 2). When compared with baseline, E/A increased significantly after 3 months (1.3 ± 0.4 vs. 0.9 ± 0.3, p = 0.004) (Table 2). Of note, there was a non-significant trend toward higher E/A values at pre-discharge evaluation compared to baseline (1.1 ± 0.3 vs. 0.9 ± 0.3, p = 0.25). E/e' decreased throughout serial evaluation with no significant change (13.1 ± 6.8 vs. 12.7 ± 6.8 vs. 10.6 ± 3.0, p = NS for all comparisons). At pre-discharge and at 3-months follow-up echocardiography, the LA volume indexed to BSA was unchanged compared with baseline measurements (56.6 ± 26.9 ml/mq vs. 59.2 ± 28.3 ml/mq vs. 59.3 ± 33.0 ml/mq, p = NS for all comparisons). There was no significant difference in LV EDV, LVEF and GLS of LV (Table 2). The results of 2D STE of LA for permanent AF patients compared with non-permanent AF patients are summarized in Table 3.

Follow-up

Follow up was completed and available for all 26 patients. At a median follow-up of 10.3 ± 4.7 months, no patients were on OAC, APT or heparin therapy. One (3.8%) non-cardiovascular death, 1 (3.8%) stroke and 4 (15.4%) cardiovascular hospitalizations occurred at long-term follow up. Evaluation by TEE or CT after 3 months showed stable and appropriate device position with LAA stump < 1 cm in all patients.

Discussion

The main findings of this study can be summarized as follows: (1) The amputation of LAA significantly impairs LA reservoir function after the procedure, although this function

recovers after 3 months. (2) TT-LAA exclusion results in a change in E/A that is persistent at 3 months follow-up.

The role of left atrial appendage clipping on left atrial reservoir function

The LA function consists of three components, namely: conduit, reservoir and pump. It is the result of a complex interplay between LV systolic and diastolic function, circulating blood volume and LAA function (13).

In the current study a transient impairment of LA reservoir function was observed after LAA exclusion; different mechanisms might contribute to this finding.

The sudden volume reduction of the LA after the procedure may affect LA distension, whereas its recovery might be explained with volume recovery or LA remodeling over time.

Changes in LA function could also be secondary to an altered neuro-humoral homeostasis expressed by changes in both atrial natriuretic peptide (ANP) and NT-proBNP. LAA endovascular occlusion is associated with an increase in ANP levels (14); ANP is produced by LAA and it plays an important role in LA physiology (15); its mutation is associated with a familial atrial dilated cardiomyopathy with standstill evolution (15). In a previous study on endovascular LAA closure, NT-proBNP was higher at 6 h and 24 h after procedure with no difference at 48 h (16). This is consistent with our results of a sudden increase in NT-proBNP followed by a return to baseline values.

Previous studies with percutaneous LAA closure, were characterized by heterogeneous results; different groups showed no changes in LA function after the procedure (17–19). A limitation of previous studies was the lack of routine 2D STE. Indeed, a subtle difference in LA function was evident only at 2D STE in our study. Furthermore, other groups demonstrated an improvement in LA function (20). The technical difference between the percutaneous and the surgical approach (with the latter causing a clean anatomical exclusion of the LAA) could explain the different behavior of the atrial function during the follow-up (21). In patients undergoing TT pulmonary veins isolation and LAA exclusion: De Maat et al. (21) concluded that the LAA exclusion does not impair the LA contractile function or the ejection fraction of LA, but there is only a reduction in LA reservoir function, in contrast Gelsomino et al. (22) described a gain of LA function and a reverse LA remodeling after the surgical ablation and LAA exclusion.

The recovery of reservoir strain of LA after 3 months is consistent with previous studies with 2D STE (20, 23); it might be explained by the recovery of both LA preload and neuro-humoral homeostasis. LAA exclusion might improve mechanical function of the LA and result in reverse LA remodeling (24).

Pulsed wave measures, in particular E/A remained increased at 3 months follow-up in the current study. In the pulsed wave analysis of transmitral flow, E wave represents the early fast diastolic filling and it is a measure of LA reservoir function. Its increase, with a consequent increase of E/A has been reported in previous studies (25); it could be a consequence of LA volume reduction following LAA exclusion, that represents the most distensible portion of LA (26).

Limitations

The main limitation of the study is that it is retrospective. The included number of patients was relatively small, due to strict inclusion criteria. Limitations also included referral bias, being the center specialized in TT treatment of AF and TT-LAA exclusion. The reported changes in reservoir function might depend also on the appendage volume, which may differ among individuals. Data on LAA volume are lacking in all the published studies, and in the present one. In patients with permanent AF, A wave was not measured.

Conclusion

Our data in a small cohort suggest that TT-LAA exclusion with epicardial clip can be a safe procedure with regards to the atrial function. The LAA amputation impairs the reservoir LA function on the short term, that recovers over time.

Data availability statement

The raw data supporting the conclusions of this article will be made available by the authors, without undue reservation.

Ethics statement

The studies involving human participants were reviewed and approved by the Santa Chiara Hospital Ethics Committee. The patients/participants provided their written informed consent to participate in this study.

Author contributions

MMa, LP, and CA: conception and design of the work. MMa, LP, SB, FT, GD'O, DF, and ES: substantial contributions to the acquisition of data for the work. MMa and LP: substantial contributions to the analysis of data for the work and drafting the work. AG, RB, MMe, GC, and CA: substantial contributions

to the interpretation of data for the work. FG, SQ, CM, AG, RB, MMe, GC, and CA: revising the draft of the work critically for important intellectual content. MMa, LP, SB, FT, GD'O, DF, ES, FG, SQ, CM, AG, RB, MMe, GC, and CA: final approval of the version to be published and agreement to be accountable for all aspects of the work in ensuring that questions related to the accuracy or integrity of any part of the work are appropriately investigated and resolved. All authors contributed to the article and approved the submitted version.

Conflict of interest

Author MMe was consultant for AtriCure. Author GC received compensation for teaching purposes and proctoring from Medtronic, Abbott, Biotronik, Boston Scientific, and Acutus Medical. Author CA received research grants on behalf of the center from Biotronik, Medtronic, Abbott, LivaNova, Boston Scientific, AtriCure, Philips, and Acutus Medical. Author CA received compensation for teaching purposes and proctoring from Medtronic, Abbott, Biotronik, Livanova, Boston Scientific, AtriCure, Acutus Medical, and Daiichi Sankyo.

The remaining authors declare that the research was conducted in the absence of any commercial or financial relationships that could be construed as a potential conflict of interest.

Publisher's note

All claims expressed in this article are solely those of the authors and do not necessarily represent those of their affiliated organizations, or those of the publisher, the editors and the reviewers. Any product that may be evaluated in this article, or claim that may be made by its manufacturer, is not guaranteed or endorsed by the publisher.

References

1. Hindricks G, Potpara T, Dagres N, Arbelo E, Bax JJ, Blomström-Lundqvist C, et al. 2020 ESC guidelines for the diagnosis and management of atrial fibrillation developed in collaboration with the European association for cardio-thoracic surgery (EACTS). *Eur Heart J.* (2021). 42:373–498.

2. January CT, Wann LS, Calkins H, Chen LY, Cigarroa JE, Cleveland JC, et al. 2019 AHA/ACC/HRS focused update of the 2014 AHA/ACC/HRS guideline for the management of patients with atrial fibrillation. *J Am Coll Cardiol.* (2019) 74:104–32.

3. Ruff CT, Giugliano RP, Braunwald E, Hoffman EB, Deenadayalu N, Ezekowitz MD, et al. Comparison of the efficacy and safety of new oral anticoagulants with warfarin in patients with atrial fibrillation: a meta-analysis of randomised trials. *Lancet.* (2014) 383:955–62.

4. Regazzoli D, Ancona F, Trevisi N, Guarracini F, Radinovic A, Oppizzi M, et al. Left atrial appendage: physiology, pathology, and role as a therapeutic target. *Biomed Res Int.* (2015) 2015:205013.

5. Melduni RM, Schaff HV, Lee HC, Gersh BJ, Noseworthy PA, Bailey KR, et al. Impact of left atrial appendage closure during cardiac surgery on the occurrence of early postoperative atrial fibrillation, stroke, and mortality. *Circulation.* (2017) 135:366–78.

6. Glikson M, Wolff R, Hindricks G, Mandrola J, Camm AJ, Lip GYH, et al. EHRA/EAPCI expert consensus statement on catheter-based left atrial appendage occlusion – an update. *Europace.* (2020) 22:184.

7. Branzoli S, Marini M, Guarracini F, Pederzolli C, D'Onghia G, Centonze M, et al. Standalone totally thoracoscopic left appendage clipping: safe, simple, Standardized. *Ann Thorac Surg.* (2021) 111:e61–3. doi: 10.1016/j.athoracsur.2020.04.130

8. Mitchell C, Rahko PS, Blauwet LA, Canaday B, Finstuen JA, Foster MC, et al. Guidelines for performing a comprehensive transthoracic echocardiographic examination in adults: recommendations from the American society of echocardiography. *J Am Soc Echocardiogr.* (2019) 32:1–64.

9. Lang RM, Badano LP, Mor-Avi V, Afilalo J, Armstrong A, Ernande L, et al. Recommendations for cardiac chamber quantification by echocardiography in adults: an update from the American society of echocardiography and the European association of cardiovascular imaging. *Eur Heart J Cardiovasc Imaging.* (2015) 16:1–39.e14.

10. Badano LP, Kolias TJ, Muraru D, Abraham TP, Aurigemma G, Edvardsen T, et al. Standardization of left atrial, right ventricular, and right atrial deformation imaging using two-dimensional speckle tracking echocardiography: a consensus document of the EACVI/ASE/industry task force to standardize deformation imaging. *Eur Heart J Cardiovasc Imaging.* (2018) 19:591–600. doi: 10.1093/ehjci/jey042

11. Mor-Avi V, Lang RM, Badano LP, Belohlavek M, Cardim NM, Derumeaux G, et al. Current and evolving echocardiographic techniques for the quantitative evaluation of cardiac mechanics: ASE/EAE consensus statement on methodology and indications endorsed by the Japanese society of echocardiography. *Eur J Echocardiogr.* (2011) 12:167–205.

12. Osmancik P, Budera P, Zdarska J, Herman D, Petr R, Fojt R, et al. Residual echocardiographic and computed tomography findings after thoracoscopic occlusion of the left atrial appendage using the AtriClip PRO device. *Interact Cardiovasc Thorac Surg.* (2018) 26:919–25. doi: 10.1093/icvts/ivx427

13. Leischik R, Littwitz H, Dworrak B, Garg P, Zhu M, Sahn DJ, et al. Echocardiographic evaluation of left atrial mechanics: function, history, novel techniques, advantages, and pitfalls. *Biomed Res Int.* (2015) 2015:765921. doi: 10.1155/2015/765921

14. Behnes M, Sartorius B, Wenke A, Lang S, Hoffmann U, Fastner C, et al. Percutaneous closure of left atrial appendage affects mid-term release of MR-proANP. *Sci Rep.* (2017) 7:9028. doi: 10.1038/s41598-017-08999-4

15. Disertori M, Quintarelli S, Grasso M, Pilotto A, Narula N, Favalli V, et al. Autosomal recessive atrial dilated cardiomyopathy with standstill evolution associated with mutation of natriuretic peptide precursor A. *Circ Cardiovasc Genet.* (2013) 6:27–36. doi: 10.1161/CIRCGENETICS.112.963520

16. Huakang L, Qing Y, Bing S, Zhihui Z, Zhiyuan S. The influence of left atrial appendage closure on the structure and function of the left atrium. *Int J Clin Exp Med.* (2018) 11:3845–51. doi: 10.1378/chest.128.3.1853

17. Hanna IR, Kolm P, Martin R, Reisman M, Gray W, Block PC. Left atrial structure and function after percutaneous left atrial appendage transcatheter occlusion (PLAATO): six-month echocardiographic follow-up. *J Am Coll Cardiol.* (2004) 43:1868–72. doi: 10.1016/j.jacc.2003.12.050

18. Madeira M, Teixeira R, Reis L, Dinis P, Paiva L, Botelho A, et al. Does percutaneous left atrial appendage closure affect left atrial performance? *Int J Cardiovasc Sci.* (2018) 31:569–77.

19. Jalal Z, Iriart X, Dinet ML, Corneloup O, Pillois X, Cochet H, et al. Evaluation of left atrial remodelling following percutaneous left atrial appendage closure. *J Geriatr Cardiol.* (2017) 14:496–500.

20. Ijuin S, Hamadanchi A, Haertel F, Baez L, Schulze PC, Franz M, et al. Improvement in left atrial strain among patients undergoing percutaneous left atrial appendage closure. *J Cardiovasc Echogr.* (2020) 30:15–21. doi: 10.4103/jcecho.jcecho_42_19

21. De Maat GE, Benussi S, Hummel YM, Krul S, Pozzoli A, Driessen AHG, et al. Surgical left atrial appendage exclusion does not impair left atrial contraction function: a pilot study. *Biomed Res Int.* (2015) 2015:318901.

22. Gelsomino S, Lucà F, Rao CM, Parise O, Pison L, Wellens F, et al. Improvement of left atrial function and left atrial reverse remodeling after surgical treatment of atrial fibrillation. *Ann Cardiothorac Surg.* (2014) 3:70–4.

23. Coisne A, Pilato R, Brigadeau F, Klug D, Marquie C, Souissi Z, et al. Percutaneous left atrial appendage closure improves left atrial mechanical function through frank–starling mechanism. *Hear Rhythm.* (2017) 14:710–6. doi: 10.1016/j.hrthm.2017.01.042

24. Dar T, Afzal MR, Yarlagadda B, Kutty S, Shang Q, Gunda S, et al. Mechanical function of the left atrium is improved with epicardial ligation of the left atrial appendage: insights from the LAFIT-LARIAT registry. *Hear Rhythm.* (2018) 15:955–9. doi: 10.1016/j.hrthm.2018.02.022

25. Kamohara K, Popović ZB, Daimon M, Martin M, Ootaki Y, Akiyama M, et al. Impact of left atrial appendage exclusion on left atrial function. *J Thorac Cardiovasc Surg.* (2007) 133:174–81.

26. Hondo T, Okamoto M, Yamane T, Kawagoe T, Karakawa S, Yamagata T, et al. The role of the left atrial appendage. A volume loading study in open-chest dogs. *JPN Heart J.* (1995) 36:225–34. doi: 10.1536/ihj.36.225

frontiers | Frontiers in Cardiovascular Medicine

TYPE Original Research
PUBLISHED 21 December 2022
DOI 10.3389/fcvm.2022.928974

OPEN ACCESS

EDITED BY
Matt Wright,
King's College London,
United Kingdom

REVIEWED BY
Malcolm Finlay,
Barts Heart Centre, United Kingdom
Alberto Guido Pozzoli,
Ospedale Regionale di
Lugano, Switzerland

*CORRESPONDENCE
Alexandre Almorad
✉ alexandre.almorad@uzbrussel.be
Sébastien Knecht
✉ sebastien.knecht@azsintjan.be

†These authors have contributed equally to this work

SPECIALTY SECTION
This article was submitted to Cardiac Rhythmology, a section of the journal Frontiers in Cardiovascular Medicine

RECEIVED 26 April 2022
ACCEPTED 25 November 2022
PUBLISHED 21 December 2022

CITATION
Almorad A, O'Neill L, Wielandts J-Y, Gillis K, De Becker B, Nakatani Y, De Asmundis C, Iacopino S, Pambrun T, Marc LM, Jaïs P, Haïssaguerre M, Duytschaever M, Chierchia J-B, Derval N and Knecht S (2022) Long-term clinical outcome of atrial fibrillation ablation in patients with history of mitral valve surgery. *Front. Cardiovasc. Med.* 9:928974. doi: 10.3389/fcvm.2022.928974

Long-term clinical outcome of atrial fibrillation ablation in patients with history of mitral valve surgery

Alexandre Almorad[1,2*†], Louisa O'Neill[1†], Jean-Yves Wielandts[1], Kris Gillis[1], Benjamin De Becker[1], Yosuke Nakatani[3], Carlo De Asmundis[2], Saverio Iacopino[2], Thomas Pambrun[3], La Meir Marc[2], Pierre Jaïs[3], Michel Haïssaguerre[3], Mattias Duytschaever[1], Jean-Baptista Chierchia[2], Nicolas Derval[3] and Sébastien Knecht[1*]

[1]Department of Cardiology, AZ Sint Jan Hospital Bruges, Bruges, Belgium, [2]Heart Rhythm Management Centre, Postgraduate Program in Cardiac Electrophysiology and Pacing, European Reference Networks Guard-Heart, Universitair Ziekenhuis Brussel - Vrije Universiteit Brussel, Brussels, Belgium, [3]Department of Cardiac Pacing and Electrophysiology, Hospital Cardiologique du Haut-Lévêque, CHU de Bordeaux, Avenue de Magellan, Pessac, France

Aims: Atrial fibrillation (AF) occurs frequently after mitral valve (MV) surgery. This study aims to evaluate the efficacy and long-term clinical outcomes after the first AF ablation in patients with prior MV surgery.

Methods: Sixty consecutive patients with a history of MV surgery without MAZE referred to three European centers for a first AF ablation between 2007 and 2017 (group 1) were retrospectively enrolled. They were matched (propensity score match) with 60 patients referred for AF ablation without prior MV surgery (group 2).

Results: After the index ablation, 19 patients (31.7%) from group 1 and 24 (40%) from group 2 had no recurrence of atrial arrhythmias (ATa) ($p = 0.3$). After 62 (48–84) months of follow-up and 2 (2–2) procedures, 90.0% of group 1 and 95.0% of group 2 patients were in sinus rhythm ($p = 0.49$). In group 1, 19 (31.7%) patients had mitral stenosis, and 41 (68.3%) had mitral regurgitation. Twenty-seven (45.0%) patients underwent mechanical valve replacement and 33 (55.0%) MV annuloplasty. At the final follow-up, 28 (46.7%) and 33 (55.0%) patients were off antiarrhythmic drugs ($p = 0.46$). ATa recurrence was seen more commonly in patients with prior MV surgery (54 vs. 22%, respectively, $p < 0.05$). No major complication occurred.

Conclusion: Long-term freedom of atrial arrhythmias after atrial fibrillation catheter ablation is achievable and safe in patients with a history of mitral valve surgery. In AF patients without a history of mitral valve surgery, repeated procedures are needed to maintain sinus rhythm.

KEYWORDS

atrial fibrillation, mitral valve surgery, ablation, atrial tachyarrhythmias, antiarrhythmic drugs

Introduction

Atrial tachyarrhythmias (ATa) are a common cause of morbidity in patients with mitral valve disease. Left atrial volume and pressure loading in the setting of stenotic and regurgitant mitral valvular disease results in atrial electrical and structural remodeling predisposing to atrial arrhythmogenesis (1). Although surgical correction is associated with an improvement in hemodynamics and reduction in left atrial (LA) dimensions (2), the risk of post-surgical ATa remains elevated (1–3) and is associated with increased mortality and morbidity (4, 5). As well as ongoing pre-existing arrhythmia (3) *de novo* atrial fibrillation (AF) is associated with increased age and LA size while reentry mechanisms can arise from sites of surgical incision and scarring (6). Catheter ablation can be challenging in this cohort, given the degree of intrinsic arrhythmogenic remodeling and the presence of surgical incisions and scars. Nevertheless, symptom burden is often high in this population and ablation may offer a significant quality of life benefit to the patient (7, 8).

To the best of our knowledge, little data exist on long-term efficacy, beyond 2 years, of AF catheter ablation after MV surgery. The aim of this study is, therefore, to evaluate long-term safety and efficacy outcomes of catheter ablation in this cohort.

Methods

Study population

An electronic medical database of three Europeans was screened for patients with a history of successful surgical correction of mitral stenosis or regurgitation and without concomitant MAZE surgery, referred for a first AF ablation from January 2008 to December 2017 across three European centers, were screened for inclusion (group 1). Patients with no or mild residual mitral regurgitation and with both paroxysmal and persistent AF were included. Those with a history of prior surgical or percutaneous ATa ablation or congenital cardiomyopathy were excluded. After collecting patients' written informed consent, a detailed case report form including clinical and procedural characteristics and follow-up was filled and incorporated into a common database shared by the three centers.

A comparison was made to a group of patients, matched for age, gender, body mass index, follow-up duration, and AF type with a history of AF ablation and no prior MV surgery (group 2).

Radiofrequency catheter ablation

Procedures were carried out under local or general anesthesia depending on the institution. Ablation strategy was according to operator discretion and ranged from pulmonary vein isolation (PVI) only to more extensive strategies including linear ablation at the LA roof and mitral isthmus, ablation of complex fractionated atrial electrograms, cavo-tricuspid isthmus ablation and superior vena cava isolation, depending on AF duration and persistence. The PVI-only strategy was performed either with a radiofrequency catheter or a single-shot cryoballoon.

In the case of repeat procedures for recurrent ATa, persistent isolation of the pulmonary veins and block across lines (if applicable) were evaluated with RF ablation performed, where necessary, to achieve re-isolation or block. Further ablation was eventually performed according to the operator's discretion. Electrical cardioversion was performed at the end of the procedure in the event of failure to restore sinus rhythm.

Follow-up

All patients underwent a clinical evaluation and a 12-lead electrocardiogram (ECG) at 1, 3, 6, and 12 months as well as a yearly 24-h Holter. ATa recurrence was defined according to the HRS/EHRA/ECAS expert consensus document as any recurrence of atrial arrhythmia >30 s (9) and a 3-month blanking period was applied.

Complications including vascular damage, thromboembolism, pericardial effusion, esophageal fistula, mechanical valve damage, atrioventricular block, and procedure-related death were systematically recorded.

Statistical analysis

Statistical analyses were performed in SPSS Statistics 24 (IBM Corporation, Armonk, New York, USA). Propensity-score matching with a 1:1 ratio, without replacement, and with the nearest neighbor technique was used to create groups of patients with similar characteristics out of a database of 180 patients (age, gender, body mass index, LA volume, follow-up duration, and AF type) to compare the outcomes in patients with vs. without MV surgery undergoing ablation.

Comparison of means between groups was performed using independent samples *t*-test for normally distributed data and Mann–Whitney *U*-test for non-uniformly distributed data. Continuous variables are expressed as mean ± SD if normally distributed, medians with first and third quartiles (Q1–Q3) if non-normally distributed, and dichotomous variables as percentages were compared using the χ^2 test. Kaplan–Meier plots were used to report arrhythmia-free survival curves for each group, and a time-to-event analysis was performed using the log-rank test. A bilateral p-value < 0.05 was considered statistically significant.

Results

Patients' and procedural characteristics

The baseline clinical characteristics of the study cohort are presented in Table 1. Sixty patients with prior MV surgery and a first AF ablation (Group 1; 65.5 ± 5.8 years, 50% women) and 60 matched patients (Group 2; 64.3 ± 6.9 years, 55% women) were studied. Patients' characteristics in both groups are summarized in Table 1.

In group 1, 19 (31.7%) patients had mitral stenosis and 41 (68.3%) had mitral regurgitation. Twenty-seven (45.0%) patients underwent MV replacement with mechanical valves and 33 (55.0%) MV annuloplasty. Eighteen patients underwent concomitant surgical procedures, including coronary bypass in six patients, aortic valve replacement in three patients, tricuspid valve repair in eight patients, and interatrial closure in one patient. Surgical atrial access was granted through the right atrium and the interatrial septum in 32 patients, 12 patients through the left atrium, and 16 patients through the roof.

Procedural characteristics are shown in Table 2. Substrate ablation was performed in a higher proportion of patients in group 1 (Table 2). Procedural times (p = 0.47) and fluoroscopy times were similar between groups ($p = 0.72$).

TABLE 1 Clinical and index procedure characteristics ($n = 120$).

	Group 1 ($n = 60$)	Group 2 (control, $n = 60$)	*P*-value
Female, *n* (%)	30 (50.0%)	33 (55.0%)	0.84
Age, mean ± SD yrs	65.5 ± 5.8	64.3 ± 6.9	0.29
BMI, mean ± SD kg/m^2	24.9 ± 4.1	25.5 ± 4.1	0.31
Mitral regurgitation, *n* (%)	41 (68.3%)	NA	NA
Mitral stenosis, *n* (%)	19 (31.7%)	NA	NA
Mitral valve repair, *n* (%)	33 (55.0%)	NA	NA
Mitral valve replacement, *n* (%)	27 (45.0%)	NA	NA
Mechanical valve, *n* (%)	27 (45%)	NA	NA
Type of atrial fibrillation			
Paroxysmal AF, *n* (%)	32 (53.3%)	30 (50.0%)	0.85
Non paroxysmal AF, *n* (%)	28 (46.7%)	30 (50.0%)	0.85
Time from first AF episode, months	35.8 ± 6.5	33.0 ± 8.4	0.16
CHA_2DS_2-VASc Score	2,4 ± 1.4	2.2 ± 1.1	0.92
Arterial Hypertension, *n* (%)	36 (60.0%)	39 (65.0%)	0.78
Diabetes, *n* (%)	5 (7.1%)	4 (6.7%)	0.66
Congestive heart failure, *n* (%)	12 (20.0%)	7 (11.7%)	0.32
History of stroke, *n* (%)	6 (10.0%)	4 (6.7%)	0.53
Anti-arrhythmic drug before the procedure, *n* (%)	33 (55.0%)	30 (50.0%)	0.84
Betablockers, *n* (%)	25 (*41.7%*)	36 (*60.0%*)	0.07
Flecainide, *n* (%)	25 (*41.7%*)	21 (*35.0%*)	0.57
Sotalol, *n* (%)	4 (*6.7%*)	3 (*5.0%*)	0.46
Amiodarone, *n* (%)	10 (16.7%)	5 (*7.1%*)	0.27
Direct anticoagulant, *n* (%)	37 (61.7%)	40 (66.7%)	0.71
Antivitamin K, *n* (%)	34 (56.7%)	7 (11.7%)	*0.001*
LVEF, mean ± SD %	51.8 ± 7.5	52.7 ± 3.9	0.21
Left atrial diameter	47.2 ± 6.7	44.3 ± 5.5	0.08

BMI, body mass index; AF, atrial fibrillation; LVEF, left ventricular ejection fraction.

Procedural outcomes and recurrence characteristics

Following the index ablation, 19 patients (31.6%) from group 1 and 24 patients (40.0%) from group 2 had no recurrence of ATa ($p = 0.34$). Of these, 9 (15%) and 18 (30%) respectively were not taking antiarrhythmic drugs (AADs) ($p = 0.22$, Table 3). In those with recurrent arrhythmia, the median time to the first recurrence was similar between groups [Group 1, 13 (9–17) months vs. Group 2, 19 (8–22) months] ($p = 0.06$; Figure 1). One-, 2-, and 5-years freedom of recurrence are also shown on Kaplan–Meier curves (Supplementary material).

As pointed out in Table 3, 41 patients (68.3%) from group 1 and 36 patients (60.0%) from group 2 experienced recurrence. Among them, AT was more observed in group 1 than in group 2 (22 vs. 8, respectively, $p = 0.03$), whereas AF was evenly observed in both groups (19 vs. 28; $p = 0.09$).

Each patient underwent a median of 2 (2–2) ablation procedures and was followed for 62 (48–84) months. No difference was observed in both groups regarding the outcome with 54 patients (90.0%) in sinus rhythm in group 1 vs. 57 (95.0%) in group 2 ($p = 0.49$; Table 3). Twenty-eight (46.7%) and 33 (55.0%) patients were off AADs at the final follow-up in groups 1 and 2, respectively ($p = 0.46$).

No statistical difference was seen between mitral stenosis or regurgitation in terms of overall ATa recurrence, the number of procedures, and the type of ATa.

Complications

No major peri or postoperative complications are reported. One pseudo-aneurysm and two groin hematomas were observed in groups 1 and 2 groin hematomas in group 2. Of note, mitral valve entrapment was not observed in either group.

10.3389/fcvm.2022.928974

Discussion

In the present study, we evaluated the safety and long-term efficacy of AF catheter ablation after MV surgery in 60 patients across three experienced European centers. Our results highlight the following key findings: Catheter ablation for AF in patients with a history of MV surgery; (1) offers meaningful results with repeat procedures, similar to those seen in a matched population; (2) results in a higher rate of AT recurrence compared to control patients; and (3) has a favorable safety profile.

TABLE 2 Procedural characteristics ($n = 120$).

	Group 1 ($n = 60$)	Group 2 (control, $n = 60$)	*P*-value
Sinus rhythm at index procedure, *n* (%)	27 (45.0%)	43 (71.7%)	*0.003*
PVI only at index, *n* (%)	13 (21.7%)	29 (48.3%)	*0,004*
Substrate ablation at index			
Left atrium substrate	47	31	*0,003*
Right atrium substrate	7	1	*0,001*
Superior Vena Cava Isolation	7	1	*0,001*
Cavotricuspid Isthmus	11	2	*0,001*
Index procedure time, mean ± SD minutes	137.45 ± 30.2	134.45 ± 19.7	0.47
Index fluoroscopic time, mean ± SD minutes	8.1 ± 5.2	7.9 ± 3.9	0.72

PVI, Pulmonary vein isolation.

Arrhythmia recurrence

This study represents the longest follow-up study of its nature in patients with prior MV surgery, without concomitant surgical ablation, referred for first-time catheter ablation for AF.

After one ablation procedure, arrhythmia-free survival is modest in our cohort, with the majority of patients experiencing a recurrence of an ATa. Similar outcomes were seen in the control group; however, these results are also reflected by other studies of patients with prior MV surgery (Table 4). In a recent study by Chen et al., only 33% of patients with prior MV replacement were arrhythmia-free at 42.7 ± 17.3 months post-ablation (10). Similarly, Hussein et al. (8) describe an Ata-free rate of 44.2% over 24 months after index ablation (8). Better results were reported by Mountantonakis et al. (11) with 71%

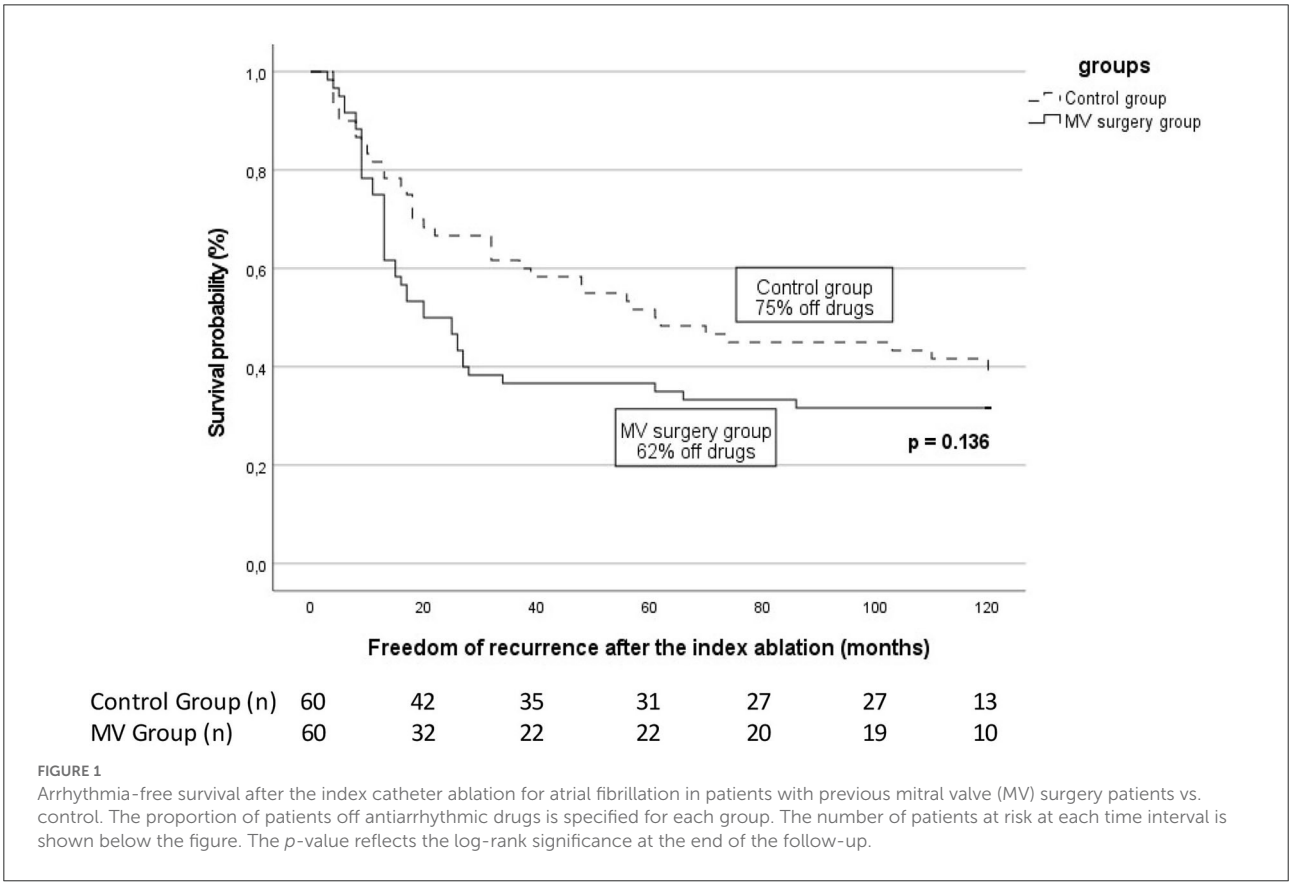

FIGURE 1
Arrhythmia-free survival after the index catheter ablation for atrial fibrillation in patients with previous mitral valve (MV) surgery patients vs. control. The proportion of patients off antiarrhythmic drugs is specified for each group. The number of patients at risk at each time interval is shown below the figure. The *p*-value reflects the log-rank significance at the end of the follow-up.

TABLE 3 Follow-up characteristics ($n = 120$).

	Group 1 ($n = 60$)	Group 2 (control, $n = 60$)	*P*-value
Free of arrhythmia after index procedure, *n* (%)	19 (31.7%)	24 (40.0%)	0.34
Free of arrhythmia and off-AAD after index procedure, *n* (%)	9 (15%)	18 (30%)	0.08
Free of arrhythmia after one repeat procedure, *n* (%)	48 (80.0%)	52 (86.7%)	0.46
Free of arrhythmia at end of follow-up, *n* (%)	54 (90.0%)	57 (95.0%)	0.49
Out of AAD after last procedure, *n* (%)	28 (46.6%)	33 (55.0%)	0.46
Without any recurrence, *n* (%)	9 (*32.1%*)	18 (*54.5%*)	0.22
Number of procedures per patient, median (Q1–Q3)	2 (2–2)	2 (2-2)	0.11
Atrial tachyarrhythmias recurrence, *n* (%)	41 (68.3%)	36 (60.0%)	0.45
Atrial fibrillation, *n* (%)	19 (*46.0%*)	28 (*78.0%*)	0.09
Atrial tachycardia	22 (*54.0%*)	8 (*22.0%*)	***0.03***
Time to first recurrence, median (Q1–Q3), *n* (%)	13 (9–17)	19 (8–22)	0.06
Major complication	0	0	0.91

AAD, Antiarrhythmic drugs.

of patients arrhythmia-free in a similar population, however, the follow-up duration was significantly shorter at only 7 ± 4 months (11) (Table 4).

While a single procedure appears to be insufficient to maintain sinus rhythm in these patients, after one repeat RF procedure, the rate of ATa freedom in our MV cohort increased to 80% (Figure 2) with 68.3% (41/60) of them undergoing a second procedure. Supporting these findings, high rates of repeat procedures have been described in similar population groups (6, 8).

Furthermore, at a median final follow-up of 62 (48–84) months, the long-term rate of sinus rhythm was high at 90%, with no difference seen with respect to the control group. These results suggest that, with repeat ablation, long-term outcomes similar to a control population are achievable in patients with prior MV surgery.

With regards to medium to long-term follow-up, conflicting reports exist in the literature, on smaller cohorts and/or shorter follow-ups (8, 12, 13). In a 2020 meta-analysis of 227 patients by Marazzato et al. (14) freedom from ATa at the end of follow-up was more modest at 49% after at least one repeat procedure with a significant decrease in arrhythmia-free survival seen after 2 years (14). While several studies in this meta-analysis included follow-up beyond 2 years, it also included studies of prior surgical ablation and those referred primarily for atrial

TABLE 4 Clinical characteristics and outcome of ablation from studies on populations with previous mitral valve surgery.

	Year	Number of patients (*n*)	Previous surgical ablation (*n*)	Follow-up (months)	Free of arrhythmia at end of follow-up	Off AAD (%)	Repeat procedure (%)	Recurrence after the index catheter ablation (%)	AT recurrence (%)
Enriquez et al. (6)	2017	67	33	12	62%	NA	42%	NA	NA
Santangeli et al. (7)	2012	178	NA	11.5 ± 8.6	NA	NA	NA	36%	NA
Hussein et al. (8)	2011	81	0	24	82.7%	69%	36%	NA	NA
Chen et al. (10)	2013	21	0	42.7 ± 17.3	33%	NA	43%	67%	43%
Mountantonakis et al. (11)	2011	21	12	7 ± 4	71%	43%	43%	43%	28%
Lang et al. (12)	2005	26	0	10	73%	NA	34%	50%	23%
Lakkireddy et al. (13)	2011	50	0	12	80%	NA	34%	NA	NA

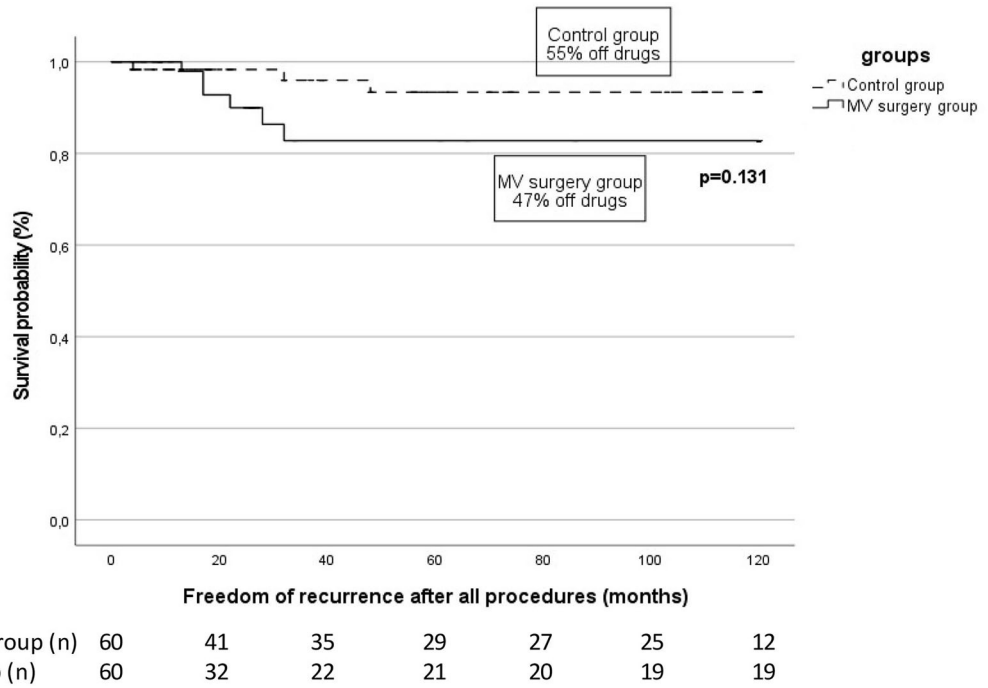

FIGURE 2
Arrhythmia-free survival in patients with previous mitral valve (MV) surgery patients vs. control at the end of follow-up after a median of 2 (2–2) catheter ablation. The proportion of patients off antiarrhythmic drugs is specified for each group. The number of patients at risk at each time interval is shown below the figure. The *p*-value reflects the Log-rank significance at the end of the follow-up.

tachycardia ablation, however, rendering direct comparison with the patients studied here difficult. Differences in reported post-ablation success rates in those with prior MV surgery may be explained by multiple factors including varying follow-up duration, multiple valve surgery, ablation technique, and post-ablation monitoring. Indeed, significant heterogeneity exists between the studies included in the meta-analysis mentioned above. The more favorable results seen at long-term follow-up in our study may reflect advances in current ablation and mapping technology.

At the end of the follow-up period, approximately 50% of patients in each group were off AADs. These ratios are comparable to previously published data from Mountantonakis et al. (8) and Hussein et al. (11) with patients off drugs at 43 and 69.1%, respectively (8, 11). Furthermore, without AADs, only a small proportion of the patients studied here remained free from any recurrence of atrial arrhythmia throughout follow-up. This highlights the complementary role of AADs and repeats ablation in the long-term maintenance of sinus rhythm in this patient cohort.

Recurrence mechanisms

We report a higher rate of atrial tachycardia (AT) recurrence in the patients who underwent surgery in our cohort. This phenomenon could be explained by several mechanisms. On the one hand, valve surgery itself can contribute to slow conduction zones facilitating the appearance of re-entry circuits (15) with the type of surgical incision previously described as predictive of the development of atrial tachycardia on follow-up (16). In addition, it is well established that multiple valve surgery and coronary bypass patients, as is the case in our cohort, are associated with a higher incidence of arrhythmia (15, 16). Atrial scar and fibrosis, slow conduction zones, or incomplete lines of previous ablation procedures may also play a role in the development of AT recurrences (6). While right atrial macro re-entry circuits appear to predominate in patients undergoing first-time ablation for AT post-MV surgery, LA ATs have been more commonly described in those who have undergone concomitant surgical ablation, and become more frequent after the index catheter ablation procedure (6). Accordingly, previous studies report that the predominant mechanism for AT recurrence in patients post-MV surgery was macro re-entry in 75–99%, mostly originating from the LA in 63–100% (14, 17, 18). These observations are comparable to ours and highlight the role of LA substrate in ATa recurrence after index catheter ablation in patients with a history of MV surgery. In contrast, AF recurrences in this population may relate less to the prior surgical procedure and rather reflect the progression of an advanced atrial arrhythmia substrate secondary to the hemodynamic consequences of the valvular lesion. This point is highlighted by the authors of the 2020 meta-analysis outlined above as a probable explanation for the relationship between

AF recurrences and follow-up duration (14). The high rate of sinus rhythm at the end of follow-up in this study may underscore the importance of adjunct atrial substrate ablation in this population.

Safety

Prior safety concerns regarding catheter ablation of atrial arrhythmia in patients post-MV surgery surround the risk of damage to the prosthetic valve (19, 20) and thromboembolic events (7, 13). In this study, we report no major complications relating to ablation. In patients with a history of MV surgery and in particular with valve prostheses, catheter maneuvering may be challenging due to the presence of atrial remodeling, scarring, and the prosthesis itself. This is reflected in frequently reported increased procedural as was the case in our study. Nevertheless, with attention, the risk of valve damage appears to be low as we report no mechanical valve entrapment or post-procedural malfunction. In addition, the maintenance of periprocedural therapeutic warfarin has been reported to mitigate the increased risk of thromboembolic events (7, 13). Our findings are supported by several studies emphasizing the safety of catheter ablation in this cohort (8, 11, 14) with no difference in complication rates between those with prior MV surgery and matched controls. While Lang et al. (12) reported more procedure-related complications among patients with MV prostheses, these did not include valvular damage or thromboembolism (12).

Clinical implications

Our study suggests that patients with symptomatic AF and a history of severe mitral valve disease requiring valvular surgery derive a potential long-term benefit from catheter ablation. Despite the need for repeat ablation procedures in most patients and the continuation of AADs in approximately half of our cohort, the results seen here were similar to a group of matched control patients, suggesting that this treatment strategy is of similar value in both cohorts. The ongoing use of AADs appears to be complimentary to repeat ablation in maintaining sinus rhythm and freedom from symptoms, and the continuation of these should not be viewed as a treatment failure in this group.

Limitations

This is a non-randomized retrospective observational study with a sample of heterogeneous patients, including the type of MV surgery (repair or replacement) but also the physiopathology of the MV disease itself: rheumastismal and degenerative MV regurgitation propensity scores are performed to reduce the heterogeneity bias and improve the power of the analysis in retrospective studies. Nevertheless, this statistical technique is limited by nature, as only few factors can be matched, and the analysis depends on the available database. Thus, the *p*-value in Kaplan–Meier curves can be only a reflection of the low power of the study. Also, ATa recurrences were assessed by ECG rather than continuous monitoring, thus, the overall success rate may have been overestimated. Moreover, performing ablation on an operated heart, especially on the MV, is challenging and could lead to an incomplete ablation and, thus, considered a cause of the recurrence of ATa. Furthermore, due to its retrospective design, no quality of life assessment was performed during this study preventing to draw off any conclusion regarding the symptoms. In the index procedure, the PVI-only rate between groups is different, this could have impacted the final result regarding the ATa freedom, but this parameter is comparable between groups at the end of the follow-up. Whether the PVI-only strategy plays a role in the type of recurrence (AF vs. AT) is highly speculative as the number of patients would be limited to draw a powerful conclusion. In addition, over the long period covered by this study, a lot of changes in the guidelines and improvements occurred not only from a technological point of view (3D map, ContactForce, irrigation, and power control) but also technically (Ablation Index and Close protocol), this could have impacted the results of ATa freedom on the long run. Finally, this study was performed in experienced centers with strict patient selection making the results entrusted exclusively to experienced teams.

Conclusion

In this long-term follow-up study, freedom from atrial arrhythmias after catheter ablation for atrial fibrillation is achievable and safe in patients with a history of mitral valve surgery. With repeated procedures and the use of antiarrhythmic drugs, high rates of sinus rhythm can be achieved in the long term, emphasizing the value of this treatment strategy in this cohort.

Data availability statement

The raw data supporting the conclusions of this article will be made available by the authors, without undue reservation.

Ethics statement

The studies involving human participants were reviewed and approved by Univeristeit Ziekenhuis Brussel Ethics Committee.

The patients/participants provided their written informed consent to participate in this study.

Author contributions

All authors listed have made a substantial, direct, and intellectual contribution to the work and approved it for publication.

Conflict of interest

The authors declare that the research was conducted in the absence of any commercial or financial relationships that could be construed as a potential conflict of interest.

Publisher's note

Supplementary material

The Supplementary Material for this article can be found online at: https://www.frontiersin.org/articles/10.3389/fcvm.2022.928974/full#supplementary-material

References

1. Darby AE, Di Marco JP. Management of atrial fibrillation in patients with structural heart disease. *Circulation.* (2012) 125:945–57. doi: 10.1161/CIRCULATIONAHA.111.019935

2. Pande S, Agarwal SK, Mohanty S, Bansal A. Effect of mitral valve replacement on reduction of left atrial size. *Asian Cardiovasc Thorac Ann.* (2013) 21:288–92. doi: 10.1177/0218492312453142

3. Gillinov AM, Gelijns AC, Parides MK, DeRose JJ, Moskowitz AJ, Voisine P, et al. Surgical ablation of atrial fibrillation during mitral-valve surgery. *N Engl J Med.* (2015) 372:1399–409. doi: 10.1056/NEJMoa1500528

4. Bramer S, Van Straten AHM, Soliman Hamad MA, Van Den Broek KC, Maessen JG, Berreklouw E. New-onset postoperative atrial fibrillation predicts late mortality after mitral valve surgery. *Ann Thorac Surg.* (2011) 92:2091–6. doi: 10.1016/j.athoracsur.2011.06.079

5. Jovin A, Oprea DA, Jovin IS, Hashim SW, Clancy JF. Atrial fibrillation and mitral valve repair. *Pacing Clin Electrophysiol.* (2008) 31:1057–63. doi: 10.1111/j.1540-8159.2008.01135.x

6. Enriquez A, Santangeli P, Zado ES, Liang J, Castro S, Garcia FC, et al. Postoperative atrial tachycardias after mitral valve surgery: mechanisms and outcomes of catheter ablation. *Heart Rhythm.* (2017) 14:520–6. doi: 10.1016/j.hrthm.2016.12.002

7. Santangeli P, Di Biase L, Bai R, Horton R, David Burkhardt J, Sanchez J, et al. Advances in catheter ablation: atrial fibrillation ablation in patients with a mitral mechanical prosthetic valve. *Curr Cardiol Rev.* (2012) 8:362–7. doi: 10.2174/157340312803760767

8. Hussein AA, Wazni OM, Harb S, Joseph L, Chamsi-Pasha M, Bhargava M, et al. Radiofrequency ablation of atrial fibrillation in patients with mechanical mitral valve prostheses safety, feasibility, electrophysiologic findings, and outcomes. *J Am Coll Cardiol.* (2011) 58:596–602. doi: 10.1016/j.jacc.2011.03.039

9. Calkins H, Hindricks G, Cappato R, Kim YHH, Saad EB, Aguinaga L, et al. *2017 HRS/EHRA/ECAS/APHRS/SOLAECE Expert Consensus Statement on Catheter and Surgical Ablation of Atrial Fibrillation: Executive Summary.* (2017). Available online at: http://www.ncbi.nlm.nih.gov/pubmed/29021841 (accessed March 8, 2019).

10. Chen H, Yang B, Ju W, Zhang F, Gu K, Li M, et al. Long-term outcome following ablation of atrial tachycardias occurring after mitral valve replacement in patients with rheumatic heart disease. *Pacing Clin Electrophysiol.* (2013) 36:795–802. doi: 10.1111/pace.12153

11. Mountantonakis S, Frankel DS, Hutchinson MD, Dixit S, Riley M, Callans DJ, et al. Feasibility of catheter ablation of mitral annular flutter in patients with prior mitral valve surgery. *Heart Rhythm.* (2011) 8:809–14. doi: 10.1016/j.hrthm.2011.01.019

12. Lang CC, Santinelli V, Augello G, Ferro A, Gugliotta F, Gulletta S, et al. Transcatheter radiofrequency ablation of atrial fibrillation in patients with mitral valve prostheses and enlarged atria: safety, feasibility, and efficacy. *J Am Coll Cardiol.* (2005) 45:868–72. doi: 10.1016/j.jacc.2004.11.057

13. Lakkireddy D, Nagarajan D, Di Biase L, Vanga SR, Mahapatra S, Jared Bunch T, et al. Radiofrequency ablation of atrial fibrillation in patients with mitral or aortic mechanical prosthetic valves: a feasibility, safety, and efficacy study. *Heart Rhythm.* (2011) 8:975–80. doi: 10.1016/j.hrthm.2011.02.012

14. Marazzato J, Cappabianca G, Angeli F, Crippa M, Golino M, Ferrarese S, et al. Catheter ablation of atrial tachycardias after mitral valve surgery: A systematic review and meta-analysis. *J Cardiovasc Electrophysiol.* (2020) 31:2632–41. doi: 10.1111/jce.14666

15. Nielsen JC, Lin YJ, De Oliveira Figueiredo MJ, Sepehri Shamloo A, Alfie A, Boveda S, et al. European Heart Rhythm Association (EHRA)/Heart Rhythm Society (HRS)/Asia Pacific Heart Rhythm Society (APHRS)/Latin American Heart Rhythm Society (LAHRS) expert consensus on risk assessment in cardiac arrhythmias: use the right tool for the right outcome, in the right population. *J Arrhythmia.* (2020) 36:553–607. doi: 10.1002/joa3.12338

16. Kernis SJ, Nkomo VT, Messika-Zeitoun D, Gersh BJ, Sundt TM, Ballman KV, et al. Atrial fibrillation after surgical correction of mitral regurgitation in sinus rhythm: incidence, outcome, and determinants. *Circulation.* (2004) 110:2320–5. doi: 10.1161/01.CIR.0000145121.25259.54

17. Huo Y, Schoenbauer R, Richter S, Rolf S, Sommer P, Arya A, et al. Atrial arrhythmias following surgical AF ablation: electrophysiological findings, ablation strategies, and clinical outcome. *J Cardiovasc Electrophysiol.* (2014) 25:725–38. doi: 10.1111/jce.12406

18. Trumello C, Pozzoli A, Mazzone P, Nascimbene S, Bignami E, Cireddu M, et al. Electrophysiological findings and long-term outcomes of percutaneous ablation of atrial arrhythmias after surgical ablation for atrial fibrillation. *Eur J Cardiothorac Surg.* (2016) 49:273–80. doi: 10.1093/ejcts/ezv034

19. Bridgewater BJM, Levy RD, Hooper TL. Mitral valve prosthesis disk embolization during transeptal atrioventricular junction ablation. *J Interv Cardiol.* (1994) 7:535–7. doi: 10.1111/j.1540-8183.1994.tb00493.x

20. Kesek M, Englund A, Jensen SM, Jensen-Urstad M. Entrapment of circular mapping catheter in the mitral valve. *Heart Rhythm.* (2007) 4:17–9. doi: 10.1016/j.hrthm.2006.09.016

frontiers | Frontiers in Cardiovascular Medicine

TYPE Original Research
PUBLISHED 06 January 2023
DOI 10.3389/fcvm.2022.1050744

OPEN ACCESS

EDITED BY
Mien-Cheng Chen,
Kaohsiung Chang Gung Memorial Hospital, Taiwan

REVIEWED BY
Hwan-Cheol Park,
Hanyang University Guri Hospital, Republic of Korea
Yung-Hsin Yeh,
Linkou Chang Gung Memorial Hospital, Taiwan

*CORRESPONDENCE
Boyoung Joung
✉ cby6908@yuhs.ac
Pil-Sung Yang
✉ psyang01@cha.ac.kr

†These authors have contributed equally to this work

‡These authors share senior authorship

SPECIALTY SECTION
This article was submitted to Cardiac Rhythmology, a section of the journal Frontiers in Cardiovascular Medicine

RECEIVED 22 September 2022
ACCEPTED 12 December 2022
PUBLISHED 06 January 2023

CITATION
Yu G-I, Kim D, Sung J-H, Jang E, Yu HT, Kim T-H, Pak H-N, Lee M-H, Lip GYH, Yang P-S and Joung B (2023) Impact of frailty on early rhythm control outcomes in older adults with atrial fibrillation: A nationwide cohort study. *Front. Cardiovasc. Med.* 9:1050744. doi: 10.3389/fcvm.2022.1050744

Impact of frailty on early rhythm control outcomes in older adults with atrial fibrillation: A nationwide cohort study

Ga-In Yu[1†], Daehoon Kim[1†], Jung-Hoon Sung[2], Eunsun Jang[1], Hee Tae Yu[1], Tae-Hoon Kim[1], Hui-Nam Pak[1], Moon-Hyoung Lee[1], Gregory Y. H. Lip[3], Pil-Sung Yang[2*‡] and Boyoung Joung[1*‡]

[1]Division of Cardiology, Department of Internal Medicine, Yonsei University College of Medicine, Seoul, Republic of Korea, [2]Division of Cardiology, CHA Bundang Medical Center, CHA University, Seongnam, Republic of Korea, [3]Liverpool Centre for Cardiovascular Science, University of Liverpool and Liverpool Heart & Chest Hospital, Liverpool, United Kingdom

Purpose: Rhythm-control therapy administered early following the initial diagnosis of atrial fibrillation (AF) has superior cardiovascular outcomes compared to rate-control therapy. Frailty is a key factor in identifying older patients' potential for improvement after rhythm-control therapy. This study evaluated whether frailty affects the outcome of early rhythm-control therapy in older patients with AF.

Methods: From the Korean National Health Insurance Service database (2005–2015), we collected 20,611 populations aged ≥65 years undergoing rhythm- or rate-control therapy initiated within 1 year of AF diagnosis. Participants were emulated by the EAST-AFNET4 trial, and stratified into non-frail, moderately frail, and highly frail groups based on the hospital frailty risk score (HFRS). A composite outcome of cardiovascular-related mortality, myocardial infarction, hospitalization for heart failure, and ischemic stroke was compared between rhythm- and rate-control.

Results: Early rhythm-control strategy showed a 14% lower risk of the primary composite outcome in the non-frail group [weighted incidence 7.3 vs. 8.6 per 100 person-years; hazard ratio (HR) 0.86, 95% confidence interval (CI) 0.79–0.93, $p < 0.001$] than rate-control strategy. A consistent trend toward a lower risk of early rhythm-control was observed in the moderately frail (HR 0.91, 95% CI 0.81–1.02, $p = 0.09$) and highly frail (HR 0.93, 95% CI 0.75–1.17, $p = 0.55$) groups.

Conclusion: Although the degree attenuated with increasing frailty, the superiority of cardiovascular outcomes of early rhythm-control in AF treatment was maintained without increased risk for safety outcomes. An individualized approach is required on the benefits of early rhythm-control therapy in older patients with AF, regardless of their frailty status.

KEYWORDS

atrial fibrillation, rhythm-control, rate-control, frailty, older adults

Introduction

Atrial fibrillation (AF) has the highest proportion among persistent arrhythmias, and its prevalence increases with aging (1, 2). It can be related with ischemic stroke, hospitalization, heart failure (HF), as well as cognitive dysfunction, depression, and impaired quality of life. It ultimately increases mortality (3, 4). Many major clinical studies have been conducted to compare rate-control and rhythm-control treatment strategy in AF treatment (5–8). The results have shown the superiority of rhythm-control, strengthened by recent studies on the development of newer medications and advances in ablation capable of overcoming the limitations of the initial rhythm-control strategies (9). Additionally, it has been shown that these reference trial results are equally reflected in real world observational data (10). However, the outcome of rhythm-control for older patients is still controversial. In an analysis of the AFFIRM trial for ages between 70 and 80 years, rate-control therapy had lower mortality and hospitalization rates than rhythm-control therapy (11). However, a study showed that active rhythm-control with ablation is advantageous in the older population (12).

Frailty refers to a condition in which the physiological system that copes with external stress weakens and becomes functionally vulnerable with increasing age. It has a significant impact on medical outcomes of the older population (13), and has been found to be an important factor in predicting older patients' potential for improvement after catheter ablation (14, 15). Therefore, the assessment of frailty plays a meaningful role in generating management plans for older patients (16). The method of measuring frailty is systematic and sufficiently objective, and validation has already been made through the results of studies on older population in various countries (17–19).

The results of studies on rhythm-control in compared to rate-control the older AF population have been mostly associated with age. However, the effects of variables apart from age have been insufficiently studied. In this study, the effect of frailty on the results of early rhythm-control compared to rate-control therapy in the older AF population was evaluated.

Materials and methods

The present study is a retrospective observational cohort analyses based on the National Health Claims Database (NHIS-2016-4-009) provided by the National Health Insurance Service (NHIS) of Republic of Korea. The start of the observation period was 1 January 2005. The NHIS is the single insurer managed by the Korean Government, with the majority (97.1%) of Korean citizens as mandatory subscribers, and the remaining (3%) under the Medical Aid program. As the NHIS database contains the information of Medical Aid users as well, it is essentially based on the entire Korean population (4, 20–23). The data can be accessed through the National Health Insurance Data Sharing Service homepage.[1]

This study was approved by the Institutional Review Board of the Yonsei University Health System (4-2016-0179), and following strict confidentiality guidelines, personally identifiable information was removed after the cohort was created, and it was therefore exempt from prior consent requirements. Applications to use the NHIS data will be reviewed by the inquiry committee of research support and, once approved, raw data will be provided to the authorized researcher with a fee at several permitted sites. Through this study, we attempted to closely emulate the protocol of the EAST-AFNET4 trial, as summarized in **Table 1**.

Study population

This observational cohort study evaluated whether the degree of frailty affects the outcome of rhythm- and rate-control therapies in older AF populations. AF was defined based on the cases registered with the National Health Claims Database as International Classification of Diseases 10th Revised Edition (ICD-10) code I48, and the time of initial diagnosis was judged to be the time when the code was first registered. The code I48 registration was only possible when AF was documented in electrocardiogram (ECG). The reliability of

1 http://nhiss.nhis.or.kr

TABLE 1 Summary of strategies for emulating target trial.

Components	Target trial (EAST-AFNET4)	This study
Inclusion period	28 July 2011 – 30 December 2016	1 January 2005 – 31 December 2015
Eligibility criteria	1) Adults (≥18 years of age) who were older than 75 years of age, had had a previous transient ischemic attack or stroke, or met two of the following criteria: age greater than 65 years, female sex, heart failure, hypertension, diabetes mellitus, severe coronary artery disease, chronic kidney disease, and left ventricular hypertrophy 2) Early AF (diagnosed ≤12 months before enrollment)	1) Selected older adults (≥65 years of age) that received a rhythm-control or rate-control treatments and have no prior history of prescriptions and no records of ablation in the database who were older than 75 years of age, had a previous transient ischemic attack or stroke, or met two of the following criteria: age greater than 65 years, female sex, heart failure, hypertension, diabetes mellitus, myocardial infarction, and chronic kidney disease 2) Early AF (defined as AF diagnosed ≤12 months before enrollment) 3) Undergoing oral anticoagulation (>90 days of supply within 180 days after their first recorded prescription of rhythm- or rate-control medications or ablation procedure)
Exposed group	Rhythm control: antiarrhythmic drugs, AF ablation, cardioversion of persistent AF, to be initiated early after randomization	Rhythm control: a prescription of more than a 90-day supply of any antiarrhythmic drugs in the 180-day period since the first prescription or the performance of an ablation procedure for AF.
Unexposed group	Usual care: initially treated with rate-control therapy without rhythm-control therapy	Rate control: a prescription of more than a 90-day supply of any rate-control drugs in the 180-day period since the first prescription and with no prescription of rhythm-control drug and no ablation within this period. Patients prescribed rhythm-control drugs for more than 90 days or who underwent ablation within the 180-day period since the initiation of rate-control drugs were classified as intention-to-treat with rhythm control.
Primary outcome	1) A composite of death from cardiovascular causes, stroke, or hospitalization with worsening of heart failure or acute coronary syndrome 2) The number of nights spent in the hospital per year.	1) A composite of death from cardiovascular causes, ischemic stroke, hospitalization for heart failure, or acute myocardial infarction 2) The number of nights spent in the hospital per year.
Secondary outcome	Each component of the primary outcome, rhythm, left ventricular function, quality of life, AF-related symptom	Each component of the primary outcome
Safety outcome	A composite of death from any cause, stroke, or pre-specified serious adverse events of special interest capturing complications of rhythm-control therapy	A composite of death from any cause, intracranial or gastrointestinal bleeding requiring hospitalization, or pre-specified serious adverse events of special interest capturing complications of rhythm control
Follow-up	From randomization until the end of the trial, death, or withdrawal from the trial.	From 180 days after their first recorded prescription or procedure to avoid immortal time bias until the end of follow-up of the database (31 December 2016) or death.

AF diagnosis using this method in the NHIS database was verified as a positive predictive value of 94.1% in a previous study (22).

We designed this study based on the criteria of the EAST-AFNET 4 trial, which has been approved for the study of AF early rhythm control (9). We collected AF populations above 65 years of age with a medical history of an ischemic stroke or transient ischemic attack, or ones that met the following standards: female, with the presence of any of the related medical history (hypertensive disorders, diabetes, chronic renal disease, HF, or previous myocardial infarction) between 1 January 2005 and 31 December 2015 (details of inclusion and exclusion standards are described in **Table 1**).

Patients underwent rhythm-control or rate-control treatments according to a new-user and intention-to-treat design. A "new-user" was defined as a patient with no previous record of prescription or treatment during the observation period, while "intention-to-treat-with-rhythm-control" was defined as a patient prescribed with rhythm control drugs for 90 days within 180 days from the first prescription after AF diagnosis, or the first prescription after AF procedure. In the case of patients who underwent ablation, the intention-to-treat-with-rhythm-control group was considered only if the procedure was carried out within 180 days after the initial diagnosis of AF. Conversely, "intention-to-treat-with-rate-control" was defined as having been prescribed a rate-control drug for 90 days within 180 days from the first prescription after AF diagnosis, and not receiving any rhythm-control drug prescriptions or ablation within this period. Definitions and ICD-10 codes used for defining rhythm- and rate- control drugs treatments and procedures for AF are presented in **Supplementary Table 1**.

The present study excluded the following: (1) patients who had not been prescribed anticoagulants (warfarin or direct oral anti-coagulant) for 90 days or more within 180 days of starting (rhythm-control or rate-control) drugs therapy or receiving

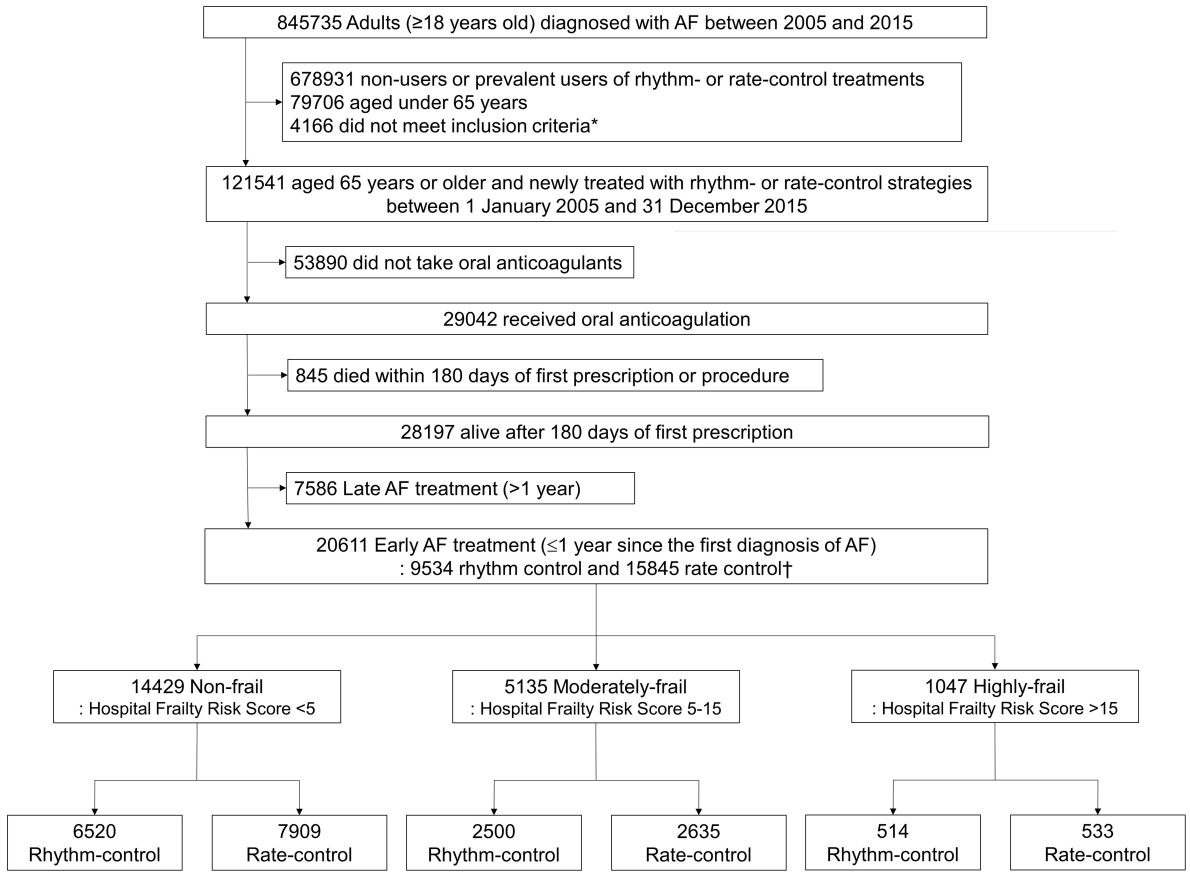

FIGURE 1
Flowchart of enrollment and analysis of the study population. AF, atrial fibrillation. *AF populations above 65 years of age with a medical history of an ischemic stroke or transient ischemic attack, or ones that met the following standards: female, with the presence of any of the related medical history (hypertensive disorders, diabetes, chronic renal disease, heart failure, or previous myocardial infarction).

ablation for AF, and (2) those who died within 180 days of starting drugs therapy or undergoing ablation (**Figure 1**).

This study assessed the frailty of individual patients using hospital frailty risk score (HFRS) based on administrative data (18). The HFRS has been validated using data from Canada, the UK, and Korea; therefore, it is a reliable and objective indicator (17, 19, 24). The HFRS for each patient was estimated using ICD-10 codes registered before 180 days from the first prescription date after AF diagnosis. The ICD-10 code-based HFRS is a scoring method based on the selection of 109 diagnostic ICD codes related to frailty, assigning a specific value proportional to how strongly it was reflected for each code (17). The variables and their corresponding ICD codes are described in **Supplementary Table 2**.

We classified the enrolled populations into three levels of frailty groups according to the calculated HFRSs. Populations were divided into the non-frail (low-risk) (<5), moderately frail (5–15), and highly frail (>15) groups with reference to previously reported cut-off points (17). The interaction tests were performed among three groups.

Outcomes and covariates

Outcomes and covariates were obtained from the Korea NHIS data. To avoid immortal time bias, the investigation of clinical outcomes was begun 180 days after the first prescription or first ablation post AF diagnosis, and the observation ended (31 December 2016) according to the protocol or with the death of the participant. The types and definitions of AF procedures and the corresponding ICD-10 codes are summarized in **Supplementary Table 1** in detail. The endpoint of the study also followed the EAST-AFNET 4 trial with evidence (9).

The primary outcome was a composite of ischemic stroke, acute myocardial infarction, hospitalization for HF, and cardiovascular mortality. Additionally, the number of days in hospital per year during each patient's individual follow-up period was also identified and calculated. The safety outcome was a composite of all-cause death, major bleeding (intracranial or gastrointestinal bleeding), and critical adverse events associated with rhythm-control (complications related to ablation such as cardiac tamponade, and the development

of bradyarrhythmia related to antiarrhythmic drugs). The definition of study outcomes and the ICD codes corresponding to each element are detailed in **Supplementary Table 3**.

Statistical analysis

Descriptive statistics were employed to analyze the baseline characteristics of participants. In order to eliminate bias between the rhythm- and rate-control groups, propensity score overlap weighting was performed on the baseline characteristics (25). Propensity scores for the probability of receiving rhythm-control were estimated by logistic regression based on demographics, time since diagnosis of AF, year of treatment initiation, level of care at which the initial prescription was provided, clinical risk scores, medical history, and concurrent medication use (variables in **Supplementary Table 4**). We estimated the balance between enrolled patients by standardized differences of every qualitative and quantitative covariates using a threshold of 0.1 to manifest imbalance (26). The distribution of propensity scores before and after overlap weighting is shown in **Supplementary Figure 1**. We did subgroup analyses for the primary composite outcome stratified by sex, age, HF, chronic kidney disease, and ischemic stroke. Interaction tests were done for all subgroups. We used the test variable from the weighting procedure to recreate the overlap weighting.

The weighted incidence rates of clinical outcomes were evaluated by dividing the weighted number of events by 100 person-years at risk, with a 95% confidence interval (CI). The significance of the difference in outcome between the rhythm-control group and the rate-control group was confirmed using the log-rank test, and the results were expressed through failure curves. Fine and Gray competing risk regression with time-varying covariates was used to estimate the relative hazards of all-cause mortality as a main outcome (27). The proportional hazards assumption was checked using the Schoenfeld residual test (28).

Cox models were stratified on frailty score, with treatment as the exposure. Cox proportional hazards model for the total weighted study population was used to evaluate whether the degree of frailty (non-frailty, moderately frailty, or highly frailty) affects the primary composite outcome and safety outcome of the early AF treatment strategy (rhythm-control vs. rate-control). The balance of baseline characteristics before and after propensity overlap weighting in the overall study population is summarized in **Supplementary Table 5**.

A two-sided p-value < 0.05 was judged to be objectively significant. All statistical work was performed with the R version 4.1.2 (The R Foundation[2], Vienna, Austria) and the SAS version 9.4 (SAS Institute, Cary, NC, USA).

2 www.R-project.org

Sensitivity analyses

Sensitivity analysis was carried out according to the on-treatment principle, by censoring treatments for patients who dropped out mid-therapy or switched strategies between rhythm- and rate-control. Time-varying regression was performed considering a time-dependent variable for the switch between treatments. The above analytical process is schematically represented in **Supplementary Figure 2**. Next, we performed one-to-one propensity score matching test without replacement with a caliper of 0.01. The balance of baseline characteristics after propensity score matching is summarized in **Supplementary Table 6**. We evaluated the association between intention-to-treat with rhythm control, which was defined as the performance of a cardioversion for AF as well as the use of antiarrhythmic drug or ablation, and cardiovascular outcomes. We defined the treatment strategies of rhythm or rate control as a prescription for more than a 20-day supply of the drugs in the 30-day period since the first prescription, instead of the 180-day period in the main analyses. Follow-up began 30 days after the first recorded prescription or procedure to avoid immortal time bias. Any systematic bias in the present study was excluded by using falsification analysis with 30 pre-specified falsification endpoints with a true hazard ratio (HR) of 1 (29). The component and their corresponding ICD codes for falsification endpoints are described in **Supplementary Table 7**.

Results

A total of 20,611 patients aged ≥65 years [median 73, interquartile range (IR) 69–78] at an early stage of AF diagnosis (within 1 year) were included (**Figure 1**). Before propensity overlap weighting, compared with those in the rate-control group, populations in the rhythm-control group were younger, mostly female, had a higher income, and more comorbidities, irrespective of frailty risk (**Supplementary Table 4**). After propensity overlap weighting, the baseline characteristics were well balanced between the rhythm-control and rate-control groups (**Table 2**). The small sized hospital showed a preference for rate-control approach independent of frailty status (**Supplementary Table 4**). The distribution of HFRS in the population recently diagnosed with AF receiving rhythm-control or rate-control strategies is presented in **Figure 2**. In rhythm-control therapy, class III antiarrhythmic drug, amiodarone, had the highest proportion (40% in the non-frail, 47.1% in the moderately frail, and 53.1% in the highly frail groups), followed by the class Ic antiarrhythmic drugs (**Figure 3**). Ablation strategy was performed as an initial treatment in 1.5, 1.2, and 0.2% of the patients in the non-frail, moderately frail, and highly frail groups, respectively, and as a final therapy during the entire study period in 5.4, 3.2, and 0.4% of the patients in each group, respectively (**Figure 3**).

TABLE 2 Baseline characteristics before overlap weighting.

	Non-frail (*n* = 14,429)			Moderately frail (*n* = 5,135)			Highly frail (*n* = 1,047)		
Variables	Rhythm control (*n* = 6,520)	Rate control (*n* = 7,909)	ASD (%)	Rhythm control (*n* = 2,500)	Rate control (*n* = 2,635)	ASD (%)	Rhythm control (*n* = 514)	Rate control (*n* = 533)	ASD (%)
Age (years)	72 (68–76)	73 (69–78)	23.9	74 (70–79)	75 (71–80)	18.6	76 (71–81)	77 (72–83)	18.8
65–74	4,349 (66.7)	4,548 (57.5)	19.0	1,314 (52.6)	1,166 (44.3)	16.7	215 (41.8)	194 (36.4)	11.1
≥75	2,171 (33.3)	3,361 (42.5)	19.0	1,186 (47.4)	1,469 (55.7)	16.7	299 (58.2)	339 (63.6)	11.1
Male	1,776 (49.5)	1,827 (51.6)	7.5	1,121 (44.8)	1,247 (47.3)	5.0	187 (36.4)	234 (43.9)	15.4
AF duration (months)	0.1 (0.0–1.2)	0.0 (0.0–0.0)	30.5	0.0 (0.0–1.2)	0.0 (0.0–0.2)	22.9	0.0 (0.0–1.3)	0.0 (0.0–1.0)	1.9
Enrollment year:									
2005	353 (5.4)	1,078 (13.6)	28.3	65 (2.6)	146 (5.5)	14.9	7 (1.4)	18 (3.4)	13.3
2006	374 (5.7)	841 (10.6)	17.9	83 (3.3)	157 (6.0)	12.6	8 (1.6)	21 (3.9)	14.6
2007	351 (5.4)	632 (8.0)	10.5	92 (3.7)	146 (5.5)	8.9	13 (2.5)	16 (3.0)	2.9
2008	339 (5.2)	628 (7.9)	11.1	106 (4.2)	193 (7.3)	13.2	13 (2.5)	30 (5.6)	15.7
2009	378 (5.8)	555 (7.0)	5.0	122 (4.9)	133 (5.0)	0.8	22 (4.3)	29 (5.4)	5.4
2010	454 (7.0)	526 (6.7)	1.2	166 (6.6)	189 (7.2)	2.1	29 (5.6)	38 (7.1)	6.1
2011	569 (8.7)	539 (6.8)	7.1	212 (8.5)	230 (8.7)	0.9	42 (8.2)	39 (7.3)	3.2
2012	655 (10.0)	615 (7.8)	8.0	242 (9.7)	261 (9.9)	0.8	55 (10.7)	47 (8.8)	6.3
2013	800 (12.3)	739 (9.3)	9.4	369 (14.8)	320 (12.1)	7.7	78 (15.2)	79 (14.8)	1.0
2014	937 (14.4)	731 (9.2)	15.9	426 (17.0)	348 (13.2)	10.7	112 (21.8)	76 (14.3)	19.7
2015	1,310 (20.1)	1,025 (13.0)	19.3	617 (24.7)	512 (19.4)	12.7	135 (26.3)	140 (26.3)	<0.1
High tertile of income	3,419 (52.4)	3,168 (40.1)	25.0	1,219 (48.8)	1,164 (44.2)	9.2	256 (49.8)	263 (49.3)	0.9
Number of OPD visits ≥12/year	5,813 (89.2)	6,313 (79.8)	26.0	2,174 (87.0)	1,964 (74.5)	31.9	387 (75.3)	346 (64.9)	22.8
Living in metropolitan areas	3,230 (49.5)	3,284 (41.5)	16.2	1,097 (43.9)	994 (37.7)	12.6	203 (39.5)	196 (36.8)	5.6
Level of care initiating treatment									
Tertiary	4,019 (61.6)	3,120 (39.4)	45.5	1,348 (53.9)	1,030 (39.1)	30.1	257 (50.0)	176 (33.0)	35.0
Secondary	2,199 (33.7)	3,899 (49.3)	32.0	1,104 (44.2)	1,489 (56.5)	24.9	251 (48.8)	338 (63.4)	29.7
Primary	302 (4.6)	890 (11.3)	24.7	48 (1.9)	116 (4.4)	14.2	6 (1.2)	19 (3.6)	15.8
CHA_2DS_2-VASc score	4 (3–5)	4 (3–5)	15.2	5 (4–6)	5 (4–6)	20.7	6 (5–7)	6 (5–7)	33.3
mHAS-BLED score*	3 (2–3)	2 (2–3)	38.8	3 (3–4)	3 (2–4)	34.7	4 (3–4)	3 (3–4)	37.4
Charlson comorbidity index	3 (2–5)	2 (1–4)	53.4	5 (3–7)	4 (2–6)	49.1	7 (5–9)	6 (4–8)	44.9
Hospital frailty risk score	0.8 (0.0–2.5)	0.0 (0.0–2.2)	13.1	8.0 (6.2–10.3)	8.0 (6.2–10.4)	1.2	19.0 (16.8–23.2)	19.0 (16.6–23.1)	3.0
Medical history									
Heart failure	2,761 (42.3)	4,049 (51.2)	17.8	1,331 (53.2)	1,276 (48.4)	9.6	315 (61.3)	256 (48.0)	26.9
Previous hospitalization for heart failure	705 (10.8)	1,288 (16.3)	16.0	427 (17.1)	397 (15.1)	5.5	106 (20.6)	65 (12.2)	22.9
Hypertension	5,432 (83.3)	4,945 (62.5)	48.1	2,187 (87.5)	1,821 (69.1)	45.7	476 (92.6)	410 (76.9)	44.7
Diabetes	1,700 (26.1)	1,553 (19.6)	15.4	929 (37.2)	744 (28.2)	19.1	246 (47.9)	199 (37.3)	21.4
Dyslipidaemia	5,234 (80.3)	4,493 (56.8)	52.2	2,183 (87.3)	1,945 (73.8)	34.6	465 (90.5)	449 (84.2)	18.8

(Continued)

TABLE 2 (Continued)

Variables	Non-frail (*n* = 14,429)			Moderately frail (*n* = 5,135)			Highly frail (*n* = 1,047)		
	Rhythm control (*n* = 6,520)	Rate control (*n* = 7,909)	ASD (%)	Rhythm control (*n* = 2,500)	Rate control (*n* = 2,635)	ASD (%)	Rhythm control (*n* = 514)	Rate control (*n* = 533)	ASD (%)
Ischemic stroke	1,456 (22.3)	1,678 (21.2)	2.7	1,279 (51.2)	1,478 (56.1)	9.9	385 (74.9)	420 (78.8)	9.2
Transient ischemic attack	577 (8.8)	401 (5.1)	14.9	410 (16.4)	290 (11.0)	15.7	126 (24.5)	87 (16.3)	20.4
Intracranial bleeding	50 (0.8)	66 (0.8)	0.8	94 (3.8)	113 (4.3)	2.7	56 (10.9)	57 (10.7)	0.6
Myocardial infarction	548 (8.4)	442 (5.6)	11.1	383 (15.3)	256 (9.7)	17.0	112 (21.8)	82 (15.4)	16.5
Peripheral arterial disease	962 (14.8)	625 (7.9)	21.7	485 (19.4)	297 (11.3)	22.7	130 (25.3)	91 (17.1)	20.2
Valvular heart disease	517 (7.9)	876 (11.1)	10.7	230 (9.2)	167 (6.3)	10.7	29 (5.6)	21 (3.9)	8.0
Chronic kidney disease	267 (4.1)	202 (2.6)	8.6	265 (10.6)	128 (4.9)	21.6	99 (19.3)	49 (9.2)	29.1
Proteinuria	366 (5.6)	358 (4.5)	5.0	171 (6.8)	124 (4.7)	9.2	33 (6.4)	28 (5.3)	5.0
Hyperthyroidism	756 (11.6)	559 (7.1)	15.6	379 (15.2)	255 (9.7)	16.7	96 (18.7)	52 (9.8)	25.8
Hypothyroidism	799 (12.3)	533 (6.7)	18.9	408 (16.3)	246 (9.3)	21.0	106 (20.6)	68 (12.8)	21.2
Malignancy	1,407 (21.6)	1,243 (15.7)	15.1	797 (31.9)	659 (25.0)	15.3	188 (36.6)	168 (31.5)	10.7
COPD	1,969 (30.2)	2,165 (27.4)	6.2	1,120 (44.8)	952 (36.1)	17.7	269 (52.3)	251 (47.1)	10.5
Chronic liver disease	2,498 (38.3)	2,031 (25.7)	27.3	1,165 (46.6)	972 (36.9)	19.8	255 (49.6)	223 (41.8)	15.6
Hypertrophic cardiomyopathy	165 (2.5)	101 (1.3)	9.2	71 (2.8)	22 (0.8)	15.0	16 (3.1)	4 (0.8)	17.2
Osteoporosis	2,331 (35.8)	2,233 (28.2)	16.2	1,320 (52.8)	1,220 (46.3)	13.0	361 (70.2)	336 (63.0)	15.3
Sleep apnea	25 (0.4)	10 (0.1)	5.1	7 (0.3)	3 (0.1)	3.7	0 (0.0)	3 (0.6)	10.6
Concurrent drugs[†]									
Oral anticoagulant	6,520 (100.0)	7,909 (100.0)	<0.1	2,500 (100.0)	2,635 (100.0)	<0.1	514 (100.0)	533 (100.0)	<0.1
Warfarin	5,627 (86.3)	7,320 (92.6)	20.4	2,090 (83.6)	2,334 (88.6)	14.4	421 (81.9)	443 (83.1)	3.2
NOAC	1,142 (17.5)	774 (9.8)	22.7	540 (21.6)	410 (15.6)	15.6	118 (23.0)	112 (21.0)	4.7
Beta blocker	2,866 (44.0)	4,965 (62.8)	38.4	1,100 (44.0)	1,639 (62.2)	37.1	236 (45.9)	318 (59.7)	27.8
Non-DHP CCB	923 (14.2)	1,386 (17.5)	9.2	330 (13.2)	457 (17.3)	11.5	72 (14.0)	103 (19.3)	14.3
Digoxin	601 (9.2)	3,692 (46.7)	91.9	223 (8.9)	990 (37.6)	72.1	54 (10.5)	180 (33.8)	58.4
Aspirin	1,803 (27.7)	2,002 (25.3)	5.3	655 (26.2)	557 (21.1)	11.9	133 (25.9)	97 (18.2)	18.6
P2Y12 inhibitor	630 (9.7)	565 (7.1)	9.1	299 (12.0)	285 (10.8)	3.6	90 (17.5)	68 (12.8)	13.3
Statin	2,621 (40.2)	2,468 (31.2)	18.9	1,182 (47.3)	1,128 (42.8)	9.0	267 (51.9)	249 (46.7)	10.5
DHP-CCB	1,522 (23.3)	962 (12.2)	29.6	585 (23.4)	400 (15.2)	20.9	122 (23.7)	93 (17.4)	15.6
ACEI/ARB	3,720 (57.1)	4,634 (58.6)	3.1	1,341 (53.6)	1,334 (50.6)	6.0	272 (52.9)	235 (44.1)	17.7
Loop/thiazide diuretics	2,792 (42.8)	4,932 (62.4)	39.9	1,140 (45.6)	1,336 (50.7)	10.2	238 (46.3)	214 (40.2)	12.4
K+ sparing diuretics	884 (13.6)	2,164 (27.4)	34.7	382 (15.3)	528 (20.0)	12.5	81 (15.8)	83 (15.6)	0.5
Alpha blocker	194 (3.0)	221 (2.8)	1.1	70 (2.8)	88 (3.3)	3.1	13 (2.5)	19 (3.6)	6.0

Values are presented as median (interquartile range) or *n* (%).

*Modified HAS-BLED = hypertension, 1 point; >65 years old, 1 point; stroke history, 1 point; bleeding history or predisposition, 1 point; labile international normalized ratio, not assessed; ethanol or drug abuse, 1 point; drug predisposing to bleeding, 1 point.

[†]Defined as a prescription fill of >90 days within 180 days after the first prescription for rhythm- or rate-control drugs or the performance of an ablation procedure for AF.

AAD, antiarrhythmic drug; ACEI, angiotensin converting enzyme inhibitor; AF, atrial fibrillation; ARB, angiotensin II receptor blocker; ASD, absolute standardized difference; CCB, calcium channel blocker; COPD, chronic obstructive pulmonary disease; DHP, dihydropyridine; NOAC, non-vitamin K antagonist oral anticoagulant; OPD, outpatient department.

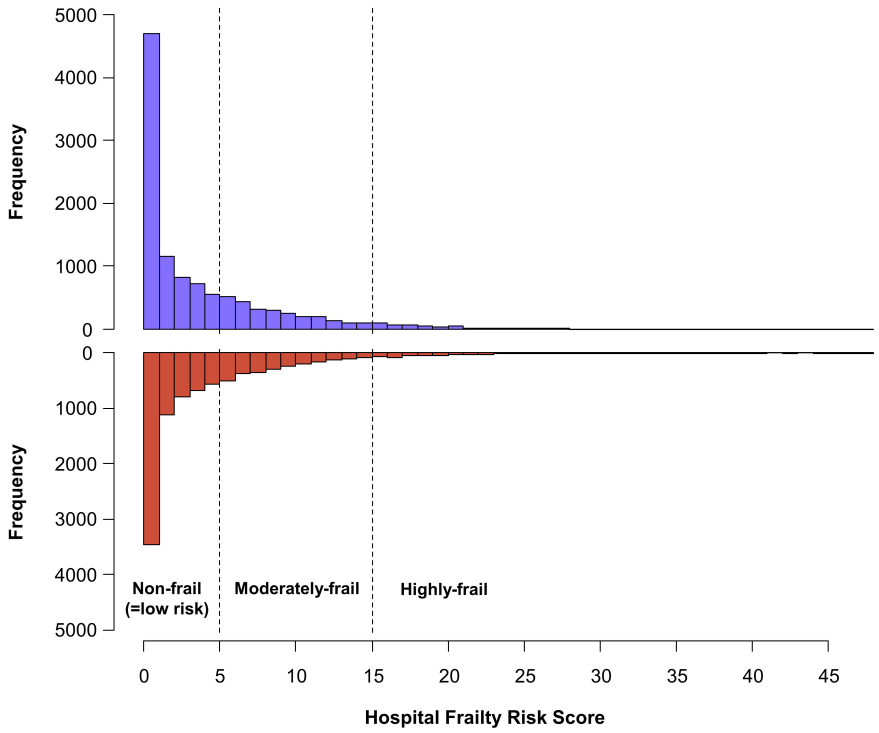

FIGURE 2
Distribution of the hospital frailty risk score in study population recently diagnosed with atrial fibrillation. The patients were diagnosed within 1 year, receiving new rhythm-control or rate-control treatments among patients.

Outcomes of early rhythm-control according to different frailty risks

In non-frail patients (HFRS <5), 6,520 and 7,909 patients started rhythm-control and rate-control therapies at an early stage of AF diagnosis (within 1 year), respectively. During a median follow-up of 4.1 (IR 2.2–7.1) years, early rhythm-control had a lower risk of primary composite outcome compared to rate-control therapy (weighted incidence rate 7.3 vs. 8.6 events per 100 person-years; HR 0.86, 95% CI 0.79–0.93; **Table 3** and **Figure 4A**). For each component of the primary composite outcome, early rhythm-control was related with reduced risks of ischemic stroke (HR 0.75, 95% CI 0.66–0.84), hospitalization for HF (HR 0.86, 95% CI 0.77–0.97) and acute myocardial infarction (HR 0.60, 95% CI 0.43–0.85) when compared to rate-control (**Table 3**).

In the moderately frail group (HFRS 5–15), 2,500 and 2,635 patients started rhythm-control and rate-control, respectively, with a median follow-up duration of 2.9 (IR 1.7–5.0) years. In the highly frail group (HFRS >15), rhythm-control and rate-control treatments were started in 514 and 533 patients, respectively, with a median follow-up of 2.1 (IR 1.3–3.7) years. There was no interaction between frailty risk and treatment effect in the primary composite outcome (p for interaction = 0.180), any of its components, or the composite safety outcome (p for interaction = 0.716). The early rhythm-control strategy showed a non-significant trend toward a lower risk of the primary composite outcome than the rate-control strategy in both the moderately frail (weighted incidence rate 12.3 vs. 13.7 events per 100 person-years; HR 0.91, 95% CI 0.81–1.02; **Table 3** and **Figure 4B**) and highly frail (weighted incidence rate 20.4 vs. 21.6 events per 100 person-years; HR 0.93, 95% CI 0.75–1.17; **Table 3** and **Figure 4C**) groups. Among patients in the moderately frail group, early rhythm-control was related with a reduced risk of ischemic stroke (HR 0.80, 95% CI 0.67–0.95).

We also calculated the number of days in hospital per year during each patient's individual follow-up period. In both the non-frail and moderately frail groups, the mean number of days in hospital was lower with the early rhythm-control than with the early rate-control group (17.6 vs. 21.7 days per year; $p < 0.001$ and 46.9 vs. 52.5 days per year; $p = 0.025$ respectively; **Table 3**). In case of the highly frail group, there was no significant difference in the number of days in hospital between the early rhythm-control and early rate-control groups (110.4 vs. 112.2 days per year; $p = 0.829$; **Table 3**).

In addition, a subgroup analysis according to sex, old age over 75 years, HF, CKD, and ischemic stroke showed that factors other than ischemic stroke in highly frail group did not affect

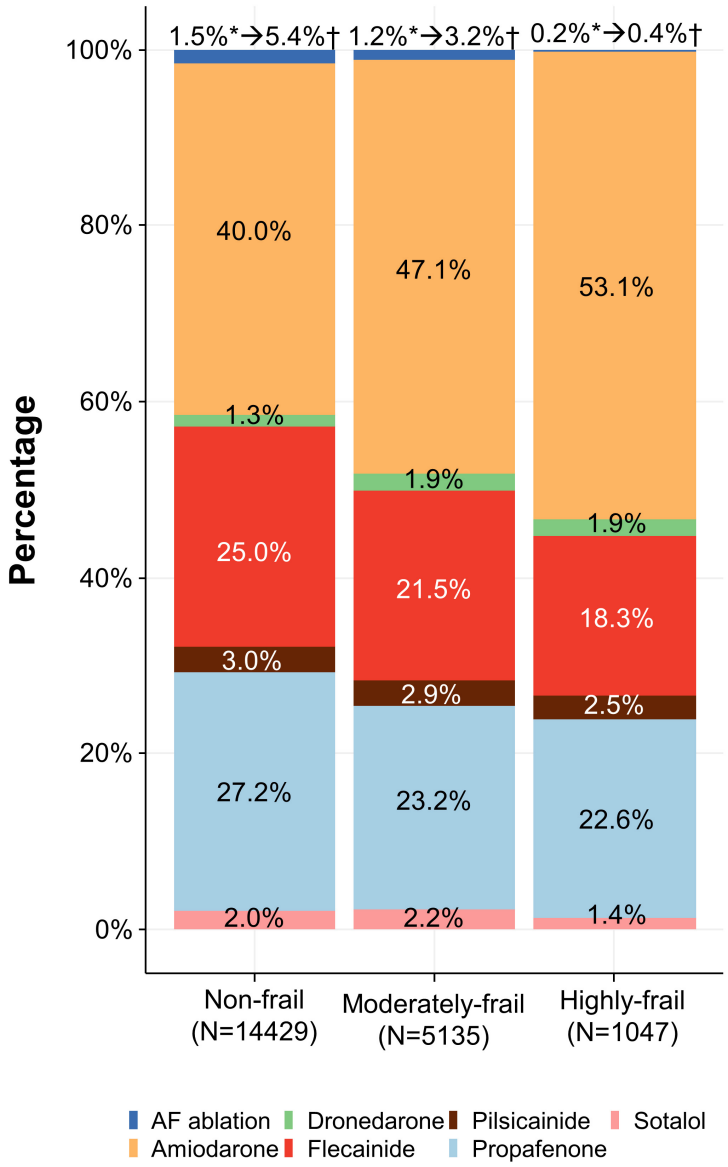

FIGURE 3
Initial choice of rhythm-control strategy. Treatments according to different frailty risk categories among patients who were recently (within 1 year) diagnosed with atrial fibrillation.

the benefit of the early rhythm control strategy for frail patients (**Supplementary Figure 3**).

Among all frail groups, there was no significant difference in the risk of composite safety outcome between early rhythm-control and rate-control (**Table 4**). The weighted incidence rates of early rhythm-control therapy vs. rate-control therapy were 9.0 vs. 9.1 events per 100 person-years (HR 0.99, 95% CI 0.89–1.01, $p = 0.850$); 15.8 vs. 14.1 events per 100 person-years (HR 1.11, 95% CI 0.96–1.30; $p = 0.149$); and 27.3 vs. 27.2 events per 100 person-years (HR 1.00, 95% CI 0.82–1.23; $p = 0.995$) in the non-frail, moderately frail and highly frail groups, respectively (**Table 4**).

Sensitivity analysis

Some patients switched between treatment strategies: 1,003 (9.1%) patients from rate control switched to rhythm control, whereas 5,013 (52.6%) patients switched from rhythm control

TABLE 3 Efficacy outcomes in weighted patients undergoing rhythm or rate control stratified according to frailty.

	Rhythm control			Rate control			Absolute rate difference per 100 person-years* (95% CI)	Weighted hazard ratio (95% CI)	*p*-value	*p* for interaction*
Outcome	Number of events	Person-years	Event rate	Number of events	Person-years	Event rate				
Non-frail (HFRS <5)	*n* = 2,165.2			*n* = 2,165.2						
Primary composite outcome	581	8,006	7.3	654	7,582	8.6	−1.4 (−2.3 to −0.5)	0.86 (0.79–0.93)	<0.001	0.180
Components of primary outcome										
Cardiovascular death	218	9,291	2.3	233	9,085	2.6	−0.2 (−0.7 to 0.2)	0.93 (0.82–1.06)	0.287	0.604
Ischemic stroke	242	8,675	2.8	316	8,332	3.8	−1.0 (−1,5 to −0.5)	0.75 (0.66–0.84)	<0.001	0.245
Hospitalization for heart failure	285	8,526	3.3	326	8,246	4.0	−0.6 (−1.2 to −0.0)	0.86 (0.77–0.97)	0.010	0.168
Acute myocardial infarction	27	9,231	0.3	45	8,976	0.5	−0.2 (−0.4 to −0.0)	0.60 (0.43–0.85)	0.004	0.823
Night spent in hospital/year†	17.6 ± 43.5			21.7 ± 52.1			−4.0 (−5.6 to −2.5)		<0.001	
Moderately frail (HFRS 5–15)	*n* = 848.2			*n* = 848.2						
Primary composite outcome	270	2,197	12.3	292	2,132	13.7	−1.4 (−3.6 to 0.7)	0.91 (0.81–1.02)	0.093	
Components of primary outcome										
Cardiovascular death	118	2,624	4.5	112	2,633	4.3	0.2 (−0.9 to 1.3)	1.06 (0.89–1.27)	0.511	
Ischemic stroke	110	2,406	4.6	136	2,373	5.7	−1.1 (−2.5 to 0.1)	0.80 (0.67–0.95)	0.011	
Hospitalization for heart failure	122	2,386	5.1	132	2,354	5.6	−0.5 (−1.8 to 0.8)	0.92 (0.77–1.09)	0.324	
Acute myocardial infarction	12	2,600	0.5	13	2,602	0.5	−0.0 (−0.4 to 0.3)	0.93 (0.54–1.60)	0.794	
Night spent in hospital/year†	46.9 ± 87.5			52.5 ± 92.9			−5.6 (−10.6 to −0.7)		0.025	
Highly frail (HFRS >15)	*n* = 177.2			*n* = 177.2						
Primary composite outcome	65	317	20.4	71	326	21.6	−1.2 (−8.3 to 5.9)	0.93 (0.75–1.17)	0.552	
Components of primary outcome										
Cardiovascular death	32	391	8.2	35	411	8.4	−0.2 (−4.2 to 3.8)	0.96 (0.69–1.33)	0.866	
Ischemic stroke	27	348	7.7	30	365	8.1	−0.4 (−4.5 to 3.7)	0.93 (0.65–1.33)	0.689	
Hospitalization for heart failure	23	357	6.5	23	376	6.1	0.4 (−3.3 to 4.0)	1.03 (0.69–1.55)	0.873	
Acute myocardial infarction	1	391	0.2	4	398	1.1	−0.8 (−1.9 to 0.3)	0.22 (0.05–1.07)	0.061	
Night spent in hospital/year†	110.4 ± 129.7			112.2 ± 131.4			−1.7 (−17.6 to 14.1)		0.829	

Event rates are presented as per 100 person-years. CI, confidence interval; HFRS, hospital frailty risk score.

**p* for interactions between frailty risk (non-frail/intermediate-frailty/high-frailty) and treatment strategy (rhythm control or rate control).

†Results are reported as mean (standard deviation) and the difference between the treatment groups was estimated using a two-sample weighted t test.

10.3389/fcvm.2022.1050744

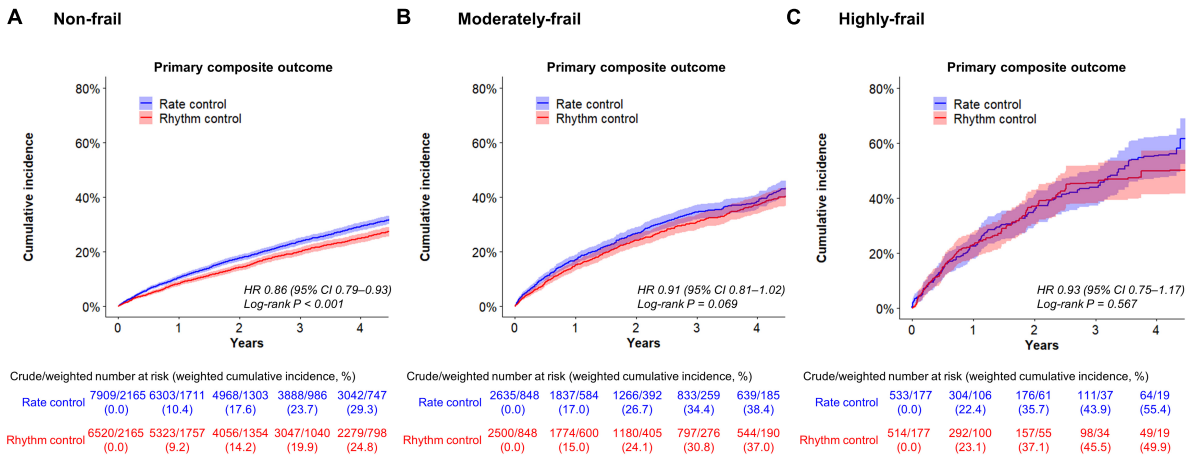

FIGURE 4
Weighted cumulative incidence curves for primary composite outcome. Curves shown for non-frail **(A)**, moderately frail **(B)**, and highly frail **(C)** patients who were recently (within 1 year) diagnosed with atrial fibrillation.

to rate control during follow-up (**Supplementary Table 8**). The results of on-treatment analyses (**Supplementary Table 9**) and time-varying regression analyses (**Supplementary Table 10**) were consistent with the main results. Similar outcomes were obtained in the one-to-one propensity score matched patients as in the main analysis (**Supplementary Table 11**). The sensitivity analyses in which cardioversion was also included as a rhythm-control strategy, and the results were consistent (**Supplementary Table 12**). When analyzed using a 30-day observational period (within the period, more than 20 days of drug supply was defined as intention-to-treat), and the results were consistent with the main findings (shown in **Supplementary Table 13**). In the falsification analysis, the 95% CIs of the correlations between rhythm-control and each falsification endpoint (30 in total) covered 1 of 29 (96.7%), 1 of 29 (96.7%), and 1 of 30 (100%) endpoints in the non-frail, moderately frail, and highly frail groups, respectively (**Supplementary Table 14**).

Discussion

Our previous study demonstrated that early rhythm control was associated with less frequent cardiovascular events than rate control in patients with AF (10). In the present study, we conducted a stratified analysis according to frailty, and the main finding were that, compared to early rate-control treatment, early rhythm-control treatment among non-frail patients with AF was related to a 14% decreased risk (absolute decrease in risk: 1.4 events per 100 person-years) in primary efficacy composite outcomes without an increased risk of safety outcomes. These results are consistent with the EAST-AFNET 4 trial that we emulated.

Further, although statistical significance was decreased, a consistent trend toward a lower risk of early rhythm-control was seen in the moderately frail (HR 0.91, 95% CI 0.81–1.02) and highly frail (HR 0.93, 95% CI 0.75–1.17) groups.

Third, there was no difference in the risk of composite safety outcomes across the different frailty groups, which is noteworthy for this study due to the concern that frailty may affect the safety outcome of active rhythm-control therapy.

Efficacy of early rhythm-control strategy in frail patients

Although current AF guidelines recommend anticoagulation and treatment for comorbidities in all patients who are eligible, rhythm-control treatment is limited to only those who have related symptoms (1, 2). However, the ATHENA and EAST-AFNET 4 trials reported that rhythm-control strategy may reduce cardiovascular events in patients who have received dronedarone (ATHENA) or early rhythm-control therapy (EAST-AFNET 4) (9, 30). We have confirmed through previous works that the results of a reference trial on the benefits of early rhythm-control are equally reflected in real world observational data in old age (10). Nevertheless, it is not yet clear which patients should be targeted for early rhythm-control, especially in elderly patients.

This study is meaningful as it suggests rhythm-control as a suitable target by stratifying the patients according to frailty and extending the inferences. We showed that early rhythm-control strategy was related with a reduced risk of primary outcomes in non-frail patients with AF and there was a consistent trend toward a lower risk of early rhythm-control in the moderate as

TABLE 4 Safety outcomes in weighted patients undergoing rhythm or rate control stratified according to frailty.

	Rhythm control			Rate control			Absolute rate difference per 100 person-years (95% CI)	Weighted hazard ratio (95% CI)	*p*-value
Outcome	Number of events	Person-years	Event rate	Number of events	Person-years	Event rate			
Non-frail (HFRS <5)	*n* = 2,165.2			*n* = 2,165.2					
Composite safety outcome*	733	8,110	9.0	746	8,183	9.1	−0.1 (−1.0 to 0.8)	0.99 (0.89–1.01)	0.850
All-cause death	473	9,291	5.1	533	9,085	5.9	−0.8 (−1.5 to −0.1)	0.86 (0.76–0.98)	0.020
Intracranial bleeding	64	9,191	0.7	79	8,938	0.9	−0.2 (−0.5 to 0.1)	0.80 (0.58–1.12)	0.196
Gastrointestinal bleeding	169	8,910	1.9	191	8,694	2.2	−0.3 (−0.7 to 0.1)	0.88 (0.72–1.09)	0.243
SAE related to rhythm control									
Cardiac tamponade	7	9,282	0.1	3	9,074	0.0	0.0 (−0.0 to 0.1)	2.09 (0.56–7.84)	0.273
Syncope	129	8,866	1.5	93	8,795	1.1	0.4 (0.0 to 0.7)	1.38 (1.06–1.80)	0.018
Sick sinus syndrome	90	8,783	1.0	26	8,973	0.3	0.7 (0.5 to 1.0)	3.56 (2.30–5.49)	<0.001
Atrioventricular block	41	9,028	0.5	25	8,931	0.3	0.2 (−0.0 to 0.4)	1.70 (1.03–2.81)	0.037
Pacemaker implantation	48	9,019	0.5	16	9,013	0.2	0.3 (0.2 to 0.5)	3.00 (1.71–5.26)	<0.001
Sudden cardiac arrest	59	9,268	0.6	53	9,067	0.6	0.1 (−0.2 to 0.3)	1.12 (0.77–1.61)	0.565
Moderately frail (HFRS 5–15)	*n* = 848.2			*n* = 848.2					
Composite safety outcome*	356	2,251	15.8	335	2,381	14.1	1.7 (−0.5 to 4.0)	1.11 (0.96–1.30)	0.149
All-cause death	260	2,624	9.9	263	2,633	10.0	−0.1 (−1.8 to 1.6)	0.99 (0.84–1.18)	0.928
Intracranial bleeding	27	2,582	1.1	25	2,598	1.0	0.1 (−0.4 to 0.6)	1.12 (0.65–1.93)	0.684
Gastrointestinal bleeding	80	2,495	3.2	84	2,497	3.4	−0.2 (−1.2 to 0.9)	0.96 (0.70–1.30)	0.780
SAE related to rhythm control									
Cardiac tamponade	2	2,621	0.1	0	2,632	0.0	0.1 (−0.0 to 0.2)	22.5 (2.76–182.7)	0.004
Syncope	50	2,481	2.0	34	2,552	1.3	0.7 (−0.0 to 1.4)	1.52 (0.98–2.36)	0.060
Sick sinus syndrome	25	2,428	1.0	11	2,582	0.4	0.6 (0.1 to 1.1)	2.43 (1.19–4.99)	0.015
Atrioventricular block	16	2,536	0.6	5	2,588	0.2	0.4 (0.1 to 0.8)	3.12 (1.17–8.35)	0.024
Pacemaker implantation	11	2,502	0.4	7	2,600	0.3	0.2 (−0.2 to 0.5)	1.57 (0.61–4.03)	0.352
Sudden cardiac arrest	17	2,619	0.7	25	2,626	1.0	−0.3 (−0.8 to 0.2)	0.70 (0.38–1.28)	0.247

(Continued)

10.3389/fcvm.2022.1050744

TABLE 4 (Continued)

Outcome	Rhythm control			Rate control			Absolute rate difference per 100 person-years (95% CI)	Weighted hazard ratio (95% CI)	*p*-value
	Number of events	Person-years	Event rate	Number of events	Person-years	Event rate			
Highly frail (HFRS > 15)	*n* = 177.2			*n* = 177.2					
Composite safety outcome*	91	335	27.3	96	351	27.2	0.1 (−7.7 to 8.0)	1.00 (0.82–1.23)	0.995
All-cause death	74	391	18.8	78	411	19.1	−0.3 (−6.3 to 5.8)	0.98 (0.78–1.22)	0.842
Intracranial bleeding	9	382	2.4	6	405	1.5	0.9 (−1.1 to 2.8)	1.55 (0.73–3.25)	0.252
Gastrointestinal bleeding	22	364	5.9	24	376	6.5	−0.6 (−4.1 to 3.0)	0.89 (0.59–1.35)	0.597
SAE related to rhythm control									
Cardiac tamponade	1	391	0.2	0	411	0.1	0.2 (−0.4 to 0.7)	3.21 (0.22–47.4)	0.395
Syncope	5	380	1.2	10	390	2.6	−1.4 (−3.4 to 5.4)	0.45 (0.20–0.99)	0.048
Sick sinus syndrome	5	371	1.4	0	410	0.1	1.3 (0.1 to 2.6)	13.4 (2.45–73.1)	0.003
Atrioventricular block	2	380	0.6	1	407	0.2	0.4 (−0.5 to 1.3)	2.64 (0.64–11.0)	0.182
Pacemaker implantation	1	381	0.3	0	409	0.1	0.3 (−0.4 to 0.9)	5.44 (0.59–50.2)	0.135
Sudden cardiac arrest	5	385	1.3	8	408	1.9	−0.5 (−2.3 to 1.2)	0.68 (0.32–1.47)	0.503

Event rates are presented as per 100 person-years. CI, confidence interval; SAE, serious adverse event(s).

*p for interactions between frailty risk (non-frail/intermediate frailty/high frailty) and treatment strategy (rhythm control or rate control) was 0.716.

10.3389/fcvm.2022.1050744

well as highly frail groups. Thus, early rhythm-control can be carried out without hesitation regardless of the degree of frailty.

Safety outcomes after early rhythm-control strategy in frail patients

Major guidelines have no specific recommendations on age or frailty assessment for choosing rate- or rhythm-control treatment, such as electrical shock delivery and ablation therapy (1, 2). For safety concerns, rhythm-control therapy is not an active treatment in elderly frail patients; based on the findings of this study, it tends to be a more passive treatment option in primary or secondary institutions. Contrary to common perception however, the results of the present study consistently showed that the degree of frailty had no effect on the safety outcomes of early rhythm-control strategy in older AF populations.

Although the importance of integrated AF management, including symptom control, is consistent in frail patients, the outcome of rhythm-control at an advanced age cannot be guaranteed as frail older patients are predisposed to a decline in both renal and hepatic function, leading to hesitation in its use (19). However, this study showed that early rhythm-control did not affect safety outcomes in older frail AF populations, therefore suggesting that the treatment direction should be decided by evaluating, characterizing, and individualizing each patient's condition rather than basing it simply on age and frailty. This is also emphasized in the recently revised 2019 AHA/ACC/HRS and 2020 ESC guidelines (1, 2).

Study limitations

The present research has some limitations, however. First, this study was retrospectively performed using all patients with AF in Korea National Health Insurance Service databases, and needed more validation in general population group. Second, this study used ICD-10 codes for the AF diagnosis, medications and procedure complications. Although AF definition and study outcomes are validated (**Supplementary Table 3**), there is the possibility of mis-diagnosis of AF and AF ablation state. Third, the number of participants who underwent ablation among patients who chose early rhythm-control as a treatment strategy was low. This is because the reimbursement of ablation therapy is allowed only for AF patients who have not achieved sinus rhythm even after receiving drug treatment, including antiarrhythmic drugs, for 6 weeks or more. The use of catheter ablation therapy was minimal, such that no conclusions could be drawn for this specific form of rhythm-control therapy. Fourth, this study used per-protocol analysis, so there may be an attrition bias resulting from patients who do not have similar characteristics among the groups. Fifth, although the results of the falsification analysis showed that the probability of a major systematic bias was unlikely, unmeasured confounders (such as the adequacy of anticoagulant treatment or health-related habits like drinking, smoking, and physical activity) may have affected the results. Finally, because the aim of the present study was to evaluate the effectiveness of therapeutic interventions for rhythm-control and rate-control, non-users were excluded. However, as some non-users included frail patients that did not need rate-control drugs due to a low baseline heart rate, future studies may need to take this into consideration.

Conclusion

In the non-frail population, the superiority of cardiovascular outcomes of early rhythm-control in the treatment of AF was observed without any effect on the safety outcomes, showing a consistent trend toward a lower risk of adverse cardiovascular outcomes without an increased risk of safety outcomes. And frailty does not have a detrimental effect on rhythm-control treatment. Thus, an individualized approach is required on the early rhythm-control strategy in older patients with AF, regardless of their frailty status.

Data availability statement

The datasets presented in this study can be found in online repositories. The names of the repository/repositories and accession number(s) can be found in the article/**Supplementary material**.

Ethics statement

This study was approved by the Institutional Review Board of the Yonsei University Health System (4-2016-0179), and following strict confidentiality guidelines, personally identifiable information was removed after the cohort was created, and it was therefore exempt from prior consent requirements. Written informed consent for participation was not required for this study in accordance with the national legislation and the institutional requirements.

Author contributions

G-IY and DK conceived and designed the study. EJ analyzed the clinical data and drafted the manuscript. HY, T-HK, H-NP, J-HS, and M-HL assisted with data analysis. BJ, P-SY, and GL reviewed the study and put forward constructive suggestions. All authors gave final approval of the version to be published and agreed to be accountable for all aspects of the work.

Funding

This work was supported by a grant from the Patient-Centered Clinical Research Coordinating Center (PACEN) funded by the Ministry of Health and Welfare, Republic of Korea (grant number: HC19C0130). The funders had no role in the study design, collection, analysis and interpretation of data, writing of the report, or the decision to submit the report for publication.

Acknowledgments

The database used in this study was provided by the NHIS of Korea. The authors would like to thank them for their cooperation.

Conflict of interest

BJ has served as a speaker for Bayer, BMS/Pfizer, Medtronic, Johnson & Johnson, and Daiichi-Sankyo, and received research funds from Samjin, Hanmi Pharmaceutical Co., Ltd., Huino, Medtronic, Abbott, Boston, and Biotronik. GL has served as a consultant for Bayer/Janssen, BMS/Pfizer, Biotronik, Medtronic, Boehringer Ingelheim, Novartis, Verseon, and Daiichi Sankyo, and as a speaker for Bayer, BMS/Pfizer, Medtronic, Boehringer Ingelheim, and Daiichi Sankyo. No fees were received either directly or personally from any of the institutions mentioned above.

The remaining authors declare that the research was conducted in the absence of any commercial or financial relationships that could be construed as a potential conflict of interest.

Publisher's note

All claims expressed in this article are solely those of the authors and do not necessarily represent those of their affiliated organizations, or those of the publisher, the editors and the reviewers. Any product that may be evaluated in this article, or claim that may be made by its manufacturer, is not guaranteed or endorsed by the publisher.

Supplementary material

The Supplementary Material for this article can be found online at: https://www.frontiersin.org/articles/10.3389/fcvm.2022.1050744/full#supplementary-material

References

1. January, C, Wann L, Calkins H, Chen L, Cigarroa J, Cleveland J Jr, et al. 2019 Aha/Acc/Hrs focused update of the 2014 Aha/Acc/Hrs guideline for the management of patients with atrial fibrillation: a report of the American college of cardiology/American heart association task force on clinical practice guidelines and the heart rhythm society. *J Am Coll Cardiol.* (2019) 74:104–32. doi: 10.1016/j.jacc.2019.01.011

2. Hindricks G, Potpara T, Dagres N, Arbelo E, Bax J, Blomstrom-Lundqvist C, et al. 2020 Esc guidelines for the diagnosis and management of atrial fibrillation developed in collaboration with the European association for cardio-thoracic surgery (Eacts): the task force for the diagnosis and management of atrial fibrillation of the European society of cardiology (Esc) developed with the special contribution of the European heart rhythm association (Ehra) of the Esc. *Eur Heart J.* (2021) 42:373–498. doi: 10.1093/eurheartj/ehaa612

3. Weber C, Hung J, Hickling S, Nedkoff L, Murray K, Li I, et al. Incidence, predictors and mortality risk of new heart failure in patients hospitalised with atrial fibrillation. *Heart.* (2021) 107:1320–6. doi: 10.1136/heartjnl-2020-318648

4. Kim D, Yang P, Yu H, Kim T, Jang E, Sung J, et al. Risk of dementia in stroke-free patients diagnosed with atrial fibrillation: data from a population-based cohort. *Eur Heart J.* (2019) 40:2313–23. doi: 10.1093/eurheartj/ehz386

5. Corley S, Epstein A, DiMarco J, Domanski M, Geller N, Greene H, et al. Relationships between Sinus rhythm, treatment, and survival in the atrial fibrillation follow-up investigation of rhythm management (Affirm) study. *Circulation.* (2004) 109:1509–13. doi: 10.1161/01.CIR.0000121736.16643.11

6. Hohnloser S, Kuck K, Lilienthal J. Rhythm or rate control in atrial fibrillation–pharmacological intervention in atrial fibrillation (Piaf): a randomised trial. *Lancet.* (2000) 356:1789–94. doi: 10.1016/s0140-6736(00)03230-x

7. Wyse D, Waldo A, DiMarco J, Domanski M, Rosenberg Y, Schron E, et al. A comparison of rate control and rhythm control in patients with atrial fibrillation. *N Engl J Med.* (2002) 347:1825–33. doi: 10.1056/NEJMoa021328

8. Carlsson J, Miketic S, Windeler J, Cuneo A, Haun S, Micus S, et al. Randomized trial of rate-control versus rhythm-control in persistent atrial fibrillation: the strategies of treatment of atrial fibrillation (Staf) study. *J Am Coll Cardiol.* (2003) 41:1690–6. doi: 10.1016/s0735-1097(03)00332-2

9. Kirchhof P, Camm A, Goette A, Brandes A, Eckardt L, Elvan A, et al. Early rhythm-control therapy in patients with atrial fibrillation. *N Engl J Med.* (2020) 383:1305–16. doi: 10.1056/NEJMoa2019422

10. Kim D, Yang P, You S, Sung J, Jang E, Yu H, et al. Treatment timing and the effects of rhythm control strategy in patients with atrial Fibrillation: nationwide cohort study. *BMJ.* (2021) 373:n991. doi: 10.1136/bmj.n991

11. Shariff N, Desai R, Patel K, Ahmed M, Fonarow G, Rich M, et al. Rate-control versus rhythm-control strategies and outcomes in septuagenarians with atrial fibrillation. *Am J Med.* (2013) 126:887–93. doi: 10.1016/j.amjmed.2013.04.021

12. Metzner I, Wissner E, Tilz R, Rillig A, Mathew S, Schmidt B, et al. Ablation of atrial fibrillation in patients >/=75 years: long-term clinical outcome and safety. *Europace.* (2016) 18:543–9. doi: 10.1093/europace/euv229

13. Clegg A, Young J, Iliffe S, Rikkert M, Rockwood K. Frailty in elderly people. *Lancet.* (2013) 381:752–62. doi: 10.1016/S0140-6736(12)62167-9

14. Yang P, Sung J, Kim D, Jang E, Yu H, Kim T, et al. Frailty and the Effect of catheter ablation in the elderly population with atrial fibrillation- a real-world analysis. *Circ J.* (2021) 85:1305–13. doi: 10.1253/circj.CJ-20-1062

15. Bahnson T, Giczewska A, Mark D, Russo A, Monahan K, Al-Khalidi H, et al. Association between age and outcomes of catheter ablation versus medical therapy for atrial fibrillation: results from the cabana trial. *Circulation.* (2022) 145:796–804. doi: 10.1161/Circulationaha.121.055297

16. Rockwood K, Theou O, Mitnitski A. What are frailty instruments for? *Age Ageing.* (2015) 44:545–7. doi: 10.1093/ageing/afv043

17. Gilbert T, Neuburger J, Kraindler J, Keeble E, Smith P, Ariti C, et al. Development and validation of a hospital frailty risk score focusing on older people in acute care settings using electronic hospital records: an observational study. *Lancet.* (2018) 391:1775–82. doi: 10.1016/S0140-6736(18)30668-8

18. Kundi H, Valsdottir L, Popma J, Cohen D, Strom J, Pinto D, et al. Impact of a claims-based frailty indicator on the prediction of long-term mortality after transcatheter aortic valve replacement in medicare beneficiaries. *Circ-Cardiovasc Qual.* (2018) 11:e005048. doi: 10.1161/CIRCOUTCOMES.118.005048

19. Yang P, Sung J, Jang E, Yu H, Kim T, Lip G, et al. Application of the simple atrial fibrillation better care pathway for integrated care management in frail patients with atrial fibrillation: a nationwide cohort study. *J Arrythm.* (2020) 36:668–77. doi: 10.1002/joa3.12364

20. Kim D, Yang P, Jang E, Yu H, Kim T, Uhm J, et al. 10-year nationwide trends of the incidence, prevalence, and adverse outcomes of non-valvular atrial fibrillation nationwide health insurance data covering the entire Korean population. *Am Heart J.* (2018) 202:20–6. doi: 10.1016/j.ahj.2018.04.017

21. Kim D, Yang P, Jang E, Yu H, Kim T, Uhm J, et al. Increasing trends in hospital care burden of atrial fibrillation in Korea, 2006 through 2015. *Heart.* (2018) 104:2010–7. doi: 10.1136/heartjnl-2017-312930

22. Kim D, Yang P, Kim T, Jang E, Shin H, Kim H, et al. Ideal blood pressure in patients with atrial fibrillation. *J Am Coll Cardiol.* (2018) 72:1233–45. doi: 10.1016/j.jacc.2018.05.076

23. Kim T, Yang P, Yu H, Jang E, Shin H, Kim H, et al. Effect of hypertension duration and blood pressure level on ischaemic stroke risk in atrial fibrillation: nationwide data covering the entire Korean population. *Eur Heart J.* (2019) 40:809–19. doi: 10.1093/eurheartj/ehy877

24. McAlister F, van Walraven C. External validation of the hospital frailty risk score and comparison with the hospital-patient one-year mortality risk score to predict outcomes in elderly hospitalised patients: a retrospective cohort study. *BMJ Qual Saf.* (2019) 28:284–8. doi: 10.1136/bmjqs-2018-008661

25. Desai R, Franklin J. Alternative approaches for confounding adjustment in observational studies using weighting based on the propensity score: a primer for practitioners. *BMJ.* (2019) 367:l5657. doi: 10.1136/bmj.l5657

26. Austin P. Balance diagnostics for comparing the distribution of baseline covariates between treatment groups in propensity-score matched samples. *Stat Med.* (2009) 28:3083–107. doi: 10.1002/sim.3697

27. Austin P, Latouche A, Fine J. A review of the use of time-varying covariates in the fine-gray subdistribution hazard competing risk regression model. *Stat Med.* (2020) 39:103–13. doi: 10.1002/sim.8399

28. Park S, Hendry D. Reassessing schoenfeld residual tests of proportional hazards in political science event history analyses. *Am J Polit Sci.* (2015) 59:1072–87. doi: 10.1111/ajps.12176

29. Lipsitch M, Tchetgen E, Cohen T. Negative controls a tool for detecting confounding and bias in observational studies. *Epidemiology.* (2010) 21:383–8. doi: 10.1097/EDE.0b013e3181d61eeb

30. Hohnloser S, Crijns H, Van E, Gaudin C, Page R, Torp-Pedersen C, et al. Effect of dronedarone on cardiovascular events in atrial fibrillation. *N Engl J Med.* (2009) 360:668–78.

frontiers | Frontiers in Cardiovascular Medicine

TYPE Original Research
PUBLISHED 12 April 2023
DOI 10.3389/fcvm.2023.1086791

OPEN ACCESS

EDITED BY
François Regoli,
University of Zurich, Switzerland

REVIEWED BY
Serge Boveda,
Clinique Pasteur, France
Stepan Havranek,
Charles University, Czechia

*CORRESPONDENCE
Carlo de Asmundis
✉ carlo.deasmundis@uzbrussel.be;
carlodeasmundis@me.com

†These authors have contributed equally to this work

SPECIALTY SECTION
This article was submitted to Cardiac Rhythmology, a section of the journal Frontiers in Cardiovascular Medicine

RECEIVED 01 November 2022
ACCEPTED 27 March 2023
PUBLISHED 12 April 2023

CITATION
Pannone L, Eltsov I, Ramak R, Cabrita D, De Letter P, Chierchia G-B and de Asmundis C (2023) Compatibility assessment of a temperature-controlled radiofrequency catheter with a novel electroanatomical mapping system.
Front. Cardiovasc. Med. 10:1086791.
doi: 10.3389/fcvm.2023.1086791

Compatibility assessment of a temperature-controlled radiofrequency catheter with a novel electroanatomical mapping system

Luigi Pannone[1†], Ivan Eltsov[1,2†], Robbert Ramak[1], David Cabrita[2], Paul De Letter[3], Gian-Battista Chierchia[1] and Carlo de Asmundis[1*]

[1]Heart Rhythm Management Centre, Postgraduate Program in Cardiac Electrophysiology and Pacing, Universitair Ziekenhuis Brussel—Vrije Universiteit Brussel, European Reference Networks Guard-Heart, Brussels, Belgium, [2]Medtronic Inc., Minneapolis, MN, United States, [3]Abbott Laboratories, St Paul, MN, United States

Background: The novel DiamondTemp ablation system (DTA) and EnSiteX mapping System (EAM) are both CE-Marked and FDA approved medical devices. The DTA has been validated by its manufacturer only in combination with previous version of EnSite System—EnSite Precision. The aim of this study was to evaluate compatibility of DTA with EnSite X with a previously developed protocol.
Methods: Three configurations were tested: 3.1. Medtronic Generator connection Box (GCB) and AmpereConnect cable; 3.2. the Medtronic GCB-E and electrogram out cable from GCB to EAM; 3.3. Direct connection of DTA to EAM using intracardiac out cable with no GCB.
Results: The previously developed universal method for compatibility assessment of ablation catheters and navigation systems was used with success for assessing DTA and EnSite X EAM compatibility, with reproducible results. Accuracy of DTA visualization with different setups was evaluated with a phantom model measuring distances between DTA and reference points. DTA is compatible with EnSiteX EAM with a safety and reliability profile guaranteed, if within the described specifications. In particular, careful setup is mandatory to achieve good clinical outcomes as only setup 3.2 is viable for both NavX and Voxel Mode and demonstrated satisfactory results and accuracy. Setup 3.3 showed a significant shift immediately after catheter insertion. Catheter position was away from baseline points and the dislocation increased during the radiofrequency delivery.
Conclusions: Previously developed method for compatibility assessment of ablation catheters and navigation systems has been used for a new EAM. DTA is compatible with EnSiteX EAM with proper configuration.

KEYWORDS
catheter ablation, universal compatibility, diamondTemp ablation system, ensite electroanatomic mapping system, cardiac arrhythmias

Introduction

Fast development of the medical device industry in the last decades has led to novel technologies from different manufacturers. Electrophysiology products are one of the most dynamic parts of the entire medical device market and the cross-compatibility between electrophysiological devices is not always investigated. As compatibility is not

guaranteed "out of the box" the need for compatibility assessment methods between devices from different manufacturers becomes crucial.

Our group has previously developed a novel universal compatibility assessment method to evaluate the safety and accuracy of a new temperature-controlled radiofrequency (RF) catheter ablation system with 3rd party electro anatomical mapping systems (1).

The aim of this research is to the apply our bench testing protocol to assess the compatibility between a temperature-controlled RF catheter ablation and a novel Electroanatomical mapping system (EAM), EnSiteX™ (Abbott, St. Paul, MN).

EnSiteX™, offers both a primary impedance mode (NavX) and a primary magnetic mode (Voxel) (2).

Magnetic based systems are constantly sending localization information based on magnetic field measurements, which allows the system to track it and represent it in the 3D model, but it is possible only for catheters manufactured by the same company.

Impedance-based tracking allows to visualize and tracking virtually any catheter using the impedance measurement between external patches and an electrode on the catheter. However, the precision of this tracking needs to be assessed. Hybrid tracking of EnSiteX system in Voxel mode uses both magnetic and impedance-based methods, where magnetic tracking is enhancing localization accuracy of impedance tracked catheter by acquisition of Voxels.

The novel DiamondTemp™ ablation system (DTA), (Medtronic Inc, Minneapolis, MN) and EnSiteX™ EP System (Abbott, St. Paul, MN) are both CE-Marked and FDA approved medical devices (3, 4). The DTA has been validated by its manufacturer only in combination with previous version of EnSite System—EnSite Precision™ System (Abbott, St. Paul, MN) (5). The aim of this study was to evaluate compatibility between DTA and EnSiteX with a previously developed protocol (1). Furthermore, different configurations have been tested to ensure accuracy of DTA visualization in the novel mapping system.

Methods

Ablation catheter and mapping system

The DTA ablation catheter is a 7.5-F irrigated RF catheter; the 4.1-mm composite tip electrode delivers RF. The ablation electrode tip is embedded with 3 interconnected diamonds, which allows rapid RF delivery (due to electric and thermal diamond properties) and shunting heath from externalized thermocouples, Figure 1. This allows accurate temperature measurement at tip-tissue interface. The catheter operates in temperature control mode and a dedicated RF generator (RFG), titrates rapidly the delivered power to the target temperature. The dual composite ablation tip behaves as a single electrode during ablation and electrically insulation of the tip allows for high-resolution EGM sensing (3, 4).

EnSite X™ EP System is a novel EAM which is result of further development of EnSite Product Family. The system can operate in 2 different modes—Voxel mode and NavX mode. NavX mode is an enhanced version of the previous feature of the EnSite™ Precision Cardiac Mapping System. Catheter location is purely based on impedance data, Figure 2. Magnetic data is optional and used to improve impedance tracking. Tracking is also dependent on local changes in thoracic impedance (lungs, sheath, etc.). In Voxel Mode the inflexible portion of sensor enabled (SE) catheter location is based on magnetic localization, Figure 2. The system collects Voxels (Impedance Fiducials) which allow Impedance-based electrodes to be shown. SE catheter location is based on impedance & magnetic data. Catheter shape is consistent despite local impedance changes. Non-SE catheters are visualized using Voxels as well which allows better precision compared to NavX mode, Figure 2.

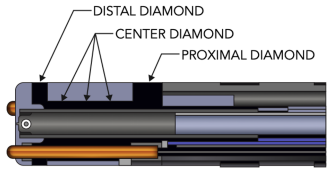

FIGURE 1
Diamondtemp™ catheter composite tip structure. The tip of the catheter consists of a diamond network—distal, proximal and center diamond. Three thermally isolated thermocouples protrude from the distal tip to ensure enhanced tip-tissue interface temperature readings; another 3 thermocouples are embedded in the proximal part to allow correct measurements.

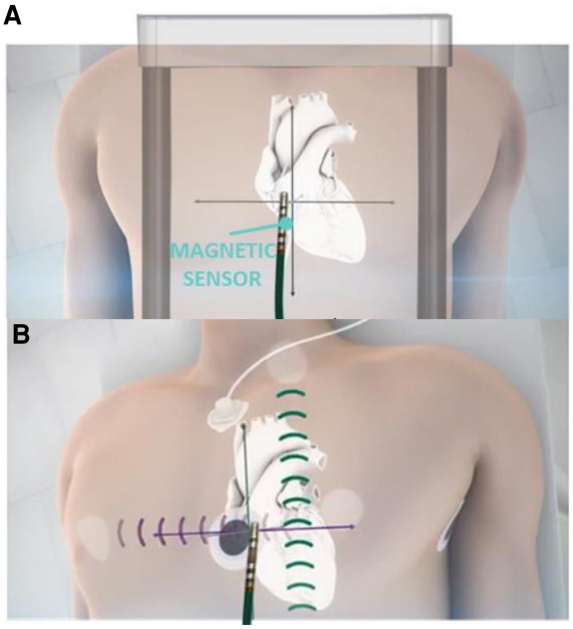

FIGURE 2
Ensite X voxel and NavX modes tracking. Panel A: schematic mechanism of magnetic based tracking of sensor enabled (SE) catheters (Voxel Mode). Panel B: impedance-based visualization of catheters without magnetic sensor (NavX mode).

Assessment endpoints

This study has 3 endpoints

1) Safety and efficiency of RF energy delivery when a specific setup is used. To ensure that RF energy and current emitted by the system does not leak throughout the setup and can be entirely delivered to the tissue.
2) The DTA is correctly represented inside the 3D model, with a precise and reliable position not influenced by external factors, especially RF energy delivery. Four different configurations have been tested.
3) Reproducibility of results, in comparison with earlier testing according to the described compatibility assessment method (1).

The DTA can be connected to the navigation system either by using electrogram (EGM) out cables from RF generator or from dedicated GenConnect interface to be able to filter out RF energy so it does not affect localization. Previous version of EnSite has been validated to be used in combination with Genconnect connected to the EAM directly—so this configuration was tested as well. In addition, the new EnSite X system has 2 operating modes NavX and Voxel mode. As the DTA can be visualized using impedance mode—testing have been performed in NavX mode. Compatibility of DTA with EnSiteX in VoXel mode has been also assessed for investigational purposes, however qualificative data is not available as in this mode it is impossible perform reliable measurements, so results of this evaluation can be considered only speculative.

Test configurations (setups), Figure 3:

1.0. DTA connected only to the DTA RFG—No GenConnect (GC) nor Genconnect Cable (GCC) connected to the DTA;
2.0. DTA not connected to a MS but connected to:
  2.1. The Medtronic (MDT) Generator Connection Box E (MDT GCB-E)
  2.2. The MDT GCB-E and intracardiac (IC) out *via* the MDT GCB-E;
3.0. DTA connected to the EnSiteX EAM using:
  3.1. MDT GCB and AmpereConnect cable
  3.2. The MDT GCB-E and EGM out cable from GCB to EAM (**Figures 3**, **4**)
  3.3. The direct connection of DTA to EAM using IC out cable with no GCB.

Configurations 1.x and 2.x were used for functional and safety assessment only.

Functional and safety parameters assessment

To assess functional and safety parameters of the DTA with the different setups proposed, a calibrated electrosurgery analyzer "FLUKE Biomedical QA-ESII" was used (6). This device allows for continuous measurement of power, current, peak-to-peak voltage (closed load only) and crest factor for each RF application. The test and connectivity of the FLUKE Biomedical QA-ESII Electrosurgery Analyzer equipment to different components is performed in "continuous operation mode" with no footswitch. The test is interrupted by pressing the "stop" key. The Analyzer acts like a meter during the test, showing increasing and decreasing values as received from the unit being tested, in this case the DTA RFG. The DTA RFG is connected to the connection for the electrode outputs of an internal variable resistance. An active connection (Red) is directly connected to the catheter tip alligator clip wired to Red pin. The neutral connection is direct wired from the DTA neutral plate connection and the analyzer neutral pin (Black).

The functional and safety parameters of the DTA and its RFG were assessed at 3 different loads, namely 50 Ohms, 100 Ohms and 150 Ohms and 3 different maximum power outputs 50 W, 30 W and 15 Watts. For each load and maximum power output, measurements were repeated 3 times to assess the following parameters: (1) Maximum power output indicated on the DTA RFG; (2) Power output measured at the tip of the DTC; (3) Current measured at the tip of the DTC; (4) Peak-to-peak

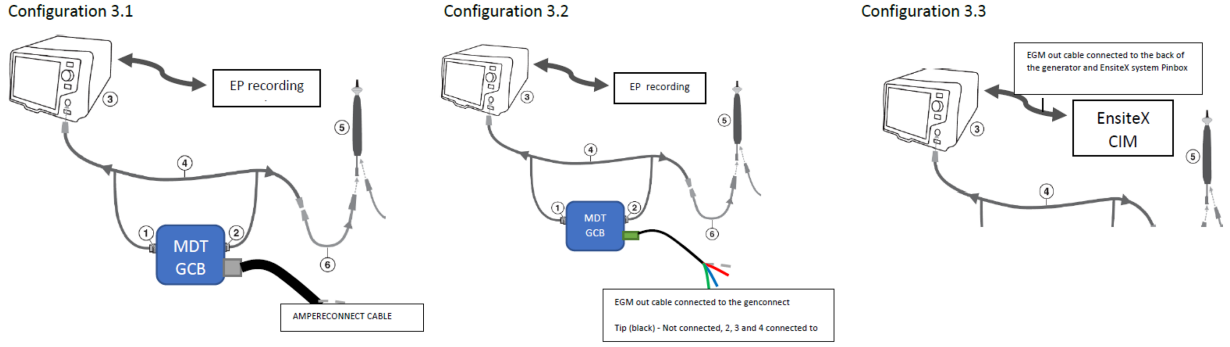

FIGURE 3
Test configurations (setups). Configuration 3.1—DTA connected to the EnsiteX *via* AmpereConnect cable connected to the MDT Genconnect. Configuration 3.2—DTA connected *via* EGM out cable from the genconnect to the Ensite CIM (without distal as it is not wired). Configuration 3.3 EGM cable from RFG back to CIM and not from genconnect.

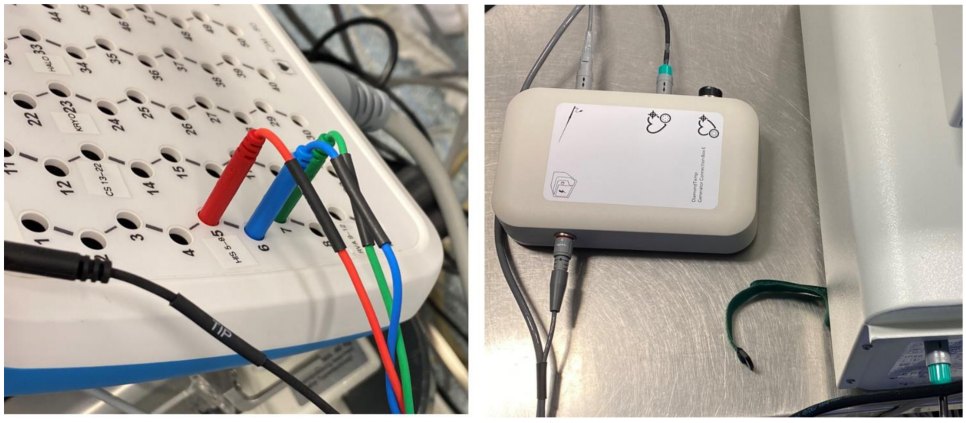

FIGURE 4
Configuration 3.2 details. Electrogram (EGM) out cable connected to the Genconnect and to the EnsiteX CIM pins 2–4.

voltage measured at the tip of the DTC; (5) Maximum current variation among the 3 measurements.

Accuracy assessment

The accuracy assessment of DTA visualization when using the Ensite X^{TM} EAM was assessed using a dedicated EAM phantom emulating the patient with patches connected. The phantom was similar to the one used during EAM installation prior to certification for clinical use. Different components were connected to the DTA RFG and EAM according to the different setup to be tested.

In NavX mode no geometry model was created; reference locations have been reached with ring electrode of Advisor HD Grid Mapping Catheter, Sensor Enabled (Abbott, St. Paul, MN) and tagged to create a baseline point set. Then DTA has been inserted into the phantom and its proper visualization has been visually assessed. Then the DTA has been moved to reference locations to ensure accuracy.

To assess the reliability of the catheter location on the EAM, the DTA was placed back at each reference location and an additional point was collected. An assessment was made regarding the reproducibility of the baseline point locations by measuring the distance between tags (in mm) on the EAM.

Each reinsertion and reconnection were performed 5 times prior to energy delivery. RF was delivered 3 times at each point.

For each setup, three different RF pulses were tested: (1) RF energy for 45 s with a target temperature of 60°C (longest application time and highest temperature allowed by the DTA in a clinical setting), with zero sec of power ramp delay, 1 s of pre-cooling and 0 s of cooling post ablation (RF1); or (2) RF energy for 10 s with a target temperature of 55°C (longest application time and highest temperature allowed by the DTA in a clinical setting) with zero sec of power ramp delay, 1 s of pre-cooling and 0 s of cooling post ablation (RF2); or (3) RF energy for 5 s with a target temperature of 50°C (longest application time and highest temperature allowed by the DTAS in a clinical setting) with zero sec of power ramp delay, 1 s of pre-cooling and 0 s of cooling post ablation (RF3).

Between each RF delivery the DTA was removed and reinserted in the phantom and the DTA cable was disconnected and re-connected without moving the catheter.

After each RF application, the catheter was manually placed at each reference location by looking at the phantom directly. An additional point was collected at each reference location. Distance between every taken point and its corresponding baseline marker were measured using EAM software (**Figure 5**).

Distance measurements (in mm) between baseline points and collected points were repeated for every reference location on the phantom model after each RF pulse. At the next step, the DTA was placed once again back at each reference location and an additional final point was collected.

Voxel mode testing has been performed only for configuration 3.2 as using configuration 3.1 in Voxel mode is not possible according to the instruction for use (IFU). The phantom anatomy was built using a dedicated mapping catheter, Advisor HD Grid Mapping Catheter, Sensor Enabled, (Abbott, St. Paul, MN). Reference locations from the phantom were reached with the tip of this catheter and reference locations were added to the surface of the phantom as baseline. Then the tracking of the DTA was verified by visual comparison of physical catheter movements and its representation on the map (**Figure 6**). The exact accuracy measurements in this mode were not possible as the system does not allow to tag locations from non-SE catheters.

Configurations and settings of EnSiteX EAM and DTA

In configuration 3.1 DTA has been configured as an ablation catheter connected to the AmpereConnect. The original setup has been modified by connecting AmpereConnect cable between EAM and MDT GCB.

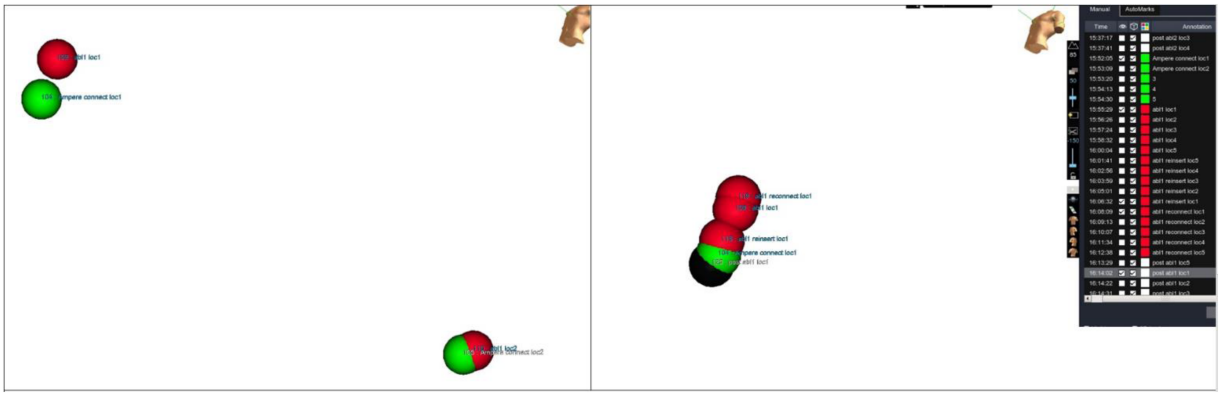

FIGURE 5
Accuracy measurements. Distance measurements between tags collected at same location during different moments of evaluation. Tip location has been tagged at each testing step and then distance has been measured.

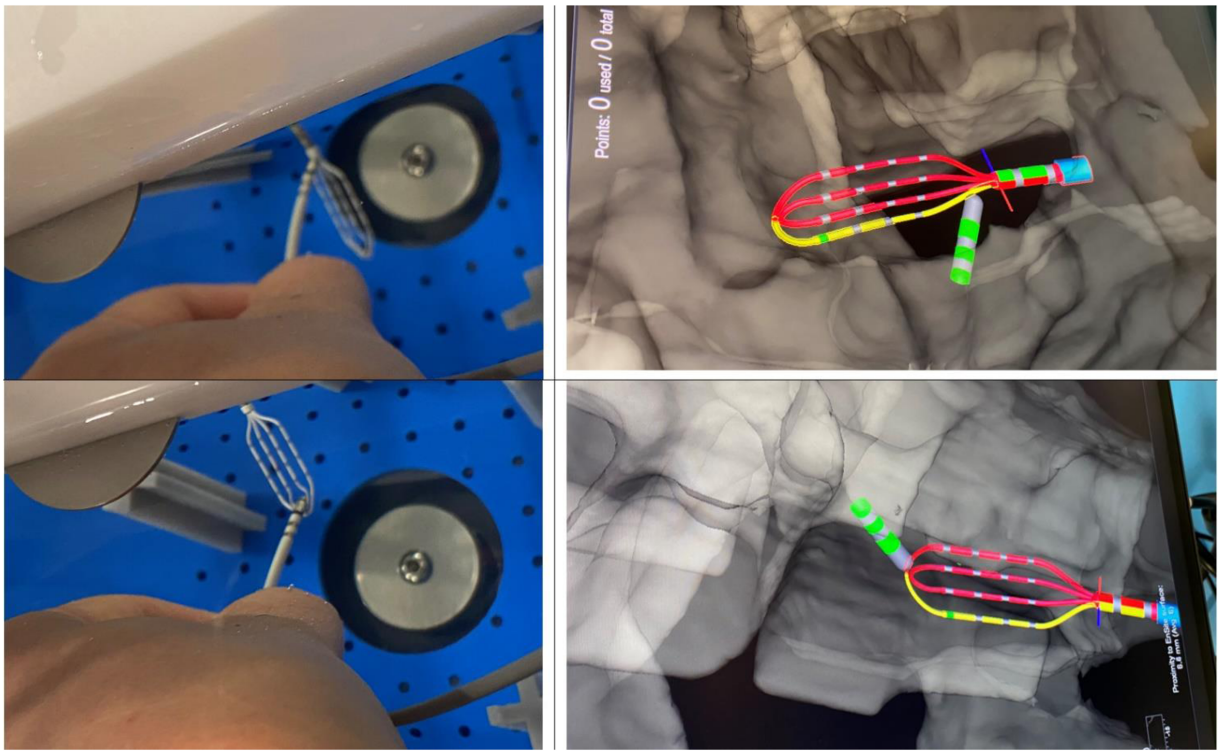

FIGURE 6
Visualization of DiamondTemp™ catheter in voXel mode. Photo of real location of HD-Grid mapping catheter and DiamondTemp™ (DTA) within the phantom and their representation on the Ensite System in Voxel mode.

For configurations 3.2 and 3.3 the DTA has been configured as AUX catheter connected to the IC module of EnSite X and no modifications to the original setup has been done.

The accuracy assessment of the DTA visualization in the Voxel mode was based on the fact that Voxel mode uses a hybrid tracking mechanism. In this mode, the EAM system collects Voxels using SE catheter and aligns impedance values with magnetic points. This allows to accurately track non SE catheters.

Statistical analysis

All variables were tested for normality with Shapiro–Wilk test. Normally distributed variables were described as mean ± standard deviation and the groups were compared through ANOVA, paired or unpaired t-test as appropriate, while the non-normally distributed variables were described as median (Inter Quartile Range) and compared by Kruskal-Wallis test, Mann-Whitney test

or Wilcoxon signed-rank test as appropriate. The categorical variables were described as frequencies (percentages) and compared by Chi-squared test or Fisher's exact test as appropriate.

A *p*-value less than 0.05 was considered statistically significant.

The analysis was performed using R software version 3.6.2 (R Foundation for Statistical Computing, Vienna, Austria).

Results

DTA functional and safety parameters assessment with different setups

The data collected on the functional and safety parameters of the DTA connected to the EnSite X™ EAM are detailed in Table 1 and Supplementary Table S1.

At the lowest load setting of 50 Ohm, a maximum discrepancy of 5 W, could be observed between the maximum power programmed to be delivered by the DTA RFG, the actual power output indicated on the DTA RFG and the power output measured at the tip of the DTA.

Variations on the current measured at the tip of the DTA by RF analyzer could be observed between the 3 measurements performed with the same settings; All variations were within limits specified by the manufacturer of the device (7). The results are summarized in Table 1 and Supplementary Table S1.

Accuracy of DTA visualization

The DTA location was represented in real-time for all configurations. A proper tracking of the DTA was observed by visual comparison of physical catheter movements and its representation on EAM. This was consistent with all setups tested.

TABLE 1 Functional and safety parameters of DiamondTemp™ radiofrequency generator.

	Reference	Setup 3.1	Setup 3.2	Setup 3.3
15 Watt setting				
RFG Power Value (W)	15	15	15	15
Measured power (W)	15	15	15	15
Peak-to-Peak Voltage (V)	116	116	116	116
Current measured at tip (mA)	384	383	383	384
30 Watt setting				
RFG Power Value (W)	30	30	30	30
Measured power (W)	30	30	30	30
Peak-to-Peak Voltage (V)	164	164	164	165
Current measured at tip (mA)	542	541	541	542
50 Watt setting				
RFG Power Value (W)	50	50	50	50
Measured power (W)	50	50	50	50
Peak-to-Peak Voltage (V)	213	212	212	213
Current measured at tip (mA)	700	698	698	697

Measurements have been performed with 3 different loads (50 Ohm, 100 Ohm and 150 Ohm). Each measurement has been repeated 3 times. Data for 100 Ohm is shown in Table 1 (other measurements are available in Supplementary Table S1). *P* value = not significant (NS) for all comparisons.

Baseline points were taken using HD Grid Mapping Catheter tracked either using magnetic (Voxel mode) or impedance based (NavX mode) localization. The verification of the location of baseline points was established by taking points at the reference markers on the wet tank.

In setups 3.1 and 3.2 no major shifts were observed in the DTC location after RF1, RF2 or RF3 were performed with all setups tested, Table 2 and Supplementary Table S2. The location of the DTC did not significantly shift in space when compared to baseline reference points. This was consistent: after reinsertion and reconnection as well as following RF energy delivery. The distances measured between the baseline points after each variable, for each setup tested, are described in Table 2 and Supplementary Table S2.

Specific observations related to the setup 3.3

In this configuration a significant shift was observed immediately after catheter insertion. Catheter position was away from baseline points and this dislocation increased during the RF delivery. This may be linked to the fact that in this configuration no proper RF filtering is used. Due to huge baseline shift, further RF applications were not delivered as could be harmful for the EAM system with no added value as this configuration was suboptimal, Table 2 and Supplementary Table S2.

Observations related to the setup 3.1 and 3.2

In these configurations no significant shift has been observed. All points were taken within the EnSiteX accuracy specifications (1), Table 2 and Supplementary Table S2.

Specific observations related to voxel mode evaluation

Voxel mode evaluation has been performed only for the configurations 3.2 and 3.3 as per EnSite X IFU. Setup 3.3 showed a baseline shift in catheter position as in NavX mode. No RF application has been delivered in configuration 3.3 to avoid potential damage of the system.

Due to impossibility of adequately measuring accuracy in Voxel mode, a visual assessment of accuracy in Voxel mode has been performed. DTA has been placed on the surface of HDGrid and their relative visualizations on the EAM were compared. DTA was deemed as stable and accurate, Figure 6.

Discussion

The main results of the current study are: (1) Previously developed universal method for compatibility assessment of

TABLE 2 Accuracy of DiamondTemp™ visualization in EnsiteX system with different setups and different radiofrequency applications.

	Reference	Setup 3.1	Setup 3.2	Setup 3.3	*P* value
Distance after reinsertion (mm)	1.14 ± 0.4	1.49 ± 0.5	1.19 ± 0.1	5.16 ± 2.2	0.49/0.75/0.011
Distance after reconnection (mm)	1.26 ± 0.3	1.65 ± 0.7	1.44 ± 0.4	4.26 ± 1.6	0.37/0.38/0.013
Shift during RF (mm)	1.31 ± 0.2	1.35 ± 0.7	1.21 ± 0.3	13.81 ± 4.7	0.74/0.69/0.01
Shift after RF (mm)	1.09 ± 0.1	1.67 ± 0.6	1.12 ± 0.2	11.15 ± 3.2	0.31/0.68/0.002
Maximum shift observed (mm)	2.50 ± 0.4	4.00 ± 0.9	2.70 ± 0.6	21.40 ± 4.6	0.22/0.55/0.008

Each reinsertion and reconnection were performed 5 times prior to energy delivery. Radiofrequency (RF) was delivered 3 times at each point. The table summarizes average and maximal distance from catheter tip to the reference point after each step for 5 different points on the model. *P* value is reported for each comparison as follows: Reference-Setup 3.1/Reference-Setup 3.2/Reference-Setup 3.3. Details are available in Supplementary Table S2.

ablation catheters and navigation systems has been used for a new EAM with reproducible results; (2) DTA is compatible with EnSiteX EAM. Safety and reliability profile is guaranteed within described specifications; (3) Careful setup is mandatory to achieve good clinical outcomes as only setup 3.2 is viable for both NavX and Voxel Mode and demonstrated satisfactory results.

3D mapping systems are considered as a standard of care for the diagnosis and treatment of cardiac arrythmias. They reduce radiation time and dose and improve the precision of ablation treatment (2, 5, 8). However, the use of third-party ablation catheters is limited as there is no compatibility out of the box. Extending the range of compatible ablation systems with various EAM allows new therapeutic modalities, which may be associated with clinical benefit.

The *in vitro* compatibility assessment is a crucial step, which must be done prior to clinical trials (3, 4). In the current study a previously developed universal method for compatibility assessment was used (1). It demonstrated to be reproducible with different EAM. This is of clinical relevance as it could be used for future standard bench evaluation before commercialization of novel components by different manufacturers.

Compared to our previous study, assessing compatibility between DTA and Rhythmia™ EAM (Boston Scientific) (1), the current study is the first to evaluate the compatibility between DTA and another EAM, namely EnSiteX. The results showed that the same *in vitro* method can be applied to different EAM. Indeed, the experimental dataset hereby presented is completely new and this further reinforces the generalizability of the approach.

Furthermore, DTA has been demonstrated as compatible with EnSiteX EAM. Despite the current clinical use of DTA with EnSiteX EAM is feasible, configuration choice is of utmost importance. Indeed, safety and reliability of tracking is guaranteed within described settings. Both configurations 3.1 and 3.2 might be used for DTA in NavX mode. However only configuration 3.2 is possible for Voxel mode. If switching from NavX mode to Voxel mode can be required during procedure, careful pre procedural planning and proper connection setting should be considered.

Limitations

This study is based on a phantom model. There was no test *in vivo*.

Conclusions

Previously developed universal method for compatibility assessment of ablation catheters and navigation systems has been used for a new EAM with reproducible results. DTA is compatible with EnSiteX EAM with proper configuration.

Data availability statement

The original contributions presented in the study are included in the article/**Supplementary Material**, further inquiries can be directed to the corresponding author/s.

Author contributions

Conception and design of the work: LP, IE and CA. Substantial contributions to the acquisition of data for the work: RR, DC and PDL. Substantial contributions to the analysis of data for the work: RR. Substantial contributions to the interpretation of data for the work: LP, IE and RR. Drafting the work: LP and IE. Revising the draft of the work critically for important intellectual content: DC, PDL, GBC and CA. Final approval of the version to be published: LP, IE, RR, DC, PDL, GBC and CA. Agreement to be accountable for all aspects of the work in ensuring that questions related to the accuracy or integrity of any part of the work are appropriately investigated and resolved: LP, IE, RR, DC, PDL, GBC and CA. All authors contributed to the article and approved the submitted version.

Conflict of interest

IE and DC are employees of Medtronic, Inc. PDL is an employee of Abbott, Inc. GBC received compensation for teaching purposes and proctoring from Medtronic, Abbott, Biotronik, Boston Scientific, Acutus Medical. CA receives research grants on behalf of the center from Biotronik, Medtronic, Abbott, LivaNova, Boston Scientific, AtriCure, Philips, and Acutus; CA received compensation for teaching purposes and proctoring from Medtronic, Abbott, Biotronik, Livanova, Boston Scientific, Atricure, Acutus Medical Daiichi Sankyo. The remaining authors declare that the research

was conducted in the absence of any commercial or financial relationships that could be construed as a potential conflict of interest.

Publisher's note

All claims expressed in this article are solely those of the authors and do not necessarily represent those of their affiliated organizations, or those of the publisher, the editors and the reviewers. Any product that may be evaluated in this article, or claim that may be made by its manufacturer, is not guaranteed or endorsed by the publisher.

Supplementary material

The Supplementary Material for this article can be found online at: https://www.frontiersin.org/articles/10.3389/fcvm.2023.1086791/full#supplementary-material.

References

1. Pannone L, Eltsov I, Ramak R, Cabrita D, Verherstraeten M, Gauthey A, et al. Universal method of compatibility assessment for novel ablation technologies with different 3D navigation systems. *Front Cardiovasc Med.* (2022) 9(June):1–12. doi: 10.3389/fcvm.2022.917218

2. Singh HR. ALARA in pediatric electrophysiology laboratory. *Children*. (2022) 9(6):866. doi: 10.3390/children9060866

3. Iwasawa J, Koruth JS, Petru J, Dujka L, Kralovec S, Mzourkova K, et al. Temperature-controlled radiofrequency ablation for pulmonary vein isolation in patients with atrial fibrillation. *J Am Coll Cardiol.* (2017) 70(5):542–53. doi: 10.1016/j.jacc.2017.06.008

4. Ramak R, Lipartiti F, Mojica J, Monaco C, Bisignani A, Eltsov I, et al. Comparison between the novel diamond temp and the classical 8-mm tip ablation catheters in the setting of typical atrial flutter. *J Interv Card Electrophysiol.* (2022) 64(3):751–7. doi: 10.1007/s10840-022-01152-w

5. Ellermann C, Frommeyer G, Eckardt L. High-resolution 3D mapping: opportunities and limitations of the Rhythmia™ mapping system. *Herzschrittmachertherapie und Elektrophysiologie*. (2018) 29(3):284–92. doi: 10.1007/s00399-018-0580-0

6. Fluke Biomedical. QA-ES II Electrosurgical Analyzer—Users Manual. 2006—Fluke Corporation, USA.

7. Medtronic. *Instruction for use—ePIX therapeutics—diamondTemp catheter*. Medtronic MN, USA. (2021). Available at: https://manuals.medtronic.com/content/dam/emanuals/crdm/M016135C001A_view.pdf

8. Pani A, Belotti G, Bonanno C, Bongiorni MG, Bottoni N, Brambilla R, et al. Predictors of zero x-ray ablation for supraventricular tachycardias in a nationwide multicenter experience. *Circ Arrhythmia Electrophysiol.* (2018) 11(3):e005592. doi: 10.1161/CIRCEP.117.005592

frontiers | Frontiers in Cardiovascular Medicine

TYPE Original Research
PUBLISHED 01 August 2023
DOI 10.3389/fcvm.2023.1110707

OPEN ACCESS

EDITED BY
Daniel M. Johnson,
The Open University, United Kingdom

REVIEWED BY
Peter Backx,
York University, Canada
Jasmeet S. Reyat,
University of Birmingham, United Kingdom

*CORRESPONDENCE
Tong Liu
✉ liutongdoc@126.com
Xue Liang
✉ liangxue19841219@126.com

†These authors share first authorship

RECEIVED 29 November 2022
ACCEPTED 20 July 2023
PUBLISHED 01 August 2023

CITATION
Shangguan W, Gu T, Cheng R, Liu X, Liu Y, Miao S, Wang W, Song F, Wang H, Liu T and Liang X (2023) Cfa-circ002203 was upregulated in rapidly paced atria of dogs and involved in the mechanisms of atrial fibrosis.
Front. Cardiovasc. Med. 10:1110707.
doi: 10.3389/fcvm.2023.1110707

Cfa-circ002203 was upregulated in rapidly paced atria of dogs and involved in the mechanisms of atrial fibrosis

Wenfeng Shangguan[1†], Tianshu Gu[1†], Rukun Cheng[1†], Xing Liu[1], Yu Liu[2], Shuai Miao[1], Weiding Wang[1], Fang Song[3], Hualing Wang[1], Tong Liu[1*] and Xue Liang[1*]

[1]Tianjin Key Laboratory of Ionic-Molecular Function of Cardiovascular Disease, Department of Cardiology, Tianjin Institute of Cardiology, The Second Hospital of Tianjin Medical University, Tianjin, China, [2]Department of Cardiology, Taikang Ningbo Hospital, Ningbo, China, [3]Department of Geriatric, The Second Hospital of Tianjin Medical University, Tianjin, China

Background and aims: The role of circular RNAs (circRNAs) in the pathophysiology of cardiovascular disease is gradually being elucidated; however, their roles in atrial fibrillation (AF)-related fibrosis are largely unknown. This study aimed to characterize the different circRNA profiles in the rapid-pacing atria of dogs and explore the mechanisms involved in atrial fibrosis.

Methods: A rapid right atrial-pacing model was established using electrical stimulation from a pacemaker. After 14 days, atrial tissue was collected for circRNA sequencing analysis. *In vitro* fibrosis was established by stimulating canine atrial fibroblasts with angiotensin II (Ang II). The fibroblasts were transfected with siRNA and overexpressing plasmids to explore the effects of cfa-circ002203 on fibroblast proliferation, migration, differentiation, and the expression of fibrosis-related proteins.

Results: In total, 146 differentially expressed circRNAs were screened, of which 106 were upregulated and 40 were downregulated. qRT-PCR analysis showed that cfa-circ002203 was upregulated in both *in vivo* and *in vitro* fibroblast fibrosis models. The upregulation of cfa-circ002203 enhanced proliferation and migration while weakening the apoptosis of fibroblasts. Western blotting showed that cfa-circ002203 overexpression increased the protein expression levels of fibrosis-related indicators (Col I, Col III, MMP2, MMP9, and α-SMA) and decreased the protein expression levels of pro-apoptotic factors (Bax and Caspase 3) in Ang II-induced fibroblast fibrosis.

Conclusion: Cfa-circ002203 might serve as an active promoter of the proliferation, migration, and fibrosis of atrial fibroblasts and is involved in AF-induced fibroblast fibrosis.

KEYWORDS

atrial fibrillation, atrial fibrosis, high-throughput sequencing, bioinformatics, cfa-circ002203

1. Introduction

Atrial fibrillation (AF) is the most common arrhythmia and is associated with heart failure, which leads to high morbidity and mortality (1). The long-term persistence of AF may result in the remodeling and deposition of atrial fibrous tissue. Cardiac fibrosis is one of the major factors resulting in cardiac remodeling in patients with AF (2, 3).

In addition, endomysial fibrosis is the strongest determinant of AF complexity compared with other structural alterations (4). Cardiac fibrosis is characterized by notable changes in the synthesis and degradation of collagen I and III, the main components of the extracellular matrix (ECM), and the malfunction of matrix metalloproteinases (MMP2 and MMP9) (5). The cellular and molecular mechanisms underlying the development of cardiac fibrosis have not been completely elucidated. Studies have indicated that phenotypic changes in cardiac fibroblasts, a class of small fusiform cells that control the composition and structure of the ECM, contribute to AF-induced cardiac fibrosis. When activated by pro-fibrotic stimulation, such as mechanical stress, and growth factors, such as angiotensin II (Ang II), fibroblasts proliferate and differentiate into a secretory phenotype, namely myofibroblasts, with α-smooth muscle actin (α-SMA) expression acting as a marker of the myofibroblast phenotype (6). Consequently, cardiac fibrosis might directly involve in the occurrence and perpetuation of AF and its related disease.

Cellular circular RNAs (circRNAs) are a class of stable, single-stranded RNAs with covalently closed head-to-tail circularized transcripts (7). Owing to improvements in RNA sequencing and bioinformatics tools, thousands of circRNAs in various organisms have been identified. CircRNAs play an important role in the pathogenesis of heart disease, as previous studies have revealed that they play regulatory roles in heart failure (8, 9) and pathological hypertrophy (10). For example, Ni et al. found that circHIPK3 inhibited Ang II-induced cardiac fibrosis by sponging miR-29b-3p (11). In a diabetic db/db mouse model, circRNA_010567 was found upregulated and knockdown of circRNA_010567 could reduce synthesis of Col I, Col II and α-SMA in Ang II-treated cardiac fibroblasts (12). Wu et al. uncovered that circYAP was significantly decreased in the hearts of patients with cardiac hypertrophy and the pressure overload mouse model (13). Most of these studies based on cells or mice. Our research group previously performed circRNA sequencing analysis in the atrial tissue of a rapid atrial pacing dog model and screened several differentially expressed circRNAs (14), indicating that they may be involved in the pathology of AF and fibrosis. Based on this, this study focuses on the function of the molecular mechanism of circRNA's involvement in the fibrosis of atrial fibroblasts. Given the extensive influence of circRNAs on the activity of microRNA (miRNA), there is great interest in understanding the effect of circRNAs on the gene regulatory functions of miRNAs (15). In this molecular mechanism, circRNAs act as sponges and compete with miRNAs to bind to the untranslated regions of messenger RNA (mRNA) and regulate the expression of target genes. As post-transcriptional regulators, circRNAs participate in mammalian physiological and pathological processes. Each circRNA acts as a competing endogenous RNA (ceRNA) with multiple miRNAs, generating a complex and fine-tuned system that regulates the pathology of diseases.

Based on the above information, the objective of this study was to identify circRNAs associated with AF in dogs by producing an interaction network diagram of circRNA-miRNA-mRNA and performing qRT-PCR verification, and to further identify the role of circRNAs in fibroblast inflammation, proliferation, and fibrosis in an *in vitro* atrial fibroblast fibrosis model induced by Ang II.

2. Methods

2.1. Rapid right atrial pacing model establishment

This study was conducted in compliance with the ARRIVE guidelines and approved by the Laboratory Animal Ethics Committee of the Institute of Radiation Medicine, Chinese Academy of Medical Sciences (approval number: IRM-DWLL-2019018).

Twelve healthy mongrel dogs of either sex weighing between 12 and 14 kg were randomly divided into two groups, a control group ($n = 6$) and an AF group ($n = 6$) with the established rapid right atrial pacing model. After randomization, sex and body weight were equally distributed between the two groups by artificial adjustment to reduce system errors. The dogs were fasted for 12 h and anesthetized with an intravenous injection of 3% (w/v) isopentobarbital sodium (dissolved in normal saline, 30 mg/kg) into the right upper limb. After endotracheal intubation, an ALC-V8 animal ventilator (tidal volume 12–15 ml/kg, frequency 25 bpm; Shanghai Alcott Biotech Co., Ltd, Shanghai, China) was connected to maintain mechanical ventilation. The dog was fixed in the supine position on the operating table, and their electrocardiography (ECG), blood pressure, and oxyhemoglobin saturation were monitored using a multichannel electrophysiological system (Shanghai Hongtong Industrial Co. Ltd., Shanghai, China) during anesthesia before and after 14 days of pacing. A longitudinal incision of 3 cm was made on the right side of the middle of the trachea, a modified pacemaker electrode (St. Jude Medical, St. Paul, MN, USA) was inserted along the external jugular vein into the right atrium, and electrical stimulation of 5 V and 200 bpm was applied using an electrophysiological stimulator (Suzhou Oriental Electronic Instrument Factory, Suzhou, China). The pacing frequency was adjusted to 500 bpm, and the electrode was fixed when the pacing was good. A surgical incision was made in the interscapular region and a pacemaker pocket was buried subcutaneously. Electrical stimulation with a pacing voltage of 5 V, pulse width of 0.2 ms, and frequency of 500 bpm was applied continuously. The control group underwent the same operation as described above, with pacemaker placement, but no electrical stimulation. Aseptic procedures were strictly followed during the operation, and antibiotics (1 g of cefuroxime sodium dissolved in 50 ml of normal saline) were administered to each dog by an intravenous drip three times a day for 3 days after the operation to prevent pacemaker pocket infection.

After 14 days of pacing, the anesthetized dog was fixed on the operating table, the pacing electrode was removed, and the mapping electrodes (diameter:1.5 mm; distance between poles:1.5 mm) were stitched onto the left and right atrial

epicardia and four limbs to monitor the atrial epicardial electrocardiography and limb-lead electrocardiography using a multi-channel electrophysiological recorder. AF susceptibility was assessed according to preprocedural cardiac stimulation (S1S2). AF was induced by four times the threshold and 600 bpm rapid stimulation for 2 min, and was regarded as successful when the electrocardiogram sinus *P* wave was replaced by a rapid and disorderly fibrillation wave and the duration of this electrical activity disorder was more than 1 s.

2.2. Tissue preparation for sequencing

The dogs were euthanized by an intravenous injection of overloaded 3% isopentobarbital sodium (85 mg/kg). The hearts of the experimental dog in each group were quickly removed and washed with pre-cooled phosphate-buffered saline (PBS) at 4°C. The right atrium was separated and weighed. The right atria of three dogs from each group were randomly fixed in 10% neutral formalin for histomorphological examination. The remaining tissue of the right atrium was placed in a cryopreservation tube and stored at −80°C for qRT-PCR detection. The remaining three atrial tissues of dogs were washed with pre-cooled PBS solution at 4°C and then placed in a cryopreservation tube and stored in the refrigerator at −80°C until the total RNA was extracted for high-throughput sequencing.

2.3. Hematoxylin-Eosin (HE) staining and Masson staining

HE staining and Masson staining were performed using a HE staining kit (Solarbio, Beijing, China) and Masson staining kit (Solarbio, Beijing, China), respectively, on the right atria fixed in 10% neutral formalin. Briefly, the atria were dehydrated using an ethanol gradient, cleared with xylene, and embedded in paraffin. The paraffin-embedded atria were cut into 5-μm sections and dewaxed with xylene, hydrated with an ethanol gradient, and stained with hematoxylin and eosin or Masson trichrome. The sections were observed under an optical microscope (Olympus, Tokyo, Japan) at a magnification of 200×.

2.4. High-throughput sequencing

The total RNA was isolated using Trizol Reagent (Invitrogen, Carlsbad, CA, USA) and resuspended in sterile water for RNA quality control. The RNA purity is suitable for sequencing when the OD260/OD280 value ranges from 1.8 to 2.1. Ribosomal RNAs (rRNAs) were removed using RiboZero rRNA removal kits (Illumina, San Diego, CA, USA). A circRNA sequencing library was constructed using the TruSeq Stranded Total RNA Library Prep Kit (Illumina, San Diego, CA, USA). Library quality control was performed using a BioAnalyzer 2,100 instrument. CircRNA sequencing was performed in the two-terminal mode on an Illumina HiSeq 4,000 sequencer (Illumina, San Diego, CA, USA). Q30 was the quality control standard, and Q30 > 80% indicates good sequencing quality. Cutadapt software (version 1.9.3) was used to remove connectors and obtain high-quality reads for statistical analysis.

For circRNA expression profile screening, clean reads were compared with the dog reference genome (UCSC canFam3) using Bowtie2 software, and, under the guidance of Ensembl Transcriptome GTF files, find_circ software (7) was used for circRNA detection. The number of spliced reads reflects the abundance of circRNAs. The identified circRNAs were annotated using the circBase database (16) according to their genomic locations. In this study, the standardized reads number was used to screen differentially expressed circRNAs between two groups with multiple changes of ≥ 2.0 and $P \leq 0.05$ as the threshold of differential circRNAs. The differentially expressed circRNAs screened from the atrial tissue were analyzed by clustering with fragments per kilobase of exon model per million mapped fragment values using the heatmap2 function of R. A circRNA-miRNA-mRNA network diagram was constructed using Cytoscape software based on the binding information available in online databases, including TargetScan, miRNet, and ENCORI (Starbase V3.0), and the relationship between them was visualized.

2.5. Culture of atrial fibroblasts

The myocardial tissue from the posterior wall of the right atrium was cut into 1 × 1 × 1-cm pieces. After the residual blood was washed with PBS, the pieces were placed in Petri dishes in RPMI-1640 medium. The tissue was digested with 0.125% trypsin, prepared into a suspension, and cultured in a culture flask at 37°C. After 1.5 h of culturing, the medium was replaced with fresh medium every other day. Cells were passaged at the logarithmic growth stage until they reached 90% confluence. The mixture in the culture flask was digested with 0.25% trypsin. When the cells became spherical, PBS was added to stop the digestion. The cell suspension was centrifuged at 1,500 rpm for 5 min, and the cell precipitate was suspended. The cells were passaged at a ratio of 1:2 and cultured in a cell incubator. Two to three generations of fibroblasts were used in subsequent experiments.

2.6. *In vitro* Ang-II induced fibroblast fibrosis

The fibroblasts were maintained in RPMI-1640 (supplemented with 10% fetal bovine serum, 2 mm L-glutamine, 100 U/ml penicillin G, and 100 μg/ml streptomycin) (Invitrogen, Carlsbad, CA, USA) and cultured at 37°C in a humidified incubator with 5% CO_2 (Thermo Fisher, Waltham, MA, USA). Fibroblasts were seeded in a six-well plate at 5×10^4 cells/well. After 12 h of culture, the medium was replaced with the L-15 basic medium without serum and penicillin-streptomycin (Gibco, Carlsbad, CA, USA). After 12 h of culture, 5.0 μmol/L angiotensin II (AngII) (ab120183, Abcam, Waltham, MA, USA) was added to stimulate

the fibroblasts. The cells were collected at various time points for subsequent detection.

2.7. Cell transfection

The cells were seeded in six-well plates at a density of 2×10^6 cells/well, and basic culture medium without penicillin–streptomycin was added to each well. When the cells grew to about 80% confluence, 200 pmol of siRNA or 4 μg of pcDNA3.1+ plasmid (Invitrogen, Carlsbad, CA, USA) plus 10 μl of lipofectamine^{TM}2000 (Invitrogen, Carlsbad, CA, USA) were added to each well. The six-well plate was placed in a cell incubator at 37°C for 6–8 h and then replaced with complete medium. Twenty-four hours after transfection, Ang II was added and the cells were collected after 24 h for subsequent tests.

2.8. Western blot

To each well of six-well plates, 200 μl of prepared cell lysate was added (radio immunoprecipitation assay: phenylmethanesulfonyl fluoride = 100:1) and the plates were shaken slowly at 4°C for 30 min. Protein samples were obtained by centrifugation, quantified using a bicinchoninic acid kit (Sigma-Aldrich, St. Louis, MO, USA), and loaded into sodium dodecyl sulfate polyacrylamide gel electrophoresis mixed with loading buffer. Proteins were transferred from the gels to the polyvinylidene fluoride (PVDF) membranes using a Bio-Rad Trans-Blot Turbo system (Hercules, CA, USA). After transfer, the PVDF membrane was placed in 5% defatted milk powder dissolved in TBST-Tween-20, blocked at room temperature for 1 h, and incubated overnight with primary antibodies. On the second day, the rinsed PVDF membranes were immersed in the secondary antibodies and incubated at room temperature for 1 h. Enhanced chemiluminescence was added to the PVDF membrane and developed and photographed using a Gel Imaging System.

TABLE 1 Primary and secondary antibodies used in western blot.

Primary antibodies	Dilution	Solvent
Rabbit Anti-Collagen I antibody (ab233080)	1:1,000	TBST
Rabbit Anti-Collagen III antibody (ab7778)	1:5,000	TBST
Rabbit anti-MMP2 (ab97779)	1:2,000	TBST
Rabbit anti-MMP9 (ab219372)	1:1,000	TBST
Goat anti-α-SMA (ab21027)	1:1,000	TBST
Rabbit anti-TIMP1 (ab216432)	1:1,000	TBST
Rabbit anti-POSTN (ab92460)	1:1,000	TBST
Rabbit anti-Bax (ab104156)	1:1,000	TBST
Mouse anti-Bcl2 (ab692)	1:1,000	TBST
Rabbit anti-Caspase3 (ab13874)	1:500	TBST
Mouse anti-β-actin (ab8226)	1:5,000	TBST
Secondary antibodies	**Dilution**	**Solvent**
Goat anti-rabbit IgG-HRP (ab7090)	1:5,000	TBST
Goat anti-mouse IgG-HRP (ab97040)	1:5,000	TBST
Donkey anti-goat IgG-HRP (ab7125)	1:5,000	TBST

Detailed information on the primary and secondary antibodies is provided in Table 1.

2.9. qRT-PCR

To each well of six-well plates, 1 ml of Trizol reagent (Invitrogen, Carlsbad, CA, USA) was added and lysed for 30 min. Extracted RNA samples were dissolved in sterile water. RNA purity was detected using a NanoDrop ND-2000 instrument, and the OD260/OD280 value ranged from 1.8 to 2.1, indicating that the purity of the RNA was sufficient. RNA was reverse-transcribed into cDNA using a FastQuant RT Kit (with gDNase) (KR106, Tiangen, Beijing, China). The cDNA product served as a template for the PCR using the SYBR Premix Ex Taq II kit (Takara, Kyoto, Japan) on an Applied Biosystems^{TM} 7,500 Fast Dx Real-Time PCR (Thermo Fisher, Waltham, MA, USA). The primer sequences are listed in Table 2.

2.10. Cell scratch test

One day before transfection, cells were seeded into six-well plates at a density of 2×10^6 cells/well and transfected with siRNA or an overexpressed plasmid when the cell density

TABLE 2 Primers used in real-time PCR.

Primer	Species	Sequence (5′-3′)	Tm (°C)
GFI	Dog	F: CGTCATTAACATCGGCATTG	58.0
		R: TGGTCTCCTGGGTGGTAAAG	
cfa-circ001021	Dog	F: GATTATTAGGACACAACGGAGC	58.0
		R: CTGGCAATAATGACTGGTTTCT	
cfa-circ002168	Dog	F: ACCAACTCAGAGTGGGTAA	58.0
		R: GGTCTGAATGATCTGTGGTG	
cfa-circ002203	Dog	F: ATCACATGAACGTTGTCCG	58.0
		R: TGATGGCAACAGCCCTAA	
cfa-circ009305	Dog	F: AACCAAGTACCAAGTGAAGAC	58.0
		R: CAATCATCTGTTCAGGAGTAGT	
Collagen I	Dog	F: TTCAGCTTTGTGGACCTCCG	60.0
		R: GGGTTTCCATACGTCTCGGT	
Collagen III	Dog	F: GTATGAAAGGACATAGAGGCTTTGA	59.0
		R: ACGAGCACCATCGTTACCTC	
MMP2	Dog	F: GTGCTCCACCACCTACAACT	60.0
		R: TGGAAGCGGAACGGGAACT	
MMP9	Dog	F: TCGACGTGAAGACGCAGAC	60.0
		R: TCACACGCCAGTAGAAGCG	
α-SMA	Dog	F: GAATGCTACCACAGCCCTGA	59.0
		R: CCACAACGCAGGTTTCTCTC	
TIMP1	Dog	ACTTGCACAGGTCCCAGA	58.0
		GGGATGGATGAACAGGTAAACA	
POSTN	Dog	TCTCTACTCTTGCTGGTTGTTGT	58.0
		TTTCCTTCCACAGATGGCAC	
Bax	Dog	GTGAGGTCTTCTTCCGAGTGG	60.0
		TCCAGTGTCCAGCCCATGA	
Bcl2	Dog	TCATGTGTGTGGAGAGCGTC	60.0
		TCAAACAGAGGCTGCATGGT	
Caspase3	Dog	CCTGCCGAGGTACAGAACT	59.0
		GCGTATAGTTTCAGCATCGCAC	

reached approximately 80% influence. After culturing for another 24 h, the cells were scratched in a straight line at an angle perpendicular to the bottom of the culture plate. PBS preheated at 37°C was used to infiltrate the plate and remove the cell debris floating on the cell surface, and the cells were then placed under a microscope to record the size of the scratch space by photography. The basic medium was replaced with Ang II medium. The cells were cultured at 37°C for 24 h. The migration of cells in each well was photographed. At least three images were taken for each group of cells, and "Image-Pro Plus 6.0" software was used to calculate the scratch area and perform statistical analysis.

2.11. Immunofluorescence staining

The cells were seeded in glass dishes and transfected with siRNA or an overexpressed plasmid when the cell density reached approximately 80%influence. After culturing for another 48 h, the cells were washed with PBS, fixed with pre-cooled methyl alcohol for 10 min, and treated with 0.5% Triton X-100 for 20 min. Cells were blocked with goat serum for 30 min and incubated with primary antibody and Alexa Fluor®647-labeled IgG(H + L)/fluorescein isothiocyanates (FITCs) (Beyotime, Shanghai, China). The cells were counterstained with 4′,6-diamidino-2-phenylindole (DAPI, Beyotime, Shanghai, China). Fluorescent staining was performed and images were captured using a confocal microscope (Leica, Wetzlar, Germany).

2.12. Cell apoptosis

The fibroblasts were digested with trypsin and centrifuged at 3,000 rpm for 10 min. After adding pre-cooled PBS to the supernatant, the cells were centrifuged again at 1,000 rpm for 10 min. Then, binding buffer, Annexin V-FITC, and 7-Aminoactinomycin D were added to an Annexin V-FITC Apoptosis Detection Kit (BD Sciences, Franklin Lake, NJ, USA) in sequence and placed in the dark for 30 min at 4°C. Cell apoptosis was assessed within 1 h using a flow cytometer (BD FACSverse, BD Sciences, Franklin Lake, NJ, USA).

2.13. Statistical analysis

Statistical analysis was performed using SPSS 22.0 and GraphPad Prism (version 6.0; Boston, MA, USA), and Adobe Photoshop CS5 (San Jose, CA, USA) was used for plotting. Measurement data were expressed as the mean ± standard deviation, and comparisons between groups were performed using the independent samples *t*-test. $P < 0.05$ indicates a statistically significant difference.

3. Results

3.1. Establishment of rapid atrial pacing model

ECG showed that the sinus *P* waves disappeared and were replaced by fibrillation waves with varying amplitudes and frequencies (**Supplementary Figure S1**). In addition, HE staining revealed obvious myocardial fractures, disordered atrial myocytes, abnormal cell morphology, and increased intercellular spacing in the pacing group (**Figure 1A**). Masson staining indicated clear blue collagen deposition in the atrial myocyte space of the pacing group. The collagen volume fraction was significantly higher in the pacing group than that in the control group ($P < 0.05$; **Figure 1B**). These results indicate the successful establishment of a rapid atrial pacing model.

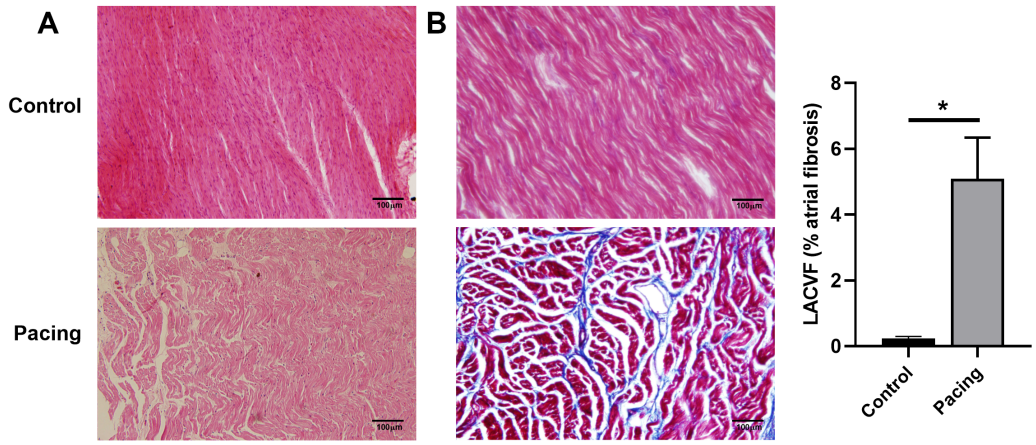

FIGURE 1
Establishment of a rapid atrial pacing model in dogs. (A) HE staining of the right atria from control and pacing group dogs. Clear myocardial fractures, disordered atrial myocytes, abnormal cell morphology, and increased intercellular space in the pacing group were observed. (B) Masson staining of the right atria from control and pacing group dogs. Collagen volume fraction was calculated. Data are expressed as the mean ± standard deviation, and comparisons between groups are performed using the independent samples *t*-test. $n = 6$, * indicates $P < 0.05$.

3.2. CircRNA expression profiles in the right atria of the rapid atrial pacing model

A total of 15,990 circRNAs were detected using high-throughput sequencing. According to the positions of the adjacent coding RNAs, the circRNAs obtained by sequencing could be roughly classified into five categories: exon circRNAs (11,060, 69%), justice overlap circRNAs (3,025, 19%), intergenic circRNAs (720, 5%), antisense circRNAs (673, 4%), and intron circRNAs (512, 3%) (**Figure 2A**). 15,990 circRNAs are widely distributed in all chromosomes including the mitochondrial genome (**Figure 2B**). The length of the circRNA exons ranged from 79 to 99,731 nucleotides, and that of most circRNAs (89%) ranged from 200 to 2,000 nucleotides. Only 1% of the circRNAs had lengths of over 5,000 nucleotides (**Figure 2C**). The analysis of different circRNA expression profiles showed 146 differentially expressed circRNAs in the pacing group compared with the control group, including 106 upregulated and 40 downregulated circRNAs (**Figure 2D**). Heatmap analysis showed that the 146 differentially expressed circRNAs could distinguish the samples in the control and pacing groups, suggesting the reliability of the differentially expressed circRNAs (**Figure 2E**).

3.3. Prediction of circRNA-miRNA-mRNA interactions

We selected inflammation-related mRNAs from the literature (17–19) and constructed a ceRNA network between the top-25 differentially expressed circRNAs and inflammation-related mRNAs. Based on the abundance of binding miRNAs, free energy level, and size of the ceRNA score, several circRNAs with significant binding abilities were selected as representatives to draw the network diagram (**Figure 3A**), where a single circRNA interacted with different miRNAs in a family and different circRNAs also acted on the same miRNA (**Figure 3A**). qRT-PCR verification of the expression levels of the four circRNAs in the ceRNA network showed that, compared with the control group, the expression levels of three circRNAs were significantly upregulated in the pacing group (**Figure 3B**), including

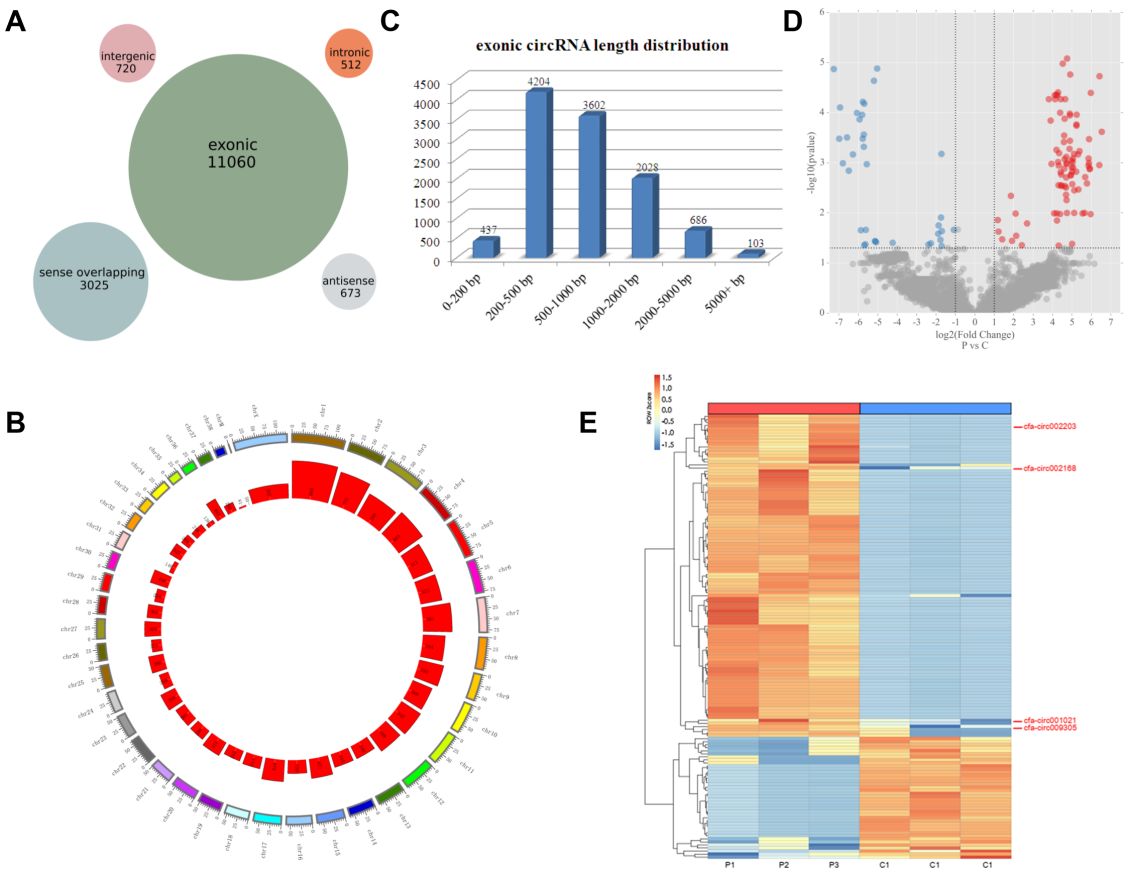

FIGURE 2
CircRNA expression profiles detected by high-throughput sequencing. (**A**) Number of circRNAs in the five classifications. (**B**) Distribution of circRNAs on the chromosome. (**C**) Number of exon circRNAs at each length interval. (**D**) Volcano plot of differentially expressed circRNAs (red plot represents upregulated circRNAs; blue plot represented downregulated circRNAs). (**E**) Heatmaps of the 146 differentially expressed circRNAs. The four circRNAs in the ceRNA network are indicated.

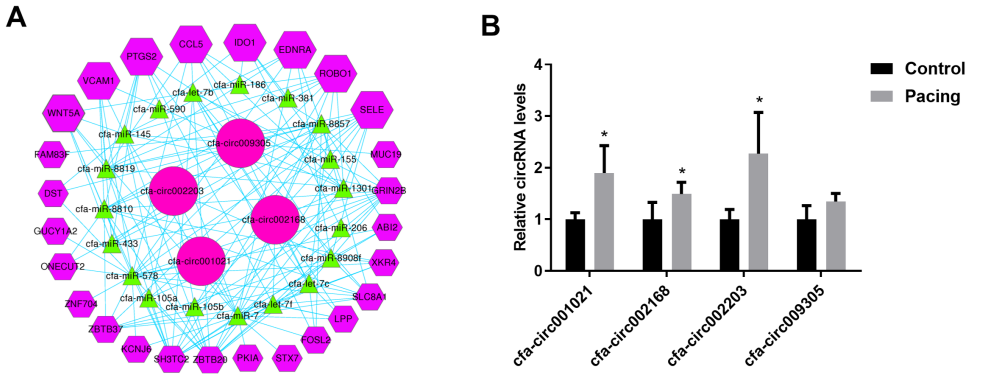

FIGURE 3
Prediction of circRNA-miRNA-mRNA interactions. (A) CeRNA network of circRNA-miRNA-mRNA. (B) Validation of four circRNAs in the ceRNA network by qRT-PCR. Compared with the control group, the expression levels of three circRNAs were significantly up-regulated in the pacing group. All experiments were conducted in triplicate. Data are expressed as the mean ± standard deviation, and comparisons between groups are performed using the independent samples *t*-test. $n = 6$, $^*P < 0.05$.

cfa-circ002203, cfa-circ002168, and cfa-circ001021. Cfa-circ002203, with the highest fold change, was selected to explore whether it was associated with fibrosis in atrial fibroblasts induced by Ang II *in vitro*.

3.4. Validation of cfa-circ002203 silenced and overexpressed cell line construction in Ang II-induced fibrosis

Atrial fibroblasts may play a key role in myocardial fibrosis, and their proliferation leads to collagen remodeling. Therefore, we examined the effect of cfa-circ002203 on atrial fibroblasts. In Ang II-treated fibroblasts, the expression of cfa-circ002203 was significantly upregulated at time dependent manner (Figure 4A). Atrial fibroblasts with cfa-circ002203 silencing or overexpression were generated and verified by qRT-PCR. Among the three siRNAs of cfa-circ002203, si-cfa-circ002203-3 had the best silencing effect, with a 90% reduction (Figure 4B). The transfection of the cfa-circ002203-pcDNA3.1$^+$ plasmid into atrial myofibroblasts significantly upregulated the cfa-circ002203 level (Figure 4C).

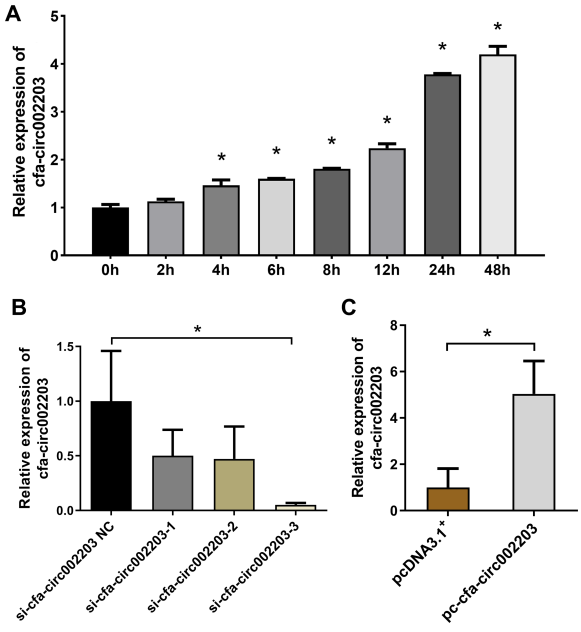

FIGURE 4
Cfa-circ002203 expression in atrial fibroblasts after cfa-circ002203 silencing or overexpression vector transfection. (A) Expression of cfa-circ002203 detected by qRT-PCR was significantly increased after AngII treatment with a time-dependent manner. (B) qRT-PCR showing that the cfa-circ002203 expression levels were significantly decreased after 48 h transfection of three siRNAs. (C) qRT-PCR showing that the cfa-circ002203 expression level was significantly increased after 48 h of pc-circRNA vector transfection. All experiments were conducted in triplicate. $^*P < 0.05$.

3.5. Cfa-circ002203 promoted the expression of inflammatory factors in atrial fibroblasts

We collected supernatants of atrial fibroblasts transfected with si-cfa-circ002203 and overexpression vector, and then detected the changes in the proinflammatory factors interleukin (IL)-6, tumor necrosis factor (TNF)-α, monocyte chemoattractant protein-1 (MCP-1), and IL-1β. The results showed that the levels of IL-6, TNF-α, MCP-1, and IL-1β decreased significantly after transfection with si-cfa-circ002203 (Figures 5A–D), while they increased significantly after transfection with cfa-circ002203 overexpression vector (Figures 5A–D), indicating that cfa-circ002203 affected the secretion of inflammatory factors in myofibroblasts fibrosis induced by Ang II.

3.6. Cfa-circ002203 promoted fibroblast fibrosis and inhibited apoptosis

In fibroblast fibrosis induced by Ang II, we detected cells using a confocal laser microscope and found that the expression of α-SMA decreased significantly after the cells were transfected with si-cfa-circ002203, while it was significantly upregulated after transfection with the cfa-circ002203 overexpression vector (Figure 6).

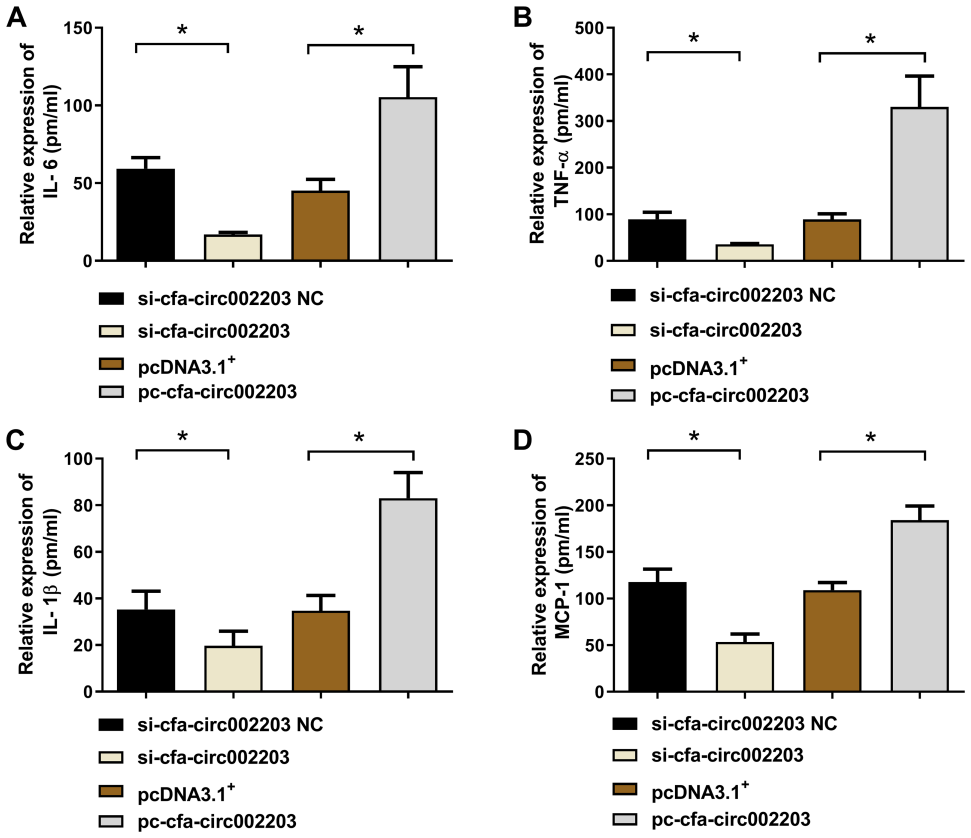

FIGURE 5
Expression levels of IL-6 (A), TNF-α (B), IL-1β (C), and MCP-1 (D) measured by ELISA after the silencing and overexpression of cfa-circ002203 in atrial fibroblasts. Compared with si-circRNA NC (negative control), the expression levels of IL-6, TNF-α, IL-1β, and MCP-1 were significantly decreased, while their levels were significantly increased after transfecting pc-circRNA compared with the empty vector, pcDNA3.1$^+$. pm/ml, pmol/ml. *$P < 0.05$.

Western blotting and qRT-PCR were used to detect the expression of the fibrosis indicators collagen I, collagen III, MMP2, MMP9, α-SMA, TIMP1 and POSTN as well as the apoptosis factors Bax, Bcl-2, and Caspase 3. The results showed that the expression of fibrosis indicators was significantly decreased after transfection with si-cfa-circ002203 compared with that in the control (Figures 7A,B,D) and was significantly upregulated after transfection with the si-cfa-circ002203 overexpression vector (Figures 7A,C,E). These results suggest that cfa-circ002203 might be important in promoting the differentiation of fibroblasts into myofibroblasts. In addition, the expression of Bax and Caspase3 was significantly upregulated after transfection with si-cfa-circ002203 compared with that in the control group (Figures 7A,B,D), while it was significantly decreased when cfa-circ002203 was overexpressed (Figures 7A,C,E). The expression of Bcl-2 showed the opposite trend. These results suggest that cfa-circ002203 represses fibroblast apoptosis.

3.7. Effects of cfa-circ002203 on the proliferation and migration of fibroblasts

A cell scratch assay was performed to detect fibroblast migration after the silencing and overexpression of cfa-circ002203, and the CCK8 assay was used to detect fibroblast proliferation. The results showed that, 24 h after the cell scratching experiment, the mobility of the si-cfa-circ002203 group was lower than that of the si-cfa-circ002203 NC (negative control) group and increased after the overexpression of cfa-circ002203 (Figures 8A,B). The CCK8 results showed that, compared with the NC group, the proliferative ability of fibroblasts was weakened after transfection with si-cfa-circ002203, and the proliferative ability of cfa-circ002203-overexpressed fibroblasts was significantly increased (Figure 8C).

3.8. Effects of cfa-circ002203 on fibroblast apoptosis

Fibroblasts were stained with Annexin V/PI, and cell apoptosis was measured by flow cytometry. Compared with the control group, si-cfa-circ002203 increased the number of late apoptotic cells in Q2 and decreased the number of living cells in Q1 ($P < 0.05$). In contrast, the overexpression of cfa-circ002203 inhibited fibroblast apoptosis ($P < 0.05$; Figure 9).

4. Discussion

The regulatory and functional roles of circRNAs in the progression of heart disease have been proposed (8, 20) and their

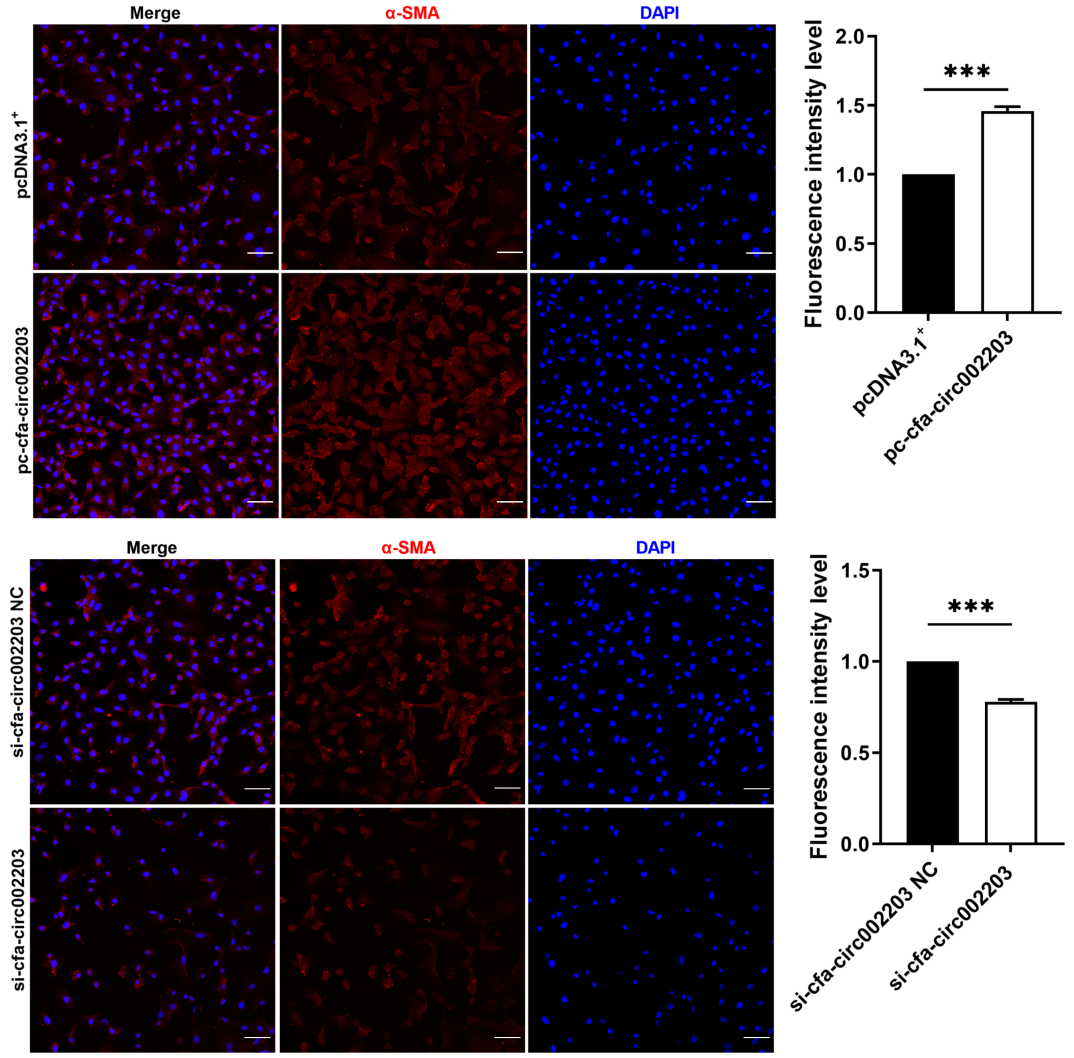

FIGURE 6
Immunofluorescence staining of α-SMA expression in atrial fibroblasts transfected with si-cfa-circ002203 or overexpression vector. α-SMA was labelled with Alexa Fluor®647-labeled IgG(H + L)/FITCs and cell nuclei were stained with DAPI. All experiments were conducted in triplicate. Scale bar, 20 μm. Data are expressed as the mean ± standard deviation, and comparisons between groups are performed using the independent samples *t*-test. ***$P < 0.001$.

regulatory role in AF-induced fibrosis is the focus of the present study. This is the first study to demonstrate that cfa-circ002203 plays an important role in AF-induced atrial fibrosis and is critical for the progression of atrial fibroblast inflammation and fibrosis.

Fibrosis is part of the pathological remodeling of atrial tissue and clinical cardiac disease. Although corresponding treatments have been adopted according to the different mechanisms of AF, there is currently no effective treatment for atrial fibrosis, and the prevention and reversal of atrial fibrosis is still a major problem in medicine (6). CircRNA is a potential target for preventing or even reversing the progression of tissue fibrosis, because previous studies have reported the role of circRNAs in inhibiting myocardial fibrosis. For instance, circRNA_000203 regulates the expression of fibrosis-associated genes in cardiac fibroblasts (21). circHIPK3 and mmu_circ_0005019 prevent the proliferation and migration of cardiac fibroblasts (11, 22). These data reveal the function of circRNAs in influencing the expression of fibroblast-related genes and the phenotypic change from fibroblasts to fibrotic phenotypes. In our experiments using high-throughput sequencing of fibrotic atrial tissue in an AF dog model, we found that 15,990 circRNAs were widely distributed in all chromosomes, and 146 circRNAs were dysregulated in AF-induced fibrosis, indicating the potential of circRNAs to participate in AF and AF-induced myocardial fibrosis.

Although circRNAs have been suggested to perform various biological functions, such as acting as miRNAs or protein inhibitors ("sponges"), regulating protein functions, or self-translation (23), their regulatory networks with miRNAs and mRNAs are widely accepted to play key roles in disease progression, including cancer and immune system, metabolic, and endocrine diseases (24–27). This also applies to the molecular mechanisms underlying cardiovascular diseases (28, 29). Based on the circRNA-miRNA-mRNA network, we

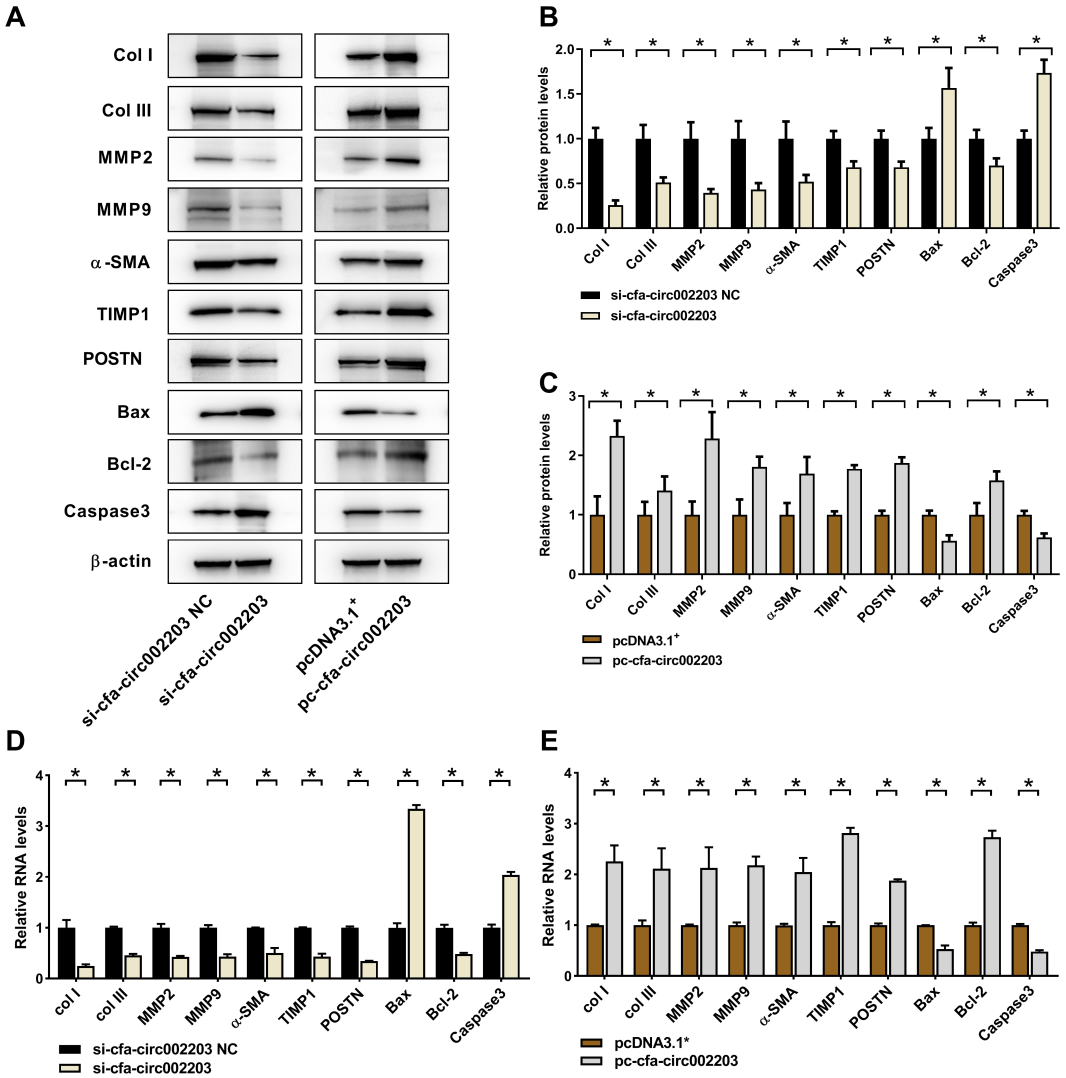

FIGURE 7
Protein and mRNA expression levels of fibrosis- and apoptosis-associated proteins in atrial fibroblasts transfected with cfa-circ002203 silencing or overexpression vectors. (A) Representative western blotting images. (B,C) Relative expression of proteins calculated from three independent samples in cfa-circ002203-silencing and cfa-circ002203-overexpressing cells. (D,E) Relative expression of fibrosis- and apoptosis-associated genes detected by qRT-PCR. Data are expressed as the mean ± standard deviation, and comparisons between groups are performed using the independent samples *t*-test. $n = 3$, $^*P < 0.05$.

screened circRNAs that might have affected the expression of atrial fibrosis-related mRNA and verified them in the atrial tissues of the AF dog model. Finally, cfa-circ002203 was selected as a candidate gene for the further analysis of the involvement of circRNAs in fibroblast fibrosis. Cfa-circ002203 is located on chr20:33297388–33298499+ in the dog genome, and its function has not yet been elucidated. Therefore, we investigated the role of cfa-circ002203 in Ang II-induced fibrosis.

First, cfa-circ002203 is thought to be associated with fibroblast inflammation, which is an important factor in the occurrence, maintenance, and recurrence of AF (30). In atrial tissue from patients with AF, there was a significant, positive correlation between the serum proinflammatory cytokine TNF-α and IL-6 levels and the collagen volume fraction (31). Fibrosis is a pathological process of AF substrate formation and is affected by inflammation (32). Our data showed that the Ang-II-induced expressions of proinflammatory cytokines IL-6, TNF-α, IL-1β, and chemokine MCP-1 in fibroblasts changed, along with cfa-circ002203 silencing and overexpression. This led to the interesting speculation that cfa-circ002203 is an active regulator of the inflammatory activation of fibroblasts.

Atrial fibrosis entailing fibrous collagen types I and III is a typical characteristic of AF. Collagen is a relatively hard material with high tensile strength, and even small changes in its quality, indicated by its concentration, proportion, and degree of crosslinking, have been proven to significantly affect cardiac functional properties, resulting in diastolic and contractile properties (33). Our results showed that the expression of collagen types I and III significantly decreased in the cfa-circ002203-silenced fibroblasts, and were up-regulated in cfa-circ002203-overexpressed fibroblasts. Furthermore, we examined the expression of MMP-2 and MMP-9, proteins in fibrotic fibroblasts that are essential for normal and pathological tissue

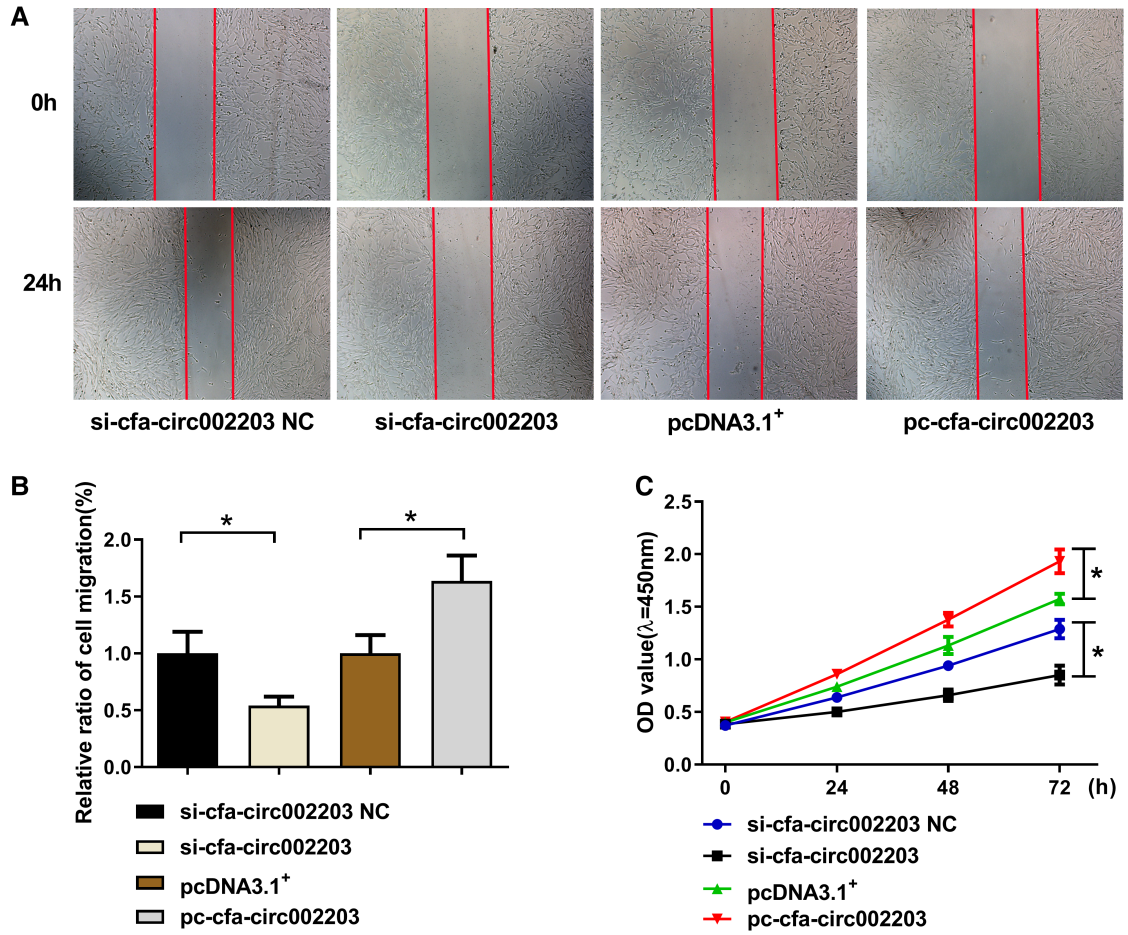

FIGURE 8
Effects of cfa-circ002203 on the proliferation and migration of fibroblasts. (A,B) The cell scratch assay was used to detect the migration of fibroblasts after silencing and overexpressing cfa-circ002203. The red lines depict the edges of cells. The mobility of the si-cfa-circ002203 group was lower than that of the si-cfa-circ002203 NC group and increased after the overexpression of cfa-circ002203. (C) CCK8 was used to detect the proliferation of fibroblasts. All experiments were conducted in triplicate. *$P < 0.05$. Compared with the NC group, the proliferation ability of fibroblasts was weakened after transfecting with si-cfa-circ002203, and the proliferation ability of cfa-circ002203-overexpressing fibroblasts was significantly increased.

remodeling, by controlling the degree of ECM remodeling (34). Our data showed that the silencing or overexpression of cfa-circ002203 promoted the downregulation and upregulation of MMP-2 and MMP-9 expression, respectively. It Cfa-circ002203 appears to function in the ECM remodeling of fibroblasts.

Additionally, we verified the role of cfa-circ002203 in the transformation of fibroblasts into activated myofibroblasts. The transformation from fibroblasts to myofibroblasts occurs during the late proliferative stage and is characterized by the expression of SMA (35). Our data suggest that α-SMA expression and cell migration induced by Ang II changed with the silencing or overexpression of cfa-circ002203. Collectively, cfa-circ002203 exerts an active function on the expression levels of the remarkable proteins of fibrotic fibroblasts, including collagen I, collagen III, MMP2, MMP9, and α-SMA, and is considered as a promotor of the fibrosis of fibroblasts.

We also examined the effect of cfa-circ002203 on apoptosis. Western blotting showed that the expression of Bax and Caspase3 was significantly upregulated after transfection with si-cfa-circ002203, whereas it was significantly decreased when cfa-circ002203 was overexpressed compared with the control group. The expression of Bcl-2 showed the opposite trend. In addition, flow cytometry showed that the overexpression of cfa-circ002203 decreased the number of late apoptotic cells in Q2 and increased the number of living cells in Q1 compared with the control group ($P < 0.05$). AF may result in cardiac apoptosis by downregulating protective mechanisms and activating proapoptotic pathways. Xu et al. identified increased levels of BAX and lower levels of BCL-2 in AF and determined that the protein expression of BAX and BCL-2 was correlated with the frequency of apoptosis in AF (36). These results suggest that cfa-circ002203 promotes the apoptosis of fibroblasts and may serve as a target for the treatment of AF.

This study had some limitations. First, the role of cfa-circ002203 on cell proliferation was not checked by EDU incorporation assay. Second, the expression of circRNA_002203 over the timecourse of the proliferation assay should also be checked. Therefore, further research is required to investigate the role of circ002203 in fibrosis.

In summary, the results of the present study suggest that several circRNAs exhibit aberrant expression patterns in canine AF-induced

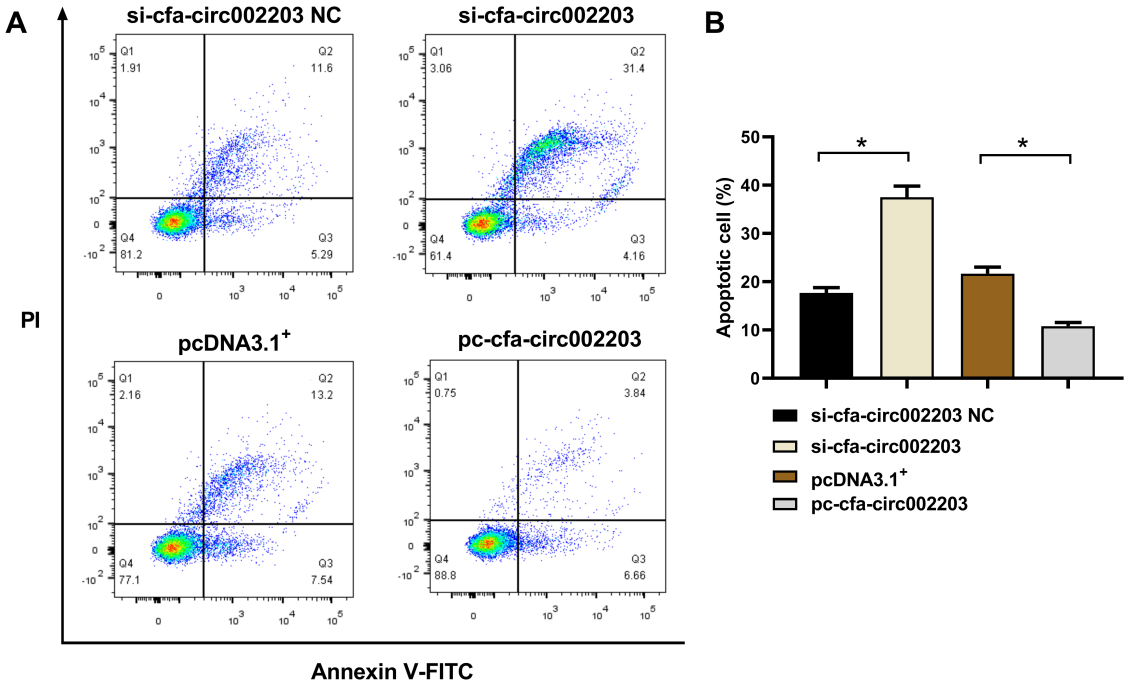

FIGURE 9
Effects of cfa-circ002203 on fibroblast apoptosis detected by flow cytometry. (A) Representative picture of fibroblast apoptosis detected by flow cytometry. (B) Quantitative analysis of apoptotic cells in each group. All experiments were conducted in triplicate. Compared with the control group, si-cfa-circ002203 increased the number of late apoptotic cells in Q2 and decreased the number of living cells in Q1. In contrast, the overexpression of cfa-circ002203 inhibited fibroblast apoptosis. *$P < 0.05$.

fibrosis. Among these circRNAs, cfa-circ002203 was closely associated with fibrosis, inflammatory activation, and fibroblast apoptosis. The findings of this study strengthen the role of circRNAs in AF-induced fibrosis in dogs and provide a perspective on the disease mechanisms and therapeutic targets for AF.

Data availability statement

The original contributions presented in the study are publicly available. This data can be found here: https://www.ncbi.nlm.nih.gov/geo/, GSE225086.

Ethics statement

The animal study was reviewed and approved by the Laboratory Animal Ethics Committee of the Institute of Radiation Medicine, Chinese Academy of Medical Sciences (approval number: IRM-DWLL-2019018).

Author contributions

All authors contributed to the study conception and design. Conception and design of the research: XL and TL; Acquisition of data: WS, TG, and RC; Analysis and interpretation of data: SM and WW; Statistical analysis: HW, YL, and FS; Drafting the manuscript: XL and WS; Obtaining funding: XL, WW, WS, SM, and XL, Revision of manuscript for important intellectual content: TL and XL. All authors contributed to the article and approved the submitted version.

Funding

This work was supported by the National Natural Science Foundation of China Youth Science Foundation Project [No. 81700304, No. 81900314 and No. 82000313]; Tianjin Health Research Project [No. TJWJ2023MS007]; The Scientific Research Fund Project of Key Laboratory of Second Hospital of Tianjin Medical University [No. 2019ZDSYS11, No. 2019ZDSYS10, No. 2019ZDSYS07]; The Research Fund for Central Laboratory of Second Hospital of Tianjin Medical University [No. 2020ydey05]; The Science and Technology Development Fund of Tianjin Education Commission for Higher Education [No. 2020KJ168] and Tianjin Key Medical Discipline (Specialty) Construction Project [TJYXZDXK-029A].

Conflict of interest

The authors declare that the research was conducted in the absence of any commercial or financial relationships that could be construed as a potential conflict of interest.

Handling editor has stated in acceptance email: “Please could you adjust the title of the manuscript whilst this is going through the proof process” (Case 10930722).

Publisher's note

Supplementary material

The Supplementary Material for this article can be found online at: https://www.frontiersin.org/articles/10.3389/fcvm.2023.1110707/full#supplementary-material

SUPPLEMENTARY FIGURE S1
ECG of the body surface (III lead) and epicardium (LAA, left atrial appendage; RAA, right atrial appendage; LLA, low left atrial; LRA, low right atria; HLA, high left atria; HRA, high right atria).

References

1. Kirstein B, Neudeck S, Gaspar T, Piorkowski J, Wechselberger S, Kronborg MB, et al. Left atrial fibrosis predicts left ventricular ejection fraction response after atrial fibrillation ablation in heart failure patients: the Fibrosis-HF study. *Europace*. (2020) 22(12):1812–21. doi: 10.1093/europace/euaa179

2. Sohns C, Marrouche NF. Atrial fibrillation and cardiac fibrosis. *Eur Heart J*. (2020) 41(10):1123–31. doi: 10.1093/eurheartj/ehz786

3. Xintarakou A, Tzeis S, Psarras S, Asvestas D, Vardas P. Atrial fibrosis as a dominant factor for the development of atrial fibrillation: facts and gaps. *Europace*. (2020) 22(3):342–51. doi: 10.1093/europace/euaa009

4. Maesen B, Verheule S, Zeemering S, La Meir M, Nijs J, Lumeij S, et al. Endomysial fibrosis, rather than overall connective tissue content, is the main determinant of conduction disturbances in human atrial fibrillation. *Europace*. (2022) 24(6):1015–24. doi: 10.1093/europace/euac026

5. Polyakova V, Miyagawa S, Szalay Z, Risteli J, Kostin S. Atrial extracellular matrix remodelling in patients with atrial fibrillation. *J Cell Mol Med*. (2008) 12(1):189–208. doi: 10.1111/j.1582-4934.2008.00219.x

6. Nattel S. Molecular and cellular mechanisms of atrial fibrosis in atrial fibrillation. *JACC Clin Electrophysiol*. (2017) 3(5):425–35. doi: 10.1016/j.jacep.2017.03.002

7. Memczak S, Jens M, Elefsinioti A, Torti F, Krueger J, Rybak A, et al. Circular RNAs are a large class of animal RNAs with regulatory potency. *Nature*. (2013) 495 (7441):333–8. doi: 10.1038/nature11928

8. Devaux Y, Creemers EE, Boon RA, Werfel S, Thum T, Engelhardt S, et al. Circular RNAs in heart failure. *Eur J Heart Fail*. (2017) 19(6):701–9. doi: 10.1002/ejhf.801

9. Sun C, Ni M, Song B, Cao L. Circulating circular RNAs: novel biomarkers for heart failure. *Front Pharmacol*. (2020) 11:560537. doi: 10.3389/fphar.2020.560537

10. Wang K, Long B, Liu F, Wang JX, Liu CY, Zhao B, et al. A circular RNA protects the heart from pathological hypertrophy and heart failure by targeting MiR-223. *Eur Heart J*. (2016) 37(33):2602–11. doi: 10.1093/eurheartj/ehv713

11. Ni H, Li W, Zhuge Y, Xu S, Wang Y, Chen Y, et al. Inhibition of Circhipk3 prevents angiotensin II-induced cardiac fibrosis by sponging MiR-29b-3p. *Int J Cardiol*. (2019) 292:188–96. doi: 10.1016/j.ijcard.2019.04.006

12. Zhou B, Yu JW. A novel identified circular RNA, circrna_010567, promotes myocardial fibrosis via suppressing MiR-141 by targeting Tgf-β1. *Biochem Biophys Res Commun*. (2017) 487(4):769–75. doi: 10.1016/j.bbrc.2017.04.044

13. Wu N, Xu J, Du WW, Li X, Awan FM, Li F, et al. YAP circular RNA, CircYAP, attenuates cardiac fibrosis via binding with tropomyosin-4 and gamma-actin decreasing actin polymerization. *Mol Ther*. (2021) 29(3):1138–50. doi: 10.1016/j.ymthe.2020.12.004

14. Shangguan W, Liang X, Shi W, Liu T, Wang M, Li G. Identification and characterization of circular RNAs in rapid atrial pacing dog atrial tissue. *Biochem Biophys Res Commun*. (2018) 506(1):1–6. doi: 10.1016/j.bbrc.2018.05.082

15. Panda AC. Circular RNAs act as MiRNA sponges. *Adv Exp Med Biol*. (2018) 1087:67–79. doi: 10.1007/978-981-13-1426-1_6

16. Glazar P, Papavasileiou P, Rajewsky N. Circbase: a database for circular RNAs. *RNA*. (2014) 20(11):1666–70. doi: 10.1261/rna.043687.113

17. Vezzani A, Balosso S, Ravizza T. Neuroinflammatory pathways as treatment targets and biomarkers in epilepsy. *Nat Rev Neurol*. (2019) 15(8):459–72. doi: 10.1038/s41582-019-0217-x

18. Zeemering S, Isaacs A, Winters J, Maesen B, Bidar E, Dimopoulou C, et al. Atrial fibrillation in the presence and absence of heart failure enhances expression of genes involved in cardiomyocyte structure, conduction properties, fibrosis, inflammation, and endothelial dysfunction. *Heart Rhythm*. (2022) 19(12):2115–24. doi: 10.1016/j.hrthm.2022.08.019

19. Wang L, Duan C, Wang R, Chen L, Wang Y. Inflammation-Related genes and immune infiltration landscape identified in kainite-induced temporal lobe epilepsy based on integrated bioinformatics analysis. *Front Neurosci*. (2022) 16:996368. doi: 10.3389/fnins.2022.996368

20. Wang Y, Liu B. Circular RNA in diseased heart. *Cells*. (2020) 9(5):1240. doi: 10.3390/cells9051240

21. Tang CM, Zhang M, Huang L, Hu ZQ, Zhu JN, Xiao Z, et al. Circrna_000203 enhances the expression of fibrosis-associated genes by derepressing targets of miR-26b-5p, Col1a2 and CTGF, in cardiac fibroblasts. *Sci Rep*. (2017) 7:40342. doi: 10.1038/srep40342

22. Wu N, Li C, Xu B, Xiang Y, Jia X, Yuan Z, et al. Circular RNA mmu_circ_0005019 inhibits fibrosis of cardiac fibroblasts and reverses electrical remodeling of cardiomyocytes. *BMC Cardiovasc Disord*. (2021) 21(1):308. doi: 10.1186/s12872-021-02128-w

23. Patop IL, Wust S, Kadener S. Past, present, and future of circRNAs. *EMBO J*. (2019) 38(16):e100836. doi: 10.15252/embj.2018100836

24. Liang ZZ, Guo C, Zou MM, Meng P, Zhang TT. Circrna-miRNA-mRNA regulatory network in human lung cancer: an update. *Cancer Cell Int*. (2020) 20:173. doi: 10.1186/s12935-020-01245-4

25. Zhang J, Liu Y, Shi G. The circRNA-miRNA-mRNA regulatory network in systemic lupus erythematosus. *Clin Rheumatol*. (2021) 40(1):331–9. doi: 10.1007/s10067-020-05212-2

26. Yang F, Chen Y, Xue Z, Lv Y, Shen L, Li K, et al. High-throughput sequencing and exploration of the LncRNA-circRNA-miRNA-mRNA network in type 2 diabetes mellitus. *Biomed Res Int*. (2020) 2020:8162524. doi: 10.1155/2020/8162524

27. Zhang Z, Yue L, Wang Y, Jiang Y, Xiang L, Cheng Y, et al. A circRNA-miRNA-mRNA network plays a role in the protective effect of diosgenin on alveolar bone loss in ovariectomized rats. *BMC Complement Med Ther*. (2020) 20(1):220. doi: 10.1186/s12906-020-03009-z

28. Zhang F, Zhang R, Zhang X, Wu Y, Li X, Zhang S, et al. Comprehensive analysis of CircRNA expression pattern and circRNA-miRNA-mRNA network in the pathogenesis of atherosclerosis in rabbits. *Aging (Albany NY)*. (2018) 10(9):2266–83. doi: 10.18632/aging.101541

29. Su Q, Lv X. Revealing new landscape of cardiovascular disease through circular RNA-MiRNA-MRNA axis. *Genomics*. (2020) 112(2):1680–5. doi: 10.1016/j.ygeno.2019.10.006

30. Guo Y, Lip GY, Apostolakis S. Inflammation in atrial fibrillation. *J Am Coll Cardiol*. (2012) 60(22):2263–70. doi: 10.1016/j.jacc.2012.04.063

31. Qu YC, Du YM, Wu SL, Chen QX, Wu HL, Zhou SF. Activated nuclear factor-kappab and increased tumor necrosis factor-alpha in atrial tissue of atrial fibrillation. *Scand Cardiovasc J*. (2009) 43(5):292–7. doi: 10.1080/14017430802651803

32. Harada M, Van Wagoner DR, Nattel S. Role of inflammation in atrial fibrillation pathophysiology and management. *Circ J*. (2015) 79(3):495–502. doi: 10.1253/circj.CJ-15-0138

33. Baicu CF, Stroud JD, Livesay VA, Hapke E, Holder J, Spinale FG, et al. Changes in extracellular collagen matrix alter myocardial systolic performance. *Am J Physiol Heart Circ Physiol*. (2003) 284(1):H122–32. doi: 10.1152/ajpheart.00233.2002

34. Parthasarathy A, Gopi V, Umadevi S, Simna A, Sheik MJ, Divya H, et al. Suppression of atrial natriuretic peptide/natriuretic peptide receptor-a-mediated signaling upregulates angiotensin-II-induced collagen synthesis in adult cardiac fibroblasts. *Mol Cell Biochem*. (2013) 378(1-2):217–28. doi: 10.1007/s11010-013-1612-z

35. Felisbino MB, McKinsey TA. Epigenetics in cardiac fibrosis: emphasis on inflammation and fibroblast activation. *JACC Basic Transl Sci*. (2018) 3(5):704–15. doi: 10.1016/j.jacbts.2018.05.003

36. Xu GJ, Gan TY, Tang BP, Chen ZH, Mahemuti A, Jiang T, et al. Accelerated fibrosis and apoptosis with ageing and in atrial fibrillation: adaptive responses with maladaptive consequences. *Exp Ther Med*. (2013) 5(3):723–9. doi: 10.3892/etm.2013.899

frontiers | Frontiers in Cardiovascular Medicine

TYPE Original Research
PUBLISHED 29 September 2023
DOI 10.3389/fcvm.2023.1144988

OPEN ACCESS

EDITED BY
Yoshiaki Kaneko,
Gunma University, Japan

REVIEWED BY
Nikolaos Fragakis,
Aristotle University Medical School, Greece
Giuseppe Mascia,
University of Genoa, Italy

*CORRESPONDENCE
E. Chieffo
✉ enri.chieffo@gmail.com

RECEIVED 21 January 2023
ACCEPTED 28 August 2023
PUBLISHED 29 September 2023

CITATION
Chieffo E, D'Amore S, De Regibus V, Dossena C, Frigerio L, Taravelli E, Ferrazzano C, De Iuliis P, Cacucci M and Landolina ME (2023) Atrioventricular nodal reentry tachycardia treatment using CARTO 3 V7 activation mapping: a new era of slow pathway radiofrequency ablation is under coming. Front. Cardiovasc. Med. 10:1144988. doi: 10.3389/fcvm.2023.1144988

Atrioventricular nodal reentry tachycardia treatment using CARTO 3 V7 activation mapping: a new era of slow pathway radiofrequency ablation is under coming

Enrico Chieffo[1]*, Sabato D'Amore[1], Valentina De Regibus[1], Cinzia Dossena[1], Laura Frigerio[1], Erika Taravelli[2], Carolina Ferrazzano[3], Pasquale De Iuliis[3], Michele Cacucci[1] and Maurizio E. Landolina[1]

[1]Department of Cardiology, ASST Ospedale Maggiore, Crema, Italy, [2]Department of Cardiology, S. Croce e Carle Hospital, Cuneo, Italy, [3]Biosense Webster, Johnson & Johnson Medical S.p.A., Pomezia, Italy

Background: Slow pathway (SP) ablation is the cornerstone for atrioventricular nodal reentry tachycardia (AVNRT) treatment, and a low-voltage bridge offers a good target during mapping using low x-ray exposure. We aimed to assess a new tool to identify SP by activation mapping using the last CARTO3® version, i.e., CARTO PRIME® V7 (Biosense Webster, Diamond Bar, CA, USA)

Methods and results: Right atrial septum and triangle of Koch 3D-activation map were obtained from intracardiac contact mapping during low x-ray CARTO 3® procedure. In 60 patients (mean age 60.3 ± 14.7, 61% females) undergoing ablation for AVNRT, an automatic activation map using a DECANAV® mapping catheter and CARTO® Confidense™, Coherent, and FAM DX software modules were obtained. The SP was identified in all patients as the latest atrioventricular node activation area; RF catheter ablation (RFCA) in that region elicited junctional beats. The mean procedural time was 150.3 ± 48.3 min, the mean fluoroscopy time exposure was 2.9 ± 2 min, the mean dose-area product (DAP) was 16.5 ± 2.7 cGy/cm^2. The mean number of RF applications was 3.9 ± 2, the mean ablation index was 428.6 ± 96.6, and the mean contact force was 8 ± 2.8 g. There were no adverse event during the procedure, and no AVNRT recurrences occurred during a mean follow-up of 14.3 ± 8.3 months.

Conclusion: Ablation of the SP by automatic mapping using Confidense™, Coherent, and FAM DX software modules is an innovative, safe, and effective approach to AVNRT ablation. The CARTO3® V7 system shows on a 3D map the latest AV node activation area during sinus rhythm allowing low fluoroscopy time and highly effective RFCA.

KEYWORDS

slow pathway, atrioventricular nodal reentry tachycardia, RF ablation, CARTO 3 version 7, activation map, Confidense module

Introduction

Atrioventricular nodal reentry tachycardia (AVNRT) is the most common supraventricular tachycardia in clinical practice (1), and catheter ablation is the treatment of choice for symptomatic patients (2) improving quality of life. The success rate is high (91%–99% of patients) and recurrences are seen in 5%–9%, considering both

radiofrequency (RF) and cryogenic application, and AV block is a rare complication (about 1% of the patients) (3, 4). The slow pathway (SP), generally located in the lower one-third of the Koch triangle in the postero-septal region anterior to the ostium of the coronary sinus (CS), is targeted during ablation using either RF energy or cryoablation, with the aim of rendering the tachycardia not inducible at the end of procedure. During effective ablation, RF energy elicits junctional beats whereas cryoenergy results in non-inducibility with or without echo beats during freezing. Recently, non-fluoroscopic 3D mapping has been used to identify in the postero-septal region a low-voltage bridge as a new target for SP ablation, especially in children (5). The objective of our study was to assess, in a consecutive adult population undergoing SP ablation, how to identify SP location by activation mapping using the last CARTO 3 version, i.e., CARTO PRIME V7 (Biosense Webster, Diamond Bar, CA, USA) (6). The study also aimed to evaluate whether this technique may have an impact on the complexity of the procedure, on the success rate, and on the risk of complications.

Methods

We performed a single-center prospective observational study in 60 consecutive patients (females 61%, mean age 60.3 ± 14.7 years) who underwent catheter ablation for AVNRT between May 2020 and November 2021. All patients had structural normal heart confirmed by echocardiogram. The study was in accordance with the guiding principles of the Declaration of Helsinki; written informed consent was obtained prior to the ablation procedure. Each patient provided informed consent for data collection and analysis.

Electrophysiological study

In all patients, a low x-ray exposure protocol was applied during the Electrophysiological study (EP). The procedure was performed in conscious sedation without general anesthesia. Antiarrhythmic drugs were discontinued for at least five half-lives before the procedure. A quadripolar 2-5-2 mm and a decapolar 2-8-2 mm (DECANAV®, Biosense Webster, CA, USA) catheters were inserted into the left femoral vein and positioned at the His bundle area and in the coronary sinus, respectively, after fast anatomical mapping (FAM) reconstruction. A SMARTTOUCH 4 mm ablation catheter (Biosense Webster©, Inc., Irvine, CA, USA) was inserted into right femoral vein and positioned in the right ventricle (RV) without x-ray exposure. Incremental atrial pacing and programmed atrial or ventricular stimulation were delivered to induce supraventricular tachycardia: the same stimulation protocol was repeated under isoproterenol infusion (0.01–0.04 μg/kg/min) in case of non-induction in baseline condition. An atrial-His jump was considered diagnostic of dual AV node physiology if a sudden prolongation of AH interval by 50 ms was documented following a shortening of the coupling interval of the atrial extrastimulus by 10 ms. During tachycardia, RV reset and entrainment maneuvers were delivered to exclude accessory pathway/atrial tachycardia and to confirm AVNRT. During sinus rhythm para-Hisian pacing was performed to exclude concealed antero-septal accessory pathway. Typical (slow–fast) AVNRT was defined by an atrial-His/His-atrial ratio (AH/HA) >1 and HA interval ≤70 ms; atypical AVNRT (slow–slow and fast–slow) was defined by a delayed retrograde atrial activation HA > 70 ms (2, 7). In the absence of inducible tachycardia, the evidence of an AH jump with an echo beat together with previous electrocardiographic records of a narrow complex tachycardia consistent with AVNRT were considered reasonable features suggestive of this tachycardia.

CARTO 3 mapping

Using the DECANAV catheter and the FAM DX© module (Biosense Webster©, Inc., Irvine, CA, USA), FAM of the right atrium, coronary sinus, and Koch triangle were performed and a voltage gradient and late activation time (LAT) maps were created during sinus rhythm generating a 3D color endocardial gradient map. After FAM reconstruction, quadripolar and decapolar catheters were positioned, respectively, on the His bundle and in the coronary sinus without fluoroscopy exposure. Using Confidense and Coherent© modules, a window of interest (WOI) from −300 to −80 ms before the P wave onset was set. Tissue proximity, LAT stability (5), and cycle length range (925–1,100 ms) were activated too. His potential was accurately marked on the map but excluded during LAT acquisition. The latest atrial activation in correspondence with the Koch triangle at the LAT map was considered a marker of the SP position and was used as a target for ablation (**Figure 1**). A low-voltage bridge was defined from the voltage gradient map as previously described by Drago et al. (5, 8).

Ablation procedure

Once the diagnosis of AVNRT was established, the ablation catheter was moved from RV to Koch Triangle. In correspondence of Koch triangle's latest activation area identified with the techniques described above (**Figure 1**), a "hump and spike" signal (9, 10) was recorded during sinus rhythm, and the maximum local atrial-His delay (ms) and the local distance (mm) from the His bundle were evaluated (**Figure 2**). RF energy [power 30 W, not irrigated tip, temperature setting of 55°C, minimum contact force (CF) 5 g, up to 60 s] was delivered in correspondence to the latest activation area to obtain junctional beats with 1:1 retrograde ventriculo-atrial (VA) conduction. In case of absence of VA retrograde conduction during junctional rhythm, RF delivery was immediately interrupted. Once junctional rhythm with VA conduction was recorded, energy delivery was continued up to 60 s or until junctional rhythm cessation. Following ablation, arrhythmia induction at baseline and under isoproterenol infusion was attempted. End points for ablation success were non-inducibility of AVNRT and elimination of atrial-His jump; in case of modulation of slow

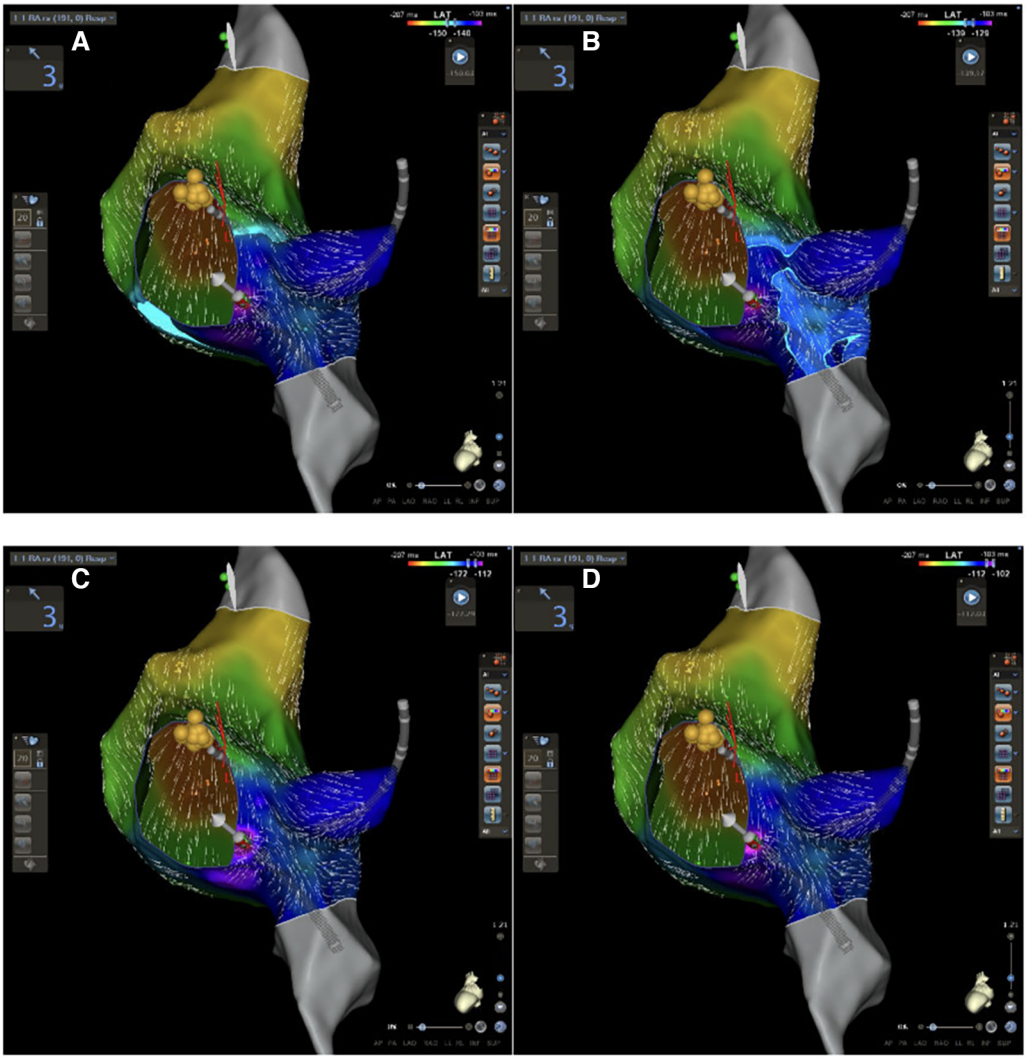

FIGURE 1
CARTO 3 PRIME V7 atrial and Koch's triangle activation during sinus rhythm in LAO view. (A–D) Progressive activation of Koch's triangle: slow pathway is located at the area of latest activation (purple area in D).

pathway, single atrial-His jump eventually followed by single reentry was tolerated without tachycardia induction (6).

Follow-up

After successful ablation, patients were discharged within 24 h on aspirin and no antiarrhythmic drugs. All patients were followed up for at least 12 months; follow-up visit and 24 h ECG Holter were programmed at 3 and 12 months. No patients were lost to follow-up. Documentation of AVNRT at 12 lead ECG or 24 h ECG Holter or emergency room admission for symptoms compatible with supraventricular tachycardia were considered arrhythmia recurrences.

Statistical analysis

Descriptive statistics (mean ± SD, counts and percentages) were used to summarize the data. A two-sample Student's *t*-test were used to compare distance (mm) from ablation point to His potential between subgroups of patient (<75 and ≥75 years). Receiver operating characteristic (ROC) curve analysis was performed to identify the optimal cut-off of the ablation index (AI) and CF for predicting effective radiofrequency ablation.

Results

The results are reported in **Table 1**. All patient enrolled in our study underwent electrophysiological study and ablation procedure. No major complications occurred during and after the procedure. Procedural success rate was 100%, and there were no tachycardia recurrences during a mean follow of 14.3 ± 8.3 months. No acute or late AV block was documented. Slow–fast AVNRT was induced in 58 (96%) patient, slow–slow AVNRT was documented in 1 (2%) patient, and a fast–slow tachycardia was found in 1 (2%). A residual SP function with an echo beat

10.3389/fcvm.2023.1144988

FIGURE 2
An example of AH measurement on His catheter and at the ablation site during slow pathway ablation: the difference represents delay of the local atriogram to His atriogram (40 ms in this case).

TABLE 1 Demographic and procedural characteristics of the overall population.

Overall population	
Age (years)	60.3 ± 14.7
Sex (M/F, %)	39/61
Symptomatic (%)	100
Access to ER (%)	46.6
Tachycardia CL (ms)	375 ± 65.1
AVNRT	
Slow–fast (%)	96
Fast–slow (%)	2
Slow–slow (%)	2
Slow pathway	
Ablation (%)	60
Modulation (%)	40
Cardiomyopathy (%)	1.5
Fluoroscopy time (min)	2.9 ± 2
Radiofrequency total time (s)	200 ± 121
Procedural time (min)	150.3 ± 48.3
DAP (cGy/cm^2)	16.5 ± 2.7
RF applications	3.9 ± 2
Follow-up (months)	14.3 ± 8.3
Acute procedural success (%)	100
Arrhythmic recurrences at follow-up (%)	
3 months	0
12 months	0
AV block (%)	
Acute	0
Late	0
AH–His cath (ms)	96.3 ± 27
AH (abl site) (ms)	52.3 ± 20
AI (ablation site)	428.6 ± 96.6
CF (g)	8 ± 2.8
Distance Abl site–His bundle (mm)	18.6 ± 4.5

DAP, dose-area product; AI, ablation index; CF, contact force.

was remained at 40% of clinical cases (24 patients) after RF application: no AVNRT recurrences were reported at clinical follow-up. The mean procedural time was 150.3 ± 48.3 min, the mean fluoroscopy time exposure was 2.9 ± 2 min, and the mean dose-area product (DAP) 16.5 ± 2.7 cGy/cm^2. The mean number of RF applications was 3.9 ± 2, the mean ablation index was 428.6 ± 96.6, and the mean contact force was 8 ± 2.8 g.

Distance from the ablation site to the His bundle was 18.6 ± 4.5 mm, and no significant differences were found between young and old patients ($p = 0.64$), after dividing our population into two groups and considering 75 years elderly threshold. Delay of the local atriogram to His atriogram was 44 ± 7 ms (Table 1). Ablation points were located at the postero-septal area (88%), at medio-septal area (6%), and at coronary sinus ostium (6%). No ablation site was located inside the coronary sinus, at the antero-septal region or at the postero-septal aspect of the mitral valve. We found that A/V ratio at the target point was 1/2 in all our procedure (Figure 2). Furthermore, ROC curves were created to identify the cut-off value for AI (>380, AUC: 0.90, $p < 0,001$, sensitivity 90.2, specificity 88.2) and for CF (>6 g, AUC: 0.69, $p = 0.04$, sensitivity 73.5, specificity 57.1) (Figure 3).

Discussion

In 60 consecutive patients, undergoing EP study and catheter ablation for AVNRT, was used a new mapping tool by Biosense CARTO 3® PRIME® V7 system including Confidense, Coherent, and FAM DX modules. The reduction of radiological exposure in the electrophysiology lab has become a decisive point for everyday activity due to the stochastic and deterministic effects that x-rays could have on our patient's health (11). For this reason, our ablation technique was different from the conventional one: we used the latest technological innovations by Biosense CARTO 3 to reduce radiological exposure and cancer risk without reducing the effectiveness of ablation (absence of recurrences) or increasing procedure-related complications. As described by Mascia and Giaccardi (12), electrophysiologists should ensure that x-ray exposure is low as reasonably achievable without sacrificing quality of care: zero and near-zero fluoroscopic approaches represent a milestone for cancer prevention in ablation procedure. For these reasons, we used the Confidense, Coherent, and FAM DX modules that allowed a high-definition mapping as well as an accurate selection of electrical activation points under low radiological exposure. In particular, using DECANAV® catheters and CARTO® 3 FAM DX software, we performed a fast electroanatomical reconstruction and activation map of the right atrium/Koch's triangle/tricuspid valve in sinus rhythm by creating a high-density mapping points without using an ablator catheter. The CARTO® 3 Confidence Module allowed us to collect a large number of atriograms by selecting them and discarding points not pertinent to the ongoing reconstruction. CARTO® 3 Coherent Module integrated vector and velocity information to every electroanatomical point in a vector map allowing us to identify easily the ablation site.

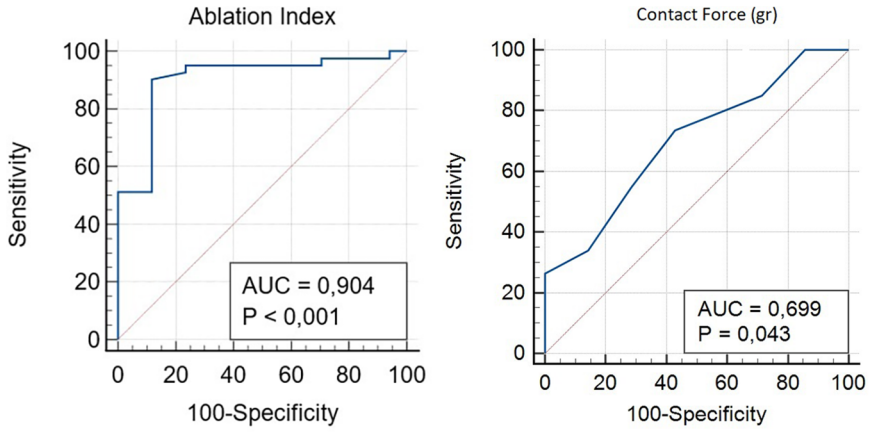

FIGURE 3
ROC curve analysis was performed to identify the optimal cut-off of the AI and CF for predicting effective radiofrequency ablation.

These new CARTO® 3 system technologies may offer a fast method to evaluate Koch's triangle activation and to perform AVNRT ablation. All atriograms were annotated excluding the His bundle signal to create an annotation map of the right atrium, in particular, of Koch's triangle: in this way, it was possible to identify the latest activation of Koch's triangle which may be an expression of the AV nodal slow pathway. This hypothesis agrees with the first descriptions of Spach and Josephson (13, 14) according to which AV nodal slow pathway cannot be identified by a single endocavitary signal (such as His bundle), and it is not a defined region with a set of specialized cells but a wide variation of a local non-uniform anisotropic conduction. No areas of conduction block were identified as previously described by Pandozi et al. (15). A convergence of the activation front has been identified in correspondence with the slow conduction pathway: a wavefront coming from the apex of Koch's triangle (fast conduction pathway) and another coming from the base (tricuspid valve), which is activated laterally along the cavo-tricuspid isthmus (**Figure 1**).

Our mapping and ablation approach using new technologies for identifying the area of slow conduction seems to militate in this direction (**Figure 1**). We suggest that this new method has several advantages: it is simple (it uses the same number of catheters as a traditional ablation), fast (it takes a few minutes more than traditional methods that are compensated by shorter ablation time), reproducible (in all our cases it was possible to identify it the latest activation of Koch's triangle), and safe (no temporary or permanent AV blocks or other complications occurred). Furthermore, our study suggests new cut-off settings for AVNRT ablation procedure: a successful procedure needs an ablation index of more than 380 and a CF of more than 6 g (**Figure 3**). No AI or CF values were previously described for AVNRT ablation procedures. Our approach with low x-ray exposure achieved an average DAP of 16.5 ± 2.7 cGy/cm^2, it corresponds to an effective dose (ED) of 0.032 ± 0.005 mSv for an adult patient calculated with the formula DAP (Gy) $\times$ 0.2. When compared with the ED data reported in the work of Picano and Piccaluga (11) for an AVNRT ablation (ED 4.4 mSv), it represents a big step forward in terms of x-ray exposure reduction for electrophysiologists and patients, equal to an additional lifetime risk of fatal and non-fatal cancer between $1/10^5$ and $1/10^6$.

The follow-up period is not excessively long due to the recent introduction of these CARTO 3 system tools, and we have not documented acute or late AV conduction blocks (16, 17): it was never necessary to perform the ablation in proximity of areas where a far field of the Hisian potential was recorded or to redo the ablation procedure for arrhythmic recurrences.

Conclusions

Activation mapping of Koch's triangle with new CARTO PRIME® V7 modules (Confidense, Coherent and FAM DX) during a procedure of AVNRT ablation allows to correctly identify the slow conduction pathway, to perform an effective ablation and to minimize the risk of complications such as atrioventricular block even in cases without a low-voltage bridge identification. Furthermore we suggest new cut-off settings for AVNRT ablation procedure such as the effective ablation index, the delay in ms of target signal compared to the Hisian atriogram and the mean catheter force at the ablation site. As expected, this new method significantly reduces radiological exposure which is a current theme in electrophysiological labs.

Study limitation

The limitations of the current analysis are the same as those of other single-center observational studies, such as potential bias in patient selection and lack of a control group. Nevertheless, possible bias is mitigated by the fact that patients were consecutively and prospectively included. It may not be

ruled out that the absence of recurrences could be either due to the relatively limited number of patients or the duration of follow-up. Moreover, the absence of recurrence could have influenced and limited the relevance of some mapping and activation parameters such as the presence of areas of slow conduction inside the coronary sinus or at postero-septal aspect of the mitral valve. Thus, larger multicenter studies could be helpful to evaluate better the relevance of this new mapping method for AVNRT ablation.

Data availability statement

The raw data supporting the conclusions of this article will be made available by the authors, without undue reservation.

Ethics statement

The studies involving humans were approved by ASST OSPEDALE MAGGIORE DI CREMA. The studies were conducted in accordance with the local legislation and institutional requirements. Written informed consent for participation was not required from the participants or the participants' legal guardians/next of kin in accordance with the national legislation and institutional requirements.

Author contributions

All authors listed have made a substantial, direct, and intellectual contribution to the work and approved it for publication.

Conflict of interest

ML is a member of speaker bureau of Medtronic and Boston Scientific. CF and PD are employed by Biosense Webster Corporation, a Johnson and Johnson Company. CF and PD did not have access to study results.

The remaining authors declare that the research was conducted in the absence of any commercial or financial relationships that could be construed as a potential conflict of interest.

The reviewer GM declared a past co-authorship with the author ML to the handling editor.

Publisher's note

References

1. Porter MJ, Morton JB, Denman R, Lin AC, Tierney S, Santucci PA, et al. Influence of age and gender on the mechanism of supraventricular tachycardia. *Heart Rhythm*. (2004) 1:393–6. doi: 10.1016/j.hrthm.2004.05.007

2. Goldberg AS, Bathina MN, Mickelsen S, Nawman R, West G, Kusumoto FM. Long-term outcomes on quality-of-life and health care costs in patients with supraventricular tachycardia (radiofrequency catheter ablation versus medical therapy). *Am J Cardiol*. (2002) 89:1120–3. doi: 10.1016/S0002-9149(02)02285-3

3. Clague JR, Dagres N, Kottkamp H, Breithardt G, Borggrefe M. Targeting the slow pathway for atrioventricular nodal reentrant tachycardia: initial results and longterm follow-up in 379 consecutive patients. *Eur Heart J*. (2001) 22:82. doi: 10.1053/euhj.2000.2124

4. Chan NY, Mok NS, Lau CL, Lo YK, Choy CC, Lau ST, et al. Treatment of atrioventricular nodal re-entrant tachycardia by cryoablation with a 6 mm-tip catheter vs. radiofrequency ablation. *Europace*. (2009) 11:1065–70. doi: 10.1093/europace/eup121

5. Drago F, Battipaglia I, Russo MS, Remoli R, Pazzano V, Grifoni G, et al. Voltage gradient mapping and electrophysiologically guided cryoablation in children with AVNRT. *Europace*. (2018) 20(4):665–72. doi: 10.1093/europace/eux021

6. Lindsay BD, Chung MK, Carolyn Gamache M, Luke RA, Schechtman KB, Osborn JL, et al. Therapeutic end points for the treatment of atrioventricular node reentrant tachycardia by catheter-guided radiofrequency current. *J Am Coll Cardiol*. (1993) 22:733–40. doi: 10.1016/0735-1097(93)90184-3

7. Katritsis DG, Sepahpour A, Marine JE, Katritsis GD, Tanawuttiwat T, Calkins H, et al. Atypical atrioventricular nodal reentrant tachycardia: prevalence, electrophysiologic characteristics, and tachycardia circuit. *Europace*. (2015) 17:1099–106. doi: 10.1093/europace/euu387

8. Drago F, Calvieri C, Russo MS, Remoli R, Pazzano V, Battipaglia I, et al. Low-voltage bridge strategy to guide cryoablation of typical and atypical atrioventricular nodal re-entry tachycardia in children: mid-term outcomes in a large cohort of patients. *Europace*. (2021) 23(2):271–7. doi: 10.1093/europace/euaa195

9. Bailin SJ, Korthas MA, Weers NJ, Hoffman CJ. Direct visualization of the slow pathway using voltage gradient mapping: a novel approach for successful ablation of atrioventricular nodal reentry tachycardia. *Europace*. (2011) 13(8):1188–94. doi: 10.1093/europace/eur112

10. Jentzer JH, Goyal R, Williamson BD, Man KC, Niebauer M, Daoud E, et al. Analysis of junctional ectopy during radiofrequency ablation of the slow pathway in patients with atrioventricular nodal reentry tachycardia. *Circulation*. (1994) 90(6):2820–6. doi: 10.1161/01.cir.90.6.2820

11. Picano E, Piccaluga E. Risks related to fluoroscopy radiation associated with electrophysiology procedure. *J Atr Fibrillation*. (2014) 7(2):1044. doi: 10.4022/jafib.1044

12. Mascia G, Giaccardi M. A new era in zero x-ray ablation. *Arrhythm Electrophysiol Rev*. (2020 Nov) 9(3):121–7. doi: 10.15420/aer.2020.02

13. Spach M, Josephson M. Initiating re-entry: the role of non uniform anisotropy in small circuits. *J Cardiovasc Electrophysiol*. (1994) 5:182–209. doi: 10.1111/j.1540-8167.1994.tb01157.x

14. McGuire M, de Bakker JM, Vermeulen JT, Opthof T, Becker AE, Janse MJ, et al. Origin and significance of double potentials near the atrioventricular node. Correlation of extracellular potentials, intracellular potentials and histology. *Circulation*. (1994) 89:2351–60. doi: 10.1161/01.CIR.89.5.2351

15. Pandozi C, Matteucci A, Galeazzi M, Ficili S, Malacrida M, Colivicchi F, et al. New insights into atrioventricular nodal anatomy, physiology, and immunochemistry: a comprehensive review and proposed model of the slow-fast atrioventricular nodal reentrant tachycardia circuit in agreement with direct potential recordings in the Koch's triangle area. *Heart Rhythm*. (2023) 20(4):614–26. doi: 10.1016/j.hrthm.2023.01.004

16. Bohnen M, Stevenson WG, Tedrow UB, Michaud GF, John RM, Epstein LM, et al. Incidence and predictors of major complications from contemporary catheter ablation to treat cardiac arrhythmias. *Heart Rhythm*. (2011) 8:1661–6. doi: 10.1016/j.hrthm.2011.05.017

17. Feldman A, Voskoboinik A, Kumar S, Spence S, Morton JB, Kistler PM, et al. Predictors of acute and long-term success of slow pathway ablation for atrioventricular nodal reentrant tachycardia: a single center series of 1,419 consecutive patients. *Pacing Clin Electrophysiol*. (2011) 34:927–33. doi: 10.1111/j.1540-8159.2011.03092.x

Frontiers in
Cardiovascular Medicine

Innovations and improvements in cardiovascular treatment and practice

Focuses on research that challenges the status quo of cardiovascular care, or facilitates the translation of advances into new therapies and diagnostic tools.

Discover the latest Research Topics

See more →

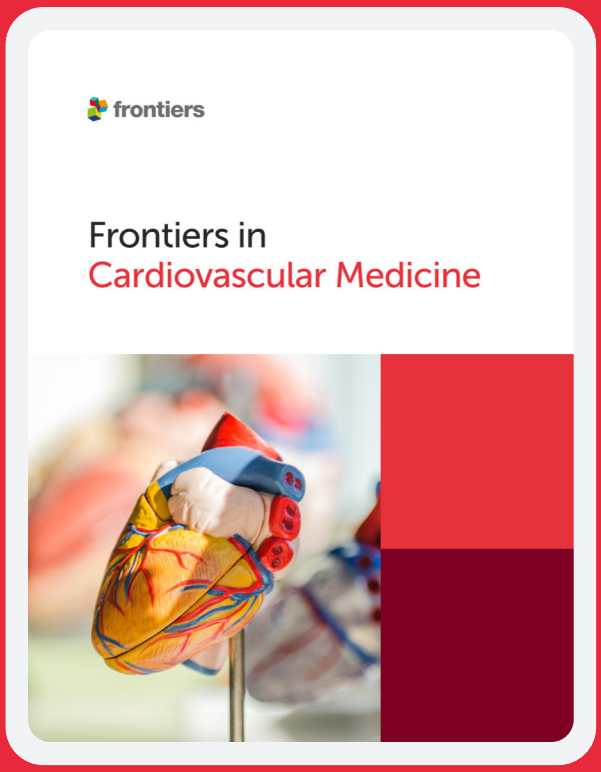

Frontiers

Avenue du Tribunal-Fédéral 34
1005 Lausanne, Switzerland
frontiersin.org

Contact us

+41 (0)21 510 17 00
frontiersin.org/about/contact